

EMERGING INFECTIOUS DISEASES[®]



Respiratory Infections

October 2019



EMERGING INFECTIOUS DISEASES®

EDITOR-IN-CHIEF

D. Peter Drotman

ASSOCIATE EDITORS

Paul M. Arguin, Atlanta, Georgia, USA
 Charles Ben Beard, Fort Collins, Colorado, USA
 Ermias Belay, Atlanta, Georgia, USA
 David M. Bell, Atlanta, Georgia, USA
 Sharon Bloom, Atlanta, Georgia, USA
 Richard Bradbury, Bratislava, Slovakia
 Mary Brandt, Atlanta, Georgia, USA
 Corrie Brown, Athens, Georgia, USA
 Charles H. Calisher, Fort Collins, Colorado, USA
 Benjamin J. Cowling, Hong Kong, China
 Michel Drancourt, Marseille, France
 Paul V. Effler, Perth, Australia
 Anthony Fiore, Atlanta, Georgia, USA
 David O. Freedman, Birmingham, Alabama, USA
 Peter Gerner-Smidt, Atlanta, Georgia, USA
 Stephen Hadler, Atlanta, Georgia, USA
 Matthew J. Kuehnert, Edison, New Jersey, USA
 Nina Marano, Atlanta, Georgia, USA
 Martin I. Meltzer, Atlanta, Georgia, USA
 David Morens, Bethesda, Maryland, USA
 J. Glenn Morris, Jr., Gainesville, Florida, USA
 Patrice Nordmann, Fribourg, Switzerland
 Johann D.D. Pitout, Calgary, Alberta, Canada
 Ann Powers, Fort Collins, Colorado, USA
 Didier Raoult, Marseille, France
 Pierre E. Rollin, Atlanta, Georgia, USA
 David H. Walker, Galveston, Texas, USA
 J. Todd Weber, Atlanta, Georgia, USA
 J. Scott Weese, Guelph, Ontario, Canada

Managing Editor

Byron Breedlove, Atlanta, Georgia, USA

Copy Editors

Kristina Clark, Dana Dolan, Karen Foster,
 Thomas Gryczan, Amy Guinn, Michelle Moran, Shannon O'Connor,
 Jude Rutledge, P. Lynne Stockton, Deborah Wenger

Production

Thomas Eheman, William Hale, Barbara Segal,
 Reginald Tucker

Journal Administrator

Susan Richardson

Editorial Assistants

Kelly Crosby, Kristine Phillips

Communications/Social Media

Sarah Logan Gregory,
 Tony Pearson-Clarke, Deanna Altomara (intern)

Founding Editor

Joseph E. McDade, Rome, Georgia, USA

EDITORIAL BOARD

Barry J. Beaty, Fort Collins, Colorado, USA
 Martin J. Blaser, New York, New York, USA
 Christopher Braden, Atlanta, Georgia, USA
 Arturo Casadevall, New York, New York, USA
 Kenneth G. Castro, Atlanta, Georgia, USA
 Vincent Deubel, Shanghai, China
 Christian Drostén, Charité Berlin, Germany
 Isaac Chun-Hai Fung, Statesboro, Georgia, USA
 Kathleen Gensheimer, College Park, Maryland, USA
 Rachel Gorwitz, Atlanta, Georgia, USA
 Duane J. Gubler, Singapore
 Richard L. Guerrant, Charlottesville, Virginia, USA
 Scott Halstead, Arlington, Virginia, USA
 David L. Heymann, London, UK
 Keith Klugman, Seattle, Washington, USA
 Takeshi Kurata, Tokyo, Japan
 S.K. Lam, Kuala Lumpur, Malaysia
 Stuart Levy, Boston, Massachusetts, USA
 John S. Mackenzie, Perth, Australia
 John E. McGowan, Jr., Atlanta, Georgia, USA
 Jennifer H. McQuiston, Atlanta, Georgia, USA
 Tom Marrie, Halifax, Nova Scotia, Canada
 Nkuchia M. M'ikanatha, Harrisburg, Pennsylvania, USA
 Frederick A. Murphy, Bethesda, Maryland, USA
 Barbara E. Murray, Houston, Texas, USA
 Stephen M. Ostroff, Silver Spring, Maryland, USA
 Mario Raviglione, Milan, Italy, and Geneva, Switzerland
 David Relman, Palo Alto, California, USA
 Guenael R. Rodier, Saône-et-Loire, France
 Connie Schmaljohn, Frederick, Maryland, USA
 Tom Schwan, Hamilton, Montana, USA
 Frederic E. Shaw, Atlanta, Georgia, USA
 Rosemary Soave, New York, New York, USA
 P. Frederick Sparling, Chapel Hill, North Carolina, USA
 Robert Swanepoel, Pretoria, South Africa
 David E. Swayne, Athens, Georgia, USA
 Phillip Tarr, St. Louis, Missouri, USA
 Duc Vugia, Richmond, California, USA
 Mary E. Wilson, Cambridge, Massachusetts, USA

Emerging Infectious Diseases is published monthly by the Centers for Disease Control and Prevention, 1600 Clifton Rd NE, Mailstop H16-2, Atlanta, GA 30329-4027, USA. Telephone 404-639-1960, fax 404-639-1954, email eideditor@cdc.gov.

The conclusions, findings, and opinions expressed by authors contributing to this journal do not necessarily reflect the official position of the U.S. Department of Health and Human Services, the Public Health Service, the Centers for Disease Control and Prevention, or the authors' affiliated institutions. Use of trade names is for identification only and does not imply endorsement by any of the groups named above.

All material published in Emerging Infectious Diseases is in the public domain and may be used and reprinted without special permission; proper citation, however, is required.

Use of trade names is for identification only and does not imply endorsement by the Public Health Service or by the U.S. Department of Health and Human Services.

EMERGING INFECTIOUS DISEASES is a registered service mark of the U.S. Department of Health & Human Services (HHS).

∞ Emerging Infectious Diseases is printed on acid-free paper that meets the requirements of ANSI/NISO Z39.48-1992 (Permanence of Paper)

EMERGING INFECTIOUS DISEASES®

Respiratory Infections

October 2019



On the Cover

Robert Lee Kocher (1929–), *Two Birds* (1959). Oil on wood, 12 in x 7.75 in/30.5 cm x 19.7 cm. Image used by permission of the artist. Private collection, Fayetteville, Georgia, USA. Photography by James Gathany

About the Cover p. 1999

Synopses

Localized Outbreaks of Epidemic Polyarthrititis among Military Personnel Caused by Different Sublineages of Ross River Virus, Northeastern Australia, 2016–2017

W. Liu et al. 1793

Related material available online:
http://wwwnc.cdc.gov/eid/article/25/10/18-1610_article

Transmissibility of MERS-CoV Infection in Closed Setting, Riyadh, Saudi Arabia, 2015

M.D. Van Kerkhove et al. 1802



Related material available online:
http://wwwnc.cdc.gov/eid/article/25/10/19-0130_article

Emergence and Containment of Canine Influenza Virus A(H3N2), Ontario, Canada 2017–2018

J.S. Weese et al. 1810



***Edwardsiella tarda* Bacteremia, Okayama, Japan, 2005–2016**

We observed more severe underlying diseases, susceptibility of isolated strains to most antimicrobial drugs, and no seasonal distribution.

S. Kamiyama et al. 1817



Case Studies and Literature Review of Pneumococcal Septic Arthritis in Adults

We saw an increase in this condition related to emergence of *Streptococcus pneumoniae* serotype 23B.

A. Dernoncourt et al. 1824

Global Epidemiology of Diphtheria, 2000–2017

K.E.N. Clarke et al. 1834



Related material available online:
http://wwwnc.cdc.gov/eid/article/25/10/19-0271_article

Research

Economic Burden of West Nile Virus Disease, Quebec, Canada, 2012–2013

N. Ouhoumane et al. 1843

VAR2CSA Serology to Detect *Plasmodium falciparum* Transmission Patterns

A.M. Fonseca et al. 1851



Related material available online:
http://wwwnc.cdc.gov/eid/article/25/10/18-1177_article

Risk Factors for Carbapenem-Resistant *Pseudomonas aeruginosa*, Zhejiang Province, China

Y.-Y. Hu et al. 1861



Related material available online:
http://wwwnc.cdc.gov/eid/article/25/10/18-1699_article

Sensitive and Specific Detection of Low-Level Antibody Responses in Mild Middle East Respiratory Syndrome Coronavirus Infections

N.M.A. Okba et al. 1868



Related material available online:
http://wwwnc.cdc.gov/eid/article/25/10/19-0051_article

Comparison of Serologic Assays for Middle East Respiratory Syndrome Coronavirus

R. Harvey et al. 1878



Related material available online:
http://wwwnc.cdc.gov/eid/article/25/10/19-0497_article

Prevalence of Tuberculosis in Children After Natural Disasters, Bohol, Philippines

K.O. Murray et al. 1884



Related material available online:
http://wwwnc.cdc.gov/eid/article/25/10/19-0619_article

Sporotrichosis in the Highlands of Madagascar, 2013–2017

T. Rasamoelina et al. 1893



Related material available online:
http://wwwnc.cdc.gov/eid/article/25/10/19-0070_article

Serologic Evidence of Exposure to Highly Pathogenic Avian Influenza H5 Viruses in Migratory Shorebirds, Australia

M. Wille et al. 1903



Related material available online:
http://wwwnc.cdc.gov/eid/article/25/10/19-0699_article



Risk for Invasive Streptococcal Infections among Adults Experiencing Homelessness, Anchorage, Alaska, USA, 2002–2015

We detected a disproportionately high incidence of these infections in this population.

E. Mosites et al. 1911

Early Diagnosis of Tularemia by Flow Cytometry, Czech Republic, 2003–2015

A. Chrdle et al. 1919

EMERGING INFECTIOUS DISEASES®

October 2019



Dispatches

Control and Elimination of Extensively Drug-Resistant *Acinetobacter baumannii* in an Intensive Care Unit

A. Chamieh et al. 1928

Antigenic Variation of Avian Influenza A(H5N6) Viruses, Guangdong Province, China, 2014–2018

R. Bai et al. 1932



Related material available online:
http://wwwnc.cdc.gov/eid/article/25/10/19-0274_article

***Plasmodium cynomolgi* as Cause of Malaria in Tourist to Southeast Asia, 2018**

G.N. Hartmeyer et al. 1936

Bidirectional Human–Swine Transmission of Seasonal Influenza A(H1N1)pdm09 Virus in Pig Herd, France, 2018

A. Chastagner et al. 1940



Related material available online:
http://wwwnc.cdc.gov/eid/article/25/10/19-0068_article

Tick-Borne Encephalitis in Auvergne-Rhône-Alpes Region, France, 2017–2018

E. Botelho-Nevers et al. 1944

Factoring Prior Treatment into Tuberculosis Infection Prevalence Estimates, United States, 2011–2012

L.A. Vonnahme et al. 1949

Melioidosis after Hurricanes Irma and Maria, St. Thomas/St. John District, US Virgin Islands, October 2017

I. Guendel et al. 1952

Possible Prognostic Value of Serial Brain Magnetic Resonance Imaging for Powassan Virus Encephalitis

J. Allgaier et al. 1956

Rapid Screening of *Aedes aegypti* Mosquitoes for Susceptibility to Insecticides as Part of Zika Emergency Response, Puerto Rico

R.R. Hemme et al. 1959



Related material available online:
http://wwwnc.cdc.gov/eid/article/25/10/18-1847_article

New Exposure Location for Hantavirus Pulmonary Syndrome Case, California, USA, 2018

A.M. Kjemtrup et al. 1962

Two Cases of *Borrelia miyamotoi* Meningitis, Sweden, 2018

A.J. Henningsson et al. 1965



Related material available online:
http://wwwnc.cdc.gov/eid/article/25/10/19-0416_article

Susceptibility of Influenza A, B, C, and D Viruses to Baloxavir

V.P. Mishin et al. 1969



Related material available online:
http://wwwnc.cdc.gov/eid/article/25/10/19-0607_article

Genetic Characterization and Zoonotic Potential of Highly Pathogenic Avian Influenza Virus A(H5N6/H5N5), Germany 2017–2018

A. Pohlmann et al. 1973



Related material available online:
http://wwwnc.cdc.gov/eid/article/25/10/18-1931_article

Research Letters

Lassa Virus in Pygmy Mice, Benin, 2016–2017

A. Yadouleton et al. 1977



Related material available online:
http://wwwnc.cdc.gov/eid/article/25/10/18-0523_article

Genomic Characterization of Rift Valley Fever Virus, South Africa, 2018

A. van Schalkwyk, M. Romito 1979



Related material available online:
http://wwwnc.cdc.gov/eid/article/25/10/18-1748_article

Estimated Incubation Period and Serial Interval for Human-to-Human Influenza A(H7N9) Virus Transmission

L. Zhou et al. 1982



Related material available online:
http://wwwnc.cdc.gov/eid/article/25/10/19-0117_article

Pulmonary Infection Associated with *Mycobacterium canariense* in Suspected Tuberculosis Patient, Iran

F. Sakhaee et al. 1984



Related material available online:
http://wwwnc.cdc.gov/eid/article/25/10/19-0156_article

EMERGING INFECTIOUS DISEASES®

October 2019



Mycobacterium conceptionense Pneumonitis in Patient with HIV/AIDS

S.M. Michienzi et al. 1986

Emergence of Influenza A(H7N4) Virus, Cambodia

D. Vijaykrishna et al. 1988



Related material available online:
http://wwwnc.cdc.gov/eid/article/25/10/19-0506_article

Mycobacterium marseillense Infection in Human Skin, China, 2018

B. Xie et al. 1991



Related material available online:
http://wwwnc.cdc.gov/eid/article/25/10/19-0695_article

Geospatial Variation in Rotavirus Vaccination in Infants, United States, 2010–2017

M.A.M. Rogers et al. 1993

Letters

Databases for Research and Development

M.G. Head 1996

Self-Flagellation as Possible Route of Human T-Cell Lymphotropic Virus Type 1 Transmission

C.E. Styles et al. 1996

Books and Media

Flu Hunter: Unlocking the Secrets of a Virus

S.W. Boktor, S. Ostroff 1998

About the Cover

A Study in Stillness and Symmetry

B. Breedlove 1999

Etymologia

Edwardsiella tarda

R. Henry 1833

Corrections

1997

Vol. 25, No. 3

Figure 2 contained incorrect values in Cross-Border Movement of Highly Drug-Resistant *Mycobacterium tuberculosis* from Papua New Guinea to Australia through Torres Strait Protected Zone, 2010–2015.

Vol. 25, No. 9

Clostridioides was misspelled in Risk for *Clostridioides difficile* Infection among Older Adults with Cancer.

DECEMBER 2019 WILL BE EID'S FINAL PRINT ISSUE



Emerging Infectious Diseases will transition to an online-only journal starting with the January 2020 issue, the beginning of Volume 26.

Bookmark the journal's website so you can access and search all of EID's new and archived content, and sign up for email notifications for monthly table of contents alerts and topics of interest.

<https://wwwnc.cdc.gov/eid/>

Localized Outbreaks of Epidemic Polyarthriti s among Military Personnel Caused by Different Sublineages of Ross River Virus, Northeastern Australia, 2016–2017

Wenjun Liu, Joanne R. Kizu, Luke R. Le Grand, Christopher G. Moller, Tracy L. Carthew, Ian R. Mitchell, Ania J. Gubala, John G. Aaskov

Two outbreaks of epidemic polyarthriti s occurred among Australian Defence Force personnel during and following short military exercises in the Shoalwater Bay Training Area, northeastern Australia, in 2016 and 2017. Ross River virus (RRV) IgM was detected in acute-phase serum samples from most patients (28/28 in 2016 and 25/31 in 2017), and RRV was recovered from 4/38 serum samples assayed (1/21 in 2016 and 3/17 in 2017). Phylogenetic analyses of RRV envelope glycoprotein E2 and nonstructural protein nsP3 nucleotide sequences segregated the RRV isolates obtained in 2016 and 2017 outbreaks into 2 distinct sublineages, suggesting that each outbreak was caused by a different strain of RRV. The spatiotemporal characteristics of the 2016 outbreak suggested that some of the infections involved human-mosquito-human transmission without any intermediate host. These outbreaks highlight the importance of personal protective measures in preventing vectorborne diseases for which no vaccine or specific prophylaxis exists.

Epidemic polyarthriti s (EPA) caused by Ross River virus (RRV) infection is the most frequently reported arboviral disease in Australia; $\approx 55,000$ cases have been reported over the past decade (1). RRV is a positive-sense, single-strand RNA, enveloped virus in the *Alphavirus* genus of the *Togaviridae* family. Other viruses in this genus include chikungunya virus (CHIKV), Barmah Forest virus (BFV), Sindbis virus, and Eastern and Western equine encephalitis viruses. The prototype strain of RRV (T48) was isolated in

1959 from *Aedes vigilax* mosquitoes captured near the Ross River in Townsville, Queensland, Australia (2). Since then, outbreaks have been recorded in all the states of Australia (3) and in the South Pacific and Western Pacific regions, including Fiji (4), Samoa (5,6), the Cook Islands (7), New Caledonia (8), and Papua New Guinea (9,10). In Australia, most RRV infections occur during February–May or after periods of high rainfall or spring tides (11).

RRV is endemic and enzootic in Australia and has a natural animal-mosquito-animal transmission cycle. Humans can become infected incidentally by virus spillover, resulting in seasonal disease outbreaks. RRV has a complex ecology; >40 different mosquito species have been implicated as vectors, and ≥ 18 different wild and domestic animals and birds could serve as amplifying hosts (12–14). Humans can carry the virus from endemic to epizootic regions, and human-mosquito-human transmission is thought to be the most common means of transmission during large epidemics (15,16).

The RRV disease state varies widely between persons. This variation is readily apparent during outbreaks of the virus, wherein most persons in an infected population have asymptomatic or subclinical infection and only a few patients are substantially affected by the virus (ratio $\approx 3:1$) (4). Among patients reporting clinical symptoms, most will recover in 4–6 weeks. However, in some cases, joint pain, muscle pain, and fatigue can persist for several months or years (17). RRV-caused EPA is characterized by arthritis, particularly in the small joints of the hands and feet. About 20%–60% of patients also have rash, fever, malaise, or a combination of these signs and symptoms (18–21). Symptoms similar to EPA occur after infection with BFV, CHIKV, Epstein-Barr virus (22), rubella virus (23), and parvovirus B19 (24). BFV co-circulates with RRV; $\approx 1,600$ cases of BFV infection are reported each year in Australia (1,20). Although transmission of CHIKV does not occur in

Author affiliations: Australian Defence Force Malaria and Infectious Disease Institute, Enoggera, Queensland, Australia (W. Liu, J.R. Kizu, L.R. Le Grand, C.G. Moller, T.L. Carthew); Australian Defence Science and Technology Group, Fishermans Bend, Victoria, Australia (I.R. Mitchell, A.J. Gubala); Queensland University of Technology, Brisbane, Queensland, Australia (J.G. Aaskov)

DOI: <https://doi.org/10.3201/eid2510.181610>

Australia, clinical infections have been reported in travelers returning to Australia from endemic areas (25,26).

During 2016–2017, two outbreaks of EPA occurred in Australian Defence Force (ADF) personnel during and after short military exercises in the Shoalwater Bay Training Area (SWBTA) in northeastern Australia. We conducted an investigation to confirm whether the 2 outbreaks of EPA among ADF personnel in SWBTA were attributable to RRV infection by identifying RRV RNA in patient serum samples and to determine whether the viruses were novel genotypes (and, if so, their phylogenetic origin).

Material and Methods

Ethics Statement

This study was a retrospective study approved by the ADF Joint Health Command Ethics Review Committee (Joint Health Command low-risk ethics panel no. 16-021). We obtained written formal consent from all participants.

Study Area

SWBTA is a 4,545-km² expanse of naturally vegetated coastal region ≈80 km north of the city of Rockhampton, Queensland, in northeastern Australia. ADF and allied forces use it regularly for military training. Because of its large size, restricted access, and protected ecology, regular mosquito surveillance or control is not conducted in the area. SWBTA is populated with large numbers of mammal and bird species, which could serve as hosts for RRV, as well as >40 species of mosquitoes, including major RRV vectors *Aedes vigilax* and *Culex annulirostris* mosquitoes (11,18,27). Weather conditions in SWBTA during March–May are typically hot and humid.

Epidemiologic Data Collection

Laboratory confirmation of a RRV infection is achieved by isolating RRV or detecting viral RNA in patient serum samples or through observing seroconversion within 8–10 weeks of onset of symptoms consistent with RRV infection (28). Clinical records for patients could not be accessed for this investigation, so we collected information about clinical symptoms and what personal protective measures (PPMs) patients had undertaken during the exercise by using questionnaires completed by ADF personnel who had EPA symptoms and had given their consent to participate in this study.

Virus Isolation and Genotyping

We obtained acute-phase serum samples from EPA patients who consented to participate in this study from Queensland Medical Laboratories on completion of routine RRV testing for RRV IgM and IgG with Panbio ELISA kits (<http://www.panbiosystems.com>). We recovered virus by culturing

100 μL of a patient serum sample on monolayers of C6–36 cells. We detected RRV infection in these cells 3 days postinfection by indirect immunofluorescence using an RRV-specific monoclonal antibody D7 (29).

We extracted viral RNA from serum and cell culture fluid by using the QIAamp viral RNA Mini Kit (QIAGEN, <https://www.qiagen.com>) according to the manufacturer's instructions. The glycoprotein E2 and nonstructural protein nsP3 genes were amplified by using reverse transcription PCR, and amplicons were purified from Tris-acetate-EDTA (TAE) agarose gels and sequenced at the Australian Genome Research Facility, as described previously (30). We edited and assembled all sequences by using Geneious 11.2 (<https://www.geneious.com>). An additional 20 strains of RRV collected previously by our laboratory were sequenced in the same manner and submitted to GenBank (Appendix Table 1, <https://wwwnc.cdc.gov/EID/article/25/10/18-1610-App1.pdf>).

Phylogenetic Analysis

We aligned nucleotide sequences of 58 RRV E2 genes and 32 nsP3 genes (Appendix Table 1) by using the ClustalW program in Geneious. E2 and nsP3 sequences for 24 of these viruses were derived in this study. We converted the alignment file to NEXUS format by using MEGAX for use with BEAST (<http://beast.community>) and associated tools to postulate a phylogenetic tree for the RRV E2 and nsP3 proteins. We determined the nucleotide-substitution model by using the model test capability in MEGAX and confirmed the findings by using jModelTest 2.1.3 (31). Although the general time reversible plus gamma distribution with invariant sites (GTR+Γ+I) and Hasegawa–Kishino–Yano (HKY) substitution models were considered in BEAST, TN93+Γ had the lowest Bayesian information criterion score (32–34) (Appendix Table 2) and was selected for the phylogenetic analysis of the E2 gene.

Isolation dates of RRV at the tips of phylogenetic trees were taken from the GenBank “collection date” field and estimated to have a precision of ±1.5 years. We conducted initial analyses assuming a strict molecular clock model because the evolutionary timeframe for this study was comparatively short. However, we also acknowledged that the environmental conditions were sufficiently diverse to warrant a relaxed clock (lognormal). We used the Bayesian skyline as the demographic model for the phylogenetic trees. We performed Markov chain Monte Carlo analysis by using BEAST version 1.8.1 with a 10 million chain length and sampling every 1,000 generations and assessed convergence of parameters on the basis of the ESS value >200, which was viewed by using Tracer 1.6.0. We subsequently generated maximum clade credibility trees after a 10% burn-in protocol by using TreeAnnotator version 1.8.1 and formatted the final trees in FigTree 1.3.1. We obtained

all software for these analyses, except Geneious, from <http://beast.community>.

Results

The first EPA outbreak was reported after a 12-day exercise (February 29–March 11, 2016). Forty-four personnel from a combat unit of 128 sought care at the Regimental Aid Post (RAP) with rash, headache, nausea, fatigue, lethargy, and joint and muscle pain at the conclusion of the exercise. RRV IgM was detected in acute- or convalescent-phase serum samples collected from 28 of these 44 persons 14–50 days after symptom onset (Table); attack rates ranged from 22% (confirmed cases only, 28/128 [22%]) to 34% (all suspected cases, 44/128 [34%]) (Figure 1, panel A).

Troops from the affected unit (referred to hereafter as the combat unit) had spent 3 days in heavy rain near Camp Growl in the training area (Figure 1, panel B). During the following 3 days, the unit moved over varied terrain, including dense bushland, in hot and humid conditions to an urban operation training facility (UOTF). Once at the UOTF, they conducted urban assault maneuvers against a 36 member opposition force for an additional 5 days. Upon conclusion of the UOTF component of the exercise, the combat unit marched back to Camp Growl, where they spent the night before returning to Brisbane, ≈630 km south of SWBTA. An administration unit of 30 persons was stationed in SWBTA during the same period but remained at Camp Growl throughout the exercise. In addition to the 44 members of the combat unit affected by EPA, 1 member

from the administration unit reported symptoms of EPA, and RRV IgM was detected in this patient's serum sample upon return to Brisbane (attack rate 3.3%) (Figure 1, panel A). None of the 36 members of the opposition force reported symptoms of EPA (Figure 1, panel A). This localized EPA outbreak had 2 distinct epidemic curves, with gaps of 7 days and ≈15 days between the peaks (Figure 1, panel C).

In 2017, a total of 43 members from 3 different units had symptoms of EPA during an exercise conducted from late April to mid-May in the same area as the combat unit affected in the 2016 outbreak. Thirty-one of the 43 patients provided a serum sample. Of these, 25 samples contained RRV IgM (Table). Neither the advancing routes of these 3 units through SWBTA nor the epidemiologic timeline of the 2017 EPA outbreak could be obtained because of ADF operational restrictions. Additional EPA cases might have occurred during both outbreaks, given that anecdotal evidence suggests that members who were unwell at that time chose not to seek care at the RAP. ADF members were not screened for RRV seroconversions over the course of the exercise, so asymptomatic RRV infections could not be detected. Because most RRV infections are asymptomatic, the number of infections during these outbreaks was probably higher than the number of cases reported.

The most common symptoms experienced in the 2016 and 2017 outbreaks were, respectively, polyarthritis and muscle pain (71% and 88%), arthralgia (67% and 88%), fatigue (71% and 88%), loss of appetite (52% and 75%), stiff neck (38% and 71%), fever (33% and 47%), rash (9.5%

Table. Epidemiologic characteristics of RRV outbreaks among ADF personnel during and after training in SWBTA, northeastern Australia, 2016–2017*

Characteristic	Outbreak	
	2016	2017
Total no. reported EPA cases	44	43
% RRV IgM antibody-reactive cases/tested cases	100 (28/28)	80.6 (25/31)
No. participants who consented	21	17
Average age, y (range)	ND	27 (20–45)
Sex, no.	ND	16 M, 1 F
History of arbovirus infection before this infection	0	0
Outdoor training experience in SWBTA	100 (21)	100 (17)
Clinical symptoms		
Severe headache	28.6 (6/21)	41.2 (7/17)
Nausea	4.8 (1/21)	17.7 (3/17)
Rash	9.5 (2/21)	64.7 (11/17)
Fever, chills, or sweats	33.3 (7/21)	47.1 (8/17)
Arthralgia	66.7 (14/21)	88.2 (15/17)
Muscle pain	71.4 (15/21)	88.2 (15/17)
Fatigue	71.4 (15/21)	88.2 (15/17)
Loss of appetite	52.4 (11/21)	70.1 (12/17)
Stiff neck	38.1 (8/21)	64.7 (11/17)
Mosquito bite experiences	100 (21/21)	100 (17/17)
Personal protection measures		
Mosquito repellents	100 (21/21)	100 (17/17)
Trousers and long-sleeve shirts	85.7 (18/21)	47.1 (8/17)
Slept under ADF-issued mosquito nets	57.1 (12/21)	82.4 (14/17)
Awareness of permethrin uniform and bed net treatment	100 (21/21)	100 (17/17)
Use of ADF-recommended permethrin treatment	0 (0/21)	0 (0/17)

*Data are % (no. positive/total no.) unless otherwise indicated. ADF, Australian Defence Force; EPA, epidemic polyarthritis; ND, not done; RRV, Ross River virus; SWBTA, Shoalwater Bay Training Area.

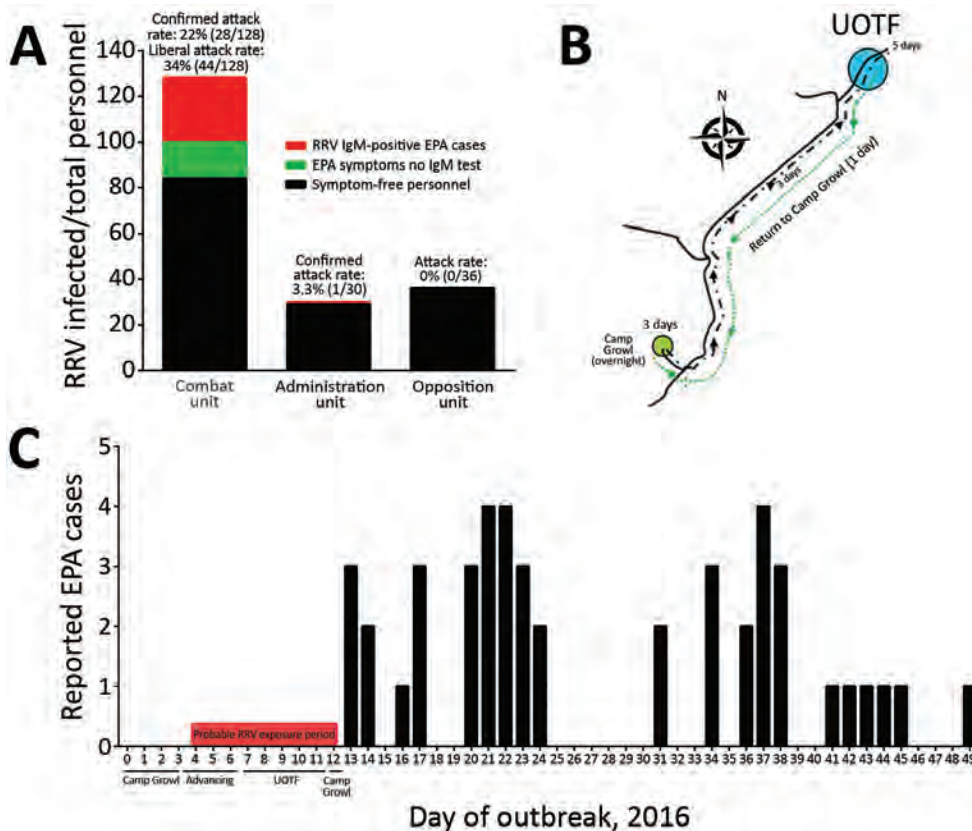


Figure 1. Characteristics of an RRV outbreak among Australian Defence Force (ADF) personnel during and after training in Shoalwater Bay Training Area (SWBTA), northeastern Australia, 2016. A) RRV attack rates among 3 ADF units. B) Routes of ADF units during exercises in SWBTA. C) Timeline of outbreak. EPA, epidemic polyarthrits; RRV, Ross River virus; UOTF, urban operation training facility.

and 65%), headache (28% and 41%), and sore throat (14% and 24%) (Table). Most personnel recovered within 4–6 weeks of symptom onset, except for 3 from the 2016 outbreak who were unfit for deployment 3 months after illness onset because of ongoing signs and symptoms.

All study participants were aware of the ADF policy of dipping uniforms and bed nets in permethrin, but none of the participants, nor their unit commanders, requested support from the Preventive Medicine Company to undertake this procedure before or during either exercise, citing time constraints (Table). More than half of the personnel failed to comply with the sleeves-down policy because of the hot and humid weather conditions. All participants stated that they used commercial repellents, which contain relatively low concentrations of N,N-Diethyl-metoluamide (DEET) compared with the repellents issued by the ADF. About 57% (2016) and 82% (2017) of personnel reported sleeping under bed nets at night but noted that nets at times were abandoned because of their incompatibility with the tactical situation. Five soldiers from the 2017 outbreak reported constantly being assailed with mosquito bites (concentrated around their hands and legs) during the night even when inside their nets. Gloves and socks were worn when sleeping to address this issue. All participants reported being bitten by mosquitoes on a regular basis.

Bayesian phylogenetic analyses of 58 RRV complete E2 sequences (1,266 nt) were performed by using TN93+ Γ , HKY+ Γ , and the GTR+ Γ +I substitution models with both strict and relaxed clock models. All phylogenies placed the ADF RRV isolates collected in 2016 and 2017 (MIDI13.2016, MIDI4.2017, MIDI9.2017, and MIDI32.2017) into 2 distinct sublineages of lineage III (IIIE and IIIF). The TN93+ Γ substitution model was the most highly ranked of those used, having the lowest Bayesian information criterion score (32–34) (Appendix Table 1), and coupled with the strict clock to produce the E2 phylogenetic tree (Figure 2). The remaining trees are provided in Appendix Figures 1–5.

Although the confidence level for the separation of the 2 sublineages differs depending on the model used (posterior probabilities range from 0.63 for HKY+ Γ relaxed clock to 0.89 for GTR+ Γ +I relaxed clock), the bifurcation of the 2 sublineages occurs in all of the trees produced (Figure 2; Appendix Figures 1–5). Furthermore, an analysis of 32 nsP3 sequences (1,650 nt) similarly demonstrates the bifurcation of the 2 proposed sublineages but with high posterior probability (≈ 1) for each of the HKY and GTR+ Γ +I substitutional models with both strict and relaxed clocks. The tree for nsP3 based on the HKY substitution model with a strict clock (Figure 3) is also presented with alternative substitution models and clocks (Appendix Figures 6–8).

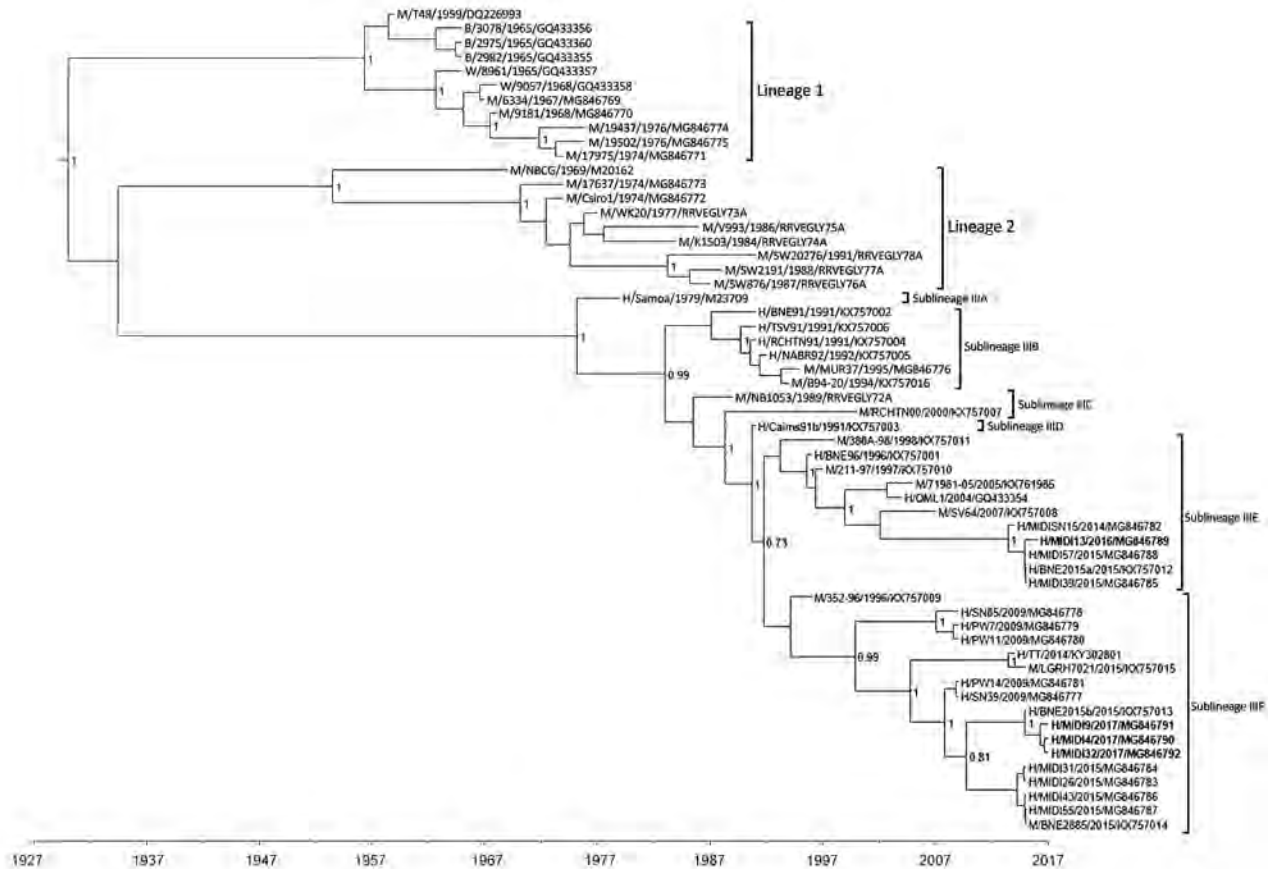


Figure 2. Maximum clade credibility tree based on analysis of 58 complete Ross River virus E2 sequences (1,266 nt) from outbreaks among Australian Defence Force personnel during and after training in Shoalwater Bay Training Area, northeastern Australia, 2016–2017. Isolates were classified into 2 distinct sublineages in lineage III. We used Bayesian phylogenetic analysis method in BEAST software (<http://beast.community>) to analyze the aligned E2 sequences, applying the TN93 plus gamma substitution model with a strict clock model, a chain length of 10 million, and a 10% burn-in using TreeAnnotator (<https://beast.community/treeannotator>). Numbers at nodes indicate the posterior probability values ≥ 0.8 except the value for the bifurcation of the sublineages III E and III F. The naming convention of the strains was name of host/strain/year of isolation/GenBank accession number. B, birds; H, humans; M, mosquitoes; W, wallabies.

Collectively, these results suggest that different lineages of RRV were responsible for the 2016 and 2017 outbreaks. The 2016 isolate (MIDI13.2016) resembled strains of RRV recovered from patients in Brisbane (≈ 600 km south of SWBTA) in 2014 and 2015 and belongs to sublineage III E. Lineage III is thought to have evolved from 2 other lineages of RRV that are believed to be extinct. The 3 isolates recovered in 2017 (MIDI4.2017, MIDI9.2017, and MIDI32.2017) shared 99.8% nucleotide identity in pairwise comparisons and have been assigned to sublineage III F, which contains strains of RRV recovered from the east and west coasts of Australia in 2009 and in an isolate identified in Brisbane in 2015 (BNE 2885.2015).

We observed 6 amino acid differences between the 2016 (sublineage III E) and 2017 (sublineage III F) isolates from SWBTA (N132D, Y296H, T369A, I376M, A384T, and A389T) of which only 1 (I376M) was a conservative change. All substitutions are located in the A and C

domains of the E2 protein, in areas involved in the interaction with other proteins (E1, capsid, and 6k), as well as in the process of budding of alphavirus envelope proteins from host cell membranes (35,36). The 2 glycosylation sites on the E2 protein were conserved in all 4 of the SWBTA isolates.

Discussion

The state of Queensland, where SWBTA is situated, has the highest rates of EPA in Australia, consistently recording $>1,000$ cases each year (1). RRV-caused EPA cases are reported routinely in the areas surrounding Rockhampton (37), the nearest city to SWBTA. In 1997, nineteen RRV-caused EPA cases were reported among US Navy personnel during a joint Australia–US military exercise located at SWBTA (27). In 2004, RRV RNA was detected in multiple mosquito species collected in this training area (27,38). The most recent common ancestor of RRV (strain T48) originated from

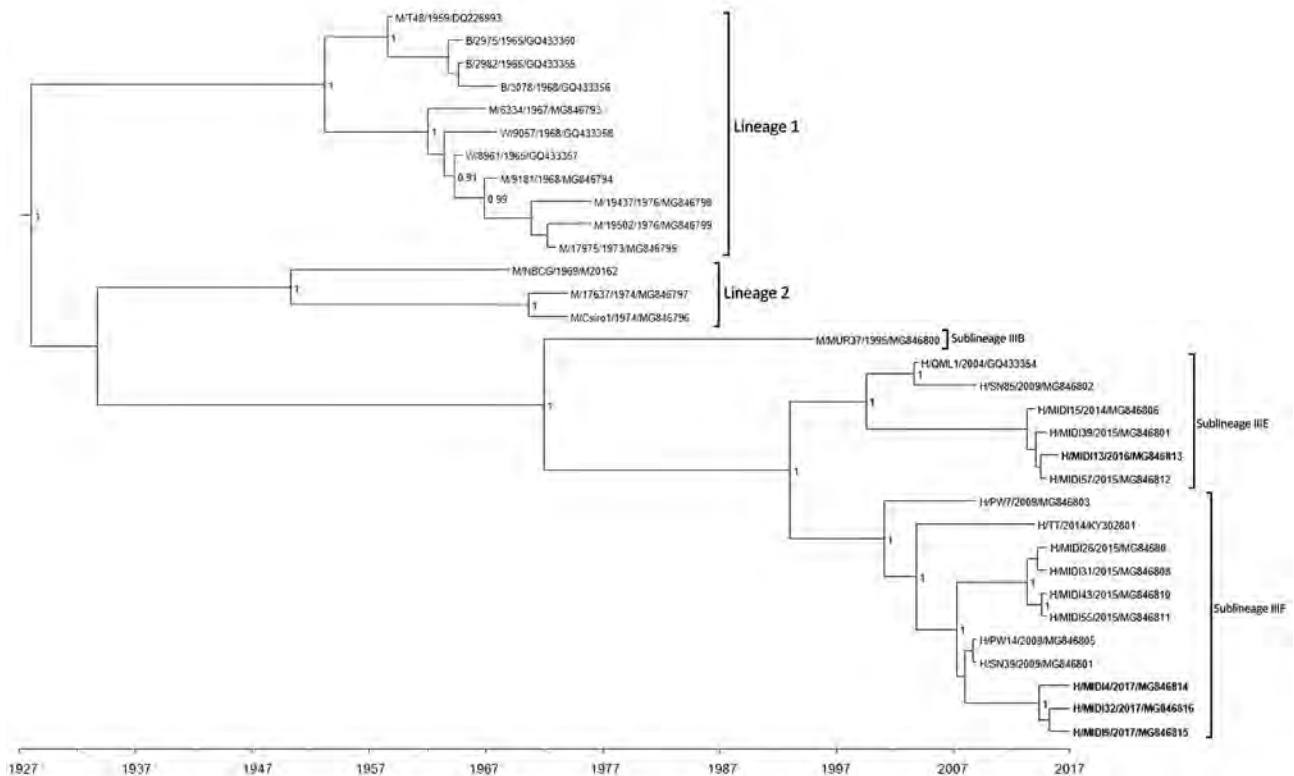


Figure 3. Maximum clade credibility tree based on analysis of 32 complete Ross River virus nsP3 sequences (1,650 nt) from outbreaks among Australian Defence Force personnel during and after training in Shoalwater Bay Training Area, northeastern Australia, 2016–2017. Isolates were classified into 2 distinct sublineages in lineage III. We used Bayesian phylogenetic analysis method in BEAST software (<http://beast.community>) to analyze the aligned nsP3 sequences, applying the TN93 plus gamma substitution model with a strict clock model, a chain length of 10 million, and a 10% burn-in using TreeAnnotator (<https://beast.community/treeannotator>). Numbers at nodes indicate the posterior probability values ≥ 0.8 . The naming convention of the strains was name of host/strain/year of isolation/GenBank accession number. B, birds; H, humans; M, mosquitoes; W, wallabies.

northeastern Australia (2,18), and this finding is in agreement with our phylogenetic analysis (Figure 2).

In light of these data, we reasonably believe that RRV has established its natural endemic cycle in SWBTA. The recurrent outbreaks of RRV infection within SWBTA and the intermittent presence of humans in this region suggests that the 2016 and 2017 infections were spillover events in which the virus was incidentally acquired by ADF soldiers from the natural endemic animal-mosquito-animal transmission cycle made possible by large populations of native animals (e.g., kangaroos and wallabies) and the wide variety of RRV vectors (21). However, phylogenetic analyses of nucleotide sequences of the E2 and nsP3 genes of RRV recovered from the ADF personnel in our study and from patients and mosquitoes from other parts of Australia do not support the notion of RRV strains being sequestered in endemic pockets across Australia. Instead, SWBTA isolates bore a remarkable similarity to those circulating in the wider community (Figures 2, 3; Appendix Figures 1–8). A more likely explanation is that strains of RRV are not regionally locked but spread around Australia by the

movement of humans, as most likely occurred in the RRV outbreak in the Pacific during 1979–1980 (4–8). More surveillance and exhaustive genetic analysis might help to resolve the precise origin and nature of these outbreaks.

The spatiotemporal characteristics of the 2016 outbreak suggested that the virus was transmitted among soldiers by local mosquitoes after the initial infection. The first wave of soldiers who sought care at the RAP at Gallipoli Barracks, Brisbane, did so within a 2-week period of leaving the SWBTA, which is consistent with the 2–15-day incubation period proposed for RRV infection in humans (18) (Figure 1, panel C). Although this first wave of soldiers might have been infected with RRV by spillover from the suspected natural, endemic animal–mosquito–animal transmission cycle in SWBTA, few (if any) intermediate host macropods exist in Gallipoli Barracks from which soldiers would become infected upon their return. Soldiers who sought care for EPA signs and symptoms 19–37 days after returning to the barracks are indicative of a potential secondary human-mosquito-human infection cycle in Gallipoli Barracks, possibly involving asymptomatic but viremic

persons. This conclusion is further supported by the high level of homology shared by 3 RRV isolates from 2017.

No EPA cases were reported (except 1 case from the administration unit attached to the combat team at SWB-TA) from other units at Gallipoli Barracks (a base containing >5,600 personnel who operate across 30 different units) upon the return of the infected personnel. This finding might simply reflect the probability of an extremely small number of infected mosquitoes finding a susceptible and unprotected human host among other units headquartered at discrete localities spread over an area of >200 hectares. However, without concurrent isolation of the virus from local mosquitoes in the vicinity of Gallipoli Barracks, this 2-wave theory, however plausible, remains speculative. Delayed or failed reporting of health concerns or symptoms of infected personnel can be a confounding issue when surveying soldiers attached to combat units. This difficulty is caused in part by a cultural resistance to seek medical attention for ailments of low to moderate severity; soldiers often opt to press on in the face of adversity.

A previous study based on phylogenies derived from short E2 gene sequences identified 2 lineages of RRV (3), whereas a more recent study (39) using longer sequences identified 3 (1 from eastern Australia, 1 from western Australia, and 1 from northeastern Australia). The phylogenetic analyses in our study, which used the complete nucleotide sequences of RRV E2 and nsP3 genes, confirm the presence of 3 lineages but suggest that lineage III should be divided into 6 sublineages. Lineage I viruses were classified as the northeastern Australia lineage; examples of this lineage have not been isolated since 1977. Lineage II was classified as the western Australia lineage; examples of this lineage have not been isolated since 1991 (Figures 2, 3; Appendix Table 1, Figures 1–8). The virus strain of RRV that was responsible for the outbreaks in Fiji, the Cook Islands, and Samoa during 1979–1980 has been classified as sublineage IIIA. The results of our study suggest that the lineage III viruses have been responsible for outbreaks of RRV infection in Australia since 1991. The temporal structure of the maximum clade credibility trees suggest that RRV is continuing to diversify under the pressure of natural selection and potential for further diversification exists given changes in the virus' ecologic niche, cycles of transmission, or both. The importance of the 5 nonconservative changes in the amino acid sequences of the E2 proteins that occurred from 2016 to 2017 warrants further investigation to determine what role they might play in viral fitness. The implementation of continuous and routine viral sequencing, analysis, and monitoring will increase confidence in the proposed delineation of the sublineages within lineage III and further clarify the evolutionary process.

With the ADF's commitment to maintaining the natural environment in its training areas, an ongoing risk for

infection with RRV persists for personnel who do not have natural immunity through prior exposure to RRV and who are required to spend prolonged periods in this RRV-endemic area. A further risk is the potential for RRV to be exported to other countries through infected, asymptomatic personnel participating in multinational exercises, which occur on a regular basis in SWB-TA. This risk is of particular concern for countries with mosquitoes known to be RRV vectors (40). The largest outbreak of RRV infection ever recorded occurred in the Pacific during 1979–1980 (4) and is a testament to the epidemic potential of the virus. The recent experience with Zika and chikungunya viruses underscores the serious threat posed to global health by the potential for previously obscure arboviruses to move from their historical cycles of transmission (41,42).

In conclusion, this investigation confirmed through viral isolation and sequence analysis that the outbreaks of EPA in the ADF in 2016 and 2017 were caused by 2 distinct sublineages of lineage III strains of RRV. Further, these outbreaks are most likely attributable to human-mosquito-human transmission.

Acknowledgments

The authors would like to thank all participants of the study and Australian Defence Force 2nd General Health Battalion for supporting the investigation.

Role of funding source: Joint Health Command of the Australian Defence Force funded this investigation. The funder had no role in the study design, data collection and analysis, decision to publish, or preparation of the manuscript.

About the Author

Dr. Liu is head of the Arbovirology Department at the Australian Defence Force Malaria and Infectious Disease Institute. His primary research interests are epidemiology, evolution, and transmission of emerging arboviral diseases.

References

1. Australian Government Department of Health National Notifiable Diseases Surveillance System. Number of notifications of Ross River virus and Barmah Forest virus infection, Australia, in the period of 1991 to 2018 and year-to-date notifications for 2019 [cited 2018 Oct 15]. http://www9.health.gov.au/cda/source/rpt_3.cfm
2. Doherty RL, Carley JG, MacKerras MJ, Marks EN. Studies of arthropod-borne virus infections in Queensland. III. Isolation and characterization of virus strains from wild-caught mosquitoes in North Queensland. *Aust J Exp Biol Med Sci.* 1963;41:17–39. <http://dx.doi.org/10.1038/icb.1963.2>
3. Sammels LM, Coelen RJ, Lindsay MD, Mackenzie JS. Geographic distribution and evolution of Ross River virus in Australia and the Pacific Islands. *Virology.* 1995;212:20–9. <http://dx.doi.org/10.1006/viro.1995.1449>
4. Aaskov JG, Mataika JU, Lawrence GW, Rabukawaqa V, Tucker MM, Miles JA, et al. An epidemic of Ross River virus

- infection in Fiji, 1979. *Am J Trop Med Hyg.* 1981;30:1053–9. <http://dx.doi.org/10.4269/ajtmh.1981.30.1053>
5. Lau C, Aubry M, Musso D, Teissier A, Paulous S, Desprès P, et al. New evidence for endemic circulation of Ross River virus in the Pacific Islands and the potential for emergence. *Int J Infect Dis.* 2017;57:73–6. <http://dx.doi.org/10.1016/j.ijid.2017.01.041>
 6. Tesh RB, McLean RG, Shroyer DA, Calisher CH, Rosen L. Ross River virus (Togaviridae: *Alphavirus*) infection (epidemic polyarthritis) in American Samoa. *Trans R Soc Trop Med Hyg.* 1981;75:426–31. [http://dx.doi.org/10.1016/0035-9203\(81\)90112-7](http://dx.doi.org/10.1016/0035-9203(81)90112-7)
 7. Rosen L, Gubler DJ, Bennett PH. Epidemic polyarthritis (Ross River) virus infection in the Cook Islands. *Am J Trop Med Hyg.* 1981;30:1294–302. <http://dx.doi.org/10.4269/ajtmh.1981.30.1294>
 8. Fauran P, Donaldson M, Harper J, Oseni RA, Aaskov JG. Characterization of Ross River viruses isolated from patients with polyarthritis in New Caledonia and Wallis and Futuna Islands. *Am J Trop Med Hyg.* 1984;33:1228–31. <http://dx.doi.org/10.4269/ajtmh.1984.33.1228>
 9. Scrimgeour EM. Suspected Ross River virus encephalitis in Papua New Guinea. *Aust N Z J Med.* 1999;29:559. <http://dx.doi.org/10.1111/j.1445-5994.1999.tb00759.x>
 10. Scrimgeour EM, Aaskov JG, Matz LR. Ross River virus arthritis in Papua New Guinea. *Trans R Soc Trop Med Hyg.* 1987;81:833–4. [http://dx.doi.org/10.1016/0035-9203\(87\)90045-9](http://dx.doi.org/10.1016/0035-9203(87)90045-9)
 11. Yu W, Mengersen K, Dale P, Mackenzie JS, Toloo GS, Wang X, et al. Epidemiologic patterns of Ross River virus disease in Queensland, Australia, 2001–2011. *Am J Trop Med Hyg.* 2014;91:109–18. <http://dx.doi.org/10.4269/ajtmh.13-0455>
 12. Claffin SB, Webb CE. Ross River virus: many vectors and unusual hosts make for an unpredictable pathogen. *PLoS Pathog.* 2015;11:e1005070. <http://dx.doi.org/10.1371/journal.ppat.1005070>
 13. Boyd AM, Hall RA, Gemmell RT, Kay BH. Experimental infection of Australian brushtail possums, *Trichosurus vulpecula* (Phalangeridae: Marsupialia), with Ross River and Barmah Forest viruses by use of a natural mosquito vector system. *Am J Trop Med Hyg.* 2001;65:777–82. <http://dx.doi.org/10.4269/ajtmh.2001.65.777>
 14. Potter A, Johansen CA, Fenwick S, Reid SA, Lindsay MD. The seroprevalence and factors associated with Ross River virus infection in western grey kangaroos (*Macropus fuliginosus*) in Western Australia. *Vector Borne Zoonotic Dis.* 2014;14:740–5. <http://dx.doi.org/10.1089/vbz.2014.1617>
 15. Marshall IDMJ. Ross River virus and epidemic polyarthritis. In: Harris KF, editor. *Current topics in vector research*. New York: Praeger; 1984. p. 31–56.
 16. Lindsay M, Condon R, Mackenzie J, Johansen C, D'Ercole MDS. A major outbreak of Ross River virus infection in the southwest of Western Australia and the Perth metropolitan area. *Commun Dis Intell.* 1992;16:290–4.
 17. Fraser JR, Tait B, Aaskov JG, Cunningham AL. Possible genetic determinants in epidemic polyarthritis caused by Ross River virus infection. *Aust N Z J Med.* 1980;10:597–603. <http://dx.doi.org/10.1111/j.1445-5994.1980.tb04238.x>
 18. Harley D, Sleight A, Ritchie S. Ross River virus transmission, infection, and disease: a cross-disciplinary review. *Clin Microbiol Rev.* 2001;14:909–32. <http://dx.doi.org/10.1128/CMR.14.4.909-932.2001>
 19. Mackenzie JS, Lindsay MDA, Smith DW, Imrie A. The ecology and epidemiology of Ross River and Murray Valley encephalitis viruses in Western Australia: examples of One Health in action. *Trans R Soc Trop Med Hyg.* 2017;111:248–54. <http://dx.doi.org/10.1093/trstmh/trx045>
 20. Jacups SP, Whelan PI, Currie BJ. Ross River virus and Barmah Forest virus infections: a review of history, ecology, and predictive models, with implications for tropical northern Australia. *Vector Borne Zoonotic Dis.* 2008;8:283–97. <http://dx.doi.org/10.1089/vbz.2007.0152>
 21. Russell RC. Ross River virus: ecology and distribution. *Annu Rev Entomol.* 2002;47:1–31. <http://dx.doi.org/10.1146/annurev.ento.47.091201.145100>
 22. Ray CG, Gall EP, Minnich LL, Roediger J, De Benedetti C, Corrigan JJ. Acute polyarthritis associated with active Epstein-Barr virus infection. *JAMA.* 1982;248:2990–3. <http://dx.doi.org/10.1001/jama.1982.03330220034032>
 23. McCormick JN, Duthie JJ, Gerber H, Hart H, Baker S, Marmion BP. Rheumatoid polyarthritis after rubella. *Ann Rheum Dis.* 1978;37:266–72. <http://dx.doi.org/10.1136/ard.37.3.266>
 24. Varache S, Narbonne V, Jousse-Joulin S, Guennoc X, Dougados M, Daurès JP, et al. Is routine viral screening useful in patients with recent-onset polyarthritis of a duration of at least 6 weeks? Results from a nationwide longitudinal prospective cohort study. *Arthritis Care Res (Hoboken).* 2011;63:1565–70. <http://dx.doi.org/10.1002/acr.20576>
 25. Huang B, Pyke AT, McMahon J, Warrilow D. Complete coding sequence of a case of chikungunya virus imported into Australia. *Genome Announc.* 2017;5:e00310–7. <http://dx.doi.org/10.1128/genomeA.00310-17>
 26. Jansen CC, Williams CR, van den Hurk AF. The usual suspects: comparison of the relative roles of potential urban chikungunya virus vectors in Australia. *PLoS One.* 2015;10:e0134975. <http://dx.doi.org/10.1371/journal.pone.0134975>
 27. Hueston L, Yund A, Cope S, Monteville M, Marchetti M, Haniotis J, et al. Ross River virus in a joint military exercise. *Commun Dis Intell.* 1997;21:193.
 28. Australian Government Department of Health. River virus infection case definition [cited 2018 Oct 15]. http://www.health.gov.au/internet/main/publishing.nsf/Content/cda-surveil-ndss-casedef-cd_rrv.htm
 29. Jupille HJ, Medina-Rivera M, Hawman DW, Oko L, Morrison TE. A tyrosine-to-histidine switch at position 18 of the Ross River virus E2 glycoprotein is a determinant of virus fitness in disparate hosts. *J Virol.* 2013;87:5970–84. <http://dx.doi.org/10.1128/JVI.03326-12>
 30. Liu WJ, Rourke MF, Holmes EC, Aaskov JG. Persistence of multiple genetic lineages within intrahost populations of Ross River virus. *J Virol.* 2011;85:5674–8. <http://dx.doi.org/10.1128/JVI.02622-10>
 31. Posada D. jModelTest: phylogenetic model averaging. *Mol Biol Evol.* 2008;25:1253–6. <http://dx.doi.org/10.1093/molbev/msn083>
 32. Evans J, Sullivan J. Approximating model probabilities in Bayesian information criterion and decision-theoretic approaches to model selection in phylogenetics. *Mol Biol Evol.* 2011;28:343–9. <http://dx.doi.org/10.1093/molbev/msq195>
 33. Vrieze SI. Model selection and psychological theory: a discussion of the differences between the Akaike information criterion (AIC) and the Bayesian information criterion (BIC). *Psychol Methods.* 2012;17:228–43. <http://dx.doi.org/10.1037/a0027127>
 34. Lu ZH, Chow SM, Loken E. A comparison of Bayesian and frequentist model selection methods for factor analysis models. *Psychol Methods.* 2017;22:361–81. <http://dx.doi.org/10.1037/met0000145>
 35. Jose J, Snyder JE, Kuhn RJ. A structural and functional perspective of alphavirus replication and assembly. *Future Microbiol.* 2009;4:837–56. <http://dx.doi.org/10.2217/fmb.09.59>
 36. Li L, Jose J, Xiang Y, Kuhn RJ, Rossmann MG. Structural changes of envelope proteins during alphavirus fusion. *Nature.* 2010;468:705–8. <http://dx.doi.org/10.1038/nature09546>
 37. Moody S. Virus outbreak: 101 locals diagnosed with Ross River virus. *The Morning Bulletin* [cited 2018 Oct 15]. <https://www.themorningbulletin.com.au/news/mosquitoes-buzzy-infecting-rocky-locals-with-disea/3203125>
 38. Frances SP, Cooper RD, Rowcliffe KL, Chen N, Cheng Q. Occurrence of Ross River virus and Barmah Forest virus in

- mosquitoes at Shoalwater Bay military training area, Queensland, Australia. *J Med Entomol*. 2004;41:115–20. <http://dx.doi.org/10.1603/0022-2585-41.1.115>
39. Jones A, Lowry K, Aaskov J, Holmes EC, Kitchen A. Molecular evolutionary dynamics of Ross River virus and implications for vaccine efficacy. *J Gen Virol*. 2010;91:182–8. <http://dx.doi.org/10.1099/vir.0.014209-0>
40. Flies EJ, Lau CL, Scott C, Weinstein P. Another emerging mosquito-borne disease? Endemic Ross River virus transmission in the absence of marsupial reservoirs. *Bioscience*. 2018;68:288–93. <http://dx.doi.org/10.1093/biosci/biy011>
41. Metsky HC, Matranga CB, Wohl S, Schaffner SF, Freije CA, Winnicki SM, et al. Zika virus evolution and spread in the Americas. *Nature*. 2017;546:411–5. <http://dx.doi.org/10.1038/nature22402>
42. Thiberville SD, Moya N, Dupuis-Maguiraga L, Nougaiere A, Gould EA, Roques P, et al. Chikungunya fever: epidemiology, clinical syndrome, pathogenesis and therapy. *Antiviral Res*. 2013;99:345–70. <http://dx.doi.org/10.1016/j.antiviral.2013.06.009>

Address for correspondence: Wenjun Liu, Australian Defence Force Malaria and Infectious Disease Institute, Weary Dunlop Dr, Gallipoli Barracks, Enoggera, Brisbane 4051, Australia; email: wenjun.liu@defence.gov.au



**EMERGING
INFECTIOUS DISEASES™**

June 2016

Respiratory Diseases

- Debate Regarding Oseltamivir Use for Seasonal and Pandemic Influenza
- Perspectives on West Africa Ebola Virus Disease Outbreak, 2013–2016
- Human Infection with Influenza A(H7N9) Virus during 3 Major Epidemic Waves, China, 2013–2015
- Integration of Genomic and Other Epidemiologic Data to Investigate and Control a Cross-Institutional Outbreak of *Streptococcus pyogenes*
- Infectious Disease Risk Associated with Contaminated Propofol Anesthesia, 1989–2014
- Improved Global Capacity for Influenza Surveillance
- Reemergence of Dengue in Southern Texas, 2013
- Transmission of *Mycobacterium chimaera* from Heater–Cooler Units during Cardiac Surgery despite an Ultraclean Air Ventilation System
- Extended Human-to-Human Transmission during a Monkeypox Outbreak in the Democratic Republic of the Congo
- Use of Population Genetics to Assess the Ecology, Evolution, and Population Structure of *Coccidioides*, Arizona, USA
- Infection, Replication, and Transmission of Middle East Respiratory Syndrome Coronavirus in Alpacas
- Human Adenovirus Associated with Severe Respiratory Infection, Oregon, 2013–2014
- Heterogeneous and Dynamic Prevalence of Asymptomatic Influenza Virus Infections
- High MICs for Vancomycin and Daptomycin and Complicated Catheter-Related Bloodstream Infections with Methicillin-Sensitive *Staphylococcus aureus*
- Population-Level Effect of Cholera Vaccine on Displaced Populations, South Sudan, 2014
- Experimental Infection and Response to Rechallenge of Alpacas with Middle East Respiratory Syndrome Coronavirus
- Scarlet Fever Upsurge in England and Molecular-Genetic Analysis in North-West London, 2014
- Possible Case of Novel Spotted Fever Group Rickettsiosis in Traveler Returning to Japan from India
- *Shigella* Antimicrobial Drug Resistance Mechanisms, 2004–2014
- MERS-CoV Antibodies in Humans, Africa, 2013–2014
- Microcephaly in Infants, Pernambuco State, Brazil, 2015
- Prospective Validation of Cessation of Contact Precautions for Extended-Spectrum β -Lactamase-Producing *Escherichia coli*
- Whole-Genome Analysis of *Cryptococcus gattii*, Southeastern United States
- Prevalence of Nontuberculous Mycobacterial Pulmonary Disease, Germany, 2009–2014
- Rapid Detection of Polymyxin Resistance in *Enterobacteriaceae*

To revisit the June 2016 issue, go to:

<https://wwwnc.cdc.gov/eid/articles/issue/22/6/table-of-contents>

Transmissibility of MERS-CoV Infection in Closed Setting, Riyadh, Saudi Arabia, 2015

Maria D. Van Kerkhove,¹ Sadoof Aswad, Abdullah Assiri, Ranawaka A.P.M. Perera, Malik Peiris, Hassan E. El Bushra, Abdulaziz A. BinSaeed²

To investigate a cluster of Middle East respiratory syndrome (MERS) cases in a women-only dormitory in Riyadh, Saudi Arabia, in October 2015, we collected epidemiologic information, nasopharyngeal/oropharyngeal swab samples, and blood samples from 828 residents during November 2015 and December 2015–January 2016. We found confirmed infection for 19 (8 by reverse transcription PCR and 11 by serologic testing). Infection attack rates varied (2.7%–32.3%) by dormitory building. No deaths occurred. Independent risk factors for infection were direct contact with a confirmed case-patient and sharing a room with a confirmed case-patient; a protective factor was having an air conditioner in the bedroom. For 9 women from whom a second serum sample was collected, antibodies remained detectable at titers $\geq 1:20$ by pseudoparticle neutralization tests ($n = 8$) and 90% plaque-reduction neutralization tests ($n = 2$). In closed high-contact settings, MERS coronavirus was highly infectious and pathogenicity was relatively low.

Middle East respiratory syndrome (MERS) coronavirus (CoV) is a zoonotic virus (1). Approximately 2,266 laboratory-confirmed cases of MERS have been reported to the World Health Organization (WHO) (2) since the identification of the first human cases in 2012 (3,4).

Although the primary source of human infections is MERS-CoV-infected dromedaries, the modes of transmission from dromedaries to humans remain unclear (5). Human-to-human transmission has occurred primarily in healthcare settings (6), sometimes resulting in large explosive outbreaks (7,8). However, to date, no sustained human-to-human infection has been detected. Few outbreaks of MERS-CoV outside of healthcare settings have been documented, and

limited transmission within families has been reported, but secondary attack rates in households or in settings outside of healthcare facilities (e.g., farms) seem to be low (9).

The nonspecificity of clinical definitions for MERS-CoV and the tendency of surveillance to focus on severe cases suggest that the prevalence of mild or asymptomatic infection cannot be estimated from case-based clinical surveillance alone (10). Mild or asymptomatic cases have been identified from contact tracing of laboratory-confirmed case-patients in several countries, including Saudi Arabia, the United Arab Emirates, Qatar, and South Korea (11–16).

In early October 2015, a cluster of MERS-CoV infections was identified among expatriate women working for a women-only university in Riyadh, Saudi Arabia. At the time the outbreak investigation was initiated, Kingdom of Saudi Arabia (KSA) Ministry of Health officials had identified 8 MERS case-patients by reverse transcription PCR (RT-PCR) (17); all patients were epidemiologically linked through their place of residence, a dormitory that housed expatriate women. Two additional laboratory-confirmed cases were identified among healthcare workers who had been exposed to the first case-patient, who had sought treatment at a medical clinic near the residence (17).

As part of this outbreak investigation, we conducted a molecular and seroepidemiologic study of the residents of an expatriate dormitory where the initial case-patients lived. Our goal was to describe and characterize the outbreak, determine potential source(s) of the outbreak, estimate the extent of MERS-CoV infection among residents, and evaluate risk factors for infection among residents.

Methods

Selection and Recruitment of Study Participants

We used the MERS-CoV standardized serologic investigation protocol developed by WHO and the Consortium for the Standardization of Influenza Seroepidemiology (18)

¹Current affiliation: World Health Organization, Geneva, Switzerland.

²Current affiliation: King Saud University, Riyadh, Saudi Arabia.

Author affiliations: Institut Pasteur, Paris, France (M.D. Van Kerkhove); Ministry of Health, Riyadh, Saudi Arabia (S. Aswad, A. Assiri, H.E. El Bushra, A.A. BinSaeed); Jubail General Hospital, Riyadh (S. Aswad); The University of Hong Kong, Hong Kong, China (R.A.P.M. Perera, M. Peiris); HKU-Pasteur Research Pole, Hong Kong (M. Peiris)

DOI: <https://doi.org/10.3201/eid2510.190130>

and adapted it to the context of this outbreak. All 828 residents of the women-only expatriate dormitory in Riyadh were informed of the purpose of the outbreak investigation by KSA Ministry of Health official field teams and asked in person to participate. The KSA Ministry of Health, WHO, and Institut Pasteur field teams provided information sessions about the study and about MERS-CoV. The response team established a nursing station within the residential compound and assigned 2 nurses to reside within the compound to follow up with exposed persons and keep a log of any medical complaints from the residents throughout the outbreak period. Because this outbreak investigation was part of a public health response, it was not considered by the KSA Ministry of Health, Institut Pasteur, or The University of Hong Kong to be research that was subject to review by an institutional review board. As such, written informed consent was not required.

Included in the investigation were all residents of the dormitory who orally provided consent for completion of a questionnaire; collection of a nasopharyngeal or oropharyngeal swab sample, or both; and collection of a blood sample for serologic testing. Exclusion criteria included being <16 years of age at the time of recruitment, having any contraindication to venipuncture, or both.

The interviewers were trained to use the data collection forms developed for this investigation; because most residents were from the Philippines, the questionnaire was translated into Tagalog (Appendix, <https://wwwnc.cdc.gov/EID/article/25/10/19-0130-App1.pdf>). Each question was read aloud to women in groups of 15–25 in the dormitory while they filled in the questionnaire by hand. A subset of more sensitive questions was administered one-on-one by a member of the investigation team over the course of the 3-day field investigation. Before study implementation, frontline staff, including all outbreak investigation personnel, were trained with regard to infection control procedures, including proper hand hygiene and the correct use of respiratory face masks, to minimize their own risk for infection when in close contact with patients during home visits and elsewhere and to minimize the potential risk for MERS-CoV transmission between participants or between households.

Specimen Collection and Testing for MERS-CoV

Any participant who reported respiratory symptoms during the initial investigation (October 19–28, 2015) or during a 14-day follow-up period (after last contact with a confirmed/suspected MERS-CoV patient) was immediately isolated, and nasopharyngeal/oropharyngeal swab samples were collected and tested for MERS-CoV by RT-PCR. RT-PCR testing of human biological specimens was conducted at the Riyadh Regional Laboratory by use of standardized RT-PCR methods for MERS-CoV testing (19). Any participants with a positive MERS-CoV result by RT-PCR

according to WHO criteria (10) were reported to WHO under the requirements of the International Health Regulations (2005) (<https://www.who.int/ihr/9789241596664/en>).

On November 1–2, 2015, a total of 5 mL of blood was collected from consenting residents of the compound. The blood was collected in a serum collection tube according to standard procedures and labeled with a coded identification number linked to the data collection forms. Transport of specimens within national borders complied with the applicable national regulations of Saudi Arabia. International transport of MERS-CoV specimens followed applicable international regulations (20).

Serologic assays used to detect and confirm seropositivity in the serum samples were MERS-CoV S1 IgG ELISA (EUROIMMUN EI 2604–9601G kit, <https://www.euroimmun.com>), MERS-CoV spike pseudoparticle neutralization test (ppNT), and 90% plaque-reduction neutralization test (PRNT₉₀). Serologic testing for MERS-CoV antibodies was conducted at the University of Hong Kong, as previously described (21). All serum samples were screened by MERS-CoV S1 ELISA, and positive or equivocal samples were further tested by ppNT and PRNT₉₀. Serologic results were interpreted as positive if PRNT₉₀ or ppNT titer for either the first or second serum specimen was $\geq 1:20$.

Statistical Analyses

We entered all data for analysis in the entry form in Epi Info 3.5.4 (<https://www.cdc.gov/epiinfo>) and exported it to statistical software Stata 14 (<https://www.stata.com>). We estimated risk factors for infection among case-patients and non-case-patients (risk ratios [RRs] and 95% CIs) and within a nested case-control study (odds ratios [ORs] and 95% CIs) by restricting analyses to residents living in villas in which laboratory-confirmed cases had been identified.

Results

The first patient in this cluster who had laboratory-confirmed MERS was a 27-year-old woman who worked as a janitor in a women-only university in Riyadh. She reported experiencing dry cough and fatigue on October 1, 2015; she sought care at a private healthcare clinic on October 4 and was provided treatment and sent home the same day. On October 7, after signs and symptoms worsened to include fever, shortness of breath, productive cough, and signs of pneumonia, she again sought care in the same healthcare clinic, and a diagnosis of MERS was suspected. On October 8, a nasopharyngeal sample was collected and the patient was transferred to a public hospital in Riyadh, designated for isolation and treatment of MERS patients. MERS-CoV infection was confirmed on October 9. A second case in this cluster has recently been described (22).

The first patient resided in an enclosed, women-only, expatriate dormitory composed of 24 villas (Figure 1). Each

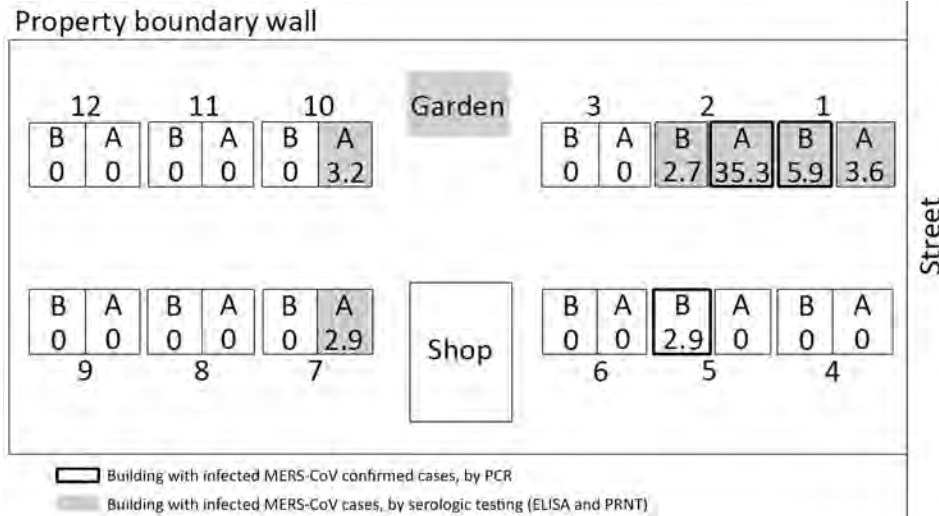


Figure 1. Schematic of expatriate dormitory (the residence, buildings 1–12) and MERS-CoV infection attack rates (IARs), Riyadh, Saudi Arabia, 2015. Each building contained 2 villas on 3 floors. The distance between buildings is ≈5 m. During the initial investigation (October 2015), 8 residents were positive for MERS-CoV by PCR (indicated by black boxes); they lived in buildings 1B, 2A, and 5B. A vegetable garden separated buildings 3 and 10, and a convenience store (shop) separated buildings 6 and 7. IARs are shown as percentages inside each villa. MERS-CoV, Middle East respiratory syndrome coronavirus; PRNT, plaque-reduction neutralization test.

villa is a 3-story building with 7 bedrooms (2 on the ground floor, 3 on the first floor, and 2 on the second floor) and is inhabited by 24–50 women. On inspection of the living quarters, the field team found that most of the windows in the bedrooms were closed and sealed and that ventilation within the bedrooms was poor. Initial open-ended interviews with some residents informed the study team that residents shared the same kitchen and dining room within the villa but did not typically eat together or share food at mealtimes. There were no designated social spaces; however, residents reported gathering around laptops to watch movies together.

A total of 828 women who lived in the residence complex were included in the seroepidemiologic study; none of the eligible women refused to participate. All participants were female, and median age was 35.1 (26.6–41.3) years. None were Saudi Arabia nationals; they were from the Philippines (84.6%), Sri Lanka (6.4%), Indonesia (2.9%), Nepal (1.6%), and India (1.1%) (Table 1). A total of 49 participants (1 case-patient and 48 non-case-patients) reported having ≥1 chronic condition (e.g., asthma, diabetes, heart disease, hypertension, breast cancer) (Table 1). The MERS case-patient reported having asthma; among non-case-patients, the most common chronic conditions reported were asthma (31%), diabetes (25%), and hypertension (18%).

In terms of occupation, almost half (49.1%) of participants reported working at the women-only university in Riyadh, including 17 (89.5%) of the MERS case-patients (Table 1). Participants reported working in 1 of 4 hospitals as either their primary or secondary occupation (Table 1).

Contact tracing of the initial patient and molecular and serologic laboratory test results identified an additional 18 MERS-CoV infections (Figure 2; Table 2). Of the 19 total case-patients, 12 (63.2%) were from villa 2A; 2 (10.5%) were from a facing villa (1B); and 1 case (5.3%) was reported from each of 5 villas either close to the mostly

affected villa (2A) or 2 other villas (10A and 7A) populated with residents from the Philippines (Figure 1).

Among the 8 MERS-CoV cases positive by PCR, 8 were also serologically positive for MERS-CoV (Table 2). According to PRNT₉₀ or ppNT serology results for either the first or second serum sample, an additional 11 persons were serologically positive for MERS-CoV infections. Therefore, a total of 19 of the 828 dormitory residents had evidence of MERS-CoV infection by molecular or serologic testing or both; the infection attack rate [IAR] for the cohort was 2.3%.

Of the 9 patients from whom a second sample was collected in March 2016, a total of 8 had ppNT titers of ≥1:20, and only 2 of these had PRNT₉₀ titers of ≥1:20. For 2 of these 8 patients, ppNT indicated a ≥4-fold fall in antibody titer; for the others, ppNT antibody levels remained within 2-fold that of the initial serum sample.

Bivariate analyses indicated significant associations between MERS and the following risk factors: having direct contact with a known MERS patient (RR 10.9, 95% CI 6.7–17.6); sharing a bedroom (RR 25.5, 95% CI 10.3–63.1), kitchen (RR 15.5, 95% CI 5.4–44.2), bathroom (RR 25.5, 95% CI 10.3–63.1), meal (RR 19.4, 95% CI 7.5–50.3), or transportation vehicle (RR 11.8, 95% CI 4.9–28.5); and having indirect contact with a known patient (RR 15.5, 95% CI 5.4–44.2) (Table 3). The presence of a chronic condition did not vary by MERS infection status. According to multivariate analyses, direct contact with a known MERS patient (OR 27.6, 95% CI 8.4–91.0) and sharing a bedroom with a MERS patient (OR 5.7, 95% CI 1.5–22.5) remained statistically significant. Having a functioning air conditioner in the bedroom was protective (OR 0.15, 95% CI 0.03–0.82). None of the women reported traveling outside of Saudi Arabia in the 14 days before symptom onset (data not shown).

Table 1. Demographic characteristics of participants with and without MERS-CoV infection in study of MERS-CoV transmissibility in a closed setting, Riyadh, Saudi Arabia, 2015*

Characteristics	All participants, no. (%), n = 828	Case-patients, no. (%), n = 19†	Non-case-patients, no. (%), n = 809
Sex			
F	814/814 (100)‡	19/19 (100)‡	795/795 (100)‡
M	0	0	0
Nationality	779	19	760
Filipino	659 (84.6)	19 (100)	640 (84.2)
Sri Lankan	50 (6.4)	0	50 (6.6)
Nepali	12 (1.5)	0	12 (1.6)
Bangladeshi	28 (3.6)	0	28 (3.7)
Indonesian	22 (2.8)	0	22 (2.9)
Indian	8 (1.0)	0	8 (1.0)
Highest level of education reached	779	19	761
Primary school	80 (10.3)	1 (5.3)	79 (10.4)
High school	377 (48.4)	10 (52.6)	368 (48.4)
University/diploma	234 (30.0)	4 (21.1)	230 (30.3)
Postgraduate degree	77 (9.9)	4 (21.1)	73 (9.6)
No education	11 (1.4)	0	11 (1.4)
Primary occupation	770	19	751
Women-only university	378 (49.1)	17 (89.5)	361 (48.1)
Public university	12 (1.6)	0	12 (1.6)
Hospital A	32 (4.2)	0	32 (4.3)
Hospital B	238 (30.9)	2 (10.5)	236 (31.4)
Hospital C	54 (7.0)	0	54 (7.2)
Hospital D	56 (7.3)	0	56 (7.5)
Secondary occupation	83/805 (10.3)	3 (15.8)	80 (10.7)
Hospital A	NA	2 (10.5)	17 (2.3)
Hospital D	NA	1 (5.3)	10 (1.3)
Other (health club)	NA	0	53 (7.0)
Any underlying medical conditions	49/780 (6.3)	1 (5.0)	48/761 (6.3)
Regularly smoke (% daily)	10/773 (1.3)	1/19 (5.6)	9/755 (1.2)
Current chronic conditions§	49/780 (6.3)	1/19 (5.3)	48/761 (6.3)

*Median age (interquartile range): for all, 35.1 (26.6–41.3) years; for case-patients, 29.8 (28–37.2) years; for non-case-patients, 35.2 (29.6–41.4) years. CoV, coronavirus; MERS, Middle East respiratory syndrome; NA, not applicable.

†Molecular or serologic evidence of MERS-CoV infection.

‡Denominator indicates the number of women who answered the question.

§Included asthma, diabetes, heart disease, hypertension, and breast cancer.

Discussion

This study details the comprehensive investigation of a cluster of MERS cases reported outside a healthcare-associated or camel industry-associated occupational setting. In this women-only, expatriate worker dormitory in Riyadh, Saudi Arabia, the overall IAR of 2.3% is similar to that found in a household contact study conducted in 2014 (IAR of 4.3%) (9). However, in this outbreak, the residential setting was more crowded than typical single-family households. Although we found the IAR in some villas to be low, we identified IARs as high as 35.3% (12/34) in 1 villa (2A), probably because of the exceptionally crowded living and sleeping conditions. Within this villa, 12 women were infected with MERS-CoV but only 10 reported any symptoms. Rates of IAR were not affected by the presence or absence of underlying conditions or the median age of residents by villa.

This study identified the independent risk factors for infection to be direct contact and sharing a bedroom with a MERS patient. Findings from other serologic studies have been similar (23). We hypothesize that the increased human-to-human transmission within villas resulted from

the clustering of the women's activities. For example, the same women who lived together typically ate and socialized together, worked together, and traveled to and from work together. These activities added to the likelihood of intense direct physical contact among the women and probably led to limited but effective human-to-human transmission within their residence.

Globally, the extent of human-to-human transmission outside of healthcare facilities is uncertain, and whether MERS-CoV has the potential for sustained community transmission is unclear. Transmission among family members seems to be limited but can be amplified in healthcare settings (24,25) among persons with underlying medical conditions and to healthcare workers. Contributors to propagation of MERS-CoV infection in healthcare facilities include aerosol-generating procedures such as intubation, suction, and collection of nasopharyngeal swabs (26). Compared with the total number of MERS-CoV infections reported to WHO to date, patients in our study cohort were significantly younger (median age 32 vs. 52 years, respectively), healthier (6.3% vs. 41.0% reporting ≥ 1 chronic condition), and more likely to be female (0 vs. 68.1% male) (27).

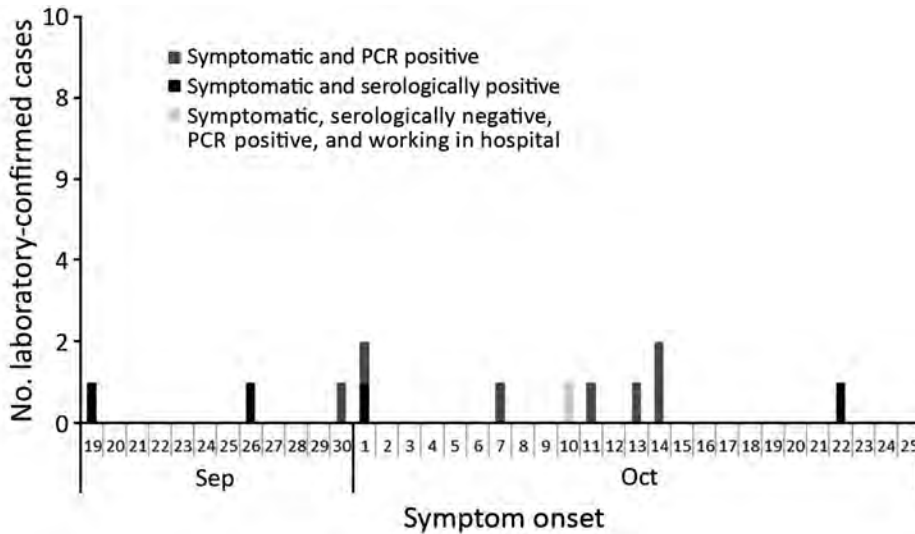


Figure 2. Epidemiologic curve for symptomatic laboratory-confirmed case-patients with Middle East respiratory syndrome coronavirus infection, Riyadh, Saudi Arabia, 2015. The curve includes only the 12 case-patients for whom symptom onset was reported, not the 7 case-patients for whom infection was serologically confirmed but no symptoms were reported in the preceding 4 weeks.

Healthcare staff can prevent human-to-human transmission of MERS-CoV through stringent adherence and implementation of detailed and clear protocols for standard, droplet, and aerosol infection prevention and control (IPC) measures among the various persons within a healthcare setting (i.e., healthcare workers, patients, and visitors) (28). Such IPC measures were not followed by the inhabitants of the dormitory in this study.

Although we were able to rule out a connection to dromedary camels, we were not able to specifically determine the

source of this outbreak. Of the 19 laboratory-confirmed case-patients, 17 reported working at the same women-only university in Riyadh and the other 2 worked primarily as cleaners at the same healthcare facility in Riyadh (hospital B). Of these 19 case-patients, 3 also reported having a secondary place of employment, including working as cleaners at 2 other hospitals in Riyadh (hospitals A and D). We hypothesize that 1 of the 19 infected women identified in this investigation may have been exposed to and infected with MERS-CoV while working as a cleaner in a healthcare facility

Table 2. Characteristics of MERS-CoV–positive participants identified from molecular and serologic assay results in study of MERS-CoV transmissibility in a closed setting, Riyadh, Saudi Arabia, 2015*

Age, y	Bldg no.	Signs/symptoms†	Symptom onset date	RT-PCR‡	Serologic test						Serologic test result§
					SI ELISA		ppNT		PRNT ₉₀		
					First sample	Second sample	First sample	Second sample	First sample	Second sample	
23	1B	Yes	Oct 11	+	1.586	0.523	80	20	20	10	+
28	5B	Yes	Oct 14	+	2.225	NA	80	NA	40	NA	+
29	2A	Yes	Oct 13	+	1.181	NA	20	NA	10	NA	+
29	2A	Yes	Oct 14	+	4.57	NA	160	NA	80	NA	+
28	2A	Yes	Oct 1	+	3.154	2.741	160	160	40	40	+
26	2A	Yes	Oct 7	+	3.154	NA	160	NA	40	NA	+
39	2A	Yes	Sep 30	+	1.553	NA	40	NA	20	NA	+
53	2A	No	NS	+	4.242	NA	160	NA	80	NA	+
41	1B	No	NS	NA	1.311	0.33	20	10	10	<10	+
37	2A	Yes	Oct 10	–	1.214	0.569	40	20	10	<10	+
30	2A	Yes	Oct 22	–	0.759	0.605	20	20	0	<10	+
24	2A	Yes	Oct 1	–	1.422	NA	80	NA	20	NA	+
32	2A	Yes	Sep 26	–	3.381	1.012	80	20	20	10	+
28	2A	Yes	Sep 19	–	1.999	1.654	40	40	10	20	+
30	1A	No	NS	NA	3.295	1.496	40	20	10	<10	+
36	2B	No	NS	–	1.419	NA	20	NA	20	NA	+
42	7A	No	NS	NA	0.576	NA	10	NA	20	NA	+
37	10A	No	NS	NA	1.115	NA	80	NA	80	NA	+
45	2A	No	NS	–	1.111	0.563	20	20	<10	<10	+

*First samples collected November 13, 2015; second samples collected March 22, 2015. Bldg, building; CoV, coronavirus; MERS, Middle East respiratory syndrome; NA, not available/not collected; NS, no signs/symptoms reported; ppNT, pseudoparticle neutralization test; PRNT₉₀, 90% plaque-reduction neutralization test; RT-PCR, reverse transcription PCR; +, positive; –, negative.

†Self-reported or observed signs/symptoms in the 14 d before epidemiologic interview.

‡According to World Health Organization criteria (http://www.who.int/csr/disease/coronavirus_infections/mers-laboratory-testing).

§Serologic test result was defined as positive if either PRNT₉₀ or ppNT titers were ≥20. SI ELISA results are shown for information only; they were not used in designating infection status.

Table 3. Bivariate analyses of reported exposures to known MERS patient, including overall cohort, in study of MERS-CoV transmissibility in a closed setting Riyadh, Saudi Arabia, 2015*

Reported exposure	Case-patients, no. (%), n = 19	Non-case-patients, no. (%), n = 809	p value†	RR (95% CI)
Direct contact with known (symptomatic) MERS-CoV case-patient	11 (57.9)	43 (5.3)	<0.001	10.9 (6.7–17.6)
Shared bedroom with known case-patient	6 (31.6)	10 (1.2)	<0.001	25.5 (10.3–63.1)
Shared kitchen with known case-patient	4 (21.1)	11 (1.4)	<0.001	15.5 (5.4–44.2)
Shared bathroom with known case-patient	6 (31.6)	10 (1.2)	<0.001	25.5 (10.3–63.1)
Shared meal with known case-patient	5 (26.3)	11 (1.4)	<0.001	19.4 (7.5–50.3)
Shared transportation to/from place of employment with known case-patient	5 (26.3)	18 (2.2)	<0.001	11.8 (4.9–28.5)
Reported nondirect contact with case-patient‡	4 (21.1)	11 (1.4)	<0.001	15.5 (5.4–44.2)

*CoV, coronavirus; MERS, Middle East respiratory syndrome; RR, risk ratio.
†By χ^2 test.
‡No physical contact, nonphysical contact (including talk to the known case-patient).

where persons with undiagnosed MERS had been cared for. In August 2015, hospital B, reportedly the primary occupation location for 2 women who were MERS-CoV positive according to PCR, was the location of a small cluster of laboratory-confirmed MERS cases (n = 5). Unfortunately, viral genetic sequencing was conducted on only 1 of those patients (22); without further epidemiologic and sequencing data from other patients in this cluster, or from the laboratory-confirmed patients in the small cluster in hospital B in August 2015, we cannot surmise further.

The time lag between identification of MERS patients in hospital B in August 2015 and the timing of this outbreak in October 2015 suggests that persons with subclinical cases may have been in or working in this hospital during August–October 2015; however, because testing for MERS-CoV in Saudi Arabia was substantial (29), missing symptomatic cases was unlikely. A subject of some debate and recent focus has been the potential role of mildly symptomatic or asymptomatic infections and possible environmental contamination in the spread of MERS-CoV in healthcare facilities (22,30–33). The rapid initiation of this investigation and use of an existing protocol (34) (developed for such use after the rapid isolation of close contacts regardless of the development of symptoms and the implementation of a no-fly policy among residents of the compound until the full 14-day follow-up was completed) probably limited further human-to-human transmission inside and potentially outside of Saudi Arabia.

Our study highlights the potential role of healthcare workers not responsible for direct patient care (e.g., hospital cleaners) in the spread of MERS-CoV. Often, hospital cleaning staff may be from other countries, may speak several languages, and may be missed by efforts to increase IPC specific to MERS-CoV. Specific MERS-CoV IPC training should be directed to cleaning staff in healthcare facilities, in addition to healthcare providers, in appropriate languages, particularly to protect them from infection and from facilitating virus spread within the healthcare facility.

For the 8 women with RT-PCR–confirmed infection, antibody titers ranged from 1:10 to 1:80 by PRNT and from 1:20

to 1:160 by ppNT. For 9 of the 19 women with confirmed evidence of infection by RT-PCR, serologic testing, or both, for whom follow-up serum samples were available 3 months after the putative exposure, 7 women had PRNT titers of <1:20 and 1 woman had ppNT titers of <1:20. Thus, the ppNT antibody test was somewhat more sensitive for detecting evidence of past infection. A ppNT titer of 1:20 is therefore an optimal indicator of past infection in seroepidemiologic assays. The ppNT, although more sensitive, correlated well with PRNT among persons with RT-PCR–confirmed MERS-CoV infection (35) and was uniformly negative in serum from persons in areas where MERS-CoV is not endemic (e.g., Hong Kong [36]). For this study, we categorized those without RT-PCR evidence of MERS-CoV infection but PRNT or ppNT antibody titers \geq 1:20 as being MERS-CoV infected.

Of the 8 women who had RT-PCR–confirmed infection, 2 were asymptomatic, as were 6 of the 11 women whose diagnosis was made solely by serologic testing. Serologic studies of cohorts of patients positive for MERS-CoV by RT-PCR have shown that milder disease and asymptomatic infections may not be associated with detectable serologic responses (37). Thus, our serologic testing probably underestimates the true number of MERS-CoV infections that may have occurred. However, our data provide evidence that even asymptomatic infections can sometimes lead to detectable serologic responses and that such investigations are useful. Furthermore, the serologic results at 5 months after putative exposure show evidence of antibody titers waning to below diagnostic limits in some patients but also show that antibodies may remain detectable in others. This information is useful when interpreting seroepidemiologic studies in high-risk populations.

Our study had several limitations. Because of multicollinearity of the exposure variables (38), the accuracy of individual predictors may be compromised. The lack of collection of acute blood samples during the outbreak limited our ability to detect seroconversion. In addition, we were not able to conduct sequencing for patients of this outbreak and therefore were not able to use this information to potentially confirm that all 19 infected women acquired their infection from a common source or to identify the source of the outbreak.

The rapid initiation of contact tracing, isolation, and subsequent investigation probably contributed to the quick halt of human-to-human transmission in this outbreak. On the basis of the possible source of infection, to reduce secondary human-to-human transmission outside the occupational setting, our study indicates that IPC measures introduced in healthcare facilities should focus on not only healthcare personnel but also those working within the wider facility, including cleaners.

Acknowledgments

We thank the KSA Ministry of Health field staff for their support in collecting biological samples and administering questionnaires during the study.

Serologic testing for this study was supported by a research grant from the US National Institutes of Health (contract no. HHSN272201400006C).

About the Author

Dr. Van Kerkhove is an infectious disease epidemiologist who specializes in outbreaks of emerging and re-emerging high-threat pathogens. She is the MERS-CoV technical lead at the WHO Health Emergencies Programme in Geneva, Switzerland. Her research interests include zoonotic, respiratory, and emerging/re-emerging viruses, and her work focuses on investigating factors associated with transmission between animals and humans, studying the epidemiology of zoonotic pathogens, and ensuring that research on infectious diseases directly informs public health policy for action.

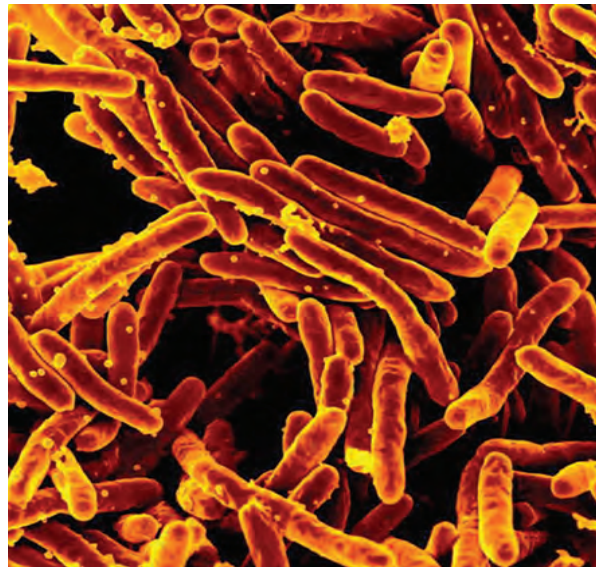
References

- Memish ZA, Mishra N, Olival KJ, Fagbo SF, Kapoor V, Epstein JH, et al. Middle East respiratory syndrome coronavirus in bats, Saudi Arabia. *Emerg Infect Dis*. 2013;19:1819–23. <https://doi.org/10.3201/eid1911.131172>
- World Health Organization. Middle East respiratory syndrome–coronavirus—update: 29 May 2013 [cited 2013 May 30]. http://www.who.int/csr/don/2013_05_29_ncov
- Zaki AM, van Boheemen S, Bestebroer TM, Osterhaus AD, Fouchier RA. Isolation of a novel coronavirus from a man with pneumonia in Saudi Arabia. *N Engl J Med*. 2012;367:1814–20. <https://doi.org/10.1056/NEJMoa1211721>
- Hijawi B, Abdallat M, Sayaydeh A, Alqasrawi S, Haddadin A, Jaarour N, et al. Novel coronavirus infections in Jordan, April 2012: epidemiological findings from a retrospective investigation. *East Mediterr Health J*. 2013;19(Suppl 1):S12–8. <https://doi.org/10.26719/2013.19.supp1.S12>
- FAO-OIE-WHO MERS Technical Working Group. MERS: progress on the global response, remaining challenges and the way forward. *Antiviral Research*. 2018;159:35–44.
- Ben Embarek PK, Van Kerkhove MD. Middle East respiratory syndrome coronavirus (MERS-CoV): current situation 3 years after the virus was first identified. *Wkly Epidemiol Rec*. 2015; 90:245–50.
- Drosten C, Muth D, Corman VM, Hussain R, Al Masri M, HajOmar W, et al. An observational, laboratory-based study of outbreaks of Middle East respiratory syndrome coronavirus in Jeddah and Riyadh, Kingdom of Saudi Arabia, 2014. *Clin Infect Dis*. 2015;60:369–77. <https://doi.org/10.1093/cid/ciu812>
- Ki M. 2015 MERS outbreak in Korea: hospital-to-hospital transmission. *Epidemiol Health*. 2015;37:e2015033.
- Drosten C, Meyer B, Müller MA, Corman VM, Al-Masri M, Hossain R, et al. Transmission of MERS-coronavirus in household contacts. *N Engl J Med*. 2014;371:828–35. <https://doi.org/10.1056/NEJMoa1405858>
- World Health Organization. Middle East respiratory syndrome coronavirus (MERS-CoV) [cited 2019 Jul 30]<http://www.who.int/emergencies/mers-cov>
- Al Hosani F, Pringle K, Al Mulla M, Kim L, Pham H, Alami NN, et al. Response to emergence of Middle East respiratory syndrome coronavirus, Abu Dhabi, United Arab Emirates, 2013–2014. *Emerg Infect Dis*. 2016;22:1162–8. <https://dx.doi.org/10.3201/eid2207.160040>
- Alraddadi B, Bawareth N, Omar H, Alsalmi H, Alshukairi A, Qushmaq I, et al. Patient characteristics infected with Middle East respiratory syndrome coronavirus infection in a tertiary hospital. *Ann Thorac Med*. 2016;11:128–31. <https://doi.org/10.4103/1817-1737.180027>
- World Health Organization. Disease outbreak news [cited 2019 Jul 30]. <http://www.who.int/csr/don/22-june-2016-mers-saudi-arabia>
- Memish ZA, Zumla AI, Assiri A. Middle East respiratory syndrome coronavirus infections in health care workers. *N Engl J Med*. 2013;369:884–6. <https://doi.org/10.1056/NEJMc1308698>
- Obobo IK, Tomczyk SM, Al-Asmari AM, Banjar AA, Al-Mugti H, Aloraini MS, et al. 2014 MERS-CoV outbreak in Jeddah—a link to health care facilities. *N Engl J Med*. 2015;372:846–54. <https://doi.org/10.1056/NEJMoa1408636>
- Moon SY, Son JS. Infectivity of an asymptomatic patient with Middle East respiratory syndrome coronavirus infection. *Clin Infect Dis*. 2017;64:1457–8.
- Kingdom of Saudi Arabia Ministry of Health. Weekly monitor MERS-CoV. 3 November 2015 [cited 2019 Jul 24]. <https://www.moh.gov.sa/en/CCC/Documents/Volume-2-Issue-11-Tuesday-March-15-2016.pdf>
- World Health Organization. Seroepidemiological investigation of contacts of Middle East respiratory syndrome coronavirus (MERS-CoV) patients [cited 2019 Aug 1]. https://www.who.int/csr/disease/coronavirus_infections/who-close-non-hcw-contact-protocol-mers-cov.docx?ua=1
- Command and Control Center SAB. Kingdom of Saudi Arabia Ministry of Health. Middle East respiratory syndrome coronavirus guidelines for healthcare professionals [cited 2019 Aug 1]. <https://www.moh.gov.sa/CCC/healthp/regulations/Documents/MERS-CoV%20Guidelines%20for%20Healthcare%20Professionals%20-%20May%202018%20-%20v5.1%20%281%29.pdf>
- World Health Organization. Guidance on regulations for the transport of infectious substances 2015–2016 [cited 2019 Jun 5]. http://www.who.int/ihr/publications/who_hse_ihr_2015.2
- Choe PG, Perera RAPM, Park WB, Song K-H, Bang JH, Kim ES, et al. MERS-CoV antibody responses 1 year after symptom onset, South Korea, 2015. *Emerg Infect Dis*. 2017;23:1079–84. <https://dx.doi.org/10.3201/eid2307.170310>
- Al-Abdely HM, Midgley CM, Alkhamis AM, Abedi GR, Tamin A, Binder AM, et al. Infectious MERS-CoV isolated from a mildly ill patient, Saudi Arabia. *Open Forum Infect Dis*. 2018;5:ofy111. <https://doi.org/10.1093/ofid/ofy111>
- Arwady MA, Alraddadi B, Basler C, Azhar EI, Abuelzein E, Sindy AI, et al. Middle East respiratory syndrome coronavirus transmission in extended family, Saudi Arabia, 2014. *Emerg Infect Dis*. 2016;22:1395–402. <https://doi.org/10.3201/eid2208.152015>
- Breban R, Riou J, Fontanet A. Interhuman transmissibility of Middle East respiratory syndrome coronavirus: estimation of pandemic risk. *Lancet*. 2013;382:694–9. [https://doi.org/10.1016/S0140-6736\(13\)61492-0](https://doi.org/10.1016/S0140-6736(13)61492-0)

25. Cauchemez S, Fraser C, Van Kerkhove MD, Donnelly CA, Riley S, Rambaut A, et al. Middle East respiratory syndrome coronavirus: quantification of the extent of the epidemic, surveillance biases, and transmissibility. *Lancet Infect Dis.* 2014;14:50–6.
26. Hui DS, Azhar EI, Kim Y-J, Memish ZA, Oh M-d, Zumla A. Middle East respiratory syndrome coronavirus: risk factors and determinants of primary, household, and nosocomial transmission. *Lancet Infect Dis.* 2018;18:e217–e27.
27. World Health Organization. WHO MERS global summary and assessment of risk: August 2018 [cited 2019 Jun 5]. https://www.who.int/csr/disease/coronavirus_infections/risk-assessment-august-2018.pdf
28. World Health Organization. Infection prevention and control during health care for probable or confirmed cases of Middle East respiratory syndrome coronavirus (MERS-CoV) infection [cited 2019 Jun 5]. https://www.who.int/csr/disease/coronavirus_infections/ipc-mers-cov
29. BinSaeed AA, Abedi GR, Alzahrani AG, Salameh I, Abdirizak F, Alhakeem R, et al. Surveillance and testing for Middle East respiratory syndrome coronavirus, Saudi Arabia, April 2015–February 2016. *Emerg Infect Dis.* 2017;23:682–5. <https://doi.org/10.3201/eid2304.161793>
30. Van Kerkhove MD, Peiris MJS, Malik MR, Ben Embarek P. Interpreting results from environmental contamination studies of Middle East respiratory syndrome coronavirus. *Clin Infect Dis.* 2016;63:1142. <https://doi.org/10.1093/cid/ciw478>
31. Kim S-H, Chang SY, Sung M, Park JH, Bin Kim H, Lee H, et al. Extensive viable Middle East respiratory syndrome (MERS) coronavirus contamination in air and surrounding environment in MERS outbreak units. *Clin Infect Dis.* 2016;63:363–9.
32. Bin SY, Heo JY, Song M-S, Lee J, Kim E-H, Park S-J, et al. Environmental contamination and viral shedding in MERS patients during MERS-CoV outbreak in South Korea. *Clin Infect Dis.* 2016;62:755–60. <https://doi.org/10.1093/cid/civ1020>
33. van Doremalen N, Bushmaker T, Munster VJ. Stability of Middle East respiratory syndrome coronavirus (MERS-CoV) under different environmental conditions. *Euro Surveill.* 2013;18:20590. <https://doi.org/10.2807/1560-7917.ES2013.18.38.20590>
34. World Health Organization. Assessment of potential risk factors of Middle East respiratory syndrome coronavirus (MERS-CoV) infection among health care personnel in a health care setting [cited 2019 Jan 1]. https://www.who.int/csr/disease/coronavirus_infections/who-generic_healthcare-mers-seroepi-investigation.docx
35. Park SW, Perera RA, Choe PG, Lau EH, Choi SJ, Chun JY, et al. Comparison of serological assays in human Middle East respiratory syndrome (MERS)-coronavirus infection. *Euro Surveill.* 2015;20:30042. <https://doi.org/10.2807/1560-7917.ES.2015.20.41.30042>
36. Perera RA, Wang P, Gomaa MR, El-Shesheny R, Kandeil A, Bagato O, et al. Seroepidemiology for MERS coronavirus using microneutralisation and pseudoparticle virus neutralisation assays reveal a high prevalence of antibody in dromedary camels in Egypt, June 2013. *Euro Surveill.* 2013;18:20574. <https://doi.org/10.2807/1560-7917.ES2013.18.36.20574>
37. Ko JH, Müller MA, Seok H, Park GE, Lee JY, Cho SY, et al. Serologic responses of 42 MERS-coronavirus-infected patients according to the disease severity. *Diagn Microbiol Infect Dis.* 2017;89:106–11.
38. Vatcheva KP, Lee M, McCormick JB, Rahbar MH. Multicollinearity in regression analyses conducted in epidemiologic studies. *Epidemiology (Sunnyvale).* 2016;6:227.

Address for correspondence: Maria D. Van Kerkhove, World Health Organization, High Threat Pathogens, Global Infectious Hazards Management Health Emergencies Program, Avenue Appia, Geneva 1211, Switzerland; email: vankerkhovem@who.int

EID podcast Tuberculosis Surveillance and Control in Puerto Rico



The WHO has recognized Puerto Rico as a promising candidate for the elimination of tuberculosis by 2035, but many challenges remain before this goal can be achieved. Before going forward, researchers must look back at the historical patterns and developments that have brought them here.

In this EID podcast, Dr. Emilio Dirlikov, a CDC epidemiologist, tells the story of TB surveillance in Puerto Rico from 1898 to 2015.

Visit our website to listen:
<https://go.usa.gov/xysv>

**EMERGING
INFECTIOUS DISEASES®**

Emergence and Containment of Canine Influenza Virus A(H3N2), Ontario, Canada, 2017–2018

J. Scott Weese, Maureen E.C. Anderson, Yohannes Berhane, Kathleen F. Doyle, Christian Leutenegger, Roxanne Chan, Michelle Chiunti, Katerina Marchildon, Nicole Dumouchelle, Theresa DeGelder, Kiera Murison, Catherine Filejski, Davor Ojkic

Canine influenza virus (CIV) A(H3N2) was identified in 104 dogs in Ontario, Canada, during December 28, 2017–October 30, 2018, in distinct epidemiologic clusters. High morbidity rates occurred within groups of dogs, and kennels and a veterinary clinic were identified as foci of infection. Death attributable to CIV infection occurred in 2 (2%) of 104 diagnosed cases. A combination of testing of suspected cases, contact tracing and testing, and 28-day isolation of infected dogs was used, and CIV transmission was contained in each outbreak. Dogs recently imported from Asia were implicated as the source of infection. CIV H3N2 spread rapidly within groups in this immunologically naive population; however, containment measures were apparently effective, demonstrating the potential value of prompt diagnosis and implementation of CIV control measures.

Canine influenza virus (CIV) is a regional cause of disease in dogs that has emerged from other host species of influenza A viruses (IAVs) as a result of adaptation and subsequent transmission within the naïve dog population (1,2). Two main CIV strains are currently recognized. CIV A(H3N8) is an equine-origin virus that was identified in

dogs in the United States in the early 2000s (1) but that is rarely identified now. In contrast, CIV H3N2 emerged in Asia from an avian influenza virus (H3N2) (2,3) and can be found in different regions in Asia (2–4). It was subsequently introduced to the United States on multiple occasions through importation of dogs from South Korea and China (5,6). Within an immunologically naive canine population, CIV can spread widely when introduced to a new dog population, and result in widespread illness and sporadic death. There is also some concern about the potential for CIV H3N2 to recombine with other IAVs (7), including human IAVs, potentially resulting in antigenic shift and creating relatively novel IAVs with broader host range and pandemic potential.

Novel CIVs are of concern for canine health because of the naive population and potential for rapid and widespread transmission. International, including transcontinental, movement of dogs is common, and CIV is one of many pathogens that can accompany transported dogs. In 2015, CIV H3N2 was introduced into the United States through the importation of dogs from Asia; the virus continues to circulate in the canine population within the country from that or subsequent importations (5,6,8). Despite its presence in the United States, CIV H3N2 had not been identified in Canada until the end of 2017. We describe the introduction and containment of CIV H3N2 in Ontario, Canada.

Outbreak Investigation

Clinical testing identified CIV H3N2 in Ontario in December 2017, prompting prospective surveillance and interventions. Initial clinical diagnoses were based on positive H3N2 PCR results from a commercial respiratory PCR panel (IDEXX Laboratories, <https://ca.idexx.com>). Subsequent testing was performed at the Animal Health Laboratory, University of Guelph (Guelph, ON, Canada), using IAV matrix gene real-time PCR (rPCR) testing of nasal or pharyngeal swab specimens or a repeat of the respiratory PCR panel test. H3N2-specific hemagglutination inhibition (HI) testing was performed at the Animal Health Diagnostic Center, Cornell

Author affiliations: University of Guelph, Guelph, Ontario, Canada (J.S. Weese, K. Murison, D. Ojkic); Ontario Ministry of Agriculture, Food and Rural Affairs, Guelph (M.E.C. Anderson); National Centre for Foreign Animal Disease, Canadian Food Inspection Agency, Winnipeg, Manitoba, Canada (Y. Berhane); Chidiac Animal Hospital Gravenhurst, Gravenhurst, Ontario, Canada (K.F. Doyle); IDEXX Laboratories, West Sacramento, California, USA (C. Leutenegger); IDEXX Laboratories, Markham, Ontario, Canada (R. Chan); Northumberland Veterinary Services, Colborne, Ontario, Canada (M. Chiunti); Lake Country Animal Hospital, Severn, Ontario, Canada (K. Marchildon); Fort Malden Animal Hospital, Amherstburg, Ontario, Canada (N. Dumouchelle); Forest Glade Animal Hospital, Windsor, Ontario, Canada (T. DeGelder); Ontario Ministry of Health and Longterm Care, Toronto, Ontario, Canada (C. Filejski)

DOI: <https://doi.org/10.3201/eid2510.190196>

University (Ithaca, NY, USA), on serum samples collected from dogs that were suspected to have been infected recently but whose PCR results might have been negative by the time testing was performed. After identification of cases (dogs with CIV-positive PCR results), contact tracing was performed, with potentially exposed dogs tested whenever possible. Longitudinal testing was performed whenever possible, and an attempt was made to get weekly samples from all positive dogs until 2 negative results were obtained. Partial sequencing of the hemagglutinin gene was performed as previously described (9).

Outbreak Cluster 1

Two dogs received diagnoses of CIV H3N2 shortly after their arrival in southwestern Ontario (Figure 1) from South Korea. The dogs had been part of a larger group flown to Chicago, Illinois, USA; the 2 affected dogs were driven to Canada immediately after arrival. Both dogs had signs consistent with upper respiratory disease, characterized by fever, productive cough, and purulent nasal discharge. Samples were collected on December 28, 2017, within 24 hours of arrival in Canada.

The 2 imported dogs went to separate foster homes; all 6 canine contacts in those homes were identified on January 5, 2018, as infected with CIV H3N2. Two feline household contacts were negative. A 28-day isolation period was recommended; compliance was good, and no further cases were identified. Two dogs were clinically normal but still shedding CIV on January 18, but all were negative by January 31.

Outbreak Cluster 2

This cluster occurred in a nearby community in southwestern Ontario; CIV H3N2 was identified in a dog with upper respiratory illness. Disease was first noted on January 20, 2018; samples were collected for an upper respiratory disease PCR panel on January 22. There was no known contact with dogs from cluster 1. The owner was a veterinary clinic employee who had handled a dog with severe and presumably infectious respiratory tract disease a few days before the onset of disease. That dog had died without testing being performed. Both canine household contacts developed respiratory disease that was diagnosed as CIV H3N2 from samples collected January 31.

The index case dog also had contact with a group of other dogs as part of a recurring canine group activity. Ten contacts were tested, and 1 dog tested positive. That dog developed mild respiratory disease; CIV H3N2 was detected on January 31.

Because the source of exposure of the index case was unclear, serologic testing was performed on the group of canine contacts in an attempt to determine whether other dogs might have been previously infected but had ceased shedding by the time of investigation. The only seropositive dogs were the affected household dogs and a single affected contact, which developed disease well after the index case.

The local public health unit implemented a mandatory 28-day confinement order for the affected dogs. No further cases were identified, and all dogs recovered uneventfully.

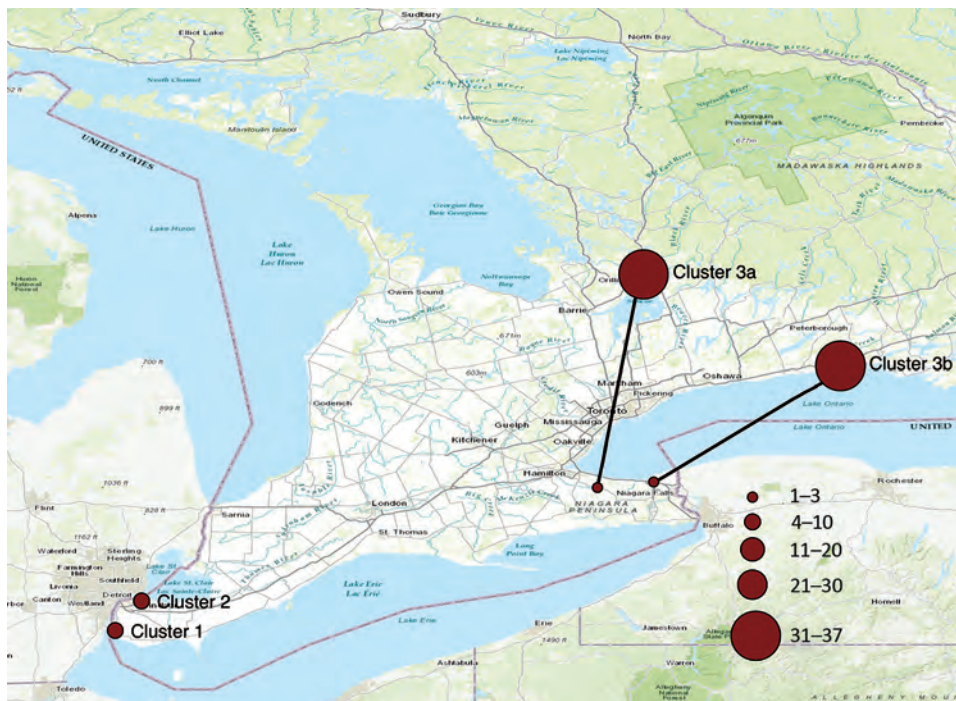


Figure 1. Approximate locations and number of dogs with diagnoses of canine influenza virus infection, Ontario, Canada, 2017–2018.

Outbreak Cluster 3a

This cluster was initially identified in central Ontario, starting February 26, 2018 (Figures 2, 3), during testing of a high-morbidity respiratory disease outbreak in a boarding kennel. Fourteen dogs at that kennel were infected.

Contact tracing raised suspicion of a rescue facility (rescue A) that had recently imported dogs from China as the source, because 1 of the imported dogs was fostered by the owner of 3 dogs that went to the affected kennel. Those 3 dogs developed upper respiratory tract disease on February 17, four days after contact with the imported dog.

The rescue facility also offered boarding and dog walking services. One dog that was walked by rescue A tested positive for CIV (February 23 and March 1); CIV was then transmitted to a household canine contact, which transmitted CIV to a grooming service it visited. Two of the groomer’s own dogs were infected; 1 was euthanized because of severe respiratory disease. One additional dog was then infected at the groomer’s.

Other cases linked to the rescue facility were identified, including 5 dogs (diagnosed March 2 and 5) whose owner resided adjacent to rescue A, 1 dog (diagnosed March 2) that had boarded at the rescue during February 17–24, a dog that had been at rescue A for day care, another dog that had visited for dog walking (diagnosed March 3), and a dog that became sick shortly after being adopted from the rescue facility. One additional case without a known origin was identified in a dog that developed respiratory disease around March 12; CIV was diagnosed on March 19. This

dog had no known contact with other affected dogs but was regularly walked along a public trail. Follow-up information was not available for the remaining 3 infected dogs.

Another linked case was identified in a different city ≈300 km away. A dog imported from China in the same shipment that went to rescue A was transferred to another group (rescue B); respiratory disease subsequently developed in an unclear number of contacts. Nasal swab specimens were collected from 15 dogs associated with rescue B on March 9, and 1 was CIV positive. It was suspected that other dogs were also infected but had ceased shedding by the time of sampling (24 days after the imported dog arrived), given the delay in identifying this group.

With 9 separate epidemiologic links and a history of importation of dogs from China, rescue A was the presumed source of CIV H3N2. It had received imported dogs from China on February 13. Upper respiratory tract disease was reported in 42/64 (66%) dogs at the rescue during February 16–March 2. Testing of 10 dogs at the facility was performed until March 8, at which point none of the dogs were found to be shedding CIV. One death attributable to respiratory disease was reported at rescue A, but testing was not performed.

A 28-day isolation period was recommended for all infected dogs; owners were receptive to isolation and infection control recommendations. The affected boarding kennel was closed until all dogs tested negative. The affected grooming facility was also closed until the owner’s dogs tested negative and the facility had been cleaned and disinfected.

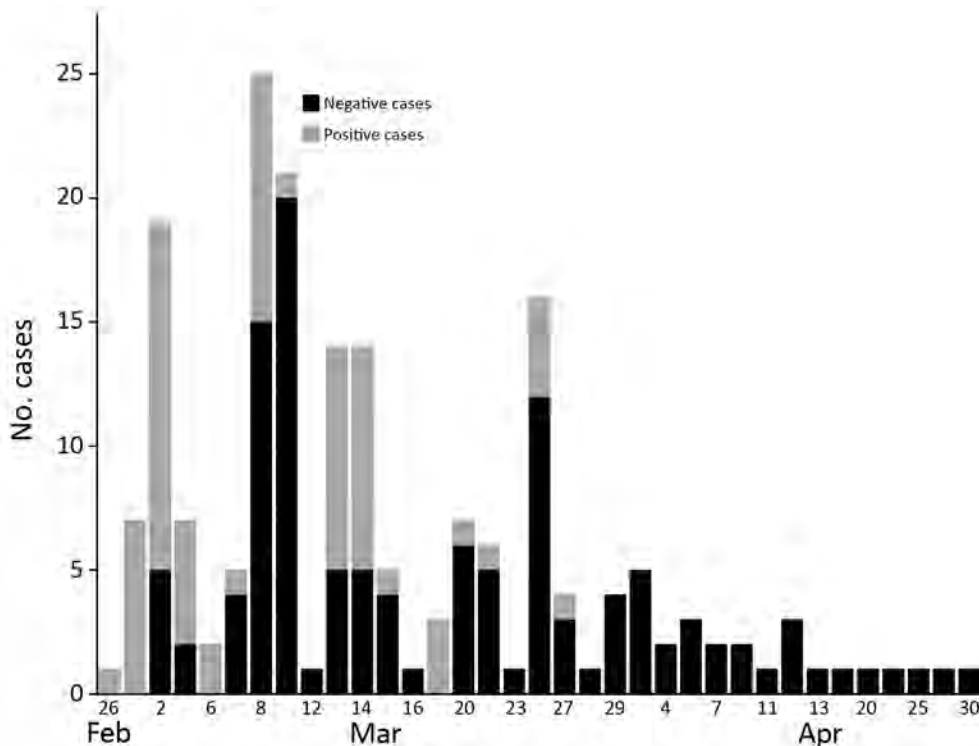


Figure 2. Time series of canine influenza diagnoses in clusters 3a and 3b, Ontario, Canada, 2017–2018. Transmission events within households are not depicted.

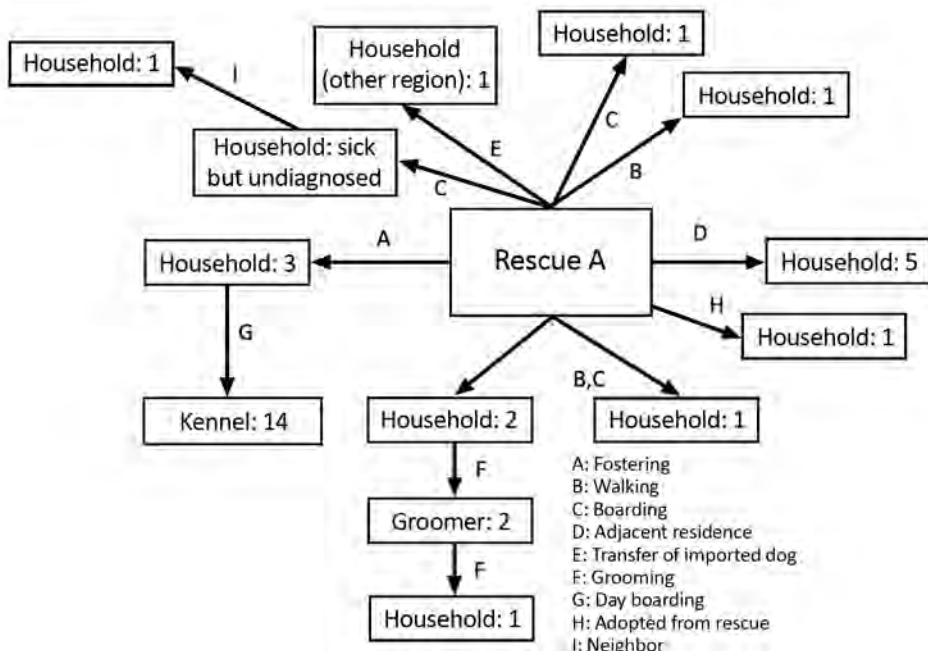


Figure 3. Suspected transmission pathways for canine influenza cluster 3a, Ontario, Canada, 2017–2018. Numbers in each box denote the number of confirmed (PCR positive) CIV infections.

Outbreak Cluster 3b

A secondary cluster was identified in eastern Ontario, ≈250 km from the central Ontario outbreak. The first diagnosed case was from a group of 3 orphaned puppies that were being cared for by personnel from a veterinary clinic, but infection was ultimately linked to a dog (dog A) from a humane society ≈250 km away (Figure 4). A local rescue group (rescue C) had obtained dog A from a shelter in the Niagara, Ontario, region (≈300 km away from cluster 3a and 250 km from the veterinary clinic, but only 25 km from where 1 of the imported dogs was transferred). Dog A was surrendered to the shelter on February 12 and transferred to rescue C on February 21. This dog was taken to the veterinary clinic after arrival at rescue C, at which time nasal discharge, sneezing, and coughing were noted. Testing was

not performed, and the dog was not available for testing until March 18. Serologic testing was performed because of the time that had passed, and the dog was seropositive (hemagglutinin inhibition [HI] titer 1:256; ≥1:16 indicates exposure). Because this dog had no history of travel outside Canada or CIV vaccination, this result provided a presumptive CIV diagnosis. Two dogs at rescue C that developed respiratory disease after dog A arrived were also seropositive on samples collected March 18; HI titers were 1:64 and 1:1,024.

Furthermore, it was reported that an outbreak of upper respiratory tract disease had occurred in dogs at rescue C shortly after dog A left. Five dogs at the shelter were tested by PCR; however, testing occurred March 9, which was 16 days after departure of the affected dog, and all tests were

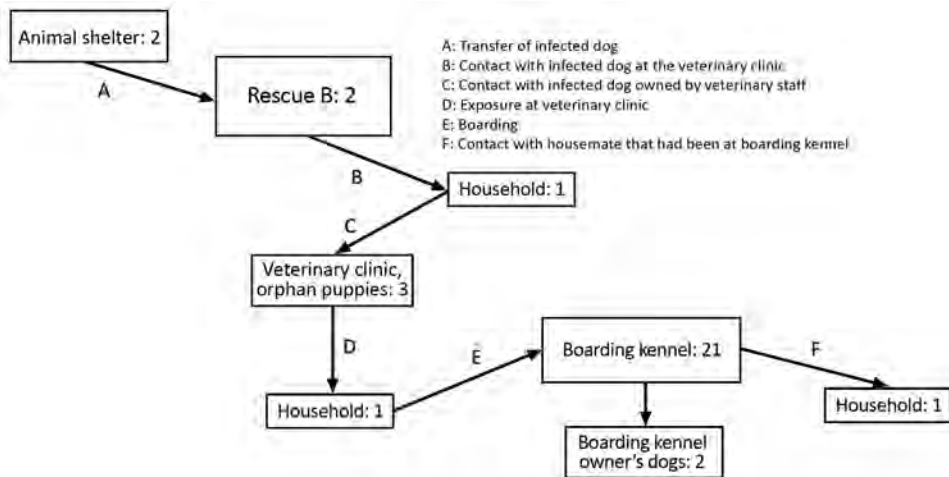


Figure 4. Suspected transmission pathways for canine influenza cluster 3b, Ontario, Canada, 2017–2018. Numbers in each box denote the number of confirmed (PCR positive) CIV infections.

negative. Serologic testing performed on 1 of those dogs was positive (HI titer of 1:1,024), supporting the presence of a CIV H3N2 cluster in that shelter, with transmission to rescue C by dog A.

The origin of CIV was unclear. Given the timing of arrival at the shelter and onset of disease, it is possible that dog A was infected at the shelter or shortly before arrival. No source of infection was identified; however, the dog was surrendered to the shelter from an area close to rescue B at the same time as the localized cluster associated with that group was active.

Dog A was at the veterinary clinic at the same time as another dog (dog B) owned by an employee of the clinic. CIV was diagnosed in dog B on February 28, and dog B's 5 household canine contacts were subsequently infected. Prior to the onset of signs of respiratory disease, dog B attended the veterinary clinic with its owner when the litter of 3 orphan puppies was in the clinic. The puppies started showing signs of respiratory tract disease on March 2; a sample was collected from 1 puppy the next day, and CIV was diagnosed by PCR.

One dog that had been at the clinic for elective surgery was infected. That dog then visited a local doggy day care. Cough was noted on the first day of stay (March 6), and the dog visited the facility for the next week. Twenty-one dogs that visited the facility were infected, along with 2 of the facility owner's dogs. A 15-year-old dog with renal disease died, with the cause attributed to CIV. The kennel was closed to all but infected dogs for the next 3 weeks and underwent thorough cleaning and disinfection; 28-day isolation of all exposed or infected dogs was recommended. To reduce the number of potential exposed animals and facilitate cleaning and disinfection, the veterinary clinic temporarily restricted elective admissions for 1 week.

Outbreak Cluster 4

In October 2018, another 2 infected dogs were identified. Both had had contact with rescue A, and it was subsequently learned that another group of dogs had been imported from China \approx 3 weeks earlier. Seven H3N2 infections among non-imported dogs were then confirmed at rescue A. Five additional H3N2-infected dogs were identified, all of which had contact with rescue A through boarding or walking. Sixty-two dogs were tested as part of the investigation and response, and no further cases were identified. Nine of the infected dogs had been vaccinated against CIV H3N2 in the spring and had received the required 2-dose initial series.

Other Cases

During the time of cluster 3, another potential case was identified in a town >200 km from the nearest affected area. The dog had mild respiratory tract disease; matrix gene rPCR testing yielded a result at the upper end of the

inconclusive range (40 cycles; reference range, positive \leq 36 cycles, inconclusive >36 but \leq 40). An affected housemate was negative, and there were no reported contacts with imported dogs or dogs from affected areas. Therefore, a false-positive result was suspected.

Sequence Analysis

Partial hemagglutinin (H) gene was amplified from 32 samples that tested positive on matrix gene rPCR for Sanger sequencing. One sample each were from clusters 1 and 2, and those samples were identical. All 20 samples from cluster 3a were genetically identical and were 99.7% identical to clusters 1 and 2. Five samples from cluster 3b were identical and were 99.5% identical to clusters 1 and 2. Three samples from cluster 3b were identical to those from cluster 3a; all 3 were from dogs in the first group of dogs in cluster 3b, suggesting that genetic drift occurred between the dogs in this household and the later cases.

Subsequent Surveillance

Overall, 104 infected dogs were identified during December 28, 2017–October 30, 2018; however, it is likely that many more dogs were infected, as testing of all affected dogs in a group was not always performed. As part of this investigation, we tested 263 dogs.

Cluster 3 was considered to be over on May 1, which was 28 days after the last known positive result. No additional cases of CIV were identified in Ontario until October 16, 2018, when cluster 4 was identified. Because a regulatory requirement for veterinarians and diagnostic laboratories to report novel influenza (which would include CIV) infection in animals to local public health units went into effect on January 1, 2018, it is likely that all diagnosed cases were identified. Although only a subset of dogs with respiratory disease are currently tested for CIV, the high infection rate of CIV would be expected to result in a greater impetus to test, given the obvious clusters of disease that can occur. Although we cannot state definitely that CIV was eradicated, no infections were identified for at least 6 months after the final cases ceased shedding CIV.

Outcome and Duration of Shedding

Deaths attributed to CIV were reported in 2 (2%) of the diagnosed cases, both of which were in older dogs with underlying diseases. CIV was also suspected in at least 1 additional death.

Multiple samples were collected from 44 CIV-positive dogs (range 2–5 samples, median 2). Of the 22 (50%) that had >1 positive sample, the interval between the 2 positive results, representing the minimal shedding period, ranged from 4 to 20 days (median 12 days). The duration from first positive to first negative ranged from 4 to 30 days (median 18 days). Two dogs had a negative sample between 2 positive samples.

Human Surveillance

In all clusters, public health units requested that potentially exposed persons report influenza-like illness so that testing could be performed. No human illnesses were reported from the undefined number of exposed human contacts.

Discussion

Multiple introductions of CIV H3N2 have occurred in Ontario, Canada, with subsequent transmission within the canine population. A unique aspect of this investigation was the degree of contact tracing and active surveillance, such that a source of exposure was identified for almost all CIV-positive dogs. The source of infection was discerned for all dogs identified after the index cases in clusters 1, 2, 3b, and 4. In cluster 3a, 1 case had no known exposure, but the dog had been walked on public trails. No information was available for 3 dogs; contact tracing identified clear or plausible links for all other cases.

The first cluster was clearly associated with importation from South Korea, because the index cases were in dogs that had been imported within days of diagnosis. The origin of the second cluster is unclear. The timing, location, and sequence data suggest a link to cluster 1, but a separate introduction cannot be excluded. The third and fourth clusters presumably originated from separate groups of dogs imported from China, given the number of epidemiologic links to that facility and the timing and sequence data.

Although virtually the entire dog population of Canada is presumably immunologically naive to CIV H3N2 because of a lack of previous exposure and very low CIV vaccination rates, this highly transmissible virus was contained. Illness rates were high within groups, but a relatively small number of distinct groups was infected. It is possible that other clusters of disease were ongoing, but the high illness rate associated with CIV, the high awareness through media reports and other communications when the outbreak was under way, and the reportable nature of the disease suggest that unidentified clusters (at least large clusters) are unlikely.

It was encouraging that CIV H3N2 was apparently eradicated multiple times. Although it is impossible to determine what actions were effective, the combination of rapid response, active surveillance of contacts, widespread communication, voluntary closure of affected facilities, and 28-day isolation of infected and exposed dogs appeared to contain this highly transmissible virus, even in an immunologically naive population. Time of year might have facilitated control; the cases occurred during periods of cold or otherwise inclement weather, something that likely reduced contact between dogs during walking, visits to parks, and similar activities. The ability to control these CIV introductions is in contrast to reports from the United States, where larger, more sustained outbreaks have occurred, perhaps

largely the result of a lack of a coordinated effort to identify and contain the disease. Although the cost–benefit ratio of CIV containment can be debated, the experience in Ontario suggests that an active approach can be effective, provided appropriate personnel and resources are available.

Information about CIV H3N2 mortality rates is limited. The 2% mortality rate reported here is consistent with the 2.5% (1/40) rate reported in a metropolitan US outbreak (8). Mortality rates for CIV can be overestimated if animals with serious illness are more likely to be tested; however, testing bias is less of a concern in this study, given the scope of the investigation. Both dogs that died were older animals, consistent with the presumed increased risk in this population. Although the true mortality rate may be lower because of lack of testing of mildly affected animals, serious respiratory disease, including death, can occur.

A bivalent CIV H3N2/H3N8 vaccine was available in Canada during the period of this investigation, but vaccination coverage is anecdotally very low because of the foreign nature of CIV. Vaccination played little role in containment of these outbreaks. Few dogs from affected areas were vaccinated, and the need for 2 doses, 14–28 days apart, reduces the potential for vaccination to help during active outbreaks. Nevertheless, vaccination of dogs in affected and adjacent communities was recommended to reduce the risk of continued spread if initial containment had failed. Most infected dogs in cluster 4 had been properly vaccinated against CIV H3N2. This raises concern about vaccine efficacy; however, interpretation is difficult because CIV vaccines are labeled as an aid for control of disease, focused on reduction of severity of disease. It is possible that vaccination reduced severity of disease. These data do not mean that vaccination is not warranted but serve as a reminder that CIV vaccination cannot be relied on as a tool to prevent entrance or dissemination of CIV in dog populations.

Sun et al. expressed concern about the potential that dogs could act as mixing vessels between human and non-human influenza viruses (7). No humans were tested as part of the surveillance of these canine cases. Response varied by health unit, but human contacts of infected dogs were generally asked to report whether they developed signs and symptoms consistent with influenza. Despite widespread human exposure in the ongoing CIV H3N2 outbreak in the United States, human cases have not been identified, suggesting that the public health risk from CIV H3N2 is limited. However, because dogs are susceptible to some influenza viruses, such as pandemic influenza A(H1N1) (10), co-infection of dogs and humans in households raises concern about the potential for reassortment.

In summary, CIV H3N2 is a highly transmissible virus with the potential to cause high-morbidity outbreaks, along with economic and social disruption in the canine

and veterinary industries. Even though human health risks are believed to be low, endemic circulation of a nonhuman influenza A virus, particularly in an animal population with such close human contact, raises concern. Clarifying transmission routes and control options is critical for CIV control; this outbreak demonstrates the likely effectiveness of a concerted approach focusing on testing, contact tracing, voluntary isolation, and communication.

Acknowledgments

The authors are grateful for the assistance of various veterinary personnel who assisted with sampling, to Cindi Wigston for assistance with data collection, and to Edward Dubovi for providing CIV H3N2 serological testing through the Cornell University Animal Health Diagnostic Center.

Funding was provided by the Ontario Veterinary College Pet Trust.

About the Author

Dr. Weese is a veterinary internist at the University of Guelph, Guelph, Ontario, Canada, whose focus is on infectious diseases. His research and clinical interests include emerging diseases, zoonoses, and antimicrobial resistance.

References

1. Crawford PC, Dubovi EJ, Castleman WL, Stephenson I, Gibbs EPJ, Chen L, et al. Transmission of equine influenza virus to dogs. *Science*. 2005;310:482–5. <https://doi.org/10.1126/science.1117950>
2. Su S, Li HT, Zhao FR, Chen JD, Xie JX, Chen ZM, et al. Avian-origin H3N2 canine influenza virus circulating in farmed dogs in Guangdong, China. *Infect Genet Evol*. 2013;14:444–9. <https://doi.org/10.1016/j.meegid.2012.11.018>
3. Song D, Kang B, Lee C, Jung K, Ha G, Kang D, et al. Transmission of avian influenza virus (H3N2) to dogs. *Emerg Infect Dis*. 2008;14:741–6. <https://doi.org/10.3201/eid1405.071471>
4. Li S, Shi Z, Jiao P, Zhang G, Zhong Z, Tian W, et al. Avian-origin H3N2 canine influenza A viruses in Southern China. *Infect Genet Evol*. 2010;10:1286–8. <https://doi.org/10.1016/j.meegid.2010.08.010>
5. Voorhees IEH, Dalziel BD, Glaser A, Dubovi EJ, Murcia PR, Newbury S, et al. Multiple incursions and recurrent epidemic fade-out of H3N2 canine influenza A virus in the United States. *J Virol*. 2018;92:e00323–18. <https://doi.org/10.1128/JVI.00323-18>
6. Voorhees IEH, Glaser AL, Toohey-Kurth K, Newbury S, Dalziel BD, Dubovi EJ, et al. Spread of canine influenza A(H3N2) virus, United States. *Emerg Infect Dis*. 2017;23:1950–7. <https://doi.org/10.3201/eid2312.170246>
7. Sun H, Blackmon S, Yang G, Waters K, Li T, Tangwangvivat R, et al. Zoonotic risk, pathogenesis, and transmission of avian-origin H3N2 canine influenza virus. *J Virol*. 2017;91:e00637–17. <https://doi.org/10.1128/JVI.00637-17>
8. Dunn D, Creevy KE, Krimer PM. Outcomes of and risk factors for presumed canine H3N2 influenza virus infection in a metropolitan outbreak. *J Am Vet Med Assoc*. 2018;252:959–65. <https://doi.org/10.2460/javma.252.8.959>
9. Phipps LP, Essen SC, Brown IH. Genetic subtyping of influenza A viruses using RT-PCR with a single set of primers based on conserved sequences within the HA2 coding region. *J Virol Methods*. 2004;122:119–22. <https://doi.org/10.1016/j.jviromet.2004.08.008>
10. Dundon WG, De Benedictis P, Viale E, Capua I. Serologic evidence of pandemic (H1N1) 2009 infection in dogs, Italy. *Emerg Infect Dis*. 2010;16:2019–21. <https://doi.org/10.3201/eid1612.100514>

Address for correspondence: J. Scott Weese, University of Guelph, Ontario Veterinary College, Department of Pathobiology, Guelph, ON N1G2W1, Canada; email: jweese@uoguelph.ca

PubMed Central

PubMed



Find *Emerging Infectious Diseases* content in the digital archives of the National Library of Medicine

www.pubmedcentral.nih.gov

Edwardsiella tarda Bacteremia, Okayama, Japan, 2005–2016

Shinya Kamiyama, Akira Kuriyama, Toru Hashimoto

Medscape **ACTIVITY**
EDUCATION

In support of improving patient care, this activity has been planned and implemented by Medscape, LLC and Emerging Infectious Diseases. Medscape, LLC is jointly accredited by the Accreditation Council for Continuing Medical Education (ACCME), the Accreditation Council for Pharmacy Education (ACPE), and the American Nurses Credentialing Center (ANCC), to provide continuing education for the healthcare team.

Medscape, LLC designates this Journal-based CME activity for a maximum of 1.00 **AMA PRA Category 1 Credit(s)**[™]. Physicians should claim only the credit commensurate with the extent of their participation in the activity.

Successful completion of this CME activity, which includes participation in the evaluation component, enables the participant to earn up to 1.0 MOC points in the American Board of Internal Medicine's (ABIM) Maintenance of Certification (MOC) program. Participants will earn MOC points equivalent to the amount of CME credits claimed for the activity. It is the CME activity provider's responsibility to submit participant completion information to ACCME for the purpose of granting ABIM MOC credit.

All other clinicians completing this activity will be issued a certificate of participation. To participate in this journal CME activity: (1) review the learning objectives and author disclosures; (2) study the education content; (3) take the post-test with a 75% minimum passing score and complete the evaluation at <http://www.medscape.org/journal/eid>; and (4) view/print certificate. For CME questions, see page 2002.

Release date: September 13, 2019; Expiration date: September 13, 2020

Learning Objectives

Upon completion of this activity, participants will be able to:

- Describe the clinical epidemiology and characteristics of *Edwardsiella tarda* bacteremia, according to a clinical series from Japan
- Determine treatment and outcomes of *E. tarda* bacteremia, according to a clinical series from Japan
- Identify seasonal distribution and other clinical implications of findings of this clinical series from Japan

CME Editor

Karen L. Foster, Technical Writer/Editor, Emerging Infectious Diseases. *Disclosure: Karen L. Foster has disclosed no relevant financial relationships.*

CME Author

Laurie Barclay, MD, freelance writer and reviewer, Medscape, LLC. *Disclosures: Laurie Barclay, MD, has disclosed no relevant financial relationships.*

Authors

Disclosures: Shinya Kamiyama, MD; Akira Kuriyama, MD, MPH; and Toru Hashimoto, MD, PhD, have disclosed no relevant financial relationships.

Edwardsiella tarda is primarily associated with gastrointestinal disease, but an increasing number of cases involving extraintestinal disease, especially *E. tarda* bacteremia, have been reported. Using clinical information of *E. tarda* bacteremia patients identified during January 2005–December 2016 in Japan, we characterized the clinical epidemiology of *E. tarda* bacteremia. A total of 182,668 sets of blood cultures were

obtained during the study period; 40 (0.02%) sets from 26 patients were positive for *E. tarda*. The most common clinical manifestations were hepatobiliary infection, including cholangitis, liver abscess, and cholecystitis. Overall 30-day mortality for *E. tarda* bacteremia was 12%, and overall 90-day mortality was 27%. The incidence of *E. tarda* infection did not vary by season. We more frequently observed hepatobiliary infection in patients with *E. tarda* bacteremia than in patients with nonbacteremic *E. tarda* infections. *E. tarda* bacteremia is a rare entity that is not associated with high rates of death.

Author affiliation: Kurashiki Central Hospital, Okayama, Japan

DOI: <https://doi.org/10.3201/eid2510.180518>

Edwardsiella tarda, a gram-negative, facultative anaerobe that is a member of the family *Enterobacteriaceae*, typically is isolated from water environments and animals that inhabit water. It is primarily associated with gastrointestinal disease, but the number of reports of extraintestinal disease, such as septicemia, meningitis, cholecystitis, and osteomyelitis, has increased (1). However, little is known about the clinical epidemiology of *E. tarda* bacteremia. Therefore, we aimed to document the clinical epidemiology of *E. tarda* bacteremia, including common sources of infection, antimicrobial susceptibility, and seasonal distribution.

Materials and Methods

We retrospectively reviewed electronic medical records and clinical microbiology records in Kurashiki Central Hospital (Okayama, Japan), a 1,166-bed, tertiary-care hospital that provides care to \approx 300,000 persons annually. Clinical specimens submitted to the microbiology laboratory included blood, sputum, urine, bile, ascites, feces, placenta, tissue, and pus. Information about identified bacteria and antimicrobial susceptibility were kept as microbiology laboratory records for each specimen. We considered bacteremia to exist when >1 set of blood cultures was positive. We identified all cultures growing *E. tarda* from clinical specimens submitted during January 2005–December 2016.

We processed blood culture samples using the BacT/Alert system (Sysmex bioMérieux Co. Ltd., <https://www.biomerieux.com>) and conducted microbial culture using KBM Chocolate HB Agar (Kohjin Bio Co. Ltd., <http://www.kohjin-bio.jp/english>), KBM Sheep Blood Agar (Kohjin Bio Co. Ltd.), and BTB agar (Kyokuto Pharmaceutical Co. Ltd., <https://ssl.kyokutoseyaku.co.jp/english/index.html>). We used different bacterial identification and antimicrobial susceptibility testing methods in our hospital throughout the study period. We used ID test EB-20 Nissui (Nissui Pharmaceutical Co. Ltd., <https://www.nissui-pharm.co.jp/english>) for bacterial identification and Kirby–Bauer disk (Eiken Chemical Co. Ltd., <http://www.eiken.co.jp>) for antimicrobial susceptibility testing from January 2005 through June 2007. EB-20 is a system to identify glucose-fermenting gram-negative rods by 20 patterns of biochemical properties, using hydrogen sulfide, indole, lysine, ONPG (2-nitrophenyl- β -D-galactopyranoside), adunit, inositol, rhamnose, mannitol, esculin, Voges-Proskauer, arginine, urea, inositol, sorbitol, arabinose, phenylpyruvic acid, citric acid, ornithine, malonic acid, raffinose, and sugar. Thereafter, automatic systems were introduced at our hospital: DPS192 (Eiken Chemical Co. Ltd, <http://www.eiken.co.jp>) during July 2007–February 2013 and MicroScan WalkAway (Beckman Coulter, Inc, <https://www.beckmancoulter.com/en>) during March 2013–March 2014. Since April 2014, we have used MALDI Biotyper

(Bruker Daltonics GmbH, <https://www.bruker.com>), using the manufacturer-provided database, for bacterial identification. We judged the drug susceptibility of a microorganism based on clinical breakpoints set by the Clinical and Laboratory Standards Institute; in particular, we used the document M100-S22 (2) during June 1, 2013–December 31, 2016.

We collected all clinical information of patients with positive *E. tarda* bacteremia results from electronic medical records, including age, sex, underlying diseases, source of infection, antimicrobial drug administered, treatment period, and outcome. We defined chronic kidney disease as a serum creatinine level of ≥ 2.0 mg/dL (reference range 0.65–1.07 mg/dL) and chronic liver disease as liver cirrhosis or chronic hepatitis B or C infection. We defined nosocomial bloodstream infection, healthcare-associated bloodstream infection, community-acquired bloodstream infection, and febrile neutropenia according to the previous study and guideline (3,4). We defined 30-day mortality as patient death within 30 days after the onset of *E. tarda* bacteremia and 90-day mortality as patient death within 90 days after onset. We also collected information of patients with *E. tarda* nonbacteremic infections.

We described the clinical characteristics and 30-day mortality of patients with *E. tarda* bacteremia, along with the source of infection and antimicrobial susceptibility. We then compared the characteristics of patients with *E. tarda* bacteremia by 30-day mortality. We also compared the characteristics of patients with bacteremic and nonbacteremic *E. tarda* infections. We also conducted an exploratory multivariable logistic regression analysis to investigate the risk for *E. tarda* bacteremia incidence among all *E. tarda* infections.

Because a previous literature review suggested seasonal variation in the occurrence of *E. tarda* bacteremia (5), we thus examined whether such variation or trend existed in the cases in our study by using Cochran-Armitage test. We tested dichotomous variables with Fisher exact test and continuous variables by Wilcoxon signed-rank test. Statistical analysis was performed using Stata version 15.1 (StataCorp, <http://www.stata.com>). We considered $p < 0.05$ to be statistically significant.

The Ethics Committee of Kurashiki Central Hospital approved this study (no. 2,527). Only persons with appropriate authorization had access to participants' records, and patient confidentiality was maintained. Given the nature of a retrospective chart review, written consent from the patients was waived.

Results

We obtained 182,668 sets of blood cultures during the study period, of which 19,234 sets were positive for some organisms and 40 sets from 26 patients were *E. tarda*-positive.

E. tarda bacteremia was diagnosed in 26 patients (13 men and 13 women); their median age was 75 years (range 45–101 years) (Table 1).

Clinical Characteristics

Some patients had ≥1 underlying disease: solid tumors (12 patients), cardiovascular diseases (4 patients), diabetes mellitus (3 patients), gallstone disease (3 patients), chronic liver disease (2 patients), cerebrovascular disease (2 patients), and hematologic malignancy (1 patient) (Table 1). Four patients had no underlying disease. Sites of solid tumors included pancreas (3 patients), gallbladder/bile duct (3 patients), colon (2 patients), and esophagus, gastric, liver, and thyroid (1 patient each). Of the 12 patients with solid tumors, 4 were receiving chemotherapy for their cancer when *E. tarda* bacteremia occurred.

Clinical diagnoses by the site of infection were cholangitis (9 patients); liver abscess (6 patients); enterocolitis (4 patients); cholecystitis (3 patients); and spontaneous

bacterial peritonitis, mycotic aneurysm, necrotizing fasciitis, empyema, osteomyelitis, and secondary peritonitis (1 patient each) (Table 2). Seventeen patients had community-acquired bloodstream infections. The source of infection was not identified in 5 patients, including 1 with febrile neutropenia; 3 patients had nosocomial bloodstream infections, and 6 had healthcare-associated bloodstream infections.

Patients with *E. tarda* bacteremia were older and more likely to have solid tumors than were patients with *E. tarda* nonbacteremic infections (Table 3). In addition, we observed hepatobiliary infection, such as cholangitis and liver abscess, more frequently in patients with bacteremia.

Because the cohort included 26 *E. tarda* bacteremia patients, we conducted a multivariable logistic regression analysis adjusted with 2 explanatory variables. We hypothesized that underlying liver disease and old age could be associated with the incidence of *E. tarda* bacteremia and selected these 2 variables as the covariates. Our analysis

Table 1. Characteristics of patients with *Edwardsiella tarda* bacteremia, Kurashiki Central Hospital, Okayama, Japan, 2005–2016*

Characteristic	Total, N = 26	Survivors, n = 23	Patients who died within 30 d after bacteremia onset, n = 3		p value
			63 (30–87)	[60–87]	
Median age, y (IQR) [range]	75 (63–85) [45–101]	75 (64–85) [45–101]	63 (30–87)	[60–87]	0.55
Sex, no. patients					
M	13	11	2		1.00
F	13	12	1		
Underlying disease, no. patients					
Solid tumor	12	10	2		0.58
Cardiovascular disease	4	4	0		1.00
Diabetes mellitus	3	3	0		1.00
Gallstone	3	3	0		1.00
Chronic liver disease	2	1	1		0.22
Cerebrovascular disease	2	2	0		1.00
Hematologic malignancy	1	1	0		1.00
Chronic kidney disease	0	0	0		NE
Ulcerative colitis	0	0	0		NE
Crohn disease	0	0	0		NE
None	4	2	2		0.052
Other	0	0	0		NE
Behavioral/dietary risk factors, no. patients					
Alcoholism	4	2	2		0.052
Exposure to raw food	3	3	0		1.00
Exposure to fresh or marine water, animal feces	1	1	0		1.00
Clinical diagnosis, no. patients					
Cholangitis	9	9	0		0.53
Liver abscess	6	6	0		1.00
Enterocolitis	4	4	0		1.00
Cholecystitis	3	3	0		1.00
Spontaneous bacterial peritonitis	1	0	1		0.115
Mycotic aneurysm	1	1	0		1.00
Necrotizing fasciitis	1	0	1		0.115
Empyema	1	0	1		0.115
Febrile neutropenia	1	1	0		1.00
Osteomyelitis	1	1	0		1.00
Secondary peritonitis	1	1	0		1.00
Focus unknown	5	4	1		0.49
Receipt of chemotherapy for cancer	4	4	0		1.00
Median duration of treatment for infection, d (IQR) [range]†	12 (7–27) [1–77]	13 (8–30) [1–77]	5 (2–11) [2–11]		0.084

*IQR, interquartile range; NE, not evaluated.

SYNOPSIS

Table 2. Clinical characteristics of 26 patients with *Edwardsiella tarda* bacteremia, Kurashiki Central Hospital, Okayama, Japan, 2005–2016*

Patient no.	Age, y/sex	Clinical diagnosis	Underlying disease	Treatment	Treatment duration, d	Concurrent organisms (source)	Outcome
1	77/M	Focus unknown	Cerebrovascular disease	LVX	3	<i>E. coli</i> , <i>B. fragilis</i> (pus)	Recovered
2	79/M	Liver abscess	Cardiovascular disease	CFP/SUL→IPM/CIL→PIP→MEP, CLI→MEM	38		Recovered
3	70/F	Cholangitis, cholecystitis	None	CFP/SUL	8		Recovered
4	87/M	Focus unknown	Hepatocellular carcinoma	FEP	11		Died at 12 d
5	62/M	Mycotic aneurysm, liver abscess, osteomyelitis	Diabetes mellitus	IPM/CIL→AMP, GEN→SAM→VCM, PNP→VCS→PZX	30		Died at 39 d
6	92/F	Focus unknown	Colon cancer	CRO	30		Died at 32 d
7	89/F	Focus unknown	Colon cancer	CRO→MEM	16		Recovered
8	85/F	Liver abscess, enterocolitis	Thyroid cancer	MEM, CLI→MEM→IPM/CIL	21		Recovered
9	88/F	Cholangitis	Cholangiocarcinoma	IPM/CIL	7		Died at 40 d
10	75/F	Cholecystitis	None	PZX	3	<i>Klebsiella</i> sp., <i>E. coli</i> (bile)	Recovered
11	101/F	Cholangitis	None	CFP/SUL	10		Recovered
12	61/M	Enterocolitis	Cardiovascular disease	CRO→LVX	10		Recovered
13	58/M	Liver abscess	Gallbladder cancer, invasion of liver	CFP/SUL→MEM→MIN→AMP, MIN	77	<i>E. faecalis</i> , <i>E. faecium</i> , <i>C. freundii</i> , <i>Bacteroides</i> sp. (pus)	Recovered
14	84/F	Cholangitis	Cardiovascular disease, cerebrovascular disease	CRO	6		Recovered
15	83/F	Cholangitis	Pancreatic cancer	CFP/SUL	1		Recovered
16	66/M	Liver abscess	Pancreatic cancer	CFZ→LEX	46		Recovered
17	85/M	Enterocolitis	Cardiovascular disease	CRO→LVX	12		Recovered
18	64/F	Enterocolitis	Chronic liver disease, diabetes mellitus	CMZ→AMP	13		Recovered
19	74/F	Secondary peritonitis	Diabetes mellitus	CMZ→TZP	27	<i>E. coli</i> , <i>K. pneumoniae</i> , <i>S. anginosus</i> , <i>F. nucleatum</i> (ascites)	Recovered
20	63/M	Necrotizing fasciitis	None	MEM, CLI	2		Died at 2 d
21	45/F	Liver abscess, cholangitis	Pancreatic cancer	CFP/SUL→AMP	31	<i>S. anginosus</i> (blood)	Died at 45 d
22	65/M	Cholangitis, cholecystitis	Gastric cancer, gallstone	CFP/SUL→AMP	13	<i>S. gallolyticus</i> (blood)	Recovered
23	81/M	Cholangitis	Gallstone, esophageal cancer	CFP/SUL→AMP	16		Recovered
24	64/M	Cholangitis	Cholangiocarcinoma, gallstone	CFP/SUL→AMP	8		Recovered
25	59/M	Focus unknown, febrile neutropenia	Peripheral T-cell lymphoma	CZO	12		Recovered
26	60/F	Spontaneous bacterial peritonitis, empyema	Chronic liver disease	TZP→AMP	5		Died at 6 d

*AMP, ampicillin; *B. fragilis*, *Bacteroides fragilis*; CFP/SUL, cefoperazone-sulbactam; *C. freundii*, *Citrobacter freundii*; CFZ, cefazolin; CLI, clindamycin; CMZ, cefmetazole; CRO, ceftriaxone; CZO, ceftiofuran; *E. faecalis*, *Enterococcus faecalis*; *E. faecium*, *Enterococcus faecium*; *E. coli*, *Escherichia coli*; FEP, cefepime; *F. nucleatum*, *Fusobacterium nucleatum*; GEN, gentamicin; IPM/CIL, imipenem-cilastatin; *K. pneumoniae*, *Klebsiella pneumoniae*; LEX, cephalexin; LVX, levofloxacin; MEM, meropenem; MIN, minocycline; PNP, panipenem; PIP, piperacillin; PZX, pazufloxacin; SAM, ampicillin sulbactam; *S. anginosus*, *Streptococcus anginosus*; *S. gallolyticus*, *Streptococcus gallolyticus*; Tx, treatment; TZP, piperacillin tazobactam. Arrows indicate the order of antimicrobial drugs used. Blank cells indicate no other concurrent organisms.

suggested that age ≥ 65 years was significantly associated with an increased risk for *E. tarda* bacteremia incidence (odds ratio 2.70; 95% CI 1.11–6.55; $p = 0.028$). However, underlying chronic liver disease was not the risk factor for *E. tarda* bacteremia (odds ratio 2.48; 95% CI 0.41–14.99; $p = 0.32$).

Treatment and Outcomes

All *E. tarda* strains isolated from blood cultures were susceptible to all tested antimicrobial drugs. *E. tarda* bacteremia patients were treated with a variety of antimicrobial drugs according to the treating physicians' discretion (Table 3). The median duration of treatment was 12 days

(range 1–77 days). Overall 30-day mortality for *E. tarda* bacteremia was 12% (3/26) and overall 90-day mortality 27% (7/26).

Patient 4 had end-stage hepatocellular carcinoma and liver failure. On day 2 after admission, *E. tarda* bacteremia developed; the source of infection was unidentified. He was treated with cefepime and promptly became afebrile. *E. tarda* bacteremia was considered controlled by cefepime; however, the patient died of hepatic failure on day 11.

In patient 20, necrotizing fasciitis was diagnosed, and *E. tarda* was detected from wound and blood cultures. Although meropenem and clindamycin were administered, he died on day 2.

Table 3. Comparison of characteristics of patients with bacteremic and nonbacteremic *Edwardsiella tarda* infection, Kurashiki Central Hospital, Okayama, Japan, 2005–2016*

Patient characteristic	Patients with bacteremic infection, n = 26	Patients with nonbacteremic infection, n = 124	p value
Median age, y (IQR) [range]	75 (63–85) [45–101]	56 (12–73) [0–89]	<0.001
Sex, no. patients			
M	13	82	0.178
F	13	42	
Underlying disease, no. patients			
Solid tumor	12	22	0.004
Cardiovascular disease	4	22	1.00
Diabetes mellitus	3	13	1.00
Gallstone	3	13	1.00
Chronic liver disease	2	7	0.65
Cerebrovascular disease	2	1	0.078
Hematologic malignancy	1	1	0.32
Chronic kidney disease	0	1	1.00
Ulcerative colitis	0	14	0.13
Crohn disease	0	1	1.00
None	4	52	0.013
Other	0	2	1.00
Behavioral/dietary risk factors, no. patients			
Alcoholism	4	9	0.24
Exposure to raw food	3	7	0.38
Exposure to fresh or marine water, animal feces	1	0	0.173
Clinical diagnosis, no. patients			
Cholangitis	9	8	<0.001
Liver abscess	6	1	<0.001
Enterocolitis	4	74	0.076
Cholecystitis	3	9	0.44
Spontaneous bacterial peritonitis	1	0	0.173
Mycotic aneurysm	1	1	0.32
Necrotizing fasciitis	1	0	0.173
Empyema	1	0	0.173
Febrile neutropenia	1	0	0.173
Osteomyelitis	1	0	0.173
Secondary peritonitis	1	0	0.173
Focus unknown	5	1	0.001
Endometriosis	0	1	1.00
Appendicitis	0	4	1.00
Congenital infection	0	1	1.00
Cystitis	0	1	1.00
Intraabdominal abscess	0	1	1.00
Perianal abscess	0	1	1.00
Pneumonia	0	2	1.00
Pyometra	0	1	1.00
Secondary peritonitis	0	2	1.00
Superficial surgical site infection	0	1	1.00
Receipt of chemotherapy for cancer, no. patients	4	7	0.099
Median duration of treatment for infection, d (IQR) [range]	12 (7–27) [1–77]	5 (3–9) [0–36]	<0.001

*IQR, interquartile range.

Patient 26, who had end-stage alcoholic liver cirrhosis, was admitted for massive pleural effusion and ascites. *E. tarda* was detected from pleural effusion but not from ascites. Empyema and spontaneous bacterial peritonitis caused by *E. tarda* were diagnosed. Although these fluids were drained and antimicrobial drugs were given, she died on day 5.

Patient 5 was admitted for evaluation of fever and back pain. Blood cultures drawn on admission day revealed *E. tarda*, and he was treated with imipenem–cilastatin. However, his fever persisted. Computed tomography scan of the chest and abdomen revealed mycotic thoracic aneurysm, liver abscess, and vertebral osteomyelitis. He was treated with multiple antimicrobial drugs but died of a ruptured mycotic aneurysm on day 39.

In patients 6, 9, and 21, *E. tarda* bacteremia developed and improved with antimicrobial therapy. However, these patients died of underlying diseases.

Seasonal Variation in *E. tarda* Bacteremia

The incidence of *E. tarda* infection did not vary by season (Figure). We found no trend of *E. tarda* bacteremia incidence among all *E. tarda* infections when we examined them by month ($p = 0.46$) or by season, defined as a set of 3 months ($p = 0.53$).

Discussion

E. tarda is associated with freshwater and marine life, including fish, reptiles, and amphibians (1). The organism resembles *Salmonella* biochemically and clinically (1). *Salmonella* usually ferments D-mannitol, urease, oxidase, and D-sorbitol, whereas *E. tarda* produces hydrogen sulfide and indole (6).

E. tarda is a rare human pathogen and is primarily associated with gastrointestinal diseases, including the

asymptomatic carrier state (1). Approximately 80% of infections are intestinal. *E. tarda* causes a *Salmonella*-like gastrointestinal infection, usually self-limited enteritis, with intermittent watery diarrhea and low-grade fever (1,7).

The pathogenesis of *E. tarda* and its disease-causing mechanism remain unclear. Twelve classes of bacterial protein secretion systems are known; these systems transport virulence proteins into the cell and, in some cases, directly into the cytoplasm of a target cell (8). The bacterial type III and type VI secretion systems (T3SS and T6SS) are believed to play an essential role in *E. tarda* survival, replication, and virulence inside the host. In particular, T6SS is proposed to enable *E. tarda* to establish inside the host, cause severe systemic infection, and eventually kill the host.

We reviewed 26 cases of *E. tarda* bacteremia. Clinical diagnoses included 15 (58%) biliary tract infections (cholangitis, cholecystitis, and liver abscess). Eight of these patients had hepatobiliary diseases including cholangiocarcinoma, gallbladder cancer, pancreatic cancer, gallstone disease. Therefore, hepatobiliary diseases may be a predisposing factor of *E. tarda* biliary tract infections. However, our multivariable logistic regression found that only age ≥ 65 years was associated with the incidence of *E. tarda* bacteremia. We acknowledge that the sample size of our study and the number of *E. tarda* bacteremia incidence were still small, and thus the finding from our multivariable analysis might be only exploratory.

Previous studies reported high rates of death for *E. tarda* bacteremia, ranging from 22.7% to 44.6% (1,5,9). In contrast, the death rate for patients with *E. tarda* bacteremia in the cohort reported here was low at 12%. However, 2 of these 3 patients had end-stage liver disease; only 1 death among these patients was attributed to *E. tarda* bacteremia.

E. tarda is susceptible to most antimicrobial drugs, including tetracyclines, aminoglycosides, quinolones, antifolates, chloramphenicol, nitrofurantoin, fosfomicin, and most β -lactams (10), and is naturally resistant to benzylpenicillin, colistin, and polymyxin B (1,11). In our study, *E. tarda* was susceptible to most commonly used antimicrobial drugs. *E. tarda* susceptibilities to colistin and polymyxin B are unknown because susceptibility testing is not routinely performed for these drugs in our institution. Previous studies have shown that all strains of *E. tarda* were positive for β -lactamase production examined with nitrocefin β -lactamase disks, but an ampicillin-resistant *E. tarda* strain has not been reported (10,11). Whether *E. tarda* isolates detected in our institution produced β -lactamase is not clear because we did not perform the β -lactamase test, but 5 cases were successfully treated with ampicillin.

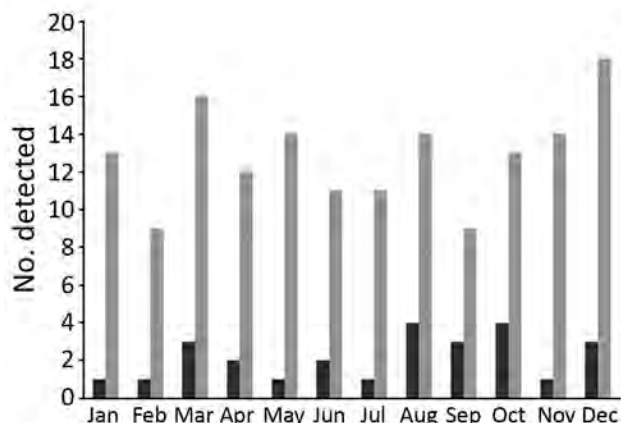


Figure. Seasonal variation in the incidence of *Edwardsiella tarda* infection, Kurashiki Central Hospital, Okayama, Japan, 2005–2016. Black bars, blood culture; gray bars, all specimens (including blood cultures).

Hirai et al. suggested that *E. tarda* bacteremia is likely to develop during summer and autumn months in the Northern Hemisphere (8). The authors conducted a literature review of 77 *E. tarda* bacteremia cases reported from diverse areas and suggested seasonal variation in incidence for 22 cases. Our study of 26 *E. tarda* bacteremia cases suggests no such seasonal distribution. Several possible reasons might account for this discrepancy. First, *E. tarda* can colonize. In our study, hepatobiliary infection (such as cholangitis, cholecystitis, and liver abscess) was diagnosed in 58% (15/26) patients, and patients colonizing *E. tarda* developed *E. tarda* bacteremia. Second, diversity might exist in the patients' dietary patterns. *E. tarda* frequently infects fish. Hirai et al. included patients from many parts of the world, so the intake of fish might have differed according to the season or geographic area across reports. In contrast, our study included only people in a single area of Japan who habitually ate raw seafood, such as sashimi, throughout the year; this tendency might have led to no seasonal variation of *E. tarda* bacteremia incidence. Third, our study had no missing clinical data for any patients, whereas Hirai et al. examined 22 of all 77 eligible patients, which might have rendered their analysis vulnerable to information bias.

Our study had some strengths. First, we elucidated that no seasonal variation existed in *E. tarda* bacteremia in this population. Second, we described the characteristics of each patient with *E. tarda* bacteremia and provided risk factors for *E. tarda* bacteremia incidence among all *E. tarda* infections.

Our study also had some limitations. First, the number of blood cultures submitted increased in recent years in our hospital. The number of blood cultures submitted in 2016 nearly doubled that for 2005. This increase might have resulted in the underestimation of *E. tarda* bacteremia in the earlier years of our study period. Second, ours was a retrospective and single-center study. However, our study had no missing data regarding clinical information. Furthermore, we successfully presented a particularly large case series of *E. tarda* bacteremia.

In conclusion, *E. tarda* bacteremia is a rare disease that is not associated with high rates of death. *E. tarda* bacteremia patients in our cohort in Japan had more severe underlying diseases, such as hepatobiliary disease and solid tumors, than did patients in previous studies. Hepatobiliary infections, such as cholangitis, cholecystitis, and liver abscess, are the most common clinical manifestations in patients with *E. tarda* bacteremia. The major underlying diseases in this study were hepatobiliary diseases and malignancy. Furthermore, *E. tarda* strains we isolated were susceptible to most antimicrobial drugs, including β -lactams, aminoglycoside, tetracycline, fosfomycin, fluoroquinolone, and trimethoprim/sulfamethoxazole, and

E. tarda bacteremia was successfully treated with ampicillin. Finally, we observed no seasonal distribution of *E. tarda* bacteremia. Risk factors for *E. tarda* bacteremia-related death remain to be investigated.

About the Author

Dr. Kamiyama is the medical director at Kurashiki Central Hospital. His primary research interests include cytomegalovirus infections in critically ill patients and transplant patients.

References

- Janda JM, Abbott SL. Infections associated with the genus *Edwardsiella*: the role of *Edwardsiella tarda* in human disease. *Clin Infect Dis*. 1993;17:742–8. <https://doi.org/10.1093/clinids/17.4.742>
- Clinical and Laboratory Standards Institute. Performance standards for antimicrobial susceptibility testing: twenty-third informational supplement (M100-S23). Wayne (PA): The Institute; 2013.
- Friedman ND, Kaye KS, Stout JE, McGarry SA, Trivette SL, Briggs JP, et al. Health care-associated bloodstream infections in adults: a reason to change the accepted definition of community-acquired infections. *Ann Intern Med*. 2002;137:791–7. <https://doi.org/10.7326/0003-4819-137-10-200211190-00007>
- Freifeld AG, Bow EJ, Sepkowitz KA, Boeckh MJ, Ito JI, Mullen CA, et al.; Infectious Diseases Society of America. Clinical practice guideline for the use of antimicrobial agents in neutropenic patients with cancer: 2010 update by the Infectious Diseases Society of America. *Clin Infect Dis*. 2011;52:e56–93. <https://doi.org/10.1093/cid/cir073>
- Hirai Y, Asahata-Tago S, Ainoda Y, Fujita T, Kikuchi K. *Edwardsiella tarda* bacteremia. A rare but fatal water- and foodborne infection: review of the literature and clinical cases from a single centre. *Can J Infect Dis Med Microbiol*. 2015;26:313–8. <https://doi.org/10.1155/2015/702615>
- Wilson JP, Waterer RR, Wofford JD Jr, Chapman SW. Serious infections with *Edwardsiella tarda*. A case report and review of the literature. *Arch Intern Med*. 1989;149:208–10. <https://doi.org/10.1001/archinte.1989.00390010170025>
- Schlenker C, Surawicz CM. Emerging infections of the gastrointestinal tract. *Best Pract Res Clin Gastroenterol*. 2009;23:89–99. <https://doi.org/10.1016/j.bpg.2008.11.014>
- Green ER, Meccas J. Bacterial secretion systems: an overview. *Microbiol Spectr*. 2016;4.
- Wang IK, Kuo HL, Chen YM, Lin CL, Chang HY, Chuang FR, et al. Extraintestinal manifestations of *Edwardsiella tarda* infection. *Int J Clin Pract*. 2005;59:917–21. <https://doi.org/10.1111/j.1742-1241.2005.00527.x>
- Clark RB, Lister PD, Janda JM. In vitro susceptibilities of *Edwardsiella tarda* to 22 antibiotics and antibiotic- β -lactamase-inhibitor agents. *Diagn Microbiol Infect Dis*. 1991;14:173–5. [https://doi.org/10.1016/0732-8893\(91\)90054-J](https://doi.org/10.1016/0732-8893(91)90054-J)
- Stock I, Wiedemann B. Natural antibiotic susceptibilities of *Edwardsiella tarda*, *E. ictaluri*, and *E. hoshinae*. *Antimicrob Agents Chemother*. 2001;45:2245–55. <https://doi.org/10.1128/AAC.45.8.2245-2255.2001>

Address for correspondence: Shinya Kamiyama, Kurashiki Central Hospital, Department of Laboratory Medicine and Infectious Diseases, 1-1-1 Miwa Kurashiki Okayama 710-8602, Japan; email: kamiyama-knz@umin.ac.jp

Case Studies and Literature Review of Pneumococcal Septic Arthritis in Adults

Amandine Dernoncourt,¹ Youssef El Samad, Jean Schmidt, Jean Philippe Emond, Charlotte Gouraud, Anne Brocard, Mohamed El Hamri, Claire Plassart, Florence Rousseau, Valéry Salle, Momar Diouf, Emmanuelle Varon, Farida Hamdad¹

Medscape **ACTIVITY** EDUCATION

In support of improving patient care, this activity has been planned and implemented by Medscape, LLC and Emerging Infectious Diseases. Medscape, LLC is jointly accredited by the Accreditation Council for Continuing Medical Education (ACCME), the Accreditation Council for Pharmacy Education (ACPE), and the American Nurses Credentialing Center (ANCC), to provide continuing education for the healthcare team.

Medscape, LLC designates this Journal-based CME activity for a maximum of 1.00 **AMA PRA Category 1 Credit(s)**[™]. Physicians should claim only the credit commensurate with the extent of their participation in the activity.

Successful completion of this CME activity, which includes participation in the evaluation component, enables the participant to earn up to 1.0 MOC points in the American Board of Internal Medicine's (ABIM) Maintenance of Certification (MOC) program. Participants will earn MOC points equivalent to the amount of CME credits claimed for the activity. It is the CME activity provider's responsibility to submit participant completion information to ACCME for the purpose of granting ABIM MOC credit.

All other clinicians completing this activity will be issued a certificate of participation. To participate in this journal CME activity: (1) review the learning objectives and author disclosures; (2) study the education content; (3) take the post-test with a 75% minimum passing score and complete the evaluation at <http://www.medscape.org/journal/eid>; and (4) view/print certificate. For CME questions, see page 2003.

Release date: September 12, 2019; Expiration date: September 12, 2020

Learning Objectives

Upon completion of this activity, participants will be able to:

- Describe clinical and epidemiological features of pneumococcal SA in adults >18 years old reported to the "Picardie Regional Pneumococcal Network" from January 2005 to December 2016, according to results from a retrospective case series and literature review
- Determine diagnosis and treatment of pneumococcal SA in adults >18 years old reported to the "Picardie Regional Pneumococcal Network" from January 2005 to December 2016, according to results from a retrospective case series and literature review
- Identify outcomes and implications of pneumococcal SA in adults >18 years old reported to the "Picardie Regional Pneumococcal Network" from January 2005 to December 2016, according to results from a retrospective case series and literature review

CME Editor

Amy J. Guinn, BA, MA, Copyeditor, Emerging Infectious Diseases. Disclosure: Amy J. Guinn, BA, MA, has disclosed no relevant financial relationships.

CME Author

Laurie Barclay, MD, freelance writer and reviewer, Medscape, LLC. Disclosure: Laurie Barclay, MD, has disclosed no relevant financial relationships.

Authors

Disclosures: **Amandine Dernoncourt, MD; Youssef El Samad, MD; Jean Schmidt, MD, PhD; Jean Philippe Émond, PhD; Charlotte Gouraud, MD; Anne Brocard, PharmD; Mohamed El Hamri, MD; Claire Plassart, MD; Florence Rousseau, PharmD, PhD; Valéry Salle, MD, PhD; Momar Diouf, PhD; and Farida Hamdad, PharmD, PhD**, have disclosed no relevant financial relationships. **Emmanuelle Varon, MD, MSc**, has disclosed the following relevant financial relationships: support to attend European Congress of Clinical Microbiology & Infectious Diseases and European Society for Pediatric Infectious Diseases from Pfizer Inc.

Author affiliations: Amiens-Picardie University Medical Center, Amiens, France (A. Dernoncourt, Y. El Samad, J. Schmidt, J.P. Emond, A. Brocard, M. El Hamri, C. Plassart, F. Rousseau, V. Salle, M. Diouf, F. Hamdad); Compiègne Hospital, Compiègne, France (J.P. Emond, C. Gouraud); Senlis Hospital, Senlis, France (A. Brocard); Laon Hospital, Laon, France (M. El Hamri); Beauvais

Hospital, Beauvais, France (C. Plassart); Intercommunal Hospital of Creteil, Paris, France (E. Varon)

DOI: <https://doi.org/10.3201/eid2510.181695>

¹These authors contributed equally to this article.

We conducted a retrospective study on all cases of pneumococcal septic arthritis (SA) in patients ≥ 18 years of age reported to the Picardie Regional Pneumococcal Network in France during 2005–2016. Among 1,062 cases of invasive pneumococcal disease, we observed 16 (1.5%) SA cases. Although SA is uncommon in adult patients, the prevalence of pneumococcal SA in the Picardie region increased from 0.69% during 2005–2010 to 2.47% during 2011–2016 after introduction of the pneumococcal 13-valent conjugate vaccine. We highlight the emergence of SA cases caused by the 23B serotype, which is not covered in the vaccine.

Septic arthritis (SA) constitutes a medical emergency and is associated with high rates of illness and death (1–3). The annual incidence of proven or probable SA in industrialized countries is 4–10/100,000 patients in the general population and 30–70/100,000 in patients with rheumatoid arthritis or history of prosthetic joint replacement surgery (1–3). The increasing prevalence over recent decades is related to an aging population, use of immunosuppressive drugs, and the growing number of orthopedic procedures (1–3). Large studies of SA have identified *Staphylococcus aureus* as the most common organism involved, along with *Streptococcus pyogenes* to a lesser degree (1–4). *Streptococcus pneumoniae* is considered an uncommon cause of SA in adults (3–11).

S. pneumoniae is a common cause of bacterial community-acquired pneumonia, acute otitis, maxillary sinusitis, and severe invasive infections, especially in patients < 2 or ≥ 65 years of age and in patients with underlying conditions, such as diabetes, malignancy, immune deficiency, chronic alcoholism, and splenectomy (12–15). Invasive pneumococcal disease (IPD) is a major public health concern worldwide, with a reported incidence of 7–97/100,000 persons ≥ 18 years of age annually (14). IPD is defined as isolation of pneumococci from normally sterile body fluids. According to a review from 1952–2008, pneumococcal SA occurred in 0.6%–2.2% of all cases of IPD (14). Similarly, in a large case study published by Marrie et al. (16), 1.6% of patients with IPD had pneumococcal SA.

Antimicrobial drug therapy and vaccination have been central elements of the clinical approach to pneumococcal disease. Literature from the 1990s also emphasized the spread of pneumococcal strains resistant to β -lactams and other antimicrobial agents (1,2,5–10,12–15). Pneumococcal vaccination has since become a global public health focus (15,17–21).

We analyzed all cases of pneumococcal SA in patients ≥ 18 years of age reported to the Picardie Regional Pneumococcal Network in France during 2005–2016. We also reviewed scientific publications on SA from the 1950s through 2017. Our aim was to determine prevalence of *S. pneumoniae* in SA and assess whether introduction of

pneumococcal 13-valent conjugate vaccine (PCV13) might contribute to increased rates of pneumococcal SA.

Patients and Methods

The Picardie region of France has a population of ≈ 2 million. Cases of IPD are reported to the Picardie Regional Pneumococcal Network, a collection of 12 public hospital-based clinical bacteriology departments across the region. We conducted a retrospective study of pneumococcal SA in patients ≥ 18 years of age reported to the network during January 1, 2005–December 31, 2016. We defined cases by either an *S. pneumoniae*-positive culture from synovial fluid, an *S. pneumoniae*-positive blood culture with purulent or inflammatory joint fluid, medical imaging consistent with the diagnosis of arthritis, or a combination of these.

We collected patient demographic characteristics, including age, sex, and underlying conditions; clinical signs and symptoms; whether patients had other sites of pneumococcal infection; laboratory findings; antimicrobial therapy; and clinical outcomes. We performed statistical analyses by using SAS version 9.4 (SAS Institute Inc., <https://www.sas.com>) software, and estimated p values for comparison of relative frequencies by using χ^2 test. We considered $p < 0.05$ the threshold for statistical significance. This study was conducted in compliance with French legislation and the Declaration of Helsinki regarding ethics principles for medical research involving human subjects.

We also conducted a review of the largest case studies (≥ 3 patients) of pneumococcal SA in patients ≥ 18 years of age published in the medical literature during 1950–2017 by using the search terms “*Streptococcus pneumoniae* infection” and “Septic arthritis” in the PubMed database. We excluded studies reporting on patients < 18 years of age, in vitro and animal studies, and other factors. We retrieved 15 studies for full-text review and identified 7 studies meeting our inclusion criteria (Figure).

Results

During January 1, 2005–December 31, 2016, we observed 16 (1.5%) cases of pneumococcal SA out of 1,062 cases of IPD reported (Table 1). The prevalence of pneumococcal SA increased during the study period, ranging from 0.69% during 2005–2010 to 2.47% during 2011–2016 ($p = 0.02$).

Of patients with pneumococcal SA, the mean age was 69.7 (34–93) years, and 62.5% were ≥ 65 years of age; 9 were women and 7 were men. Fourteen (87.5%) patients had monoarticular infection; the other 2 (12.5%) cases had polyarticular infection, 1 case involving the knee and shoulders and the other sacroiliac joints.

For 14 patients, data on medical history, clinical characteristics, and time to diagnosis were available (Table 2). We found that 11 (78.57%) patients had 1–2 underlying

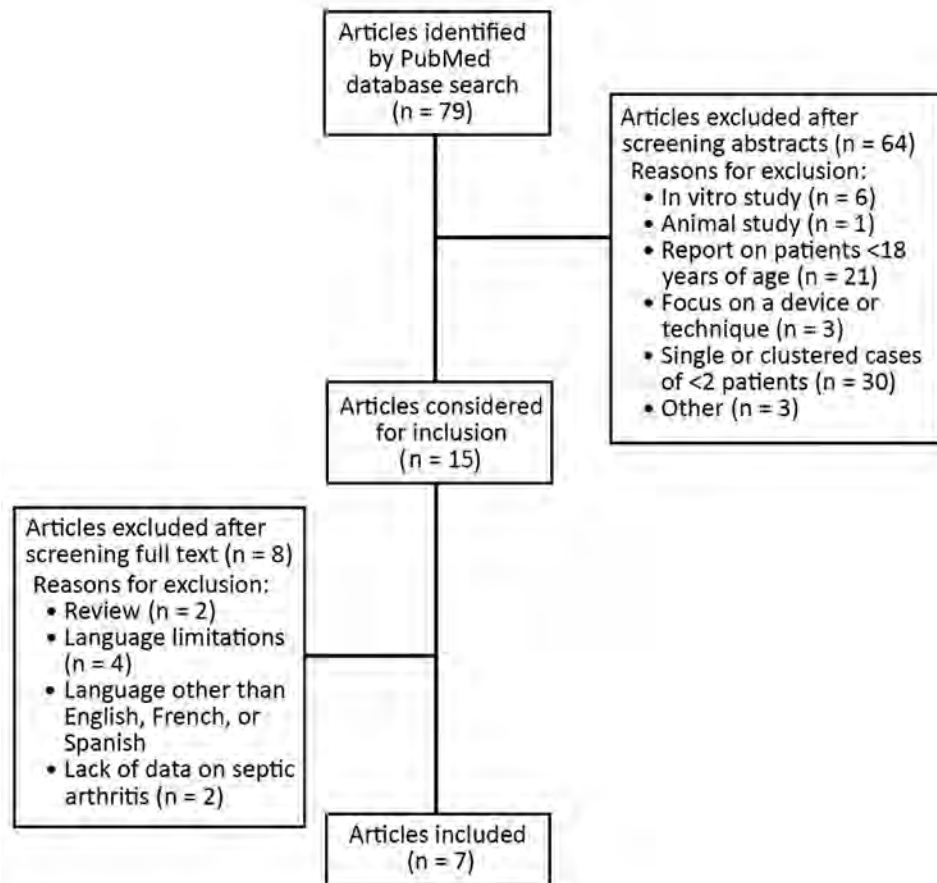


Figure. Selection process for systematic review of published data on pneumococcal septic arthritis in adults.

conditions predisposing them to pneumococcal SA, 5 (35.71%) had 1 condition, and 6 (42.86%) had >1 condition; 3 (21.42%) had no risk factors but were among the oldest patients, and 5 (35.71%) had concurrent respiratory tract infections. Most joint infections involved the knee, 11/16 (68.75%) SA cases; 9 (56.25%) patients had native joint infections; and 5 (31.25%) patients had infections after prosthetic joint surgery, 4 involving a knee and 1 involving a hip.

Of note, 1 patient had undergone surgery for inguinal hernia, which was complicated by abdominal wall hematoma and pneumococcal SA with concomitant crystal-induced arthritis (gout). Another patient received a diagnosis of multiple myeloma while hospitalized for pneumococcal SA. An additional patient developed pneumococcal SA 2 years after the joint infection.

Vaccination status was available for 11 (78.57%) of the 14 patients with clinical data. Only 2 patients had been vaccinated against pneumococci, both after splenectomy.

Two patients were admitted to the intensive care unit with septic shock and severe renal failure. All patients reported pain of the infected joint; only half were febrile (>38°C) at admission; and 10 (71.42%) patients had joint swelling. The median interval between admission and diagnosis was 1 day (range 1–60 days). The patient with infection of the prosthetic hip joint had few symptoms, which might explain the delay in diagnosis of pneumococcal SA, which took 60 days.

Leukocyte scintigraphy was helpful for 3 patients, 1 with prosthetic hip joint infection and 2 with sacroiliac joint infection. Positron emission tomography was performed for a patient with infection of a single sacroiliac joint, which showed increased radionuclide uptake.

We noted increased white cell count, >10,000/mm³, in 13 (81.25%) cases with a mean of 13,800 cells/mm³ (range 6,020–78,000 cells/mm³). Fourteen patients had serum C-reactive protein (CRP) results, and 13 (92.82%) had CRP >100 mg/L (mean 325 mg/L [range 28–552 mg/L]) (Table

Table 1. Cases of septic arthritis and IPD, Picardie region, France, 2005–2016*

Year	2005	2006	2007	2008	2009	2010	2011	2012	2013	2014	2015	2016
IPD cases, no.	130	39	108	92	141	67	83	58	106	60	89	89
No. (%) pneumococcal SA	0	0	3 (2.8)	0	0	1 (1.5)	1 (1.2)	3 (5.2)	1 (0.9)	2 (3.3%)	0	5 (5.6)

*IPD, invasive pneumococcal disease; SA, septic arthritis

Table 2. Demographic data, clinical characteristics, underlying conditions, and other sites of pneumococcal infection for 16 patients with pneumococcal septic arthritis in the Picardie region, France, 2005–2016*

Patient age, y/sex	Affected joint	Days from admission to diagnosis	Underlying conditions, risk factors	Vaccination, type	Clinical signs and symptoms	Other infection
90/M	Hip, prosthetic joint surgery 1 y before SA	60	Multiple myeloma diagnosed 2 y after septic arthritis	ND	Joint pain	None
93/F	Knee, prosthetic joint surgery 5 y before SA	2	None	ND	Joint pain and swelling	Pneumonia
34/M	Hip	1	Chronic alcoholism	N	Fever, joint pain	None
68/M	Knee	4	Gout, heart disease	N	Fever, joint pain and swelling	Hematoma in abdominal muscles
75/M	Knee	1	Diabetes mellitus, heart disease	N	Joint pain and swelling	None
42/F	One knee, both shoulders	1	Splenectomy, Immunosuppressive drug	Y, PPV23	Joint pain and swelling	None
80/F	Knee	1	Chronic alcoholism	N	Joint pain and swelling	None
61/F	Knee	2	COPD, multiple myeloma diagnosed while hospitalized for septic arthritis	N	Fever, joint pain and swelling	None
57/F	Shoulder	1	COPD, MGUS	N	Joint pain and swelling	Bronchitis 3 weeks prior
82/F	Knee, prosthetic joint	ND	ND	ND	ND	ND
90/F	Knee	ND	ND	ND	ND	ND
53/F	Both sacroiliac joints	2	Splenectomy	Y, PCV13	Fever, joint pain	Sinusitis 3 weeks prior
69/M	Knee, prosthetic joint surgery 1 mo before SA	1	Malignant disease MGUS	N	Fever, joint pain and swelling	None
82/F	Knee, prosthetic joint surgery 1 y before SA	1	None	N	Fever, joint pain and swelling	Pneumonia
57/M	Knee	1	Chronic alcoholism	ND	Fever, joint pain and swelling	None
82/M	Sacroiliac joint	5	None	N	Joint pain	Pneumonia

*COPD, chronic obstructive pulmonary disease; MGUS, monoclonal gammopathy of undetermined significance; SA, septic arthritis; ND, no data.

3). Procalcitonin test (PCT) was performed on 8 patients, and 6 (75%) had levels >0.5 ng/mL. Urinary pneumococcal antigen detection was performed for 5 patients, and 4 (80%) patients had positive results.

Joint aspiration was performed in 15 cases; a patient with sacroiliac joint SA was excluded. All joint aspirates had white blood cell counts >10,000/mm³ on cytological analysis and were purulent in 10 (66.67%) cases. Gram staining showed gram-positive cocci in 11 (73.33%) cases. Joint fluid was cultured for *S. pneumoniae*, and 14 (93.33%) cases had positive cultures; *S. pneumoniae* strains were recovered from both joint aspirate and blood cultures from 9 (56.25%) cases. In 2 (12.5%) cases, bacteriological diagnosis of arthritis was made exclusively on the basis of blood culture, and in 5 (31.25%) cases, the positive culture was only obtained for joint aspirate.

Of the 16 *S. pneumoniae* strains we recovered, 4 (25%) had low-level penicillin resistance, 1 (6.25%) also had low-level ceftriaxone resistance, and 1 (6.25%) had high-level ceftriaxone resistance (MIC 4 mg/L). Three (75%) of 4

strains from 2005–2010 had low-level penicillin resistance, whereas only 1 (8.3%) of 12 strains from 2011–2016 had low-level penicillin resistance ($p < 0.01$). All strains isolated from cases of nonbacteremic SA were penicillin susceptible. We serotyped 15 isolates and found 33.33% were strain 23B, 13.33% were 19F, and 13.33% were serotype 1 (Table 3). Serotype 23B was always penicillin susceptible, but other the serotypes had low-level penicillin resistance.

All patients were treated with a combination of 2 intravenous antimicrobial drugs, mainly amoxicillin and gentamicin (68.75%). The median duration for intravenous antimicrobial therapy was 6 days (range 1–27 days). After intravenous antimicrobial drug therapy, patients were prescribed oral antimicrobial drugs, such as amoxicillin, rifampin, levofloxacin, or clindamycin, alone or in combination (Table 4). The median overall duration of antimicrobial therapy was 42 days (range 42–84 days) for patients with native joint infection and 47 days (range 42–120 days) for patients with infection in prosthetic joints. In addition to antimicrobial therapy, all patients with prosthetic joint

Table 3. Laboratory findings, joint analysis, antimicrobial susceptibility, and serotypes of *Pneumococcus*-positive cultures for 16 patients with pneumococcal septic arthritis, Picardie region, France, 2005–2016*

Patient age, y/sex	Laboratory findings					Joint analysis			MIC, mg/L			Serotype
	CRP†	Leuk‡	PCT§	Bact	Ag U	Characteristics	Gram stain	Culture	PEN	AMOX	CEF	
90/M	100	10,400	0.14	Y	+	Inflammation	–	+	2	2	0.5	19F
93/F	505	11,900	5.6	Y	+	Purulent	+	+	0.016	0.016	0.016	3
34/M	290	14,000	0.36	N	NA	Purulent	+	+	0.016	0.016	0.016	10A
68/M	28	78,000	NA	Y	NA	Purulent	+	+	0.5	0.25	0.25	1
75/M	360	13,800	NA	Y	NA	Purulent	+	+	0.064	0.016	0.016	NA
42/F	203	44,000	13	Y	NA	Inflammation	–	+	0.016	0.016	0.016	23B¶
80/F	385	18,200	NA	Y	NA	Purulent	+	+	0.016	0.016	0.032	23B¶
61/F	552	6,020	155	Y	NA	Purulent	+	+	0.5	0.5	1	1
57/F	391	11,310	NA	N	NA	Inflammation	NA	+	0.008	0.016	0.016	23B¶
82/F	NA	12,200	NA	N	NA	Inflammation	+	+	0.016	0.016	0.032	6A#
90/F	NA	NA	NA	Y	+	Purulent	+	–	1	0.5	4	19F
53/F	110	12,800	69.9	Y	–	NA	NA	NA	0.016	0.016	0.016	24F¶
69/M	552	8,740	NA	Y	NA	Purulent	+	+	0.016	0.016	0.016	9N
82/F	178	19,480	3.72	Y	NA	Purulent	+	+	0.016	0.016	0.016	8
57/M	450	15,550	NA	N	NA	Purulent	–	+	0.032	0.016	0.016	23B¶
82/M	240	21,000	0.96	N	+	Inflammation	+	+	0.016	0.016	0.016	23B¶

*Ag U, pneumococcal antigen in urine; AMOX, amoxicillin; Bact, bacteremia; CEF, ceftriaxone; CRP, C-protein reactive; leuk, leukocytes; NA, not available; PCT, procalcitonin; PEN, penicillin; PCV13, pneumococcal 13-valent conjugate vaccine; PPV23, pneumococcal 23-valent polysaccharide vaccine; +, positive; –, negative.

†In mg/L.

‡In cells/mm³.

§In ng/mL.

¶Serotypes not covered by PCV13 or PPV23.

#Serotype covered by PCV13 but not by PPV23.

infection also underwent surgical drainage, and 1 patient also required replacement of the prosthetic hip joint.

Most patients survived, but 1 (6.25%) patient died from colchicine-related multiorgan failure 2 days after admission. The remaining patients recovered well 8 (57.14%) of 14 patients completely recovered, and 5 (35.71%) had moderately reduced range of motion in the affected joint (Table 4).

Literature Review

We reviewed the largest case studies published during 1950–2017 (Table 5) and identified 121 cases of *S. pneumoniae* SA in adults in the literature (4,6–10,16). The age of affected patients was 47–75 years. Case-patients included 71 men and 50 women, 87.6% (106/121) of whom had underlying conditions that might have been predisposing factors for pneumococcal SA, including rheumatoid arthritis, gout and degenerative joint disease, diabetes, alcoholism, immunosuppression, cardiovascular disease, chronic obstructive pulmonary disease, malignancy, corticosteroid use, and splenectomy.

The clinical characteristics of pneumococcal infection, laboratory findings, antimicrobial therapy, and clinical outcomes were not available for all cases, and immunization status rarely was described. Among 70 patients for whom clinical characteristics were available, 36 (51.42%) had either prior or concurrent pneumococcal infections other than SA, including 24 (35.71%) cases of pneumonia, 10 (14.29%) cases of meningitis, and 4 (5.71%) cases of endocarditis. The knee was the joint most commonly involved in SA (66/121), but other affected sites included the shoulder

(19/105), ankle (11/105), hip (10/112), and elbow (9/105). Polyarticular involvement was reported in 23% of patients (28/121). Of 70 patients with prosthetic joint replacement, 4 (5.71%) had *S. pneumoniae* infections and 61 (87.14%) had joint cultures that were positive for bacteremia.

Concomitant bacteremia was documented in 98/119 (82.35%) patients for whom blood culture results were reported. Of 59 documented isolates, 5 (8.47%) demonstrated low-level penicillin resistance and 3 (5.1%) had low-level ceftriaxone resistance. Serotype data were seldom available, but a study by Marrie et al. (16) listed serotypes 4, 8, and 22F as the most commonly isolated.

Of the 121 patients we identified, 117 (96.7%) received antimicrobial therapy. Of those, 41 cases had detailed data on treatment regimens. Penicillin was the first-line treatment in 29 (70.7%) cases; third-generation cephalosporins, vancomycin, and rifampin were administered less frequently.

Among the 63 patients for whom clinical outcome data were available, 58 (92.1%) underwent joint drainage, and 11.1%–66.7% experienced sequelae of the joint infection. Death rates were variable among the studies but ranged as high as 32%.

Discussion

We report 16 (1.5%) cases of pneumococcal SA in a cohort of 1,062 IPD patients in France. Our study only includes data on *S. pneumoniae*-positive cultures from patients who were treated in public-sector hospitals. The true number of cases of pneumococcal SA in the region likely would be higher if data from private-sector hospitals were included. We found that the prevalence

Table 4. Clinical data on 16 patients with pneumococcal septic arthritis, Picardie region, France, 2005–2016*

Patient age, y/sex	Antimicrobial drugs, initial intravenous therapy; duration, d	Antimicrobial drugs, change to oral therapy	Surgical intervention	Duration of antimicrobial therapy, d	Clinical outcome
90/M	Ceftriaxone and rifampin; 4	Levofloxacin and rifampin	Arthrotomy and replacement of prosthetic joint	42	Recovered, regained baseline joint function
93/F	Ceftriaxone and gentamicin; 5	Levofloxacin and clindamycin	Arthrotomy and synovectomy	120	Recovered, regained baseline joint function
34/M	Amoxicillin and gentamicin; 4	Levofloxacin and amoxicillin	None	42	Recovered, moderately reduced range of motion
68/M	Amoxicillin and gentamicin; 2	NA	None	2	Died 2 d after admission from multiorgan failure related to colchicine overdose
75/M	Amoxicillin and gentamicin, then amoxicillin and levofloxacin; 11	Levofloxacin	None	42	Recovered, regained baseline joint function
42/F	Vancomycin and gentamicin; 6	Levofloxacin and rifampin	Arthrotomy	42	Recovered, moderately reduced range of motion
80/F	Ofloxacin and cloxacillin; 1	Amoxicillin	None	42	Recovered, regained baseline joint function
61/F	Amoxicillin and levofloxacin and rifampin; 7	Amoxicillin and rifampin	Arthrotomy	42	Recovered, regained baseline joint function
57/F	Amoxicillin and gentamicin; 5	Amoxicillin	None	42	Recovered, moderately reduced range of motion
82/F	ND	ND	ND	ND	ND
92/F	ND	ND	ND	ND	ND
53/F	Ceftriaxone and gentamicin; 15	Levofloxacin	None	84	Recovered, regained baseline joint function
69/M	Amoxicillin and gentamicin; ND	ND	ND	ND	Recovered, regained baseline joint function
82/F	Cefotaxime and gentamicin; 7	Levofloxacin and rifampin	Arthrotomy	47	Recovered, moderately reduced range of motion
57/M	Amoxicillin and gentamicin; 27	Amoxicillin	Arthrotomy and synovectomy	42	Recovered, moderately reduced range of motion
82/M	Amoxicillin and gentamicin; 10	Amoxicillin	None	42	Recovered, regained baseline joint function

*NA, not applicable; ND, no data.

of pneumococcal SA reported to the Picardie Regional Pneumococcal Network increased 4-fold after introduction of PCV13 in 2010.

We observed slight female predominance in our case-patients, which is in line with other studies (8,9). However, some studies describe male predominance (4,7,10,16). We found that older adults were more susceptible to pneumococcal SA; 62.5% of our patients were ≥ 65 , but this proportion was lower than reported in previous studies (4,6–10,16,22). Underlying conditions that could predispose patients to pneumococcal SA were observed in 79% of cases, and 21% of pneumococcal joint infections occurred in apparently healthy patients, which is in line with the results reported by others (23).

Among our cohort, 2 cases of multiple myeloma were revealed by pneumococcal SA. Because multiple myeloma causes immunosuppression, patients with multiple myeloma are more likely to become infected by encapsulated bacteria. Clinicians should consider multiple myeloma when pneumococcal SA is diagnosed in patients with no apparent predisposing factor (24,25).

Some studies report a history of concomitant extra-articular infection in 40%–60% of patients with pneumococcal joint infection (6–8,10). We noted pneumococcal respiratory tract infection in 36% of our cohort, but the respiratory tract was the only site of concomitant extra-articular infection reported. The knee was the joint affected most commonly. Among our cohort, 62.5% had SA in the knee and 12.5% had SA in the hip, a site reported less commonly overall; only 1%–7.8% of SA cases in the literature involved the hip (9,10,26). SA involved a prosthetic joint in 31% of cases, a higher rate than previously reported (6,7,9,10,26). Joint prosthesis in older adults appears to be an added risk factor for SA.

For most patients, the time to diagnosis was a few days. However, the diagnosis of prosthetic joint SA, particularly in the hip, was sometimes longer, as seen in previous findings (4,9,26).

Clinical signs and conventional laboratory markers, such as elevated white blood cell count, and CRP cannot differentiate infectious from noninfectious inflammation, and these tests should not be used alone to diagnose SA. Serum

Table 5. Detailed analysis of reports of septic arthritis in patients >18 years of age reported in medical literature during 1950–2019*

Study details	Study authors, year published (reference)							
	This study	Ros, et al., 2003 (10)	Ispahani et al., 1999 (8)	Dubost et al., 2004 (4)	Raad et al., 2004 (6)	James et al., 2000 (7)	Belkhir et al., 2014 (9)	Marrie et al., 2017 (16)
No. patients	16	11	25	7	4	14	9	51
Median age, y (IQR)	69.7 (±25)	60 (±18.5)	69 (NA)	63 (NA)	47 (±3.25)	63 (±21.75)	75 (±26)	56 (±17)
Sex, M/F	7/9	6/5	11/14	4/3	2/2	9/5	4/5	35/16
Impaired joints, no.								
Knee	11	6	12	4	0	10	7	26
Hip	2	0	0	0	2	0	0	0
>1 joint	2	3	5	0	3	6	0	9
Prosthetic joint	5	2	2	0	0	0	0	NA
Extraarticular infections, no.	6†	5	11	1	2	7	5	NA
Underlying conditions, no.	11†	9	23	5	4	10	3	48
Known vaccination status, no.								
No. immunized	2	–	–	–	–	–	0	–
Laboratory data, no. positive/no. tested								
Bacteremia	11/16	9/11	20/24	4/6	1/4	8/14	5/9	51/51
Gram stain	11/14	NA	23/25	4/5	NA	NA	5/9	NA
Culture	14/15	11/11	19/25	7/7	4/4	13/14	7/9	NA
Serotypes, no.	6	1	1	NA	NA	NA	4	29
Strains	23B and 24F	6A	24F	–	–	–	NA	NA
Covered by PCV13 and PPV23	N	Y	N	–	–	–	Y	–
Susceptibility								
Penicillin S	4	3	25	NA	2	NA	5	NA
Ceftriaxone S	1	1	25	NA	1	1	NA	NA
Ceftriaxone R	1	–	–	–	–	–	NA	NA
Median duration of antimicrobial therapy, d	42	42	49	27	49	NA	44.7	NA
Surgical intervention, no.‡	6†	8†	21	3	2	11	6	NA
Clinical outcome								
Death	1	2	8	0	0	3	1	6
Sequelae	5	4	10	4	1	2	1	NA

*IQR, interquartile range; NA, not available; PCV13, pneumococcal 13-valent conjugate vaccine; PPV23, pneumococcal 23-valent polysaccharide vaccine; R, resistant; S, susceptible.

†Data not available for all patients in study.

‡Including arthrotomy or synovectomy of affected joint or prosthetic joint replacement.

PCT levels also increase in various forms of inflammation and microbial infections. PCT is <0.5 ng/mL in healthy patients but rapidly increases with systemic bacterial infections, such as SA (27). Some studies have reported falsely low PCT during the early phase of infection or in localized infections, such as SA (27). In our study, all patients had elevated CRP and 75% had elevated PCT. Synovial fluid almost always had an inflammatory appearance and often was purulent, as also described in prior studies (4,6–10,28). Positive gram staining results were reported in 80% of cases, and positive culture was reported in 93% of cases, similar to the rates from previous studies (4,6–10).

In the literature, pneumococcal bacteremia was complicated by joint infection in 0.3%–0.6% of cases (10,29,30); bacteremia was observed in 55%–100% of adults with pneumococcal SA (4,6,8–10,16) and appeared to be more frequent when a prosthetic joint was infected (6). In our study, we observed bacteremia in 69% of cases

of native SA and in 80% of cases of prosthetic joint infection. The frequency of documented concurrent bacteremia emphasizes the importance of obtaining blood cultures in addition to joint fluid cultures before initiating antimicrobial therapy. Isolation of pathogenic microorganisms from both synovial fluid and blood culture can be considered the gold standard for SA diagnosis.

Most reported pneumococcal SA strains for which antimicrobial susceptibility data were available were susceptible to penicillin (6–10,28). A few strains with low- or high-level penicillin and ceftriaxone resistance have been reported in the literature (6,7,10); in our study, 25% of the strains had low-level penicillin resistance, and 12.5% had low- or high-level ceftriaxone resistance. Regardless, the frequency of low-level β-lactam resistance decreased from 2005–2010 to 2011–2016 (p<0.01). Despite the poor immunization coverage in this population, the decreased rate of resistance is related to a reduction in resistant serotypes, achieved by herd immunity.

Radiography, computed tomography, scintigraphy, and magnetic resonance imaging can be useful to assess the presence and extent of bone and joint inflammation and destruction but cannot distinguish between infections and other causes of acute inflammatory arthritis (3). Septic inflammation of a joint also can lead to radio-nuclide uptake in scintigraphy (31). However, diagnosis of pyogenic sacroiliitis often was made on the basis of patient history, physical examination, and positive skeletal scintigraphy or computed tomography of the sacroiliac joint.

No consensus has been reached concerning the optimal duration of intravenous antimicrobial therapy and the role of switching to oral therapy (3,28). The median duration reported in the literature ranged from 17–30.1 days for intravenous therapy and 30.6–49 days for oral antimicrobial agents (4,6,8–10). The median duration of intravenous therapy in our study was shorter, 1–23 days with a mean of 5.5 days, but the overall duration of antimicrobial therapy was comparable to reports in the literature. In several studies, penicillin was the most commonly used antimicrobial drug, then third-generation cephalosporins; gentamicin rarely was used (7,8,10,28). In contrast, 68.75% of cases in our study received a combination therapy of a β -lactam antimicrobial drug and gentamicin.

Antimicrobial therapy in the absence of drainage can be successful in certain patients. However, arthrotomy in combination with antimicrobial therapy typically is considered the best treatment for SA (4,6–10). In our cohort, arthrotomy was performed in 46% of cases. In the literature, when information regarding management was available, joint drainage always was performed on patients with SA in a prosthetic joint. Several cases of pneumococcal prosthetic joint SA required extended courses of antimicrobial drugs or even lifetime antimicrobial therapy, open surgical drainage, and sometimes replacement of the prosthetic joint (3,7,8,26,28).

Pneumococcal SA usually has a favorable prognosis when appropriate treatment is instituted rapidly (3,28). In our study and others we reviewed, most patients recovered and achieved their initial joint range of motion or had only minor sequelae with mildly reduced range of motion (7,9,10). Nevertheless, extensive physical damage sometimes was described (4), and mortality rates of up to 32% were reported in patients with pneumococcal SA (6–8,10,16). Risk of death appeared to be higher in cases of pneumococcal SA associated with bacteremia (24%) than those without bacteremia (6%) (15). In our study, 1 (7%) patient died with SA infection caused by a strain with low-level penicillin resistance.

Because the prevalence of antimicrobial drug-resistant *S. pneumoniae* has increased, pneumococcal vaccination has become a greater focus for public health (12,15,17–

21). In the Picardie region, and in France as a whole, both PCV13 and pneumococcal 23-valent polysaccharide vaccine (PPV23) are indicated in adults with underlying conditions that predispose them to pneumococcal disease (15,17). In the Picardie Regional Pneumococcal Network, 82% (9/14) of patients with known vaccination status had not been vaccinated; of those, 5 (55.5%) had underlying conditions that would have justified pneumococcal vaccination. Of the strains isolated, 60% are covered by either PCV13 or PPV23. Of the 40% not covered by either vaccine, 5 were 23B serotype and 1 was the 24F serotype. Although several studies have demonstrated the effectiveness of pneumococcal vaccines in preventing IPD in adults (17,18,20,21), a large retrospective study of patients with pneumococcal SA reported *S. pneumoniae* serotypes 22F and 12F, both of which are covered by PPV23, frequently occur (16), findings that emphasize the importance of following the immunization guidelines.

In June 2010, health authorities in France introduced PCV13 for children <2 years of age; older children with ≥ 1 underlying conditions, such as innate or acquired immunodeficiency, malignancy, impaired splenic function, cochlear implants, cerebrospinal fluid leakage, or recurrent IPD; and adults at risk for pneumococcal infections, such as those with immunosuppression or history of splenectomy. According to studies in France, after the introduction of PCV13, the incidence of all IPD types decreased during 2008–2012 by 20% in adults 16–64 years of age and by 15% in patients ≥ 65 years of age (17). Decreases in *S. pneumoniae* isolates with reduced antimicrobial sensitivity also were noted (15), but the frequency of serotypes not covered by the vaccine increased (15,17).

In our study, serotype 23B in pneumococcal SA or IPD emerged 2 years after the introduction of PCV13 (data not shown), and these strains were always penicillin susceptible. The 2 patients in our study who had *S. pneumoniae* vaccination after splenectomy were not protected against infection by serotypes 23B and 24F. Our data are consistent with trends observed in other countries (32–35). For example, Germany and the United States report a rise in serotype 23B after implementation of PCV13 (32–35) and a high proportion of the 23B isolates displayed a low-level penicillin resistance. However, the serotype 23B strain we saw in the Picardie region was always penicillin-susceptible. If confirmed by future studies, 23B and 24F serotypes should be considered when developing next-generation PCVs (36).

In conclusion, the prevalence of pneumococcal SA in adults in the Picardie Regional Pneumococcal Network of France increased over the 5 years reported, apparently in relation to emergence of serotype 23B. Vaccination in the region might not comply fully with the current guidelines; 60% of the strains isolated from patients in this study are

covered by PCV13 and PPV23, suggesting that these pneumococcal infections could have been prevented.

Authors' contributions: Y.E.S., A.D., V.S., J.S., and C.G. performed clinical examinations. J.P.E., A.B., M.E.H., C.P., F.R., and F.H. performed bacteriological diagnoses, E.V. serotyped the *S. pneumoniae* strains, and M.D. performed the statistical analysis. A.D. and F.H. drafted the manuscript. All authors read and approved the final manuscript.

About the Author

Mrs. Dernoncourt is an internal medicine resident at the University Hospital of Amiens-Picardie, Amiens, France. Her research interests include immune-related diseases and vaccine-preventable infections. Dr. Hamdad is a senior clinical microbiologist and PhD at the University Hospital of Amiens-Picardie, Amiens, France. Her research interests include emerging infectious diseases and antimicrobial resistance.

References

- Mathews CJ, Weston VC, Jones A, Field M, Coakley G. Bacterial septic arthritis in adults. *Lancet*. 2010;375:846–55. [https://doi.org/10.1016/S0140-6736\(09\)61595-6](https://doi.org/10.1016/S0140-6736(09)61595-6)
- García-Arias M, Balsa A, Mola EM. Septic arthritis. *Best Pract Res Clin Rheumatol*. 2011;25:407–21. <https://doi.org/10.1016/j.berh.2011.02.001>
- Goldenberg DL. Septic arthritis. *Lancet*. 1998;351:197–202. [https://doi.org/10.1016/S0140-6736\(97\)09522-6](https://doi.org/10.1016/S0140-6736(97)09522-6)
- Dubost J-J, Soubrier M, De Champs C, Ristori J-M, Sauvezie B. Streptococcal septic arthritis in adults. A study of 55 cases with a literature review. *Joint Bone Spine*. 2004;71:303–11. [https://doi.org/10.1016/S1297-319X\(03\)00122-2](https://doi.org/10.1016/S1297-319X(03)00122-2)
- Ryan MJ, Kavanagh R, Wall PG, Hazleman BL. Bacterial joint infections in England and Wales: analysis of bacterial isolates over a four year period. *Br J Rheumatol*. 1997;36:370–3. <https://doi.org/10.1093/rheumatology/36.3.370>
- Raad J, Peacock JE Jr. Septic arthritis in the adult caused by *Streptococcus pneumoniae*: a report of 4 cases and review of the literature. *Semin Arthritis Rheum*. 2004;34:559–69. <https://doi.org/10.1016/j.semarthrit.2004.04.002>
- James PA, Thomas MG; Paul A. James, Mark G. Thomas. *Streptococcus pneumoniae* septic arthritis in adults. *Scand J Infect Dis*. 2000;32:491–4. <https://doi.org/10.1080/003655400458758>
- Ispahani P, Weston VC, Turner DP, Donald FE. Septic arthritis due to *Streptococcus pneumoniae* in Nottingham, United Kingdom, 1985–1998. *Clin Infect Dis*. 1999;29:1450–4. <https://doi.org/10.1086/313526>
- Belkhir L, Rodriguez-Villalobos H, Vandercam B, Marot JC, Cornu O, Lambert M, et al. Pneumococcal septic arthritis in adults: clinical analysis and review. *Acta Clin Belg*. 2014;69:40–6. <https://doi.org/10.1179/0001551213Z.00000000015>
- Ross JJ, Saltzman CL, Carling P, Shapiro DS. Pneumococcal septic arthritis: review of 190 cases. *Clin Infect Dis*. 2003;36:319–27. <https://doi.org/10.1086/345954>
- Seng P, Vernier M, Gay A, Pinelli P-O, Legré R, Stein A. Clinical features and outcome of bone and joint infections with streptococcal involvement: 5-year experience of interregional reference centres in the south of France. *New Microbes New Infect*. 2016;12:8–17. <https://doi.org/10.1016/j.nmni.2016.03.009>
- Dockrell DH, Whyte MKB, Mitchell TJ. Pneumococcal pneumonia: mechanisms of infection and resolution. *Chest*. 2012;142:482–91. <https://doi.org/10.1378/chest.12-0210>
- Lynch JP III, Zhanel GG. *Streptococcus pneumoniae*: epidemiology, risk factors, and strategies for prevention. *Semin Respir Crit Care Med*. 2009;30:189–209. <https://doi.org/10.1055/s-0029-1202938>
- Rueda AM, Serpa JA, Matloobi M, Mushtaq M, Musher DM. The spectrum of invasive pneumococcal disease at an adult tertiary care hospital in the early 21st century. *Medicine (Baltimore)*. 2010;89:331–6. <https://doi.org/10.1097/MD.0b013e3181f2b824>
- Varon E. Epidemiology of *Streptococcus pneumoniae*. *Med Mal Infect*. 2012;42:361–5. <https://doi.org/10.1016/j.medmal.2012.04.002>
- Marrie TJ, Tyrrell GJ, Majumdar SR, Eurich DT. Rates of, and risk factors for, septic arthritis in patients with invasive pneumococcal disease: prospective cohort study. *BMC Infect Dis*. 2017;17:680. <https://doi.org/10.1186/s12879-017-2797-7>
- Lepoutre A, Varon E, Georges S, Dorléans F, Janoir C, Gutmann L, et al.; Microbiologists of Epibac; ORP Networks. Impact of the pneumococcal conjugate vaccines on invasive pneumococcal disease in France, 2001–2012. *Vaccine*. 2015;33:359–66. <https://doi.org/10.1016/j.vaccine.2014.11.011>
- Webber C, Patton M, Patterson S, Schmoele-Thoma B, Huijts SM, Bonten MJM; CAPiTA Study Group. Exploratory efficacy endpoints in the Community-Acquired Pneumonia Immunization Trial in Adults (CAPiTA). *Vaccine*. 2017;35:1266–72. <https://doi.org/10.1016/j.vaccine.2017.01.032>
- Richard C, Le Garlantezec P, Lamand V, Rasamijao V, Rapp C. Anti-pneumococcal vaccine coverage for hospitalized risk patients: Assessment and suggestions for improvements [in French]. *Ann Pharm Fr*. 2016;74:244–51. <https://doi.org/10.1016/j.pharma.2015.10.007>
- Falkenhorst G, Remschmidt C, Harder T, Hummers-Pradier E, Wichmann O, Bogdan C. Effectiveness of the 23-valent pneumococcal polysaccharide vaccine (PPV23) against pneumococcal disease in the elderly: systematic review and meta-analysis. *PLoS One*. 2017;12:e0169368. <https://doi.org/10.1371/journal.pone.0169368>
- Bonten MJ, Huijts SM, Bolkenbaas M, Webber C, Patterson S, Gault S, et al. Polysaccharide conjugate vaccine against pneumococcal pneumonia in adults. *N Engl J Med*. 2015;372:1114–25. <https://doi.org/10.1056/NEJMoa1408544>
- Butler JC, Schuchat A. Epidemiology of pneumococcal infections in the elderly. *Drugs Aging*. 1999;15(Suppl 1):11–9. <https://doi.org/10.2165/00002512-199915001-00002>
- Forestier E, Sordet C, Cohen-Solal J, Remy V, Javier RM, Kuntz JL, et al. Bone and joint infection due to *Streptococcus pneumoniae* in two immunocompetent adults. *Joint Bone Spine*. 2006;73:325–8. <https://doi.org/10.1016/j.jbspin.2005.07.004>
- Riachy MA. *Streptococcus pneumoniae* causing septic arthritis with shock and revealing multiple myeloma. *BMJ Case Rep*. 2011;2011:bcr1220103664. <https://doi.org/10.1136/bcr.12.2010.3664>
- Kalambokis GN, Christou L, Tsianos EV. Multiple myeloma presenting with an acute bacterial infection. *Int J Lab Hematol*. 2009;31:375–83. <https://doi.org/10.1111/j.1751-553X.2009.01154.x>
- Bertani A, Drouin C, Demortière E, Gonzalez J-F, Candoni P, Di Schino M. A prosthetic joint infection caused by *Streptococcus pneumoniae*: a case report and review of the literature [in French]. *Rev Chir Orthop Reparat Mot*. 2006;92:610–4. [https://doi.org/10.1016/S0035-1040\(06\)75921-9](https://doi.org/10.1016/S0035-1040(06)75921-9)
- Zhao J, Zhang S, Zhang L, Dong X, Li J, Wang Y, et al. Serum procalcitonin levels as a diagnostic marker for septic arthritis: a meta-analysis. *Am J Emerg Med*. 2017;35:1166–71. <https://doi.org/10.1016/j.ajem.2017.06.014>

28. Baraboutis I, Skoutelis A. *Streptococcus pneumoniae* septic arthritis in adults. *Clin Microbiol Infect*. 2004;10:1037–9. <https://doi.org/10.1111/j.1469-0691.2004.00968.x>
29. Gransden WR, Eykyn SJ, Phillips I. Pneumococcal bacteraemia: 325 episodes diagnosed at St Thomas's Hospital. *Br Med J (Clin Res Ed)*. 1985;290:505–8. <https://doi.org/10.1136/bmj.290.6467.505>
30. Burman LA, Norrby R, Trollfors B. Invasive pneumococcal infections: incidence, predisposing factors, and prognosis. *Rev Infect Dis*. 1985;7:133–42. <https://doi.org/10.1093/clinids/7.2.133>
31. Bhattarai A, Nakajima T, Sapkota S, Arisaka Y, Tokue A, Yonemoto Y, et al. Diagnostic value of 18F-fluorodeoxyglucose uptake parameters to differentiate rheumatoid arthritis from other types of arthritis. *Medicine (Baltimore)*. 2017;96:e7130. <https://doi.org/10.1097/MD.00000000000007130>
32. van der Linden M, Falkenhorst G, Perniciaro S, Imöhl M. Effects of infant pneumococcal conjugate vaccination on serotype distribution in invasive pneumococcal disease among children and adults in Germany. *PLoS One*. 2015;10:e0131494. <https://doi.org/10.1371/journal.pone.0131494>
33. van der Linden M, Perniciaro S, Imöhl M. Increase of serotypes 15A and 23B in IPD in Germany in the PCV13 vaccination era. *BMC Infect Dis*. 2015;15:207. <https://doi.org/10.1186/s12879-015-0941-9>
34. Steens A, Bergsaker MA, Aaberge IS, Rønning K, Vestheim DF. Prompt effect of replacing the 7-valent pneumococcal conjugate vaccine with the 13-valent vaccine on the epidemiology of invasive pneumococcal disease in Norway. *Vaccine*. 2013;31:6232–8. <https://doi.org/10.1016/j.vaccine.2013.10.032>
35. Richter SS, Diekema DJ, Heilmann KP, Dohrn CL, Riahi F, Doern GV. Changes in pneumococcal serotypes and antimicrobial resistance after introduction of the 13-valent conjugate vaccine in the United States. *Antimicrob Agents Chemother*. 2014;58:6484–9. PubMed <https://doi.org/10.1128/AAC.03344-14>
36. Ouldali N, Levy C, Varon E, Bonacorsi S, Béchet S, Cohen R, et al.; French Pediatric Meningitis Network. Incidence of paediatric pneumococcal meningitis and emergence of new serotypes: a time-series analysis of a 16-year French national survey. *Lancet Infect Dis*. 2018;18:983–91. [https://doi.org/10.1016/S1473-3099\(18\)30349-9](https://doi.org/10.1016/S1473-3099(18)30349-9)

Address for correspondence: Amandine Dernoncourt, Amiens-Picardie University Medical Center, Department of Internal Medicine, Place Victor Pauchet, F-80054 Amiens CEDEX 01, France; email: amandine.dernoncourt@wanadoo.fr

etymologia

Edwardsiella tarda

Ronnie Henry

In 1965, a group of CDC researchers described a species of gram-negative, facultatively anaerobic bacteria in the family *Enterobacteriaceae*, which they named *Edwardsiella* (for CDC microbiologist Philip R. Edwards) *tarda* (Latin, “slow,” referring to biochemical inactivity and the fact that it ferments few carbohydrates). These organisms infect a variety of fish, reptiles, and amphibians and are opportunistic pathogens for humans.

Dr. P.R. Edwards of the US Public Health Service, seated in the background, and George Herman working in the Enteric Bacteriology Unit Laboratory.

Dr. Edwards joined the staff of the Communicable Disease Center of the Public Health Service in 1948 and served as Chief of the Enteric Bacteriology Unit until June 1962 when he accepted the post of Chief of the Bacteriology Section at CDC. Image source, Public Health Image Library.



Sources

1. Ewing WH, McWhorter AC, Escobar MR, Lubin AH. *Edwardsiella*, a new genus of *Enterobacteriaceae* based on a new species, *E. tarda*. *Int Bull Bacteriol Nomencl Taxon*. 1965;15:33–8. <https://doi.org/10.1099/00207713-15-1-33>
2. Abbott SL, Janda JM. The genus *Edwardsiella*. In: Dworkin M, editor. *The prokaryotes*. New York: Springer; 2006. p. 72–89.

Address for correspondence: Ronnie Henry, Centers for Disease Control and Prevention, 1600 Clifton Rd NE, Mailstop E28, Atlanta, GA 30329-4027, USA; email: boq3@cdc.gov

DOI: <https://doi.org/10.3201/eid2510.ET2510>

Global Epidemiology of Diphtheria, 2000–2017¹

Kristie E.N. Clarke, Adam MacNeil, Stephen Hadler,
Colleen Scott, Tejpratap S.P. Tiwari, Thomas Cherian²

In 2017, a total of 8,819 cases of diphtheria were reported worldwide, the most since 2004. However, recent diphtheria epidemiology has not been well described. We analyzed incidence data and data from the literature to describe diphtheria epidemiology. World Health Organization surveillance data were 81% complete; completeness varied by region, indicating underreporting. As national diphtheria–tetanus–pertussis (DTP) 3 coverage increased, the proportion of case-patients <15 years of age decreased, indicating increased protection of young children. In countries with higher case counts, 66% of case-patients were unvaccinated and 63% were <15 years of age. In countries with sporadic cases, 32% of case-patients were unvaccinated and 66% were ≥15 years of age, consistent with waning vaccine immunity. Global DTP3 coverage is suboptimal. Attaining high DTP3 coverage and implementing recommended booster doses are necessary to decrease diphtheria incidence. Collection and use of data on subnational and booster dose coverage, enhanced laboratory capacity, and case-based surveillance would improve data quality.

Diphtheria was a leading cause of childhood death in the prevaccine era (1). Incidence in industrialized countries decreased rapidly with diphtheria–tetanus–pertussis (DTP) vaccine introduction after World War II. Incidence in less developed countries also decreased after the launch of the World Health Organization (WHO) Expanded Programme on Immunization in 1974 (2), which recommended that all infants receive a 3-dose series of DTP vaccine by 6 months of age. A spike in incidence in the newly independent states of the former Soviet Union occurred in the 1990s (Figure 1), resulting in >157,000 cases and 5,000 deaths (1). This spike demonstrated the potential for severe outbreaks of diphtheria in communities that have a large population of nonimmune adults and poor vaccination coverage for children.

Although several comprehensive reviews were published after that outbreak peaked (3–5), only sporadic

documentation of diphtheria outbreaks has been published since, and no examination of global epidemiologic trends has been published. During 2016–2019, diphtheria outbreaks were reported in multiple countries, including Bangladesh, Yemen, and Venezuela. Several outbreaks were among vulnerable populations or in areas of social disruption and conflict. Authors in some low- and middle-income countries have reported a resurgence of the disease or a shift to older populations (6–8). However, the quality of reported surveillance data varies; 26 of 130 responding countries report no diphtheria surveillance system, and only 55 report case-based surveillance with laboratory confirmation (9). In this context, a review of recent epidemiologic trends is needed to better characterize recent outbreaks.

Given a previous lack of global guidance on diphtheria-containing booster doses after the 3-dose primary series, a wide variety of schedules had been adopted by different countries as of 2018 (10–12). Twenty-four percent of countries used the 3-dose series alone, and other countries offered 1–3 booster doses on varying schedules; 24% of countries also included ≥1 adult booster doses, defined as a dose recommended at or after 18 years of age (Figure 2). Although there are no global estimates of coverage for booster doses, available data suggest coverage is lower than that for the primary series in many countries (13).

In August 2017, WHO released revised recommendations for diphtheria vaccination (14). In addition to the 3-dose primary series in infancy, new recommendations include 3 diphtheria toxoid-containing booster doses given at 12–23 months of age, 4–7 years of age, and 9–15 years of age. These recommendations, which harmonize with the updated recommendations for tetanus boosters released in February 2017 (15), emphasize the need for a life course vaccination approach and present new opportunities for synergies with other vaccines and healthcare activities, such as measles second dose, preventive care at school

Author affiliations: Centers for Disease Control and Prevention, Atlanta, Georgia, USA (K.E.N. Clarke, A. MacNeil, S. Hadler, C. Scott, T.S.P. Tiwari); World Health Organization, Geneva, Switzerland (T. Cherian)

¹Preliminary results from this study were presented at the meeting of the Strategic Advisory Group of Experts on Immunization, Geneva, Switzerland, April 25–27, 2017.

²Retired.

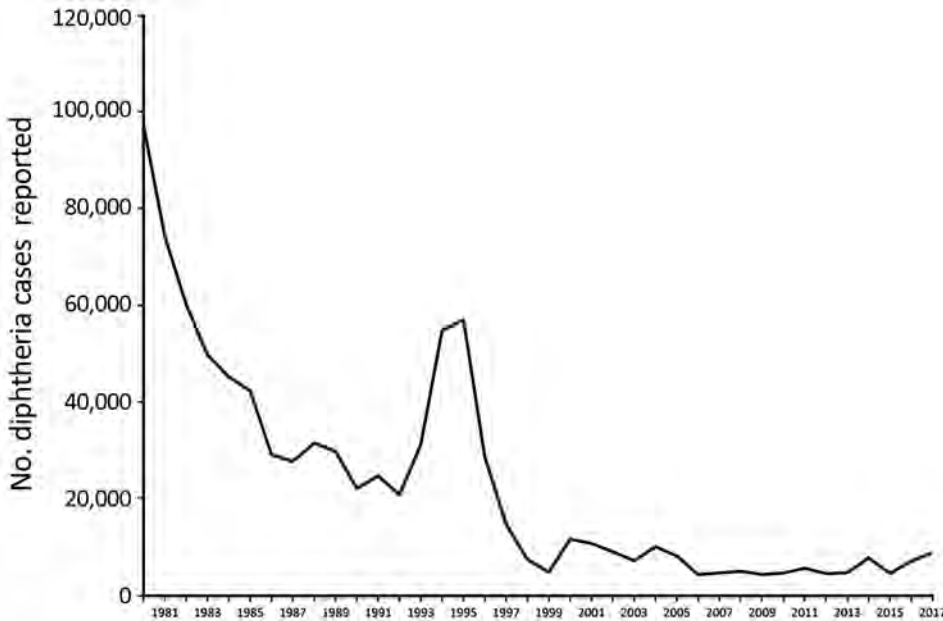


Figure 1. Cases of diphtheria as reported to the World Health Organization and the United Nations Children’s Fund, through the Joint Reporting Form, worldwide, 1980–2017.

entry, and human papillomavirus vaccination. In addition, it is now recommended that the combined tetanus toxoid and diphtheria toxoid vaccine be used during pregnancy and when tetanus prophylaxis is required because of injury, rather than using tetanus toxoid alone. The objective of this study was to review the epidemiology of diphtheria since 2000, including global aggregate surveillance data, vaccination coverage data, and available data regarding the age and vaccination status of infected persons.

Methods

We examined aggregate diphtheria surveillance data reported annually to WHO and the United Nations Children’s Fund (UNICEF) from each country through the Joint Reporting Form (JRF) for global and regional epidemiologic incidence trends during 2000–2017. JRF data include the

aggregate number of cases of diphtheria reported by countries in a given year and do not provide information on case-patient age or vaccination status.

We obtained information on the age or vaccination status of diphtheria case-patients from accessible published or gray literature (publications produced by organizations outside traditional commercial or academic publishing and distribution channels), presentation reports, and regional case-based surveillance data. We performed systematic searches covering publication dates during January 2000–September 2018 (Table 1). Searches returned 1,080 unique abstracts; 2 researchers reviewed each abstract to determine relevance. Discrepancies were discussed until consensus was reached. To meet inclusion criteria, manuscripts had to contain data about the age or vaccination status of case-patients with respiratory

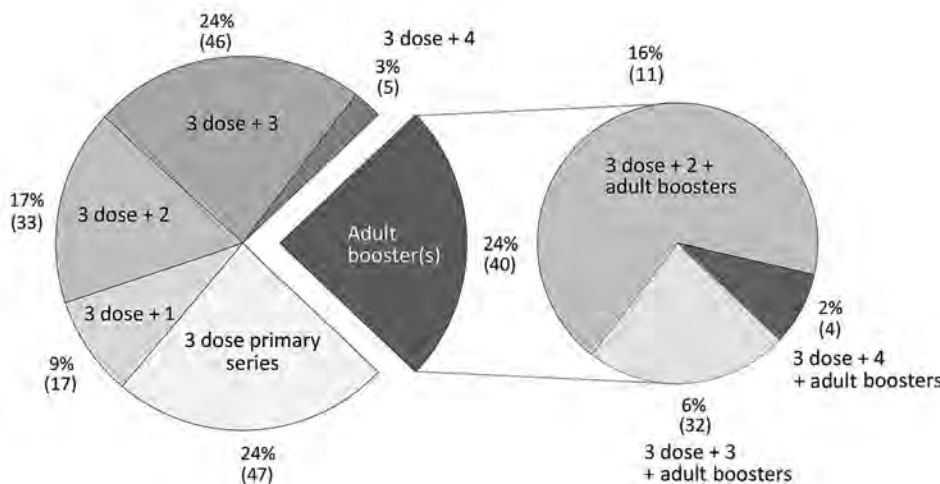


Figure 2. Percentage (number) of countries reporting each diphtheria vaccination schedule, 2018. The number after the plus sign indicates the number of booster doses on the national schedule after the 3-dose primary series and before the age of 18 years.

Table 1. Strategy for systematic literature search for diphtheria, January 1, 2000–September 18, 2018*

Database	Initial search strategy
Medline	(Diphtheria/ AND Disease Outbreaks/) OR (diphtheria.ti AND (outbreak* OR cluster* OR epidemic*).ti,ab.) OR (diphtheria ADJ3 (outbreak* OR cluster* OR epidemic*).ab.
Embase	(Diphtheria/ AND Disease Outbreaks/) OR (diphtheria.ti AND (outbreak* OR cluster* OR epidemic*).ti,ab.) OR (diphtheria ADJ3 (outbreak* OR cluster* OR epidemic*).ab.
Scopus	TITLE-ABS-KEY(diphtheria W/2 outbreak*)
Database	Secondary Search Strategy
Medline	*diphtheria/ or diphtheria.ti,ab. AND Epidemics/ OR Disease Outbreaks/ OR (outbreak* OR cluster* OR epidemic*).ti,ab. AND Limit 2000–
Embase	*diphtheria/ or diphtheria.ti,ab. AND Epidemic/ OR (outbreak* OR cluster* OR epidemic*).ti,ab. AND Limit 2000–
Global Health	diphtheria/ OR diphtheria.ti,ab,sh. AND Epidemics/ OR (outbreak* OR cluster* OR epidemic*).ti,ab,sh. AND Limit 2000–
CINAHL	(MJ diphtheria) or (TI diphtheria) OR (AB diphtheria) AND (MH "Disease Outbreaks") OR (MH Epidemics) OR (TI (outbreak* OR cluster* OR epidemic*)) OR (AB (outbreak* OR cluster* OR epidemic*)) AND Limit 2000- ; Exclude Medline records
Cochrane Library	[mh diphtheria] or diphtheria:ti,ab AND [mh "Disease Outbreaks"] OR [mh Epidemics] OR (outbreak* OR cluster* OR epidemic*):ti,ab AND Limit 2000–
LILACS	Diphtheria AND (outbreak* OR cluster* OR epidemic*)
Scopus	INDEXTERMS(Diphtheria) AND INDEXTERMS("disease outbreak*" OR epidemic*) AND (LIMIT-TO(PUBYEAR,2015) OR LIMIT-TO(PUBYEAR,2014) OR LIMIT-TO(PUBYEAR,2013) OR LIMIT-TO(PUBYEAR,2012) OR LIMIT-TO(PUBYEAR,2011) OR LIMIT-TO(PUBYEAR,2010) OR LIMIT-TO(PUBYEAR,2009) OR LIMIT-TO(PUBYEAR,2008) OR LIMIT-TO(PUBYEAR,2007) OR LIMIT-TO(PUBYEAR,2006) OR LIMIT-TO(PUBYEAR,2005) OR LIMIT-TO(PUBYEAR,2004) OR LIMIT-TO(PUBYEAR,2003) OR LIMIT-TO(PUBYEAR,2002) OR LIMIT-TO(PUBYEAR,2001) OR LIMIT-TO(PUBYEAR,2000)) AND (LIMIT-TO(DOCTYPE,"ar") OR LIMIT-TO(DOCTYPE,"re")) AND (LIMIT-TO(EXACTKEYWORD,"Diphtheria"))

*CINAHL, Cumulative Index to Nursing and Allied Health Literature; LILACS, Latin American and Caribbean Health Sciences Literature.

diphtheria caused by *Corynebacterium diphtheriae* during 2000–2017, with availability of full text in English or Spanish. Twenty-nine abstracts were excluded for language, as were 779 abstracts not relevant to the review. Two additional articles were not retrievable in full text.

Of 107 manuscripts reviewed in full text, 28 met inclusion criteria for the analysis (Appendix references 1–28, <https://wwwnc.cdc.gov/EID/article/25/10/19-0271-App1.pdf>). The full text of each manuscript was reviewed by 2 investigators, and relevant data were compiled in an Excel (Microsoft, <https://www.microsoft.com>) database. An additional 19 published manuscripts were identified through the reference lists (Appendix references 29–47). A review of the gray literature resulted in 12 additional sources (Appendix, references 48–59), and communications with colleagues resulted in access to 11 unpublished reports (Pan American Health Organization: T.S.P. Tiwari [2]; R. Kaiser; Centers for Disease Control and Prevention; WHO Punjab; J. Crucena; Republic of Philippines Epidemiology Bureau; T. Nguyen; A. Nihal; and L. Sangal).

Diphtheria data from the European Surveillance System were provided by Spain, Latvia, Germany, Italy, Lithuania, the Netherlands, the United Kingdom, Finland, Sweden, France, Austria, and Belgium and released by the European Centre for Disease Prevention and Control (Stockholm, Sweden) (Appendix reference 60). Similar case-based diphtheria data were not available from other regions. Because of multiple data sources, we conservatively excluded cases identified as potential duplicates when matching by age group, location, and year. The final dataset

consisted of 15,380 cases of diphtheria (15,068 including age data and 7,242 including vaccination status data) from 34 countries.

We compared cases included in the final dataset with the number of cases in the aggregate JRF data for each country over the same period to cross-reference the completeness of the diphtheria data reported in the JRF. Because DTP 3 coverage is a major risk factor for disease transmission in a population, we took the average of the national WHO–UNICEF estimates of DTP3 coverage (16) for the 5 years previous to the cases for each set of reported cases. For analysis, we classified countries with data included in the review as either countries with higher case counts (defined as reporting ≥ 10 cases in each of ≥ 3 years of JRF incidence data during 2000–2017, or reporting ≥ 100 cases in a single year) or as countries with sporadic cases.

The age distribution analysis was complicated by the diverse ways in which age data were aggregated in different manuscripts. Our analysis used an age of 15 years for disaggregation of age data because this age was most frequently mentioned in the historical literature as a benchmark for the age shift in diphtheria incidence over time. However, on the basis of availability of age data from source documents, we made classifications by using heterogeneous age cutoffs in the initial analysis. To address this limitation, we compiled a more precise dataset ($n = 9,334$ cases from 32 countries) for sensitivity analyses that contained only data that classified case-patients as ≥ 15 or < 15 years of age (± 1 year).

Sources also aggregated vaccination status data differently and had varying definitions for fully vaccinated depending on the vaccination schedule of the country or criteria of the investigators. For this review we defined fully vaccinated, at a minimum, as having received all 3 doses of the primary series. Cases with partial vaccination (≥ 1 dose of infant DTP) were grouped with fully vaccinated cases in several sources; we conservatively designated these cases as partially vaccinated in the full dataset. Reports of cases with unknown or partial vaccination status were grouped with unvaccinated cases in other sources; we conservatively designated these cases as unvaccinated in the full dataset. To address this limitation, we compiled a dataset (1,534 cases from 27 countries) that contained only cases that were reported in ≥ 3 different groups (unvaccinated, partially vaccinated, or fully vaccinated). We also

provide additional information on datasets compiled from the literature and gray literature review (Table 2).

We analyzed distribution of case-patients by age and vaccination status by using descriptive methods in Excel 2016. We performed sensitivity analysis to test for consistency of findings between those analyses performed by using the full dataset and those performed by using a dataset with enhanced precision around the variable of interest. Because cases from India represented $>50\%$ of cases in the full dataset, we conducted a final sensitivity analysis to check for consistency of trends for all analyses when data from India were excluded.

Finally, to examine the relationship between vaccination coverage with the primary series and age distribution, we combined the total number of cases for each country in the dataset. We compared the proportion of case-patients

Table 2. Overview of datasets with information on age and vaccination status compiled from review compared with aggregate diphtheria incidence data reported by countries on the joint reporting form over the same period, 2000–2017*

Country	Classification	Datasets for sensitivity analysis							
		Full dataset, n = 15,380		Age data, n = 9,334†		Vaccination status data, n = 1,534‡		Joint reporting form data 2000–2017, n = 103,138	
		Years of data	Total cases	Years of data	Total cases	Years of data	Total cases	Years ≥ 1 case reported	Total cases
Afghanistan	Higher case count	1	50	1	37	NA	NA	8	1,380
Australia	Sporadic	1	1	1	1	1	1	7	26
Austria	Sporadic	1	2	1	2	NA	NA	2	4
Bangladesh§	Higher case count	1	3,581	1	3,567	NA	NA	18	804
Belgium	Sporadic	2	2	2	2	1	1	7	15
Brazil	Higher case count	3	32	2	28	3	32	16	331
Colombia	Sporadic	1	8	1	8	1	6	4	17
Dominican Republic	Higher case count	2	82	2	82	1	1	15	372
Finland	Sporadic	2	2	2	2	2	2	3	3
France	Sporadic	7	22	7	22	4	4	10	54
Germany	Sporadic	7	24	7	24	3	3	13	77
Haiti	Higher case count	6	314	3	92	3	41	14	230
India¶	Higher case count	20	8,720	18	3,303	12	544	18	79,034
Indonesia	Higher case count	2	582	2	566	1	52	17	7,160
Italy	Sporadic	1	1	1	1	NA	NA	1	1
Laos	Higher case count	2	62	2	62	2	27	15	578
Latvia	Higher case count	10	133	10	133	6	45	18	612
Lithuania	Sporadic	2	3	2	3	NA	NA	4	10
Malaysia	Higher case count	1	1	1	1	NA	NA	14	106
Myanmar	Higher case count	2	156	2	154	1	50	17	512
Netherlands	Sporadic	3	5	3	5	3	4	5	12
Nigeria	Higher case count	6	118	6	118	3	8	4	7,565
Norway	Sporadic	3	8	3	8	1	3	3	5
Pakistan	Higher case count	2	406	2	406	2	372	18	1,176
Paraguay	Sporadic	1	47	NA	NA	1	12	5	59
Philippines	Higher case count	7	553	7	512	6	280	15	1,019
South Africa	Sporadic	1	15	1	15	1	8	6	26
Spain	Sporadic	2	2	2	2	2	2	2	2
Sweden	Sporadic	6	12	6	12	5	7	6	12
Thailand	Higher case count	2	47	2	35	NA	NA	18	342
United Kingdom	Sporadic	8	23	8	22	4	4	13	40
United States	Sporadic	1	1	1	1	1	1	5	6
Venezuela	Higher case count	2	244	NA	NA	1	11	3	818
Vietnam	Higher case count	2	121	1	108	1	13	18	730

*NA, not available.

†Includes all case-patients for which age was clearly designated as above or below an age cutoff point of 15 y (± 1 y).

‡Includes all cases for which vaccination status was clearly designated as fully vaccinated, partially vaccinated, or unvaccinated.

§Population of Rohingya refugees from Myanmar housed in a refugee camp in Bangladesh.

¶Data from India include 2 articles with aggregate data including the late 1990s (Appendix references 15,18, <https://wwwnc.cdc.gov/EID/article/25/10/19-0271-App1.pdf>).

≥15 years of age in each country with the average of DTP3 coverage for the 5 years preceding the year(s) when the cases were reported. We excluded countries with <5 cases in the dataset from this analysis, leaving 24 countries in the primary analysis and 23 countries in the sensitivity analysis.

Results

General Epidemiologic Trends

Since 2000, the number of reported diphtheria cases worldwide in JRF data initially decreased, then leveled at 4,300–5,700 reported cases/year during 2006–2013. Subsequently, the annual number of reported cases became more variable; 8,819 cases were reported in 2017, the most cases in a single year since 2004 (Figure 3). The average number of annual cases reported worldwide over the most recently reported 5-year period (2013–2017) was 6,582, an increase of 37% compared with the previous 5-year average of 4,809 cases during 2008–2012.

Since 2000, the WHO South-East Asia region has reported most of the global diphtheria incidence each year. India has reported the largest proportion of diphtheria cases in aggregate JRF data since 2000 (64%); similarly, in data compiled from the literature review, >50% of cases with age and vaccination status were from India in the full dataset (8,720 [57%]). Collectively, India, Nepal, and Indonesia have reported 96%–99% of the cases in the South-East Asia region since 2000. Meanwhile, cases reported from the WHO Europe region decreased as the impact of the large outbreak in the former Soviet Republics during the 1990s attenuated.

Surveillance Data Completeness and Accuracy

During 2000–2017, each country (except South Sudan) had the opportunity to submit 18 years of JRF data on

diphtheria incidence to WHO, which provided a maximum of 3,481 potential country-years of data. Although these surveillance data are known to have limitations (17), they represent the most complete existing database for worldwide disease incidence. However, 19% of country-years were missing globally. Missing JRF diphtheria data were not equally distributed among regions. The Africa region had the highest percentage of missing country-years (40%); this percentage included substantial periods of missing data from populous countries, including Nigeria (66% of country-years missing data), Kenya (78%), Uganda (89%), and Ethiopia (100%). The Western Pacific (22%) and Eastern Mediterranean (22%) regions also had an above average proportion of missing country-years. In the remaining regions, 2%–11% of country-years were missing.

We cross-referenced the years and countries with cases in the full review dataset with JRF data. Overall, when data were cross-checked between aggregate JRF data and case data compiled from manuscripts and outbreak reports, we identified 36 instances in which diphtheria data reported through the JRF were inconsistent with those reported in the published literature. In 20 instances, we found case data during the review from countries with missing JRF data for diphtheria in the corresponding year(s); in 7 instances, countries had reported 0 cases for the corresponding year(s); and in 9 additional instances, the number of cases found in the review exceeded the number reported in the JRF.

Vaccination Status of Diphtheria Case-Patients

Analysis showed that 65% of case-patients in the full dataset were unvaccinated, 13% were partially vaccinated, and 22% were vaccinated with ≥3 doses of diphtheria toxoid-containing vaccine. In a sensitivity analysis that

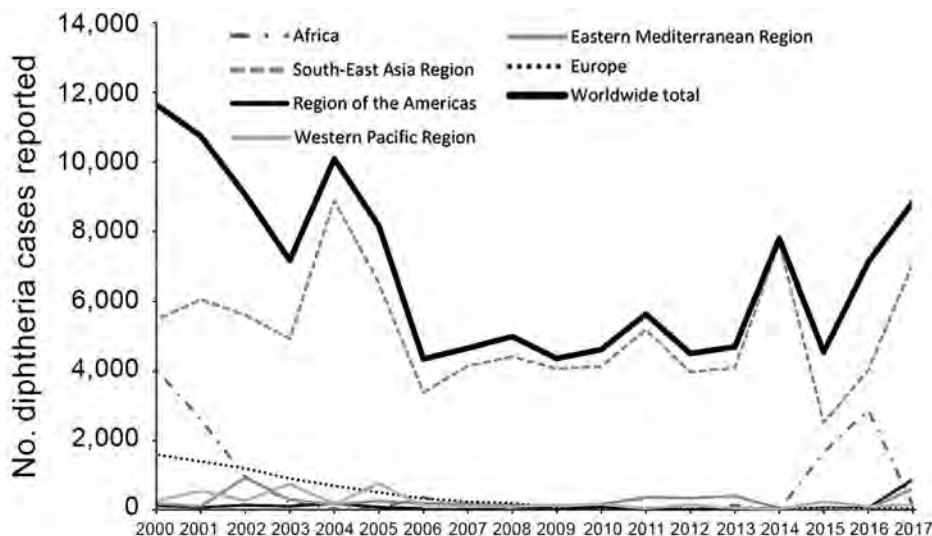


Figure 3. Reported cases of diphtheria per Joint Reporting Form, by World Health Organization region and worldwide, 2000–2017.

only included cases that had more precise data on vaccination status, we found that the proportion of unvaccinated case-patients increased to 72%.

In countries with higher case counts, most case-patients were unvaccinated (Figure 4). Among case-patients with known vaccination status in the full review dataset ($n = 7,242$), 66% were unvaccinated in higher case count countries; this percentage was 73% in the sensitivity analysis restricted to case-patients with precise vaccination status data ($n = 1,534$). Excluding cases from India showed that these percentages were similar (63% in the primary dataset and 66% in the sensitivity analysis dataset). In countries with sporadic incidence, vaccination status of case-patients was more evenly distributed; the largest proportion was in the partially vaccinated category in both the main analysis (46%) and the sensitivity analysis (38%).

Age of Diphtheria Case-Patients

In the dataset overall (15,068 case-patients with age data), 37% of case-patients were ≥ 15 years of age. In a sensitivity analysis of the dataset with more precise age data, we found that 34% were ≥ 15 years of age.

Proportions of case-patients ≥ 15 years of age differed markedly between countries with sporadic incidence and those with higher case counts (Figure 5); this finding was consistent across the primary and sensitivity analyses. In higher case-count countries, there was a lower proportion of cases ≥ 15 years of age when examined in the full dataset (37%) and the dataset with more precise age data (34%). When data from India were further excluded among higher case count countries, there was an even lower proportion of case-patients ≥ 15 years of age in the main dataset (25%) and the dataset with more precise age data (34%). Conversely, in sporadic incidence countries, 66% of the case-patients were ≥ 15 years of age in the full dataset and on sensitivity analysis.

Relationship between Age of Case-Patients and Vaccination Coverage

When we examine the relationship between vaccination coverage with the primary series and age distribution, we found a visible trend toward a higher percentage of case-patients ≥ 15 years of age in countries with higher DTP3 coverage in both the full dataset (Figure 6) and a sensitivity analysis on the dataset with more precise age data. In particular, in almost all countries with DTP3 coverage $>90\%$, $>50\%$ of diphtheria cases occurred among persons ≥ 15 years of age.

Discussion

It is clear from aggregate incidence data that progress in decreasing diphtheria incidence worldwide has stalled, and reported cases have recently increased. Larger societal

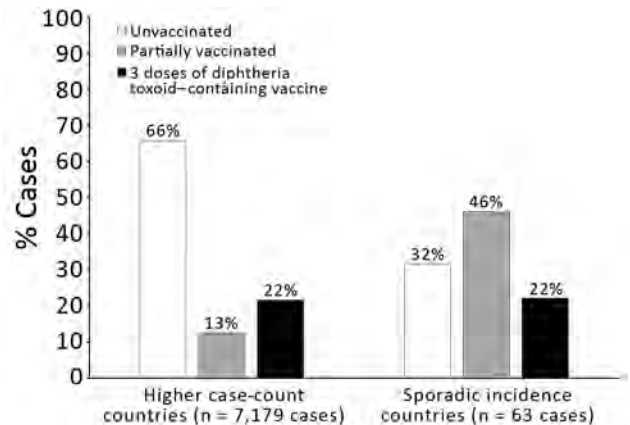


Figure 4. Vaccination status of diphtheria cases in higher case count versus sporadic incidence countries (full dataset, 34 countries), 2000–2017.

factors, such as population migration or political instability, can create conditions favorable to an outbreak; the largest recent outbreaks (January 2016–February 2019) were reported in the Rohingya refugee population in Bangladesh (8,403 cases), as well as areas experiencing conflict or social disruption, such as Yemen (3,340 cases) and Venezuela (2,512 cases) (19). The South-East Asia region has reported most of the diphtheria cases since 2000, which might be caused by the large populations of several countries in the region that have endemic disease. However, incomplete data from other regions could be obscuring additional major foci of disease incidence. Global and regional trends can be shaped by incomplete data, including years of nonreporting or underreporting by populous and high-incidence countries.

The diphtheria data reported annually to WHO and UNICEF on the JRF have substantial limitations in terms of quality and reflect opportunities to improve disease surveillance. We found these data to be incomplete when

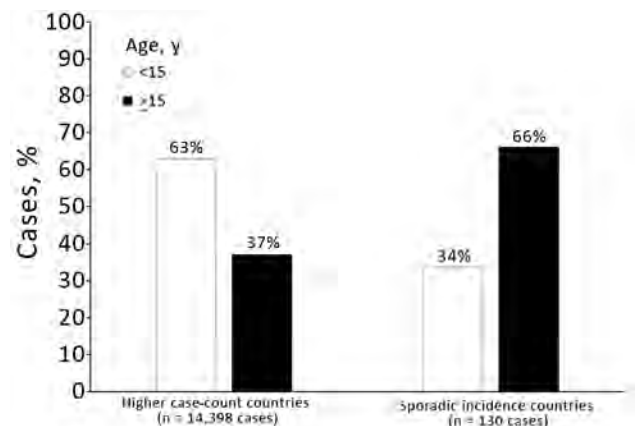


Figure 5. Proportion of diphtheria case-patients <15 years and ≥ 15 years of age in higher case count versus sporadic incidence countries (full dataset, 34 countries), 2000–2017.

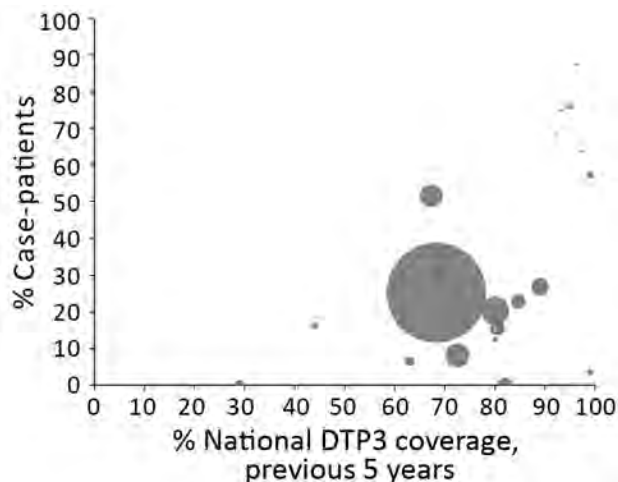


Figure 6. Percentage of diphtheria case-patients ≥ 15 years of age, by national DTP3 coverage, 2000–2017. Each circle represents a country, and its size is proportionate to the average number of cases reported from the country per year of data in the dataset. The largest data point represents a large number of cases in a single year among Rohingya refugees from Myanmar. The vaccination coverage of the Rohingya population is unknown; therefore, the average of DTP3 coverage of Rakhine State in Myanmar from 2016–2017 was used (18). DTP3, diphtheria–tetanus–pertussis vaccine; UNICEF, United Nations Children’s Fund; WHO, World Health Organization.

cross-referenced with the literature, indicating a likely underestimate of incidence worldwide and a decreased understanding of the burden of disease. However, in some countries with lower laboratory capacity, only a small proportion of cases are laboratory confirmed, which could result in overreporting in some settings (19). The ability to use aggregate data for action is limited by the lack of key variables, including vaccination status, age, and subnational location.

Implementation of case-based surveillance for diphtheria, combined with availability of subnational coverage data, would result in improved understanding of diphtheria epidemiology and enhanced capability to prevent and respond to outbreaks. A 2017 gap analysis of diphtheria diagnostic capacity in the European Union found substantial gaps, including lack of sufficient laboratory systems with methods to determine toxigenicity, difficulty obtaining primary media culture, and challenges to obtaining diphtheria antitoxin for both laboratory diagnosis and clinical management of cases (20). Similar assessments are currently being conducted to more fully understand the scope of challenges in other regions (A. Efstratiou, National Infection Service, London, UK, pers. comm., 2019 Aug 1). Worldwide, only 55 countries report conducting national, case-based surveillance for diphtheria with laboratory confirmation (9). In response to the limitations of current disease surveillance systems, WHO has released

new comprehensive surveillance recommendations (21). For diphtheria, immediate investigation and collection of case-based data are recommended for all outbreaks. These guidelines provide a set of recommended minimum data elements to collect, as well as recommended analyses and uses of data collected. These standards represent an opportunity to improve and standardize available data with widespread implementation but will require investments in both surveillance and laboratory capacity.

Accounts of outbreaks in the peer-reviewed literature, gray literature, presentations, and other reports were compiled as the best available sources of information on case-patient age and vaccination status. When examining these data, we found that most diphtheria cases occur in unvaccinated persons, particularly in countries with higher case counts where most disease is among children < 15 years of age. Therefore, achieving adequate coverage with the primary series is urgently needed. Ensuring high primary series coverage is especially useful in the context of vaccine hesitancy, which has wide variability among countries and regions (22). DTP3 coverage worldwide has stagnated at 84%–85% since 2010 (23), and improving this coverage through increased equity of and access to routine immunization services is key to the efforts to combat diphtheria. Countries with sporadic incidence of diphtheria have a more even distribution of vaccination status among cases. Age data from these countries also reflect a higher proportion of cases in the adolescent and adult populations. The predominance of older case-patients in these countries, taken together with the higher proportion of case-patients who have received, at a minimum, 3 doses of diphtheria-containing vaccine in infancy, indicate that waning immunity is also a major issue. This issue can be addressed through widespread adoption of the 3 diphtheria toxoid-containing booster doses recommended in 2017 by WHO and recently approved as a future investment in the 2021–2025 Gavi Vaccine Investment Strategy (24).

In our dataset, as vaccination coverage in a country increased, the percentage of case-patients ≥ 15 years of age also increased. This increase in the proportion of older case-patients is not unique to diphtheria because similar changes have been seen in the epidemiology of other vaccine-preventable diseases as coverage increased (25). This finding indicates that the large proportion of case-patients ≥ 15 years of age in countries with sporadic incidence probably represents a proportional, rather than an absolute, increase because high vaccination coverage in childhood resulted in fewer susceptible persons in this age group. Many adults might have grown up during a time when no or fewer booster doses were given, although information on historical changes to vaccination schedules is incomplete. As countries implement or modify booster dose schedules according to the new WHO recommendation, data on booster

dose coverage would improve understanding of susceptibility to disease in different age groups.

Limitations of this analysis include heterogeneous methods used by available sources to aggregate data on case-patient age and vaccination status. Because the available data might not be representative, findings might not be generalizable to all contexts. Because of lack of laboratory capacity in some settings, many cases in the literature are not confirmed by culture. Strengths of the analysis include the compilation of all known available data on the age and vaccination status of diphtheria case-patients, which highlight that data from published disease outbreaks are a useful resource for describing epidemiologic changes and to triangulate with other existing data sources. Limitations of the dataset were addressed as comprehensively as possible through sensitivity analyses of subsets of cases with more precise data to validate trends observed on analysis of the full dataset.

In light of a recent increase in reported cases, action is needed to make progress in combating diphtheria. However, many national immunization schedules lag behind current recommendations, and the lack of case-based diphtheria data limits the ability to take targeted action. Intensified efforts to improve routine immunization coverage with DTP3 and to implement recommended booster doses would help to decrease diphtheria cases by both decreasing the susceptibility of children and addressing the problem of waning immunity among adolescents and adults. Implementing new WHO guidelines (21) would result in case-based diphtheria surveillance data with laboratory confirmation that could be analyzed by using standardized age categories. This implementation would greatly enhance available data and highlights the need for enhanced laboratory capacity to provide these case confirmations, particularly in countries with endemic disease and other lower-middle-income and low-income countries. Increased availability of booster dose coverage data, subnational coverage data, and more complete historical records of changes to immunization schedules would lend context to data on incidence and epidemiologic trends. An improvement in the quality and consistency of data collected on diphtheria would create a stronger evidence base for future research, timely interventions, and recommendations to combat this deadly disease.

Acknowledgments

We thank Steve Cochi, Eric Mast, and Peter Bloland for providing early conceptual contributions to the analysis; Nita Patel for assistance with abstract review; and Howard Gary and Qian An for providing thoughtful feedback on appropriate analytic methods. We also thank international organizations and colleagues for sharing available data from individual outbreak responses to better inform this global analysis.

About the Author

Dr. Clarke is a medical epidemiologist in the Division of Global Immunization, Center for Global Health, Centers for Disease Control and Prevention, Atlanta, GA. Her primary research interest is global child health, especially how the quality and use of data on immunization rates and vaccine-preventable disease incidence can be leveraged and improved to optimize the health of children.

References

- Zakikhany K, Efstratiou A. Diphtheria in Europe: current problems and new challenges. *Future Microbiol.* 2012;7:595–607. <https://doi.org/10.2217/fmb.12.24>
- World Health Organization. World Health Organization expanded programme on immunization. WHA2757. Geneva: The Organization; 1974. p. 28–9.
- Galazka A. Implications of the diphtheria epidemic in the Former Soviet Union for immunization programs. *J Infect Dis.* 2000;181(Suppl 1):S244–8. <https://doi.org/10.1086/315570>
- Galazka A. The changing epidemiology of diphtheria in the vaccine era. *J Infect Dis.* 2000;181(Suppl 1):S2–9. <https://doi.org/10.1086/315533>
- Golaz A, Hardy IR, Strebel P, Bisgard KM, Vitek C, Popovic T, et al. Epidemic diphtheria in the Newly Independent States of the Former Soviet Union: implications for diphtheria control in the United States. *J Infect Dis.* 2000;181(Suppl 1):S237–43. <https://doi.org/10.1086/315569>
- Dravid MN, Joshi SA. Resurgence of diphtheria in Malegaon and Dhule regions of north Maharashtra. *Indian J Med Res.* 2008;127:616–7.
- Landazabal García N, Burgos Rodríguez MM, Pastor D. Diphtheria outbreak in Cali, Colombia, August–October 2000. *Epidemiol Bull.* 2001;22:13–5.
- Dandinarsaiah M, Vikram BK, Krishnamurthy N, Chetan AC, Jain A. Diphtheria re-emergence: problems faced by developing countries. *Indian J Otolaryngol Head Neck Surg.* 2013;65:314–8. <https://doi.org/10.1007/s12070-012-0518-5>
- World Health Organization. JRF supplementary questionnaire on surveillance. Geneva: The Organization; 2018 [cited 2018 Oct 20]. https://www.who.int/immunization/monitoring_surveillance/burden/vpd/JRF_Supplementary_Questionnaire_Surveillance_18Mar.pdf
- World Health Organization. Reported immunization schedules by vaccine. Geneva: The Organization; 2018 [cited 2018 Oct 20]. http://www.who.int/immunization/monitoring_surveillance/data
- European Centre for Disease Prevention and Control. Vaccine Scheduler: vaccine schedules in all countries of the European Union. Stockholm: The Centre; 2018 [cited 2018 Oct 20]. <https://vaccine-schedule.ecdc.europa.eu>
- World Health Organization. Immunization provided at school. Geneva: The Organization; 2017 [cited 2018 Oct 20]. http://www.who.int/immunization/monitoring_surveillance/data
- World Health Organization. Reported estimates of DTP4 coverage. Geneva: The Organization; 2018 [cited 2018 Aug 29]. http://apps.who.int/immunization_monitoring/globalsummary/timeseries/tscoveredtp4.html
- World Health Organization. Diphtheria vaccine: WHO position paper—August 2017. Geneva: The Organization; 2017 [cited 2019 Jul 16]. https://www.who.int/immunization/policy/position_papers/diphtheria
- World Health Organization. Tetanus vaccines: WHO position paper—February 2017. Geneva: The Organization, 2017 [cited 2019 Jul 16]. https://www.who.int/immunization/policy/position_papers/tetanus

16. World Health Organization. WHO–UNICEF estimates of DTP3 coverage 1980–2017. Geneva: The Organization; 2018 [cited 2018 Oct 20]. http://apps.who.int/immunization_monitoring/globalsummary/timeseries/tswucoveredtp3.html
17. MacNeil A, Dietz V, Cherian T. Vaccine preventable diseases: time to re-examine global surveillance data? *Vaccine*. 2014;32:2315–20. <https://doi.org/10.1016/j.vaccine.2014.02.067>
18. Bahl S, editor. Diphtheria outbreak response—Cox’s Bazar, Bangladesh. World Health Organization Strategic Advisory Group of Experts. Geneva: The Organization; 2018 [cited 2019 Jul 16]. <http://www.searo.who.int/bangladesh/reportdiph>
19. Hadler SC, Acosta A, Tiwari T, Patel M, editors. Diphtheria: a re-emerging threat in countries affected by conflict, migration, and social disruption. Atlanta: Emory University; 2019.
20. European Centre for Disease Prevention and Control. Gap analysis on securing diphtheria diagnostic capacity and diphtheria antitoxin availability in the EU/EEA. Stockholm: The Centre; July 2017 [cited 2019 May 21]. <https://ecdc.europa.eu/en/publications-data/gap-analysis-securing-diphtheria-diagnostic-capacity-and-diphtheria-antitoxin>
21. World Health organization. WHO–recommended standards for surveillance of selected vaccine-preventable diseases. Geneva: The Organization; 2014. p. 10–2 [cited 2018 Oct 20]. https://www.who.int/immunization/monitoring_surveillance/burden/vpd/WHO_SurveillanceVaccinePreventable_04_Diphtheria_R2.pdf
22. Larson HJ, de Figueiredo A, Xiaohong Z, Schulz WS, Verger P, Johnston IG, et al. The state of vaccine confidence 2016: global insights through a 67-country survey. *EBioMedicine*. 2016;12:295–301. <https://doi.org/10.1016/j.ebiom.2016.08.042>
23. VanderEnde K, Gacic-Dobo M, Diallo MS, Conklin LM, Wallace AS. Global routine vaccination coverage—2017. *MMWR Morb Mortal Wkly Rep*. 2018;67:1261–4. <https://doi.org/10.15585/mmwr.mm6745a2>
24. Gavi. Gavi board starts framing alliance’s approach to 2021–2025 period. Geneva: Gavi; 2018 [cited 2018 Nov 29]. <https://www.gavi.org/library/news/press-releases/2018/gavi-board-starts-framing-alliance-s-approach-to-2021-2025-period>
25. Durrheim DN, Crowcroft NS, Strebel PM. Measles: the epidemiology of elimination. *Vaccine*. 2014;32:6880–3. <https://doi.org/10.1016/j.vaccine.2014.10.061>

Address for correspondence: Kristie E.N. Clarke, Centers for Disease Control and Prevention, 1600 Clifton Rd NE, Mailstop A04, Atlanta, GA 30329-4027, USA; email: kclarke2@cdc.gov

EID Podcast

Tickborne *Ehrlichia* in North Carolina

While caring for patients in North Carolina, Dr. Ross Boyce began to suspect that tickborne *Ehrlichia* was being underdiagnosed. His study showed that *Ehrlichia*, despite being relatively common, was only tested for in about a third of patients thought to have a tickborne illness.

In this EID podcast, Dr. Ross Boyce, an infectious disease physician at the University of North Carolina at Chapel Hill, examines the prevalence and diagnosis of *Ehrlichia* in North Carolina.

Visit our website to listen: <https://go.usa.gov/xy6UH> **EMERGING
INFECTIOUS DISEASES**

Economic Burden of West Nile Virus Disease, Quebec, Canada, 2012–2013

Najwa Ouhoumane, Eric Tchouaket, Anne-Marie Lowe, Ann Fortin, Dahlia Kairy, Anne Vibien, Jessica Kovitz-Lensch, Terry-Nan Tannenbaum,¹ François Milord

The economic burden of West Nile virus (WNV) infection is not known for Canada. We sought to describe the direct and indirect costs of WNV infection in the province of Quebec, Canada, up to 2 years after onset of signs and symptoms. We conducted a retrospective cohort study that included WNV cases reported during 2012 and 2013. For 90 persons infected with WNV, persons with encephalitis accounted for the largest proportion of total cost: a median cost of \$21,332 per patient compared with \$8,124 for West Nile meningitis ($p = 0.0004$) and \$192 for West Nile fever ($p < 0.0001$). When results were extrapolated to all reported WNV patients, the estimated total cost for 124 symptomatic cases was ≈\$1.7 million for 2012 and that for 31 symptomatic cases was ≈\$430,000 for 2013. Our study provides information for the government to make informed decisions regarding public health policies and infectious diseases prevention and control programs.

West Nile virus (WNV) infection is endemic to North America. More than 41,000 cases of WNV-related illnesses and 2,000 deaths were reported in the United States between the introduction of the virus in 1999 and 2015 (1). During the same period, 5,310 cases were reported in Canada (2). In Quebec, the first cases were documented in 2002. After a quiet period (2004–2010), this province experienced an outbreak in 2012 (124 symptomatic cases);

Author affiliations: Institut National de Santé Publique du Quebec, Quebec City, Canada (N. Ouhoumane, A. Fortin, F. Milord); Université du Quebec en Outaouais, Gatineau, Quebec, Canada (E. Tchouaket); Public Health Agency of Canada, Montreal, Quebec, Canada (A.-M. Lowe); Université de Montreal, Montreal (D. Kairy); Centre de Recherche Interdisciplinaire en Réadaptation du Montreal Métropolitain, Montreal (D. Kairy); Centre Intégré de Santé et de Services Sociaux de la Montérégie Est-Hôpital Honoré Mercier, St.-Hyacinthe, Quebec, Canada (A. Vibien, J. Kovitz-Lensch); Institut National de Santé Publique de Montreal, Montreal (T.-N. Tannenbaum); Université de Sherbrooke, Sherbrooke, Quebec, Canada (F. Milord)

DOI: <https://doi.org/10.3201/eid2510.181608>

since 2013, the number of cases has remained stable (average of 30 cases/year) (3).

WNV causes an asymptomatic infection in 80% of cases, but in <1% of cases, a severe illness occurs with neurologic involvement, such as aseptic meningitis, encephalitis, or acute flaccid paralysis (4,5). WNV infection and particularly neurologic disease have been associated with mild to severe clinical manifestations, might require hospitalization, and lead to long-term sequelae and death (6).

To date, 3 studies in the United States have estimated the economic burden of WNV disease (7–9). These estimates can be used in assessing the cost-effectiveness of various interventions designed to decrease WNV disease risk (8). In the province of Quebec, Canada, a cost-effectiveness analysis was conducted during 2006 (10). However, this study was based on a hypothetical simulation of 2 scenarios (high activity of the virus versus low-activity season); therefore, the cost estimations could be speculative. Thus, in Canada, no data are available on the actual costs of WNV disease, and results from the United States cannot be extrapolated because of differences in the organization of the healthcare systems and costs, WNV disease prevention programs, mean income, and standards of living. Furthermore, exchange rate differences do not accurately reflect real differences in purchasing power (11). The objective of this study was to estimate direct and indirect costs of WNV disease cases in the province of Quebec, Canada, up to 2 years after symptom onset.

Materials and Methods

Study Population

WNV infection is a reportable disease in Quebec. Physicians and laboratories must report all WNV-positive cases to regional public health boards, which conduct epidemiologic investigations to document the infection; determine the likely place of acquisition; and collect sociodemographic and clinical information, such as date of illness

¹Deceased.

onset and clinical syndrome (i.e., uncomplicated fever, meningitis, encephalitis, and acute flaccid paralysis). The data are entered into the integrated system for public health monitoring of West Nile virus, a provincial electronic surveillance system for WNV disease that includes information on humans, mosquitoes, and animals (12). During 2012–2013, a total of 155 symptomatic WNV cases were reported in Quebec.

We asked regional public health boards to contact each of the case-patients to see whether they were willing to participate in a study. A research nurse obtained written consent from all eligible case-patients to participate in a telephone interview and to enable access to their medical charts. Consent was obtained from parents or family of patients who were <18 years of age and for patients who had died. More details on the methods are available in a previous article (6). The study protocol was submitted to the public health research ethics board of the Institut National de Santé Publique du Québec, which provided a favorable recommendation for the study (13).

Case Definitions

A WNV-positive case includes a laboratory diagnosis of WNV infection by IgM capture enzyme immunoassays for either serum or cerebrospinal fluid samples. In Quebec, after a first IgM-positive case has been confirmed by using a plaque reduction neutralization test, all other IgM-positive cases in the same season are considered to be laboratory confirmed. Cases are further classified according to their clinical manifestations: West Nile fever (WNF, an acute systemic febrile illness), West Nile meningitis (WNM, with stiff neck and cerebrospinal fluid pleocytosis), West Nile encephalitis (WNE, with altered mental status), West Nile meningoencephalitis, and acute flaccid paralysis (AFP, polio-like myelitis, or Guillain-Barré syndrome) (14).

Data Collection

For all eligible patients, we administered a telephone questionnaire 24 months after sign or symptom onset to document medical service, productivity losses, and expenses up to 2 years after the acute phase of WNV disease. We developed the questionnaire on the basis of the study by Staples et al. (8). Participants were asked to document the following items related to their WNV disease after initial hospitalization or consultation: subsequent hospitalization, stay in a

rehabilitation center, physiotherapy, occupational therapy, speech therapy, home care, primary care physician consultations, neurologist consultations, medications, medical equipment, recruitment for household chores, and all other personal expenses incurred by the WNV disease. We also considered time off from work for the patient and for family members (to care for the patient). For hospitalized patients, we obtained data for hospital stay, intensive care unit admission, and inpatient rehabilitation from medical records.

Costs Estimation

We based the estimation of costs on the principle of human capital and a societal perspective (relevant costs regardless of who paid) (15). For their initial care, eligible patients either were hospitalized (n = 71), were seen in an emergency department but not hospitalized (n = 10), or consulted with doctor in a clinic (n = 12). For the third group, we did not collect any costs associated with their initial care.

Hospitalization

We obtained costs for initial hospitalization (no subsequent hospitalization was reported) by using the All Patient Refined–Diagnosis-Related Groups (APR-DRG) and the relative use of resources. The APR-DRG provides average costs incurred for inpatient services. These costs include all inpatient allied healthcare, surgical and medical procedures, medication, and laboratory tests. Because permission to access individual costs data was not obtained, we created 19 groups of patients on the basis of 4 criteria: the principal diagnosis of each patient (by using the International Classification of Diseases, 10th Revision), patient's age (<60 vs. ≥60 years of age), admission to intensive care unit (yes or no), and diagnostic year (2012 or 2013). Nearly 60% of hospitalized participants had specific principal International Classification of Diseases, 10th Revision, diagnosis code of WNV (A923) (Table 1). For other participants with no specific principal diagnosis code of WNV, WNV infection had to be coded as secondary diagnosis in the APR-DRG database to ensure specificity. The mean and median costs in the APR-DRG for each group were attributed to each patient in the group.

Inpatient Rehabilitation

Cost for inpatient rehabilitation was based on the average daily cost of services in a rehabilitation center for physical

Table 1. Principal diagnoses for 71 hospitalized case-patients with West Nile virus infection, Quebec, Canada*

Principal diagnosis	ICD-10 code	No. (%) patients
West Nile virus infection	A923	42 (59)
Viral meningitis, unspecified	A879	16 (23)
Viral infection, unspecified	B349	7 (10)
Unspecified viral encephalitis	A86	3 (4)
Guillain-Barré syndrome	G610	2 (3)
Headache	R51	1 (1)

*ICD-10, International Classification of Diseases, 10th Revision.

disabilities in 2012–2013. This factor was multiplied by the number of days spent in a center, which was obtained from the medical record.

Emergency Department Consultations

For patients seen in an emergency department, the physician service claims database was used to estimate the cost of medical consultations in the emergency department (Canadian \$109.90) (16). This rate includes only the physician remuneration. Costs associated with emergency department stays and laboratory examinations and accommodations were not included.

Medical and Paramedical Care up to 2 Years after Sign/Symptom Onset

During the telephone interview, patients were asked to provide information on types and numbers and duration of outpatient medical and paramedical services that they sought after the acute-care period. We obtained estimated costs for these services by multiplying type-specific cost estimates by the number of visits reported (Table 2) (16). The number of follow-up physician visits was missing for 2 participants; a minimum of 1 visit was used for those case-patients.

Medical Equipment

Patients were asked about the acquisition of specific equipment and associated costs. Costs were assigned a value of 0 if the equipment was provided by government or was borrowed.

Recruitment for Household Chores

We obtained information for patients who needed aids for household chores. We also asked them to provide associated costs.

Absence from Work

We obtained information about missed workdays by patients or family members to care for a patient. Patients or family members having a job at the time of their WNV infection were asked to provide their occupation, the number of days they worked per week, and the number of days they missed work (including hospital stay).

Income data for each patient or family member were obtained from the wage guide by occupation in Quebec according to their occupation. Productivity losses were estimated by multiplying the time taken off work by a weekly wage.

Occupation data were missing for 2 patients and 2 family members. For these 4 persons, we used the minimum wage. One patient reported stopping work because of his WNV infection. For this patient, we estimated the associated cost as the number of potential years of lost employment (65 minus age at infection). All persons (n = 11) who died during their initial hospitalization were ≥ 65 years of age. Therefore, productivity losses caused by death were not taken into account.

Other Personal Expenses

Patients were asked about other costs that they had to assume. For ambulance transportation, the basic cost of Canadian \$125 was used.

Data Analysis

For data analysis, we combined West Nile meningoencephalitis cases (n = 18) and AFP cases (n = 2) with WNE cases (n = 28) because of similar clinical manifestations; 1 case with missing information about clinical syndrome was excluded. All analyses were performed according to 3 clinical categories (WNF, WNM, and WNE). We compared proportions by using the χ^2 test or Fisher exact test when appropriate. We compared distributions of age and hospital stay by using nonparametric tests (Wilcoxon rank-sum or Kruskal-Wallis tests).

Because cost distributions were not normal, we calculated mean and median values with the interquartile range (IQR). In this study, participants and nonparticipants were comparable with regard to demographic and illness severity (see Results). Thus, we assumed that participants were representative of the total number of WNV cases during 2012 and 2013, and we extrapolated estimated costs to all reported WNV cases according to clinical syndrome, cost category, and year. For each category, we estimated total number of cases (except for hospitalization, for which the exact number of cases was known) and total cost. For example, the total number of

Table 2. Physician service claims billing codes and costs for outpatient paramedical services, Quebec, Canada, 2012–2013*

Medical/paramedical service	Régie de l'Assurance maladie du Québec billing code	Patient age, y: rate in 2014/visit
Primary care physician visit	08874	<60: \$40.00
	00074	60–69: \$42.05
	08879	70–79: \$48.60
	08881	≥ 80 : \$50.80
Neurologist visit	09162: initial visit	\$70.60
	09164: control visit	\$40.00
Physiotherapy, occupational and speech therapy	None	\$79.00
Home care	09171	\$44.00

*Costs are in Canadian dollars.

WNE case-patients admitted to inpatient rehabilitation (N_t) = total number of WNE case-patients \times proportion of WNE case-patients admitted to inpatient rehabilitation. The total cost for this category = $N_t \times C_p$, in which C_p is the inpatient rehabilitation median costs per WNE case-patient.

We performed analyses by using SAS version 9.1 (SAS Institute Inc., <https://www.sas.com>). A 2-sided $p < 0.05$ was considered statistically significant.

Results

Of the 155 symptomatic WNV patients during 2012–2013, a total of 93 (60%) agreed to participate in the study, but 2 of them could not be reached for the telephone interview and 1 with missing information about clinical syndrome was excluded from analyses. Medical records were available for 81 (87%) patients (71 hospitalizations and 10 emergency department visits). Participants and nonparticipants were comparable with regard to demographics (except for sex; more women agreed to participate [54% vs. 36%; $p = 0.026$]) and illness severity (hospitalization, clinical syndrome, and death).

Demographic and Clinical Characteristics

We obtained demographic and clinical characteristics of patients (Table 3). For 90 patients, WNF accounted for 27%, WNM 20%, and WNE 53%. Patients with WNE were significantly older than patients with WNM or WNF; 71% of WNE patients were ≥ 60 years of age compared with 22% of WNM patients and 29% of WNF patients ($p < 0.0001$). Most patients with neurologic syndrome were hospitalized. The median hospital stay was longer for WNE patients than for WNM patients ($p < 0.0001$) or WNF patients ($p = 0.010$). Ten (21%) WNE patients and 1 (6%) WNM patient died during hospitalization. In addition, 3 WNE patients, 2 who were discharged to home with support and 1 requiring rehabilitation services, died during the follow-up period, but their deaths were not considered to be directly related to WNV infection.

Use of Medical and Paramedical Services and Absence of Work

We obtained data for use of medical and paramedical services up to 2 years after the acute phase of WNV disease (Table 4). When we excluded in-hospital deaths, the most common services used by participants were physician visits (66%), followed by medications (41%) and neurologist visits (26%). In general, WNE and WNM patients used more services and WNM participants needed more physician ($p = 0.016$) and neurologist ($p = 0.029$) visits. Six WNE patients were admitted to rehabilitation (median length of stay 75 days, range 30–120 days). Most patients who had a job missed work because of their infection (median absence 60 days, range 5–365 days).

Although 41% of patients reported outpatient medication expenses, they could not accurately recall the names and amounts of medication taken. Therefore, we did not compute medication costs.

Direct and Indirect Costs

We determined direct and indirect costs according to illness severity (Table 5). WNE patients accounted for the largest proportion of total cost (median cost \$21,332, IQR \$12,131–\$28,101) per participant compared with \$8,124 (IQR \$4,025–\$13,631) for WNM patients ($p = 0.0004$) and \$192 (IQR \$20–\$5,359) for WNF patients ($p < 0.0001$). For WNE patients, costs were attributable mostly to hospitalization, which accounted for 65% of the total cost, followed by inpatient rehabilitation (20%). For WNM patients, indirect costs (47%), followed by hospitalization (38%), contributed to the largest proportion of total costs. For WNF patients, hospitalization (44%) and indirect costs (44%) contributed to the same proportion of total cost. Median indirect costs were significantly higher for WNM patients than for WNE ($p = 0.004$) or WNF ($p = 0.0005$) patients. Physician visit costs were also significantly higher for WNM patients than for WNE ($p = 0.041$) or WNF ($p = 0.038$) patients.

Table 3. Demographic and clinical characteristics of 90 WNV patients by clinical syndrome, Quebec, Canada, 2012–2013*

Characteristic	WNF, n = 24	WNM, n = 18	WNE, n = 48†
Age group, y			
<50	7 (29)	7 (39)	6 (12)
50–59	10 (42)	7 (39)	8 (17)
≥ 60	7 (29)	4 (22)	34 (71)
Sex			
M	7 (29)	8 (44)	24 (50)
F	17 (71)	10 (56)	24 (50)
Hospitalization	5 (21)	17 (94)	47 (98)
Days hospitalized, median (range)	4 (2–12)	4 (1–36)	12 (3–663)
Intensive care	0	0	22/47 (47)
Complications	0	3/17 (18)	21/47 (45)
Death in hospital	0	1/17 (6)	10/47 (21)

*Values are no. (%) or no. occurrences/no. hospitalized (%) unless otherwise indicated. WNE, West Nile encephalitis; WNF, West Nile fever; WNM, West Nile meningitis; WNV, West Nile virus.

†Includes WNE (n = 28), meningoencephalitis (n = 18), and acute flaccid paralysis (n = 2).

Table 4. Characteristics for 79 WNV patients needing medical and paramedical services and other expenses by clinical syndrome ≤ 2 y after the acute phase of infection Quebec, Canada, 2012–2013*

Characteristic	WNF, n = 24	WNM, n = 17	WNE, n = 38†
Inpatient rehabilitation			
No. (%)	0	1 (6)	6 (13)
No. days, median (range)	0	21	75 (30–120)
Physiotherapy			
No. (%)	2 (8)	3 (18)	6 (16)
No. visits, median (range)	20‡	28 (8–48)‡	32 (24–48)
Occupational therapy			
No. (%)	0	0	4 (11)
No. visits, median (range)	0	0	24 (3–32)
Speech therapy			
No. (%)	0	0	3 (8)
No. visits, median (range)	0	0	3 (1–3)
Home care			
No. (%)	1 (4)	0	2 (5)
No. hours, median (range)	1	0	2 (1–3)
Primary care physician visits			
No. (%)	15 (63)	12 (71)	25 (66)
No. visits, median (range)	2 (1–12)	4 (2–18)	2 (1–12)
Neurologist visits			
No. (%)	1 (4)	6 (35)	14 (37)
No. visits, median (range)	1	3 (2–4)	1 (1–4)
Medications			
No. (%)	7 (29)	10 (59)	15 (39)
Medical equipment			
No. (%)	1 (4)	1 (6)	6 (16)
No. using equipment, median (range)	3	2	2 (1–3)
Household chores			
No. (%)	0	0	2 (5)
Absence from work among workers			
No. (%)	6/8 (75)	15/15 (100)	16/16 (100)
No. days, median (range)	21 (5–60)	60 (7–180)	90 (30–365)§
Absence from work to care for a patient			
No. (%)	1 (4)	8 (47)	10 (26)
No. days, median (range)	3	5 (2–14)	7 (1–60)
Other personal expenses			
No. (%)	5 (21)	11 (65)	26 (68)

*WNE, West Nile encephalitis; WNF, West Nile fever; WNM, West Nile meningitis; WNV, West Nile virus.

†Includes WNE (n = 19), meningoencephalitis (n = 18), and acute flaccid paralysis (n = 1).

‡Visits number missing for 1 participant.

§Excluding 1 participant who reported stopping work because of his WNV infection.

During 2012, a total of 124 symptomatic WNV patients were reported in the province of Quebec, and during 2013, a total of 31 symptomatic WNV patients were reported. Based on our study, the estimated total cost of these cases was \approx \$1.7 million for 2012 and \approx \$430,000 for 2013. We determined the estimated total cost by category (Table 6). For both years, WNF accounted for $<5\%$ of the total, and WNM accounted $<10\%$ of the total, and WNE accounted for $>85\%$ of extrapolated costs.

Discussion

In this study, we estimated direct and indirect costs of WNV disease cases in Quebec, Canada, up to 2 years after the acute phase of WNV disease. We found that costs varied considerably according to disease manifestations. Patients with WNE accounted for the largest proportion of the total cost, which could be attributable mainly to their worse hospital course, including severe clinical manifestations, longer stay in the hospital, admission to

the intensive care unit, and complications (6). When we compared WNM with WNE patients, we found that WNE patients had lower indirect costs (absence from work), which could be explained by their older age ($\approx 70\%$ were retired at the time of their WNV infection vs. only 17% of patients with WNM).

Although most WNM patients were hospitalized, hospital costs accounted for only 38% of the total cost. WNM is generally associated with a favorable outcome and shorter hospital stay. However, in our study, WNM patients required more physician visits after hospitalization than patients with WNE or WNF. WNF patients accounted for only 3% of the total cost, which was mostly associated with the 5 hospitalized case-patients. For these patients, the median cost of hospitalization was similar to that for the 17 hospitalized WNM patients ($p = 0.901$) (Table 7). In our previous study (6), we showed that hospitalized WNF patients had similar demographic and clinical profiles as WNE patients, and we assumed that

Table 5. Economic costs for 90 patients with WNV diseases by clinical syndrome, Quebec, Canada, 2012–2013*

Cost	WNF, n = 24	WNM, n = 18	WNE, n = 48†
Direct			
Mean (SD)	1,113 (2,048)	5,794 (7,625)	26,085 (28,363)
Median (IQR)	151 (20–685)	2,699 (2,483–7 703)	15,963 (7,881–28,065)
Total	27,271	106,167	1,257,249
Hospital			
Mean (SD)	892 (1,930)	4,221 (3,682)	19,259 (17,488)
Median (IQR)	0 (0–0)	2,333 (2,295–5,604)	15,839 (7,603–27,931)
Total	21,401	75,977	924,447
Emergency department visits			
Mean (SD)	55 (110)	110 (110)	110 (110)
Median (IQR)	55 (0–110)	110 (110–110)	110 (110–110)
Total	1,319	1,978	5,275
Inpatient rehabilitation			
Mean (SD)	0	1,019 (4,323)	6,004 (18,120)
Median (IQR)	0	0 (0–0)	0 (0–0)
Total	0	18,340	288,209
Outpatient readaptation‡			
Mean (SD)	74 (323)	289 (1,052)	480 (1,320)
Median (IQR)	0 (0–0)	0 (0–0)	0 (0–0)
Total	1,780	5,194	23,068
Physician visits§			
Mean (SD)	74 (106)	180 (185)	89 (124)
Median (IQR)	41 (0–93)	126 (0–277)	60 (0–136)
Total	1,781	3,242	4,279
Additional costs¶			
Mean (SD)	41 (104)	80 (66)	250 (673)
Median (IQR)	0 (0–0)	100 (0–100)	100 (0–100)
Total	990	1,435	11,971
Indirect costs (absence from work)#			
Mean (SD)	896 (2,198)	5,169 (6,116)	3,454 (9,101)
Median (IQR)	0 (0–556)	2,550 (650–9,000)	0 (0–3,374)
Total	21,506	93,042	165,772
Total costs			
Mean (SD)	2,009 (2,904)	10,963 (9,072)	29,539 (31,067)
Median (IQR)	192 (20–5,359)	8,124 (4,025–13,631)	21,332 (12,131–28,101)
Total	48,777	199,209	1,423,021

*Costs are in Canadian dollars. Total costs are the sum of all category costs. Mean and median costs are expressed as per-patient cost for all participants (including patients with 0 costs). Total is the costs sum for all participants. IQR, interquartile range; WNE, West Nile encephalitis; WNF, West Nile fever; WNM, West Nile meningitis; WNV, West Nile virus.

†Includes WNE encephalitis (n = 28), meningoencephalitis (n = 18), and acute flaccid paralysis (n = 2).

‡Includes physiotherapy, occupational therapy, speech therapy, and home care costs.

§Includes primary care physician and neurologist consultations costs.

¶Includes medical equipment purchase, recruitment for household chores costs, and other personal expenses.

#Includes participants' and families' missed work costs.

some of them could have undetected mild neuroinvasive disease because 3 of 5 hospitalized WNF patients did not have a lumbar puncture. However, half of WNF patients had consulted only a clinic, and costs associated with their initial care were not available. Thus, the total WNF costs could be underestimated.

These results are similar to those reported by Staples et al. (8), who estimated the initial and 5 years post-WNV infection costs among hospitalized patients in Colorado, USA, during 2003. These authors reported that initial costs were higher for AFP and WNE patients, and long-term costs were higher for AFP and WNM patients. However, this study focused on hospitalized case-patients and might not be a true reflection of all reported WNV patients. Two other studies have evaluated the economic burden of WNV outbreaks in the United States, but both evaluated only initial costs (7,9).

When we extrapolated our results to all reported WNV cases in the province of Quebec, we estimated that WNV infections could cost ≈\$1.7 million during an epidemic, such as during 2012; during a low activity year, such as 2013, the cost could be ≈\$430,000. These results are consistent with those of the cost-effectiveness simulation study of Bonneau et al. (10), which estimated total direct and indirect cost of ≈\$400,000 during a hypothetical year of low activity (25 cases of WNV infection) and >\$13 million during a hypothetical year of high activity (840 cases of WNV infection). In that analysis, direct costs included hospitalization, rehabilitation, and outpatient consultations, and indirect costs included productivity losses caused by absence from work and death.

Our study had several limitations. Although participation rate was high and participants were similar to non-participants, analyses by clinical categories were based on

Table 6. Total extrapolated costs for WNV cases by clinical syndrome, Quebec, Canada, 2012–2013*

Cost	2012, n = 124						2013, n = 31					
	WNV		WNM		WNE		WNV		WNM		WNE	
	No.	Cost	No.	Cost	No.	Cost	No.	Cost	No.	Cost	No.	Cost
Hospitalization	11	61,644	23	54,556	62	982,018	1	5,604	7	16,604	16	253,424
ED visit	19	2,090	24	2,640	62	6,820	4	385	7	770	17	1,870
Inpatient rehabilitation	0	0	1	24,453	8	304,583	0	0	0	0	2	83,515
Outpatient readaptation†	3	2,818	4	2,528	9	34,286	1	519	1	737	2	9,401
Physician visit‡	24	1,900	17	4,004	37	4,158	4	350	5	1,168	10	1,140
Additional§	8	792	16	1,600	45	4,521	1	146	5	467	12	1,240
Indirect¶	11	14,054	21	68,267	23	104,625	2	2,589	6	19,911	6	28,688
Total	38	83,298	24	158,048	62	1,441,010	7	9,593	7	39,657	17	379,277

*Costs are in Canadian dollars. Total costs are the sum of all category costs. ED, emergency department; WNE, West Nile encephalitis; WNF, West Nile fever; WNM, West Nile meningitis; WNV, West Nile virus.

†Includes physiotherapy, occupational therapy, speech therapy, and home care costs.

‡Includes primary care physician and neurologist consultations costs.

§Includes medical equipment purchase, recruitment for household chores costs, and other personal expenses.

¶Includes participants' and families' missed work costs.

a small number of cases. However, this number is similar to those for 3 studies in the United States (7–9). Some costs, such as initial consultations in private practice and medication expenses during follow-up, were not included because they were unavailable or they lacked precision. However, these costs accounted for a small proportion of total cost. Recall biases were also possible for costs incurred during follow-up.

Calculation of productivity losses varies between studies. Because of ethical issues related to the evaluation of productivity losses for a dead person (e.g., is an old person less worthy than a young person because of the fact that he or she is retired or less productive?) (15), we decided not to include the indirect costs associated with death in our results. This decision resulted in an underestimation of the WNV economic burden, particularly for WNE patients, because 10 of them plus 1 WNM patient died during their initial hospitalization. Grosse et al. (17) estimated for the United States the productivity value by age and sex on a daily, annual, and lifetime basis (in 2007 US dollars). Such productivity tables are not available for Canada and Quebec. However, when we used daily production values and age and sex distribution of Grosse et al. (17) for

our cases, we estimated the loss of productivity caused by WNV deaths over a 2-year period after the infection. To take into account time preference, we applied a discount rate of 3%, 5%, and 8% and converted the results to 2013 Canadian dollars on the basis of methods suggested by Montmarquette and Scott (18) and Tchouaket et al. (19). These estimates ranged from \$467,000 (3% discount rate) to \$589,000 (8% discount rate) and would represent a 35% increase over costs we calculated (Table 5).

In comparison, Zohrabian et al. (7) calculated lifetime lost productivity for persons who died, and this productivity loss represented half of the total costs of illness. Staples et al. (8) valued productivity losses for those who died but not for older persons who were retired at the time of their illness, and evaluation led to lower indirect costs for WNE than for WNM. In their simulation study, Bonneau et al. (10) showed that nearly 70% of total costs were attributable to indirect costs (deaths and absence from work).

In summary, we found that the overall cost of WNV infection in Quebec was ≈1.7 million for 2012 (24 symptomatic cases) and ≈430,000 for 2013 (31 symptomatic cases) and that costs were significantly higher for patients who had more severe forms of disease. Our study

Table 7. Median economic costs of WNV diseases per patient by clinical syndrome, Quebec, Canada, 2012–2013*

Cost	Disease, no. patients; cost (IQR)		
	WNV	WNM	WNE†
Hospitalization	5; 5,604 (2,295–5,604)	17; 2,372 (2,295–5,604)	47; 15,839 (7,603–27,931)
ED visit	12; 110 (110–110)	18; 110 (110–110)	48; 110 (110–110)
Inpatient rehabilitation	0, 0	1; 18,340 (18,340–18,340)	6; 39,301 (26,200–78,602)
Outpatient readaptation‡	2; 890 (200–1,580)	3; 632 (100–4,462)	7; 3,792 (2,540–4,661)
Physician visit§	15; 80 (42–160)	13; 231 (126–280)	29; 111 (71–152)
Additional¶	5; 100 (100–340)	12; 100 (100–125)	35; 100 (100–115)
Indirect (absence from work)#	7; 1,268 (961–5,434)	16; 3,200 (1,259–9,418)	18; 4,500 (3,000–8,653)

*Costs are in Canadian dollars. Median costs are expressed as per-patient cost on the basis of participants who incurred costs in each category (excluding patients with 0 costs). ED, emergency department; IQR, interquartile range; WNE, West Nile encephalitis; WNF, West Nile fever; WNM, West Nile meningitis; WNV, West Nile virus.

†Includes WNE (n = 28), meningoencephalitis (n = 18), and acute flaccid paralysis (n = 2).

‡Includes physiotherapy, occupational therapy, speech therapy, and home care costs.

§Includes primary care physician and neurologist consultations costs.

¶Includes medical equipment purchase, recruitment for household chores costs, and other personal expenses.

#Includes participants, and families, missed work costs.

provides information to government and public health organizations to make informed decisions regarding preventive and intervention programs for WNV infection. Public health monitoring of costs, both direct and indirect, associated with different clinical manifestations of infectious diseases is essential to enable adequate planning for public health policies and infectious diseases prevention and control programs.

Acknowledgments

We thank the regional public health boards for contacting patients, research nurses for collecting data, Melissa Trudeau for performing data entry, and all patients for agreeing to participate in the study.

About the Author

Dr. Ouhoumane is an epidemiologist at the Institut National de Santé Publique du Québec, Montreal, Quebec, Canada. Her research interests include vectorborne diseases, such as Lyme disease and West Nile virus infection.

References

- Centers for Disease Control and Prevention. West Nile virus: statistics and maps [cited 2017 May 15]. <https://www.cdc.gov/westnile/statsmaps/index.html>
- Public Health Agency of Canada. Surveillance of West Nile virus [cited 2017 May 15]. <https://www.canada.ca/en/public-health/services/diseases/west-nile-virus/surveillance-west-nile-virus.html>
- Ouhoumane N, Turcotte ME, Irace-Cima A, et al. Report on surveillance of the West Nile Virus and other arboviruses in Québec: 2016 season. Montreal: Institut National de Santé Publique du Québec; 2018. p. 11.
- Carson PJ, Borchardt SM, Custer B, Prince HE, Dunn-Williams J, Winkelman V, et al. Neuroinvasive disease and West Nile virus infection, North Dakota, USA, 1999–2008. *Emerg Infect Dis*. 2012;18:684–6. <https://doi.org/10.3201/eid1804.111313>
- Mostashari F, Bunning ML, Kitsutani PT, Singer DA, Nash D, Cooper MJ, et al. Epidemic West Nile encephalitis, New York, 1999: results of a household-based seroepidemiological survey. *Lancet*. 2001;358:261–4. [https://doi.org/10.1016/S0140-6736\(01\)05480-0](https://doi.org/10.1016/S0140-6736(01)05480-0)
- Ouhoumane N, Lowe A-M, Fortin A, Kairy D, Vibien A, K-Lensch J, et al. Morbidity, mortality and long-term sequelae of West Nile virus disease in Québec. *Epidemiol Infect*. 2018;146:867–74. <https://doi.org/10.1017/S0950268818000687>
- Zohrabian A, Meltzer MI, Ratard R, Billah K, Molinari NA, Roy K, et al. West Nile virus economic impact, Louisiana, 2002. *Emerg Infect Dis*. 2004;10:1736–44. <https://doi.org/10.3201/eid1010.030925>
- Staples JE, Shankar MB, Sejvar JJ, Meltzer MI, Fischer M. Initial and long-term costs of patients hospitalized with West Nile virus disease. *Am J Trop Med Hyg*. 2014;90:402–9. <https://doi.org/10.4269/ajtmh.13-0206>
- Barber LM, Schleier JJ III, Peterson RKD. Economic cost analysis of West Nile virus outbreak, Sacramento County, California, USA, 2005. *Emerg Infect Dis*. 2010;16:480–6. <https://doi.org/10.3201/eid1603.090667>
- Bonneau V. Strategic impact assessment of the government response plan for public health protection against West Nile virus: sector report 10: cost-benefit analysis [in French]. Institut National de Santé Publique du Québec; 2008 [cited 2109 Jul 3]. <http://www.inspq.qc.ca/publications/498>
- De Wals P, Blackburn M, Guay M, Bravo G, Blanchette D, Douville-Fradet M. Burden of chickenpox on families: a study in Quebec. *Can J Infect Dis*. 2001;12:27–32. <https://doi.org/10.1155/2001/361070>
- Gosselin P, Lebel G, Rivest S, Douville-Fradet M. The Integrated System for Public Health Monitoring of West Nile Virus (ISPHM-WNV): a real-time GIS for surveillance and decision-making. *Int J Health Geogr*. 2005;4:21. <https://doi.org/10.1186/1476-072X-4-21>
- Public Health Ethics Committee. Opinion on the proposed study of the burden of WNV infection in Quebec: cohorts 2012 and 2013 [in French]. Quebec City (Canada): Institut National de Santé Publique du Québec; 2014. p. 2 [cited 2019 Jul 3]. <https://www.inspq.qc.ca/publications/1751>
- Ministry of Health and Social Services of Quebec. Surveillance of notifiable diseases in Québec – diseases of infectious origin: case definitions, 11th ed. [in French] Québec City: Ministry of Health; 2018. p. 116 [cited 2019 Jul 9] <http://publications.msss.gouv.qc.ca/msss/document-000480>
- Drummond MF, Sculpher MJ, Claxton K, Stoddart GL, Torrance GW. Methods for the economic evaluation of health care programmes. 4th ed. Oxford: Oxford University Press; 2015.
- Régie de l'Assurance maladie du Québec. Pricing of visits; 2016 [in French] [cited 2019 Jul 3]. http://www.ramq.gouv.qc.ca/SiteCollectionDocuments/professionnels/manuels/150-facturation-specialistes/012_b_tarif_visites_acte_spec.pdf
- Grosse SD, Krueger KV, Mvundura M. Economic productivity by age and sex: 2007 estimates for the United States. *Med Care*. 2009;47 (Suppl 1):S94–103. <https://doi.org/10.1097/MLR.0b013e31819c9571>
- Montmarquette C, Scott I. Discount rate for the valuation of public investments in Quebec [in French]. Montreal: Centre for Interuniversity Research and Analysis on Organizations; 2007.
- Tchouaket E, Dubois CA, D'Amour D. The economic burden of nurse-sensitive adverse events in 22 medical-surgical units: retrospective and matching analysis. *J Adv Nurs*. 2017;73:1696–711. <https://doi.org/10.1111/jan.13260>

Address for correspondence: François Milord, Centre Intégré de Santé et de Services Sociaux Montréal-Centre, 1255 Beauregard, Longueuil QC, Canada J4K 2M3; email: francois.milord@usherbrooke.ca

VAR2CSA Serology to Detect *Plasmodium falciparum* Transmission Patterns in Pregnancy

Ana Maria Fonseca, Raquel González, Azucena Bardají, Chenjerai Jairoce, Maria Rupérez, Alfons Jiménez, Llorenç Quintó, Pau Cisteró, Anifa Vala, Charfudin Sacoor, Himanshu Gupta, Jennifer Hegewisch-Taylor, Joe Brew, Nicaise Tuikue Ndam, Simon Kariuki, Marta López, Carlota Dobaño, Chetan E. Chitnis, Peter Ouma, Michael Ramharter, Salim Abdulla, John J. Aponte, Achille Massougbdji, Valerie Briand, Ghyslain Mombo-Ngoma, Meghna Desai, Michel Cot, Arsenio Nhacolo, Esperança Sevene, Eusebio Macete, Clara Menéndez, Alfredo Mayor

Pregnant women constitute a promising sentinel group for continuous monitoring of malaria transmission. To identify antibody signatures of recent *Plasmodium falciparum* exposure during pregnancy, we dissected IgG responses against VAR2CSA, the parasite antigen that mediates placental

sequestration. We used a multiplex peptide-based suspension array in 2,354 samples from pregnant women from Mozambique, Benin, Kenya, Gabon, Tanzania, and Spain. Two VAR2CSA peptides of limited polymorphism were immunogenic and targeted by IgG responses readily boosted during infection and with estimated half-lives of <2 years. Seroprevalence against these peptides reflected declines and rebounds of transmission in southern Mozambique during 2004–2012, reduced exposure associated with use of preventive measures during pregnancy, and local clusters of transmission that were missed by detection of *P. falciparum* infections. These data suggest that VAR2CSA serology can provide a useful adjunct for the fine-scale estimation of the malaria burden among pregnant women over time and space.

Author affiliations: ISGlobal, Hospital Clinic–Universitat de Barcelona, Barcelona, Spain (A.M. Fonseca, R. González, A. Bardají, M. Rupérez, A. Jiménez, L. Quintó, P. Cisteró, H. Gupta, J. Hegewisch-Taylor, J. Brew, C. Dobaño, J.J. Aponte, C. Menéndez, A. Mayor); ICBAS–Universidade do Porto, Porto, Portugal (A.M. Fonseca); Centro de Investigação em Saúde da Manhica, Maputo, Mozambique (R. González, A. Bardají, C. Jairoce, M. Rupérez, A. Vala, C. Sacoor, C. Dobaño, J.J. Aponte, A. Nhacolo, E. Sevene, E. Macete, C. Menéndez, A. Mayor); Universidade Eduardo Mondlane, Maputo (E. Sevene); CIBER Epidemiología y Salud Pública, Madrid, Spain (R. González, A. Jiménez, A. Mayor, A. Bardají); Université d'Aboméy Calavi, Cotonou, Benin (N.T. Ndam, A. Massougbdji); Kenya Medical Research Institute, Kisumu, Kenya (S. Kariuki, P. Ouma); BCNatal–Barcelona Center for Maternal-Fetal and Neonatal Medicine–Hospital Clínic and Hospital Sant Joan de Deu, Barcelona (M. López); Vrije Universiteit Amsterdam, Amsterdam, the Netherlands (J. Brew); MERIT, Institut de Recherche pour le Développement, Paris, France (N.T. Ndam, V. Briand, M. Cot); Institut Pasteur, Paris (C.E. Chitnis); Institute of Tropical Medicine, University of Tübingen, Tübingen, Germany (G. Mombo-Ngoma); Bernhard Nocht Institute for Tropical Medicine, Hamburg, Germany (M. Ramharter, G. Mombo-Ngoma); University Medical Center Hamburg-Eppendorf, Hamburg (M. Ramharter); Ifakara Health Institute, Dar es Salaam, Tanzania (S. Abdulla); Centre de Recherches Médicales de Lambaréné, Lambaréné, Gabon (G. Mombo-Ngoma); Centers for Disease Control and Prevention, Atlanta, Georgia, USA (M. Desai)

DOI: <https://doi.org/10.3201/eid2510.181177>

Agile malaria surveillance and response systems that can be sustained over time are needed for the optimal design of control programs (1,2). Rates of *Plasmodium falciparum* infection among pregnant women are sensitive to changes in transmission (3,4) and correlate well with infection in infants (5) and children (6,7). Thus, passive detection of malaria cases at maternal health care services constitutes a promising approach to providing contemporary data on the levels, and changes in levels, of malaria burden in the population for successful malaria control and elimination (8).

After exposure to *P. falciparum* parasites that sequester in the placenta (9), antibodies against VAR2CSA, a multidomain variant antigen of the *P. falciparum* erythrocyte membrane protein 1 family, develop in pregnant women (10). VAR2CSA is expressed on the surface of infected erythrocytes and mediates placental sequestration of parasites through binding to chondroitin sulfate A (11). Levels of antibodies against VAR2CSA are affected by variables that influence the risk for *P. falciparum* exposure (12–14) and mirror malaria trends during pregnancy (3). Moreover,

levels of VAR2CSA IgG at delivery correlate with the risk for malaria in the offspring (14), suggesting the value of these antibodies for pinpointing areas of high malaria transmission (15). Because VAR2CSA antibodies persist after the infection is cleared (16), they can provide a sensitive adjunct for *P. falciparum* monitoring, especially in areas of low malaria endemicity, where the chances of detecting antibodies are higher than those of detecting the parasite (17).

The utility of serosurveillance depends mainly on specific properties of the antigen, including immunogenicity, polymorphism, cross-reactivity, and longevity of the antibodies. Because different VAR2CSA domains elicit IgG responses with varying magnitudes and dynamics (16,18,19), we hypothesized that short-lived antibodies against immunogenic nonpolymorphic VAR2CSA epitopes would enable a fine-scale estimation of recent *P. falciparum* transmission during pregnancy (17). We examined plasma from pregnant women living in areas in which *P. falciparum* transmission varied from high to low and absent (Benin, Gabon, Mozambique, Kenya, Tanzania, and Spain) against a quantitative suspension array containing VAR2CSA and general parasite antigens. We first selected IgG responses that were rapidly acquired after *P. falciparum* infection, did persist in circulation, and were sensitive to the level of parasite exposure in pregnant women from Mozambique and Spain. We then used the serologic assay to quantify the relationship of VAR2CSA antibody responses with *P. falciparum* infection as well as with temporal, spatial, and intervention-driven changes in malaria burden among pregnant women.

Methods

Study Sites, Population, and Procedures

We included in our study pregnant women who participated in 3 clinical trials of intermittent preventive treatment during pregnancy (IPTp) during 2003–2005 in Mozambique (NCT00209781) (20) and during 2010–2012 in Mozambique, Benin, Gabon, Kenya, and Tanzania (NCT00811421) (21,22). Participants were recruited at their first antenatal visit, and all received a long-lasting insecticide-treated bed net. During 2003–2005, all received 2 doses of sulfadoxine/pyrimethamine (20); during 2010–2012, they received 2 doses of mefloquine or sulfadoxine/pyrimethamine if they were not HIV infected (21) and 3 doses of mefloquine or placebo plus daily cotrimoxazol prophylaxis if they were HIV infected (22). At delivery, tissue samples from the maternal side of the placenta, as well as 50 μ L peripheral and placental dried blood spots (DBS), were collected. Peripheral and placental blood from pregnant women in Mozambique and Benin were also collected into EDTA Vacutainer tubes (Becton Dickinson, <https://www.bd.com>) and centrifuged; plasma was stored

at -20°C . From a subset of pregnant women in Mozambique who delivered during 2011–2012, peripheral blood samples were also collected at the first antenatal visit and before administration of the second IPTp dose. We geocoded the households of women in Mozambique by using a global information system. Clinical malaria episodes were treated according to national guidelines at the time of the study (20–22). DBS and plasma samples were also collected from 49 pregnant women never exposed to *P. falciparum* who delivered in 2010 at the Hospital Clinic of Barcelona (Barcelona, Spain).

The study was approved by the ethics committees from the Hospital Clínic of Barcelona, the Comité Consultatif de Déontologie et d'Éthique from the Institut de Recherche pour le Développement (Marseille, France), the Centers for Disease Control and Prevention (Atlanta, GA, USA), and national ethics review committees from each malaria-endemic country participating in the study. Written informed consent, which included permission to test for immune markers by using stored biological samples, was obtained from all participants.

Laboratory Determinations

At recruitment, we assessed HIV serostatus by using rapid diagnostic tests according to national guidelines and hemoglobin level at delivery by using following mobile devices on capillary blood samples: HemoCue (Danaher, <http://www.hemocue.com>), Hemocontrol (EKF Diagnostics, <http://www.ekfdiagnostics.com>), and KX analyzer (Sysmex, <http://www.sysmex.com>). Thick and thin blood films and placental biopsy samples were checked for *Plasmodium* spp. according to standard, quality-controlled procedures (3). We tested blood on filter paper for the presence of *P. falciparum* in duplicate by means of a real-time quantitative PCR (qPCR) targeting 18S ribosomal DNA (3).

Antibody Measurements

We measured IgG in plasma (Benin and Mozambique) or on DBS (Gabon, Kenya, and Tanzania) in appropriate conditions for plasma elution (19) by using the xMAP technology and the Luminex 100/200 System (<https://www.luminexcorp.com>) for 37% of pregnant women participating in the clinical trials with samples available. We constructed 2 multiplex suspension array panels (Appendix 1, <https://wwwnc.cdc.gov/EID/article/25/10/18-1177-App1.pdf>) (19), 1 including *P. falciparum* recombinant proteins (VAR2CSA Duffy binding-like recombinant domains DBL3X, DBL5E, and DBL6E; apical membrane antigen 1 [AMA1]; and 19-kDa fragment of the merozoite surface protein-1 [MSP1₁₉], from 3D7 strain) and 1 consisting of synthetic peptides (25 VAR2CSA peptides covering conserved and semiconserved regions of VAR2CSA and a circumsporozoite peptide [pCSP]) (19). To assess unspecific

IgG recognition, we used bovine serum albumin in both arrays (19). Procedures for reconstitution of DBS and quality control, bead-based immunoassay, data normalization, and definition of seropositivity cutoffs are described in Appendix 1.

var2csa Sequencing and 3D Protein Modeling

We used DNA extracted from 50 DBS that were *P. falciparum* positive by qPCR for Sanger sequencing of *var2csa* PCR amplification products covering peptides of interest (Appendix 1). Sequence variability with respect to the peptide included in the array was assessed after amino acid alignment, and a 3D model of the DBL1X-ID1 region was developed by using Chimera version 1.5.3 (<https://www.cgl.ucsf.edu>; Appendix 1).

Definitions and Statistical Analyses

We included in the analysis pregnant women for whom all information was available for IPTp, date of delivery, HIV status, age, parity, and antibody responses. We classified women as primigravid (first pregnancy) or multigravid (≥1 previous pregnancy) and categorized age as <20, 20–24, or ≥25 years (13). Anemia was defined as hemoglobin level at delivery <11 mg/L. We compared proportions by using the Fisher exact test. We used univariate regression models to evaluate the association of log-transformed IgG levels (linear) and seropositivity (logistic) with study periods (2004–2005 and 2010–2012) and country, *P. falciparum*

infection, parity, anemia, and IPTp intervention, taking into account potential confounding variables (HIV and age) in multivariate models. We assessed the modification of the associations by HIV infection or parity by including interaction terms into the regression models. To control the false discovery rate in the selection of antigens, we computed adjusted p values (q-values) by using the Simes procedure (23). We used multilevel mixed-effect linear regression analysis to estimate half-life and time to double (T_{2x}) IgG levels in the longitudinal cohort of pregnant women from Mozambique (Appendix 1). We identified spatial clusters of *P. falciparum* infection and seropositivity as well as the most likely hotspots by using the Ward hierarchical cluster analysis and Kulldorf spatial scan method (Appendix 1). We performed statistical analyses by using Stata/SE software version 12.0 (StataCorp, <https://www.stata.com>), R statistics software version 3.2.1 (<https://www.r-project.org>), and Graphpad Prism version 6 (<https://www.graphpad.com>).

Results

Study Participants and *P. falciparum* Prevalence

Study participants consisted of 2,354 pregnant women (Table; Appendix 1 Figure 2) recruited during 2004–2005 (n = 146) and 2010–2012 (n = 2,208) in the context of IPTp clinical trials (20–22). Among them, 993 were from Mozambique, 854 from Benin, 131 from Gabon, 296 from Kenya,

Table. Participants in study of VAR2CSA serologic testing to detect *Plasmodium falciparum* transmission patterns, by country and HIV status*

Variable	HIV-uninfected, no. (%)					HIV-infected, no. (%)		
	2004–2005	2010–2012				2004–2005	2010–2012	
	Mozambique, n = 65	Mozambique,† n = 485	Benin, n = 854	Gabon, n = 131	Tanzania, n = 31	Mozambique, n = 81	Mozambique,† n = 362	Kenya, n = 296
Parity								
Primigravid	17 (26)	181 (37)	188 (22)	38 (29)	16 (52)	28 (35)	46 (13)	22 (7)
Multigravid	48 (74)	304 (63)	666 (78)	93 (71)	15 (48)	53 (65)	316 (87)	274 (93)
Age, y								
<20	19 (29)	181 (37)	86 (10)	42 (32)	5 (16)	27 (33)	41 (11)	15 (5)
20–24	17 (26)	123 (25)	281 (33)	45 (34)	14 (45)	26 (32)	84 (23)	96 (32)
≥25	29 (45)	181 (37)	487 (57)	44 (34)	12 (39)	28 (35)	237 (65)	185 (62)
IPTp								
Sulfadoxine/pyrimethamine	65 (100)	151 (31)	288 (34)	55 (42)	11 (35)	81 (100)	0	0
Mefloquine	0	334 (69)	566 (66)	76 (58)	20 (65)	0	178 (49)	139 (47)
Placebo‡	0	0	0	0	0	0	184 (51)	157 (53)
Microscopy§¶								
Positive	9 (14)	13 (3)	110 (15)	3 (2)	1 (3)	8 (10)	8 (2)	15 (5)
Negative	56 (86)	468 (97)	616 (85)	125 (98)	30 (97)	73 (90)	323 (98)	268 (95)
qPCR¶#								
Positive	16 (25)	28 (6)	332 (46)	9 (10)	0	21 (26)	13 (4)	22 (8)
Negative	49 (75)	424 (94)	393 (54)	80 (90)	31 (100)	60 (74)	314 (96)	251 (92)

*IPTp, intermittent preventive treatment during pregnancy; qPCR, quantitative PCR.
 †40% (196/485) of HIV-uninfected and 12% (43/362) of HIV-infected participants were pregnant women with samples collected also at recruitment and second IPTp administration.
 ‡All HIV-infected women who received placebo were also receiving cotrimoxazol prophylaxis.
 §Maternal microscopic infection defined by the presence of *P. falciparum* parasites in peripheral blood or in placenta on microscopic or histologic examination, respectively.
 ¶Not determined: 179 microscopy and 196 qPCR.
 #Maternal qPCR-positive infection was defined by a positive result on qPCR testing in peripheral or placental blood.

31 from Tanzania, and 49 from Spain. The baseline characteristics of the women selected for this trial were similar to those of the 6,216 women participating in the randomized clinical trials (Appendix 2 Table 1, <https://wwwnc.cdc.gov/EID/article/25/10/18-1177-App2.xlsx>).

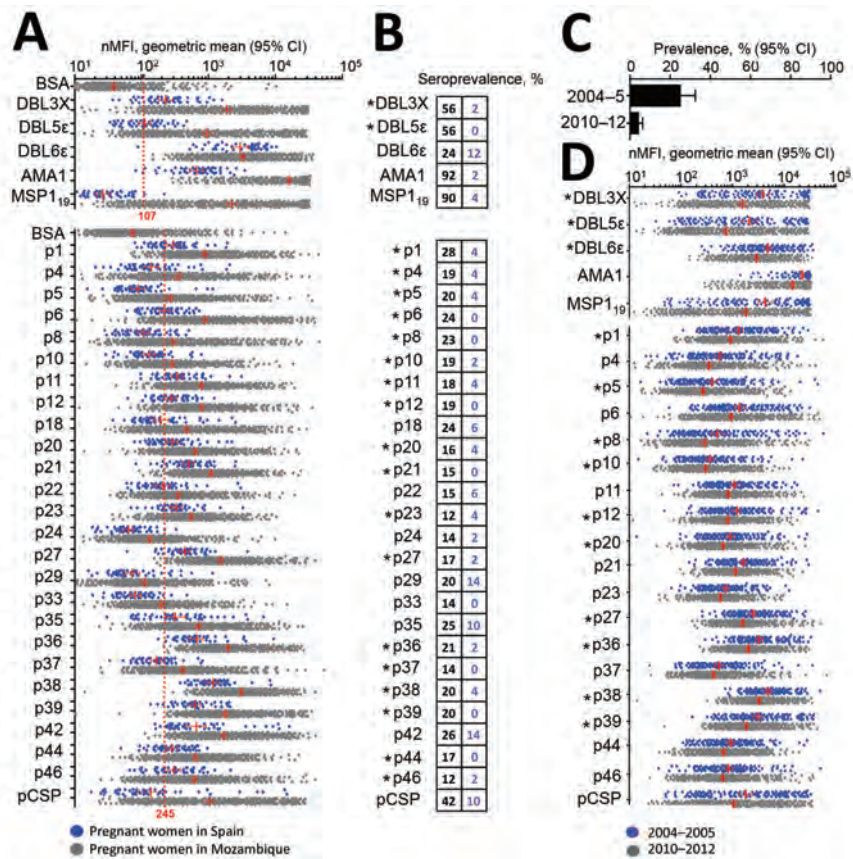
The study areas represented 5 sites in sub-Saharan Africa with different intensities of malaria transmission. Prevalence of *P. falciparum* infection detected by qPCR at delivery, in either peripheral or placental blood (averaged for 2010–2012), among HIV-uninfected women was 46% (332/725) in Benin, 10% (9/89) in Gabon, and 6% (28/452) in Mozambique and among HIV-infected women was 8% (22/273) in Kenya and 4% (13/327) in Mozambique (Table). The prevalence of *P. falciparum* infection among pregnant women in Mozambique decreased from 25% (37/146) in 2004–2005 to 2% (3/176) in 2010 and increased to 6% (4/72) in 2012. A subset of 239 pregnant women from Mozambique recruited during 2011–2012 was followed during pregnancy; prevalence of *P. falciparum* infection detected by qPCR was 16% (38/239) at first antenatal visit (mean gestational age \pm SD, 20.7 \pm 5.45 weeks), 3% (8/239) at the second IPTp administration (25.9 \pm 4.98 weeks), and 5% (13/239) at delivery (38.4 \pm 2.26 weeks).

P. falciparum infection was detected at unscheduled visits for 2% (5/239) of the women. Overall, *P. falciparum* infection was detected at any of these time points for 21% (49/239) of the women.

***P. falciparum*–Specific Antibody Profiles and Parasite Exposure during Pregnancy**

Mean antiparasite IgG levels in pregnant women from Mozambique delivering from 2010 through 2012 were above levels against bovine serum albumin plus 3 SD and higher than IgG levels in pregnant women from Spain except for DBL6E and 3 of 25 VAR2CSA peptides (Figure 1, panel A; Appendix 2 Table 3). Five VAR2CSA peptides, DBL6E, and pCSP were recognized by IgG from \geq 5% of the pregnant women from Spain who had never been exposed to *P. falciparum* (Figure 1, panel B), suggesting unspecific recognition; thus, these peptides were excluded from subsequent analysis. To further narrow down the VAR2CSA peptide candidates, we compared IgG levels in pregnant women from Mozambique delivering in 2004–2005 and 2010–2012, a period when *P. falciparum* prevalence assessed by qPCR at delivery in peripheral or placental blood dropped from 25% to 5% (Figure 1, panel C) (3). This

Figure 1. *Plasmodium falciparum* VAR2CSA IgG in malaria-exposed and -nonexposed pregnant women. A) nMFI measured in pregnant women from Mozambique and Spain. Red dashed line represents the mean nMFI from bovine serum albumin + 3 SDs. B) Seroprevalence among pregnant women from Spain (blue) and Mozambique (black). Asterisks indicate antigens recognized by pregnant women from Mozambique at levels above IgG against bovine serum albumin + 3 SDs and above levels in pregnant women from Spain (q-value <0.05 by Simes procedure) and those antigens poorly recognized by pregnant women from Spain (seroprevalence <5%). C, D) Prevalence of *P. falciparum* infection in peripheral and placental blood by quantitative PCR (C) and nMFIs (D) among pregnant women from Mozambique delivering in 2004–2005 and 2010–2012. Red lines represent the geometric mean and T-bars the 95% CI. Asterisks indicate antigens recognized by IgG whose levels dropped between 2004 and 2012, as assessed by linear regression adjusted by intermittent preventive treatment during pregnancy, parity, age, and HIV status (q-value <0.05 by Simes procedure). nMFI, normalized median fluorescent intensity.



decline in infection rates was mirrored by drops of IgG levels against 10 of the 18 previously selected VAR2CSA peptides (p1, p5, p8, p10, p12, p20, p27, p36, p38, p39) (Figure 1, panel D; Appendix 2 Table 4).

Acquisition and Decay of IgG Responses against VAR2CSA

We assessed the dynamics of IgG responses in a longitudinal cohort of 239 pregnant women from Mozambique (Figure 2, panel A). At delivery, compared with uninfected women, the 49 (21%) women infected with *P. falciparum*

during pregnancy had higher IgG levels against the 10 down-selected peptides (Figure 2, panel B; Appendix 2 Table 5). At delivery, seroprevalence rates for p1 (23%), p5 (26%), p8 (26%), and p39 (31%) antibodies were above the cumulative prevalence of *P. falciparum* infection during pregnancy (Figure 2, panel C; Appendix 2 Table 5). No difference in IgG levels was observed between primigravid and multigravid women (Figure 2, panel D; Appendix 2 Table 5). T_{2x} after *P. falciparum* infection ranged from 0.45 years (95% CI 0.31–0.80 years) for p5 to 1.07 years (95% CI 0.60–5.23 years) for p27 (Figure 2, panel E; Appendix

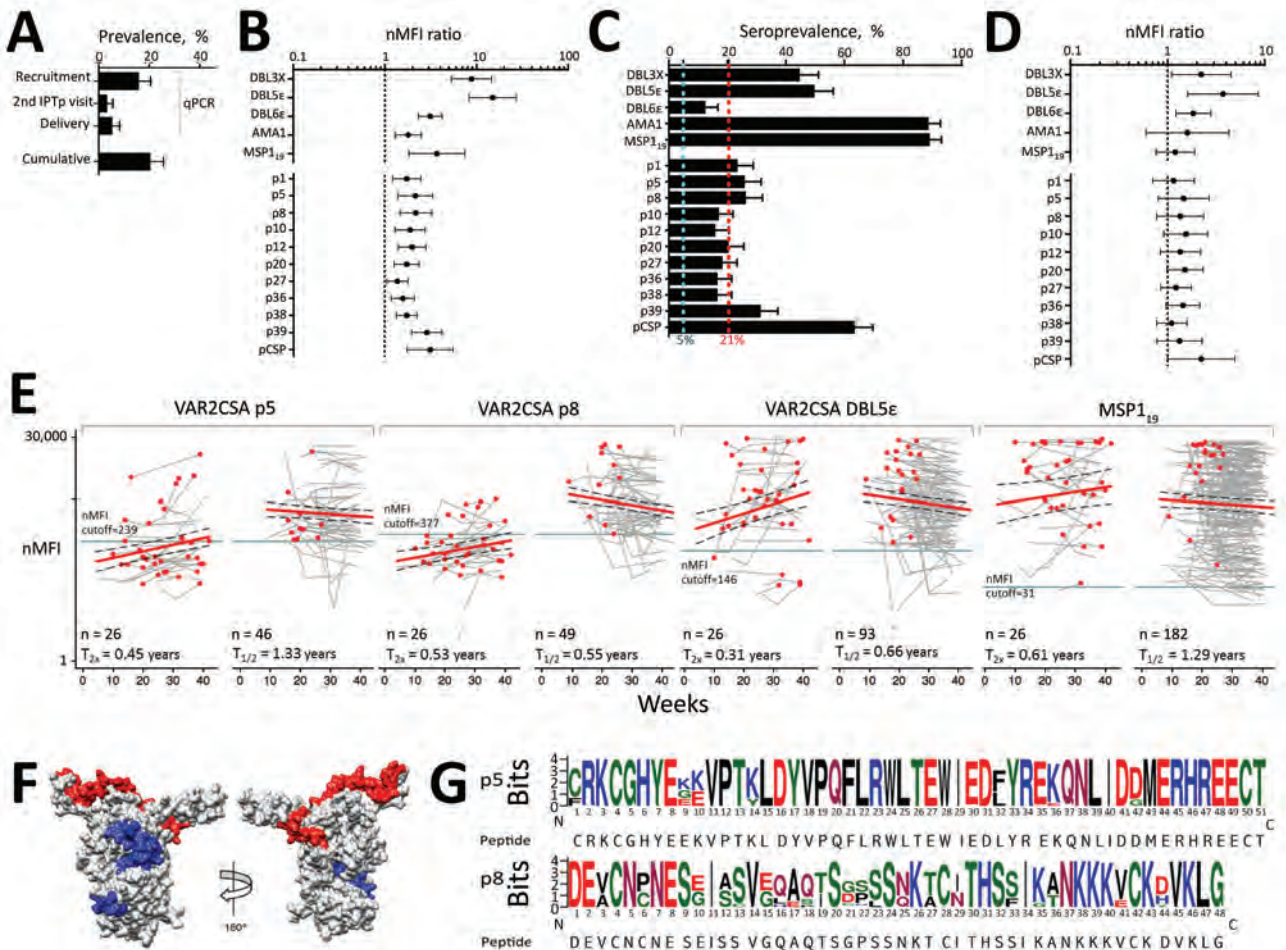


Figure 2. IgG responses during pregnancy against selected VAR2CSA antigens and polymorphism in target sequences in serology study of *Plasmodium falciparum* in pregnant women. A) *P. falciparum* prevalence by quantitative PCR (qPCR) in 239 pregnant women from Mozambique at recruitment, second administration of IPTp, and delivery. Cumulative prevalence at delivery refers to peripheral or placental infection detected by microscopy, qPCR, or histology at any time point. B) Ratio of nMFIs at delivery in women from Mozambique infected during pregnancy compared with uninfected women. Error bars indicate 95% CIs. C) Seroprevalence at delivery, showing the cumulative prevalence of infection during pregnancy (red dashed line) and the prevalence at delivery by qPCR (light blue line). D) Ratio of nMFIs at delivery in multigravid compared with primigravid women, adjusted by IPTp, parity, age, and HIV status. Error bars indicate 95% CIs. E) IgG dynamics during pregnancy with estimates of time to double (T_{2x}) and half-life ($T_{1/2}$) obtained from linear mixed-effect regression model. Red points represent *P. falciparum* infection, dark gray lines the seropositivity cutoff, red lines the fitted-estimation, and dashed lines the 95% CI. F) Space-filling representation of DBL1X-ID1 showing p5 (blue) and p8 (red). G) Logo representation of p5 and p8 sequences obtained from 50 *P. falciparum* isolates (20 from Mozambique, 10 from Benin, 10 from Gabon, and 10 from Kenya). IPTp, intermittent preventive treatment during pregnancy; nMFI, normalized median fluorescent intensity.

2 Table 6). IgG half-life among seropositive women at recruitment without evidence of *P. falciparum* infection during follow-up ranged from 0.55 (95% CI 0.38–1.02) years for p8 to 3.66 (95% CI 0.98–∞) years for p1 (Figure 2, panel E; Appendix 2 Table 6). Among recombinant antigens, IgG DBL5E showed the lowest T_{2x} (0.31 [95% CI 0.21–0.61] years) and half-life (0.66 [95% CI 0.42–1.65] years), whereas AMA1 IgG showed the highest T_{2x} (1.76 [95% CI 0.76–∞] years) and half-life (4.18 [95% CI 1.86–∞] years).

Among the down-selected VAR2CSA peptides (p1, p5, p8, and p39), IgG against p5 (51 amino acids) and p8 (48 amino acids) showed the lowest half-lives (0.55 [95% CI 0.38–1.02] years for p8; 1.33 [95% CI 0.65–∞] years for p5) and the largest increase in women exposed to *P. falciparum* during pregnancy compared with uninfected women (adjusted ratio [AR]_{p5} 2.15 [95% CI 1.39–3.31] and AR_{p8} 2.17 [95% CI 1.46–3.23]; Figure 2, panel B; Appendix 1 Figure 5; Appendix 2 Table 5). IgG levels and seroprevalence rates at delivery for p5 and p8 were higher among pregnant women with active or past malaria infection than among women with no parasite or pigment in the placenta, as assessed by histologic examination (Appendix 2 Table 7). 3D modeling mapped both sequences on the exposed surface of DBL1X-ID1 region of VAR2CSA (Figure 2, panel F). Amino acid variability obtained from 50 *P. falciparum* isolates collected at study sites was 5% ± 2 SD for p5 sequences and 16% ± 5 SD for p8 sequences, compared with the consensus peptide sequence included in the array (Figure 2, panel G; Appendix 1 Figures 3, 4).

Performance of Selected VAR2CSA Peptides for Assessing Spatial and Temporal Differences in *P. falciparum* Exposure

In pregnant women from Mozambique at delivery, p5 and p8 seroprevalence rates, as well as the composite of both (p5+8), decreased from 2004–2005 to 2010 (adjusted odds ratio [AOR]_{p5+8} 0.27 [95% CI 0.11–0.68]), followed by an increase from 2010 to 2012 (AOR_{p5+8} 2.49 [95% CI 1.34–4.61]; Figure 3, panel A; Appendix 2 Table 8). This decrease and subsequent increase mirrored *P. falciparum* prevalence by qPCR. HIV infection and parity did not modify the associations observed (p value for interaction >0.05 for all cases; Appendix 2 Table 8). Similar to *P. falciparum* prevalence determined by qPCR, seroprevalence rates were the highest in HIV-uninfected women from Benin, followed by those from Gabon (AOR_{p5+8} 0.31 [95% CI 0.21–0.47]) and Mozambique (AOR_{p5+8} 0.21 [95% CI 0.16–0.28]; Figure 3, panel B; Appendix 2 Table 9). At delivery, pregnant women living in an area from Tanzania where no *P. falciparum* infection was detected by qPCR were seronegative against p5, p8, and p5+8 antibodies; 42% were seropositive against AMA1 and 48% were seropositive

against MSP1₁₉ antibodies (Figure 3, panel B). Among HIV-infected women, seroprevalence rates for p8 and p5+8 were lower in Mozambique than in Kenya (AOR_{p5+8} 0.58 [95% CI 0.38–0.88]; Figure 3, panel C; Appendix 2 Table 9). p5 and p5+8 seroprevalence rates were higher among anemic than among nonanemic women (AOR_{p5+8} 1.26 [95% CI 1.03–1.55]; Figure 3, panel D; Appendix 2 Table 10). Seroprevalence rates were lower among HIV-uninfected women who received IPTp with mefloquine than among those who received sulfadoxine/pyrimethamine (AOR_{p5+8} 0.74 [95% CI 0.59–0.94]; Figure 3, panel E; Appendix 2 Table 11). Seroprevalence rates among HIV-infected women were lower among those who received mefloquine than among those who received placebo, although differences were not significant (AOR_{p5+8} 0.76 [95% CI 0.50–1.15]; Figure 3, panel F; Appendix 2 Table 11).

Geographic Patterns of *P. falciparum* Transmission through VAR2CSA Serologic Testing

Spatial geocoordinates were available for 698 pregnant women from Mozambique residing in Manhiça District (southern Mozambique). Geographic areas experiencing significantly higher seroprevalence rates than would be expected by chance were observed for p5 (radius 2.82 km; p = 0.024) and p5+8 (radius 1.06 km; p = 0.049) but not for MSP1₁₉ and AMA1 (Figure 4; Appendix 2 Table 12). The distribution of HIV infection, parity, age, and IPTp was similar among women inside and outside the serologic hotspot (p>0.05; Appendix 2 Table 12).

Discussion

Routine *P. falciparum* testing of easily accessible pregnant women at maternal healthcare services has the potential to offer a rapid, consistent, and cost-effective method for evaluating the malaria burden in different communities and tracking progress of interventions. IgGs against 2 VAR2CSA peptides, selected according to their ability to maximize the information about recent *P. falciparum* exposure during pregnancy, reflected differences in malaria burden over time and space in multiple settings in Africa and changes in parasite rates associated with the use of different preventive regimens. Overall, our results indicate that in areas with well-attended maternal healthcare services, this pregnancy-specific serologic test may serve as a useful sentinel surveillance tool for flagging changes in malaria burden and progress in the path toward elimination.

p5 (51 amino acids) is localized in the DBL1X domain and p8 (48 amino acids) in the ID1 region of VAR2CSA. Limited diversity (5%) of p5 sequence was observed in *P. falciparum* isolates from a variety of regions of Africa, in accordance with estimates from previous studies for the DBL1X domain (24). p8 corresponds to a more diverse (16%) variant of the ID1 region in VAR2CSA (25). Both

peptides are exposed on the DBL1X-ID1 N terminal region of VAR2CSA (18,26) and recognized by IgG from malaria-exposed pregnant women at levels higher than those of pregnant women from Spain and men from Mozambique (19). IgG responses against both VAR2CSA peptides increased with *P. falciparum* infection during pregnancy. Moreover, higher risk for anemia among p5 and p5+8 sero-responders support these antibodies as markers of recent infection, which adversely affects the women's health (3). In contrast to the slow decay of IgG responses against AMA1, the half-life of IgG against p5 and p8 was <2 years, the

average time reported in Mozambique for a second pregnancy to occur (27). The short half-life of p5 and p8 IgG, together with the similar IgG levels in multigravid and primigravid women, suggests that antibodies acquired during one pregnancy are not maintained over multiple pregnancies; thus, antibodies can be used as a reliable indicator of recent exposure for pregnant women, regardless of parity.

Sero-prevalence rates for p5, p8, and the composite of both peptides (p5+8) mirrored trends in *P. falciparum* prevalence among pregnant women from Mozambique delivering during 2004–2012 (3), a temporal pattern that was also

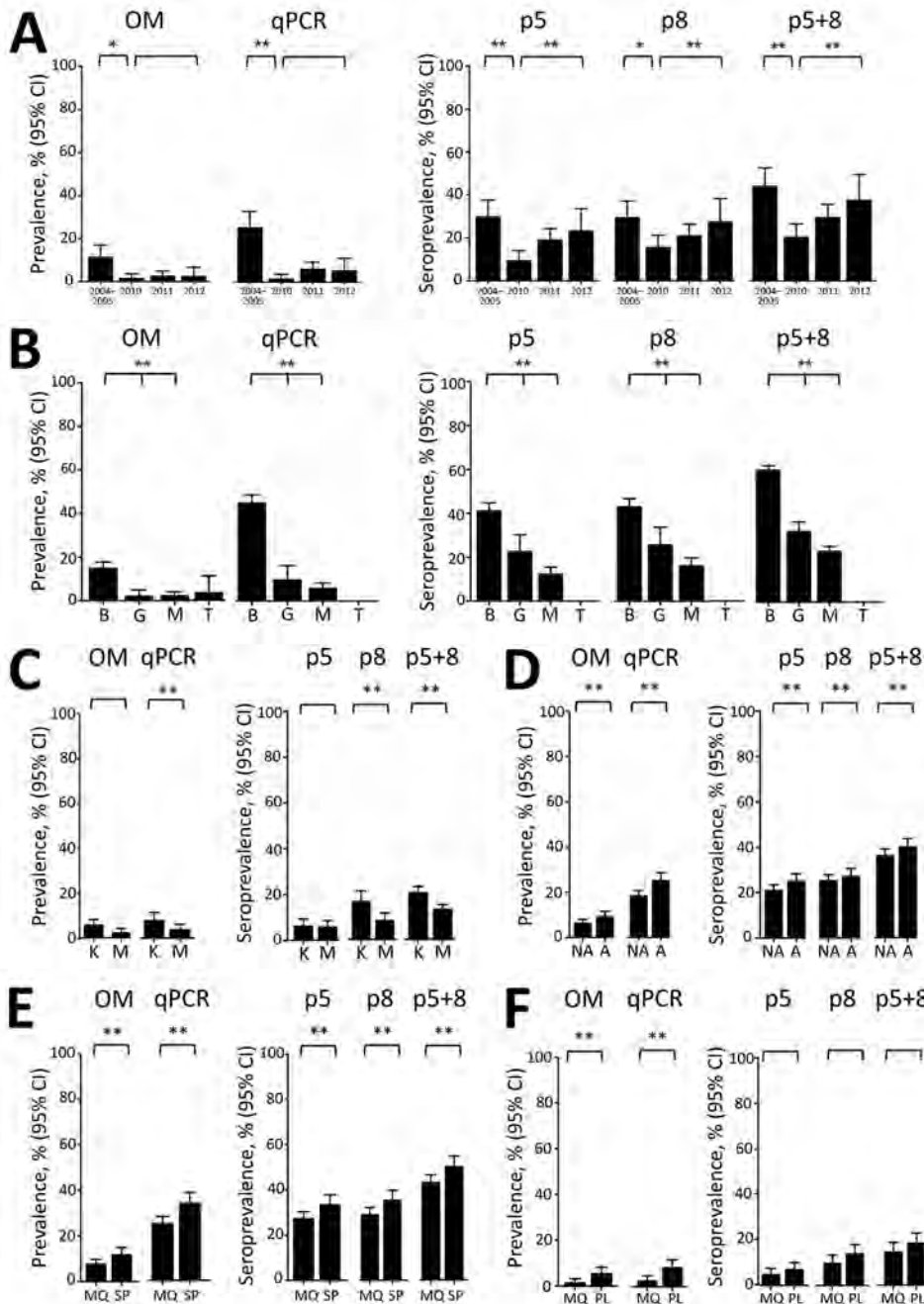


Figure 3. IgG seroprevalence against VAR2CSA selected antigens according to study period, country, anemia status and intermittent preventive treatment group in serologic study of *Plasmodium falciparum* in pregnant women. A) Pregnant women from Mozambique delivering during different periods. B) HIV-uninfected pregnant women from Benin, Gabon, Mozambique, and Tanzania. C) HIV-infected pregnant women from Kenya and Mozambique. D) Nonanemic (NA) and anemic (A) pregnant women. E) HIV-uninfected pregnant women receiving mefloquine (MQ) or sulfadoxine/pyrimethamine (SP) as intermittent preventive treatment during pregnancy (IPTp). F) HIV-infected pregnant women receiving MQ or placebo (PL) as IPTp. Maternal microscopic infection was defined by the presence of *P. falciparum* parasites in peripheral blood or in placenta on microscopic or histologic examination, respectively. Maternal quantitative PCR (qPCR)-positive infection was defined by a positive result on qPCR of peripheral or placental blood. P-values were obtained from multivariate regression models adjusted for HIV, parity, age, IPTp, and country when applicable. T-bars represent 95% CIs. *Crude p<0.05; **adjusted p<0.05. B, Benin; G, Gabon; K, Kenya; M, Mozambique; OM, optical microscopy; T, Tanzania.

observed for PfPR₂₋₁₀ (28). Trends were similar among HIV-uninfected and infected women, suggesting that impairment of *P. falciparum*-specific antibody responses driven by viral infection (29) may not affect short-lived IgG responses against p5 and p8. Seroprevalence also reflected the burden of malaria among pregnant women residing in a variety of settings in Africa, as well as reductions in infection rates resulting from the use of mefloquine as IPTp among HIV-uninfected women (21). Similar trends, although not statistically significant, were observed among HIV-infected women receiving cotrimoxazol prophylaxis alone or in combination with mefloquine (22), possibly because of the longer duration of protection provided by 3 IPTp doses in HIV-infected women compared with the 2 doses in HIV-uninfected women. We also found that pregnant women living in an area from Tanzania where no *P. falciparum* infection was detected by qPCR as well as pregnant women from Spain never exposed to malaria were seronegative against p5 and p8, suggesting that pregnancy-specific serology might be used to confirm the eventual interruption of transmission.

Geographic distribution of pregnant women from Mozambique who were seropositive against p5 and p5+8 revealed a serologic hotspot in an area close to the river and sugar cane plantations, where the density of anopheline mosquitoes can be expected to be higher. In contrast, antibodies against MSP1₁₉ and AMA1 were not able to identify these malaria transmission patterns because of saturation of antibody responses after lifelong exposure to *P. falciparum*. These results support the value of using VAR2CSA serologic testing to amplify signals of recent exposure and

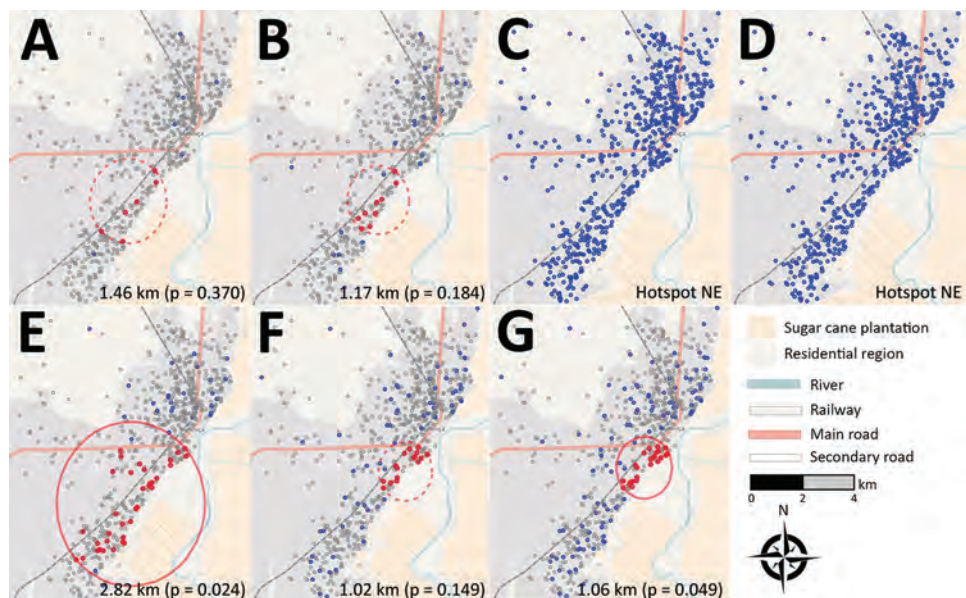
suggest its potential to trigger targeted interventions to persons living in close proximity to passively detected seropositive pregnant women.

Our study has several limitations. First, the peptide array we used may have missed some conformational nonlinear epitopes. Second, different transmission dynamics and host genetic factors may affect the acquisition and decay of antibodies (16). Third, steeper decay of antibodies may be observed out of pregnancy when infecting parasites express non-VAR2CSA variants. Fourth, the reduction of data from median fluorescence intensity to seroprevalence to simplify the serologic information of the assay may reduce the depth of serologic information. Developing alternative mathematical models that use antibody levels (30) may increase the sensitivity to detect temporal and spatial changes in malaria transmission. Fifth, small numbers of pregnant women from malaria-free areas in Tanzania and Spain limit the generalizability of our data to support pregnancy-specific serologic testing as a tool to confirm interruption of transmission. Last, antibody assessments in this study were conducted mainly at delivery; further studies should assess the performance of this testing at antenatal visits or soon after delivery (i.e., during infant immunization). Future research is needed to describe the relationship between pregnancy-specific serologic testing and malaria transmission in the general population and its value for confirming interruption of malaria transmission and providing early signals of *P. falciparum* resurgence after local elimination.

In summary, this study shows that IgG against 2 VAR2CSA peptides from the DBL1X-ID1 domain reveal

Figure 4. Geographic patterns of *Plasmodium falciparum* infection and IgG seropositivity in pregnant women living in southern Mozambique.

Geographic distribution of seropositive pregnant women (HIV-uninfected and HIV-infected) living in Manhiça District, Mozambique, who delivered during 2010–2012 and for whom microscopy, quantitative PCR (qPCR), and spatial geocoordinates were available. Distribution shows pregnant women with and without *P. falciparum* infection at delivery, either in peripheral or in placental blood, detected by microscopy or histology (A) or qPCR (B), as well as AMA1 (C), MSP1₁₉ (D), p5 (E), p8 (F), and p5+8 (G) seropositive and seronegative pregnant women at delivery. Grey dots indicate seronegative women, blue dots indicate seropositive women, red dots indicate seropositive women selected by the hotspot cluster algorithm; red circles indicate the most likely hotspot (continuous line $p < 0.05$, dashed line $p > 0.05$). Maps were generated by using OpenStreetMap (<https://www.openstreetmap.org>). Hotspot NE, not estimated because of low prevalence of seroposponders.



Hotspot NE, not estimated because of low prevalence of seroposponders.

temporal and spatial differences in malaria burden among pregnant women and reductions in exposure associated with the use of preventive measures during pregnancy. These antibodies enable the identification of local clusters of transmission that are missed by detection of *P. falciparum* infections. Our results suggest that inferring recent exposure through VAR2CSA serologic testing would amplify signals of ongoing malaria transmission and increase the power to detect changes, either natural or driven by deliberate efforts, as well as malaria hotspots, among pregnant women (2). Moreover, peptides such as p1 targeted by long-lasting IgG responses may be useful for capturing past changes in transmission by sampling women of child-bearing age and relating seroprevalence with the number and timing of previous pregnancies. Operationally suitable serologic tests (31) capable of detecting antibodies against VAR2CSA synthetic peptides may be used in programmatic environments to stratify areas based on malaria burden, measure the effects of interventions, and document year-to-year changes in transmission.

Acknowledgments

We thank the women from Benin, Gabon, Kenya, Mozambique, Tanzania, and Spain who participated in the study, as well as the staff of the hospitals, clinical officers, field supervisors, and data manager. We also thank Laura Puyol, Diana Barrios, Gemma Moncunill, Pau Cisteró, Lazaro Mussacate, Nelito Ernesto Jose, and Ana Rosa Manhiça for their contribution to the collection and organization of sample shipment and Joe Campo, Aida Valmaseda, Marta Vidal, Eduard Rovira-Vallbona, Pedro Aide, Beatriz Galatas, Patrick G.T. Walker, and Peter Gething for providing important inputs for standardization of the Luminex technology, the design of protein 3D models, the interpretation of results and PfPR₂₋₁₀ data.

This study was supported by the Malaria Eradication Scientific Alliance; the European and Developing Countries Clinical Trials Partnership; the Malaria in Pregnancy Consortium; and grants from Banco de Bilbao, Vizcaya, Argentaria Foundation (BBVA 02-0), Instituto de Salud Carlos III (PS09/01113, PI13/01478, and CES10/021-I3SNS, to A. Mayor), and Ministerio de Ciencia e Innovación (RYC-2008-02631, to C.D.), the Fundação para a Ciência e Tecnologia (SFRH/BD/51696/2011, to A.M.F.), the Department of Science & Technology, Government of India (SB/OS/PDF-043/2015-16, to H.G.) and the Department d'Universitats i Recerca de la Generalitat de Catalunya (AGAUR; 2017SGR664, to A.M.).

The Centro de Investigação em Saúde da Manhica receives core support from the Spanish Agency for International Cooperation and Development. The Malaria in Pregnancy Consortium is funded by a grant from the Bill & Melinda Gates Foundation to the Liverpool School of Tropical Medicine and the Malaria Eradication Scientific Alliance is funded by a grant from the

Barcelona Institute of Global Health. ISGlobal is a member of the CERCA Programme, Generalitat de Catalunya.

A patent application has been filed for the use of p5 and p8 for serologic surveillance (US 376 patent application no. 62523828, filed on June 23, 2017, by A.M.).

About the Author

Dr. Fonseca is a doctoral fellow at ISGlobal, Barcelona Institute for Global Health, Hospital Clínic, Universitat de Barcelona, Barcelona, Spain. Her research focus includes malaria immune epidemiology in pregnant women and strategies to improve malaria surveillance in disease-endemic regions experiencing a low burden of infection.

References

1. World Health Organization. The world malaria report. Geneva: The Organization; 2018. p. 32.
2. Mogeni P, Omedo I, Nyundo C, Kamau A, Noor A, Bejon P, et al. on behalf of the Hotspot Group authors. Effect of transmission intensity on hotspots and micro-epidemiology of malaria in sub-Saharan Africa [cited 2019 Aug 2]. <https://bmccmedicine.biomedcentral.com/articles/10.1186/s12916-017-0887-4>
3. Mayor A, Bardají A, Macete E, Nhampossa T, Fonseca AM, González R, et al. Changing trends in *P. falciparum* burden, immunity, and disease in pregnancy. *N Engl J Med*. 2015; 373:1607–17. <http://dx.doi.org/10.1056/NEJMoa1406459>
4. Ndam NT, Mbuba E, González R, Cisteró P, Kariuki S, Sevene E, et al. Resisting and tolerating *P. falciparum* in pregnancy under different malaria transmission intensities. *BMC Med*. 2017;15:130. <http://dx.doi.org/10.1186/s12916-017-0893-6>
5. Willilo RA, Molteni F, Mandike R, Mugalura FE, Mutafungwa A, Thadeo A, et al. Pregnant women and infants as sentinel populations to monitor prevalence of malaria: results of pilot study in Lake Zone of Tanzania. *Malar J*. 2016;15:392. <http://dx.doi.org/10.1186/s12936-016-1441-0>
6. Walton GA. On the control of malaria in Freetown, Sierra Leone; control methods and the effects upon the transmission of *Plasmodium falciparum* resulting from the reduced abundance of *Anopheles gambiae*. *Ann Trop Med Parasitol*. 1949;43:117–39. <https://doi.org/10.1080/00034983.1949.11685399>
7. van Eijk AM, Hill J, Noor AM, Snow RW, ter Kuile FO. Prevalence of malaria infection in pregnant women compared with children for tracking malaria transmission in sub-Saharan Africa: a systematic review and meta-analysis. *Lancet Glob Health*. 2015;3:e617–28. [http://dx.doi.org/10.1016/S2214-109X\(15\)00049-2](http://dx.doi.org/10.1016/S2214-109X(15)00049-2)
8. Ataíde R, Mayor A, Rogerson SJ. Malaria, primigravidae, and antibodies: knowledge gained and future perspectives. *Trends Parasitol*. 2014;30:85–94. <http://dx.doi.org/10.1016/j.pt.2013.12.007>
9. Brabin BJ, Romagosa C, Abdelgalil S, Menéndez C, Verhoeff FH, McGready R, et al. The sick placenta—the role of malaria. *Placenta*. 2004;25:359–78. <http://dx.doi.org/10.1016/j.placenta.2003.10.019>
10. Salanti A, Staalsoe T, Lavstsen T, Jensen AT, Sowa MP, Arnot DE, et al. Selective upregulation of a single distinctly structured var gene in chondroitin sulphate A-adhering *Plasmodium falciparum* involved in pregnancy-associated malaria. *Mol Microbiol*. 2003;49:179–91. <https://doi.org/10.1046/j.1365-2958.2003.03570.x>
11. Fried M, Duffy PE. Adherence of *Plasmodium falciparum* to chondroitin sulfate A in the human placenta. *Science*. 1996; 272:1502–4. <https://doi.org/10.1126/science.272.5267.1502>

12. Aitken EH, Mbewe B, Luntamo M, Kulmala T, Beeson JG, Ashorn P, et al. Antibody to *P. falciparum* in pregnancy varies with intermittent preventive treatment regime and bed net use. *PLoS One*. 2012;7:e29874. <https://doi.org/10.1371/journal.pone.0029874>
13. Mayor A, Kumar U, Bardají A, Gupta P, Jiménez A, Hamad A, et al. Improved pregnancy outcomes in women exposed to malaria with high antibody levels against *Plasmodium falciparum*. *J Infect Dis*. 2013;207:1664–74. <http://dx.doi.org/10.1093/infdis/jit083>
14. Serra-Casas E, Menéndez C, Bardají A, Quintó L, Dobaño C, Sigauque B, et al. The effect of intermittent preventive treatment during pregnancy on malarial antibodies depends on HIV status and is not associated with poor delivery outcomes. *J Infect Dis*. 2010;201:123–31. <http://dx.doi.org/10.1086/648595>
15. Bejon P, Williams TN, Liljander A, Noor AM, Wambua J, Ogada E, et al. Stable and unstable malaria hotspots in longitudinal cohort studies in Kenya. *PLoS Med*. 2010;7:e1000304. <http://dx.doi.org/10.1371/journal.pmed.1000304>
16. Fowkes FJ, McGready R, Cross NJ, Hommel M, Simpson JA, Elliott SR, et al. New insights into acquisition, boosting, and longevity of immunity to malaria in pregnant women. *J Infect Dis*. 2012;206:1612–21. <http://dx.doi.org/10.1093/infdis/jis566>
17. Drakeley C, Cook J. Chapter 5: Potential contribution of sero-epidemiological analysis for monitoring malaria control and elimination: historical and current perspectives. *Adv Parasitol*. 2009;69:299–352.
18. Andersen P, Nielsen MA, Resende M, Rask TS, Dahlbäck M, Theander T, et al. Structural insight into epitopes in the pregnancy-associated malaria protein VAR2CSA. *PLoS Pathog*. 2008;4:e42. <http://dx.doi.org/10.1371/journal.ppat.0040042>
19. Fonseca AM, Quinto L, Jiménez A, González R, Bardají A, Maculve S, et al. Multiplexing detection of IgG against *Plasmodium falciparum* pregnancy-specific antigens. *PLoS One*. 2017;12:e0181150. <https://doi.org/10.1371/journal.pone.0181150>
20. Menéndez C, Bardají A, Sigauque B, Romagosa C, Sanz S, Serra-Casas E, et al. A randomized placebo-controlled trial of intermittent preventive treatment in pregnant women in the context of insecticide treated nets delivered through the antenatal clinic. *PLoS One*. 2008;3:e1934. <https://doi.org/10.1371/journal.pone.0001934>
21. González R, Mombo-Ngoma G, Ouédraogo S, Kakolwa MA, Abdulla S, Accrombessi M, et al. Intermittent preventive treatment of malaria in pregnancy with mefloquine in HIV-negative women: a multicentre randomized controlled trial. *PLoS Med*. 2014;11:e1001733. <http://dx.doi.org/10.1371/journal.pmed.1001733>
22. González R, Desai M, Macete E, Ouma P, Kakolwa MA, Abdulla S, et al. Intermittent preventive treatment of malaria in pregnancy with mefloquine in HIV-infected women receiving cotrimoxazole prophylaxis: a multicenter randomized placebo-controlled trial. *PLoS Med*. 2014;11:e1001735. <http://dx.doi.org/10.1371/journal.pmed.1001735>
23. Simes R. An improved Bonferroni procedure for multiple tests of significance. *Biometrika*. 1986;73:751–4. <https://doi.org/10.1093/biomet/73.3.751>
24. Bockhorst J, Lu F, Janes JH, Keebler J, Gamain B, Awadalla P, et al. Structural polymorphism and diversifying selection on the pregnancy malaria vaccine candidate VAR2CSA. *Mol Biochem Parasitol*. 2007;155:103–12. <http://dx.doi.org/10.1016/j.molbiopara.2007.06.007>
25. Doritchamou J, Sabbagh A, Jespersen JS, Renard E, Salanti A, Nielsen MA, et al. Identification of a major dimorphic region in the functionally critical N-terminal ID1 domain of VAR2CSA. *PLoS One*. 2015;10:e0137695. <https://doi.org/10.1371/journal.pone.0137695>
26. Nunes-Silva S, Gangnard S, Vidal M, Vuchelen A, Dechavanne S, Chan S, et al. Llama immunization with full-length VAR2CSA generates cross-reactive and inhibitory single-domain antibodies against the DBL1X domain. *Sci Rep*. 2014;4:7373. <http://dx.doi.org/10.1038/srep07373>
27. Mandomando IM, Macete EV, Ruiz J, Sanz S, Abacassamo F, Vallès X, et al. Etiology of diarrhea in children younger than 5 years of age admitted in a rural hospital of southern Mozambique. *Am J Trop Med Hyg*. 2007;76:522–7. <https://doi.org/10.4269/ajtmh.2007.76.522>
28. Bhatt S, Weiss DJ, Cameron E, Bisanzio D, Mappin B, Dalrymple U, et al. The effect of malaria control on *Plasmodium falciparum* in Africa between 2000 and 2015. *Nature*. 2015;526:207–11. <http://dx.doi.org/10.1038/nature15535>
29. Nanche D, Serra-Casas E, Bardají A, Quintó L, Dobaño C, Sigauque B, et al. Reduction of antimalarial antibodies by HIV infection is associated with increased risk of *Plasmodium falciparum* cord blood infection. *J Infect Dis*. 2012;205:568–77. <http://dx.doi.org/10.1093/infdis/jir815>
30. Sepúlveda N, Stresman G, White MT, Drakeley CJ. Current mathematical models for analyzing anti-malarial antibody data with an eye to malaria elimination and eradication. *J Immunol Res*. 2015;2015:738030. <https://doi.org/10.1155/2015/738030>
31. Welch RJ, Anderson BL, Litwin CM. Rapid immunochromatographic strip test for detection of anti-K39 immunoglobulin G antibodies for diagnosis of visceral leishmaniasis. *Clin Vaccine Immunol*. 2008;15:1483–4. <https://doi.org/10.1128/CVI.00174-08>

Address for correspondence: Alfredo Mayor, ISGlobal, Hospital Clínic, Universitat de Barcelona, Carrer Rosselló 153 (CEK Bldg), E-08036 Barcelona, Spain; email: alfredo.mayor@isglobal.org

Risk Factors for Carbapenem-Resistant *Pseudomonas aeruginosa*, Zhejiang Province, China

Yan-Yan Hu, Jun-Min Cao, Qing Yang, Shi Chen, Huo-Yang Lv, Hong-Wei Zhou, Zuwei Wu, Rong Zhang

Carbapenem-resistant *Pseudomonas aeruginosa* (CRPA) is a public health concern worldwide, but comprehensive analysis of risk factors for CRPA remains limited in China. We conducted a retrospective observational study of carbapenem resistance in 71,880 *P. aeruginosa* isolates collected in Zhejiang Province during 2015–2017. We analyzed risk factors for CRPA, including the type of clinical specimen; the year, season, and region in which it was collected; patient information, including age, whether they were an outpatient or inpatient, and whether inpatients were in the intensive care unit or general ward; and the level of hospital submitting isolates. We found CRPA was more prevalent among isolates from patients ≥ 60 years of age and in inpatients, especially in intensive care units. In addition, specimen types and seasons in which they were collected were associated with higher rates of CRPA. Our findings can help hospitals reduce the spread of *P. aeruginosa* and optimize antimicrobial drug use.

The bacterium *Pseudomonas aeruginosa* is a particularly concerning nosocomial pathogen because of its intrinsic resistance to multiple antimicrobial agents (1,2). In 2016, surveillance of nosocomial infections in China showed *P. aeruginosa* was the fifth most frequently isolated pathogen, accounting for 8.7% of hospital-acquired infections, and the fourth most common (8.0%) in Zhejiang Province (3,4). *P. aeruginosa* often causes severe infections and results in high rates of illness and death among infected patients (1). A survey in the United States revealed that *P. aeruginosa* was the second-leading cause of nosocomial pneumonia (14%–16%), third main contributor of urinary tract infections (7%–11%), and seventh major cause of bloodstream infections (2%–6%) (5,6).

Author affiliations: Second Affiliated Hospital of Zhejiang University, School of Medicine, Hangzhou, China (Y.-Y. Hu, H.-W. Zhou, R. Zhang); First Affiliated Hospital of Zhejiang University, School of Medicine, Hangzhou (Q. Yang); Zhejiang Provincial Hospital of Traditional Chinese Medicine, Hangzhou (J.-M. Cao, H.-Y. Lv); Hangzhou Third People's Hospital, Hangzhou (S. Chen); Iowa State University, Ames, Iowa, USA (Z. Wu)

DOI: <https://doi.org/10.3201/eid2510.181699>

Carbapenems are the most effective antimicrobial agents against severe *P. aeruginosa* nosocomial infections involving bacteria producing cephalosporinase AmpC or extended-spectrum β -lactamases (7). However, *P. aeruginosa* has become increasingly resistant to carbapenems. A 2016 World Health Organization survey ranked carbapenem-resistant *P. aeruginosa* (CRPA) as the second most critical-priority bacterium among 20 antimicrobial-resistant bacterial species (8).

CHINET surveillance (<http://www.chinets.com>) revealed that CRPA in Zhejiang Province, China, increased annually from 22% in 2015 to 38.67% in 2017 and that Zhejiang had the highest rates of CRPA of all provinces in China in 2017. In addition, Zhejiang reported the local emergence of carbapenem-resistant *Klebsiella pneumoniae* carbapenemase-producing *P. aeruginosa* in 2015 (9). Given the clinical importance of CRPA, we analyzed short-term trends and various risk factors related to the occurrence of carbapenem resistance in *P. aeruginosa* in Zhejiang, as well as co-resistance to other commonly used antimicrobial agents.

Materials and Methods

Bacterial Species and Strain Identification

We obtained data from the Annual Review of Hospital Infection Resistance Survey in Zhejiang Province, collected during 2015–2017 (4,10,11). Each of the ≥ 78 secondary or tertiary hospitals enrolled in the surveillance each year (Table 1) imported and shared data of routine antimicrobial susceptibility testing using WHONET 5.6 software (<http://www.whonet.org>). Enrolled hospitals are distributed in 11 cities of Zhejiang Province: Hangzhou, Huzhou, Jiaxing, Shaoxing, Ningbo, Taizhou, Jinhua, Quzhou, Lishui, Wenzhou, and Zhoushan. Each hospital laboratory cultured isolates on blood agar plates and identified antimicrobial-resistant strains by using matrix-assisted laser desorption/ionization time of flight (MALDI-TOF) mass spectrometry, the VITEK 2 Compact system (bioMérieux, <https://www.biomerieux.com>), or the Phoenix 100 system (Becton Dickinson, <https://www.bd.com>).

Table 1. *Pseudomonas aeruginosa* isolates obtained from hospitals in Zhejiang Province, China, 2015–2017

Year	No. hospitals*				No. isolates	Isolation rate, %†	Gram-negative isolates, %	Imipenem-resistant isolates, %	
	Total	3A	3B	2A					2B
2015	78	41	23	13	1	22,464	8.1	11.9	35.4
2016	88	44	23	19	2	24,303	8.0	12.0	37.1
2017	84	41	24	18	1	25,113	7.8	12.0	39.1

*Hospital classification is performed by the National Health Commission of China on the basis of the number of beds and comprehensive evaluation scores. Comprehensive evaluation covers the number of departments, staffing levels, management, technical level, work quality, and supporting facilities. Class 3 hospitals have >500 beds, class 2 hospitals have 100–499 beds. Grade levels are given on the basis of scores from a comprehensive evaluation; grade A hospitals received >900 points, grade B hospitals received 750–899 points.

†*P. aeruginosa* was the fourth most commonly isolated pathogen in the region in each of the reported years.

Antimicrobial Susceptibility Testing

We performed antimicrobial susceptibility testing on 71,880 *P. aeruginosa* isolates submitted during 2015–2017. We tested for susceptibility to gentamicin, amikacin, piperacillin/tazobactam, ceftazidime, cefepime, aztreonam, imipenem, meropenem, ciprofloxacin, levofloxacin, colistin, and polymyxin B. We selected these 12 antimicrobial agents because all are used routinely in clinical settings in the province and we could include 1–2 from each antimicrobial category, per guidelines from the Clinical and Laboratory Standards Institute (CLSI; 12). We imported susceptibility data into WHONET, deleted duplicated strains, used only the first isolate from each patient, and interpreted results according to CLSI guidelines (12).

Hospitals prepared isolates for susceptibility testing by using the Kirby-Bauer method and interpreted results manually according to CLSI guidelines (12) or by using broth microdilution for analysis by VITEK 2 or Phoenix 100 automated systems. To ensure comparable susceptibility tests between hospitals, each used the same reference strain, *P. aeruginosa* ATCC27853, and standardized procedures, following guidelines from the National Health Commission of China. We considered possible inaccuracies of susceptibility tests for colistin and polymyxin B in automated systems, especially by the Kirby-Bauer method, because of poor and slow diffusion in agar plates (13) and applied strict quality control practices by comparing results against our reference strain.

We conducted imipenem susceptibility testing of 71,880 isolates and meropenem susceptibility testing of 26,916 (37.44%). We used imipenem resistance as an indicator of carbapenem resistance and separately analyzed imipenem-resistant (IMP-R) and imipenem-susceptible (IMP-S) *P. aeruginosa* isolates against the other antimicrobial agents.

Classifications

We used year as an independent variant for occurrence analysis of IMP-R *P. aeruginosa*. Then, we calculated other variants by year. For our analysis, we categorized patient age into 6 groups: 0–2, 3–9, 10–19, 20–39, 40–59, and ≥60 years of age. Then we analyzed specific specimen

types: blood, sputum, and urine. We analyzed outpatient and inpatient data and divided inpatients into 2 categories: those in intensive care units (ICUs) and those in standard patient wards (non-ICUs). To assess seasonality of CRPA, we analyzed quarters of the year, January–March, April–June, July–September, and October–December.

We grouped hospitals into 4 levels, 3A, 3B, 2A, and 2B, according to classifications designated by the National Health Commission of China, which classifies hospitals on the basis of the number of beds and scores on a comprehensive evaluation. Class 3 hospitals have >500 beds, and class 2 hospitals have 100–499 beds. The National Health Commission grades hospitals using scores from a comprehensive evaluation of the number of departments, staffing levels, management, technical level, work quality, and supporting facilities. Grade A hospitals received >900 points; grade B hospitals received 750–899 points.

We grouped geographic regions by city (Figure 1). Then, we analyzed each variant by year (Appendix Figure 1, <http://wwwnc.cdc.gov/EID/article/25/10/18-1699-App1.pdf>).

Statistical Analysis

We analyzed antimicrobial resistance patterns of *P. aeruginosa* isolates exported from WHONET. We used unconditional logistic regression models to estimate odds ratios (ORs) and 95% CIs for univariable analysis of risk factors associated with IMP-R *P. aeruginosa*. We used either Pearson χ^2 test or Fisher exact test to compare the frequency distribution of categorical variables. For all models, we considered $p < 0.05$ statistically significant and then performed 2-sided probability on those results by using SPSS version 23.0 (IBM, <https://www.ibm.com>). We classified both intermediate and resistant isolates as IMP-R.

Results

Surveillance Data

Approximately 80 hospitals from 11 administrative districts in Zhejiang Province participated in the annual survey of antimicrobial resistance. *P. aeruginosa* was the fourth most frequently isolated nosocomial pathogen identified, accounting for 8.0% of all bacteria obtained and 12.0%

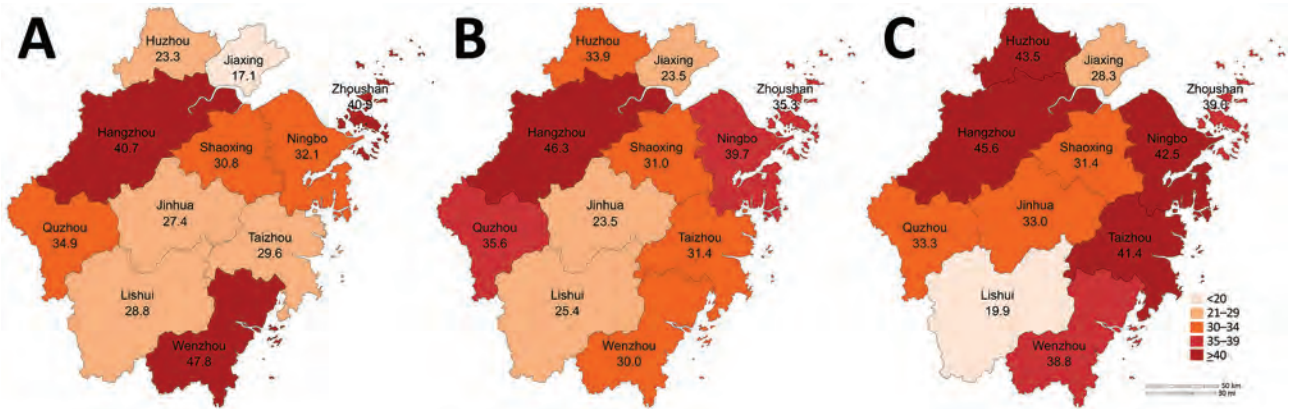


Figure 1. Heatmap of rates of carbapenem-resistant *Pseudomonas aeruginosa* each year in administrative districts in Zhejiang Province, China. A) 2015; B) 2016; C) 2017.

of gram-negative bacteria collected in Zhejiang. During 2015–2017, hospitals submitted 71,880 *P. aeruginosa* isolates, >20,000 each year; this total is much higher than the numbers analyzed in studies from the United States and Europe (14,15). The large number of isolates provides a strong dataset for our statistical analysis.

We found that 26,789 isolates (37.26%) were resistant to imipenem. The rate of IMP-R *P. aeruginosa* was >35% in each year and increased gradually during the study period. The meropenem resistance rate of ≈29% was slightly lower than that of imipenem resistance in the 3 years analyzed. In addition, we found that 29.54% of isolates were resistant to piperacillin/tazobactam and 25.11% were resistant to cefepime (Table 1; Figure 2; Appendix Table 1).

Correlation of IMP-R *P. aeruginosa* with Risk Factors

We examined the correlation between IMP-R *P. aeruginosa* and risk factors by using OR (Table 2). We investigated quarter of the year, geographic region, patient age, inpatient or outpatient status, and ICU or non-ICU status as risk factors. Our analysis showed that the year isolates were collected had a statistically significant effect on the OR for IMP-R *P. aeruginosa*: OR 1.072 (95% CI 1.032–1.115) in 2016 compared with 2015 and OR 1.167 (95% CI 1.124–1.213) for 2017 compared with 2015. Seasonality was also a factor; *P. aeruginosa* isolates collected during January–March,

April–June, and October–December were more likely to be IMP-R than those collected during July–September. We found that the capital of Zhejiang, Hangzhou, as well as Huzhou, Ningbo, Taizhou, Zhoushan, Wenzhou, and Quzhou, had higher IMP-R *P. aeruginosa* rates than other cities.

Isolates from inpatients had higher rates of imipenem resistance than those from outpatients, and isolates from patients in ICUs were more likely to be IMP-R than those from patients in non-ICU wards. When analyzed for patient age, the highest proportion of resistant isolates were collected from patients ≥60 years of age. We found no statistically significant difference in risk for IMP-R among isolates collected from patients 0–2 and 3–9 years of age. However, in other age groups, OR increased with age. In addition, we found that isolates from blood and sputum cultures were more likely to be IMP-R than isolates from urine (Table 2).

Antimicrobial Resistance Patterns of *P. aeruginosa*

Overall, *P. aeruginosa* showed high susceptibility to lipopeptides (99.07% to colistin and 98.5% to polymyxin B) and aminoglycosides (93.06% to amikacin and 85.88% to gentamicin) but high resistance to cephalosporins and fluquinolones (≈20%–30% susceptibility) and aztreonam (35.65% susceptibility) (Table 3). When we classified isolates into IMP-R and IMP-S groups, we

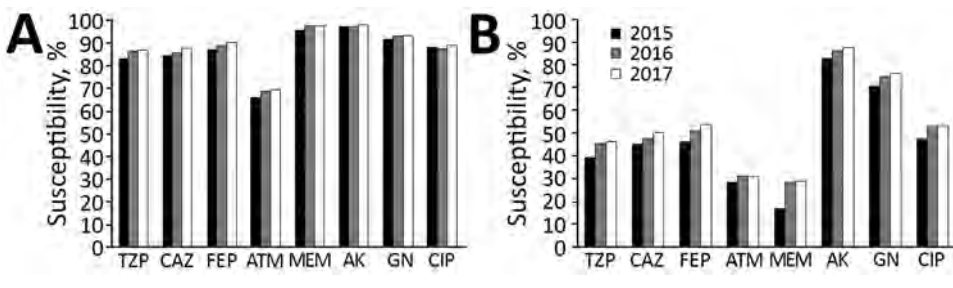


Figure 2. Annual susceptibility rates to antimicrobial agents among imipenem-susceptible (A) and imipenem-resistant (B) *Pseudomonas aeruginosa* isolates Zhejiang Province, China. AK, amikacin; ATM, aztreonam; CAZ, ceftazidime; CIP, ciprofloxacin; FEP, cefepime; GN, gentamicin; MEM, meropenem; TZP, piperacillin/tazobactam.

Table 2. Annual odds ratios for risk factors associated with carbapenem-resistant *Pseudomonas aeruginosa*, Zhejiang Province, China, 2015–2017*

Characteristics	2015		2016		2017	
	OR (95% CI)	p value	OR (95% CI)	p value	OR (95% CI)	p value
District						
Jiaxing	Referent		Referent		Referent	
Hangzhou	3.22 (2.85–3.63)	<0.001	2.83 (2.52–3.19)	<0.001	2.10 (1.91–2.31)	<0.001
Huzhou	1.42 (1.16–1.75)	0.001	1.68 (1.41–2.00)	<0.001	1.92 (1.55–2.38)	<0.001
Ningbo	2.23 (1.94–2.56)	<0.001	2.16 (1.89–2.47)	<0.001	1.85 (1.64–2.07)	<0.001
Taizhou	1.97 (1.65–2.36)	<0.001	1.50 (1.29–1.75)	<0.001	1.77 (1.51–2.07)	<0.001
Zhoushan	3.24 (2.63–4.00)	<0.001	1.79 (1.46–2.18)	<0.001	1.61 (1.31–1.97)	<0.001
Wenzhou	4.30 (3.75–4.94)	<0.001	1.40 (1.18–1.65)	<0.001	1.59 (1.40–1.80)	<0.001
Quzhou	2.99 (2.48–3.61)	<0.001	1.81 (1.53–2.14)	<0.001	1.25 (1.09–1.45)	0.002
Jinhua	1.77 (1.51–2.08)	<0.001	0.99 (0.85–1.15)	0.893	1.24 (1.09–1.40)	0.001
Shaoxing	2.09 (1.77–2.47)	<0.001	1.47 (1.26–1.71)	<0.001	1.10 (0.96–1.25)	0.165
Lishui	1.90 (1.59–2.27)	<0.001	1.11 (0.89–1.39)	0.345	0.62 (0.49–0.79)	<0.001
Specimen type						
Urine	Referent		Referent		Referent	
Blood	1.23 (0.99–1.53)	0.067	1.68 (1.35–2.08)	<0.001	1.44 (1.66–1.77)	0.001
Sputum	1.87 (1.66–2.96)	<0.001	1.97 (1.76–2.22)	<0.001	2.13 (1.90–2.39)	<0.001
Patient age, y						
0–2	Referent		Referent		Referent	
3–9	0.93 (0.58–1.49)	0.764	0.83 (0.56–1.23)	0.362	1.06 (0.73–1.54)	0.768
10–19	1.66 (0.99–2.48)	0.055	1.23 (0.84–1.80)	0.295	1.57 (1.08–2.29)	0.018
20–39	3.51 (2.48–4.97)	<0.001	2.28 (1.70–3.06)	<0.001	2.62 (1.95–3.55)	<0.001
40–59	3.93 (2.82–5.48)	<0.001	2.57 (1.95–3.39)	<0.001	3.09 (2.33–4.10)	<0.001
>60	4.34 (3.13–6.02)	<0.001	2.83 (2.15–3.71)	<0.001	3.24 (2.45–4.27)	<0.001
Quarter						
Jul–Sep	Referent		Referent		Referent	
Jan–Mar	2.11 (1.46–3.03)	<0.001	1.30 (1.17–1.44)	<0.001	1.90 (1.75–2.07)	<0.001
Apr–Jun	NA	NA	1.09 (0.97–1.22)	0.136	1.56 (1.42–1.70)	<0.001
Oct–Dec	NA	NA	1.28 (1.15–1.43)	<0.001	1.21 (1.11–1.31)	<0.001
Hospital level†						
2B	Referent		Referent		Referent	
2A	1.36 (0.71–2.63)	0.355	1.46 (0.96–2.20)	0.073	1.84 (1.11–3.04)	0.016
3B	1.13 (0.59–2.18)	0.712	0.95 (0.63–1.44)	0.819	1.35 (0.82–2.25)	0.239
3A	1.93 (1.01–3.71)	0.044	1.10 (0.72–1.68)	0.653	1.58 (0.95–2.63)	3.175
Type of patient						
Outpatient	Referent		Referent		Referent	
Inpatient, ward					1.15 (1.01–1.31)	0.039
Non-ICU	Referent		Referent		Referent	
ICU	2.60 (2.42–2.79)	<0.001	2.66 (2.49–2.85)	<0.001	2.57 (2.38–2.78)	<0.001

*Isolates from patients with missing values on the variables are not included in the analysis. Bold text indicates statistical significance. NA, not available; OR, odds ratio.

†Hospital classification is performed by the National Health Commission of China on the basis of the number of beds and comprehensive evaluation scores. Comprehensive evaluation covers the number of departments, staffing levels, management, technical level, work quality, and supporting facilities. Class 3 hospitals have >500 beds, class 2 hospitals have 100–499 beds. Grade levels are given on the basis of scores from a comprehensive evaluation; grade A hospitals received >900 points, grade B hospitals received 750–899 points.

found statistically significant differences ($p < 0.001$) in resistance rates between resistant and susceptible isolates for all analyzed antimicrobial drugs except lipopeptides. IMP-R isolates exhibited statistically lower susceptibility than IMP-S isolates to all antimicrobial drugs except the lipopeptides, colistin and polymyxin B. We saw a 2–3-fold difference in MIC₅₀ (MIC needed to inhibit 50% of cells) between IMP-S isolates and IMP-R isolates. In contrast, for each antimicrobial drug except lipopeptides, most IMP-R strains belonged to the MIC₉₀ group (MIC needed to inhibit 90% of cells), whereas the IMP-S isolates were more prevalent in the MIC₅₀ group. Similarly, the IMP-R group was highly resistant (25.36%) to meropenem, but IMP-S group was highly susceptible (96.97%) (Figure 2).

Discussion

Carbapenems are the most effective antimicrobial agents against serious infections caused by multidrug-resistant gram-negative bacilli. However, the resistance rate of *P. aeruginosa* to carbapenems has been consistently high (3,16–18). Clarifying resistance trends of CRPA and related risk factors can guide antimicrobial use and selection of effective treatment plans.

In our study, rates of IMP-R *P. aeruginosa* increased annually and were higher in Zhejiang Province than reported for other provinces in national surveillance through CHINET (3,17,18). For instance, 2017 CHINET surveillance reported national rates of 27.3% for IMP-R *P. aeruginosa* and 25.1% for meropenem-resistant *P. aeruginosa* (18), but in Zhejiang Province the rates were 39.3% for

Table 3. Antimicrobial resistance patterns of imipenem-resistant and imipenem-susceptible *Pseudomonas aeruginosa* isolates, Zhejiang Province, China, 2015–2017*

Antimicrobial drugs	No. isolates (susceptibility rate, %)		p value	Total susceptibility rate, %	MIC ₅₀ , µg/mL		MIC ₉₀ , µg/mL	
	IMP-S	IMP-R			S	R	S	R
Piperacillin/tazobactam	41,145 (85.70)	23,721 (44.01)	<0.001	70.46	8	64	64	128
Ceftazidime	30,326 (86.26)	18,348 (47.93)	<0.001	71.81	4	16	32	64
Cefepime	42,492 (89.01)	24,947 (50.83)	<0.001	74.89	2	8	16	64
Aztreonam	24,215 (68.07)	13,823 (30.32)	<0.001	54.35	8	32	32	64
Amikacin	42,106 (97.38)	24,748 (85.69)	<0.001	93.06	2	4	8	64
Gentamicin	41,207 (92.80)	24,618 (74.29)	<0.001	85.88	1	2	4	16
Ciprofloxacin	42,442 (88.28)	25,063 (51.64)	<0.001	74.67	0.25	1	2	4
Levofloxacin	41,982 (89.06)	24,593 (53.17)	<0.001	75.80	0.5	2	4	8
Meropenem	17,166 (96.97)	9,750 (25.36)	<0.001	71.03	1	8	1	16
Colistin	1,624 (99.08)	627 (99.04)	NA	99.07	1	1	1	2
Polymyxin B	5,012 (98.60)	3,746 (98.37)	0.452	98.50	1	1	2	2

*MIC₅₀ and MIC₉₀ were generated from the minimal inhibitory concentrations of antimicrobial drugs. Bold text indicates p values <0.05. IMP-R, imipenem-resistant; IMP-S, imipenem-susceptible; NA, not applicable; R, resistant; S, susceptible.

IMP-R and 28.1% for meropenem-resistant isolates. Both the CHINET surveillance and our data indicated CRPA poses a severe challenge in Zhejiang Province. The slightly lower resistance rate we saw for meropenem could be because we tested fewer isolates for meropenem resistance (n = 26,916) than for imipenem resistance (n = 71,880) or could be the result of other mechanisms, such as mutation or loss of the oprD2 in some isolates (19).

When we examined risk factors, we found that patient type and ward were associated with a higher prevalence of IMP-R *P. aeruginosa*. Inpatients and those admitted to an ICU had higher IMP-R rates than outpatients and those in non-ICU wards, in accordance with previous studies (20), indicating ICU admission is a risk factor for IMP-R *P. aeruginosa*. Patient age also factors into IMP-R *P. aeruginosa* occurrence in Zhejiang (21), which could be a result of the low immune function of patients ≥60 years of age. We saw an increase in the rate of IMP-R with increased patient age but did not see increased rates for patients 0–2, 3–9, or 10–19 years of age. However, the IMP-R rate was >10% in 2015 and increased to 20.9% in 2017 in the 10–19-year age group (data not shown), which could signal a potential increasing trend of IMP-R in subsequent years. Further studies with clinical information and data are needed to investigate this issue.

A previous study in India showed that *P. aeruginosa* isolates from sputum and blood samples from patients in the ICU were more resistant than isolates from urine (22). Other studies in China also have observed this discrepancy of *P. aeruginosa* from various specimen types (16,23). We found this observation was true, not only for isolates from patients in the ICU but for all patient isolates included in our study, indicating IMP-R *P. aeruginosa* might be a less likely agent in urinary tract infection.

Previous studies also stated that the occurrence of *P. aeruginosa* infection was associated with seasons (24,25) and that the isolation rate usually was higher in summer than in winter. However, we observed a reverse outcome for IMP-R *P. aeruginosa*: a higher prevalence in winter

than in summer (data not shown). The seasonal effect on IMP-R *P. aeruginosa* rates is unknown, but our finding could potentially inform clinical recommendations.

By OR analysis, we found that IMP-R *P. aeruginosa* was more prevalent in 7 administrative districts: Hangzhou, Huzhou, and Quzhou in the northwest and Ningbo, Taizhou, Zhoushan, and Wenzhou in the southeast of the province. However, we found no statistical differences in IMP-R related to hospital classification in Zhejiang, which is worth noting because patients in class 2 hospitals usually have mild or moderate illnesses and patients in class 3 hospitals have more severe conditions or are immunocompromised and more susceptible to infection. We weighted class 2 hospitals differently than class 3 hospitals in our statistical analysis to account for the difference in patient types. However, because we saw no statistically significant difference in imipenem resistance rates related to the hospital level, we should put the same weight on both classes of hospitals in future analyses.

Although our study showed *P. aeruginosa* was highly resistant to carbapenems and multiple other drugs, it remains highly susceptible to colistin and has some sensitivity to cephalosporins and fluoroquinolones. IMP-R *P. aeruginosa* is most sensitive to colistin in vitro, and colistin is effective against multidrug-resistant *P. aeruginosa* nosocomial infections (26). Despite its strong neurotoxicity and ototoxicity, colistin was reapproved for clinical applications in China in September 2017. However, efficacy of colistin monotherapy has been questioned in clinical trials (27), and colistin should be used in combination with other antimicrobial agents in clinical therapy.

Novel antimicrobial agents approved by the US Food and Drug Administration, such as ceftolozane/tazobactam or ceftazidime/avivactam, could be other treatment options. These drug combinations have good efficacy against CRPA isolates (28,29) but currently are not approved for use in China. Of note, ceftolozane/tazobactam might not be useful against carbapenemase-producing *P. aeruginosa* (30), and prerequisite identification of resistance mechanisms would

be needed to develop rational antimicrobial drug regimens. In addition, a novel plasmid-mediated colistin-resistant gene, *mcr*, has emerged in *Enterobacteriaceae* (31–33). To reduce the chances of its dissemination to *P. aeruginosa* under antimicrobial drug selection pressure, clinicians should prioritize colistin only for severe cases of *P. aeruginosa* infection in clinical practice. Because of limitations of susceptibility testing methods (13), MICs for polymyxins might be less reliable in strains with MICs close to the breakpoint. Therefore, clinicians also should choose polymyxin therapies carefully.

Our study had some limitations. We excluded strains without a corresponding field from the classification analysis, such as patient age, patient type, or isolation time, which might have caused a distortion in the resistance rate. A disproportionate number of class 3 to class 2 hospitals participated in the surveillance, and class 2 hospitals inevitably were biased in the statistical antimicrobial resistance rate because they submit fewer isolates. In addition, we could not include therapeutic regimens, patient outcomes, or the molecular mechanisms of resistance for CRPA strains because they were not available, but these measures could inform clinical decisions and should be included in further surveillance studies.

In summary, we conducted a comprehensive analysis of risk factors associated with CRPA in Zhejiang Province, China. We investigated potential risk factors for IMP-R *P. aeruginosa* because Zhejiang Province has higher rates of carbapenem resistance compared with other provinces (34). Our research provides insights into CRPA in China and indicates an imperative for medical institutions in China to strengthen surveillance for this organism.

Acknowledgments

We thank all the members of the Zhejiang Province Surveillance of Antimicrobial Resistance Program for supplying the data.

This work was funded by the National Natural Science Foundation of China (grant nos. 81501805 and 81772250) and Natural Science Foundation of Zhejiang Province (grant no. LQ16H200002).

Contributions: Y.-Y.H. and R.Z. were involved in the conception and design of the study. J.-M.C., S.C., Q.Y., H.Y.-L., and H.-W.Z. collected the data. Y.-Y.H. and R.Z. analyzed and interpreted the data. Y.-Y.H., Z.W., and R.Z. wrote the manuscript. All authors read and approved the final manuscript.

About the Author

Dr. Hu is a clinical laboratory technician at the Second Affiliated Hospital of Zhejiang University, School of Medicine, Zhejiang University, Hangzhou, China. Her primary research interest is antibiotic resistance mechanisms of gram-negative bacteria.

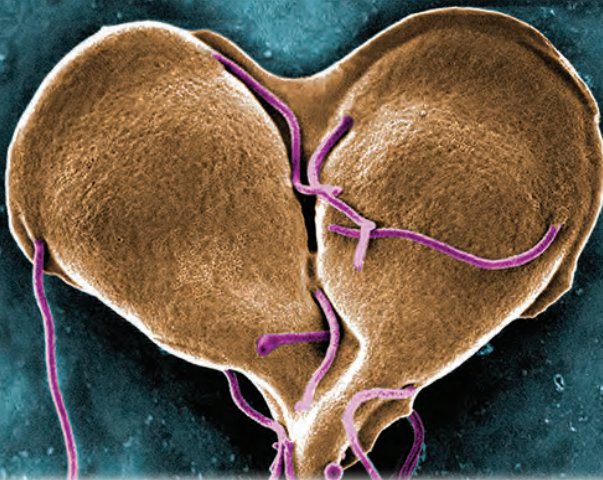
References

- Lister PD, Wolter DJ, Hanson ND. Antibacterial-resistant *Pseudomonas aeruginosa*: clinical impact and complex regulation of chromosomally encoded resistance mechanisms. *Clin Microbiol Rev*. 2009;22:582–610. <https://doi.org/10.1128/CMR.00040-09>
- Poole K. *Pseudomonas aeruginosa*: resistance to the max. *Front Microbiol*. 2011;2:65. <https://doi.org/10.3389/fmicb.2011.00065>
- Hu F, Guo Y, Zhu D, Wang F, Jiang X, Xu Y, et al. CHINET surveillance of bacterial resistance across China: report of the results in 2016. *Chin J Infect Chemother*. 2017;17:481–91. <https://doi.org/10.16718/j.1009-7708.2017.05.001>
- Xie X, Yu Y. Annual review of hospital infection resistance survey in Zhejiang Province, 2015 ed. Hangzhou (China): Zhejiang University Press; 2016.
- Emori TG, Gaynes RP. An overview of nosocomial infections, including the role of the microbiology laboratory. *Clin Microbiol Rev*. 1993;6:428–42. <https://doi.org/10.1128/CMR.6.4.428>
- National Nosocomial Infections Surveillance (NNIS) System report, data summary from October 1986–April 1998, issued June 1998. *Am J Infect Control*. 1998;26:522–33. [https://doi.org/10.1016/S0196-6553\(98\)70026-4](https://doi.org/10.1016/S0196-6553(98)70026-4)
- Zavascki AP, Carvalhaes CG, Picão RC, Gales AC. Multidrug-resistant *Pseudomonas aeruginosa* and *Acinetobacter baumannii*: resistance mechanisms and implications for therapy. *Expert Rev Anti Infect Ther*. 2010;8:71–93. <https://doi.org/10.1586/eri.09.108>
- Tacconelli E, Carrara E, Savoldi A, Harbarth S, Mendelson M, Monnet DL, et al.; WHO Pathogens Priority List Working Group. Discovery, research, and development of new antibiotics: the WHO priority list of antibiotic-resistant bacteria and tuberculosis. *Lancet Infect Dis*. 2018;18:318–27. [https://doi.org/10.1016/S1473-3099\(17\)30753-3](https://doi.org/10.1016/S1473-3099(17)30753-3)
- Hu YY, Gu DX, Cai JC, Zhou HW, Zhang R. Emergence of KPC-2–producing *Pseudomonas aeruginosa* sequence type 463 isolates in Hangzhou, China. *Antimicrob Agents Chemother*. 2015;59:2914–7. <https://doi.org/10.1128/AAC.04903-14>
- Xie XY, Yu YS, Zhang R. Annual review of hospital infection resistance survey in Zhejiang Province, 2017 ed. Hangzhou (China): Zhejiang University Press; 2019
- Xie X, Yu Y. Annual review of hospital infection resistance survey in Zhejiang Province, 2016 ed. Hangzhou (China): Zhejiang University Press; 2017.
- Clinical and Laboratory Standards Institute. Performance standards for antimicrobial susceptibility testing; twenty-eighth informational supplement (M100-S28). Wayne (PA): The Institute; 2018.
- Poirel L, Jayol A, Nordmann P. Polymyxins: antibacterial activity, susceptibility testing, and resistance mechanisms encoded by plasmids or chromosomes. *Clin Microbiol Rev*. 2017;30:557–96. <https://doi.org/10.1128/CMR.00064-16>
- Woodworth KR, Walters MS, Weiner LM, Edwards J, Brown AC, Huang JY, et al. Vital signs: containment of novel multidrug-resistant organisms and resistance mechanisms—United States, 2006–2017. *MMWR Morb Mortal Wkly Rep*. 2018;67:396–401. <https://doi.org/10.15585/mmwr.mm6713e1>
- Kazmierczak KM, de Jonge BLM, Stone GG, Sahn DF. In vitro activity of ceftazidime/avibactam against isolates of *Pseudomonas aeruginosa* collected in European countries: INFORM global surveillance 2012–15. *J Antimicrob Chemother*. 2018;73:2777–81. <https://doi.org/10.1093/jac/dky267>
- Zhang W, Sun J, Ni Y, Yu Y, Lin J, Yang Q, et al. Resistance profile of *Pseudomonas aeruginosa* in hospitals across China: the results from CHINET Antimicrobial Resistance Surveillance Program, 2005–2014 [in Chinese]. *Chin J Infect Chemother*. 2016;16:141–5.
- Hu F, Zhu D, Wang F, Jiang X, Xu Y, Zhang X, et al. Report of CHINET Antimicrobial Resistance Surveillance Program in 2015 [in Chinese]. *Chin J Infect Chemother*. 2016;16:685–94.

18. Hu F, Guo Y, Zhu D, Wang F, Jiang X, Xu Y, et al. Antimicrobial resistance profile of clinical isolates in hospitals across China: report from the CHINET Surveillance Program, 2017 [in Chinese]. *Chin J Infect Chemother*. 2018;18:241–51.
19. Shen J, Pan Y, Fang Y. Role of the outer membrane protein OprD2 in carbapenem-resistance mechanisms of *Pseudomonas aeruginosa*. *PLoS One*. 2015;10:e0139995. <https://doi.org/10.1371/journal.pone.0139995>
20. Raman G, Avendano EE, Chan J, Merchant S, Puzniak L. Risk factors for hospitalized patients with resistant or multidrug-resistant *Pseudomonas aeruginosa* infections: a systematic review and meta-analysis. *Antimicrob Resist Infect Control*. 2018;7:79. <https://doi.org/10.1186/s13756-018-0370-9>
21. Defez C, Fabbro-Peray P, Bouziges N, Gouby A, Mahamat A, Daurès JP, et al. Risk factors for multidrug-resistant *Pseudomonas aeruginosa* nosocomial infection. *J Hosp Infect*. 2004;57:209–16. <https://doi.org/10.1016/j.jhin.2004.03.022>
22. Tennant I, Harding H, Nelson M, Roye-Green K. Microbial isolates from patients in an intensive care unit, and associated risk factors. *West Indian Med J*. 2005;54:225–31. <https://doi.org/10.1590/S0043-31442005000400003>
23. Chen Y, Sun J, Ni Y, Sun Z, Chen Z, Hu Z, et al. 2012 CHINET surveillance of antimicrobial resistance in *Pseudomonas aeruginosa* in China [in Chinese]. *Chin J Infect Chemother*. 2015;15:199–203.
24. Richet H. Seasonality in Gram-negative and healthcare-associated infections. *Clin Microbiol Infect*. 2012;18:934–40. <https://doi.org/10.1111/j.1469-0691.2012.03954.x>
25. Psoter KJ, De Roos AJ, Wakefield J, Mayer J, Rosenfeld M. Season is associated with *Pseudomonas aeruginosa* acquisition in young children with cystic fibrosis. *Clin Microbiol Infect*. 2013;19:E483–9. <https://doi.org/10.1111/1469-0691.12272>
26. Lee HG, Jang J, Choi JE, Chung DC, Han JW, Woo H, et al. Blood stream infections in patients in the burn intensive care unit. *Infect Chemother*. 2013;45:194–201. <https://doi.org/10.3947/ic.2013.45.2.194>
27. Perez F, Bonomo RA. Evidence to improve the treatment of infections caused by carbapenem-resistant Gram-negative bacteria. *Lancet Infect Dis*. 2018;18:358–60. [https://doi.org/10.1016/S1473-3099\(18\)30112-9](https://doi.org/10.1016/S1473-3099(18)30112-9)
28. Spoletini G, Etherington C, Shaw N, Clifton IJ, Denton M, Whitaker P, et al. Use of ceftazidime/avibactam for the treatment of MDR *Pseudomonas aeruginosa* and *Burkholderia cepacia* complex infections in cystic fibrosis: a case series. *J Antimicrob Chemother*. 2019;74:1425–9. <https://doi.org/10.1093/jac/dky558>
29. Fernández-Cruz A, Alba N, Semiglia-Chong MA, Padilla B, Rodríguez-Macías G, Kwon M, et al. A case-control study of real-life experience with ceftolozane-tazobactam in patients with hematologic malignancy and *Pseudomonas aeruginosa* infection. *Antimicrob Agents Chemother*. 2019;63:e02340–18.
30. Munita JM, Aitken SL, Miller WR, Perez F, Rosa R, Shimose LA, et al. Multicenter evaluation of ceftolozane/tazobactam for serious infections caused by carbapenem-resistant *Pseudomonas aeruginosa*. *Clin Infect Dis*. 2017;65:158–61. <https://doi.org/10.1093/cid/cix014>
31. Liu YY, Wang Y, Walsh TR, Yi LX, Zhang R, Spencer J, et al. Emergence of plasmid-mediated colistin resistance mechanism MCR-1 in animals and human beings in China: a microbiological and molecular biological study. *Lancet Infect Dis*. 2016;16:161–8. [https://doi.org/10.1016/S1473-3099\(15\)00424-7](https://doi.org/10.1016/S1473-3099(15)00424-7)
32. Wang Y, Tian GB, Zhang R, Shen Y, Tyrrell JM, Huang X, et al. Prevalence, risk factors, outcomes, and molecular epidemiology of mcr-1-positive *Enterobacteriaceae* in patients and healthy adults from China: an epidemiological and clinical study. *Lancet Infect Dis*. 2017;17:390–9. [https://doi.org/10.1016/S1473-3099\(16\)30527-8](https://doi.org/10.1016/S1473-3099(16)30527-8)
33. Tian GB, Doi Y, Shen J, Walsh TR, Wang Y, Zhang R, et al. MCR-1-producing *Klebsiella pneumoniae* outbreak in China. *Lancet Infect Dis*. 2017;17:577. [https://doi.org/10.1016/S1473-3099\(17\)30266-9](https://doi.org/10.1016/S1473-3099(17)30266-9)
34. Zhang R, Liu L, Zhou H, Chan EW, Li J, Fang Y, et al. Nationwide surveillance of clinical carbapenem-resistant *Enterobacteriaceae* (CRE) strains in China. *EBioMedicine*. 2017;19:98–106. <https://doi.org/10.1016/j.ebiom.2017.04.032>

Address for correspondence: Rong Zhang, Zhejiang University, Second Affiliated Hospital of Zhejiang University, School of Medicine, 88 Jiefang Rd, Hangzhou 310009, China; email: zhang-rong@zju.edu.cn; Zuwei Wu, Iowa State University, Department of Veterinary Microbiology and Preventive Medicine, 1113 Vet Med, 1800 Christensen Dr, Ames, IA 50011-1134, USA; email: wuzw@iastate.edu

The Public Health Image Library (PHIL)



The Public Health Image Library (PHIL), Centers for Disease Control and Prevention, contains thousands of public health-related images, including high-resolution (print quality) photographs, illustrations, and videos.

PHIL collections illustrate current events and articles, supply visual content for health promotion brochures, document the effects of disease, and enhance instructional media.

PHIL images, accessible to PC and Macintosh users, are in the public domain and available without charge.

Visit PHIL at <http://phil.cdc.gov/phil>

Sensitive and Specific Detection of Low-Level Antibody Responses in Mild Middle East Respiratory Syndrome Coronavirus Infections

Nisreen M.A. Okba, V. Stalin Raj, Ivy Widjaja, Corine H. GeurtsvanKessel, Erwin de Bruin, Felicity D. Chandler, Wan Beom Park, Nam-Joong Kim, Elmoubasher A.B.A. Farag, Mohammed Al-Hajri, Berend-Jan Bosch, Myoung-don Oh, Marion P.G. Koopmans, Chantal B.E.M. Reusken, Bart L. Haagmans

Middle East respiratory syndrome coronavirus (MERS-CoV) infections in humans can cause asymptomatic to fatal lower respiratory lung disease. Despite posing a probable risk for virus transmission, asymptomatic to mild infections can go unnoticed; a lack of seroconversion among some PCR-confirmed cases has been reported. We found that a MERS-CoV spike S1 protein-based ELISA, routinely used in surveillance studies, showed low sensitivity in detecting infections among PCR-confirmed patients with mild clinical symptoms and cross-reactivity of human coronavirus OC43-positive serum samples. Using in-house S1 ELISA and protein microarray, we demonstrate that most PCR-confirmed MERS-CoV case-patients with mild infections seroconverted; nonetheless, some of these samples did not have detectable levels of virus-neutralizing antibodies. The use of a sensitive and specific serologic S1-based assay can be instrumental in the accurate estimation of MERS-CoV prevalence.

Middle East respiratory syndrome coronavirus (MERS-CoV) poses a public health threat; ongoing outbreaks have been reported since its detection in 2012 (1). MERS-CoV infection may be asymptomatic or may cause illness ranging from mild to fatal; fatal infections account for 35% of reported cases (2–5). Dromedary camels are the virus reservoir (6,7) and pose a high risk of infecting

humans in contact with them (4,7–9). These spillover events may seed outbreaks in the community (10), which occur mainly in healthcare settings (11,12) and, to a lesser extent, among patient household contacts (13–15). Although not sustained, human-to-human transmission accounts for most reported cases (16) and may initiate outbreaks outside endemic areas, as seen in the 2015 South Korea outbreak (17). However, the rate of human-to-human transmission and total disease burden of MERS-CoV are not fully clear because we lack accurate data on the frequency of asymptomatic and mild infections.

Diagnostic assays with validated high sensitivity and specificity are crucial to estimate the prevalence of MERS-CoV. Molecular-based assays have been developed that enable sensitive and specific diagnosis of MERS-CoV infections (18,19). Although the molecular detection of viral nucleic acid by reverse transcription PCR (RT-PCR) is the standard for MERS-CoV diagnosis, serologic detection remains necessary. Viral nucleic acid is detectable within a limited timeframe after infection, and samples from the lower respiratory tract are required for reliable results. Furthermore, whereas mutations in the viral regions where the PCR probes bind could lead to decreased sensitivity (20), genetically diverse MERS-CoV strains may retain antigenic similarity (21). Validated serologic assays are needed to ensure that the full spectrum of infections is identified; antibodies can be detected for longer periods after infection and even if viruses mutate. Several research groups and companies have developed serologic assays allowing for high-throughput surveillance for MERS-CoV infections among large populations (15,19,22–25).

Despite the number of serological assays developed, none is considered to be fully validated. There are 2 major challenges concerning specificity and sensitivity

Author affiliations: Erasmus Medical Center, Rotterdam, the Netherlands (N.M.A. Okba, V.S. Raj, C.H. GeurtsvanKessel, E. de Bruin, F.D. Chandler, M.P.G. Koopmans, C.B.E.M. Reusken, B.L. Haagmans); Utrecht University, Utrecht, the Netherlands (I. Widjaja, B.-J. Bosch); Seoul National University College of Medicine, Seoul, South Korea (W.B. Park, N.-J. Kim, M.-D. Oh); Ministry of Public Health, Doha, Qatar (E.A.B.A. Farag, M. Al-Hajri)

DOI: <https://doi.org/10.3201/eid2509.190051>

aspects of MERS-CoV serologic assays. The first challenge is that 90% of the human population have antibodies against common cold-causing human coronaviruses (HCoVs) that could cross-react, resulting in false positives in serologic assays, especially in persons infected with viruses belonging to the same genus of β -coronaviruses as human seasonal coronaviruses OC43 and HKU1 (26). The spike protein, specifically its N-terminal S1 domain, is highly immunogenic and divergent among HCoVs, so it is an ideal candidate for virus-specific serologic assays (27). The second challenge is the low antibody responses among mildly infected and asymptomatic cases. Severe MERS-CoV infections result in a robust immune response allowing serologic detection in patients with positive or negative PCR outcomes (28), but PCR-diagnosed mild or asymptomatic infections may cause variable immune responses that can be undetectable by serologic assays (5,15,17). Therefore, a sensitive assay is necessary to avoid false-negative results that can cause failure in detection of subclinical infections and underestimation of prevalence in serosurveillance studies. We evaluated the antibody responses following severe and mild laboratory-confirmed MERS-CoV infections, validating and comparing different assay platforms for the specific and sensitive detection of MERS-CoV infections.

Materials and Methods

Serum Samples

We used a total of 292 serum samples in this study (Table 1; Appendix, <https://wwwnc.cdc.gov/EID/article/25/10/19-0051-App1.pdf>). The samples represented patients with serologically identified (8) and PCR-confirmed MERS-CoV infections (17,29), a cohort of healthy blood donors as a control group, and patients confirmed by RT-PCR to have non-MERS-CoV respiratory virus infections to assess assay specificity. The use of serum samples from the Netherlands was approved by the Erasmus Medical Center local medical ethics committee (MEC approval 2014-414). The Institutional Ethics Review Board of Seoul National University Hospital approved the use of samples from patients in South Korea (approval no. 1506-093-681). The Ethics and Institutional Animal Care and Use Committees of the Medical Research Center, Hamad Medical Corporation, approved the use of samples from Qatar (permit 2014-01-001).

Serologic Assays

We tested all serum samples for MERS-CoV neutralizing antibodies using plaque reduction neutralization assay (PRNT). For S1 reactivity, we used a routine ELISA (rELISA; Euroimmun, <https://www.euroimmun.com> [15]), an

in-house ELISA (iELISA), and protein microarray (8,23). For nucleocapsid reactivity, we used luciferase immunoprecipitation assay (N-LIPS) (24). For S2 reactivity, we used ELISA (Appendix).

Statistical Analyses

We evaluated the specificity and sensitivity and predictive values of the assay platforms using serum samples from patients with PCR-diagnosed MERS-CoV infections, respiratory virus-infected patients, and healthy controls. We compared performance of assay platforms to PCR performance using Fisher exact test and used receiver operating characteristic (ROC) curve to compare performance of different platforms. We performed all statistical analyses using GraphPad Prism version 7 (<https://www.graphpad.com>).

Results

Low Antibody Responses following Mild MERS-CoV Infection

Several studies have proposed that antibody levels and longevity following MERS-CoV infection are dependent on disease severity (5,15,17). Among PCR-confirmed MERS patients, mild infections may result in undetectable or lower, short-lived immune responses when compared with severe infections. We evaluated MERS-CoV-specific antibody responses in severe and mild MERS-CoV infections using serum samples collected 6, 9, and 12 months after disease onset from PCR-confirmed MERS-CoV patients from the 2015 South Korea outbreak, 6 with severe and 5 with mild infections (17). First, we tested serum samples for MERS-CoV S1 antibodies using different assay platforms (Figure 1; Appendix Table). Consistent with the earlier report (17), the routinely used rELISA detected only 2/6 mild infections (Figure 1, panel A). In contrast, iELISA detected 5/6 mild infections (Figure 1, panel B). Similar results were obtained using the S1 protein microarray to screen for MERS-CoV-specific antibodies (Figure 1, panel C). Although these serum samples lacked MERS-CoV neutralizing antibodies (17), the presence of nucleocapsid antibodies up to 1 year postinfection in 4/6 mildly infected patients' samples confirmed the results of the S1 ELISA with an assay targeting another MERS-CoV protein (Figure 1, panel D). All severe cases, on the other hand, were found positive in all tested platforms up to 1 year after disease onset, indicating a robust immune response of high antibody titers in severe cases (Figure 1; Appendix Table). Compared with milder infections, both S1 and neutralizing antibody responses were higher in severely infected cases, confirming that antibody responses are lower following nonsevere infection.

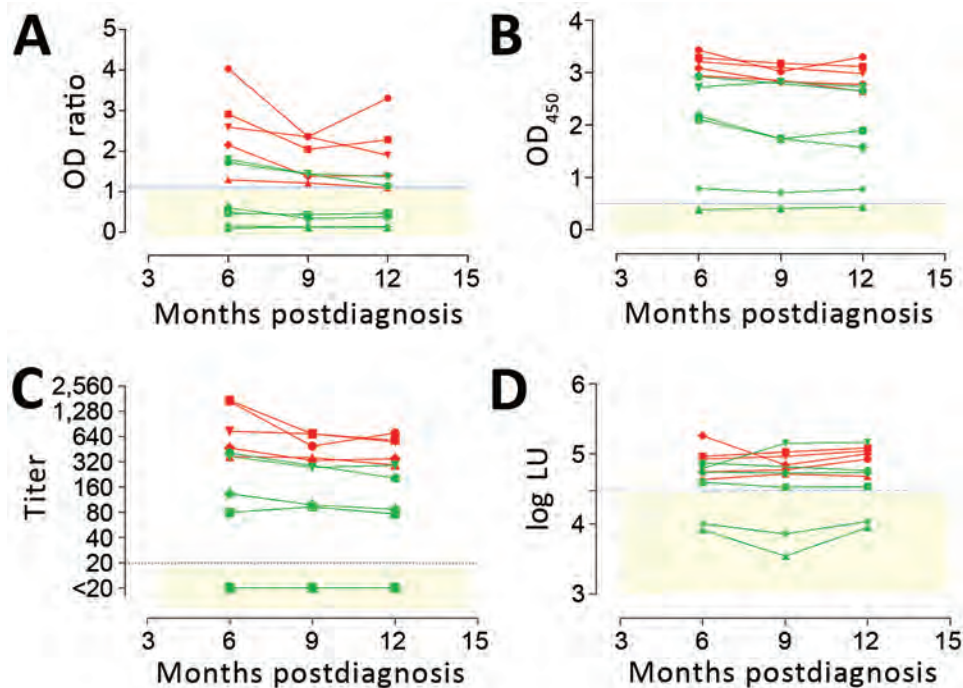


Figure 1. Detection of MERS-CoV-specific antibody responses 6–12 months following PCR-diagnosed mild and severe infections using different assays. Spike S1-specific antibody responses were tested with a routinely used S1 ELISA (rELISA) (A), in-house S1 ELISA (iELISA) (B), and S1 microarray (C). Nucleocapsid-specific antibody responses were tested using a luciferase immunoprecipitation assay (D). Severe infections (red, $n = 5$; cohort H) resulted in antibody responses detected for up to 1 year by all assays, while detection of mild infections (green, $n = 6$; cohort G) varied among assays. Horizontal dotted line indicates cutoff for each assay; yellow shaded area indicates serum undetected by each assay. CoV, coronavirus; LU, luminescence units; MERS, Middle East respiratory syndrome; OD, optical density.

Specificity and Sensitivity of In-house S1 ELISA and Microarray

To confirm that the variation in the detection of mild cases is caused by the sensitivity of the different platforms used, we further validated the platforms for specificity and sensitivity using 292 serum samples (Table 1). Using MERS-CoV neutralization as the standard for MERS-CoV serology, we tested all serum samples using plaque reduction neutralization assay (PRNT₅₀) and for S1, S2, and nucleocapsid reactivities.

We assessed the specificity of the assays using serum samples from cohorts A–C: healthy blood donors (cohort A), patients with PCR-confirmed acute respiratory non-CoV infections (cohort B), and patients with acute to convalescent PCR-confirmed α - and β -HCoV infections (cohort C). None of the serum samples from specificity cohorts A–C were reactive by iELISA at the set cutoff, indicating 100% specificity (Figure 2, panel A; Appendix). We also evaluated the sensitivity for detecting MERS-CoV infections; iELISA was able to detect MERS-CoV infections among persons with camel contact (cohort D1) who had low antibody levels as determined by protein microarray (8). Using samples from acute-phase PCR-diagnosed patients (cohort E), we detected seropositivity 6–8 days postdiagnosis (dpd). All convalescent-phase serum samples (cohort F) were positive up to the last time point tested: 228 dpd for patient 1 and 44 dpd for patient 2 (Appendix Figure 1).

These results reveal the high specificity and sensitivity of this ELISA platform, supporting our earlier findings

and confirming the sensitivity of our platform in detecting low immune responses among cases of milder infection (cohort G) (Figure 1). Overall, iELISA was 100% (95% CI 98.07%–100%) specific and 92.3% (11/13; 95% CI 66.7%–99.6%) sensitive for detection of PCR-confirmed cases (96.9% overall in the tested cohorts; 95% CI 84.3%–99.8%) (Table 2). Moreover, the iELISA performance was in accordance with that of the MERS-CoV S1 protein microarray (Figure 2, panel B). S1 microarray validation showed the same pattern of specificity with no false positives (100% specificity, 95% CI 98.07%–100%) in cohorts A–C and was 84.6% sensitive (95% CI 57.8%–97.3%) for PCR-confirmed cases and 93.8% overall (95% CI 79.9%–98.9%). Specificity of S1 as an antigen for MERS-CoV serology was further supported by the rates of seropositivity of all the serum samples from cohorts A–C: 87.4% for HCoV-HKU1, 91.3% for HCoV-OC43, 96.4% for HCoV-NL63, and 100% for HCoV-229E, as determined by microarray (Figure 2, panel C). All samples were seronegative for SARS-CoV, and no MERS-CoV false positives were detected in the iELISA and microarray. Overall, these results provided evidence for the use of S1 as a specific antigen for MERS-CoV serology.

We evaluated nucleocapsid and S2 antibody responses after MERS-CoV infections. At the set cutoff, none of the control serum samples tested positive for nucleocapsid antibodies (Figure 2, panel D). We detected seroconversion by nucleocapsid-luciferase immunoprecipitation assay among all severely infected, 4/6 (66.7%) mildly infected,

Table 1. Cohorts used in study of specificity and sensitivity of assays for MERS-CoV*

Cohort	Country	Sample source	Infection	No. samples	Postdiagnosis range
A	The Netherlands	Healthy blood donors (negative cohort)	NA	50	NA
B	The Netherlands	Non-CoV respiratory infections†	Adenovirus	5	2–4 w
			Bocavirus	2	2–4 w
			Enterovirus	2	2–4 w
			HMPV	9	2–4 w
			Influenza A	13	2–4 w
			Influenza B	6	2–4 w
			Rhinovirus	9	2–4 w
			RSV	9	2–4 w
			PIV-1	4	2–4 w
			PIV-3	4	2–4 w
			<i>Mycoplasma pneumoniae</i>	1	2–4 w
			CMV	9	2–4 w
			EBV	12	2–4 w
C	The Netherlands	Persons with recent CoV infections‡	α-CoV HCoV-229E	19	2 w–1 y
			α-CoV HCoV-NL63	18	2 w–1 y
			β-CoV HCoV-OC43	23	2 w–1 y
D1	Qatar	S1 microarray positive persons with camel contact	NA	19	NA
D2		S1 microarray negative persons with camel contact	NA	18	NA
E	The Netherlands	RT-PCR confirmed MERS case-patients‡	Acute‡	21	1–14 d
F			Convalescent‡	7	15–228 d
G	South Korea	RT-PCR confirmed MERS case-patients	Mild infection§	17	6–12 mo
H			Severe infection¶	15	6–12 mo

*Cohorts A–C were established to test assay specificity; cohorts D–H were established to test assay sensitivity. CoV, coronavirus; CMV, cytomegalovirus; EBV, Epstein-Barr virus; HCoV, human coronavirus; HMPV, human metapneumovirus; MERS, Middle East respiratory syndrome; mo, month; NA, not applicable; PIV, parainfluenza virus; RSV, respiratory syncytial virus.

†Cross-reactivity.

‡Samples taken from 2 case-patients at different time points.

§Samples taken from 6 case-patients at different time points.

¶Samples taken from 5 case-patients at different time points.

and 5/18 (28%) asymptomatic S1-positive persons with camel contact. When testing for MERS-CoV S2-specific antibody responses, none of the control serum samples in cohorts A–C was cross-reactive (Figure 2, panel E), whereas 1/17 S1-negative samples and 1/18 S1-positive samples from persons with camel contact tested positive. These findings indicate low immune responsiveness in mild MERS cases. Thus, when comparing the use of S1, S2, and N proteins for the detection of MERS-CoV infections, S1 showed the highest specificity and sensitivity among the 3 tested proteins.

rELISA Validation

Strikingly, the routinely used ELISA showed the least sensitivity among the tested S1 platforms (Table 2; Figure 1; Figure 2, panel F). We saw this difference in the cohort of persons with camel contact from Qatar who had mild to asymptomatic infections and who were identified to be seropositive for MERS-CoV in an earlier study (8) (Figure 2, panel F, cohort D1). Although they tested seropositive by iELISA and the microarray platform, only 20% of those also tested positive using the rELISA platform. We tested different coating conditions and found that a reduction in antigen coating or a loss of some conformational epitopes could have contributed to the low sensitivity seen in the rELISA versus the iELISA, despite testing the same

antigen (S1) (Figure 3). This low sensitivity confirms the likelihood of false-negative detection of some MERS-CoV cases using rELISA.

We evaluated the specificity of the rELISA platform using cohorts A–C. Among these, serum samples from 2 patients with HCoV-OC43 (a β-CoV) infection tested positive (Figure 2, panel F) but tested negative for MERS-CoV neutralization by PRNT₉₀ and S1 antibodies by iELISA and microarray (Table 3). Thus, to confirm the cross-reactivity of the 2 serum samples with MERS-CoV S1 in rELISA, we tested serum samples taken from both patients at different time points, before and after OC43 infection. All preinfection serum samples were negative, but all postinfection serum samples were positive in the rELISA (Figure 4). On the contrary, none of the serum samples was positive when tested by PRNT, Western blot, immunofluorescence assay, iELISA, or S1 protein microarray (using commercial and in-house S1 proteins), indicating a false-positive reaction in the rELISA. Overall, the rELISA was 98.97% (95% CI 96.3%–99.8%) specific in the tested cohorts (Table 3). Using a lower cutoff (optical density ratio 0.4), to show 100% specificity and sensitivity, as suggested in an earlier study (30), did increase the sensitivity (from 69.2% to 84.6%), but doing so reduced specificity; numbers of false-positive results increased from 2 to 7 and specificity decreased from 98.97% to 96.4% (Appendix Figure 2).

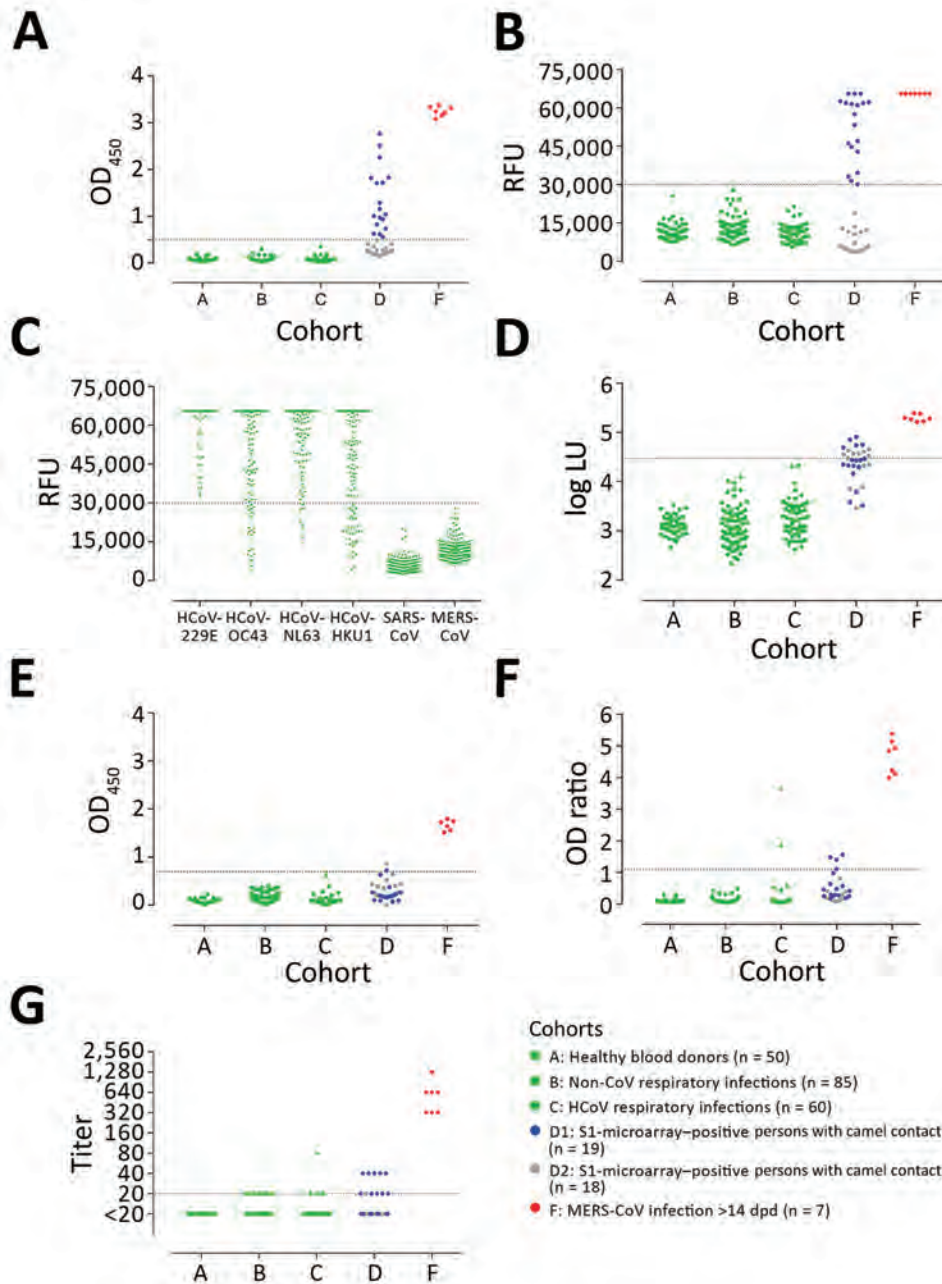


Figure 2. MERS-CoV-specific antibody responses detected by different assay platforms. A) In-house IgG of S1 ELISA (iELISA); B) MERS-CoV S1 protein microarray reactivity of non-MERS-CoV-infected serum samples to the S1 proteins of 6 different HCoVs; D) nucleocapsid luciferase immunoprecipitation assay; E) IgG S2 ELISA; F) routinely used IgG S1 ELISA expressed as the ratio of optical density of sample to kit calibrator; G) plaque reduction neutralization test (PRNT), expressed as endpoint titer for 90% plaque reduction. Serum samples tested were obtained from healthy blood donors ($n = 50$, cohort A); patients with PCR-diagnosed respiratory infections including human coronaviruses ($n = 145$, cohorts B and C); S1-microarray positive ($n = 18$, cohort D1) and negative ($n = 19$, cohort D2) camel contacts; and longitudinal serum samples from 2 PCR-confirmed MERS-CoV-infected patients taken 15–228 days after diagnosis ($n = 7$, cohort F). Cohort E is not included because patients in this cohort were in the acute phase of infection (<14 days postdiagnosis), in which seroconversion may not have occurred. Cohorts A, B, C, and F are from the Netherlands, cohort D from Qatar. Serum samples were tested at dilutions 1:101 for ELISA and N-LIPS, 1:20 for S1 microarray, and 1:20 to 1:2,560 for PRNT. Dotted lines indicate cutoff for each assay. CoV, coronavirus; LU, luminescence units; MERS, Middle East respiratory syndrome; OD, optical density; RFU, relative fluorescence units.

Mild MERS-CoV Infections and Neutralizing Antibodies

To investigate the difference in the neutralization responses produced following severe and mild infections and the reliability of neutralization assays as confirmatory assays for mild infections, we validated PRNT₉₀ for specific and sensitive detection of MERS-CoV infections. Although none of the healthy blood donors (cohort A) were reactive, the respiratory patients (cohorts B and C) showed low levels of cross-neutralization (titer 20) in 12 serum samples. One sample with a titer of 80 (Figure 2, panel G) was from an HCoV-OC43 patient; none of the serum samples

taken at 4 earlier time points from that patient showed any neutralization by PRNT (data not shown). All 13 serum samples tested negative for S1 antibodies in all tested platforms (Table 3); none of the serum samples was positive in 2 assays. For PCR-diagnosed MERS cases (cohorts E–H), PRNT₉₀ showed 100% sensitivity for detecting severe cases after the seroconversion period (>14 dpd; cohort F) and for up to 1 year (cohort H), indicating strong neutralizing antibody responses.

In contrast, results varied for mild cases (cohort G). Neutralizing antibodies were detected in 3/6 (50%) of mild

Table 2. Specificity and sensitivity of assay platforms for the detection of MERS-CoV antibodies among PCR-confirmed cases*

Test characteristic	In-house S1 ELISA	S1 microarray	PRNT ₉₀	Routinely used S1 ELISA
p value	<0.0001	<0.0001	<0.0001	<0.0001
Sensitivity, N = 13				
No. tested positive	12	11	9	9
n/N value (95% CI)	0.9231 (0.6669–0.9961)	0.8462 (0.5777–0.9727)	0.692 (0.4237–0.8732)	0.6923 (0.4237–0.8732)
Specificity, N = 195				
No. tested positive	0	0	1	2
n/N value (95% CI)	1 (0.9807–1)	1 (0.9807–1)	0.9949 (0.9715–0.9997)	0.9897 (0.9634–0.9982)
Positive predictive value				
Value (95% CI)	1 (0.7575–1)	1 (0.7412–1)	0.9 (0.5958–0.9949)	0.8182 (0.523–0.9677)
Negative predictive value				
Value (95% CI)	0.9949 (0.9717–0.9997)	0.9898 (0.9637–0.9982)	0.9798 (0.9492–0.9921)	0.9797 (0.949–0.9921)
Positive likelihood ratio	NA	NA	135	67.5
Area under the ROC curve				
Area	1	0.9893	0.7348	0.9481
SE	0	0.005409	0.07513	0.01767
95% CI	1–1	0.9787–0.9999	0.5876–0.8821	0.9134–0.9827
p value	<0.0001	<0.0001	<0.0001	<0.0001

*p value calculated by Fisher exact test. CoV, coronavirus; MERS, Middle East respiratory syndrome; NA, not applicable; PRNT, plaque reduction neutralization test; PRNT₉₀, 90% endpoint PRNT; ROC, receiver operating characteristic.

infections (Appendix Table 1), highlighting lower, shorter-lived neutralizing responses among mild cases. This finding is consistent with the results of a cohort of mild to asymptomatic MERS-CoV-infected persons with camel contact from Qatar (8) (Figure 2, panel G, cohort D1). These persons had low to undetectable neutralizing antibodies while being reactive to S1 on the protein microarray platform and in our iELISA.

Nonneutralizing Antibodies after Mild MERS-CoV Infections

For the PCR-confirmed MERS-CoV patients (cohorts E–H) and serologically positive persons with camel contact (cohort D1), S1 antibody titers as determined by iELISA strongly correlated with neutralization titers (Figure 5, panel A), showing that S1 antibody response is a reliable predictor of neutralization activity. This finding indicates that a population of mildly infected patients with S1-reactive antibodies but no detectable neutralizing antibodies could easily be missed in attempts to confirm cases by neutralization assay.

Discussion

Serologic detection of MERS-CoV exposure is valuable for identifying asymptomatic cases and virus reservoirs in population screening and epidemiologic studies, as well as for contact investigations. Detection aids in understanding the host immune response to the virus, identifying key viral immunogens, and mapping key neutralizing antibodies, which all lead to implementing appropriate preventive and therapeutic measures. Antibody responses varied among PCR-confirmed MERS-CoV cases; case-patients with mild and asymptomatic infections showed low or undetectable seroconversion, in contrast to severe infections that resulted in robust responses (5,17,31). The low-level antibody responses produced following nonsevere infections led to failure in detecting such responses in some patients by a routinely used ELISA and neutralization assays (5,17,32). This result may have impeded estimation of prevalence of virus infections in surveillance studies. We were able to detect nonneutralizing antibody responses among previously infected mild and asymptomatic cases that were previously unidentified; this finding indicates that MERS-CoV

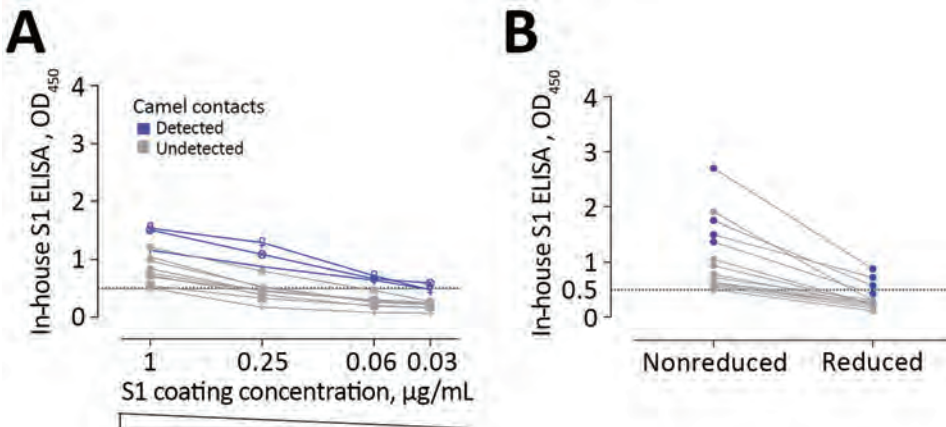


Figure 3. Low sensitivity of commercial S1 ELISA shown as the effect of lowering coating antigen concentration (A) or antigen denaturation (B) on the sensitivity of antibody detection among Middle East respiratory syndrome coronavirus-infected persons with camel contact. All samples were seropositive by in-house S1 ELISA and microarray. Dark blue indicates those that tested seropositive by commercial S1 ELISA.

Table 3. Sensitivity and specificity results of routinely used commercial S1 ELISA and PRNT₉₀ assays for MERS-CoV*

Assay parameter and sample source	Infection	No. positive/no. tested			Specificity or sensitivity, %	
		S1 rELISA†	PRNT ₉₀ (titer)		S1 rELISA	PRNT ₉₀
Specificity					98.97	93.33 (1:20); 99.5 (1:40)
Healthy blood donors	None	0/50	NA	0/50		
Non-CoV respiratory infections	Adenovirus	0/5	NA	1/5(20)		
	Bocavirus	0/2	NA	0/2		
	Enterovirus	0/2	NA	0/2		
	HMPV	0/9	NA	1/9 (20)		
	Influenza A	0/13	NA	4/13 (20, 20, 20, 20)		
	Influenza B	0/6	NA	0/6		
	Rhinovirus	0/9	NA	2/9 (20, 20)		
	RSV	0/9	NA	1/9 (20)		
	PIV-1	0/4	NA	0/4		
	PIV-3	0/4	NA	0/4		
	<i>Mycoplasma</i>	0/1	NA	0/1		
	CMV	0/9	NA	0/9		
	EBV	0/12	NA	0/12		
	Recent CoV infections‡	α-CoV HCoV-229E	0/19	NA	3/19 (20, 20, 20)	
α-CoV HCoV-NL63		0/18	NA	0/18		
β-CoV HCoV-OC43		2/23	0/2	1/21 (80)		
Sensitivity						
Persons with camel contact	S1-microarray positive§	4/19	4/4 (40, 40, 40, 20)	6/15 (40, 40, 20, 20, 20, 20)	21	52.6
	S1-microarray negative	0/18	NA	1/18 (20)	NA	NA
RT-PCR–confirmed MERS cases	≤14 d postdiagnosis	11/21	11/11	1/10 (80)	NA	NA
	>14 d postdiagnosis	7/7	7/7	NA	100	100
	6–12 mo postdiagnosis; mild infection	5/17	5/5	NA	35.3	35.3
	6–12 mo postdiagnosis; severe infection	15/15	15/15	NA	100	100

*CMV, cytomegalovirus; CoV, coronavirus; EBV, Epstein-Barr virus; ELISA, enzyme-linked immunosorbent assay; HCoV, human coronavirus; HMPV, human metapneumovirus; MERS, Middle East respiratory syndrome; NA, not applicable; PIV, parainfluenza virus; PRNT, plaque reduction neutralization test; PRNT₉₀, 90% endpoint PRNT; rELISA, routine ELISA; RSV, respiratory syncytial virus; RT-PCR, reverse transcription PCR.

†None of the serum samples from specificity cohorts tested positive by in-house S1 ELISA or microarray.

‡Cross-reactivity.

§All 19 serum samples (protein microarray positive) tested positive by in-house S1 ELISA.

prevalence could be higher than current estimates and that using sensitive platforms could lead to more precise calculation of incidence rates.

Although an earlier study evaluating serologic responses among PCR-confirmed MERS patients reported seroconversion in only 2/6 (33%) mildly infected cases (17), we were able to detect 5/6 (83.5%) by our in-house S1 ELISA and 4/6 (67%) by microarray. S1 iELISA and microarray were highly sensitive for detecting MERS-CoV infections, showing 100% specificity in the tested cohorts. Although the rELISA platform detected severe infections with no false negatives, it did not detect seroconversion among some mildly infected PCR-confirmed and asymptomatic persons with camel contact who had low antibody responses. In addition, rELISA

results showed cross-reactivity with some serum samples from HCoV-OC43–infected persons. The variation in the reactivity between the 2 ELISA platforms could be attributed to the difference in the coating protein preparations used in each or to the reduced stability of the protein during storage of the rELISA platform.

Overall, our results validate the use of S1 as a specific antigen for MERS-CoV serology if folding is correct, providing a highly specific 1-step diagnostic approach without false positives omitting the need for a confirmatory assay. In particular, neutralizing antibodies were undetectable after most asymptomatic and some mild infections. Using 50% instead of 90% reduction as a cutoff for PRNT can increase the sensitivity of the assay for confirming mild or asymptomatic

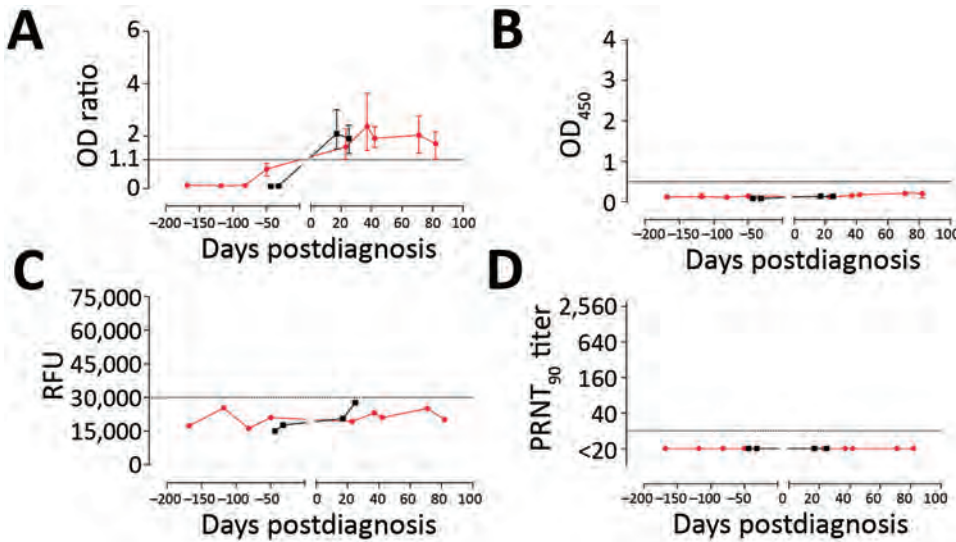


Figure 4. Reactivity to Middle East respiratory syndrome coronavirus of serum samples from 2 patients with human coronavirus OC43 in different assays. Longitudinal serum samples, collected before and after OC43 infection, from the 2 patients (red, patient 1; black, patient 2) were analyzed by commercial IgG S1 ELISA (A); in-house IgG S1 ELISA (B); S1 protein microarray (C); and PRNT₉₀ (D). Dotted line indicates the cutoff for each assay. Error bars indicate 95% CIs. OD, optical density; PRNT₉₀, 90% reduction in plaque reduction neutralization test; RFU, relative fluorescence units.

infections (15,21,33), but it is crucial to precede PRNT with a sensitive screening assay to avoid false-negative results.

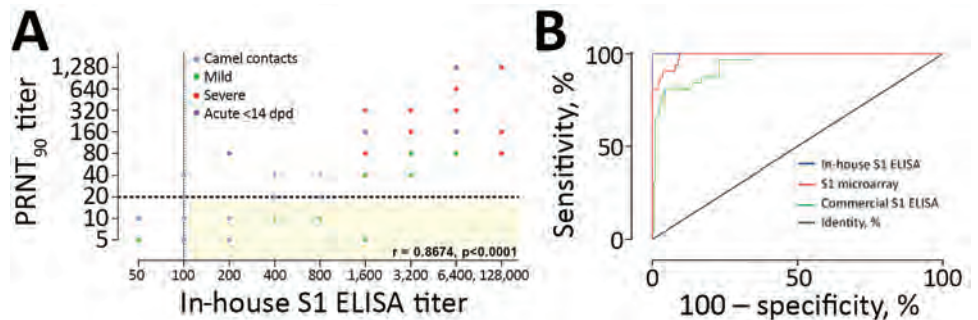
Prolonged viral shedding observed in severely infected patients but not in patients with mild infections (5,17,34) indicated that a short-lived infection in nonsevere cases may account for lower antibody responses, including functional neutralizing antibodies. A possible reason is that nonneutralizing antibodies comprise a substantial proportion of antibodies elicited after a viral infection; these antibodies can be elicited against viral proteins, including immature forms of surface proteins, released through lysis of infected cells following a short-lived abortive infection (35,36). We found that spike antibody titers were produced at higher titers than nucleocapsid antibodies and neutralizing antibodies were undetectable following nonsevere infections. These findings indicate that anti-spike antibodies are more sensitive predictors for previous MERS-CoV infections, especially mild and asymptomatic infections, and that conducting neutralization assays to confirm serologic findings, as recommended by the World Health

Organization (37), could result in potential underestimation of the true prevalence in epidemiologic studies.

Further studies testing patients with previously indeterminate infection could provide further clues on the epidemiology of MERS-CoV. A recent study reported the presence of MERS-CoV-specific CD8⁺ T-cell responses after MERS-CoV infection, irrespective of disease severity (38). Therefore, T-cell assays can be used to confirm serologic findings in epidemiologic studies (mainly asymptomatic cases) instead of neutralization assays that could yield underestimated results. However, further studies are needed to rule out possible T-cell cross-reactivity with other HCoV.

Despite the use of 90% reduction as endpoint for PRNT, we observed cross-neutralization in the respiratory panel samples (13/195). All but 1 sample had a titer of 20, and all 13 were S1 negative. We reported a similar finding in an earlier study, where 1 of 35 S1-negative serum samples had a neutralization titer of 20 (8). This finding was unexpected because neutralization assays, with their high specificity, are considered the standard for

Figure 5. Correlation between neutralizing and S1 antibody responses and comparison of different S1 platforms. A) PRNT₉₀ neutralization titers and IgG titers obtained by in-house S1 ELISA among PCR-confirmed MERS-CoV patients and persons with camel contact. Spearman correlation *r* value and 2-tailed *p*-value are shown. Yellow shading indicates S1-reactive nonneutralizing antibodies. B) Receiver operator characteristic (ROC) curves comparing the specificity and sensitivity of different MERS-CoV S1-based platforms for the diagnosis of MERS-CoV infections among PCR-confirmed cases. AUC for iELISA (blue) is 1; for S1 microarray (red) is 0.9893; for rELISA (green) is 0.9481. Dotted lines show the cutoff for each assay. AUC, area under the curve; dpd, days postdiagnosis; PRNT₉₀, 90% reduction in plaque reduction neutralization test.



MERS-CoV serodiagnosis. Such seemingly false positives could be attributed to the presence of natural antibodies or cross-reactive HCoV antibodies (15,32,35,39).

Cross-neutralization among human coronaviruses has rarely been reported. Chan et al. described cross-neutralization between SARS-CoV and MERS-CoV at low titers (≤ 20) (32). However, these serum samples also tested positive for HCoV-OC43 neutralization. This finding, along with ours, raises the probability that HCoV-OC43 antibodies caused cross-reactivity; antibodies in the serum sample could be recognizing an epitope outside S1 and thus not detected in ELISA. Of interest, we detected an HCoV-OC43 patient serum sample that could neutralize MERS-CoV at PRNT₉₀ titer ≤ 80 , but we found that the patient received an oncolytic medication shown to have antiviral activity (40). This finding could also be a probable reason for the observed cross-neutralization. Overall, while serum samples from healthy blood donors showed no cross-neutralization or cross-reactivity to S2 or N proteins, we observed some cross-neutralization and comparably higher reactivity to S2 and N proteins in serum samples of patients with respiratory infections, which we did not detect by our in-house S1 platforms. Thus, we could not avoid cross-reactivity to S2 and N proteins, leading to false positives, without loss of sensitivity. The high specificity of the S1 protein enabled us to set a cutoff high enough to ensure specificity without losing sensitivity.

Using S1 in optimized platforms enabled us to detect seroconversion among otherwise unrecognized nonsevere MERS-CoV cases with very high sensitivity and 100% specificity. Our findings indicate that our iELISA and microarray for MERS-CoV diagnostics (Table 2; Figure 5, panel B) could be reliable diagnostic tools for identifying MERS-CoV infections. For further standardization of the assay, a calibrator (e.g., monoclonal antibody) can be included in each run to avoid intraassay variations.

Although further testing on a larger cohort may be required to rule out cross-reactivity, ensure sensitivity, and thereby validate general use as a 1-step diagnostic assay, the data obtained in this study indicate that cross-reactivity between HCoVs (at least when testing for MERS-CoV and SARS-CoV reactivity) is unlikely to occur when using optimized platforms with the divergent S1 protein. A more recent follow-up study revealed that, among 454 serum samples tested using our in-house S1 ELISA, including those from persons with camel contact, only 2 samples, both MERS-CoV-neutralization positive, tested positive whereas all other serum samples were found to be negative in the iELISA (R. Bassal et al., unpub. data). Thus, in principle, low-level antibody responses among nonsevere MERS-CoV cases may be revealed by a single ELISA test.

Because patients with mild or asymptomatic infections do not develop severe illness and thus go unrecognized, they might play a role in spreading the virus into the community,

initiating outbreaks in which index case-patients report no history of camel or patient exposure. Therefore, defining the subclinical burden of infection will enable better understanding of the extent, severity, and public health threat posed by MERS-CoV, which, in turn, will guide the development and implementation of proper strategies to contain and prevent ongoing outbreaks of infection with this virus.

This work was supported by the Zoonoses Anticipation and Preparedness Initiative (ZAPI project; IMI grant agreement no. 115760), with the assistance and financial support of IMI and the European Commission, in-kind contributions from EFPIA partners.

About the Author

Ms. Okba is a PhD candidate in the viroscience department of Erasmus Medical Center, Rotterdam, the Netherlands. Her research interests include the development of diagnostic and intervention strategies for emerging viruses.

References

- Zaki AM, van Boheemen S, Bestebroer TM, Osterhaus AD, Fouchier RA. Isolation of a novel coronavirus from a man with pneumonia in Saudi Arabia. *N Engl J Med*. 2012;367:1814–20. <https://doi.org/10.1056/NEJMoa1211721>
- World Health Organization. Middle East respiratory syndrome coronavirus (MERS-CoV) [cited 2017 Jul 16]. <http://www.who.int/emergencies/mers-cov>
- Puzelli S, Azzi A, Santini MG, Di Martino A, Facchini M, Castrucci MR, et al. Investigation of an imported case of Middle East respiratory syndrome coronavirus (MERS-CoV) infection in Florence, Italy, May to June 2013. *Euro Surveill*. 2013;18:20564. <https://doi.org/10.2807/1560-7917.ES2013.18.34.20564>
- Al Hammadi ZM, Chu DK, Eltahir YM, Al Hosani F, Al Mulla M, Tarnini W, et al. Asymptomatic MERS-CoV infection in humans possibly linked to infected dromedaries imported from Oman to United Arab Emirates, May 2015. *Emerg Infect Dis*. 2015;21:2197–200. <https://doi.org/10.3201/eid2112.151132>
- Alshukairi AN, Khalid I, Ahmed WA, Dada AM, Bayumi DT, Malic LS, et al. Antibody response and disease severity in healthcare worker MERS survivors. *Emerg Infect Dis*. 2016;22. <https://doi.org/10.3201/eid2206.160010>
- Reusken CB, Haagmans BL, Müller MA, Gutierrez C, Godeke GJ, Meyer B, et al. Middle East respiratory syndrome coronavirus neutralising serum antibodies in dromedary camels: a comparative serological study. *Lancet Infect Dis*. 2013;13:859–66. [https://doi.org/10.1016/S1473-3099\(13\)70164-6](https://doi.org/10.1016/S1473-3099(13)70164-6)
- Haagmans BL, Al Dhahiry SH, Reusken CB, Raj VS, Galiano M, Myers R, et al. Middle East respiratory syndrome coronavirus in dromedary camels: an outbreak investigation. *Lancet Infect Dis*. 2014;14:140–5. [https://doi.org/10.1016/S1473-3099\(13\)70690-X](https://doi.org/10.1016/S1473-3099(13)70690-X)
- Reusken CB, Farag EA, Haagmans BL, Mohran KA, Godeke GJ V, Raj S, et al. Occupational exposure to dromedaries and risk for MERS-CoV infection, Qatar, 2013–2014. *Emerg Infect Dis*. 2015;21:1422–5. <https://doi.org/10.3201/eid2108.150481>
- Müller MA, Meyer B, Corman VM, Al-Masri M, Turkestani A, Ritz D, et al. Presence of Middle East respiratory syndrome coronavirus antibodies in Saudi Arabia: a nationwide, cross-sectional, serological study. *Lancet Infect Dis*. 2015;15:559–64. [https://doi.org/10.1016/S1473-3099\(15\)70090-3](https://doi.org/10.1016/S1473-3099(15)70090-3)
- Kayali G, Peiris M. A more detailed picture of the epidemiology of Middle East respiratory syndrome coronavirus. *Lancet Infect Dis*. 2015;15:495–7. [https://doi.org/10.1016/S1473-3099\(15\)70128-3](https://doi.org/10.1016/S1473-3099(15)70128-3)

11. Assiri AM, Biggs HM, Abedi GR, Lu X, Bin Saeed A, Abdalla O, et al. Increase in Middle East respiratory syndrome-coronavirus cases in Saudi Arabia linked to hospital outbreak with continued circulation of recombinant virus, July 1–August 31, 2015. *Open Forum Infect Dis*. 2016;3:ofw165. <https://doi.org/10.1093/ofid/ofw165>
12. Park JW, Lee KJ, Lee KH, Lee SH, Cho JR, Mo JW, et al. Hospital outbreaks of Middle East respiratory syndrome, Daejeon, South Korea, 2015. *Emerg Infect Dis*. 2017;23:898–905. <https://doi.org/10.3201/eid2306.160120>
13. Memish ZA, Zumla AI, Al-Hakeem RF, Al-Rabeeah AA, Stephens GM. Family cluster of Middle East respiratory syndrome coronavirus infections. *N Engl J Med*. 2013;368:2487–94. <https://doi.org/10.1056/NEJMoa1303729>
14. Assiri A, McGeer A, Perl TM, Price CS, Al Rabeeah AA, Cummings DA, et al.; KSA MERS-CoV Investigation Team. Hospital outbreak of Middle East respiratory syndrome coronavirus. *N Engl J Med*. 2013;369:407–16. <https://doi.org/10.1056/NEJMoa1306742>
15. Drosten C, Meyer B, Müller MA, Corman VM, Al-Masri M, Hossain R, et al. Transmission of MERS-coronavirus in household contacts. *N Engl J Med*. 2014;371:828–35. <https://doi.org/10.1056/NEJMoa1405858>
16. Aleanizy FS, Mohamed N, Alqahtani FY, El Hadi Mohamed RA. Outbreak of Middle East respiratory syndrome coronavirus in Saudi Arabia: a retrospective study. *BMC Infect Dis*. 2017;17:23. <https://doi.org/10.1186/s12879-016-2137-3>
17. Choe PG, Perera RAPM, Park WB, Song KH, Bang JH, Kim ES, et al. MERS-CoV antibody responses 1 year after symptom onset, South Korea, 2015. *Emerg Infect Dis*. 2017;23:1079–84. <https://doi.org/10.3201/eid2307.170310>
18. Corman VM, Eckerle I, Bleicker T, Zaki A, Landt O, Eschbach-Bludau M, et al. Detection of a novel human coronavirus by real-time reverse-transcription polymerase chain reaction. *Euro Surveill*. 2012;17:20285. <https://doi.org/10.2807/ese.17.39.20285-en>
19. Corman VM, Müller MA, Costabel U, Timm J, Binger T, Meyer B, et al. Assays for laboratory confirmation of novel human coronavirus (hCoV-EMC) infections. *Euro Surveill*. 2012;17:20334. <https://doi.org/10.2807/ese.17.49.20334-en>
20. Furuse Y, Okamoto M, Oshitani H. Conservation of nucleotide sequences for molecular diagnosis of Middle East respiratory syndrome coronavirus, 2015. *Int J Infect Dis*. 2015;40:25–7. <https://doi.org/10.1016/j.ijid.2015.09.018>
21. Park SW, Perera RA, Choe PG, Lau EH, Choi SJ, Chun JY, et al. Comparison of serological assays in human Middle East respiratory syndrome (MERS)–coronavirus infection. *Euro Surveill*. 2015;20:30042. <https://doi.org/10.2807/1560-7917.ES.2015.20.41.30042>
22. Al-Abdallat MM, Payne DC, Alqasrawi S, Rha B, Tohme RA, Abedi GR, et al.; Jordan MERS-CoV Investigation Team. Hospital-associated outbreak of Middle East respiratory syndrome coronavirus: a serologic, epidemiologic, and clinical description. *Clin Infect Dis*. 2014;59:1225–33. <https://doi.org/10.1093/cid/ciu359>
23. Reusken C, Mou H, Godeke GJ, van der Hoek L, Meyer B, Müller MA, et al. Specific serology for emerging human coronaviruses by protein microarray. *Euro Surveill*. 2013;18:20441. <https://doi.org/10.2807/1560-7917.ES2013.18.14.20441>
24. Alagaili AN, Briese T, Mishra N, Kapoor V, Sameroff SC, Burbelo PD, et al. Middle East respiratory syndrome coronavirus infection in dromedary camels in Saudi Arabia. *MBio*. 2014;5:e01002–14. <https://doi.org/10.1128/mBio.01002-14>
25. Perera RA, Wang P, Goma MR, El-Shesheny R, Kandeil A, Bagato O, et al. Seroepidemiology for MERS coronavirus using microneutralisation and pseudoparticle virus neutralisation assays reveal a high prevalence of antibody in dromedary camels in Egypt, June 2013. *Euro Surveill*. 2013;18:20574. <https://doi.org/10.2807/1560-7917.ES2013.18.36.20574>
26. Meyer B, Müller MA, Corman VM, Reusken CB, Ritz D, Godeke GJ, et al. Antibodies against MERS coronavirus in dromedary camels, United Arab Emirates, 2003 and 2013. *Emerg Infect Dis*. 2014;20:552–9. <https://doi.org/10.3201/eid2004.131746>
27. Meyer B, Drosten C, Müller MA. Serological assays for emerging coronaviruses: challenges and pitfalls. *Virus Res*. 2014;194:175–83. <https://doi.org/10.1016/j.virusres.2014.03.018>
28. Payne DC, Iblan I, Rha B, Alqasrawi S, Haddadin A, Al Nsour M, et al. Persistence of antibodies against Middle East respiratory syndrome coronavirus. *Emerg Infect Dis*. 2016;22:1824–6. <https://doi.org/10.3201/eid2210.160706>
29. Fanoy EB, van der Sande MA, Kraaij-Dirkzwager M, Dirksen K, Jonges M, van der Hoek W, et al. Travel-related MERS-CoV cases: an assessment of exposures and risk factors in a group of Dutch travelers returning from the Kingdom of Saudi Arabia, May 2014. *Emerg Themes Epidemiol*. 2014;11:16. <https://doi.org/10.1186/1742-7622-11-16>
30. Ko JH, Muller MA, Seok H, Park GE, Lee JY, Cho SY, et al. Suggested new breakpoints of anti-MERS-CoV antibody ELISA titers: performance analysis of serologic tests. *Eur J Clin Microbiol Infect Dis*. 2017;36:2179–86.
31. Ko JH, Müller MA, Seok H, Park GE, Lee JY, Cho SY, et al. Serologic responses of 42 MERS-coronavirus-infected patients according to the disease severity. *Diagn Microbiol Infect Dis*. 2017;89:106–11. <https://doi.org/10.1016/j.diagmicrobio.2017.07.006>
32. Chan KH, Chan JF, Tse H, Chen H, Lau CC, Cai JP, et al. Cross-reactive antibodies in convalescent SARS patients' sera against the emerging novel human coronavirus EMC (2012) by both immunofluorescent and neutralizing antibody tests. *J Infect*. 2013;67:130–40. <https://doi.org/10.1016/j.jinf.2013.03.015>
33. Liljander A, Meyer B, Jores J, Müller MA, Lattwein E, Njeru I, et al. MERS-CoV antibodies in humans, Africa, 2013–2014. *Emerg Infect Dis*. 2016;22:1086–9. <https://doi.org/10.3201/eid2206.160064>
34. Oh MD, Park WB, Choe PG, Choi SJ, Kim JI, Chae J, et al. Viral load kinetics of MERS coronavirus infection. *N Engl J Med*. 2016;375:1303–5. <https://doi.org/10.1056/NEJMc1511695>
35. Hangartner L, Zinkernagel RM, Hengartner H. Antiviral antibody responses: the two extremes of a wide spectrum. *Nat Rev Immunol*. 2006;6:231–43. <https://doi.org/10.1038/nri1783>
36. Sakurai H, Williamson RA, Crowe JE, Beeler JA, Poignard P, Bastidas RB, et al. Human antibody responses to mature and immature forms of viral envelope in respiratory syncytial virus infection: significance for subunit vaccines. *J Virol*. 1999;73:2956–62.
37. World Health Organization. Laboratory testing for Middle East respiratory syndrome coronavirus, interim guidance (WHO/MERS/LAB/15.1/Rev1/2018). Geneva: The Organization; 2018.
38. Zhao J, Alshukairi AN, Baharoon SA, Ahmed WA, Bokhari AA, Nehdi AM, et al. Recovery from the Middle East respiratory syndrome is associated with antibody and T-cell responses. *Sci Immunol*. 2017;2:eaan5393. <https://doi.org/10.1126/sciimmunol.aan5393>
39. Buchholz U, Müller MA, Nitsche A, Sanewski A, Wevering N, Bauer-Balci T, et al. Contact investigation of a case of human novel coronavirus infection treated in a German hospital, October–November 2012. *Euro Surveill*. 2013;18:20406.
40. Patel DA, Patel AC, Nolan WC, Zhang Y, Holtzman MJ. High throughput screening for small molecule enhancers of the interferon signaling pathway to drive next-generation antiviral drug discovery. *PLoS One*. 2012;7:e36594. <https://doi.org/10.1371/journal.pone.0036594>

Address for correspondence: Bart L. Haagmans, Erasmus Medical Center, Department of Viroscience, PO Box 2040, 3000 CA Rotterdam, the Netherlands; email: b.haagmans@erasmusmc.nl

Comparison of Serologic Assays for Middle East Respiratory Syndrome Coronavirus

Ruth Harvey, Giada Mattiuzzo, Mark Hassall, Andrea Sieberg, Marcel A. Müller, Christian Drosten, Peter Rigsby, Christopher J. Oxenford, and study participants¹

Middle East respiratory syndrome coronavirus (MERS-CoV) was detected in humans in 2012. Since then, sporadic outbreaks with primary transmission through dromedary camels to humans and outbreaks in healthcare settings have shown that MERS-CoV continues to pose a threat to human health. Several serologic assays for MERS-CoV have been developed globally. We describe a collaborative study to investigate the comparability of serologic assays for MERS-CoV and assess any benefit associated with the introduction of a standard reference reagent for MERS-CoV serology. Our study findings indicate that, when possible, laboratories should use a testing algorithm including ≥ 2 tests to ensure correct diagnosis of MERS-CoV. We also demonstrate that the use of a reference reagent greatly improves the agreement between assays, enabling more consistent and therefore more meaningful comparisons between results.

Since the emergence of Middle East respiratory syndrome coronavirus (MERS-CoV) in 2012 (1), more than 2,250 laboratory-confirmed cases have been reported to the World Health Organization (WHO); approximately one third of these cases were fatal. A large proportion of MERS-CoV cases have been the result of human-to-human transmission in healthcare settings (2,3); outbreaks have occurred in several countries, with the largest outbreaks seen in Saudi Arabia, United Arab Emirates, and South Korea (4). Dromedary camels are the putative reservoir hosts for MERS-CoV; they experience no or mild symptoms upon infection (5). Primary infection can occur from dromedary camels to humans, and new cases with evidence of camel contact continue to occur sporadically (6). MERS-CoV is 1 of the 10 high-threat

pathogens on the WHO Research and Development Blueprint (7), a document that sets out a roadmap for research and development of diagnostics, preventive and therapeutic products for prevention, and early detection and response to these high-priority pathogens. The WHO roadmap for MERS-CoV lists several priority activities, including improved diagnostics and vaccines for humans and camels as well as basic and translational research (8). Serologic assays are critical for the evaluation of the efficacy of new vaccines and patient treatment, as are diagnostic tools to confirm infections and perform serosurveillance. A variety of serologic assays have been developed globally, both commercially and in-house; however, there is no evidence supporting the quality of performance of these assays and their consistency with one another. Participants at the WHO intercountry meeting on MERS-CoV in Cairo, Egypt, June 20–22, 2013, recognized this issue as a public health priority and called for a study to compare currently available serologic assays (9). Therefore, we assembled a panel of human serum or plasma and polyclonal antibodies to compare the performance of serologic assays for MERS-CoV. We invited participants to use their testing algorithms to diagnose each sample as if it were a real patient sample. The assays were evaluated for sensitivity and specificity. Pas et al. described in 2015 the impact that a single international standard would have on reducing interlaboratory variability for MERS-CoV diagnostics (albeit in this case for NAT assays) (10). To this end, we included 2 samples in the panel as examples of potential WHO International Standard material, and we assessed their effectiveness in harmonization of the data from the participant laboratories.

Methods

Study Samples

The National Institute for Biological Standards and Control (NIBSC) Human Material Advisory Committee (project

Author affiliations: National Institute for Biological Standards and Control—MHRA, Potters Bar, UK (R. Harvey, G. Mattiuzzo, M. Hassall, P. Rigsby); Charité-Universitätsmedizin Berlin, Berlin, Germany (A. Sieberg, M.A. Müller, C. Drosten); German Centre for Infection Research, Berlin (M.A. Müller, C. Drosten); World Health Organization, Lyon, France (C.J. Oxenford).

DOI: <https://doi.org/10.3201/eid2510.190497>

¹Study participants who contributed data are listed at the end of this article.

16/005MP) approved this project. The Ministry of Health, Oman; Ministry of Health, Saudi Arabia; and Korea National Institute of Health, South Korea, donated convalescent serum and plasma samples from PCR-confirmed MERS-CoV-infected patients. All patient donors gave informed consent for the use of their serum or plasma, and samples were anonymized.

We treated all MERS-CoV convalescent-phase serum and plasma with solvent detergent using a validated method (11) to ensure there was no residual infectious virus. We stored all study samples at -20°C until dispatched on ice packs to participants. We blind coded the study samples provided to the participants (Table 1).

We included 5 plasma samples (samples 1, 5, 9, 11, and 12) as individual patient samples. Other smaller serum donations were pooled in 3 samples (samples 14, 16, and 18) based on their antibody titer, which we determined using the Recombivirus human MERS-CoV nucleoprotein (NP) antibody (IgG) ELISA kit (Alpha Diagnostic International, <https://4adi.com>). We categorized samples into high-, medium-, or low-positive pools (Figure 1).

We included MERS-CoV-negative serum with antibodies against other human coronavirus HCoV-229E, HCoV-NL63, HCoV-OC43, and HCoV-HKU1 (samples 3, 6, 7, 8, 13, 15, and 17) to test specificity of the assays (Table 2). Co-authors A.S., M.A.M., and C.D. precharacterized and donated these samples. Purified human MERS polyclonal antibodies from transchromosomal (Tc) cattle (12) immunized with either recombinant spike protein or whole inactivated virus (samples 2, 4, and 10) were donated by Eddie J. Sullivan (SAB Biotherapeutics, Inc., Sioux Falls, SD, USA). We diluted the material in universal buffer (10 mmol/L Tris-HCl, pH 7.4, 0.5% human serum albumin, 2% trehalose) at a concentration of 1 mg/mL.

Participants

The 10 participating laboratories (listed at the end of this article) were located in Australia, China (2 mainland, 1 Hong Kong), Germany, South Korea, the Netherlands, United States, and the United Kingdom (2 laboratories). Participating organizations included national control laboratories, diagnostic laboratories, and research laboratories.

Study Protocol

Participants tested the sample panel using their routine assays for MERS-CoV serology. We asked participants to perform 3 independent assays on different days. We provided an Excel spreadsheet (Microsoft, <http://www.microsoft.com>) for reporting the raw data for each assay and any interpretation of the results, such as positive or negative diagnosis of the samples.

Table 1. Samples used in study of serologic assays for MERS-CoV*

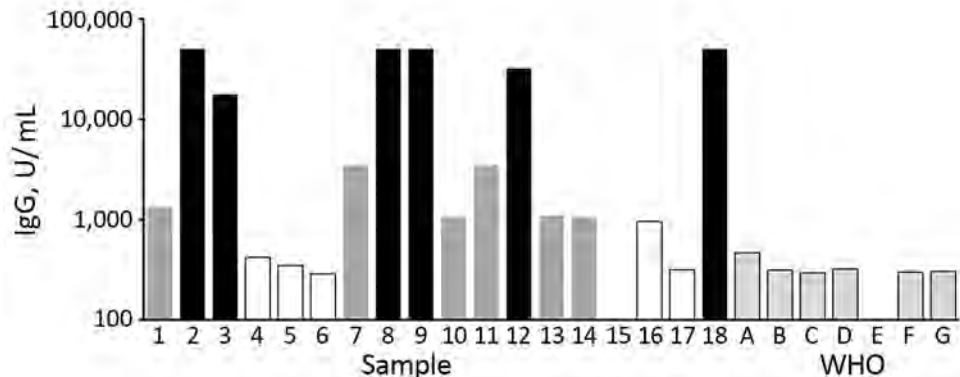
No.	Name	Description	Expected result
1	Korea 5	Single plasma from laboratory-confirmed MERS patient	Positive
2	Tc Bovine NC	Purified IgG from transchromosomal bovine, negative control	Negative
3	WHO/B	Negative control serum, high titer for other CoV	Negative
4	Tc Bovine SAB 300	Purified IgG from transchromosomal bovine, antigen whole virus	Positive
5	Korea 2	Single plasma from laboratory-confirmed MERS patient	Positive
6	WHO/G	Negative control serum, high titer for other CoV	Negative
7	WHO/A	Negative control serum, high titer for other CoV	Negative
8	WHO/D	Negative control serum, high titer for other CoV	Negative
9	Korea 3	Single plasma from laboratory-confirmed MERS patient	Positive
10	Tc Bovine SAB 301	Purified IgG from transchromosomal bovine, antigen spike protein	Positive
11	Korea 1	Single plasma from laboratory-confirmed MERS patient	Positive
12	Korea 4	Single plasma from laboratory-confirmed MERS patient	Positive
13	WHO/F	Negative control serum, high titer for other CoV	Negative
14	Pool C (low)	Pooled serum samples from laboratory-confirmed MERS patients	Positive
15	WHO/C	Negative control serum, high titer for other CoV	Negative
16	Pool A (high)	Pooled serum samples from laboratory-confirmed MERS patients	Positive
17	WHO/E	Negative control serum, high titer for other CoV	Negative
18	Pool B (medium)	Pooled serum samples from laboratory-confirmed MERS patients	Positive

*All samples were submitted as liquid in screw-cap tubes. CoV, coronavirus; MERS, Middle East respiratory syndrome; Tc, transchromosomal; WHO, World Health Organization.

Statistical Methods

We combined titers and relative potency (relative titer) estimates as unweighted geometric means (GMs) for each sample and laboratory and used these laboratory GMs to calculate overall unweighted GMs for each sample. We expressed variability between laboratories using geometric coefficients of variation ($\text{GCV} = [10^s - 1] \times 100\%$, where s is the SD of \log_{10} transformed estimates). To mitigate the effect of any potential outliers, we calculated robust estimates of s using the R package WRS2 (13).

Figure 1. Pooling of serum samples based on their ELISA titers in study of serologic assays for Middle East respiratory syndrome coronavirus. Bar shading indicates the mean ELISA unit value of 2 independent experiments run in duplicate. Black bars represent samples used in pool A (high-positive); dark gray bars indicate samples used in pool B (medium-positive); white bars, and sample 15 with no visible bar, indicate samples used in pool C (low-positive). Pale gray bars with black outline indicate results from a set of negative control samples (WHO A–G). WHO, World Health Organization.



Coding of Returned Data

We referred to all participating laboratories by code numbers, which were randomly allocated. If a laboratory returned data using different assay methods, we assayed the results separately for each method and referred to them according to their laboratory number and assay code; for example, 04 ppNT (pseudoparticle neutralization test) and 04 TCID₅₀ (50% tissue culture infectious dose).

Results

A total of 27 datasets were returned (Table 3, <https://wwwnc.cdc.gov/EID/article/25/10/19-0497-T3.htm>). Data covered a range of different assay formats: neutralization assays, ELISA, immunofluorescence tests, and 1 microarray. In general, there was good agreement between all the assays tested in this study. In assays with a quantitative measurement, the limit of detection and titer of samples varied greatly, but overall determination of positive or negative agreed between all assays except for 1 (laboratory 04 TCID₅₀ MN [micro-neutralization]), which failed to detect 2 positive samples (samples 9 and 18) that all other tests detected as positive.

The panel of negative control samples was deemed to be negative in all quantitative assays. There were 3 instances of laboratories reporting a result above cutoff for samples in 1 assay, but these samples were correctly diagnosed as negative overall by their testing algorithms: laboratory 02 detected samples 3 and 7 as above cutoff at 1:80

dilution in 1 assay only; laboratory 02 detected sample 13 as above cutoff at 1:100 and 1:400 dilutions in 1 assay; and laboratory 03 detected sample 13 as above cutoff at 1 dilution tested.

Participants detected pool A, the high-titer MERS-CoV antibody pool (sample 16) in all assays (Table 3). They detected pool B, the medium-titer pool (sample 18), in all but 1 of the quantitative assays, a TCID₅₀ MN assay from laboratory 04. In all other quantitative assays, participants detected the high pool at a higher titer than the medium pool. In the qualitative assays, 3 assays gave borderline positive or equivocal results for the medium pool; these assays were a Euroimmun S1 ELISA (<https://www.euroimmun.com>) in laboratories 01 and 10 and an in-house immunofluorescence assay in laboratory 07. The low-positive pool (pool C, sample 14) was only detected as positive in a single assay in the study, the Alpha Diagnostic International MERS NP ELISA performed in laboratory 05.

Participants scored positive the 2 purified IgG samples from MERS-CoV-immunized transchromosomal bovine samples (samples 4 and 10) in all the qualitative assays, but 2 of the quantitative assays, N ELISA from laboratory 02 and the Alpha Diagnostic International MERS NP ELISA from laboratory 05, were unable to detect these samples. We expected these 2 NP assays to fail to detect sample 10 because this antibody was raised against recombinant

Table 2. Characterization of MERS-CoV–negative control serum panel included in study of serologic assays for MERS-CoV*
Recombinant spike protein–based indirect immunofluorescence test, reciprocal endpoint titers*

Name	HCoV-229E	HCoV-NL63	HCoV-OC43	HCoV-HKU1	SARS-CoV	MERS-CoV
WHO/A	160	1,280	320	640	NR	NR
WHO/B	2,560	1,280	1,280	160	NR	NR
WHO/C	160	320	1,280	320	NR	NR
WHO/D	1,280	2,560	320	160	NR	NR
WHO/E	320	1,280	160	160	NR	NR
WHO/F	80	320	320	160	NR	NR
WHO/G	320	320	1,280	1,280	NR	NR

*All serum samples were tested in a dilution range of 1:20 to 1:5,120. CoV, coronavirus; HCoV, human CoV; MERS, Middle East respiratory syndrome; NR, nonreactive at the cutoff serum dilution of 1:20; SARS, severe acute respiratory syndrome; WHO, World Health Organization.

MERS spike protein only; however, it was surprising that the assays did not detect sample 4, which was an antibody raised against whole inactivated virus.

For the individual convalescent-phase plasma samples, we saw more variability in the results when compared with the pooled material, but despite this, 3 of the samples (samples 5, 11, and 12) were correctly identified as positive in all tests. Sample 1 was correctly diagnosed as positive in all tests but was identified as borderline positive by laboratory 01 in a Euroimmun ELISA assay. Sample 9 was the most difficult individual patient plasma to detect as positive; it was negative in the TCID₅₀ MN assay in laboratory 04; equivocal/positive in the in-house immunofluorescence assay in laboratory 07; and, in the Euroimmun ELISA, borderline/negative in lab 01, equivocal in lab 07, and weak positive in lab 10. Sample 9 was the weakest positive of the individual samples tested in the panel, as we saw from the titers in the quantitative assays that detected it as positive. We compiled the results of quantitative assays for the 5 individual positive plasma samples (Figure 2).

To simplify comparison of the assays, we reported results from the different laboratories as relative to either the transchromosomal bovine IgG sample raised against whole inactivated virus (sample 4) or the high-positive pooled human serum (pool A, sample 16). When we expressed data as a potency relative to either of the 2 chosen potential reference preparations with an assigned arbitrary value of 1,000, we observed improvement in the agreement between tests (Table 4; Figure 3). We saw the greatest reduction in the variation between laboratories (smaller SEM in Figure 3 and smaller percentage geometric coefficient of variation [GCV] in Table 4) when we used pooled human serum (sample 16) as standard. The transchromosomal bovine IgG raised against whole virus (sample 4) showed a substantial improvement in the agreement between laboratories; however, 2 ELISA methods included in this study could not identify this sample as positive.

Discussion

As detection of sporadic cases of MERS-CoV continues, development of new vaccines to combat the disease remains important, as does serosurveillance to understand exposure to the disease and the severity of illness in persons exposed to the virus (14). The importance of serologic assays for the diagnosis of MERS cases should also be considered; the WHO guideline for laboratory testing for MERS-CoV, updated in January 2018, specifically includes sample collection from suspected MERS-CoV cases for serology (15). The guideline lists 3 situations in which laboratories should conduct serologic testing for MERS-CoV: for defining a sporadic MERS-CoV case if molecular testing, such as nucleic acid amplification methods, is not possible; as part of an investigation of an ongoing outbreak;

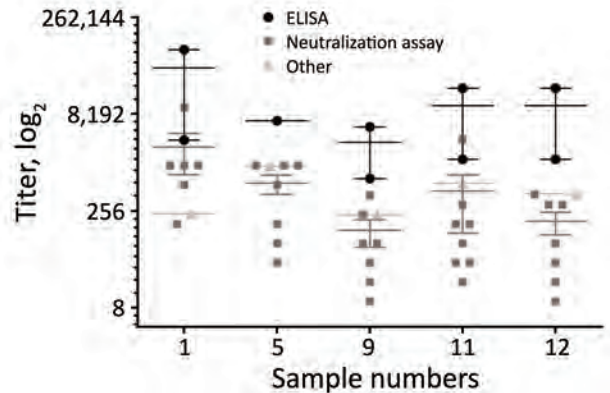


Figure 2. Endpoint titers of individual positive patient plasma samples in study of serologic assays for MERS-CoV. The titers for the 5 individual MERS-CoV-positive patient plasma were determined by ELISA (green circles), neutralization assays (blue squares), and other assays (red triangles). Horizontal lines indicate the mean for each assay type; error bars show SD between assays. MERS-CoV, Middle East respiratory syndrome coronavirus.

or serologic surveys, such as retrospective analysis of the extent of an outbreak.

In this collaborative study, we evaluated the performance of assays to detect MERS-CoV antibodies using a panel of serologic samples. All laboratories correctly identified the negative samples in the panel, including those containing antibodies against other coronaviruses, implying good specificity of the assays. Laboratories reported the positive results correctly except for sample 14, which tested negative by all but 1 assay; however, these results demonstrated the importance of a testing algorithm. We observed 14 instances of a sample being incorrectly determined as negative or borderline/equivocal in a single test in a single laboratory (Table 3). However, because each laboratory used a testing algorithm involving >1 method of analysis, all the samples with sporadic spurious results were correctly diagnosed as positive or negative; if they had used a single assay type, we would have found a higher proportion of incorrect results. The results for sample 14, which was a pool of serum samples from patients with confirmed MERS-CoV, highlight a lack of sensitivity in most of the

Table 4. GCV percentage (%GCV) for 5 individual serum samples in study of serologic assays for Middle East respiratory syndrome coronavirus*

Sample no.	% GCV		
	Endpoint	Potencies vs. sample 4	Potencies vs. sample 16
1	414	237	342
5	405	173	70
9	555	89	69
11	682	50	73
12	816	138	43

*Values derived from endpoint titers or from potencies expressed as relative to standard samples. GCV, geometric coefficient of variation.

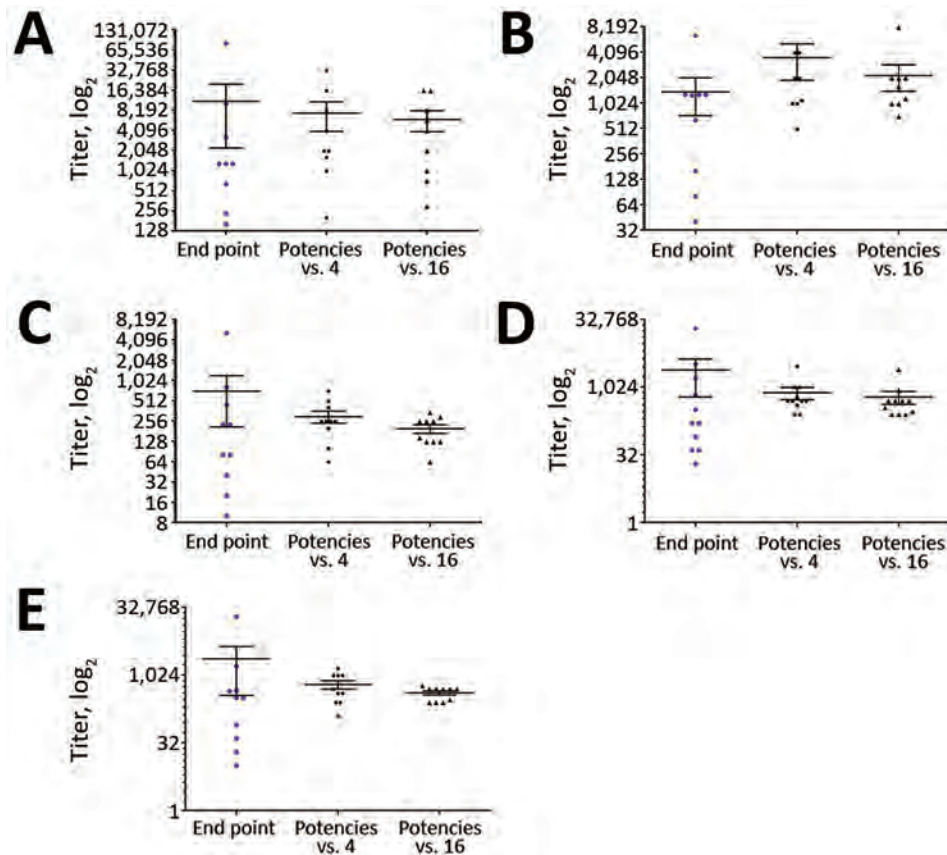


Figure 3. Relative titers of the individual positive patient plasma sample against a reference standard in study of serologic assays for MERS-CoV. Each panel represents a MERS-CoV-positive patient plasma sample: sample 1 (A), sample 5 (B), sample 9 (C), sample 11 (D), sample 12 (E). In each panel, the first data column shows the spread of endpoint titers from all quantitative assays performed; the second and third columns show quantitative results expressed as a potency relative to either sample 4 (Tc Bovine IgG raised against whole virus) or sample 16 (high-positive serum pool A). In each case the sample used as a reference was assigned nominal potency of 1,000 and all other samples were expressed as relative to the reference sample. For each dataset, horizontal line indicates the mean; error bars show SEM. MERS-CoV, Middle East respiratory syndrome coronavirus.

assays in this study; further investigation would be needed to determine why the antibody titers in this pool were below the limit of detection in all but 1 assay targeting N protein. It is important to understand whether there is a specific window of time in which clinical samples for serology should be taken or whether some patients do not mount a detectable antibody response against the spike protein during infection. Such information may lead to further updates of WHO guidelines on laboratory testing for MERS-CoV.

The raw titers reported from the laboratories performing quantitative assays varied greatly, for some samples >1,000-fold, between laboratories (Table 3). The use of a reference material in the assays tightened the values from the laboratories for all the samples, enhanced comparability (Figure 3), and reduced the GCV percentage between all laboratories (Table 4), perhaps unsurprisingly, but the magnitude of reduction in GCV percentage was noteworthy. MERS-CoV is an example of an important emerging pathogen with potential to cause outbreaks; diagnostic tests for emerging pathogens are often developed during outbreaks without proper validation or calibration.

This study showed the importance of using a standard reagent to allow better comparison of results from different laboratories or interpretation of results from different studies or clinical trials. As we continue to face emerging

pathogens, which pose significant risks to human health, it is important to use the experience gained from studies such as this to improve our response to the next threat. Standardizing assays is a key issue when different groups around the world are working to develop and produce novel assays and vaccine products. The need for a standard for MERS-CoV serology was discussed and was widely supported at the WHO–International Vaccine Institute joint symposium for MERS-CoV vaccine development in Seoul, South Korea, June 26–27, 2018. Several potential vaccines are in development, and the immune response elicited, their efficacy, and correlates of protection must be assessed. The use of a reference such as WHO International Standards (16) will enable worldwide harmonization of assays and comparability of the results from different preclinical and clinical studies. Assessing the specificity and sensitivity of methods is crucial to improve our understanding of the use and limitations of serologic assays for emerging diseases for which we have little knowledge of disease progression, antibody profiles, and other key information that is available for other infectious diseases.

Study participants who contributed data: L. Caly (Victorian Infectious Diseases Reference Laboratory, Melbourne, Australia); C. Li (National Institutes for Food and Drug Control,

Beijing, China); L. Zhao and W. Tan (National Institute for Viral Disease Control and Prevention, Chinese Center for Disease Control and Prevention, Beijing, China); M. Peiris and M. Perera (School of Public Health, The University of Hong Kong, Hong Kong, China); M. Müller and C. Drosten (Institute of Virology, Charité–Universitätsmedizin Berlin, Berlin, Germany); C. Kang and J.-S. Wang (Korea Centers for Disease Control and Prevention, Center for Laboratory Control of Infectious Diseases, Chungcheongbuk-do, South Korea); B. Haagmans and N.M.A. Okba (Department of Viroscience, Erasmus Medical Center, Rotterdam, the Netherlands); R. Gopal (High-Containment Microbiology, National Infection Service, Public Health England – Colindale, London, UK); S. Myhill and G. Mattiuzzo (National Institute for Biologic Standards and Control, South Mimms, UK); N. Thornburg (Centers for Disease Control and Prevention, Atlanta, Georgia, USA).

Acknowledgments

We thank the following institutions and organizations: Universitätsklinikum, Bonn, Germany; Charité–Universitätsmedizin, Berlin, Germany; Korea National Institute of Health; the Central Public Health Laboratory, Ministry of Health, Sultanate of Oman; Public Health Department, Supreme Council of Health, Qatar; the Ministry of Health, Public Health Directorate, Kingdom of Saudi Arabia; SAB Biotherapeutics, South Dakota, USA. We also thank Humayun Asghar from the WHO Eastern Mediterranean Regional Office for assistance obtaining the serum for the study.

C.D. was supported by the Federal Ministry of Education and Research (BMBF) grant RAPID (no. 01KI1723A) and the EU-Horizon 2020 grants COMPARE (no. 643476) and EVAg (no. 653316).

About the Author

Dr. Harvey is a principal scientist at the National Institute for Biological Standards and Control, United Kingdom. Her research interests include influenza virus vaccines and respiratory viruses including MERS coronavirus.

References

- Zaki AM, van Boheemen S, Bestebroer TM, Osterhaus AD, Fouchier RA. Isolation of a novel coronavirus from a man with pneumonia in Saudi Arabia. *N Engl J Med*. 2012;367:1814–20. <https://doi.org/10.1056/NEJMoa1211721>
- World Health Organization. WHO MERS-CoV global summary and assessment of risk. 2017 Jul 21 [cited 2019 Feb 12]. <http://www.who.int/emergencies/mers-cov/risk-assessment-july-2017.pdf>.
- Alanazi KH, Killerby ME, Biggs HM, Abedi GR, Jokhdar H, Alsharif AA, et al. Scope and extent of healthcare-associated Middle East respiratory syndrome coronavirus transmission during two contemporaneous outbreaks in Riyadh, Saudi Arabia, 2017. *Infect Control Hosp Epidemiol*. 2019;40:79–88. <https://doi.org/10.1017/ice.2018.290>
- World Health Organization. Middle East respiratory syndrome coronavirus (MERS-CoV). 2019 Mar 11 [cited 2019 Jul 31]. [http://www.who.int/en/news-room/fact-sheets/detail/middle-east-respiratory-syndrome-coronavirus-\(mers-cov\)](http://www.who.int/en/news-room/fact-sheets/detail/middle-east-respiratory-syndrome-coronavirus-(mers-cov))
- Khalafalla AI, Lu X, Al-Mubarak AI, Dalab AH, Al-Busadah KA, Erdman DD. MERS-CoV in upper respiratory tract and lungs of dromedary camels, Saudi Arabia, 2013–2014. *Emerg Infect Dis*. 2015;21:1153–8. <https://doi.org/10.3201/eid2107.150070>
- Conzade R, Grant R, Malik MR, Elkholy A, Elhakim M, Samhouri D, et al. Reported direct and indirect contact with dromedary camels among laboratory-confirmed MERS-CoV cases. *Viruses*. 2018;10:425. <https://doi.org/10.3390/v10080425>
- World Health Organization. Meeting report: 2018 annual review of diseases prioritized under the Research and Development Blueprint; February 6–7, 2018; Geneva, Switzerland. Geneva: The Organization; 2018 [cited 2019 Aug 13]. <https://www.who.int/emergencies/diseases/2018prioritization-report.pdf>
- Modjarrad K, Moorthy VS, Ben Embarek P, Van Kerkhove MD, Kim J, Kieny M. A roadmap for MERS-CoV research and product development: report from a World Health Organization consultation. *Nat Med*. 2016;22:701–5. <https://doi.org/10.1038/nm.4131>
- World Health Organization. Report on the intercountry meeting on the Middle East respiratory syndrome coronavirus (MERS-CoV) outbreak in the Eastern Mediterranean Region; June 20–22, 2013; Cairo, Egypt. Contract no.: WHO-EM/CSR/063/E/08.13. Geneva: The Organization; 2013 [cited 2019 Aug 13]. http://applications.emro.who.int/docs/IC_Meet_Rep_2013_EN_15164.pdf
- Pas SD, Patel P, Reusken C, Domingo C, Corman VM, Drosten C, et al. First international external quality assessment of molecular diagnostics for MERS-CoV. *J Clin Virol*. 2015;69:81–5. <https://doi.org/10.1016/j.jcv.2015.05.022>
- Dichtelmüller HO, Biesert L, Fabbrizzi F, Gajardo R, Gröner A, von Hoegen I, et al. Robustness of solvent/detergent treatment of plasma derivatives: a data collection from Plasma Protein Therapeutics Association member companies. *Transfusion*. 2009;49:1931–43. <https://doi.org/10.1111/j.1537-2995.2009.02222.x>
- Matsushita H, Sano A, Wu H, Jiao JA, Kasinathan P, Sullivan EJ, et al. Triple immunoglobulin gene knockout transchromosomal cattle: bovine lambda cluster deletion and its effect on fully human polyclonal antibody production. *PLoS One*. 2014;9:e90383. <https://doi.org/10.1371/journal.pone.0090383>
- Mair P, Schoenbrodt F, Wilcox R. WRS2: Wilcox robust estimation and testing. 2017 [cited 2019 Aug 13]. <http://cran.rproject.org/package=WRS2>
- FAO-OIE-WHO MERS Technical Working Group. Aguanno R, ElIdrissi A, Elkholy AA, Ben Embarek P, Gardner E, Grant R, et al. MERS: progress on the global response, remaining challenges and the way forward. *Antiviral Res*. 2018;159:35–44. <https://doi.org/10.1016/j.antiviral.2018.09.002>
- World Health Organization. Laboratory testing for Middle East respiratory syndrome coronavirus interim guidance. Contract no.: WHO/MERS/LAB/15.1/Rev1/2018. Geneva: The Organization; 2018 [cited 2019 Aug 13]. https://www.who.int/csr/disease/coronavirus_infections/mers-laboratory-testing
- World Health Organization. Recommendations for the preparation, characterization, and establishment of international and other biological reference standards (revised 2004). In: WHO Expert Committee on Biological Standardization: fifty-fifth report. WHO technical report series, no. 932. Geneva: The Organization; 2004.

Address for correspondence: Giada Mattiuzzo, NIBSC, Division of Virology, Blanche Lane, South Mimms, Hertfordshire EN6 3QG, UK; email: Giada.Mattiuzzo@nibsc.org

Prevalence of Tuberculosis in Children After Natural Disasters, Bohol, Philippines

Kristy O. Murray, Nina T. Castillo-Carandang, Anna M. Mandalakas, Andrea T. Cruz, Lauren M. Leining, Salvacion R. Gatchalian, on behalf of the PEER Health Bohol Pediatric Study Team¹

In 2013, a severe earthquake and typhoon affected Bohol, Philippines. To assess the postdisaster risk for emergence of *Mycobacterium tuberculosis* infection in children, we conducted a cross-sectional multistage cluster study to estimate the prevalence of tuberculin skin test (TST) positivity and tuberculosis (TB) in children from 200 villages in heavily affected and less affected disaster areas. Of the 5,476 children we enrolled, 355 were TST-positive (weighted prevalence 6.4%); 16 children had active TB. Fourteen (7%) villages had $\geq 20\%$ TST-positive prevalence. Although prevalence did not differ significantly between heavily affected and less affected areas, living in a shelter with ≥ 25 persons approached significance. TST positivity was independently associated with older age, prior TB treatment, known contact with a person with TB, and living on a geographically isolated island. We found a high TST-positive prevalence, suggesting that national programs should consider the differential vulnerability of children and the role of geographically isolated communities in TB emergence.

In October 2013, the island province of Bohol, Philippines, was devastated by a 7.2-magnitude earthquake, followed 3 weeks later by the landfall of Typhoon Haiyan (Super Typhoon Yolanda). These disasters resulted in the deaths of 195 persons in the province; displacement of 30% of the 1.2 million-person population (1); and disruption of routine health services, including prevention and treatment services provided by the National Tuberculosis Program (2). After other natural disasters, infrastructure loss resulted in individual patients being contagious for longer periods, and increased *Mycobacterium tuberculosis* transmission occurred because of crowding in emergency shelters (3). In complex emergencies, children are the most vulnerable population and suffer the greatest negative effects (4).

Author affiliations: Baylor College of Medicine and Texas Children's Hospital, Houston, Texas, USA (K.O. Murray, A.M. Mandalakas, A.T. Cruz, L.M. Leining); University of the Philippines, Manila, Philippines (N.T. Castillo-Carandang, S.R. Gatchalian)

DOI: <https://doi.org/10.3201/eid2509.190619>

Approximately 400,000 children live in Bohol, so the increased risk for tuberculosis (TB) emergence after these natural disasters was expected to be substantial. To further complicate matters, the main island province of Bohol includes 75 smaller islands and islets that are considered geographically isolated and disadvantaged areas (5,6). These areas are separated from mainstream society and have both physical (i.e., accessible only by boat) and socioeconomic factors that further compound their vulnerability to TB.

In this study, our primary objectives were to estimate the prevalence of *M. tuberculosis* infection and TB disease between displaced and nondisplaced children and examine risk factors for *M. tuberculosis* infection. We aimed to clarify the epidemiology of childhood TB in the late post-disaster recovery setting and provide recommendations to mitigate damage and ensure preparedness before future complex emergencies.

Methods

Study Population

We conducted this study in the island province of Bohol in the Philippines during 2016–2018. Bohol is 4,821 km² and comprises 1 city, 47 municipalities, and 1,109 villages (called barangays). In 2010, the total population of Bohol was $\approx 1,255,128$, of whom 32% were children (7). The World Health Organization estimates that $>80\%$ of children are vaccinated with *M. bovis* BCG at birth in the Philippines (8).

Study Design

To estimate the prevalence of tuberculin skin test (TST) positivity and TB in children (<15 years of age), we conducted a cross-sectional survey using a modified version of a multistage cluster sampling technique based on the World Health Organization's Expanded Programme on Immunization coverage survey methods (9). Based on our initial

¹Additional members of the PEER Health Bohol Pediatric Study Team who contributed data are listed at the end of this article.

sample size calculations, we determined that we needed to screen a minimum of 4,014 children (0–14 years of age) to identify a significant difference between our hypothesized postdisaster prevalence of *M. tuberculosis* infection (1%) and a reference value of 0.56% prevalence of infection ($\alpha = 0.05$, power = 80%) (10). To account for the possibility of missing data or incomplete or inaccurate records, we aimed to sample 4,200 children.

Using 7 households per cluster and an estimated minimum average of 3 children per household, we determined we needed 200 clusters to obtain our sample size. The 200 clusters comprised 100 clusters chosen from the municipalities that suffered the greatest effects of the natural disasters (heavily affected areas) and 100 clusters from municipalities that suffered fewer effects (less affected areas) based on data from the Provincial Health Office (Reymoses Cabagnot, Provincial Health Officer, pers. comm., 2015 Aug 17). We randomly selected 7 municipalities each from heavily affected and less affected areas, providing 14 municipalities total for sampling.

To select the 200 clusters, we alphabetically arranged the names of all villages and their population sizes (based on the 2010 census), stratified by heavily affected area and less affected area designation. We determined the sampling interval by dividing the total population of each area (224,212 in heavily affected areas and 214,072 in less affected areas) by the number of clusters needed. We identified the first cluster (village) by using a randomly generated 5-digit number and matching it to the first village in our list with a cumulative population greater than or equal to the random number. We identified the second cluster by adding the sampling interval to the random number and selected subsequent clusters by adding the sampling interval to the previously generated number until we identified 100 clusters in each area (Appendix Tables 1, 2, <https://wwwnc.cdc.gov/EID/article/25/10/19-0619-App1.pdf>).

Once we identified all 100 clusters in each area, we selected the households for enrollment using simple random sampling in the field. We worked with the barangay health stations to obtain a list of all the households within the village, which we then randomly selected using a random number generator. The household number randomly drawn was the starting point of the survey. Each subsequent household was chosen by going to the next closest front door. If no one was home, then the next house was selected, until a total of 7 households containing ≥ 1 child were obtained for each of the 200 clusters (total households 1,400). All children within the household were enrolled.

All 1,400 households had an equal chance of being selected to participate in this survey. Children were excluded if caregivers did not provide consent or if child assent for those ≥ 7 years of age was not obtained. We conducted surveys using 2 questionnaires, 1 for the household in general

and 1 for each child assessed. Surveys assessed social risk factors for *M. tuberculosis* infection, including whether or not the child was residing in Bohol during the disasters, displacement into an emergency shelter or camp, and number of new permanent or temporary residents in households who were displaced as a result of the disasters. We also assessed history of TB treatment and determined whether the children received their healthcare from the public or private sector. Caregivers completed screening for pulmonary TB using the National Tuberculosis Program questionnaire that assesses cough, weight loss, fever, and TB exposure (11); an examination for cervical lymphadenopathy ($\geq 2 \times 2$ cm); and TST (5 tuberculin units purified protein derivative-S, Serum Statens Institute, <https://en.ssi.dk>) (Figure 1).

Clinical Evaluation for TB

The study team returned to each enrolled household 48–72 hours after the initial visit to measure the TST induration transversely in accordance with National Tuberculosis Control Program guidelines (11). All children who had TSTs ≥ 10 mm (or ≥ 5 mm if recent TB exposure within the last 6 months was known), had TB-compatible signs or symptoms, or both completed further evaluation for TB. Evaluation included physical examination, chest radiography, and microbiologic testing of sputum (children > 5 years of age) or gastric aspirates (children ≤ 5 years of age) by direct smear sputum microscopy and GeneXpert PCR testing (Cepheid, <http://www.cepheid.com>); mycobacterial culture was not available. All TST-positive or symptomatic children were provided with transportation to the closest medical center along with a voucher for chest radiograph. An independent radiologist read the chest radiographs to determine the presence of lesions consistent with intrathoracic TB.

Participants in whom *M. tuberculosis* infection or TB disease was diagnosed were referred to the local health center for appropriate treatment. *M. tuberculosis* infection was defined as TST results ≥ 10 mm in asymptomatic children with normal chest radiograph results and negative direct smear sputum microscopy and PCR. In accordance with international and national guidelines (11,12), TB was diagnosed in children who met 3 of the 5 following criteria: 1) TST positive, 2) known exposure to a TB contact, 3) evidence of TB on chest radiograph, 4) direct smear sputum microscopy or PCR positive in sputum or gastric aspirates, and 5) 3 of the 6 signs and symptoms compatible with TB. Signs and symptoms of TB were cough or wheezing of ≥ 2 weeks, unexplained fever ≥ 2 weeks after common causes excluded, weight loss or failure to gain weight or weight faltering or anorexia, failure to respond to ≥ 2 weeks of antimicrobial therapy when treated for a lower respiratory tract infection, failure to return to baseline health status after ≥ 2 weeks after a viral infection or exanthema, and fatigue/

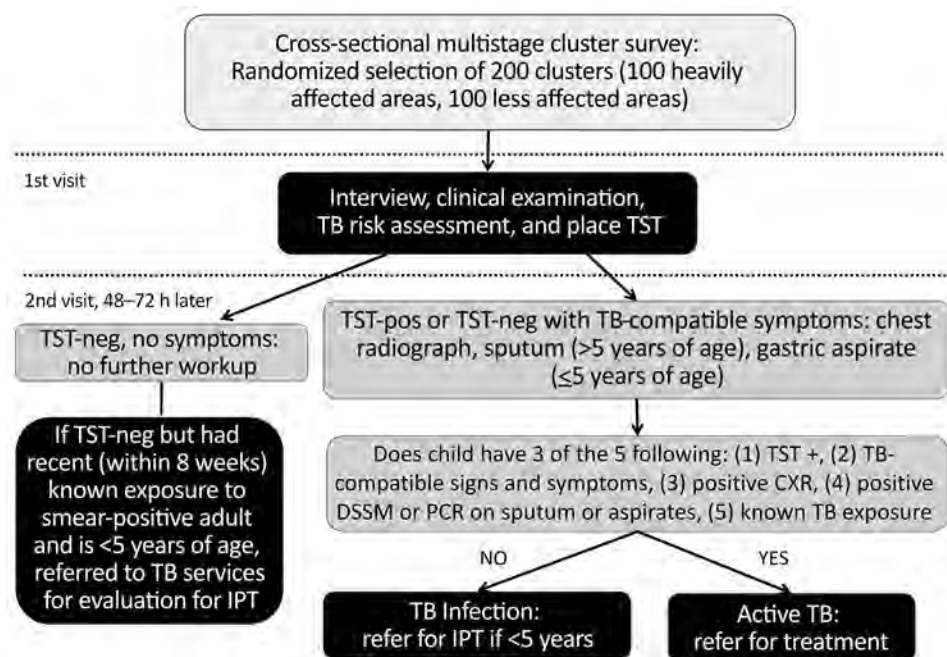


Figure 1. Procedures and decision tree for enrollment of study participants during community-based cluster survey of TB in children in areas affected by 2013 natural disasters, Bohol, Philippines. Positive result on chest radiograph means evidence of infiltrates, consolidation, or cavitory lesions suggestive of TB disease. DSSM, direct sputum smear microscopy; IPT, isoniazid preventive therapy; neg, negative; pos, positive; TB, tuberculosis; TST, tuberculin skin test.

lethargy or reduced playfulness (11). Participants in whom illnesses other than TB were diagnosed also were referred to the local health center for medical management. The Institutional Review Boards of the University of the Philippines Manila (Manila, Philippines) and Baylor College of Medicine (Houston, TX, USA) reviewed and approved this study.

Data Analysis

All data were entered into EpiInfo version 7.2 (US Centers for Disease Control and Prevention, <https://www.cdc.gov/epiinfo/index.html>) on password-protected computers and were continuously backed up to a US-based protected server accessible only by study personnel. Statistical analyses were performed using EpiInfo and NCSS (NCSS, Inc., <https://www.ncss.com>). We determined the weighted prevalence of TST positivity (including diagnosed TB) and calculated Wilson 95% CIs. We then used univariate logistic regression with calculation of odds ratios (ORs) and 95% CIs to examine whether the prevalence of TST positivity in heavily affected areas differed significantly from that in less affected areas. We also performed univariate analysis on all other collected variables that could potentially influence the risk for TST positivity. Multivariate logistic regression analysis was then performed on all variables identified on univariate analysis with a p value <0.25 to determine independent risk factors for TST positivity in Bohol. We used a stepwise-backward approach to eliminate variables with the highest p value until all remaining variables had a p value ≤ 0.05 . Model building strategies included interaction terms to determine effect modification and confounding.

Results

During 2016–2018, a total of 5,476 children (2,710 in heavily affected areas and 2,766 in less affected areas) were enrolled from the 14 municipalities from the 184 villages selected for the 200 clusters. We enrolled an average of 3.9 children per household, exceeding our original sample size estimate of 3 children per household.

A total of 355 children were TST positive (weighted prevalence 6.4% [95% CI 6.3%–6.5%]). Three of the 14 municipalities had a TST-positive prevalence $>10\%$ (1 in heavily affected areas, 2 in less affected areas; Table 1, Figure 2), and 12 villages had TST-positive prevalence $>20\%$ (Appendix Table 3). Two remote villages (1 in heavily affected areas, 1 in less affected areas) had the highest prevalence (29% each). Of the 16 island villages located offshore from mainland Bohol, 9 (56%) had prevalence $\geq 10\%$, compared with 38 (22%) of the 168 villages on mainland Bohol.

Sex was not associated with TST positivity (Table 2). Older age was significantly associated with TST positivity; prevalence increased markedly ($>10\%$) in children ≥ 10 years of age (Figure 3). Variables identified on univariate analysis as being significant risks for TST positivity were being older (≥ 6 years of age), living in 1 of the island villages away from mainland Bohol, having a history of TB treatment, having ≥ 6 persons living in the home, having a history of contact with a person with TB, and having ≥ 2 weeks of cough during the preceding month.

Most (75.4%) of the children enrolled were already born and living in Bohol during the earthquake, and almost half (47.4%) were displaced. Among those in Bohol during the earthquake, living in a shelter with ≥ 25

Table 1. Prevalence of TST positivity by municipality and area affected by 2013 natural disasters, Bohol, Philippines, 2016–2018*

Municipality†	Total population‡ of municipality‡	Total no. children enrolled	Total no. TST positive§	Prevalence, % (95% CI)
Heavily affected area				
Loon	42,729	550	14	2.5 (1.2–3.9)
Calape	30,146	260	11	4.2 (1.8–6.7)
Maribojoc	20,477	168	11	6.5 (2.8–10.3)
Clarín	20,277	267	16	6.0 (3.1–8.9)
Catigbian	22,675	624	19	3.0 (1.7–4.4)
Inabanga	43,272	537	62	11.5 (8.8–14.3)
Sagbayan	20,077	304	27	8.9 (5.7–12.1)
Less affected area				
Ubay	213,899	2,766	195	7.0 (6.1–8.0)
Bien Unido	68,482	653	48	7.4 (5.3–9.4)
Pres. Carlos P. Garcia	25,782	162	17	10.5 (5.7–15.3)
Anda	23,269	212	29	13.7 (9.0–18.3)
Mabini	16,866	327	21	6.4 (3.8–9.1)
Candijay	28,172	722	51	7.1 (5.2–8.9)
Alicia	29,043	457	27	5.9 (3.7–8.1)
Alicia	22,285	233	2	0.9 (–0.3–2.1)

*TST, tuberculin skin test.

†Heavily affected and less affected areas each comprised 100 clusters/700 households.

‡Population is based on the 2010 national census (7).

§TST Positives includes all tuberculosis cases, including the 1 child with tuberculosis who was TST negative because of malnutrition.

persons approached significance for increased risk for TST positivity on univariate analysis (OR 1.5, 95% CI 0.98–2.2; $p = 0.06$). We noted no significant difference in TST positivity between heavily affected and less affected areas (Table 3). A higher proportion of TST-positive children were from the less affected areas, but this finding was not statistically significant.

On the basis of results from the univariate analyses, we entered the following variables into the multivariate logistic regression model to determine which factors were independent risks for TST positivity: age category (6–14 years), history of TB treatment, prior contact with a person known to have TB, recent history of cough for ≥ 2 weeks, living on a remote island village, and living with ≥ 25

persons during displacement after the earthquake. Based on backward, stepwise multivariate logistic regression modeling, being older (OR 1.6; 95% CI 1.2–2.0), having a history of TB treatment (OR 3.4; 95% CI 1.7–6.7), contact with a person known to have TB (OR 4.9; 95% CI 3.8–6.2), and living on a remote island village (OR 1.5; 95% CI 1.1–2.1) were independent risk factors for TST positivity (Table 4).

According to history provided by caregivers, 57 (1%) children were previously treated for TB; only 12 (22%) were TST positive (Table 2). We were unable to assess whether the treatment administered was isoniazid preventive therapy for TB exposure or latent infection or was treatment for active disease. Of the 57 reporting prior TB treatment, 47 (82%) completed the course of treatment,

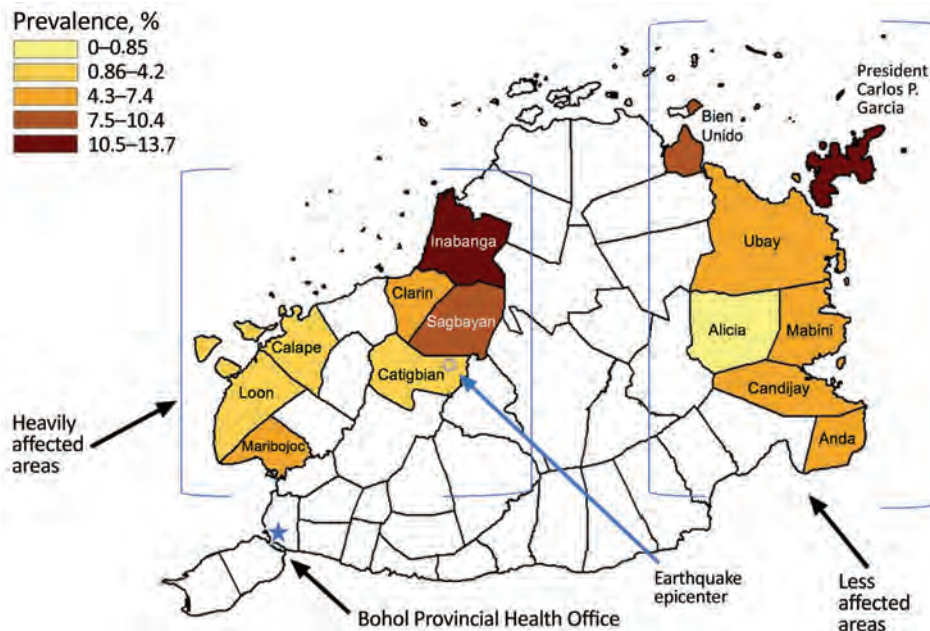


Figure 2. Prevalence of tuberculin skin test positivity by municipality obtained in study of tuberculosis in children in areas affected by 2013 natural disasters, Bohol, Philippines, 2016–2018. Epicenter of 2013 earthquake is indicated.

Table 2. Demographic, social, and clinical histories of enrolled children in cluster survey of TB in children in areas affected by 2013 natural disasters, Bohol, Philippines*

Characteristic	Total, n = 5,476 (%)	TST		OR (95% CI)	p value
		Positive† n = 355	Negative, n = 5,121		
Male sex	2,862 (52.3)	179 (50.4)	2,684 (52.4)	1.1 (0.9–1.4)	0.44
Median age, y (IQR)	5.8 (5.3)	7.8 (6.3)	5.8 (5.2)		
0–5	2,811 (51.3)	133 (37.5)	2,678 (52.3)	Reference	
6–14	2,665 (48.7)	222 (62.5)	2,443 (47.7)	1.8 (1.5–2.3)	<0.001
Island village	375 (6.8)	48 (13.5)	327 (6.4)	2.3 (1.7–3.2)	<0.001
Prior treatment for TB	57 (1.0)	12 (3.4)	45 (0.9)	4.0 (2.1–7.6)	<0.001
Median no. persons living in household before earthquake (range)	5 (1–21)	6 (1–15)	5 (1–21)	1.1 (1.0–1.1)	0.009
≥6 Persons living in home	2,586 (47.2)	193 (54.4)	2,393 (46.7)	1.4 (1.1–1.7)	0.005
Smokers in the home	3,049 (55.7)	208 (58.6)	2,841 (55.5)	1.1 (0.9–1.4)	0.23
Child had contact with person with TB	658 (12.0)	136 (38.3)	522 (10.2)	5.4 (4.3–6.8)	<0.001
Recent history of cough for ≥2 wk‡	104 (1.9)	26 (7.3)	78 (1.5)	4.9 (3.1–7.7)	<0.001

*All values are no. (%) unless indicated otherwise. IQR, interquartile range; OR, odds ratio; TB, tuberculosis; TST, tuberculin skin test.

†TST-positive includes persons with TB.

‡Within 4 wk. Active represented 9 (35%) of the 26 TST-positive persons with a recent history of a cough for ≥2 wk.

8 (14%) did not complete treatment, and 2 (4%) had unknown treatment adherence. All 8 children who did not complete treatment were from villages that were hard to reach because of distance or accessibility. Reasons for not completing treatment were inability to purchase medications (5 children); erratic medicine supply (2 children);

and distance from clinic, adverse medicine events, unpleasant taste, and difficult medication administration (1 child each). For 2 children, >1 barrier was listed for not completing treatment.

Intrathoracic TB was diagnosed in 16 (0.3%) children (median age 6 years) (Table 5). Three (24%) had

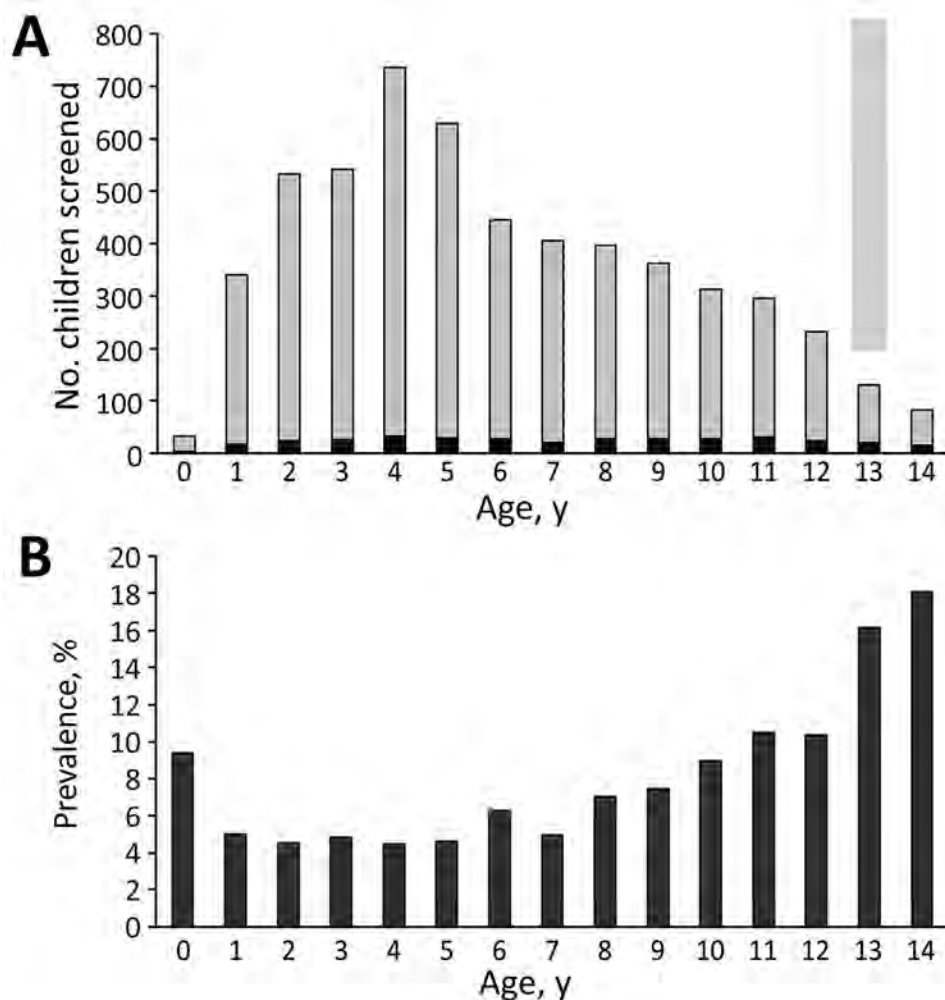


Figure 3. Distribution of patients by age in study of tuberculosis in children in areas affected by 2013 natural disasters, Bohol, Philippines. A) Number of children who screened positive by TST; B) prevalence of TST positivity. Black bars, TST positive; gray bars, TST negative. TST, tuberculin skin test.

Table 3. Factors related to 2013 earthquake and subsequent displacement on TST positivity in children in areas affected by 2013 natural disasters, Bohol, Philippines*

Factor	Total no. (%), n = 5,476	TST		Odds ratio (95% CI)	p value
		Positive, no. (%), † n = 355	Negative, no. (%), n = 5,121		
Earthquake-affected area					
Heavily affected area	2,710 (49.5)	160 (45.1)	2,550 (49.8)	1.2 (0.97–1.5)	0.09
Less affected area	2,766 (50.5)	195 (54.9)	2,571 (50.2)		
Child lived in Bohol during earthquake	4,131 (75.4)	278 (78.3)	3,853 (75.2)	1.2 (0.92–1.5)	0.20
Child was displaced	1,959/4,131 (47.4)	113/278 (40.6)	1,846/3,854 (47.9)	0.7 (0.6–0.95)	0.02
Child lived with ≥25 persons in shelter	1,081/1,959 (55.2)	72/113 (63.7)	1,009/1,846 (54.7)	1.5 (0.98–2.2)	0.06
Child displaced >7 d	777/1,956 (39.7)	50/113 (44.2)	727/1,843 (39.4)	1.2 (0.8–1.8)	0.31

*TST, tuberculin skin test.

†Includes persons with tuberculosis.

microbiological confirmation (all by GeneXpert). Seven (44%) had abnormal radiographic findings consistent with TB. The most commonly reported history of recent (within 4 weeks) symptoms were cough >2 weeks (9 [56%] children) and weight loss/anorexia (6 [38%]). On physical examination, 7 (44%) children had cervical lymphadenopathy. All 16 children with TB were included in the total number of TST-positive children in the analyses to examine risks for exposure.

Among the 1,400 households in which we conducted interviews, 148 (11%) reported a household death within the 12 months before enrollment, including 10 deaths involving a family member with known or presumed TB. Among homes of TST-positive children, 17 deaths occurred in the previous year; 6 households reported death of a family member with known or presumed TB.

Discussion

We assessed the risk for TB in a postdisaster setting among a large population of children using a methodologically rigorous study design. The prevalence of TST positivity was higher than we expected and disparate, even in a relatively small island province in the Philippines, and TST positivity in some villages approached 30%. Considering the weighted prevalence of TST positivity of 6.4% and that 422,148 children live in Bohol (7), we can estimate that ≈27,000 children are TST positive in this 1 province. At the time of this study, TST prevalence for children in the Philippines was unknown. Although we did not find TST positivity to be significantly higher in disaster-affected areas in Bohol as a result of resource interruptions as we originally hypothesized, positivity was associated with geographic barriers (i.e., island villages) and approached significance with increased risk resulting from crowding in emergency shelters. In adults, smear positivity and illness and death increased after natural and humanmade disasters in countries in Central America (13), Eastern Europe (14), and Africa (15). Our data add a perspective for children and are consistent with data reported for TB for adults in developing countries after complex humanitarian emergencies.

The high prevalence of TST positivity among subgroups of children in Bohol was unexpected. Unfortunately, we know of no prior studies in children in this region that would have enabled us to document baseline or estimate the expected prevalence. Villages with high prevalence of TST positivity might plausibly have unique risk factors for TB (e.g., geographically isolated and disadvantaged areas having poor socioeconomic status or limited access to care). TSTs also might have overestimated the incidence of *M. tuberculosis* infection resulting from cross-reactions with BCG (16). In the Philippines, BCG is administered only once, soon after birth (17), which provides a lower risk for false positive TSTs than in countries where BCG is boosted or administered to older children (18). Also, if cross-reactions were common, we would not have observed such variation in prevalence of TST positivity across Bohol, particularly in older children, which was the higher risk group.

Robust national and international data demonstrate that TB occurs in pockets of persons and varies substantially across geographic regions (19,20). Although some clustering of cases may be explained by underlying medical, social, or economic conditions (e.g., diabetes, socioeconomic status, and care access issues), explanations for clustering are not always evident. We found higher TST positivity in island villages where geographic barriers prevented immediate access to the municipal health units on mainland Bohol. Increasing distance from public health-care facilities can result in diagnostic delays and missed diagnoses, particularly for TB, where control programs often use centralized models. Late disease detection in infectious

Table 4. Independent risk factors for being TST positive in multivariate logistic regression analyses in cluster survey of TB in children in areas affected by 2013 natural disasters, Bohol, Philippines*

Variable	OR (95% CI)	p value
History of contact with a person known to have TB	4.9 (3.8–6.2)	<0.001
History of treatment for TB	3.4 (1.7–6.9)	<0.001
Older age, 6–14 y	1.6 (1.2–2.0)	<0.001
Living on a remote island village	1.5 (1.1–2.1)	0.02

*OR, odds ratio; TB, tuberculosis; TST, tuberculin skin test.

Table 5. Clinical and diagnostic findings for 16 persons with TB in cluster survey of TB in children in areas affected by 2013 natural disasters, Bohol, Philippines, 2016–2018*

Case no.	Natural disaster area	Age, y/sex	Known exposure to TB	History of signs/symptoms	Chest radiograph interpretation by radiologist	DSSM result†	GeneXpert result†
1	LAA	6/M	Yes	Cough >2 weeks, wheezing, weight loss; no improvement after taking antimicrobial drugs	Pneumonia, both paracardiac areas	Neg	Neg
2	LAA	2/M	Yes	Cough >2 weeks, weight loss, malaise; no improvement after taking antimicrobial drugs	Inflammatory process, both inner zones	Neg	Invalid, after 2 extractions
3	LAA	8/M	Yes	Cervical lymphadenopathy	Calcified hilar lymphadenopathy, likely representing a chronic process, such as pulmonary TB	Neg	Neg
4	LAA	14/M	Yes	None; history of prior TB treatment but did not complete therapy	Inflammatory process in left apical area compatible with chronic process, such as pulmonary TB with minimal apical pleural thickening	Neg	Neg
5	LAA	7/F	Yes	Cough >2 weeks	Normal	Neg	Neg
6	LAA	4/M	Yes	Cough >2 weeks, weight loss, anorexia, malaise, chest pain	Normal	Neg	Neg
7	LAA	5/M	Yes	Cervical lymphadenopathy	Inflammatory process in the left retrocardiac area	Neg	Neg
8	HAA	14/F	Yes	None	Normal	Neg	Pos
9	LAA	5/F	Yes	Cough >2 weeks, fever, weight loss	Normal	Neg	Pos
10	LAA	1/F	Yes	Cough >2 weeks, fever, dyspnea, no improvement after taking antimicrobial drugs	Normal	Neg	Neg
11	LAA	12/F	No	Coughing >2 weeks, fever, chest and back pain, weight loss, cervical lymphadenopathy	Normal	Neg	Neg
12	LAA	11/F	Yes	Cervical lymphadenopathy, no rales or wheezing	Normal	Neg	Neg
13	LAA	3/M	Yes	Cervical lymphadenopathy	Normal	Neg	Neg
14	LAA	6/M	Yes	Cervical lymphadenopathy	Normal	Neg	Neg
15	LAA	3/F	Yes	Coughing >2 weeks, weight loss	Bilateral pneumonia	Neg	Neg
16	HAA	10/M	Yes	Coughing >2 weeks, weight loss, cervical lymphadenopathy	Pneumonia, both lower lungs, minimal left pleural effusion vs. pleural thickening; consider Potts disease (extrapulmonary TB) involving T12 and L1 vertebrae with Gibbus deformity	Neg	Pos

*DSSM, direct sputum smear microscopy; HAA, heavily affected area; LAA, less affected area; neg, negative; pos, positive; TB, tuberculosis.

†Direct smears and GeneXpert (Cepheid, <http://www.cephid.com>) performed on sputum for children >5 years of age and gastric aspirates for children ≤5 years of age.

adults has substantial implications for children, including increasing *M. tuberculosis* infection and missed opportunities for preventive health services, outreach, and public health intervention.

In our study, other factors independently associated with TST positivity included older age, history of contact with a person known to have TB, and history of TB treatment. These statistical findings were expected because older children have a longer possible period of exposure risk over the course of their childhood. Similarly, known contact with a person with TB and history of TB treatment would greatly influence TST positivity. Although our finding of higher TST-positive prevalence in less affected areas than in heavily affected areas was not significant, we did not expect to find it. We hypothesize this finding was because less affected areas were much farther from the

Provincial Health Office, where TB resources are distributed to the entire province. This discrepancy is worth investigating further to understand whether availability and access to resources affects TB transmission in this region.

Historically, TB prevention and treatment efforts have focused on adults for epidemiologic, economic, and practical reasons. *M. tuberculosis*-infected children are reservoirs for future cases and transmitters of disease. Given their youth, children are less likely to experience adverse side effects of TB prevention treatment and experience greater long-term benefits than adults, presuming they are not reinfected by the original source. Additionally, in many developing nations, children account for nearly 50% of the population. Thus, changing the emphasis of treatment and prevention programs to be more inclusive of children is needed but requires modification in provider

education, expansion of diagnostic tools, caregiver support, and more readily available access to child-friendly medication formulations.

During natural disasters, disruption of TB control poses a threat to both industrialized and resource-limited nations, as seen after the 2011 earthquake in Japan, the 2010 earthquake in Haiti, and the 2005 Hurricane Katrina in the United States (15,21,22). Experience has demonstrated that major impediments to successful reconstruction of TB services include mobile populations, destroyed infrastructure, and lack of coordination, leading to poor case detection and suboptimal TB control (15). Our findings suggest that displacement after natural disasters may increase the future risk for TB in affected communities. Because public health resources are often introduced into communities after disasters, we propose that the postdisaster recovery period might provide a unique window of opportunity to introduce interventions to sustainably improve TB control.

Our study had some limitations. Epidemiologic risk factors were family-reported and subject to recall bias, particularly because this study was conducted 3–5 years after the natural disasters. Crowding in shelters with nonrelatives might have resulted in underestimating TB contacts for children. Interferon γ -release assays were unavailable; some TST positivity might have resulted from cross-reaction from BCG. However, older children were significantly more likely than younger children to be TST positive, which would not be expected if TST positivity were due solely to BCG. Although we presume that BCG uptake is high according to national data, we did not collect vaccine status individually at enrollment. The unavailability of mycobacterial cultures potentially caused an underestimation of the TB prevalence. Unfortunately, the number of active TB cases was small, so we were concerned about performing and interpreting any statistical analyses for risk; however, when active cases were examined independently in our model, the risks remained the same for this group with the exception of older age. Our findings might not be generalizable to other disaster settings in less populated regions or in areas with lower baseline TB incidence.

In conclusion, in a large, community-based screening for *M. tuberculosis* infection in children <15 years of age in the Philippines, we found a high prevalence of TST positivity, especially in geographically isolated villages. We demonstrated the feasibility and highlight the importance of implementing active TB case-finding in a resource-poor setting despite population displacement and postdisaster service-line interruption. One step to bolster postdisaster mitigation is a strong baseline national TB program that includes local stakeholders (including not only healthcare workers but also community and government leaders), reaches marginalized populations, and considers the differential vulnerability of children before a disaster.

Additional members of the PEER Health Bohol Pediatric Study Team who contributed data to this study: Hazel M. Remolador, Zarah Jane H. Tubiano, Rhea Annvi H. Lofranco, Ellen D. Lague, Riovi May S. Salmasan, Katherine Ngo, Caya R. Estoque, Fernando B. Lopos, Diozele Hazel M. Sanvictores, Carmelita D. Amora, Maureen Mae C. Riña, Catherine O. Calipes, Jeia Pondoc, Marlo Tampon, Myra Riccil Estose, Reymoses Cabagnot, Polizena Rances, Mutya Kismet T. Macuno, Crisanta Estomago, and Nelson Elle.

Acknowledgments

We thank the families and children who participated in this study. We also thank the physicians, nurses, and health workers at the Provincial Health Office, Municipal Rural Health Units, and Barangay Health Stations.

This study was funded by the US Agency for International Development and the US National Academy of Sciences through the PEER Health Program.

About the Author

Dr. Murray is a professor in pediatrics and molecular virology and microbiology and is the vice chair for research in the Department of Pediatrics, director of the William T. Shearer Center for Human Immunobiology, and assistant dean of the National School of Tropical Medicine, Baylor College of Medicine and Texas Children's Hospital, Houston, Texas, USA. Her research interests include the epidemiology and clinical investigation of infectious diseases.

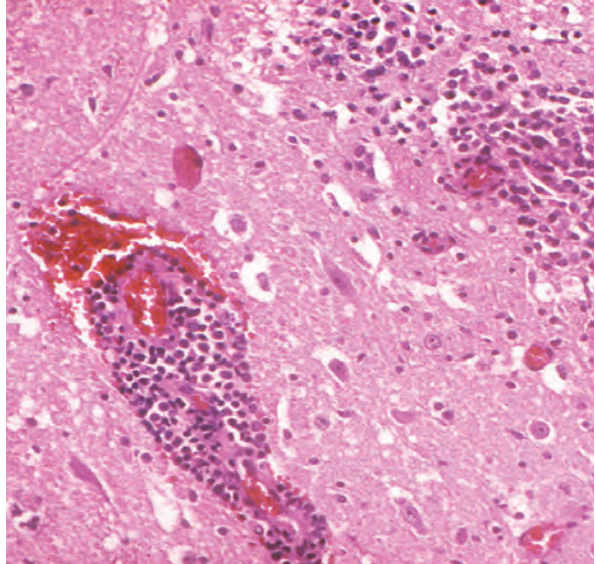
References

1. Philippine Humanitarian Country Team UNOftCoHA. Philippines: Bohol earthquake action plan (revised). January 2014 [cited 2018 Nov 30]. <https://reliefweb.int/sites/reliefweb.int/files/resources/Bohol%20Earthquake%20Action%20Plan%20%28BEAP%29%20Revision%20FINAL.pdf>
2. Survey MotPNTP. 2016 National Tuberculosis Prevalence Survey for the Department of Health, Philippines [cited 2019 Jan 22]. <http://ntp.doh.gov.ph/downloads/publications/NTPS2016.pdf>
3. Kanamori H, Hatakeyama T, Uchiyama B, Weber DJ, Takeuchi M, Endo S, et al. Clinical and molecular epidemiological features of tuberculosis after the 2011 Japan earthquake and tsunami. *Int J Tuberc Lung Dis*. 2016;20:505–14. <http://dx.doi.org/10.5588/ijtld.15.0607>
4. Moss WJ, Ramakrishnan M, Storms D, Henderson Siegle A, Weiss WM, Lejnev I, et al. Child health in complex emergencies. *Bull World Health Organ*. 2006;84:58–64. <http://dx.doi.org/10.2471/BLT.04.019570>
5. Bohol-Philippines.com Best Ecotourism Destinations. Bohol Islands [cited 2019 Apr 26]. <https://www.bohol-philippines.com/bohol-island.html>
6. Republic of the Philippines Department of Health. What is GIDA? [cited 2019 Jan 22]. <https://www.doh.gov.ph/node/1154>
7. Republic of the Philippines National Statistics Office. 2010 Census of population and housing. Report no. 2A. Demographic

- and housing characteristics (non-sample variables). Bohol [cited 2018 Nov 30]. https://psa.gov.ph/sites/default/files/BOHOL_FINAL%20PDF.pdf
8. World Health Organisation. Philippines: WHO and UNICEF estimates of immunization coverage: 2017 revision [cited 2019 Apr 24]. https://www.who.int/immunization/monitoring_surveillance/data/phl.pdf
 9. Bennett S, Woods T, Liyanage WM, Smith DL. A simplified general method for cluster-sample surveys of health in developing countries. *World Health Stat Q.* 1991;44:98–106.
 10. Vianzon R, Garfin AM, Lagos A, Belen R. The tuberculosis profile of the Philippines, 2003–2011: advancing DOTS and beyond. *Western Pac Surveill Response J.* 2013;4:11–6. <http://dx.doi.org/10.5365/wpsar.2012.3.4.022>
 11. PhilHealth. National Tuberculosis Control Program, manual of procedures. 5th ed. [cited 2018 Dec 3]. https://www.philhealth.gov.ph/partners/providers/pdf/NTCP_MoP2014.pdf
 12. Graham SM, Cuevas LE, Jean-Philippe P, Browning R, Casenghi M, Detjen AK, et al. Clinical case definitions for classification of intrathoracic tuberculosis in children: an update. *Clin Infect Dis.* 2015;61(Suppl 3):S179–87. <http://dx.doi.org/10.1093/cid/civ581>
 13. Barr RG, Menzies R. The effect of war on tuberculosis. Results of a tuberculin survey among displaced persons in El Salvador and a review of the literature. *Tuber Lung Dis.* 1994;75:251–9. [http://dx.doi.org/10.1016/0962-8479\(94\)90129-5](http://dx.doi.org/10.1016/0962-8479(94)90129-5)
 14. Toole MJ, Waldman RJ. Refugees and displaced persons. War, hunger, and public health. *JAMA.* 1993;270:600–5. <http://dx.doi.org/10.1001/jama.1993.03510050066029>
 15. Coninx R. Tuberculosis in complex emergencies. *Bull World Health Organ.* 2007;85:637–40. <http://dx.doi.org/10.2471/BLT.06.037630>
 16. Howley MM, Painter JA, Katz DJ, Graviss EA, Reves R, Beavers SF, et al.; Tuberculosis Epidemiologic Studies Consortium. Evaluation of QuantiFERON-TB gold in-tube and tuberculin skin tests among immigrant children being screened for latent tuberculosis infection. *Pediatr Infect Dis J.* 2015;34:35–9. <http://dx.doi.org/10.1097/INF.0000000000000494>
 17. Aguirre CA. Philippines childhood immunization schedule, 2016 [cited 2018 Dec 3]. <http://www.pidsphil.org/pdf/2016/16LEC-10-PIDSP-Immunization-Schedule-2016-Aguirre.pdf>
 18. Zwerling A, Behr MA, Verma A, Brewer TF, Menzies D, Pai M. The BCG World Atlas: a database of global BCG vaccination policies and practices. *PLoS Med.* 2011;8:e1001012. <http://dx.doi.org/10.1371/journal.pmed.1001012>
 19. Jenkins HE, Gegia M, Furin J, Kalandadze I, Nanava U, Chakhaia T, et al. Geographical heterogeneity of multidrug-resistant tuberculosis in Georgia, January 2009 to June 2011. *Euro Surveill.* 2014;19:20743. <http://dx.doi.org/10.2807/1560-7917.ES2014.19.11.20743>
 20. Winston CA, Menzies HJ. Pediatric and adolescent tuberculosis in the United States, 2008–2010. *Pediatrics.* 2012;130:e1425–32. <http://dx.doi.org/10.1542/peds.2012-1057>
 21. Furin J, Mathew T. Tuberculosis control in acute disaster settings: case studies from the 2010 Haiti earthquake. *Disaster Med Public Health Prep.* 2013;7:129–30. <http://dx.doi.org/10.1017/dmp.2013.7>
 22. Bieberly J, Ali J. Treatment adherence of the latently infected tuberculosis population (post-Katrina) at Wetmore TB Clinic, New Orleans, USA. *Int J Tuberc Lung Dis.* 2008;12:1134–8.

Address for correspondence: Salvacion R. Gatchalian, Section of Infectious and Tropical Diseases in Pediatrics, Department of Pediatrics, UP-PGH, Taft Avenue, Manila 1000, Philippines; email: sallymd77@yahoo.com

EID podcast Bird Migration and West Nile Virus in the U.S.



West Nile virus cycles between birds and mosquitoes that then infect humans through bites. But birds don't tend to stay in one place, and neither does the virus; a recent study has mapped how the disease has evolved along known migration routes.

In this EID podcast, Dr. Alan Barrett, Professor and Vice Chair for Research in the Department of Pathology at the University of Texas, Medical Branch, explores how bird migration patterns influence the epidemiology of West Nile virus in the U.S.

Visit our website to listen:
<https://go.usa.gov/xy6n>

**EMERGING
INFECTIOUS DISEASES®**

Sporotrichosis in the Highlands of Madagascar, 2013–2017¹

Tahinamandranto Rasamoelina, Danièle Maubon, Onivola Raharolahy, Harinjara Razanakoto, Njary Rakotozandrindrainy, Fetra Angelot Rakotomalala, Sébastien Bailly, Fandresena Sendrasoa, Irina Ranaivo, Malalaniaina Andrianarison, Benja Rakotonirina, Abel Andriantsimahavandy, Fahafahantsoa Rapelanoro Rabenja, Mala Rakoto Andrianarivelo, Lala Soavina Ramarozatovo, Muriel Cornet

Sporotrichosis is a saprozoontic fungal infection found mostly in tropical and subtropical areas. Few case reports in Madagascar have been published. To document sporotrichosis epidemiology in Madagascar, we conducted a cross-sectional study. During March 2013–June 2017, we recruited from select hospitals in Madagascar patients with chronic cutaneous lesions suggestive of dermatomycosis. Sporotrichosis was diagnosed for 63 (42.5%) of 148 patients. All but 1 patient came from the central highlands, where the prevalence was 0.21 cases/100,000 inhabitants. Frequency was high (64.7%) among patients <18 years of age. Sporotrichosis was diagnosed for 73.8% of patients with arm lesions, 32.3% with leg lesions, and 15.4% with lesions at other sites. Molecular identification identified 53 *Sporothrix schenckii* isolates. Among the 32 patients who were followed up, response to itraconazole was complete or major for 15 and minor for 17. Overall, endemicity of sporotrichosis in Madagascar was high, concentrated in the highlands.

Sporotrichosis is a chronic fungal infection of humans and animals, found mostly in tropical and subtropical regions. The causal fungi develop in the soil or on plants and infect mammals through wounds, either directly (wounds from spiky plants or thorns) or through contact with contaminated soil or infected animals. Thus, sporotrichosis is a

so-called implantation mycosis, affecting principally rural populations, particularly those who work with bare hands and feet (1–3). The disease is caused by a dimorphic fungus of the genus *Sporothrix*. These fungi display a high degree of genomic diversity, leading to the description of at least 6 cryptic species: *S. schenckii*, *S. brasiliensis*, *S. globosa*, *S. luriei*, *S. mexicana* and *S. albicans* (formerly *S. pallida*). *S. mexicana*, and *S. albicans* are mostly environmental (saprophytic and nonpathogenic) (4–7). The infection generally occurs as a lymphocutaneous form with an ulcerated subcutaneous nodule at the inoculation site and similar secondary lesions arising along the lymphatic route (1,5). Mucosal or primary pulmonary forms are less common (8). Some cases occur as disseminated forms with multiorgan involvement, most notably in HIV-infected persons (9,10).

Sporotrichosis is widespread throughout the world; several areas of known hyperendemicity are Brazil, Mexico, Peru, and China. Outbreaks from various environmental sources, involving thousands of persons, have been reported (1–3,11,12). In Brazil, a large zoonotic outbreak associated with cats is ongoing; it has been suggested that a strain of *S. brasiliensis* with enhanced virulence is involved (13–15).

In Madagascar, no epidemiologic data are available for evaluation of the sporotrichosis burden. Dermatologists and infectious disease specialists have reported encountering a large number of suspected cases during their routine medical consultations; however, the cases have not been biologically confirmed. In 2007, the dermatology department of Antananarivo University Hospital in the capital of Antananarivo confirmed a series of cases and reported 1 case (16). Since 2013, we conducted a cross-sectional study to document the current epidemiology of this fungal infection in Madagascar. To diagnose, confirm, and identify the fungal species responsible, we used conventional mycology and molecular biology methods, including matrix-assisted laser desorption/ionization-time of flight (MALDI-TOF) mass spectrometry. We describe the

Author affiliations: Centre d'Infectiologie Charles Mérieux, Université d'Antananarivo, Antananarivo, Madagascar (T. Rasamoelina, F.A. Rakotomalala, M.R. Andrianarivelo); University Grenoble Alpes, Grenoble, France (D. Maubon, S. Bailly, M. Cornet); Unité de Soins de Formation et de Recherche, Centre Hospitalier Universitaire Joseph Raseta Befelatanana, Antananarivo (O. Raharolahy, H. Razanakoto, F. Sendrasoa, I. Ranaivo, M. Andrianarison, F.R. Rabenja, L.S. Ramarozatovo); Unité Para-clinique de Formation et de Recherche, Centre Hospitalier Universitaire Joseph Ravoahangy, Antananarivo (N. Rakotozandrindrainy); Université d'Antananarivo, Antananarivo (B. Rakotonirina, A. Andriantsimahavandy); Pavillon Spécial A Centre Hospitalier Universitaire de Befelatanana, Antananarivo (L.S. Ramarozatovo)

DOI: <https://doi.org/10.3201/eid2509.190700>

¹Preliminary results from this study were presented at the 20th ISHAM Conference; June 29–July 5, 2018; Amsterdam, the Netherlands (abstract no. S1.4d).

average annual prevalence and clinical presentation of sporotrichosis in Madagascar, along with patient outcomes. We also report the species-level identification, genetic relatedness, and antifungal susceptibility of the clinical isolates.

Materials and Methods

Study Design and Patient Recruitment

We performed a cross-sectional study of patients with clinically suspected sporotrichosis or another chronic dermatomycosis (i.e., unique or multiple nodular, budding, wart-like, or plaque-like skin lesions following a lymphatic vessel, with or without ulceration, enduring for >1 month). Patients were recruited during March 2013–June 2017 (4 years and 3 months, hereafter referred to as a 4-year period) from the

Dermatology Department of the Joseph Raseta Befelatanana University Hospital (CHUJRB) in Antananarivo or during advanced consultation campaigns in regional hospitals (Figure 1, panel A). These campaigns were preceded by announcements made via radio, social media, and posters that invited patients with cutaneous or subcutaneous lesions to come to these consultations. Healthcare providers completed clinical and demographic information forms that asked about the patient's age, sex, and occupation; the probable area of contamination; anatomic location and appearance of the lesions; and treatments received. We excluded from the study 2 patients for whom this information could not be obtained. The study was approved by the Ethics Committee for Biomedical Research of the Ministry of Public Health of Madagascar (authorization no. 66-MSANP/CE). After sampling,

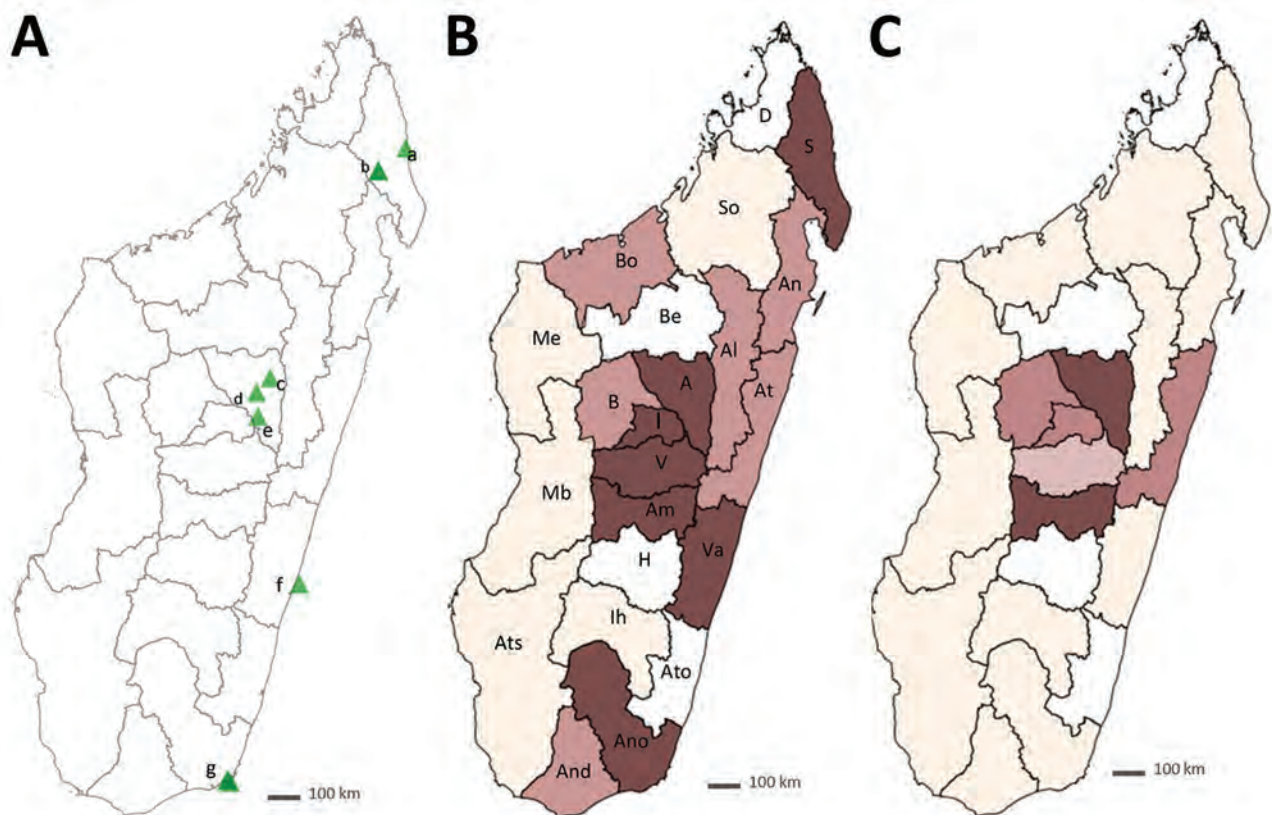


Figure 1. Recruitment of patients with chronic cutaneous and subcutaneous lesions and annual prevalence of sporotrichosis, Madagascar, March 2013–June 2017. A) Recruitment sites. Sava Region: a) Centre Hospitalier de Référence Régionale, Sambava District; b) Centre Hospitalier de District and Hôpital Adventiste, Andapa District; Analamanga Region: c) Centre de Santé de Base, Alakamisy-Anjozorobe, Anjozorobe District; d) Centre Hospitalier Universitaire Joseph Ravoahangy Befelatanana, Antananarivo District; e) Centre de Santé de Base, Andramasina District; Vatovavy Fitovinany Region; f) Fondation Médicale Ampasimanjeva, Manakara District; Anosy Region: g) Centre Médical Tolagnaro, Centre Hospitalier de Référence Régionale, Tolagnaro and Hôpital Luthérien Manambaro, Tolagnaro District. B) Patients' region of origin, from north to south: D, Diana; S, Sava; I, Itasy; A, Analamanga; V, Vakinankaratra; B, Bongolava; So, Sofia; Bo, Boeny; Be, Betsiboka; Me, Melaky; Al, Alaotra-Mangoro; At, Atsinanana; An, Analanjirofo; Am, Amoron'i Mania; H, Haute Matsiatra; Va, Vatovavy-Fitovinany; Ato, Atsimo; Ih, Ihorombe; Mb, Menabe; Ats, Atsimo Andrefana; And, Androy; Ano, Anôsy. Number of patients recruited: dark brown, $n > 6$; medium brown, $n = 3-5$; beige, $n < 3$; white, missing. Black outlines indicate regional boundaries. C) Annual prevalence of sporotrichosis, showing origins of the 63 sporotrichosis patients described in this study. Prevalence per 100,000 inhabitants: dark brown, > 0.2 ; medium brown, $0-0.2$; light brown, < 0.1 ; beige, 0 ; white, missing. Black outlines indicate regional boundaries.

treatment (200 mg/d of itraconazole) was provided free of charge to all recruited patients for at least 2 months.

Statistical Methods

We compared sporotrichosis cases and other nonsporotrichosis cases by using χ^2 or Fisher exact tests for qualitative variables and Student *t* tests for quantitative variables and a χ^2 test for trend to compare annual frequencies. We estimated the average annual prevalence as the mean number of cases per year (considering the period as a 4-year period) over the mean number of inhabitants. The mean number of inhabitants was calculated from the available figures in 2013 (obtained from the National Institute of Statistics of Madagascar, <https://www.instat.mg>) and adjusted according to the estimate of the World Bank for demographic growth of 2.7% per year (<https://donnees.banquemondiale.org/indicateur/SP.POP.GROW>). In our evaluation of the prevalence in the highlands of Madagascar, we excluded the region of Haute Matsiatra because no patients were

recruited from there. We analyzed data and generated maps by using EpiInfo version 7.2.2.1 (<https://www.cdc.gov/epiinfo/index.html>) and RStudio version 1.0.153 (<https://www.r-project.org>).

Case Definitions

We used a list of clinical, mycologic, histologic, and prognostic criteria to classify cases in this study (Table 1). Cases were identified after a monthly consultation among clinicians of the Department of Dermatology of the CHU-JRB and teams of mycologists from the Charles Mérieux Infectiology Center of Antananarivo, Madagascar, and Université Grenoble Alpes, Grenoble, France.

Clinical Samples

After obtaining patient consent, we collected specimens consisting of biopsy material, pus, or flakes of skin from all patients. All samples were sent to the laboratory of the Charles Mérieux Infectiology Center of Antananarivo,

Table 1. Criteria used to classify cases of sporotrichosis in the Highlands of Madagascar, 2013–2017*

Criteria	Description
Clinical	
Major	Cutaneous: lymphocutaneous form defined as a papule or pustule or a subcutaneous nodule at the inoculation site, then ulceration with erythematous edges and purulent secretion. Secondary lesions arise along the path of regional lymphatic vessels. Fixed or cutaneously disseminated.
Minor	Extracutaneous: disseminated, osteoarticular, ocular. Mucosal: nasal septum, with bloody secretions and detachment of crusts. Conjunctivitis, with granulomatous lesions accompanied by a serous-purulent discharge, redness, lid edema, and preauricular and submandibular lymph node enlargement. Primary pulmonary sporotrichosis: similar to that of tuberculosis. Radiologic patterns include cavitory disease, tracheobronchial lymph node enlargement, and nodular lesions. Vegetative, verrucous, infiltrated plaque, or tuberculous lesion.
Mycologic and histologic	
Major	Molecular evidence of <i>Sporothrix schenckii</i> on PCR with specific primers (targeting topoisomerase II) or ITS sequencing, directly from clinical samples or from a positive culture of a fungus morphologically suggestive of <i>Sporothrix</i> spp. MALDI-TOF mass spectrometry identification of <i>S. schenckii</i> from a positive culture of a fungus morphologically suggestive of <i>Sporothrix</i> spp.
Minor	Budding yeast cells with the characteristic cigar-shaped buds observed on direct microscopic examination or histologic analysis. Direct examination of pus and/or histologic analysis showing asteroid bodies (Splendore-Hoeppli reaction). Positive culture of a fungus morphologically suggestive of <i>Sporothrix</i> spp. from a clinical sample without molecular or MALDI-TOF mass spectrometry confirmation.
Classification	
Confirmed	≥ 1 of the major clinical criteria and ≥ 1 of the major mycologic criteria or 1 minor clinical criterion and ≥ 1 of the major mycologic criteria.
Probable	≥ 1 of the major clinical criteria and 1 minor mycologic or histologic criterion and a complete or partial response to antifungal therapy.
Possible	≥ 1 of the major clinical criteria without any (major or minor) mycologic or histologic criteria or ≥ 1 of the minor clinical criteria without any (major or minor) mycologic or histologic criteria and a complete or partial response to antifungal therapy.
Clinical response to antifungal therapy	
Cure	Complete resolution of all lesions.
Major response	Substantial improvement of most lesions with a substantial decrease in subcutaneous nodules.
Minor response	Mild improvement of most lesions with a smaller decrease in subcutaneous nodules than for a major response.
Failure	Stabilization of the lesions after ≥ 3 months of antifungal therapy or worsening of the lesions after ≥ 3 months of antifungal therapy.

*ITS, internal transcribed spacer; MALDI-TOF, matrix-assisted laser desorption/ionization time-of-flight.

where they were processed either immediately or after 24 to 48 hours of storage at 2°–8°C.

Mycologic Analyses

We directly examined the clinical specimens under a microscope (5,11). The samples were used to inoculate Sabouraud medium supplemented with chloramphenicol and incubated at 30°C for 2–3 weeks. For positive cultures, we identified the fungal isolates morphologically, extracted DNA, and froze the culture at –80°C.

Molecular Analyses

We used the QIAamp DNA Blood Mini Kit (<https://www.qiagen.com>) according to the manufacturer's instructions for DNA purification. Colonies and biopsies were crushed before processing. PCR amplification was performed in 2 steps. The first step comprised 2 panfungal PCRs targeting internal transcribed spacer (ITS) regions with the primers ITS1/ITS4 and D1D2 with the primers NL-1/NL-4 and NL-3/NL-4 (17–19). The second step was a specific *S. schenckii* PCR targeting the topoisomerase II gene with SSHF31/SSHR97 primers (20). We sequenced panfungal PCR products by LGC Genomics GmbH (<https://www.biotech.com>) by using the same primers and aligned the sequences obtained with the reference sequences in the International Society of Human and Animal Mycology (ISHAM) Barcoding Database (<http://its.mycology-lab.org>) (17) for the ITS region and the National Center for Biotechnology Information database for the D1D2 and ITS regions. We constructed the phylogenetic tree by using MEGA7 software (<https://www.megasoftware.net>).

MALDI-TOF Mass Spectrometry Analysis

We created a main spectrum profile (MSP) in-house *Sporothrix* library on the Microflex mass spectrometer, according to the MALDI Biotyper version 1.1 MSP creation protocol (Bruker Daltonics, <https://www.bruker.com>) from a reference strain of *S. schenckii* (IHEM 3787) and 18 isolates formally identified by DNA sequencing or the specific *S. schenckii* topoisomerase II PCR. We cultured isolates under 3 conditions: in Sabouraud–chloramphenicol agar for 4–7 days at 30°C, in liquid Sabouraud medium for 2–4 days at 25–30°C with shaking, and on solid peptone dextrose agar (YPD; Sigma Aldrich, <https://www.sigmaaldrich.com>) for 4–5 days at 30°C. This library was validated with the IHEM 3774 reference strain and 35 clinical strains obtained during this study but not used to create the MSPs. We used the ethanol formic acid extraction procedure on YPD subcultured strains in accordance with the MALDI BiotyperIVD protocol version 1.6. We compared the spectra obtained with the Bruker Taxonomy (7,815 entries), Bruker Filamentous Fungi (364 MSP), NIH mold (365 profiles) (21), and our new MSP in-house *Sporothrix* library,

generating identification scores with the following quality criteria: score ≥ 2 , species-level identification; score ≤ 1.7 to < 2 , genus-level identification; score < 1.7 , no identification. In addition, we applied an external control by submitting both our MSP in-house *Sporothrix* and identification spectra to an independent online database, MSI (<https://msi.happy-dev.fr>). This database contains reference spectra for *S. schenckii*, *S. brasiliensis*, *S. urviconia*, *S. fungorum*, *S. globosa*, *S. humicola*, *S. inflata*, *S. insectorum*, *S. pallida*, *S. stenoceras*, and *S. varicibatus* (22).

Susceptibility to Antifungal Drugs

To determine the MICs of antifungal agents, we used the Clinical and Laboratory Standards Institute (<https://clsi.org>) protocol for filamentous fungi on mycelial strains after subculture at 30°C (23). We tested the following agents at the concentrations indicated: posaconazole and isavuconazole (0.016 to 8 µg/mL), amphotericin B and itraconazole (0.006 to 32 µg/mL), and terbinafine (0.008 to 4 µg/mL). We determined MICs after 72 hours of culture at 30°C with a 100% inhibition endpoint for all drugs except terbinafine, for which the endpoint was 80%, as described by Espinel-Ingroff et al. (24).

Results

Demographic and Clinical Characteristics of the Patients

Total Cohort

During March 2013–June 2017, we recruited 148 patients with chronic cutaneous or subcutaneous lesions. Median patient age was 39 years (interquartile range 22–53 years). Male patients predominated ($n = 111$, 75%), and the largest number of patients ($n = 118$, 79.7%) was enrolled by CHU-JRB, the permanent recruitment center (Figure 1, panel A, triangle d). An analysis of the geographic origin of recruited patients showed that most ($n = 90$, 60.8%) came from the highlands, followed by the regions of the northeast ($n = 23$, 15.5%), east and southeast ($n = 16$, 10.8%), south and southwest ($n = 13$, 8.8%), and west ($n = 6$, 4.1%) (Figure 1, panel B). The largest proportion of recruited patients worked in agriculture ($n = 76$, 51.3%), followed by the service sector ($n = 31$, 21%); other patients were students ($n = 20$, 13.5%), craftsmen ($n = 14$, 9.5%), or unemployed ($n = 7$, 4.7%). Lesions were located mostly on the legs (62.8%) and arms (28.3%).

Patients with Sporotrichosis

At the first consultation, 47 of the 148 patients had clinically suspected sporotrichosis. A diagnosis of sporotrichosis was recognized for 63 (42.5%) patients, confirmed for 53 (35.8%), and possible for 10 (6.7%). The frequency of

sporotrichosis remained stable from 2013 through 2017 (37.5%–64%, $p = 0.16$; Table 2). From 2014 through 2016, the mean (\pm SD) number of annual sporotrichosis cases was 14 (± 5.1).

The male sex predominance was less marked among patients with sporotrichosis ($n = 44$, 69.8%) than among the other patients recruited. This difference, however, was not significant ($p = 0.29$) (Table 2).

Patients with sporotrichosis were younger than other patients (38 vs. 43 years of age), although this difference was not statistically significant ($p = 0.10$). Analysis by age group showed that this trend was linked to a high frequency of sporotrichosis in persons <18 years of age (64.7%) compared with the rest of the population (39.7%; $p = 0.08$).

The location of lesions differed significantly between sporotrichosis patients and other patients (Table 2). The principal site affected was the arms (49.2%) for patients with sporotrichosis. Sporotrichosis was diagnosed more frequently for patients with lesions on the arm (73.8%) than for patients with lesions on the leg (32.3%) or other

body sites (15.4%) ($p < 0.0001$; Table 2). The sporotrichosis lesions had been present for <1 year for 71% of patients, 1–2 years for 14.5% of patients, and >2 years for 14.5% of patients. The most frequent type of lesion for sporotrichosis patients was lymphocutaneous (69.3%). The other forms were characterized by vegetative or verrucous lesions, infiltrated plaques, or tuberculous lesions (Figure 2). We observed no fixed cutaneous forms or extracutaneous forms.

Sporotrichosis patients were predominantly farmers (52.4%), but a large number were craftsmen and tradesmen (Table 2). Sporotrichosis was diagnosed for 71.4% of the craftsmen and tradesmen and 39% of patients in other professions grouped together ($p = 0.04$).

Prevalence and Geographic Distribution of Sporotrichosis

We determined the geographic origin of patients with sporotrichosis, corresponding to the presumed origin of contamination (Figure 1, panel C). The concentration of sporotrichosis cases in the highlands was very high; almost

Table 2. Description of sporotrichosis cases in a cohort of patients with chronic cutaneous and subcutaneous lesions, Madagascar, March 2013–June 2017*

Characteristic	Sporotrichosis, no. (%), n = 63	Other, no. (%), n = 85	p value
Recruitment period			0.16†
2013, from March 1	6 (9.6)	10 (11.8)	
2014	16 (25.4)	12 (14.1)	
2015	21 (33.3)	26 (30.6)	
2016	13 (20.6)	23 (27.1)	
2017, until May 31	7 (11.1)	14 (16.4)	
Age range, y			0.2‡
3–18	11 (17.5)	6 (7.1)	
19–33	15 (23.8)	16 (18.8)	
34–48	17 (27.0)	30 (35.3)	
49–63	12 (19.1)	17 (20.0)	
64–80	8 (12.7)	16 (18.8)	
Sex			0.29‡
M	44 (69.8)	67 (78.8)	
F	19 (30.2)	18 (21.2)	
Lesion location			<0.0001‡
Leg	30 (47.6)	63 (74.2)	
Arm	31 (49.2)	11 (12.9)	
Other§	2 (3.2)	11 (12.9)	
Occupation			0.07‡
Farmer	33 (52.4)	43 (50.6)	
Service sector	8 (12.7)	23 (27.1)	
Student	9 (14.3)	11 (12.9)	
Craftsman/tradesman	10 (15.8)	4 (4.7)	
Unemployed	3 (4.8)	4 (4.7)	
Region of contamination			<0.0001‡
Highlands region			
Analamanga	38 (60.3)	18 (21.2)	
Amaron'i Mania	8 (12.7)	4 (4.7)	
Bongolava	3 (4.8)	0 (0)	
Itasy	6 (9.5)	3 (3.5)	
Vakinankaratra	7 (11.1)	3 (3.5)	
Other¶	1 (1.6)¶	57 (67.1)	

*Mean (\pm SD) ages: sporotrichosis patients 38.1 (± 19.5); other patients, 43.2 (± 18.1); $p = 0.10$ (Student t test p value to compare mean age between both groups).

† χ^2 test for trend.

‡ χ^2 or Fisher exact test to compare categorical variables between both groups.

§On trunk, leg and arm, or leg and thorax.

¶Localized to Atsinanana.

all patients with sporotrichosis ($n = 62$, 98.4%) originated from these areas. The frequency of sporotrichosis cases was much higher in the highlands (62/90, 68.9%) than on

the rest of the island (1/58, 1.7%; $p < 0.0001$). In all highland areas, the frequency of sporotrichosis was similar and very high (66.6%–100%; $p = 1.00$) (Table 2).

The average annual prevalence of sporotrichosis on the high plateaus of the Analamanga, Amoron'i Mania, Bongolava, Itasy, and Vakinankaratra regions was evaluated at 0.21 cases/100,000 inhabitants. Prevalence was highest in the Analamanga (0.27/100,000 inhabitants) and Amoron'i Mania (0.25/100,000 inhabitants) regions (Table 3; Figure 1, panel C).

Mycologic Results

We collected 192 samples from the 148 patients. Direct examination yielded negative results for all cases, and we were unable to perform histologic examinations (Appendix 1, <https://wwwnc.cdc.gov/EID/article/25/10/19-0700-App1.xlsx>).

Culture Results

We obtained 172 cultures, including 72 established with the samples of the 63 sporotrichosis patients. Overall, macroscopic and microscopic examination exhibited morphologic features consistent with *Sporothrix* spp. for 90.2% (65/72) of the cultures.

Molecular Results

Sensitivities for the 2 panfungal PCRs, for D1D2 and ITS, were lower for clinical specimens than for cultures, and the ITS PCR was less sensitive than the D1D2 PCR for clinical specimens and cultures (Appendix 2 Figure 1, <https://wwwnc.cdc.gov/EID/article/25/10/19-0700-App2.pdf>). The specific *S. schenckii* topoisomerase II PCR was unable to confirm identification for any of the clinical specimens, whereas its sensitivity for cultures was 89.2% (58/65), with features suggestive of *Sporothrix* spp.

The alignment of the ITS sequences from cultures identified 13 isolates as *S. schenckii*, according to data from the ISHAM database (Appendix 1 Table 1) (17). The phylogenetic analysis showed that the isolates from patients with sporotrichosis in our study were grouped in the *S. schenckii* clade, together with clinical strains from other regions of the world (Figure 3; Appendix 2 Figure 2). Our results confirm that ITS sequencing is suitable for separating the cryptic species of clinical importance from the strictly environmental ones (25).

The MSP in-house *Sporothrix* library performed well for *S. schenckii* identification; the score for 87.9% (29/33) of the strains was >2 and for 4 strains was >1.8 . Unfortunately, 2 strains were contaminated by *Candida* spp. and could not be identified. For sporotrichosis identification, in-house MSPs were systematically the first choice in the list of MSPs, confirming their superiority for identification at the species level over the 2 MSPs in the Bruker database



Figure 2. Clinical manifestations of sporotrichosis in patients with chronic cutaneous and subcutaneous lesions, Madagascar, March 2013–June 2017. A–C) Lymphocutaneous lesions. D) Lymphocutaneous ulcerative budding and crusty lesion. E) Ulceroerosive and erythematous lesion with irregular border, easily misdiagnosed as chromoblastomycosis.

Table 3. Prevalence of sporotrichosis in Madagascar, March 2013–June 2017

Region	Mean no. inhabitants/y*	No. cases, 2013–2017	Mean no. cases/y	Annual prevalence/100,000 inhabitants (95% CI)
North and North-Central: Analanjirofo, Sava, Sofia	3,443,999	0	0	0
Highlands	7,448,855	62	15.5	0.21 (0.2097–0.2103)
Analamanga	3,534,578	38	9.5	0.27 (0.2695–0.2705)
Amaron'i Mania	754,695	8	2.0	0.25 (0.2490–0.2510)
Bongolava	482,742	3	0.8	0.16 (0.1590–0.1610)
Itasy	773,490	6	1.5	0.17 (0.1692–0.1708)
Vakinankaratra	1,903,350	7	1.8	0.09 (0.0896–0.0904)
West: Melaky, Menabe, Boeny	1,774,661	0	0	0
East and Southeast	3,527,693	1	1.3	0.04 (0.0398–0.0402)
Alaotra Mangoro	1,084,092	0	0	0
Atsinanana	948,560	1	1.3	0.13 (0.1293–0.1307)
Vatovavy Fitovinany	1,495,041	0	0	0
South and Southwest: Androy, Anosy, Atsimo Andrefana, Ihorombe	3,203,165	0	0	0

*Mean over the period was calculated from the last figures available in 2013 adjusted for the subsequent years with a growth of 2.7% per year (World Bank estimates of the demographic growth in Madagascar, <https://donnees.banquemondiale.org/indicateur/SP.POP.GROW>).

and the 1 MSP in the NIH database. Comparison of the spectra obtained by using the MSP in-house *Sporothrix* library with those obtained from identification to the external MSI platform indicated that the most likely identification was *S. schenckii* (Appendix 1 Table 2). Percentages of similarities were consistent with accurate identification to the

species level ($\geq 20\%$) for 94.1% (48/51) (Appendix 1 Table 1); only 3 strains were not formally identified.

Taking together all results of the molecular analyses, we identified 53 *S. schenckii* strains: 51 by MALDI-TOF mass spectrometry, of which 46 were identified also by the specific *S. schenckii* topoisomerase II PCR and 13 were

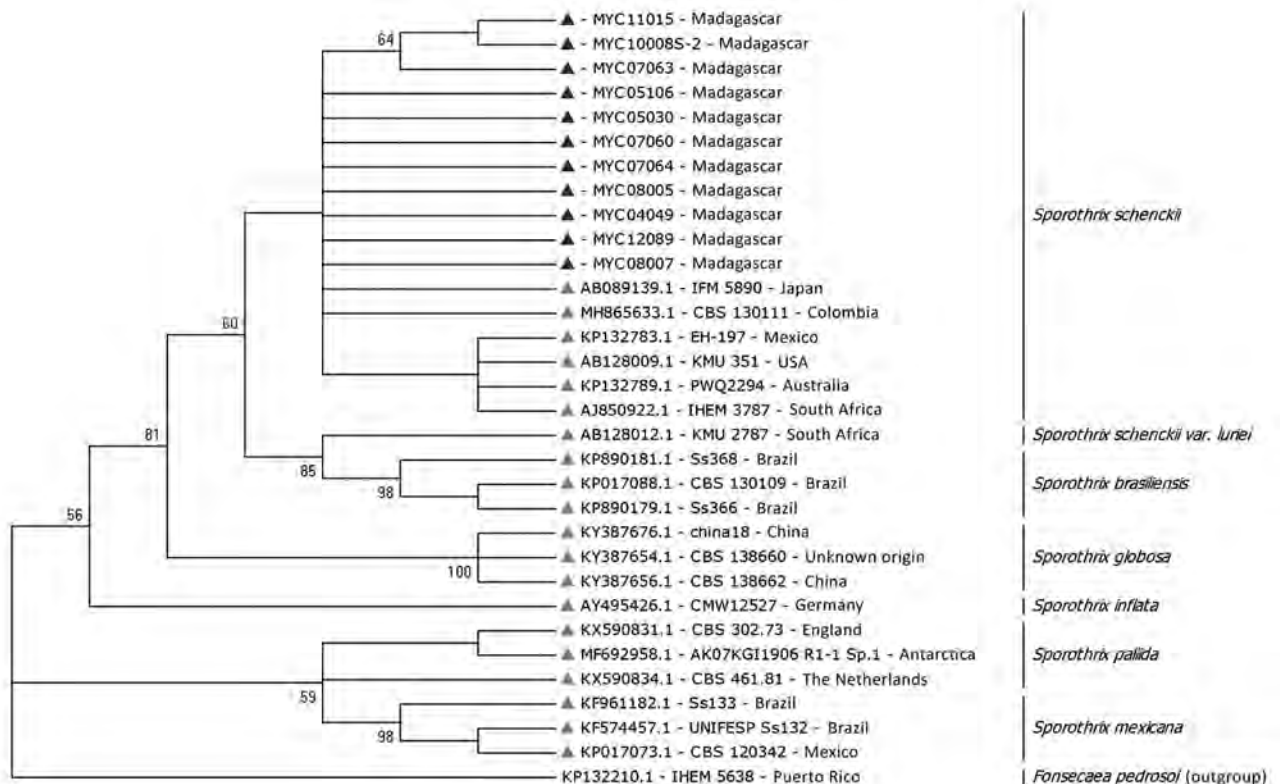


Figure 3. Phylogenetic tree of internal transcribed spacer sequences of *Sporothrix schenckii* isolates from patients with sporotrichosis, Madagascar, March 2013–June 2017 (black triangles), and reference isolates (gray triangles). *Fonsecaea pedrosoi* was considered to be out of group. The tree was built by using MEGA7.0 software (<https://www.megasoftware.net>) and applying the maximum-likelihood method based on the Kimura 2-parameter model (100 bootstrap replicates). Strains are detailed in Appendix 1 Table 1 (<https://wwwnc.cdc.gov/EID/article/25/10/19-0700-App1.xlsx>). GenBank accession numbers for isolates from this study: MYC11015, MK342563; MYC12089, MK342536; MYC10008-S2, MK342530; MYC08007, MK342562; MYC08005, MK342529; MYC07064, MK342535; MYC07063, MK342534; MYC07060, MK342533; MYC05106, MK342564; MYC05030, MK342531; MYC04049, MK249820.

Table 4. MICs of 5 antimicrobial drugs for 46 *Sporothrix schenckii* isolates in the mycelium phase, from patients in Madagascar, 2013–2017*

Drug	No. isolates with each MIC, $\mu\text{g/mL}$							MIC, $\mu\text{g/mL}$		
	<0.25	0.5	1	2	4	8	≥ 16	GM	50%	90%
Posaconazole	10	11	13	6	1	5	0	0.78	1	4
Isavuconazole	1	0	7	8	13	17	0	3.35	4	8
Amphotericin B	14	10	9	8	3	0	2	0.7	0.5	2
Itraconazole	4	10	12	6	9	2	3	1.43	1	4
Terbinafine	38	3	2	1	2	0	0	0.14	≤ 0.25	0.5

*MIC 50% and 90% represent the minimal concentrations of drug that inhibit the isolates by that percentage. GM, geometric mean.

identified also by ITS sequencing. The 2 contaminated isolates not identified by MALDI-TOF mass spectrometry were confirmed by the specific *S. schenckii* topoisomerase II PCR.

Susceptibility of *Sporothrix schenckii* to Antifungal Drugs and Patient Outcomes

A total of 46 *S. schenckii* isolates were culturable after thawing for MIC determination. We determined MICs and their geometric means for the 5 antifungal drugs tested (Table 4). Overall, of the *S. schenckii* isolates, the terbinafine MIC was low ($\leq 0.25 \mu\text{g/mL}$) for 82.3% (38/46), the itraconazole MIC was $\leq 1 \mu\text{g/mL}$ for 74% (34/46), and the posaconazole MIC was $\leq 1 \mu\text{g/mL}$ for 56.5% (26/46). However, 65% of strains had MICs $\geq 4 \mu\text{g/mL}$ for isavuconazole.

All 63 patients received treatment, but only 32 were monitored for >2 months after treatment began (23 with lymphocutaneous disease and 9 with minor forms of disease). Among those patients, the response was complete or major for 15 (47%) after 4–7 months of treatment and minor for 17 (53%) after prolonged (9 months) treatment. The remaining 31 patients received treatment for 2 months and then did not return for follow-up visits.

Discussion

This study provides recent epidemiologic data for sporotrichosis in Madagascar. We detected numerous cases and substantial endemicity despite previous reports of only sporadic cases or small series (16,26). We estimated an average annual prevalence in the highlands of 0.21 cases/100,000 inhabitants; 98% of the cases were concentrated in that area. Among sporotrichosis patients in Madagascar, we highlight the high infection risk for young persons (<18 years of age) and the particularly high frequency of lesions on the arms. On the basis of this study, we were able to develop and routinely implement molecular analyses in Madagascar, enabling positive identification of *S. schenckii* for all confirmed cases.

The high estimated prevalence (0.27 and 0.25/100,000 inhabitants) in 2 highland regions (Analamanga and Amoron'i Mania) reveals the high transmission rates in this part of the island. To date, the only published series of sporotrichosis cases in Madagascar have described disease-endemic foci in the highlands, particularly in the

Analamanga region (16), but the concentration of cases in the highlands that we observed was unexpected and striking. This almost exclusive distribution may be the result of climate conditions in this region, which differ from those on the rest of the island. This region has a tropical climate, with a mean temperature of 19.5°C and substantial rainfall, which probably favors development of fungi on plants and in the soil. A phylogeographic study focusing strictly on *S. schenckii* showed that this species was present in temperate (United States), hot and humid (South Africa, Australia, Colombia, and Venezuela), hot and dry (Australia and Uruguay), cool and dry (Peru and South Africa), and cool and humid (Uruguay) zones (27). Findings of that study therefore seem to go against the notion of a single climatic factor. The frequency of sporotrichosis in some areas of the island to the west and southwest are unknown because these areas were not investigated; thus, sporotrichosis may not be totally distributed in the highlands. In addition, some cases could have been missed because of our mode of study recruitment, the low incomes of people living in remote areas, and the limited development of the healthcare system. The concentration of sporotrichosis in the highlands is probably not the result of better access to healthcare facilities because patients with other diagnoses most frequently do not live in the highlands ($p < 0.0001$) (Table 2). However, better access to medical care in the highlands does partly explain the sporotrichosis diagnoses made relatively early in the course of disease (71% in the first year after onset).

Patients found it difficult to remember when their lesions had appeared and to associate them with a particular injury or activity; however, our survey revealed considerable involvement in rural activities: farming (rice, cassava, corn), logging, trade, and craftsmanship. Not only artisans are exposed to contamination through manual work; tradespeople are also exposed because they practice activities other than selling for living. Contamination by activities associated with the manual production of charcoal and cutting wood for cooking and heating seems likely on the basis of the predominance of arm lesions, the concentration of the disease in the coldest region of the island, and the high frequency of infections among children (who practice these activities). In northeastern China, a risk associated with the use of

wood or other fuel has been proposed as an explanation for transmission patterns (28); the authors of that study thought that contamination occurred via maize stalks (where *S. globosa* has been found) used for heating and cooking. They hypothesized that the fermentation of the plants promotes the development of yeast forms of the fungus, increasing the risk for contamination during transport and storage at home.

Other possible sources of contamination, such as soil or decaying plant material, are also possible in Madagascar. Neither we nor J.F. Carod et al. (16) observed any cases of zoonotic transmission; the identification of *S. schenckii* alone confirms the hypothesis of contamination by soil and plants.

The molecular methods that we developed in this study, including MALDI-TOF mass spectrometry, made it possible to confirm cases and to identify the species responsible (21,29). We found that it was easier to amplify the D1D2 domain (LSU) and that the amplicons obtained were easier to analyze by sequencing than were those of the ITS domain. However, the availability of a database with many verified ITS sequences and the more polymorphic and discriminant nature of these sequences makes them more suitable for cryptic species identification and phylogenetic analysis (17,25).

We added a rapid and inexpensive mass spectrometry identification approach to the molecular tools for identifying *S. schenckii* to the cryptic species level. Our results obtained by using a Bruker instrument confirm previous analyses performed with a Shimadzu instrument (29). The MSP in-house *Sporothrix* library yielded better *S. schenckii* identification scores than did the 3 preexisting MSPs. The excellent identification scores and the external validation with another mass spectrometry platform showed that *S. schenckii* identification at the species level with MALDI-TOF mass spectrometry is accurate and adapted for routine diagnoses in clinical laboratories.

In conclusion, our study reveals substantial endemicity of sporotrichosis in Madagascar. Sporotrichosis was particularly concentrated in the highlands, which have climate, vegetation, and lifestyle conditions that favor the development and transmission of the fungus. Using molecular methods and MALDI-TOF mass spectrometry, we were able to identify *S. schenckii* as the species responsible for sporotrichosis in Madagascar. Despite its high frequency, sporotrichosis remains neglected in Madagascar.

This work was supported by the Fondation Mérieux, Lyon, France; the Institut de Recherche pour le Développement; the Société Française de Mycologie Médicale; and Campus France.

M.C. received research grants from Pfizer and travel grants from Basilea, Gilead, MSD, and Pfizer.

About the Author

Dr. Rasamoelina is a scientist in the Centre d'Infectiologie Charles Mérieux in Antananarivo, Madagascar. His research interest is the laboratory diagnosis of tropical mycoses.

References

- Barros MBL, de Almeida Paes R, Schubach AO. *Sporothrix schenckii* and sporotrichosis. *Clin Microbiol Rev*. 2011;24:633–54. <https://doi.org/10.1128/CMR.00007-11>
- Queiroz-Telles F, Fahal AH, Falci DR, Caceres DH, Chiller T, Pasqualotto AC. Neglected endemic mycoses. *Lancet Infect Dis*. 2017;17:e367–77. [https://doi.org/10.1016/S1473-3099\(17\)30306-7](https://doi.org/10.1016/S1473-3099(17)30306-7)
- Chakrabarti A, Bonifaz A, Gutierrez-Galhardo MC, Mochizuki T, Li S. Global epidemiology of sporotrichosis. *Med Mycol*. 2015;53:3–14. <https://doi.org/10.1093/mmy/myu062>
- Marimon R, Cano J, Gené J, Sutton DA, Kawasaki M, Guarro J. *Sporothrix brasiliensis*, *S. globosa*, and *S. mexicana*, three new *Sporothrix* species of clinical interest. *J Clin Microbiol*. 2007;45:3198–206. <https://doi.org/10.1128/JCM.00808-07>
- Buot G, Develoux M, Hennequin C. Sporotrichose. *Encycl Méd Chir*. 2017;14:1–10.
- Mora-Montes HM, Dantas AS, Trujillo-Esquivel E, de Souza Baptista AR, Lopes-Bezerra LM. Current progress in the biology of members of the *Sporothrix schenckii* complex following the genomic era. *FEMS Yeast Res*. 2015;15:fov065. <https://doi.org/10.1093/femsyr/fov065>
- Lopes-Bezerra LM, Mora-Montes HM, Zhang Y, Nino-Vega G, Rodrigues AM, de Camargo ZP, et al. Sporotrichosis between 1898 and 2017: the evolution of knowledge on a changeable disease and on emerging etiological agents. *Med Mycol*. 2018;56(suppl 1): 126–43. <https://doi.org/10.1093/mmy/myx103>
- Rojas FD, Fernández MS, Lucchelli JM, Lombardi D, Malet J, Vetrivano ME, et al. Cavitary pulmonary sporotrichosis: case report and literature review. *Mycopathologia*. 2017;182:1119–23. <https://doi.org/10.1007/s11046-017-0197-6>
- Freitas D, Lima MA, de Almeida-Paes R, Lamas CC, do Valle AC, Oliveira MM, et al. Sporotrichosis in the central nervous system caused by *Sporothrix brasiliensis*. *Clin Infect Dis*. 2015;61:663–4. <https://doi.org/10.1093/cid/civ361>
- de Oliveira-Esteves ICMR, Almeida Rosa da Silva G, Eyer-Silva WA, Basílio-de-Oliveira RP, de Araujo LF, Martins CJ, et al. Rapidly progressive disseminated sporotrichosis as the first presentation of HIV infection in a patient with a very low CD4 cell count. *Case Rep Infect Dis*. 2017;2017:4713140. <https://doi.org/10.1155/2017/4713140>
- Rasamoelina T, Raharolahy O, Rakotozandrindrainy N, Ranaivo I, Andrianarison M, Rakotonirina B, et al. Chromoblastomycosis and sporotrichosis, two endemic but neglected fungal infections in Madagascar. *J Mycol Med*. 2017; 27:312–24. <https://doi.org/10.1016/j.mycmed.2017.08.003>
- Ramírez Soto MC. Sporotrichosis among children of a hyperendemic area in Peru: an 8-year retrospective study. *Int J Dermatol*. 2017;56:868–72. <https://doi.org/10.1111/ijd.13643>
- Rodrigues AM, de Melo Teixeira M, de Hoog GS, Schubach TM, Pereira SA, Fernandes GF, et al. Phylogenetic analysis reveals a high prevalence of *Sporothrix brasiliensis* in feline sporotrichosis outbreaks. *PLoS Negl Trop Dis*. 2013;7:e2281. <https://doi.org/10.1371/journal.pntd.0002281>
- Rodrigues AM, de Hoog GS, de Camargo ZP. *Sporothrix* species causing outbreaks in animals and humans driven by animal-animal transmission. *PLoS Pathog*. 2016;12:e1005638. <https://doi.org/10.1371/journal.ppat.1005638>
- Gremião ID, Miranda LH, Reis EG, Rodrigues AM, Pereira SA. Zoonotic epidemic of sporotrichosis: cat to human transmission.

- PLoS Pathog. 2017;13:e1006077. <https://doi.org/10.1371/journal.ppat.1006077>
16. Carod JF, Ramarozatovo L, Randrianasolo P, Ratsima E, Randrianirina F, Rapelanoro FR. Cutaneous sporotrichosis in a Malagasy patient [in French]. *Med Trop (Mars)*. 2007;67:18.
 17. Irinyi L, Lackner M, de Hoog GS, Meyer W. DNA barcoding of fungi causing infections in humans and animals. *Fungal Biol*. 2016;120:125–36. <https://doi.org/10.1016/j.funbio.2015.04.007>
 18. Kurtzman CP, Robnett CJ. Identification of clinically important ascomycetous yeasts based on nucleotide divergence in the 5' end of the large-subunit (26S) ribosomal DNA gene. *J Clin Microbiol*. 1997;35:1216–23.
 19. Abliz P, Fukushima K, Takizawa K, Nishimura K. Identification of pathogenic dematiaceous fungi and related taxa based on large subunit ribosomal DNA D1/D2 domain sequence analysis. *FEMS Immunol Med Microbiol*. 2004;40:41–9. [https://doi.org/10.1016/S0928-8244\(03\)00275-X](https://doi.org/10.1016/S0928-8244(03)00275-X)
 20. Kanbe T, Natsume L, Goto I, Kawasaki M, Mochizuki T, Ishizaki H, et al. Rapid and specific identification of *Sporothrix schenckii* by PCR targeting the DNA topoisomerase II gene. *J Dermatol Sci*. 2005;38:99–106. <https://doi.org/10.1016/j.jdermsci.2004.12.024>
 21. Lau AF, Drake SK, Calhoun LB, Henderson CM, Zelazny AM. Development of a clinically comprehensive database and a simple procedure for identification of molds from solid media by matrix-assisted laser desorption ionization–time of flight mass spectrometry. *J Clin Microbiol*. 2013;51:828–34. <https://doi.org/10.1128/JCM.02852-12>
 22. Normand AC, Becker P, Gabriel F, Cassagne C, Accoceberry I, Gari-Toussaint M, et al. Validation of a new Web application for identification of fungi by use of matrix-assisted laser desorption ionization–time of flight mass spectrometry. *J Clin Microbiol*. 2017;55:2661–70. <https://doi.org/10.1128/JCM.00263-17>
 23. Clinical and Laboratory Standards Institute. Reference method for broth dilution antifungal susceptibility testing of filamentous fungi; approved standard (document M38–A2). Wayne (PA): The Institute; 2008.
 24. Espinel-Ingroff A, Abreu DPB, Almeida-Paes R, Brilhante RSN, Chakrabarti A, Chowdhary A, et al. Multicenter, international study of MIC/MEC distributions for definition of epidemiological cutoff values for *Sporothrix* species identified by molecular methods. *Antimicrob Agents Chemother*. 2017;61:e01057-17. <https://doi.org/10.1128/AAC.01057-17>
 25. Zhou X, Rodrigues AM, Feng P, de Hoog GS. Global ITS diversity in the *Sporothrix schenckii* complex. *Fungal Divers*. 2014;66:153–65.
 26. Rapelanoro-Rabenja F, Ralandison S, Ramarozatovo L, Randrianasolo F, Ratriamoarivony C. Sporotrichose à Madagascar: une pathologie méconnue. *Nouvelles Dermatologiques*. 2007;26:10.
 27. Zhang Y, Hagen F, Stielow B, Rodrigues AM, Samerpitak K, Zhou X, et al. Phylogeography and evolutionary patterns in *Sporothrix* spanning more than 14 000 human and animal case reports. *Persoonia*. 2015;35:1–20. <https://doi.org/10.3767/003158515X687416>
 28. Li S, Cui Y, Yao L, Song Y. *Sporothrix globosa* causing sporotrichosis in Jilin Province (Northeast of China): prevalence, molecular characterization, and antifungal susceptibility. Abstract presented at the 20th Congress of the International Society for Human and Animal Mycology; Amsterdam, the Netherlands; 2018 Jun 30–Jul 4. Oxford: Oxford University Press; 2018. p. S19.
 29. Oliveira MM, Santos C, Sampaio P, Romeo O, Almeida-Paes R, Pais C, et al. Development and optimization of a new MALDI-TOF protocol for identification of the *Sporothrix* species complex. *Res Microbiol*. 2015;166:102–10. <https://doi.org/10.1016/j.resmic.2014.12.008>

Address for correspondence: Muriel Cornet, Domaine de la Merci, Laboratoire TIMC-IMAG équipe TheREX, 38706 La Tronche CEDEX, France; email: mcornet@chu-grenoble.fr

EID Podcast Developing Biological Reference Materials to Prepare for Epidemics



Having standard biological reference materials, such as antigens and antibodies, is crucial for developing comparable research across international institutions. However, the process of developing a standard can be long and difficult.

In this EID podcast, Dr. Tommy Rampling, a clinician and academic fellow at the Hospital for Tropical Diseases and University College in London, explains the intricacies behind the development and distribution of biological reference materials.

Visit our website to listen:
<https://go.usa.gov/xyfJX>

**EMERGING
INFECTIOUS DISEASES®**

Serologic Evidence of Exposure to Highly Pathogenic Avian Influenza H5 Viruses in Migratory Shorebirds, Australia

Michelle Wille, Simeon Lisovski, Alice Risely, Marta Ferenczi, David Roshier, Frank Y.K. Wong, Andrew C. Breed, Marcel Klaassen, Aeron C. Hurt

Highly pathogenic avian influenza (HPAI) H5Nx viruses of the goose/Guangdong/96 lineage continue to cause outbreaks in poultry and wild birds globally. Shorebirds, known reservoirs of avian influenza viruses, migrate from Siberia to Australia along the East-Asian-Australasian Flyway. We examined whether migrating shorebirds spending nonbreeding seasons in Australia were exposed to HPAI H5 viruses. We compared those findings with those for a resident duck species. We screened >1,500 blood samples for nucleoprotein antibodies and tested positive samples for specific antibodies against 7 HPAI H5 virus antigens and 2 low pathogenicity avian influenza H5 virus antigens. We demonstrated the presence of hemagglutinin inhibitory antibodies against HPAI H5 virus clade 2.3.4.4 in the red-necked stint (*Calidris ruficollis*). We did not find hemagglutinin inhibitory antibodies in resident Pacific black ducks (*Anas superciliosa*). Our study highlights the potential role of long-distance migratory shorebirds in intercontinental spread of HPAI H5 viruses.

Highly pathogenic avian influenza (HPAI) A(H5N1) viruses of the goose/Guangdong (gs/GD) lineage emerged in domestic birds in China in 1996, causing high morbidity and mortality rates in poultry; subsequent zoonotic spillover in 1997 caused fatal human infections (1,2). HPAI H5N1 virus reemerged in 2005 and subsequently spread throughout Asia, Europe, and Africa, becoming endemic in parts of Asia and Africa and causing economic

losses and human fatalities (3,4). The role of wild birds in the spread of HPAI H5N1 virus is uncertain, but they probably were not the main culprits in virus spread before 2014 (3–5). In 2014, and again in 2016, gs/GD lineage HPAI H5Nx virus clade 2.3.4.4 emerged and rapidly spread with wild birds from Asia to Europe, Africa, and North America (6–9). Unlike other lineages, these 2.3.4.4 clade viruses might cause low morbidity and mortality rates in wild birds, enabling their rapid intercontinental spread through bird migration (8,10,11). Asia, Europe, and Africa continue to report outbreaks of HPAI H5 viruses (10). Thus far, Australia, South America, and Antarctica remain free from gs/GD lineage viruses.

Unlike HPAI viruses, low pathogenicity avian influenza (LPAI) A viruses are part of the natural virodiversity of wild birds. Diverse subtypes and lineages circulate globally, causing no or limited clinical signs of disease (12–14). Waterfowl (Anseriformes), shorebirds, and gulls (Charadriiformes) are natural reservoirs of LPAI viruses, which have been detected in >100 wild bird species to date.

Natural annual cycles of migratory birds can contribute to the global and rapid spread of gs/GD lineage clade 2.3.4.4 when birds move from northern breeding grounds and spend nonbreeding periods in southern latitudes (8). Outbreaks of HPAI H5 virus clade 2.3.4.4 in wild birds and poultry reflect spatial patterns of bird migration, particularly waterfowl migration (8,10). Australia is part of the East-Asian-Australasian Flyway, and ≈8 million individual birds from 50 shorebird species migrate to the continent each year (15–17). In addition to Australia, birds in this flyway have stopover sites along the coast of East Asia and breed in Siberia (17).

Shorebirds are involved in the epidemiology of LPAI viruses, particularly in amplifying viruses, as occurred in Delaware Bay, NJ, USA (18), but prevalence is generally low and their role in long-distance movement of avian influenza virus (AIV) is unknown (19–22). One hypothesis

Author Affiliations: World Health Organization Collaborating Centre for Reference and Research on Influenza, Melbourne, Victoria, Australia (M. Wille, A.C. Hurt); Deakin University, Geelong, Victoria, Australia (S. Lisovski, A. Risely, M. Ferenczi, D. Roshier, M. Klaassen); Commonwealth Scientific and Industrial Research Organisation, Australian Animal Health Laboratory, Geelong (F.Y.K. Wong); Department of Agriculture and Water Resources, Canberra, Capital Territory, Australia (A.C. Breed); University of Queensland, St. Lucia, Queensland, Australia (A.C. Breed)

DOI: <https://doi.org/10.3201/eid2510.190699>

is that shorebirds play a limited role in AIV epidemiology and long-distance dispersal, explaining the absence of gs/GD lineage HPAI H5 viruses on the continent of Australia. In contrast to shorebirds, waterfowl in Australia are largely nomadic species that do not migrate outside the Australian-Papuan zone (23).

We examined whether long-distance shorebird migrants were exposed to gs/GD lineage viruses. We used the red-necked stint (*Calidris ruficollis*), which uses Australia as a nonbreeding area, as a model migratory species. The red-necked stint has known stopover locations in East and Southeast Asia, where HPAI virus is endemic. We contrasted findings from red-necked stints with those from the resident Pacific black duck (*Anas superciliosa*), a nonmigratory dabbling duck believed to be a natural reservoir for LPAI virus in Australia.

Materials and Methods

Ethics Statement

We received study approval from Deakin University Animal Ethics Committee under permit nos. A113-2010, B37-2013, and B43-2016; and from the Wildlife Ethics Committee of South Australia under permit nos. 2011/1, 2012/35, and 2013/11. The Australian Bird Banding Scheme approved catching and banding procedures under authority nos. 2915, 8000, and 8001. We obtained fauna and research permits from all relevant jurisdictions. The University of Melbourne Biochemistry & Molecular Biology, Dental Science, Medicine, Microbiology & Immunology, and Surgery Animal Ethics Committee approved ferret infections in accordance with the National Health and Medical Research Council code of practice for the care and use of animals for scientific purposes under project license no. 1714183.

Species and Sample Collection

We targeted mixed flocks of shorebirds for capture with cannon nets as part of a long-term ringing scheme. Since 2011, these birds also have been used for avian influenza surveillance (24). Red-necked stints consistently are captured in large numbers during October–March each year, predominantly in the state of Victoria. We also opportunistically collected samples from Western Australia, Northern Territory, and Queensland as part of ringing expeditions. Samples from these locations are not central to the long-term avian influenza surveillance project. Because the red-necked stint is in Australia during October–March, we analyzed and reported data for this species by using the austral summer season. We captured resident Pacific black ducks by using either baited funnel walk-in traps (25) or mist nets. We deployed walk-in traps on shorelines and baited them with a seed mix. We set these traps before dawn and

operated them during the day; at night, we left traps open so birds could enter and leave freely. To capture waterbirds at night, we erected mist nets on poles above the water surface. We collected most samples from the state of Victoria but also collected samples from South Australia and New South Wales.

After capture, we individually banded all birds with a metal ring with a unique identifier and collected ≤ 200 μL of blood from the brachial vein by using the Microvette 200 Z (Sarstedt, <https://www.sarstedt.com>) capillary blood collection system. We released all birds after banding and collecting blood samples. We stored blood samples at 4°C–8°C until we separated serum by centrifugation 12–24 hours after sampling. We collected 1,531 serum samples from red-necked stints and 394 serum samples from Pacific black ducks for this study.

General AIV Immunity

We screened serum samples for nucleoprotein (NP) antibodies to ascertain general AIV seroprevalence. We assessed NP antibodies by using a commercially available ELISA, MultiS-Screen Avian Influenza Virus Antibody Test Kit (IDEXX, <https://www.idexx.com>), following the manufacturer's recommendations, where a sample/negative (S/N) ratio of <0.5 indicates a positive result. We considered S/N ratios of 0.5–0.6 inconclusive, although this ratio has been demonstrated to correspond to antibody presence in wild birds (26,27). We calculated seroprevalence and 95% CI by using the `bioconf()` function of the `Hmisc` package in R 3.5.1 (<https://www.r-project.org>).

Hemagglutinin Inhibition Assay

After NP antibody screening, we assayed positive and inconclusive serum samples for H5 antibodies by using a hemagglutinin inhibition (HI) assay with 1% vol/vol chicken erythrocytes. We selected 7 contemporary HPAI H5 viruses from different gs/GD lineage clades and 2 LPAI H5 viruses endemic to Australia as antigens (Table). We could only test up to 8 antigens per sample because we could collect only a small volume of serum from red-necked stints; for some samples, we could only test against 4 relevant viruses.

We selected representative H5 viral lineages because of their known spatial and temporal distribution and availability of reference viral antigens, such as those selected by the World Health Organization (WHO) as candidate vaccine viruses (CVVs; http://www.who.int/influenza/vaccines/virus/candidates_reagents/a_h5n1/en/) for pandemic preparedness. WHO's CVVs are 6:2 recombinant viruses on an A/Puerto Rico/8/1934(H1N1)(PR8) backbone with the multibasic cleavage site removed. The 2 LPAI H5 viruses from Australia were gamma-irradiated antigens. We conducted a hemagglutinin assay on selected antigens to

Table. Antigens used to assess exposure of red-necked stints and Pacific black ducks to highly pathogenic avian influenza H5 viruses, Australia*

H5 virus clade†	Strain
HPAI	
1.1.1	A/Cambodia/X0810301/2013(H5N1)
2.1.3.2a	A/Indonesia/NIHRD11771/2011(H5N1)
2.3.2.1b	A/barn swallow/Hong Kong/D10-1161/2010(H5N1)
2.3.2.1c	A/duck/Vietnam/NCVD-1584/2012(H5N1)
2.3.4.2	A/Guizhou/1/2013(H5N1)
2.3.4.4	A/gyrfalcon/Washington/41088-6/2014(H5N8)
2.3.4.4	A/Hubei/29578/2016(H5N6)
LPAI H5	
	A/duck/Victoria/0305-2/2012(H5N3)
	A/wild bird/Queensland/P17-14428-30-01/2017(H5N1)‡

*All HPAI virus strains were 6:2 recombinant viruses on a PR8 backbone with the multi-basic cleavage site removed. All LPAI strains were gamma-irradiated. HPAI, highly pathogenic avian influenza; LPAI, low pathogenicity avian influenza.

†Clade notation as defined by World Health Organization/World Organization for Animal Health/Food and Agriculture Organization H5N1 Evolution Working Group (28).

‡Only used for hemagglutinin inhibition assays for serum samples from Pacific black ducks.

determine virus titer, which we then added to HI plates at a dilution of 4 hemagglutinin units. We treated all NP-positive ELISA field samples with a *Vibrio cholerae* receptor-destroying enzyme (RDE II; Denka Seiken Co., <https://denka-seiken.com>), then inactivated samples with 1.5% sodium citrate.

We raised control antiserum against all virus antigens, except the LPAI viruses A/duck/Victoria/0305-2/2012(H5N3) and A/wild bird/Queensland/P17-14428-30-01/2017(H5N1), in 6–18-month-old ferrets. In brief, we inoculated ferrets intranasally with 1 mL of virus; at 14 days postexposure, we boosted ferrets by intramuscular delivery of a concentrated dose of the same virus into the hind leg; and at 21 days postexposure, we collected a terminal blood sample. We monitored ferrets' weights,

temperatures, and clinical signs throughout. We used antibodies for all 7 H5 viruses in each assay to measure both homologous titers and cross reaction; we also ran antibodies without virus to assess nonspecific agglutination. We serially diluted all serum samples across assay plates, starting with a titer of 1:20, and calculated specificity of antigen-antibody agglutination (Appendix Table 1, <http://wwwnc.cdc.gov/EID/article/25/10/19-0699-App1.pdf>).

Results

Population Immunity to AIVs

During 2011–2018, we collected 1,531 serum samples from red-necked stints, ≈200 samples per year, most from Victoria. Overall, 20% of red-necked stints were seropositive for NP antibodies, with variations among collection years and locations (Figure 1, panel A; Appendix Table 2).

We collected 394 blood samples from Pacific black ducks during 2011–2018. Temporal structure of the data for this species was more variable, with few samples collected during 2015–2017 (Appendix Table 3). We only collected samples from the southeastern states of Australia. Overall, ≈55% of Pacific black ducks sampled were seropositive for NP antibodies. We experienced some variation across sampling events, but average seropositivity was similar across locations (Figure 1, panel B).

Differences in Exposure to HPAI H5 Virus in Migratory and Resident Birds

We assayed 307 NP ELISA-positive or -inconclusive serum samples from red-necked stints and 240 from Pacific black ducks for antibodies against H5 viruses by HI assay (Appendix Tables 2, 3). Of HI-positive serum samples, ≈12% were inconclusive by NP ELISA. Because of the small volume of serum collected from red-necked stints,

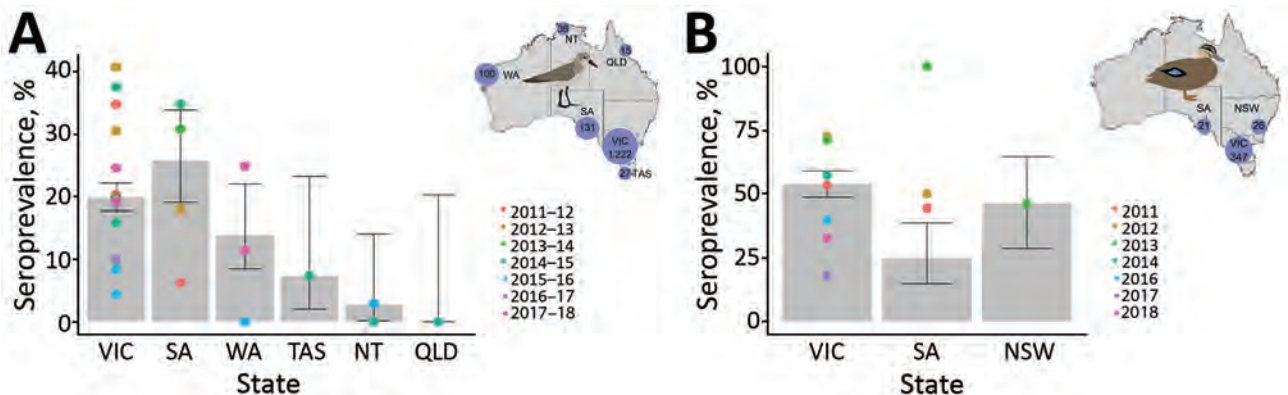


Figure 1. Seroprevalence for nucleoprotein antibodies in red-necked stints and Pacific black ducks, Australia, 2011–2018. A) For red-necked stints, year represents the austral summer period, October–April, when this species has a migratory nonbreeding stopover in Australia. B) For Pacific black duck, year represents calendar year. (No samples were collected in 2015.) Inset maps show the number of samples collected from each species in each state over the course of this study. Error bars represent seroprevalence 95% CIs for each state across all years; color dots represent estimates of seroprevalence at each sampling occasion. NSW, New South Wales; NT, Northern Territory; QLD, Queensland; SA, South Australia; TAS, Tasmania; VIC, Victoria; WA, Western Australia.

we could assay only 33 serum samples for ≤ 4 antigens each (Appendix Table 2). Nonetheless, 23 red-necked stint serum samples contained detectable HI antibodies against ≥ 1 of the 7 HPAI H5 virus antigens tested (1.5%, 95% CI 1.0%–2.3%) (Figure 2 panel A). We detected HI antibodies against antigens belonging to clade 2.3.4–derived lineages, specifically 2.3.4.2 A/Guizhou/1/2013(H5N1) ($n = 10$); 2.3.4.4 A/gyrfalcon/Washington/41088-6/2014(H5N8) ($n = 8$); and 2.3.4.4 A/Hubei/29578/2016(H5N6) ($n = 5$). We detected antibodies against A/Guizhou/1/2013(H5N1) during each sampling season, with the exception of birds captured during the 2012–13 austral summer. We detected antibodies against 2.3.4.4 A/gyrfalcon/Washington/41088-6/2014(H5N8) from the 2014–15 austral summer through the 2016–17 austral summer. We also detected antibodies against 2.3.4.4 A/Hubei/29578/2016(H5N6) in samples from the 2016–17 austral summer and the subsequent austral summer. The presence of antibodies against these 2 HPAI virus lineages corresponds with reported circulation of these lineages in Eurasia (Figure 2, panel A). Across all seasons, prevalence of HPAI H5 virus HI antibodies varied from 0.7%–2.1%, with the exception of 2016–17, when 4.5% (95% CI 2.1%–9%) of serum samples contained HI antibodies against HPAI H5Nx virus (Appendix Table 2).

Overall, HI titers were low; 9/23 serum samples had an HI titer of 20 and 14/23 an HI titer of 40. One serum sample had HI antibodies against the LP AI H5 virus A/duck/Victoria/0305-2/2012(H5N3) (Figure 2, panel A). Overall,

no red-necked stint samples were positive for both HPAI and LP AI virus antigens.

Of the 240 Pacific black duck serum samples used for HI assays, none had detectable HI antibodies against any of the HPAI H5 virus antigens (Figure 2, panel B; Appendix Table 3). However, 16 (6%) of the NP–positive serum samples contained HI antibodies that reacted with LP AI H5 virus A/duck/Victoria/0305-2/2012(H5N3), of which 2 samples also had HI antibodies that reacted with LP AI A/wild bird/Queensland/P17-14428-30-01/2017(H5N1) virus (Figure 2, panel B).

Discussion

Despite intercontinental spread of gs/GD lineage HPAI H5Nx viruses from Asia to Europe, Africa, and North America, we have no evidence that incursions of these viruses have occurred in Australia. A leading hypothesis for the lack of incursion is the absence of Anseriformes birds migrating between Asia and Australia (23,29). However, millions of shorebirds that are reservoirs for AIV migrate from Siberia to Australia, with stopover sites along the coast of East Asia (15–17,29). We demonstrated that these intercontinental migratory birds have been exposed to gs/GD lineage HPAI H5Nx viruses and have the potential to bring these viruses into Australia. The absence of HI antibodies against gs/GD lineage HPAI H5Nx viruses in a widespread and abundant Anseriformes birds in Australia and the lack of detection

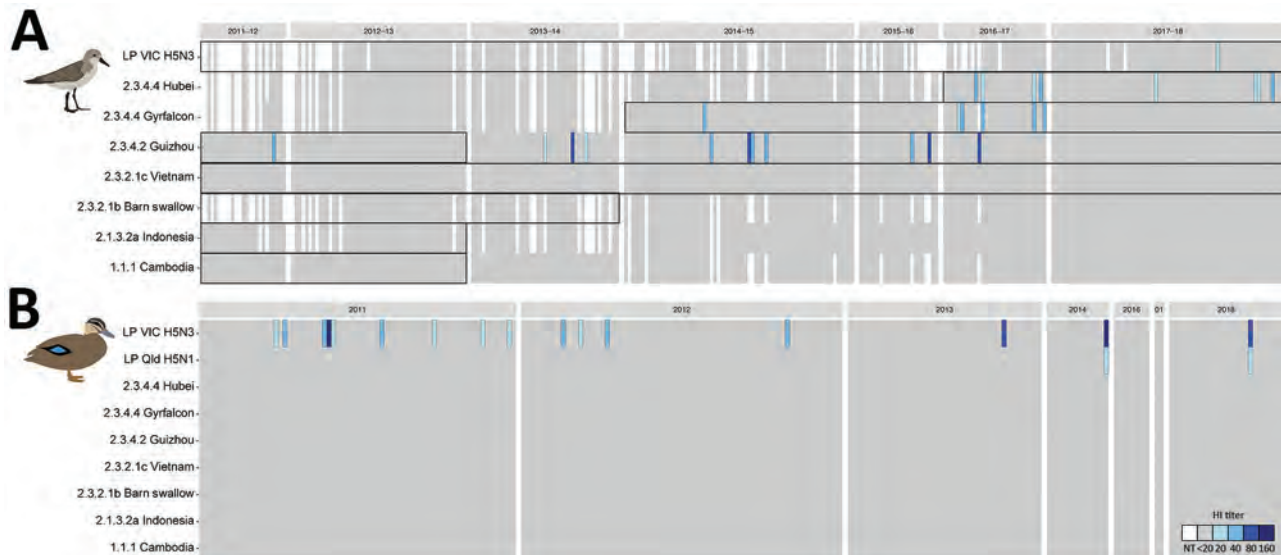


Figure 2. Avian influenza H5 virus hemagglutinin inhibition (HI) antibody patterns, Australia, 2011–2018. A) For red-necked stint, year represents the austral summer period, October–April, when this species has a migratory nonbreeding stopover in Australia. Boxes represent periods of circulation for each strain’s lineage, as determined by genomic sequences (Appendix Table 4, <https://wwwnc.cdc.gov/EID/article/25/10/19-0699-App1.pdf>). B) For Pacific black duck, year represents calendar year. White indicates untested serum samples; gray indicates a titer <20, the starting titer for this assay; blue indicates hemagglutinin inhibition (HI) antibodies, and shades vary depending on HI titer (20–160). Sample numbers are ordered by collection year and sequentially from left to right in the order in which individual birds were caught. Antigens used in this study are on the y-axis, and abbreviated with relevant clade information; full strain names are available in the Table. NT, no titer. Greater detail on positive samples appears in Appendix Figure 1.

during ongoing surveillance activities (12) suggest that a virus incursion has not occurred yet.

Overall, red-necked stints we sampled had low prevalence ($\approx 20\%$) of NP antibodies, and 1.5% of all serum samples contained HI antibodies against gs/GD lineage HPAI H5Nx virus antigen. We detected the highest seroprevalence of gs/GD lineage HPAI H5Nx virus HI antibodies, 4.5% of all serum samples collected, during the 2016–17 austral summer. A previous study in northwestern Australia during 1992–2009 showed that the red-necked stint and other members of the Scolopacidae family had higher AI virus seroprevalence than other shorebird species tested. Furthermore, H5 HI antibodies were common; 31/260 NP ELISA–positive serum samples had HI titers against HPAI H5N1 virus clade 1 A/chicken/Vietnam/8/2004 (21). Similarly, serum samples from ducks during this period also had HI antibodies against this clade but not HPAI H5N1 clade 2 viruses (21,30). One explanation for the lack of evidence for circulation of HPAI H5N1 virus clade 1 during this time is that exposure to endemic H5 virus strains in Australia produces HI antibodies with broad serologic cross-reactivity (24,31).

We found no evidence of cross-reactivity in control antibodies (Appendix Table 1) or cross-reaction in any positive serum samples, including no cross-reactivity between LPAI and HPAI virus antigens. Furthermore, the clades we detected HI antibodies against, 2.3.4.2 and particularly 2.3.4.4, are antigenically distant from previously circulating H5 viruses (32), so LPAI virus cross-reactivity is unlikely. Long-distance migratory shorebirds captured in Australia could have been exposed to HPAI H5 virus in the northern hemisphere. Indeed, a red-necked stint tested positive for HPAI H5N6 virus in Hong Kong in 2016 on its southward migration (pers. comm.), strengthening evidence of gs/GD H5Nx virus exposure in this species.

Studies of ducks in Europe and Mongolia provide further perspective. Gilbert et al. demonstrated the presence of HI antibodies against gs/GD lineage HPAI H5N1 virus in waterfowl in Mongolia. These birds had higher serologic reactivity to HPAI H5 virus than to LPAI H5 virus antigens. That study found limited or no evidence of exposure to HPAI virus antigens in a small representation of waterfowl in Europe (31). However, Gilbert et al. conducted the study before the reemergence of gs/GD HPAI virus in Europe. In 2016, Poen et al. demonstrated that 4.2% of birds they surveyed in Europe had HI antibodies against 2.3.4.4 HPAI H5Nx viruses, with much higher prevalence in some species: up to 33% in the mute swan (*Cygnus olor*) and lesser white-fronted goose (*Anser erythropus*) (33). Hill et al. reported 80% of mute swans had HI antibodies against HPAI H5N8 virus after several AI outbreaks at a swannery in the United Kingdom (34).

The prevalence of HI antibodies we detected in red-necked stints during the 2016–17 season were comparable to those reported in ducks in Europe, even though red-necked stints have a much lower seroprevalence of AIV in general. Some studies suggest that long-lived avian species, such as swans and seabirds, retain HI antibodies over the course of many years, which could enable expansion of antibody breadth, increasing the number of subtypes against which these birds have antibodies over time (35,36). An additive effect could explain why mute swans maintained high rates of HPAI H5N8 virus HI antibodies after AIV outbreaks in the United Kingdom (34). In contrast, ducks are believed to have relatively poor immune memory and to retain HI antibodies only briefly (37,38). The expected antibody longevity patterns in shorebirds such as the red-necked stint is unknown, but given the relatively high prevalence of HI antibodies, particularly during 2016–17, we hypothesize that shorebirds retain antibodies longer than ducks. We saw generally low HI titers in serum samples from red-necked stints; 82% of serum samples with detectable HI antibodies had titers <40 . Gilbert et al. also reported low titers and hypothesized that tested waterfowl were exposed months or years previously (31). Alternatively, the antigens might not have matched the antibodies tested.

Waterfowl species comprise the bulk of avian species sampled in most surveillance schemes for avian influenza and are sampled heavily for H5Nx viruses (33,39). Shorebirds are central to the ecology of AIV (13) but are tested rarely beyond the study from Delaware Bay, NJ, USA, and infection prevalence is much lower (18–22) than in waterfowl (13). However, virology and serology data from Delaware Bay suggest both ruddy turnstones (*Actinukya interpres*) and red knots (*Calidris canutus*) are exposed to a large diversity of hemagglutinin subtypes, and $\leq 36\%$ of birds tested had neutralizing antibodies against multiple subtypes, demonstrating host competency (40). Furthermore, migratory shorebirds have been implicated in the long-distance movement of LPAI viruses (41). Experimental studies have shown limited morbidity and mortality rates associated with infection of some 2.3.4.4 subclades in ducks, demonstrating their ability to act as migratory vectors for these viruses (11,42–45).

Our understanding of infection and pathogenesis of HPAI H5Nx virus in shorebirds is extremely limited. Experimental exposure of dunlins (*Calidris alpina*) and ruddy turnstones to HPAI H5N1 virus clade 2.2 resulted in contrasting outcomes (46,47). Immunologically naive dunlins showed clinical signs of infection, and 19/20 birds receiving high or mild doses of the virus died. Birds inoculated with low doses did not get infected (46). Ruddy turnstones, in contrast, were not immunologically naive, none died, and birds infected with LPAI and HPAI had similar patterns of viral shedding (47). The authors attribute

the contrasting results between dunlins and ruddy turnstones to the immunological status of birds, suggesting that cross-immunity played a key role in limiting clinical disease (47,48). In these experiments, infection rates were the same between birds that were seropositive (subtype unknown) before capture, were first exposed to a LPAI H5 virus strain, or were first exposed to an H7 virus strain, suggesting both homosubtypic and heterosubtypic immunity could play a role in protection (47,48). However, in ducks, phylogenetic distance between hemagglutinin subtypes plays a role in the degree of the heterosubtypic protective response (49), and closely related hemagglutinin subtypes likely drive protection. Red knots were more susceptible to acquiring HPAI H5N1 virus, especially clade 2.2.1, and shed higher viral titers before the onset of clinical disease during the migratory phase because of increased plasma corticosterone (50). The authors saw no difference in susceptibility to disease between birds in premigration, fueling, or migratory phases and suggested that, assuming no effect of subclinical exposure on the likelihood of migratory takeoff, red knots could spread HPAI H5 virus through migration (50). These studies demonstrate shorebirds could be exposed, survive infection, and potentially disperse HPAI H5 virus over long distances during their migratory phase.

In conclusion, we demonstrated that the long-distance migratory red-necked stint, which spends nonbreeding seasons in Australia, has been exposed to HPAI H5 virus clade 2.3.4.4. We did not detect antibodies against this or other HPAI viruses in our sample of resident Pacific black ducks, suggesting exposure has not occurred in Australia. However, our study highlights the potential for migratory shorebirds to spread HPAI H5 viruses, which should inform future avian influenza surveillance.

Acknowledgments

We thank volunteers from the Victorian Wader Study Group, Field and Game Australia (Geelong), and members of the Centre for Integrative Ecology at Deakin University for assistance in sampling birds in Australia and members from Melbourne Water, Innamincka Station, Gidgealpa Station, and Innamincka Regional Reserve for logistical support. We thank Celeste Tai and Chris Durrant for assistance in raising avian influenza antibodies in ferrets.

Sampling was supported by grants from the National Institutes of Health, National Institute of Allergy and Infectious Diseases (no. HHSN266200700010C), Australian Research Council (nos. DP 130101935 and DP160102146), and the Australian Government Department of Agriculture and Water Resources as part of its Agricultural Competitiveness White Paper (no. 4-85JCR12). The AgriBio Centre, Agriculture Victoria Research, and the Biosecurity Sciences Laboratory of the Department of Agriculture and Fisheries, Queensland, Australia,

collected samples for low pathogenic avian influenza virus antigens under the National Avian Influenza Wild Bird surveillance program.

The Australian Commonwealth Government Department of Health provided funds to the World Health Organization Collaborating Centre for Reference and Research on Influenza. The Department of Agriculture and Water Resources and the National Collaborative Research Infrastructure Strategy provided support to the Australian Animal Health Laboratory Facility.

About the Author

Dr. Wille is a postdoctoral researcher at the World Health Organization Collaborating Centre for Reference and Research on Influenza, Melbourne, Victoria, Australia. Her research interests include avian virus ecology, with a focus on avian influenza A virus.

References

1. Guan Y, Peiris JSM, Lipatov AS, Ellis TM, Dyrting KC, Krauss S, et al. Emergence of multiple genotypes of H5N1 avian influenza viruses in Hong Kong SAR. *Proc Natl Acad Sci U S A*. 2002;99:8950–5. <https://doi.org/10.1073/pnas.132268999>
2. Xu X, Subbarao, Cox NJ, Guo Y. Genetic characterization of the pathogenic influenza A/Goose/Guangdong/1/96 (H5N1) virus: similarity of its hemagglutinin gene to those of H5N1 viruses from the 1997 outbreaks in Hong Kong. *Virology*. 1999;261:15–9. <https://doi.org/10.1006/viro.1999.9820>
3. Chen H, Smith GJD, Zhang SY, Qin K, Wang J, Li KS, et al. H5N1 virus outbreak in migratory waterfowl. *Nature*. 2005;436:191–2. <https://doi.org/10.1038/nature03974>
4. Liu J, Xiao H, Lei F, Zhu Q, Qin K, Zhang XW, et al. Highly pathogenic H5N1 influenza virus infection in migratory birds. *Science*. 2005;309:1206. <https://doi.org/10.1126/science.1115273>
5. Feare CJ. Role of wild birds in the spread of highly pathogenic avian influenza virus H5N1 and implications for global surveillance. *Avian Dis*. 2010;54(Suppl):201–12. <https://doi.org/10.1637/8766-033109-ResNote.1>
6. Lee YJ, Kang HM, Lee EK, Song BM, Jeong J, Kwon YK, et al. Novel reassortant influenza A(H5N8) viruses, South Korea, 2014. *Emerg Infect Dis*. 2014;20:1087–9. <https://doi.org/10.3201/eid2006.140233>
7. Global Consortium for H5N8 and Related Influenza Viruses. Role for migratory wild birds in the global spread of avian influenza H5N8. *Science*. 2016;354:213–7. <https://doi.org/10.1126/science.aaf8852>
8. Verhagen JH, Herfst S, Fouchier RAM. How a virus travels the world. *Science*. 2015;347:616–7. <https://doi.org/10.1126/science.aaa6724>
9. Bevens SN, Dusek RJ, White CL, Gidlewski T, Bodenstien B, Mansfield KG, et al. Widespread detection of highly pathogenic H5 influenza viruses in wild birds from the Pacific Flyway of the United States. *Sci Rep*. 2016;6:222:616–7. <https://doi.org/10.1038/srep28980>
10. Bodewes R, Kuiken T. Changing role of wild birds in the epidemiology of avian influenza A viruses. *Adv Virus Res*. 2018;100:279–307. <https://doi.org/10.1016/bs.aivir.2017.10.007>
11. Pantin-Jackwood MJ, Costa-Hurtado M, Bertran K, DeJesus E, Smith D, Swayne DE. Infectivity, transmission and pathogenicity of H5 highly pathogenic avian influenza clade 2.3.4.4 (H5N8 and H5N2) United States index viruses in Pekin ducks and

- Chinese geese. *Vet Res.* 2017;48:33. <https://doi.org/10.1186/s13567-017-0435-4>
12. Grillo VL, Arzey KE, Hansbro PM, Hurt AC, Warner S, Bergfeld J, et al. Avian influenza in Australia: a summary of 5 years of wild bird surveillance. *Aust Vet J.* 2015;93:387–93. <https://doi.org/10.1111/avj.12379>
 13. Olsen B, Munster VJ, Wallensten A, Waldenström J, Osterhaus ADME, Fouchier RAM. Global patterns of influenza A virus in wild birds. *Science.* 2006;312:384–8. <https://doi.org/10.1126/science.1122438>
 14. Kuiken T. Is low pathogenic avian influenza virus virulent for wild waterbirds? *Proc Bio Sci.* 2013;280(1763):20130990. <https://doi.org/10.1098/rspb.2013.0990>
 15. Clemens RS, Kendall BE, Guillet J, Fuller RA. Review of Australian shorebird survey data, with notes on their suitability for comprehensive population trend analysis. *Stilt.* 2012;62:3–17.
 16. Studts CE, Kendall BE, Murray NJ, Wilson HB, Rogers DI, Clemens RS, et al. Rapid population decline in migratory shorebirds relying on Yellow Sea tidal mudflats as stopover sites. *Nat Commun.* 2017;8:14895. <https://doi.org/10.1038/ncomms14895>
 17. Minton C, Wahl J, Gibbs H, Jessop R, Hassell C, Boyle A. Recoveries and flag sightings of waders which spend the non-breeding season in Australia. *Stilt.* 2011;50:17–43.
 18. Krauss S, Stallknecht DE, Negovetich NJ, Niles LJ, Webby RJ, Webster RG. Coincident ruddy turnstone migration and horseshoe crab spawning creates an ecological ‘hot spot’ for influenza viruses. *Proc Biol Sci.* 2010;277(1699):3373–9. <https://doi.org/10.1098/rspb.2010.1090>
 19. Winker K, Spackman E, Swayne DE. Rarity of influenza A virus in spring shorebirds, southern Alaska. *Emerg Infect Dis.* 2008;14:1314–6. <https://doi.org/10.3201/eid1408.080083>
 20. Hanson BA, Luttrell MP, Goekjian VH, Niles L, Swayne DE, Senne DA, et al. Is the occurrence of avian influenza virus in Charadriiformes species and location dependent? *J Wildl Dis.* 2008;44:351–61. <https://doi.org/10.7589/0090-3558-44.2.351>
 21. Curran JM, Ellis TM, Robertson ID. Surveillance of Charadriiformes in northern Australia shows species variations in exposure to avian influenza virus and suggests negligible virus prevalence. *Avian Dis.* 2014;58:199–204. <https://doi.org/10.1637/10634-080913>
 22. Iverson SA, Takekawa JY, Schwarzbach S, Cardona CJ, Warnock N, Bishop MA, et al. Low prevalence of avian influenza virus in shorebirds on the Pacific Coast of North America. *Waterbirds.* 2008;31:602–10. <https://doi.org/10.1675/1524-4695-31.4.602>
 23. McCallum HI, Roshier DA, Tracey JP, Joseph L, Heinsohn R. Will Wallace’s line save Australia from avian influenza? *Ecol and Soc.* 2008;13:41.
 24. Ferenczi M, Beckmann C, Warner S, Loyn R, O’Riley K, Wang X, et al. Avian influenza infection dynamics under variable climatic conditions, viral prevalence is rainfall driven in waterfowl from temperate, south-east Australia. *Vet Res.* 2016;47:23. <https://doi.org/10.1186/s13567-016-0308-2>
 25. McNally J, Falconer DD. Trapping and banding operations Lara Lake. *Emu.* 1953;53:51–70. <https://doi.org/10.1071/MU953051>
 26. Brown JD, Stallknecht DE, Berghaus RD, Luttrell MP, Velek K, Kistler W, et al. Evaluation of a commercial blocking enzyme-linked immunosorbent assay to detect avian influenza virus antibodies in multiple experimentally infected avian species. *Clin Vaccine Immunol.* 2009;16:824–9. <https://doi.org/10.1128/CVI.00084-09>
 27. Shriner SA, VanDalen KK, Root JJ, Sullivan HJ. Evaluation and optimization of a commercial blocking ELISA for detecting antibodies to influenza A virus for research and surveillance of mallards. *J Virol Methods.* 2016;228:130–4. <https://doi.org/10.1016/j.jviromet.2015.11.021>
 28. World Health Organization/World Organisation for Animal Health/Food and Agriculture Organization (WHO/OIE/FAO) H5N1 Evolution Working Group. Revised and updated nomenclature for highly pathogenic avian influenza A (H5N1) viruses. *Influenza Other Respir Viruses.* 2014;8:384–8. <https://doi.org/10.1111/irv.12230>
 29. Tracey JP, Woods R, Roshier D, West P, Saunders GR. The role of wild birds in the transmission of avian influenza for Australia: an ecological perspective. *Emu.* 2004;104:109–24. <https://doi.org/10.1071/MU04017>
 30. Curran JM, Ellis TM, Robertson ID. Serological surveillance of wild waterfowl in Northern Australia for avian influenza virus shows variations in prevalence and a cyclical periodicity of infection. *Avian Dis.* 2015;59:492–7. <https://doi.org/10.1637/11113-043015-Reg>
 31. Gilbert M, Koel BF, Bestebroer TM, Lewis NS, Smith DJ, Fouchier RAM. Serological evidence for non-lethal exposures of Mongolian wild birds to highly pathogenic avian influenza H5N1 virus. *PLoS One.* 2014;9:e113569. <https://doi.org/10.1371/journal.pone.0113569>
 32. World Health Organization. Antigenic and genetic characteristics of zoonotic influenza viruses and development of candidate vaccine viruses for pandemic preparedness. 2019 Feb 21 [cited 2019 May 16]. https://www.who.int/influenza/vaccines/virus/201902_zoonotic_vaccinevirusupdate.pdf?ua=1
 33. Poen MJ, Verhagen JH, Manvell RJ, Brown I, Bestebroer TM, van der Vliet S, et al. Lack of virological and serological evidence for continued circulation of highly pathogenic avian influenza H5N8 virus in wild birds in the Netherlands, 14 November 2014 to 31 January 2016. *Euro Surveill.* 2016;21:e30349. <https://doi.org/10.2807/1560-7917.ES.2016.21.38.30349>
 34. Hill SC, Hansen R, Watson S, Coward V, Russell C, Cooper J, et al. Comparative micro-epidemiology of pathogenic avian influenza virus outbreaks in a wild bird population. *Philos Trans R Soc Lond B Biol Sci.* 2019;374:e20180259. <https://doi.org/10.1098/rstb.2018.0259>
 35. Hill SC, Manvell RJ, Schulenburg B, Shell W, Wikramaratna PS, Perrins C, et al. Antibody responses to avian influenza viruses in wild birds broaden with age. *Proc Biol Sci.* 2016;283(1845). <https://doi.org/10.1098/rspb.2016.2159>
 36. Ramos R, Garnier R, González-Solís J, Boulinier T. Long antibody persistence and transgenerational transfer of immunity in a long-lived vertebrate. *Am Nat.* 2014;184:764–76. <https://doi.org/10.1086/678400>
 37. Wille M, Latorre-Margalef N, Tolf C, Stallknecht DE, Waldenström J. No evidence for homosubtypic immunity of influenza H3 in Mallards following vaccination in a natural experimental system. *Mol Ecol.* 2017;26:1420–31. <https://doi.org/10.1111/mec.13967>
 38. Magor KE. Immunoglobulin genetics and antibody responses to influenza in ducks. *Dev Comp Immunol.* 2011;35:1008–17. <https://doi.org/10.1016/j.dci.2011.02.011>
 39. Poen MJ, Bestebroer TM, Vuong O, Scheuer RD, van der Jeugd HP, Kleyheeg E, et al. Local amplification of highly pathogenic avian influenza H5N8 viruses in wild birds in the Netherlands, 2016 to 2017. *Euro Surveill.* 2018;23. <https://doi.org/10.2807/1560-7917.ES.2018.23.4.17-00449>
 40. Bahnsen CS, Poulson RL, Krauss S, Webster RG, Stallknecht DE. Neutralizing antibodies to type A influenza viruses in shorebirds at Delaware Bay, New Jersey, USA. *J Wildl Dis.* 2018;54:708–15. <https://doi.org/10.7589/2017-10-252>
 41. de Araujo J, de Azevedo Júnior SM, Gaidet N, Hurtado RF, Walker D, Thomazelli LM, et al. Avian influenza virus (H1N9) in migratory shorebirds wintering in the Amazon Region, Brazil. *PLoS One.* 2014;9:e110141. <https://doi.org/10.1371/journal.pone.0110141>

42. Kwon JH, Lee DH, Swayne DE, Noh JY, Yuk SS, Jeong S, et al. Experimental infection of H5N1 and H5N8 highly pathogenic avian influenza viruses in Northern Pintail (*Anas acuta*). *Transbound Emerg Dis*. 2018;65:1367–71. <https://doi.org/10.1111/tbed.12872>
43. Son K, Kim YK, Oem JK, Jheong WH, Sleeman JM, Jeong J. Experimental infection of highly pathogenic avian influenza viruses, Clade 2.3.4.4 H5N6 and H5N8, in Mandarin ducks from South Korea. *Transbound Emerg Dis*. 2018;65:899–903. <https://doi.org/10.1111/tbed.12790>
44. Kwon J-H, Noh J-Y, Jeong J-H, Jeong S, Lee S-H, Kim Y-J, et al. Different pathogenicity of two strains of clade 2.3.4.4c H5N6 highly pathogenic avian influenza viruses bearing different PA and NS gene in domestic ducks. *Virology*. 2019;530:11–8. <https://doi.org/10.1016/j.virol.2019.01.016>
45. Pantin-Jackwood MJ, Costa-Hurtado M, Shepherd E, DeJesus E, Smith D, Spackman E, et al. Pathogenicity and transmission of H5 and H7 highly pathogenic avian influenza viruses in Mallards. *J Virol*. 2016;90:9967–82. <https://doi.org/10.1128/JVI.01165-16>
46. Hall JS, Franson JC, Gill RE, Meteyer CU, TeSlaa JL, Nashold S, et al. Experimental challenge and pathology of highly pathogenic avian influenza virus H5N1 in dunlin (*Calidris alpina*), an intercontinental migrant shorebird species. *Influenza Other Respir Viruses*. 2011;5:365–72. <https://doi.org/10.1111/j.1750-2659.2011.00238.x>
47. Hall JS, Krauss S, Franson JC, TeSlaa JL, Nashold SW, Stallknecht DE, et al. Avian influenza in shorebirds: experimental infection of ruddy turnstones (*Arenaria interpres*) with avian influenza virus. *Influenza Other Respir Viruses*. 2013;7:85–92. <https://doi.org/10.1111/j.1750-2659.2012.00358.x>
48. Fereidouni SR, Starick E, Beer M, Wilking H, Kalthoff D, Grund C, et al. Highly pathogenic avian influenza virus infection of mallards with homo- and heterosubtypic immunity induced by low pathogenic avian influenza viruses. *PLoS One*. 2009;4:e6706. <https://doi.org/10.1371/journal.pone.0006706>
49. Latorre-Margalef N, Brown JD, Fojtik A, Poulson RL, Carter D, Franca M, et al. Competition between influenza A virus subtypes through heterosubtypic immunity modulates re-infection and antibody dynamics in the mallard duck. *PLoS Pathog*. 2017;13:e1006419. <https://doi.org/10.1371/journal.ppat.1006419>
50. Reperant LA, van de Bildt MW, van Amerongen G, Buehler DM, Osterhaus AD, Jenni-Eiermann S, et al. Highly pathogenic avian influenza virus H5N1 infection in a long-distance migrant shorebird under migratory and non-migratory states. *PLoS One*. 2011;6:e27814. <https://doi.org/10.1371/journal.pone.0027814>

Address for correspondence: Michelle Wille, World Health Organization Collaborating Centre for Reference and Research on Influenza, Peter Doherty Institute for Infection and Immunity, 792 Elizabeth St, Melbourne, Victoria 3000, Australia; email: michelle.wille@influenzacentre.org

EID Podcast

Community Interventions for Pregnant Women with Zika Virus in Puerto Rico

After experiencing an alarming rise in Zika virus infections, the Puerto Rico Department of Health partnered with CDC to implement a variety of community education and prevention efforts.

But what were these efforts, and were they ultimately successful?

In this EID podcast, Dr. Giulia Earle-Richardson, a behavioral scientist at CDC, analyzes some of the Zika intervention campaigns in Puerto Rico.

Visit our website to listen:
<https://go.usa.gov/xy6nD>

**EMERGING
INFECTIOUS DISEASES**

Risk for Invasive Streptococcal Infections among Adults Experiencing Homelessness, Anchorage, Alaska, USA, 2002–2015

Emily Mosites, Tammy Zulz, Dana Bruden, Leisha Nolen, Anna Frick, Louisa Castrodale, Joseph McLaughlin, Chris Van Beneden, Thomas W. Hennessy, Michael G. Bruce

Medscape EDUCATION ACTIVITY

In support of improving patient care, this activity has been planned and implemented by Medscape, LLC and Emerging Infectious Diseases. Medscape, LLC is jointly accredited by the Accreditation Council for Continuing Medical Education (ACCME), the Accreditation Council for Pharmacy Education (ACPE), and the American Nurses Credentialing Center (ANCC), to provide continuing education for the healthcare team.

Medscape, LLC designates this Journal-based CME activity for a maximum of 1.00 **AMA PRA Category 1 Credit(s)**[™]. Physicians should claim only the credit commensurate with the extent of their participation in the activity.

Successful completion of this CME activity, which includes participation in the evaluation component, enables the participant to earn up to 1.0 MOC points in the American Board of Internal Medicine's (ABIM) Maintenance of Certification (MOC) program. Participants will earn MOC points equivalent to the amount of CME credits claimed for the activity. It is the CME activity provider's responsibility to submit participant completion information to ACCME for the purpose of granting ABIM MOC credit.

All other clinicians completing this activity will be issued a certificate of participation. To participate in this journal CME activity: (1) review the learning objectives and author disclosures; (2) study the education content; (3) take the post-test with a 75% minimum passing score and complete the evaluation at <http://www.medscape.org/journal/eid>; and (4) view/print certificate. For CME questions, see page 2004.

Release date: September 11, 2019; Expiration date: September 11, 2020

Learning Objectives

Upon completion of this activity, participants will be able to:

- Assess the epidemiology and health impact of homelessness
- Compare the profiles of persons with invasive streptococcal infections among personal experiencing homelessness (PEH) and the general population
- Analyze the risk for invasive streptococcal infection among PEH
- Evaluate the microbiology of invasive streptococcal infection among PEH and the general population.

CME Editor

Jude Rutledge, BA, Technical Writer/Editor, Emerging Infectious Diseases. *Disclosure: Jude Rutledge has disclosed no relevant financial relationships.*

CME Author

Charles P. Vega, MD, Health Sciences Clinical Professor of Family Medicine, University of California, Irvine School of Medicine, Irvine, California. *Disclosure: Charles P. Vega, MD, has disclosed the following relevant financial relationships: served as an advisor or consultant for Genentech, Inc.; GlaxoSmithKline; Johnson & Johnson Pharmaceutical Research & Development, L.L.C.; served as a speaker or a member of a speakers bureau for Shire.*

Authors

Disclosures: Emily Mosites, PhD, MPH; Tammy Zulz, MPH; Dana Bruden, MS; Leisha Nolen, MD, PhD; Anna Frick, MPH; Louisa Castrodale, DVM, MPH; Joe McLaughlin, MD, MPH; Chris A. Van Beneden, MD, MPH; Thomas Hennessy, MD, MPH; and Michael G. Bruce, MD, MPH, have disclosed no relevant financial relationships.

Author affiliations: Centers for Disease Control and Prevention, Anchorage, Alaska, USA (E. Mosites, T. Zulz, D. Bruden, L. Nolen, T.W. Hennessy, M.G. Bruce); Alaska Department of Health and Social Services, Anchorage (A. Frick, L. Castrodale, J. McLaughlin); Centers for Disease Control and Prevention, Atlanta, Georgia, USA (C. Van Beneden)

DOI: <https://doi.org/10.3201/eid2510.181408>

The risk for invasive streptococcal infection has not been clearly quantified among persons experiencing homelessness (PEH). We compared the incidence of detected cases of invasive group A *Streptococcus* infection, group B *Streptococcus* infection, and *Streptococcus pneumoniae* (pneumococcal) infection among PEH with that among the general population in Anchorage, Alaska, USA, during 2002–2015. We used data from the Centers for Disease Control and

Prevention's Arctic Investigations Program surveillance system, the US Census, and the Anchorage Point-in-Time count (a yearly census of PEH). We detected a disproportionately high incidence of invasive streptococcal disease in Anchorage among PEH. Compared with the general population, PEH were 53.3 times as likely to have invasive group A *Streptococcus* infection, 6.9 times as likely to have invasive group B *Streptococcus* infection, and 36.3 times as likely to have invasive pneumococcal infection. Infection control in shelters, pneumococcal vaccination, and infection monitoring could help protect the health of this vulnerable group.

In 2017, the number of persons experiencing homelessness (PEH) in the United States increased for the first time in 7 years to >550,000 persons, coinciding with high-profile outbreaks of infectious diseases such as hepatitis A, shigellosis, and invasive group A *Streptococcus* (GAS) infection among PEH (1–4). PEH experience unmanaged chronic disease, undernutrition, substance abuse, mental health disorders, crowding, exposure to weather, and limited access to hygiene resources, all of which can increase their risk for infectious disease (5,6). In high-income countries, baseline tuberculosis prevalence has been estimated to be 22–461 times higher, hepatitis C prevalence 4–70 times higher, and HIV prevalence up to 77 times higher among PEH than among the general population (7).

Severe manifestations of invasive streptococcal infections include pneumonia, meningitis, sepsis, cellulitis, and necrotizing fasciitis. Although PEH could be at higher risk for invasive streptococcal infection, only a few outbreaks among PEH were reported before 2015. Investigators in France described a pneumonia outbreak among homeless men during 1989–1991 caused by *Streptococcus pneumoniae* (pneumococcus) (8) and 2 invasive GAS outbreaks among PEH in 2009 (*emm* type 44) and 2010 (*emm* type 83) (9,10). During 2005–2009, an epidemic of invasive pneumococcal disease (serotype 5) was described in the homeless population in western Canada (11), and during 2009–2011, an outbreak of invasive pneumococcal disease (serotype 12F) among PEH was reported in Winnipeg, Manitoba, Canada (12). Starting in 2015, invasive GAS infections have emerged as a larger problem among PEH than previously recognized, as outbreaks began to be reported in the United States, Canada, and England (3,13,14).

The baseline risk for invasive streptococcal disease has rarely been quantified in the population experiencing homelessness. A case–control study of invasive GAS infection in Barcelona, Spain, during 1998–2003 among persons who used intravenous drugs showed that those with invasive GAS soft-tissue infections were 4 times more likely to be homeless than those without GAS infections (15). During 2002–2006, the incidence of invasive pneumococcal disease among PEH in Toronto, Ontario, Canada, was

estimated to be 30 times higher than that among the general population (273 vs. 9 infections/100,000 persons/y) (16).

To our knowledge, an estimate of the baseline relative risk for invasive streptococcal infections among PEH in the United States has not been reported. By using data from Alaska's population-based laboratory surveillance system for invasive bacterial disease, US Census data, and the Anchorage Point-in-Time count, we estimated the baseline risk for invasive disease caused by GAS, group B *Streptococcus* (GBS), and pneumococcus among adults (age ≥ 18 years) experiencing homelessness in Anchorage, Alaska, during 2002–2015.

Methods

Data Sources

In Alaska, invasive streptococcal disease cases (including pneumococcal, GAS, and GBS cases) are reportable to the Alaska Division of Public Health. In collaboration with the State of Alaska, the Centers for Disease Control and Prevention (CDC) Arctic Investigations Program (part of the National Center for Emerging and Zoonotic Diseases, Division of Preparedness and Emerging Infections) conducts statewide, population-based, and laboratory-based surveillance for invasive infections caused by these pathogens (17–19). Participating laboratories send sterile site bacterial isolates to the Arctic Investigations Program for confirmatory testing, antimicrobial-susceptibility testing, and molecular typing (*emm*-typing for GAS and serotyping for pneumococcus). Confirmed cases of invasive infection are defined as the isolation of the pathogen from a normally sterile body site (e.g., blood), isolation of GAS from a nonsterile site in persons with necrotizing fasciitis or streptococcal toxic shock syndrome, or isolation of GBS from a nonsterile site in the case of fetal demise. Standardized chart reviews are conducted on all confirmed cases, including information on demographics, associated diagnoses, alcohol abuse, injection drug use, and underlying conditions. Because many cases were detected through blood culture, bacteremia was often present in addition to other diagnoses. We report diagnosis of bacteremia as bacteremia alone, without other diagnoses. Information on homelessness was routinely collected from the medical record beginning in 2002. This routine public health surveillance is considered nonresearch by the CDC and Alaska area institutional review boards.

We did not include data from 2016 in this analysis because a large outbreak of invasive GAS infection occurred among the homeless population in Anchorage beginning in February 2016 (3). We also limited our study to cases among adults (age ≥ 18 years) because only 2 cases of invasive streptococcal disease were detected in children experiencing homelessness over the study period.

For the years 2005–2015, we used the general Anchorage adult population data from the US Census and homeless adult population data from the Anchorage Point-in-Time count (PIT) (20,21). PIT is a yearly count of sheltered and unsheltered homeless persons made on a single night in January, as mandated by the US Department of Housing and Urban Development for communities receiving federal funds from the McKinney–Vento Homeless Assistance Grants program (22). In these counts, a person is considered homeless if they are spending the night in an emergency shelter or sleeping in a car, tent, or other area considered not suitable for human habitation; persons who are staying with relatives or friends or who are in short-term or transitional housing are not included. Homeless population data were not available for 2002–2004, so we used the mean data from 2005–2015 for those years. We restricted the analysis of case and population data to Anchorage because homeless population data were available for Anchorage but not for other urban centers in Alaska (such as Juneau or Fairbanks). Limited demographic information was available for rate adjustment. Age and sex distributions were used from the US Census, but age information was not available from PIT. We estimated the age distribution of PEH in Anchorage by using data from a survey conducted during a large homeless outreach project called Project Homeless Connect from 2010 (23).

Statistical Methods

Cases of invasive GAS, GBS, and pneumococcal disease were classified as occurring in PEH if “homeless” was checked on the surveillance chart review form. Otherwise, cases were classified as being in persons in the general population. For the purposes of this analysis, the case and population data labeled as general population excluded PEH. We calculated invasive streptococcal infection incidence per 100,000 person-years for PEH and the general population, deriving annual population denominators from PIT for PEH and from the Anchorage census count minus the PIT estimate for the general population. We conducted direct age standardization of the incidence of GAS, GBS, and pneumococcal invasive disease by using the general population census age structure as the standard population. We calculated the incidence rate ratio (IRR) and 95% CIs comparing invasive streptococcal infection incidence in the homeless population to that among the general population by using Poisson exact tests. We also calculated risk differences for each invasive streptococcal infection between PEH and the general population and the percentage of each infection type associated with homelessness. We compared characteristics such as demographics, diagnoses, and coexisting conditions between cases among PEH and the general population by using χ^2 tests and Fisher exact tests.

Results

During 2005–2015, PIT counted a mean number of 970 adults (minimum 795, maximum 1,486) in Anchorage who were homeless, either sleeping in a shelter or sleeping outside. The mean general population in Anchorage during this period was 288,921 adults (minimum 264,795, maximum 300,175) who were not experiencing homelessness. The largest age stratum for both PEH and the general population was 31–50 years, but this stratum was larger for PEH (55% among PEH vs. 29% among the general population). From 2002 through 2015, the Arctic Investigations Program surveillance system detected 56 cases of invasive GAS infection, 6 cases of invasive GBS infection, and 84 cases of invasive pneumococcal infection in the adult population experiencing homelessness in Anchorage. Among the general population in Anchorage, the system detected 229 cases of invasive GAS infection, 194 cases of invasive GBS infection, and 457 cases of invasive pneumococcal infection (Table 1).

PEH with invasive GAS infection were more often male and more likely to be diagnosed with alcohol abuse but less likely to be diagnosed with diabetes than persons in the general Anchorage population with invasive GAS infection (Table 1). PEH with invasive GAS infection were also more likely to have a diagnosis of cellulitis or necrotizing fasciitis than were persons in the general population with invasive GAS infection. The most common *emm* types identified among invasive GAS infection isolates from PEH included *emm91* (19%), *emm82* (16%), and *emm49* (12%), whereas the most common *emm* types identified among persons in the general population were *emm1* (10%), *emm49* (9%), *emm82* (8%), and *emm89* (8%) (Figure 1). The crude IRR of having a detected case of invasive GAS infection for PEH compared with the general population was 53.7 (95% CI 39.3–72.2), and the age-adjusted IRR was 53.3 (95% CI 46.7–61.0) (Table 2).

PEH with invasive GBS were more likely to have alcohol abuse and less likely to have diabetes recorded in their medical record than invasive GBS patients in the general population (Table 1). The crude IRR of GBS for PEH compared with the general population was 6.8 (95% CI 2.5–15.0), and the age-adjusted IRR was 6.9 (95% CI 6.0–8.1) (Table 2).

PEH who had invasive pneumococcal infection were younger than persons with invasive pneumococcal infection among the general population (Table 1). They were also more likely than the general population to have recorded alcohol abuse and be diagnosed with pneumonia but less likely to have recorded diabetes. The most common pneumococcal infection serotypes among PEH after 2010 (the year 13-valent pneumococcal conjugate vaccine was introduced in Alaska) were 31 (19%), 16F (15%), F (a vaccine

Table 1. Demographic and clinical characteristics of adults with invasive streptococcal infection compared with the general adult population, Anchorage, Alaska, USA, 2002–2015*

Characteristic	Persons experiencing homelessness	General population	p value
Group A <i>Streptococcus</i> case-patients	56	229	
Age, y, mean (SD)	51 (11)	54 (19)	0.27
Sex			
M	43 (77)	122 (53)	<0.01
F	13 (23)	107 (47)	
Diagnosis			
Cellulitis	37 (66)	107 (47)	0.01
Pneumonia	11 (20)	43 (19)	0.88
Necrotizing fasciitis	9 (16)	14 (6)	0.01
Bacteremia	4 (7)	46 (20)	0.03
Other conditions			
Diabetes	5 (9)	68 (30)	<0.01
Intravenous drug use	5 (9)	8 (3)	0.14
Alcohol abuse	42 (75)	23 (52)	<0.01
Death during episode	6 (11)	29 (13)	0.69
Group B <i>Streptococcus</i> case-patients	6	194	
Age, y, mean (SD)	53 (11)	60 (16)	0.28
Sex			
M	4 (67)	97 (50)	0.68
F	2 (33)	97 (50)	
Diagnosis			
Cellulitis	1 (16)	63 (32)	0.67
Pneumonia	2 (33)	24 (12)	0.13
Necrotizing fasciitis	0	0	NA
Bacteremia	2 (33)	63 (32)	1.00
Other conditions			
Diabetes	0	89 (46)	0.03
Intravenous drug use	0	4 (2)	0.72
Alcohol abuse	5 (83)	21 (11)	<0.01
Death during episode	2 (33)	15(7)	0.08
<i>S. pneumoniae</i> case-patients	84	457	
Age, y, mean (SD)	48 (9)	57 (17)	<0.01
Sex			
M	55 (65)	258 (56)	0.124
F	29 (35)	199 (44)	
Diagnosis			
Cellulitis	3 (4)	8 (2)	0.39
Pneumonia	76 (90)	369 (81)	0.03
Necrotizing fasciitis	0	1 (0)	1.00
Bacteremia	4 (5)	53 (12)	0.08
Other conditions			
Diabetes	6 (7)	85 (19)	0.01
Intravenous drug use	3 (4)	8 (2)	0.39
Alcohol abuse	74 (88)	130 (28)	<0.01
Death during episode	6 (7)	60 (13)	0.15

*Values are no. (%) unless otherwise indicated. General population excludes persons experiencing homelessness. p values based on χ^2 or Fisher exact test. NA, not applicable.

type) (11%), and 9N (11%), whereas the most common serotypes among persons with invasive pneumococcal infection among the general population were 22F (12%), 7F (a vaccine type) (10%), and type 3 (a vaccine type) (9%) (Figure 1). The crude IRR of invasive pneumococcal disease for PEH compared with the general population was 40.3 (95% CI 31.5–51.0), and the age-adjusted IRR was 36.3 (95% CI 33.0–39.9) (Table 2).

During 2002–2015, an excess of 40 cases of invasive GAS, 4 cases of invasive GBS, and 54 cases of invasive pneumococcal infections per 10,000 person-years were estimated to have occurred within the homeless population in Anchorage (data not shown). Of all invasive GAS cases in Anchorage during the study period, 19.6% occurred within

the homeless population, whereas 3% of invasive GBS cases and 15.5% of invasive pneumococcal cases were within the homeless population.

Discussion

A substantial proportion of the disease burden for invasive GAS, GBS, and pneumococcal disease in Anchorage occurred among PEH. Although the estimated homeless population in 2010 accounted for only 0.4% of the total population, nearly 20% of invasive GAS infections, 3% of invasive GBS infections, and 16% of invasive pneumococcal disease occurred within this population. The risk for invasive GAS infection was 53 times higher, the risk for invasive GBS infection 7 times higher, and the risk for

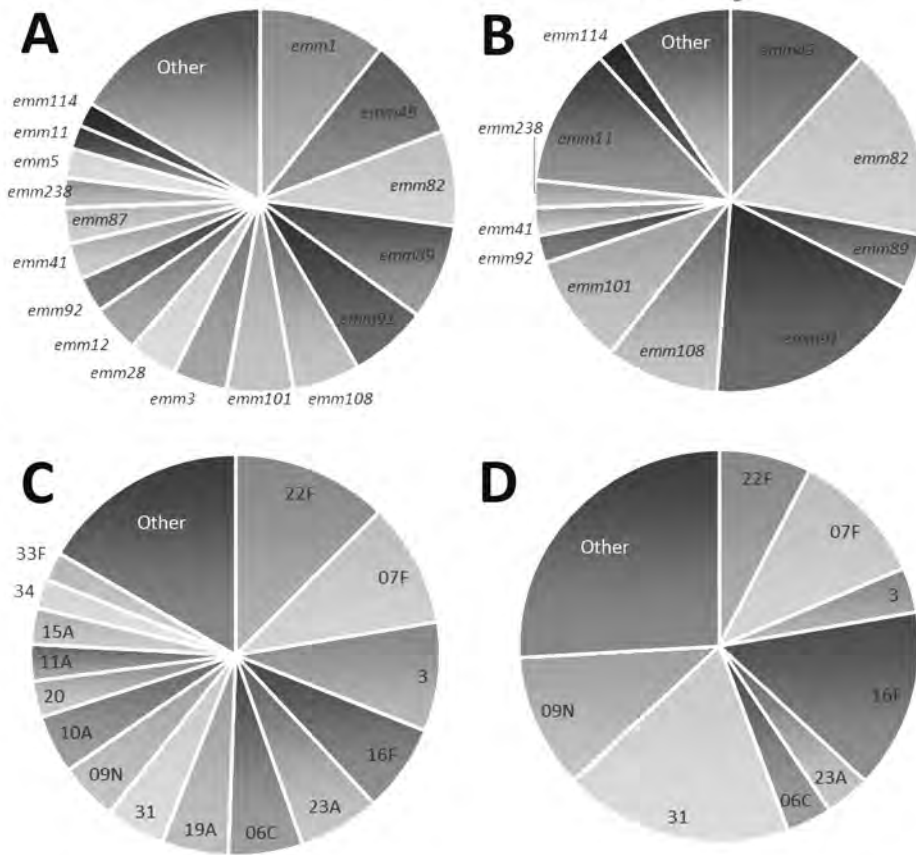


Figure 1. Group A *Streptococcus emm*-type and *Streptococcus pneumoniae* serotype distributions among the general population compared with distributions among persons experiencing homelessness, Alaska, 2002–2015. A) Group A *Streptococcus emm* types among the general population. B) Group A *Streptococcus emm* types among persons experiencing homelessness. C) *S. pneumoniae* serotypes among the general population. D) *S. pneumoniae* serotypes among persons experiencing homelessness. General population excludes persons experiencing homelessness.

invasive pneumococcal infection 36 times higher among PEH compared with the general population.

Commonly identified risk factors for invasive GAS infection among adults include older age, male sex, exposure to children, household crowding, acute and chronic skin breakdown, immune-compromising conditions, heart disease, diabetes, and intravenous drug use (24–26), whereas established risk factors for invasive GBS among adults include immune-compromising conditions, heart disease, diabetes, and older age (27,28). Homelessness has not been previously quantified as a major factor for either type of infection, despite recent outbreaks of GAS among PEH (3,13,14). For invasive pneumococcus infection, risk factors include older age, immune-compromising conditions, alcohol use, high body mass index, and cigarette smoking

(29–32). Although the overall incidence of invasive pneumococcal disease was higher in this study than the study in Toronto, Ontario (601 infections/100,000 person-years in Anchorage vs. 273 infections/100,000 person-years in Toronto), the IRR estimates were similar (adjusted IRR of 36 in Anchorage vs. crude IRR of 30 in Toronto) (16). The number of cases of invasive GBS in the homeless population over the study period was small, and the IRR was also smaller than for invasive GAS and pneumococcal infections. This finding might reflect a difference in transmission pathways and risk factors between invasive GAS, GBS, and pneumococcal infections.

For all 3 invasive streptococcal diseases, PEH were more likely than the general population to have alcohol abuse recorded but less likely to have diabetes recorded.

Table 2. Crude and age-adjusted incidence rates of invasive streptococcal infections among the adult population experiencing homelessness compared with the general adult population, Anchorage, Alaska, USA, 2002–2015*

Disease	Population experiencing homelessness			General population			Crude IRR (95% CI)	Age-adjusted IRR (95% CI)
	No. cases	Person-years	Incidence	No. cases	Person-years	Incidence		
Group A <i>Streptococcus</i>	56	13,585	412.2	229	2,983,169	7.7	53.7 (39.3–72.2)	53.3 (46.7–61.0)
Group B <i>Streptococcus</i>	6	13,585	44.2	194	2,983,169	6.5	6.8 (2.5–15.0)	6.9 (6.0–8.1)
<i>Streptococcus pneumoniae</i>	84	13,585	618.3	457	2,983,169	15.3	40.3 (31.5–51.0)	36.3 (33.0–39.9)

*General population excludes persons experiencing homelessness. Incidence expressed as no. cases/100,000 person-years. IRR, incidence rate ratio.

These differences might reflect either actual differences in invasive streptococcal disease risk factors for PEH compared with the general population or differences in distribution of these factors among each source population. For example, the difference in recorded alcohol abuse might reflect higher alcohol abuse among PEH than the general population or an elevated risk for invasive disease as a result of alcohol abuse. The difference in recorded diabetes diagnoses could reflect a truly lower prevalence of diabetes among PEH with invasive disease or a lack of access to care among PEH (and therefore a lack of diagnoses) compared with the general population.

Although GAS molecular types *emm49* and *emm82* were common among both PEH and the general population with invasive GAS, we observed some notable differences in *emm* distribution (Figure 1). For example, no cases of *emm1* infection were identified among PEH, even though it was the most commonly identified *emm* type among Anchorage general population residents with invasive GAS infection in this study. Conversely, a higher proportion of infections among PEH were *emm91* than among invasive GAS infections in the general population. These differences in *emm*-type distribution demonstrate a larger trend in *emm*-type pattern distribution (Figure 2). Among PEH, no pattern A–C strains were identified, whereas a large proportion of pattern D strains were detected. These type patterns have been associated with tissue tropism (33); pattern D strains tend to cause skin infection. This trend suggests that skin breakdown and skin-to-skin transmission could be more important risk factors for invasive GAS disease among PEH than among the general population in Anchorage, which also aligns with the differences in clinical diagnoses between the 2 groups.

As with GAS, the most common serotypes of pneumococcal isolates in persons with invasive pneumococcal infection were not the same for PEH and persons in the general population, although 7F (a 13-valent pneumococcal

conjugate vaccine type) was commonly identified in both populations (Figure 1). These differences in distribution could also be a result of social contact patterns among PEH that have low overlap with the general population.

Quantifying the number of PEH and the number of cases of disease in the homeless population is complicated by several factors. First, whether a person is experiencing homelessness could be underestimated in the medical records. To evaluate the extent of underestimation, we conducted a small analysis of the sensitivity of capture of homelessness in the context of a 2016 outbreak of invasive *emm26.3* GAS infections in Anchorage (3). In this outbreak, 24 cases of *emm26.3* that were identified through the surveillance system were independently evaluated by using chart reviews and interviews; 22 of these were determined to have occurred in PEH. Of these, 18 were captured as homeless in the standard surveillance chart review form used in our study, yielding a sensitivity of 82%. A second possible limitation is that the homeless population could be undercounted by PIT. However, even if the actual size of the homeless population were 3 times larger than estimated, the IRRs for invasive GAS, GBS, and pneumococcal disease comparing PEH to the general population would decrease proportionately but remain large and statistically significant (an adjusted IRR of 18 for GAS, 2 for GBS, and 12 for pneumococcus).

In addition, we are not able to assess the underlying risk factor distributions in the well population. Therefore, comparing the characteristics of cases in surveillance data limits our ability to assess the difference in risk factors for disease between PEH and the general population. Finally, the health-related causes and outcomes of homelessness are complex. This analysis does not isolate the effect of lacking housing from the myriad conditions that are integrated with experiencing homelessness. The effect of not having housing could lead to exposure to weather, lack of access to hygiene resources, spending time in crowded

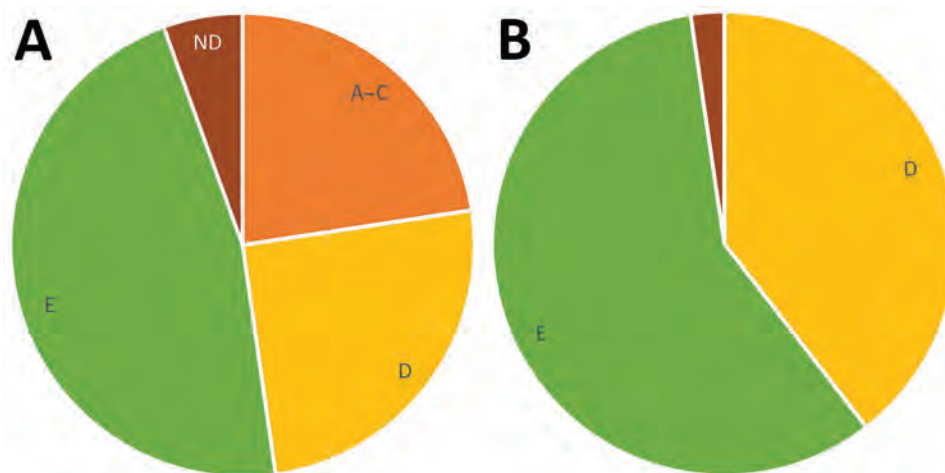


Figure 2. Group A *Streptococcus emm* pattern types among the general population (A) compared with persons experiencing homelessness (B), Anchorage, Alaska, 2002–2015. ND, not determined.

facilities, and worsening of underlying chronic illnesses, each of which could increase the transmission of invasive streptococcal disease. However, factors such as injection drug use, alcohol use, and unmanaged chronic diseases can also lead to homelessness and are independent risk factors for invasive streptococcal disease. In this analysis, we are unable to estimate how much of the increased risk for invasive streptococcal infection is a result of lacking housing or a result of the factors that led to the lack of housing. Despite these limitations, the health disparities between PEH and the general population indicate that targeted resources could prevent invasive GAS, GBS, and pneumococcal disease, regardless of the ultimate origin of risk.

In 2016, an estimated 1.42 million persons in the United States used an emergency shelter or transitional housing at some point during the year (34). According to our analysis, this population is at an increased risk for invasive streptococcal disease, especially invasive GAS and invasive pneumococcal disease. Promoting infection control in shelters, increasing the availability of pneumococcal vaccine, and improving monitoring of infections in homeless populations could improve the health of this vulnerable group.

About the Author

Dr. Mosites is an epidemiologist at the Centers for Disease Control and Prevention Arctic Investigations Program (National Center for Emerging and Zoonotic Infectious Diseases, Division of Preparedness and Emerging Infections) in Anchorage, Alaska. Her research areas include infectious disease, health disparities, and rural health.

References

- Henry M, Watt R, Rosenthal L, Shivji A. The 2017 Annual Homeless Assessment Report (AHAR) to Congress. Part 1: point-in-time estimates of homelessness. Washington: US Department of Housing and Urban Development; 2017 [cited 2018 Jun 15]. <https://files.hudexchange.info/resources/documents/2017-AHAR-Part-1.pdf>
- Kushel M. Hepatitis A outbreak in California—addressing the root cause. *N Engl J Med*. 2018;378:211–3. <http://dx.doi.org/10.1056/NEJMp1714134>
- Mosites E, Frick A, Gounder P, Castrodale L, Li Y, Rudolph K, et al. Outbreak of invasive infections from subtype *emm26.3* group A *Streptococcus* among homeless adults—Anchorage, Alaska, 2016–2017. *Clin Infect Dis*. 2018;66:1068–74. <http://dx.doi.org/10.1093/cid/cix921>
- Hines JZ, Pinsent T, Rees K, Vines J, Bowen A, Hurd J, et al. Shigellosis outbreak among men who have sex with men and homeless persons—Oregon, 2015–2016. *MMWR Morb Mortal Wkly Rep*. 2016;65:812–3. <http://dx.doi.org/10.15585/mmwr.mm6531a5>
- Aldridge RW, Story A, Hwang SW, Nordentoft M, Luchenski SA, Hartwell G, et al. Morbidity and mortality in homeless individuals, prisoners, sex workers, and individuals with substance use disorders in high-income countries: a systematic review and meta-analysis. *Lancet*. 2018;391:241–50. [http://dx.doi.org/10.1016/S0140-6736\(17\)31869-X](http://dx.doi.org/10.1016/S0140-6736(17)31869-X)
- Fazel S, Geddes JR, Kushel M. The health of homeless people in high-income countries: descriptive epidemiology, health consequences, and clinical and policy recommendations. *Lancet*. 2014;384:1529–40. [http://dx.doi.org/10.1016/S0140-6736\(14\)61132-6](http://dx.doi.org/10.1016/S0140-6736(14)61132-6)
- Beijer U, Wolf A, Fazel S. Prevalence of tuberculosis, hepatitis C virus, and HIV in homeless people: a systematic review and meta-analysis. *Lancet Infect Dis*. 2012;12:859–70. [http://dx.doi.org/10.1016/S1473-3099\(12\)70177-9](http://dx.doi.org/10.1016/S1473-3099(12)70177-9)
- Mercat A, Nguyen J, Dautzenberg B. An outbreak of pneumococcal pneumonia in two men's shelters. *Chest*. 1991;99:147–51. <http://dx.doi.org/10.1378/chest.99.1.147>
- Cady A, Plainvert C, Donnio P, Loury P, Huguenet D, Briand A, et al. Clonal spread of *Streptococcus pyogenes emm44* among homeless persons, Rennes, France. *Emerg Infect Dis*. 2011;17:315–7. <http://dx.doi.org/10.3201/eid1702.101022>
- Soriano N, Vincent P, Auger G, Cariou ME, Moullec S, Lagente V, et al. Full-length genome sequence of type M/*emm83* group A *Streptococcus pyogenes* strain STAB1101, isolated from clustered cases in Brittany. *Genome Announc*. 2015;3:e01459–14. <http://dx.doi.org/10.1128/genomeA.01459-14>
- Tyrrell GJ, Lovgren M, Ibrahim Q, Garg S, Chui L, Boone TJ, et al. Epidemic of invasive pneumococcal disease, western Canada, 2005–2009. *Emerg Infect Dis*. 2012;18:733–40. <http://dx.doi.org/10.3201/eid1805.110235>
- Schillberg E, Isaac M, Deng X, Peirano G, Wylie JL, Van Caeselele P, et al. Outbreak of invasive *Streptococcus pneumoniae* serotype 12F among a marginalized inner-city population in Winnipeg, Canada, 2009–2011. *Clin Infect Dis*. 2014;59:651–7. <http://dx.doi.org/10.1093/cid/ciu366>
- Bundle N, Bubba L, Coelho J, Kwiatkowska R, Cloke R, King S, et al. Ongoing outbreak of invasive and non-invasive disease due to group A *Streptococcus* (GAS) type *emm66* among homeless and people who inject drugs in England and Wales, January to December 2016. *Euro Surveill*. 2017;22:30446. <http://dx.doi.org/10.2807/1560-7917.ES.2017.22.3.30446>
- Teatero S, McGeer A, Tyrrell GJ, Hoang L, Smadi H, Domingo MC, et al. Canada-wide epidemic of *emm74* group A *Streptococcus* invasive disease. *Open Forum Infect Dis*. 2018;5:ofy085. <http://dx.doi.org/10.1093/ofid/ofy085>
- Sierra JM, Sánchez F, Castro P, Salvadó M, de la Red G, Libois A, et al. Group A streptococcal infections in injection drug users in Barcelona, Spain: epidemiologic, clinical, and microbiologic analysis of 3 clusters of cases from 2000 to 2003. *Medicine (Baltimore)*. 2006;85:139–46. <http://dx.doi.org/10.1097/01.md.0000224707.24392.52>
- Plevneshi A, Svoboda T, Armstrong I, Tyrrell GJ, Miranda A, Green K, et al.; Toronto Invasive Bacterial Diseases Network. Population-based surveillance for invasive pneumococcal disease in homeless adults in Toronto. *PLoS One*. 2009;4:e7255. <http://dx.doi.org/10.1371/journal.pone.0007255>
- Bruce MG, Singleton R, Bulkow L, Rudolph K, Zulz T, Gounder P, et al. Impact of the 13-valent pneumococcal conjugate vaccine (PCV13) on invasive pneumococcal disease and carriage in Alaska. *Vaccine*. 2015;33:4813–9. <http://dx.doi.org/10.1016/j.vaccine.2015.07.080>
- Rudolph K, Bruce MG, Bruden D, Zulz T, Reasonover A, Hurlburt D, et al. Epidemiology of invasive group A streptococcal disease in Alaska, 2001 to 2013. *J Clin Microbiol*. 2016;54:134–41. <http://dx.doi.org/10.1128/JCM.02122-15>
- Castrodale L, Gessner B, Hammitt L, Chimonas MA, Hennessy T. Invasive early-onset neonatal group B streptococcal cases—Alaska, 2000–2004. *Matern Child Health J*. 2007;11:91–5. <http://dx.doi.org/10.1007/s10995-006-0144-5>

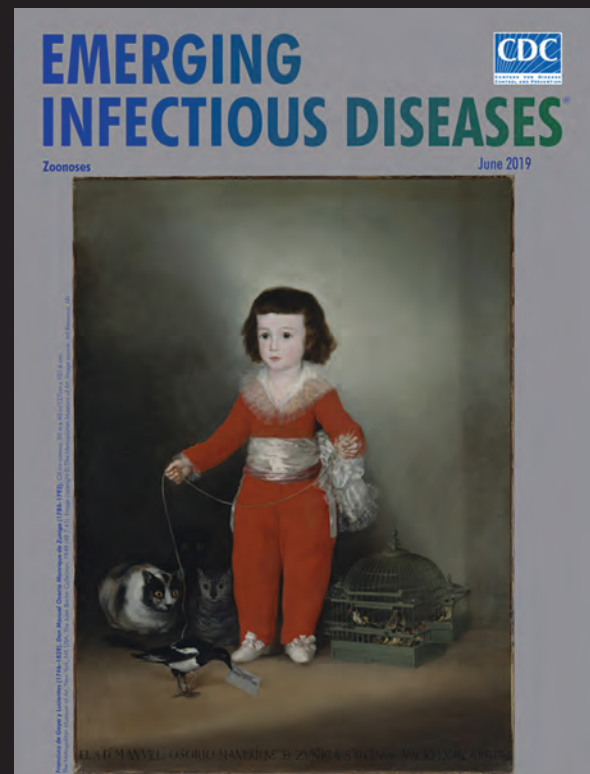
20. US Census Bureau. American FactFinder 2010 [cited 2018 May 10]. https://factfinder.census.gov/faces/nav/jsf/pages/community_facts.xhtml?src=bkmk
21. US Department of Housing and Urban Development. PIT and HIC guides, tools, and webinars [cited 2018 May 10]. <https://www.hudexchange.info/programs/hdx/guides/pit-hic/#general-pit-guides-and-tools>
22. National Alliance to End Homelessness. What is a point-in-time count? [cited 2018 Jun 12]. <https://endhomelessness.org/resource/what-is-a-point-in-time-count>
23. Anchorage Coalition to End Homelessness, Institute for Community Alliances. Alaska data and reports [cited 2018 May 10]. <https://www.icalliances.org/alaska-data-and-reports>
24. Factor SH, Levine OS, Schwartz B, Harrison LH, Farley MM, McGeer A, et al. Invasive group A streptococcal disease: risk factors for adults. *Emerg Infect Dis*. 2003;9:970–7. <http://dx.doi.org/10.3201/eid0908.020745>
25. Langley G, Hao Y, Pondo T, Miller L, Petit S, Thomas A, et al. The impact of obesity and diabetes on the risk of disease and death due to invasive group A *Streptococcus* infections in adults. *Clin Infect Dis*. 2016;62:845–52. <http://dx.doi.org/10.1093/cid/civ1032>
26. Steer AC, Lamagni T, Curtis N, Carapetis JR. Invasive group A streptococcal disease: epidemiology, pathogenesis and management. *Drugs*. 2012;72:1213–27. <http://dx.doi.org/10.2165/11634180-000000000-00000>
27. Lyytikäinen O, Nuorti JP, Halmesmäki E, Carlson P, Uotila J, Vuento R, et al. Invasive group B streptococcal infections in Finland: a population-based study. *Emerg Infect Dis*. 2003;9:469–73. <http://dx.doi.org/10.3201/eid0904.020481>
28. Skoff TH, Farley MM, Petit S, Craig AS, Schaffner W, Gershman K, et al. Increasing burden of invasive group B streptococcal disease in nonpregnant adults, 1990–2007. *Clin Infect Dis*. 2009;49:85–92. <http://dx.doi.org/10.1086/599369>
29. Watt JP, O'Brien KL, Benin AL, McCoy SI, Donaldson CM, Reid R, et al. Risk factors for invasive pneumococcal disease among Navajo adults. *Am J Epidemiol*. 2007;166:1080–7. <http://dx.doi.org/10.1093/aje/kwm178>
30. Marrie TJ, Tyrrell GJ, Majumdar SR, Eurich DT. Effect of age on the manifestations and outcomes of invasive pneumococcal disease in adults. *Am J Med*. 2018;131:100.e1–7. <http://dx.doi.org/10.1016/j.amjmed.2017.06.039>
31. Nuorti JP, Butler JC, Farley MM, Harrison LH, McGeer A, Kolczak MS, et al.; Active Bacterial Core Surveillance Team. Cigarette smoking and invasive pneumococcal disease. *N Engl J Med*. 2000;342:681–9. <http://dx.doi.org/10.1056/NEJM200003093421002>
32. Wagenvoort GH, Knol MJ, de Melker HE, Vlamincx BJ, van der Ende A, Rozenbaum MH, et al. Risk and outcomes of invasive pneumococcal disease in adults with underlying conditions in the post-PCV7 era, The Netherlands. *Vaccine*. 2016;34:334–40. <http://dx.doi.org/10.1016/j.vaccine.2015.11.048>
33. Bessen DE, Lizano S. Tissue tropisms in group A streptococcal infections. *Future Microbiol*. 2010;5:623–38. <http://dx.doi.org/10.2217/fmb.10.28>
34. Solari C, Shivji A, de Souza T, Watt R, Silverbush M. The 2016 Annual Homeless Assessment Report (AHAR) to Congress. Part 2: estimates of homelessness in the United States. Washington: US Department of Housing and Urban Development; 2016 [cited 2018 Jun 15]. <https://files.hudexchange.info/resources/documents/2016-AHAR-Part-2.pdf>

Address for correspondence: Emily Mosites, Centers for Disease Control and Prevention, 4055 Tudor Centre Dr, Anchorage, AK 99508, USA; email: lw7@cdc.gov

EID Podcast: The Red Boy, the Black Cat

A little boy, the son of aristocrats, takes his pet magpie out for a walk. Little does he realize that his beloved animal may harbor dangerous infectious diseases like psittacosis, salmonellosis, and influenza—illnesses that often prey upon young children.

In this EID podcast, Byron Breedlove, managing editor of *Emerging Infectious Diseases*, explores the sinister undertones of the cover image for July 2019, a painting of Don Manuel Osorio Manrique de Zuniga by Francisco de Goya.



Visit our website to listen:
<https://go.usa.gov/xysv5>

**EMERGING
INFECTIOUS DISEASES®**

Early Diagnosis of Tularemia by Flow Cytometry, Czech Republic, 2003–2015¹

Aleš Chrdle, Pavlína Tinavská, Olga Dvořáčková, Pavlína Filipová, Věra Hnetilová, Pavel Žampach, Květoslava Batistová, Václav Chmelík, Amanda E. Semper, Nick J. Beeching

We retrospectively assessed the utility of a flow cytometry–based test quantifying the percentage of CD3+ T cells with the CD4–/CD8– phenotype for predicting tularemia diagnoses in 64 probable and confirmed tularemia patients treated during 2003–2015 and 342 controls with tularemia-like illnesses treated during 2012–2015 in the Czech Republic. The median percentage of CD3+/CD4–/CD8– T cells in peripheral blood was higher in tularemia patients (19%, 95% CI 17%–22%) than in controls (3%, 95% CI 2%–3%). When we used 8% as the cut-off, this test's sensitivity was 0.953 and specificity 0.895 for distinguishing cases from controls. The CD3+/CD4–/CD8– T cells increased a median of 7 days before tularemia serologic test results became positive. This test supports early presumptive diagnosis of tularemia for clinically suspected cases 7–14 days before diagnosis can be confirmed by serologic testing in regions with low prevalences of tularemia-like illnesses.

Tularemia is a zoonotic disease that occurs in the Northern Hemisphere and is caused by *Francisella tularensis* (1). In Europe, >500 cases are reported annually (2); Turkey and the United States also have substantial disease burdens (3). The infection is usually acquired by direct contact with, inhalation of, or ingestion of *F. tularensis* from animal reservoirs, infected arthropod vectors, or contaminated water (4).

No clinical or laboratory manifestations are pathognomonic for tularemia; preliminary diagnosis is based on exposure risk and compatible clinical presentation (5).

Author affiliations: České Budějovice Hospital, České Budějovice, Czech Republic (A. Chrdle, P. Tinavská, P. Filipová, V. Hnetilová, P. Žampach, V. Chmelík); University of South Bohemia Faculty of Health and Social Sciences, České Budějovice, Czech Republic (A. Chrdle, O. Dvořáčková); Royal Liverpool University Hospital, Liverpool, UK (A. Chrdle, N.J. Beeching); Písek Hospital, Písek, Czech Republic (K. Batistová); Public Health England, Porton Down, UK (A.E. Semper); National Institute for Health Research Health Protection Research Unit in Emerging and Zoonotic Infections, Liverpool, UK (A.E. Semper; N.J. Beeching); Liverpool School of Tropical Medicine, Liverpool (N.J. Beeching)

DOI: <https://doi.org/10.3201/eid2510.181875>

Clinical manifestations include the ulceroglandular, glandular, oroglandular, and oculoglandular forms; septicemic (typhoidal) form; and respiratory form (6,7).

The decision to treat patients for tularemia is often based on clinical judgment, and therapy is initiated empirically days to weeks before the diagnosis is confirmed because seroconversion can take 10–20 days after symptom onset to occur (8). Culturing *F. tularensis* requires special handling because the bacterium is fastidious and needs to be cultured in Biosafety Level 3 facilities (9). To perform nucleic acid amplification testing, a sample from a swab of an ulcer or biopsy of deep tissue is required. A diagnostic test that is less invasive than tissue biopsy and supports early diagnosis of tularemia would be beneficial in guiding empiric therapy.

Peripheral blood CD3+ T lymphocytes that do not exhibit CD4 or CD8 form a heterogeneous CD3+/CD4–/CD8– T-cell population. One subset includes $\gamma\delta$ T cells, which constitute 5%–9% of circulating CD3+ T cells in healthy adults (10,11). These percentages vary according to age and race/ethnicity (12) and have been reported to not exceed 5% of total peripheral CD3+ T cells in the population of the Czech Republic (13).

An increased proportion of peripheral blood $\gamma\delta$ T cells was first reported in tularemia in 1992 (14). Subsequently, Kroca et al. observed that these T cells significantly increased in tularemia patients starting from the first week of symptom onset and persisted for months after resolution of illness (15). An increased frequency of $\gamma\delta$ T cells has also been described in individual case reports or small case series in association with infections with other intracellular pathogens (12,16), including *Mycobacterium tuberculosis* (17), *Legionella* (18), *Salmonella* (19), *Brucella* (20,21), *Ehrlichia* (22), *Coxiella burnetii* (23), *Toxoplasma* (24), *Leishmania* (25), *Plasmodium vivax* (26), and *Schistosoma* spp. in primary schistosomiasis (27).

Encouraged by local colleagues suggesting that raised $\gamma\delta$ T-cell (and by inference CD3+/CD4–/CD8– T-cell)

¹Preliminary data from this study were presented at the European Congress of Clinical Microbiology and Infectious Diseases; April 9–12, 2016; Amsterdam, the Netherlands (abstract no. O367).

percentages could be used in earlier tularemia diagnosis (28), the Immunology Laboratory of České Budějovice Hospital (České Budějovice, Czech Republic) changed its reporting practices in 2003. From this time onward, laboratory reports included comments suggesting consideration of possible tularemia if flow cytometry of peripheral blood showed an increased percentage of CD3+/CD4-/CD8- T cells or both CD3+/CD4-/CD8- and $\gamma\delta$ T cells. In turn, clinicians in the 2 cooperating infectious disease units at České Budějovice Hospital and Písek Hospital (Písek, Czech Republic) began routinely requesting that peripheral blood samples be analyzed by flow cytometry along with the serologic test when tularemia was suspected.

In this article, we review cases under consideration for a tularemia diagnosis at these 2 infectious disease units to determine whether an increase in the percentage of CD3+/CD4-/CD8- T cells in the peripheral blood is sensitive and specific for a preliminary tularemia diagnosis and, if so, to define the optimum diagnostic cutoff value. Our second objective was to compare the timing of CD3+/CD4-/CD8- T-cell count elevation with that of the first positive *F. tularensis* serologic test result. We also evaluated the correlation between CD3+/CD4-/CD8- and $\gamma\delta$ T cells to determine whether the levels of CD3+/CD4-/CD8- T cells could serve as a surrogate marker because this cell population is easier to assess.

Methods

Study Groups and Study Design

Using laboratory records and local hospital and unit diagnostic indices, we retrospectively identified all cases of tularemia that were managed in the infectious disease units at České Budějovice Hospital and Písek Hospital during January 1, 2003–December 31, 2015. The control group included a consecutive group of ill adults who were investigated for possible tularemia in the same 2 units during January 1, 2012–December 31, 2015.

We retrieved the hospital case notes for patients in each group. The study groups included patients for whom both tularemia serology and flow cytometry CD3+ T-cell population characterization were available during the same illness episode. We extracted data on demographics, signs and symptoms, final diagnoses, timing of symptom onset, and laboratory test results and recorded them onto a standardized form. Tularemia cases were categorized as probable or confirmed in keeping with published literature (4,8,29,30) and US Centers for Disease Control and Prevention 1999 and 2017 criteria (31,32): clinical illness compatible with tularemia along with detection of *F. tularensis* by culture or nucleic acid testing or a serologic test result suggestive of or confirming tularemia.

Laboratory Diagnosis of Tularemia

For serologic testing, we used a commercial agglutination test (Tularemia Diagnostic Set, Bioveta a.s., <https://www.bioveta.eu>). We assigned a probable tularemia diagnosis to patients if the antibody titer in acute phase samples was $\geq 1:20$ and illness was clinically compatible with tularemia. We assigned a confirmed tularemia diagnosis if the titer in any samples reached $\geq 1:160$ or a seroconversion (change from negative to positive of any titer) or a 4-fold increase in titer occurred between the acute and convalescent samples and illness was clinically compatible with tularemia.

We performed blood cultures using BacT/ALERT 3D (bioMérieux, <https://www.biomerieux.com>); we cultured the resulting bacteria on plates with Columbia 5% sheep blood agar (Bio-Rad Laboratories, <http://www.bio-rad.com>) and determined the species by 16S PCR. For nucleic acid analysis, we extracted DNA using the QIAamp DNA Mini Kit (QIAGEN, <https://www.qiagen.com>) and used the panbacteria primers U3 and RU8 and thermocycler protocol for 16S PCR, in accordance with Radstrom et al. (33).

Flow Cytometry

Staff of the Immunology Laboratory of České Budějovice Hospital, which acts as a reference laboratory for both participating infectious disease units, performed all tests. We stained EDTA-treated whole blood directly using CYTO-STAT tetraCHROME CD45-FITC (fluorescein isothiocyanate)/CD56-RD1 (phycoerythrin)/CD19-ECD (phycoerythrin-Texas Red-X)/CD3-PC5 (phycoerythrin cyanine 5), anti-CD4-Alexa Fluor 750, and anti-CD8-PC7 (phycoerythrin cyanine 7) (Beckman Coulter, <https://www.beckman-coulter.com>). For the subset of cases in which the CD3+/CD4-/CD8- T-cell percentage appeared high to the reporting bioscientist, the sample was further examined by staining with anti-CD3-FITC (fluorescein isothiocyanate) and anti-T-cell receptor PAN $\gamma\delta$ -PE (phycoerythrin) (Beckman Coulter) on the same day.

We processed samples using either a Cytomics FC500 (before 2014) or Navios (starting in 2013) flow cytometer and CXP (for Cytomics FC500) or Navios software (Beckman Coulter for all). In the first gate, we selected 3,000 lymphocytes on the basis of their CD45 cell surface expression and side scatter characteristics (Figure 1, panel A). Next, we selected the T cells using a B- and T-cell plot gated according to CD19 and CD3 expression (Figure 1, panel B). Then, we identified the percentage of CD3+ T cells that did not express CD4 and CD8 in CD4 versus CD8 plots (Figure 1, panel C). When high percentages of CD3+/CD4-/CD8- T cells were found, we performed a subsequent staining and analysis using anti-CD3-FITC and anti-T-cell receptor PAN $\gamma\delta$ -PE (Figure 1, panel D).

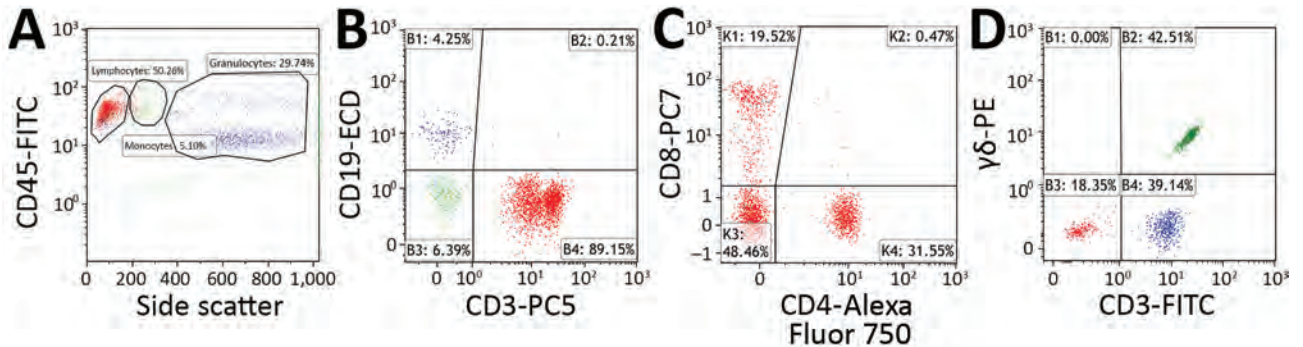


Figure 1. Flow cytometry gating strategy used to determine percentage of CD3+ lymphocytes that are CD3+/CD4–/CD8– T cells and $\gamma\delta$ T cells in peripheral blood samples acquired from patients with suspected tularemia, Czech Republic, 2003–2015. A–C) Staining with CYTO-STAT tetraCHROME CD45-FITC/CD56-RD1 (phycoerythrin)/CD19-ECD/CD3-PC5, anti-CD4-Alexa Fluor 750, and anti-CD8-PC7 (Beckman Coulter, <https://www.beckmancoulter.com>). A) CD45 versus side scatter plot. Percentages of lymphocytes (red), monocytes (green), and granulocytes (blue) are indicated. In total, 3,000 lymphocytes were selected for further analysis. B) B cells (blue) and T cells (red) plotted according to their CD19 and CD3 expression. Percentages of cells within each quadrant are indicated. T cells were selected for further analysis. C) Percentage of CD3+ T cells not displaying CD4 and CD8 (CD4–/CD8–) determined with CD4 versus CD8 plots. Percentages of cells within each quadrant are indicated. D) Staining with anti-CD3-FITC and anti-T-cell receptor PAN $\gamma\delta$ -PE (Beckman Coulter). After a side scatter and forward scatter plot (not shown), the percentage of lymphocytes that were CD3+/ $\gamma\delta$ T cells (green) was determined with a CD3 versus T-cell receptor PAN- $\gamma\delta$ plot. Percentages of cells within each quadrant are indicated. Flow cytometry was performed in the Immunology Laboratory of České Budějovice Hospital (České Budějovice, Czech Republic). ECD, phycoerythrin-Texas Red-X; FITC, fluorescein isothiocyanate; PC, phycoerythrin cyanine; PE, phycoerythrin.

Statistical Methods and Ethics Review

We tested the correlation between CD3+/CD4–/CD8– and $\gamma\delta$ T cells in tularemia cases using the Spearman correlation coefficient. To examine cell count differences by diagnosis (probable vs. confirmed), we used the Mann-Whitney U test. To test differences among the different clinical manifestations, we used the Kruskal-Wallis test.

We compared the percentage of CD3+ lymphocytes with a CD4–/CD8– phenotype between the tularemia and control group patients. In the next analysis, we compared the timing of the first elevation of CD3+/CD4–/CD8– T cells with that of the first positive serologic test result for tularemia both relative to the reported day of symptom onset. We presented these results using medians and other nonparametric rank statistics. We evaluated the difference in percentage of CD3+/CD4–/CD8– T cells between tularemia cases and controls by the Mann-Whitney U test. To assess the predictive ability of flow cytometry, we generated a receiver operating characteristic (ROC) curve and calculated the area under the ROC curve. We determined the cutoff value yielding the highest sensitivity and specificity by using the Youden index (34).

We examined the difference in days between symptom onset to elevated CD3+/CD4–/CD8– percentage (using the cutoff value determined by the ROC curve) and symptom onset to first positive serologic test result by Wilcoxon signed rank test. We present all statistical parameters with their respective 95% CIs. We performed statistical analyses using IBM SPSS Statistics 24.0 (IBM Corp., <https://www.ibm.com>) and considered p values <0.05 significant. The post hoc test power was >80% in all tests.

The ethics committee at České Budějovice Hospital reviewed the study protocol and approved this study on December 20, 2013 (reference no. 17/2013). Consent of patients was not required for case note review.

Results

Tularemia Case Group

During 2003–2015, we performed serologic tests for tularemia for 5,198 patients, and 89 patients had positive test results (Figure 2). After exclusion of 9 patients with missing case notes, 3 with resolved past infection, and 13 with missing flow cytometry results, 64 patients with tularemia had all the required information available for the same illness episode and could be included in the tularemia case group. Of 64 cases, 22 were defined as probable and 42 as confirmed (1 case positive by blood culture with a titer $\geq 1:160$, 1 case positive by PCR with a seroconversion to titer <1:160, 13 cases of titer $\geq 1:160$ including 7 seroconverters, and 27 cases of seroconversion to a titer <1:160) (Table 1).

Patients were treated according to local protocol with a drug combination of doxycycline and gentamicin or ciprofloxacin. Excision of a lymph node was necessary for 26.6% (17/64) of patients. All tularemia patients survived; median time to recovery was 50 (range 20–260) days. Five (7.8%) patients experienced a relapse and needed a second or prolonged course of antimicrobial drugs; 2 of these patients were treated with ciprofloxacin for <7 days and the remaining 3 with doxycycline and gentamicin for 3 weeks. The 3 patients needing prolonged drug treatment also

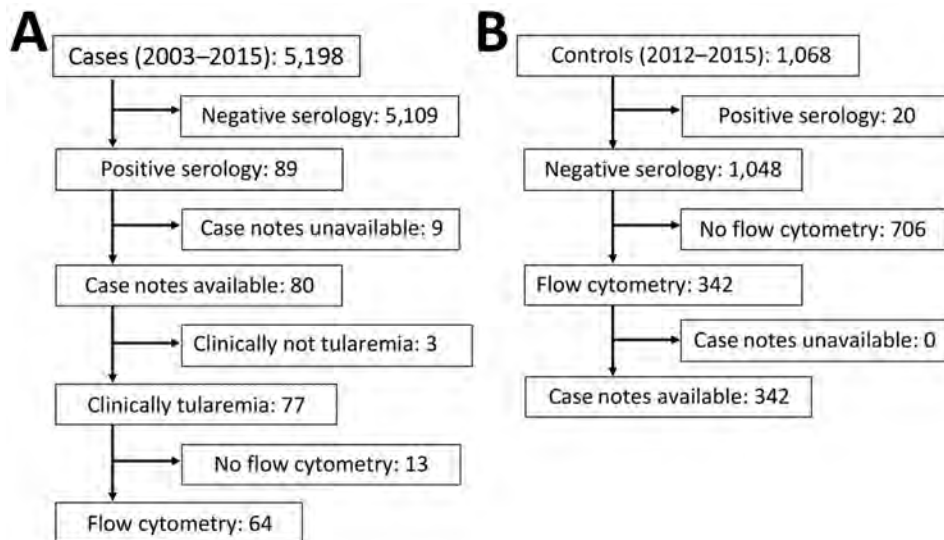


Figure 2. Selection of tularemia cases (2003–2015) and controls (2012–2015) in investigation of whether $\gamma\delta$ T cells or CD3+/CD4-/CD8- T cells can be used for early presumptive tularemia diagnosis, Czech Republic.

required drainage of progressive purulent lymphadenopathy at the end of therapy.

Control Group

During 2012–2015, tularemia serologic tests were performed for 1,068 consecutive adults; 20 of these patients had positive test results, 19 of whom had flow cytometry data available and were thus included in the tularemia case group. Of the remaining 1,048 patients with negative serologic test results, 342 had both case notes and flow cytometry results available. These patients, with various final diagnoses (Table 2), constituted the control group (Figure 2).

Patients in the case group (median age 45 [range 16–66] years) were older than those in the control group (median age 36 [range 12–85] years; $p < 0.0001$). More patients were male in the case group (67.2%, 43/64) than the control group (47.4%, 162/342; $p = 0.004$). All patients were white.

Percentage of CD3+ T Cells with CD4-/CD8- Phenotype in Peripheral Blood Samples

The Spearman correlation coefficient of the plot of the CD3+/CD4-/CD8- T-cell and $\gamma\delta$ T-cell percentages (in 48/64 tularemia cases where both parameters were known) was 0.830 (95% CI 0.679–0.906; $p < 0.0001$) (Figure 3). This strong-positive correlation suggests these 2 measures

can be used interchangeably. The percentages of these T cells did not differ by type of tularemia diagnosis (probable vs. confirmed; Mann-Whitney U test, $p = 0.102$ for CD3+/CD4-/CD8- and $p = 0.364$ for $\gamma\delta$). These subpopulations did differ by clinical manifestation (Kruskal-Wallis test, $p = 0.041$ for CD3+/CD4-/CD8- and $p = 0.033$ for $\gamma\delta$) (Figure 4), but the subgroups were too small for further analysis. Because of these results and the small sample size, we used the whole group of 64 probable and confirmed tularemia cases in further analyses.

The percentage of CD3+/CD4-/CD8- T cells was higher in the case group (median 19%, 95% CI 17%–22%, interquartile range 13%–26%) than the control group (median 3%, 95% CI 2%–3%, interquartile range 1%–5%; Mann-Whitney U = 652.5, $Z = -12.02$, $p < 0.0001$) (Figure 5). The area under the ROC curve assessing the sensitivity and specificity of this flow cytometry-based diagnostic test was 0.970 (95% CI 0.952–0.988). The optimum cutoff CD3+/CD4-/CD8- T-cell percentage was 8%, and with this cutoff, the sensitivity was 95.3% (95% CI 88.0%–98.7%) and specificity was 89.5% (95% CI 85.9%–92.4%) for discriminating between cases and controls (Figure 6). Among our cohort, 61 (95.3%) tularemia patients and 36 (10.5%) controls had a peripheral blood CD3+/CD4-/CD8- T-cell percentage $\geq 8\%$ (Table 2).

Timing in Rise of CD3+/CD4-/CD8- T-Cell Percentage and First Positive Serologic Test Result

The time of symptom onset was known for 58 of 61 tularemia patients with CD3+/CD4-/CD8- T-cell percentages $\geq 8\%$. Among these 58 patients, the increased CD3+/CD4-/CD8- T-cell percentage preceded the first positive serologic test result by a median of 7 (95% CI 1.0–12.0) days (Wilcoxon signed rank test $Z = -4.796$; $p < 0.0001$) (Table 3; Figure 7). In the subset of tularemia patients in whom an elevated

Table 1. Clinical disease manifestation of tularemia patients, by type of diagnosis, Czech Republic, 2003–2015

Manifestation	No. probable cases, n = 22	No. confirmed cases, n = 42	No. (%) total cases, n = 64*
Ulceroglandular	7	22	29 (45.3)
Glandular	6	4	10 (15.6)
Oroglandular	2	7	9 (14.1)
Pulmonary	5	4	9 (14.1)
Typhoidal	2	5	7 (11.0)

*Percentages do not total 100% because of rounding.

Table 2. Final diagnoses of 342 control group patients with negative serologic test results for tularemia and percentages of controls with elevated CD3+/CD4-/CD8- T cells, Czech Republic, 2012–2015*

Diagnosis	No. (%) controls†	No. (%) with elevated CD3+/CD4-/CD8- T cells
Nonspecific resolving lymphadenitis	99 (28.9)	7 (7.1)
Fever of unknown origin or fatigue	44 (12.9)	2 (4.5)
Epstein-Barr virus or cytomegalovirus	26 (7.6)	3 (11.5)
Lymphoma or cancer	26 (7.6)	1 (3.8)
<i>Chlamydia</i> or <i>Mycoplasma</i> respiratory infection	25 (7.3)	5 (20.0)
Recurring or nonresolving tonsilitis	17 (5.0)	4 (23.5)
Toxoplasmosis	16 (4.7)	5 (31.3)
Other‡	89 (26.0)	9 (10.1)§

*The percentage of the CD3+ T cells with a CD4-/CD8- phenotype was measured by flow cytometry and 8% was used as the cutoff value to define an elevated percentage. ANCA, anti-neutrophil cytoplasmic antibody.

†Percentages do not total 100% because of rounding.

‡Other diagnoses: 8 cases each of cellulitis or skin abscess and lower respiratory tract infection or pneumonia; 5 cases of bartonellosis; 4 cases each of ANCA-positive vasculitis, leptospirosis, purulent sialadenitis, reactive arthritis (urethritis *C. trachomatis*), and tick-borne encephalitis; 3 cases of cervical cyst; 2 cases each of HIV, human granulocytic anaplasmosis, other reactive arthritis, polymyalgia rheumatica, sarcoidosis, systemic lupus erythematosus, toxocariasis, and viral meningitis; and 1 case each of acute sinusitis, ankylosing spondylitis, bacterial endocarditis, Behçet disease, cholangitis, deep vein thrombosis, dental abscess, erythema nodosum, farmer’s lung, hantavirus, herpetic tonsilitis, hidradenitis suppurativa, hyperthyroidism, hypothyroidism, legionellosis, lipoma, liver abscess, Lyme disease, mumps, necrotizing lymphadenitis of Kikuchi-Fujimoto, nonspecific hepatitis, parvovirus B19, pertussis, recurrent bacterial conjunctivitis, rickettsial disease, ulcerative colitis, undetermined tumor of the brain and pancreatic head, urinary tract infection, and *Yersinia enterocolitica* arthritis.

§Includes 2 cases of arthralgia and 1 case each of ANCA-positive vasculitis, brain tumor, liver abscess, pneumocystis pneumonia in the setting of AIDS, rickettsial disease, skin and soft tissue infection, and toxocariasis.

CD3+/CD4-/CD8- T-cell percentage was detected while serology was still negative (58.6%, 34/58), the median delay from rise of CD3+/CD4-/CD8- T cells to positive serologic test result was 14 (95% CI 8–22) days (Table 3).

Comparison of Cases and Controls in 2012–2015 Only

To investigate the possible effects of bias introduced by comparing cases selected from a 13-year period with controls from just the last 4 years of that period, we repeated our analyses with the 19 tularemia patients and 342 controls with full data available who sought treatment during 2012–2015. When we used 8% as the cutoff, we found the percentage of CD3+/CD4-/CD8- T cells was raised in 100% (19/19) of cases and 10.5% (36/342) of controls. The 8% cutoff value had a sensitivity of 100% (95% CI 87.8%–100%) and specificity of 89.5% (95% CI 85.9%–92.4%) for distinguishing tularemia patients from controls seeking treatment during this period.

Discussion

This study confirms results of earlier reports (14,15,35) describing the potential application of flow cytometry to support early presumptive tularemia diagnosis. We showed that CD3+/CD4-/CD8- T cells can be used as a pragmatic surrogate for $\gamma\delta$ T cells in this context. The percentage of CD3+ T cells with the CD4-/CD8- phenotype was 19% in tularemia patients with differing disease presentations and 3% in control patients with a wide variety of infectious and noninfectious conditions. When we used 8% as the cutoff to define elevated CD3+/CD4-/CD8- T cells, we found this flow cytometry–based test was elevated ≥ 7 days before serologic test results became positive and had a sensitivity of 95% and specificity of 89.5% for distinguishing tularemia cases from other illnesses.

Flow cytometry is not routinely used to investigate most infections but is available in centers that care for HIV patients. The CD3+/CD4-/CD8- T-cell percentage is easily measurable and can be performed before patients seroconvert or while awaiting serologic test results (30,36). One of the strengths of this study was that the control group consisted of patients with a wide variety of illnesses, rather than a group of healthy volunteers, as in previous reports. These patients were investigated for possible tularemia as part of routine care over several years, representing real-life practice.

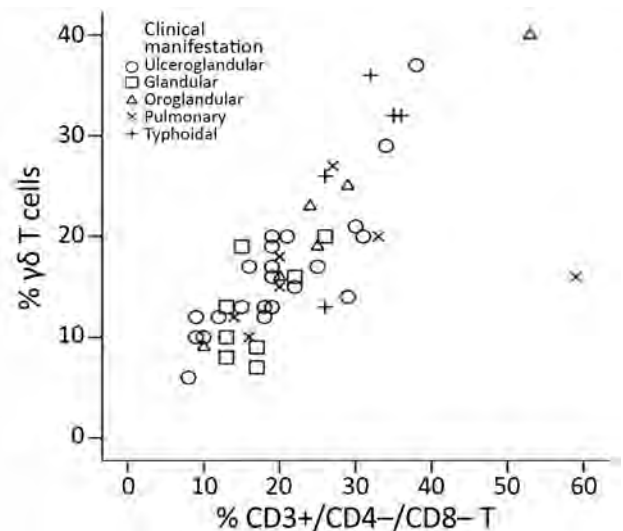
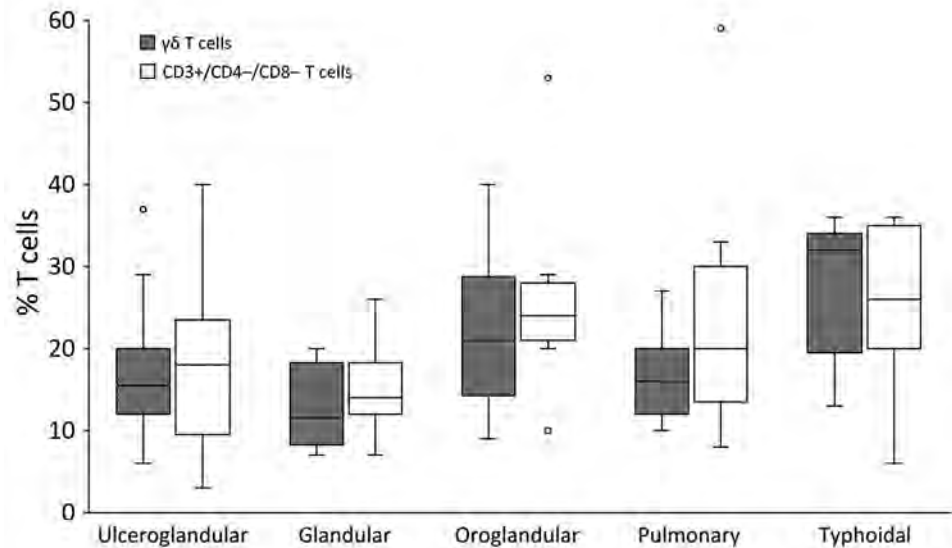


Figure 3. Correlation between percentage of CD3+ lymphocytes that are $\gamma\delta$ T cells and percentage that are CD3+/CD4-/CD8- T cells in peripheral blood samples from patients with confirmed or probable tularemia diagnoses (n = 48), Czech Republic, 2003–2015. The Spearman correlation coefficient of this plot (0.830, 95% CI 0.679–0.906; p<0.0001) indicates a strong correlation and suggests that these T cells can be used interchangeably for tularemia diagnosis.

Figure 4. Percentage of CD3+ lymphocytes that are $\gamma\delta$ T cells and CD3+/CD4-/CD8- T cells in peripheral blood samples from patients with confirmed or probable tularemia by clinical manifestation, Czech Republic, 2003–2015. The percentage of $\gamma\delta$ T cells was determined for 48 cases and percentage of CD3+/CD4-/CD8- T cells for 64 cases. Paired comparisons (Kruskal-Wallis test) reveal no significant differences except for glandular versus typhoidal in $\gamma\delta$ ($p = 0.037$) and CD3+/CD4-/CD8- T cells ($p = 0.041$). Boxes indicate interquartile ranges (IQRs), horizontal lines within boxes indicate medians, whiskers indicate range values $\leq 1.5 \times$ the IQR limits, and circles indicate outliers (i.e., values $> 1.5 \times$ the IQR limits).



Our study was conducted in the Czech Republic, a setting with a low incidence of diseases that might be mistaken for tularemia, such as brucellosis, leptospirosis, Q fever, tuberculosis, or malaria (12); our study conclusions are probably most applicable to settings with low prevalences of the intracellular pathogens that cause these diseases. This study should be repeated in other geographic areas with higher prevalences of these infections (21), which

could decrease the sensitivity and specificity of this test for predicting tularemia diagnoses.

Test results might need to be considered with more caution in less racially homogeneous populations because the reference range of CD3+/CD4-/CD8- T cells can vary by race/ethnicity and age (12). A study conducted in the United States showed a higher baseline percentage of $\gamma\delta$ T cells in healthy white persons (3.7%) than in healthy black persons

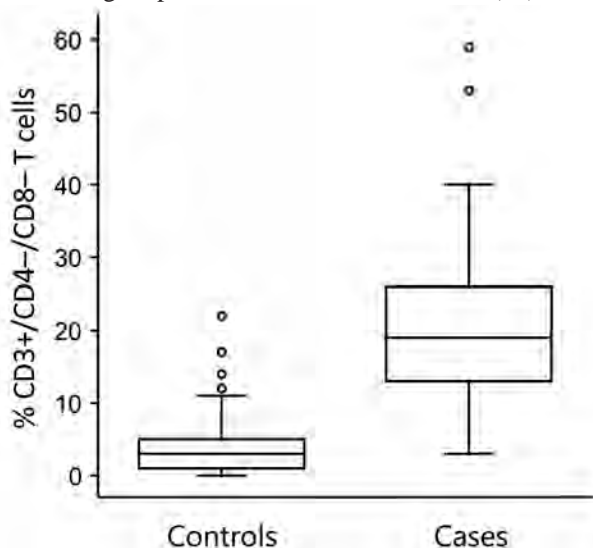


Figure 5. Comparison of percentages of CD3+ lymphocytes with CD4-/CD8- phenotype in peripheral blood samples from patients with probable or confirmed tularemia cases ($n = 64$, 2003–2015) and controls ($n = 342$, 2012–2015), Czech Republic. Boxes indicate interquartile ranges (IQRs), horizontal lines within boxes indicate medians, whiskers indicate range values $\leq 1.5 \times$ the IQR limits, and circles indicate outliers (i.e., values $> 1.5 \times$ times the IQR limits). The percentage of CD3+/CD4-/CD8- T cells is significantly higher in cases than controls (Mann-Whitney U test, $p < 0.0001$).

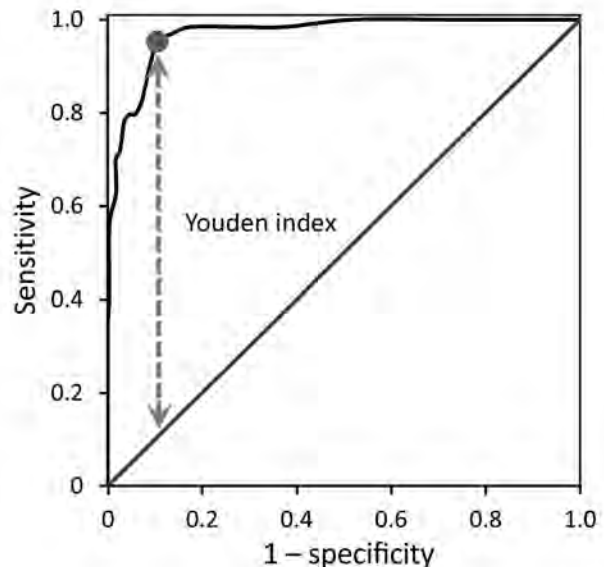


Figure 6. Receiver operating characteristic curve for diagnostic utility of raised CD3+/CD4-/CD8- T cells distinguishing probable and confirmed tularemia cases ($n = 64$, 2003–2015) from controls ($n = 342$, 2012–2015), Czech Republic. The area under the receiver operating characteristic curve is 0.970 (95% CI 0.952–0.988). The Youden index (circle on curve) is the maximal vertical distance (dashed line) of the curve from the diagonal line.

Table 3. Time to positive diagnostic test result for tularemia, by starting time point, test, and population, Czech Republic, 2003–2015*

Category	Time, d			
	Median	95% CI	Interquartile range	Range
Time relative to onset of patient symptoms				
Diagnostic test type				
Flow cytometry, n = 58	18.5	15.5–22.0	9.75–33.25	2–128
Serologic test, n = 58	29.5	24.0–37.0	21.0–42.0	2–140
Time to first positive serologic test result relative to rise in CD3+/CD4-/CD8- T cells				
Patient population				
All, n = 58	7.0	1.0–12.0	0–18.75	-50 to 62
Delayed seroconverters, n = 34	14.0	8.0–22.0	7.5–22.0	1–62

*A positive flow cytometry test result for tularemia was defined as $\geq 8\%$ of peripheral blood CD3+ T cells having the CD4-/CD8- phenotype. A positive serologic test result for tularemia included probable and confirmed diagnoses and was defined for probable cases as an antibody titer of $\geq 1:20$ in any acute phase blood sample or for confirmed cases as an antibody titer of $\geq 1:160$ in any blood sample or a seroconversion from negative to positive (any titer) or a 4-fold increase in titer between acute and convalescent patient samples (agglutination test; Tularemia Diagnostic Set, Bioveta a.s., <https://www.bioveta.eu>).

(1.18%) (11), and a study in Sweden indicated a lower percentage in persons from Sweden (4.2%) and Japan (4.5%) than from Bangladesh (9.2%) or Turkey (9.3%) (10). Higher percentages of $\gamma\delta$ T cells in inhabitants of West Africa might be a result of priming during childhood with malaria parasites (37). Likewise, a higher percentage of baseline $\gamma\delta$ T cells in populations of Turkey might be caused by Turkey's higher prevalence of latent tuberculosis compared with central Europe (10). The CD3+/CD4-/CD8- T-cell percentage might be valuable to use as a generic marker for intracellular infections when investigating fever of unknown origin, although specificity might not be adequate because these percentages can also be elevated in association with some cancers (12).

Because of the relative rarity of tularemia, we used a retrospective design to enroll sufficient numbers of tularemia patients into this pilot study, and adequate details were not available for 26% (22/86) of patients. However, the spectrum of clinical presentations of those included is representative of tularemia patients in other published series in the Czech Republic (38) and elsewhere (4,7), and bias seems unlikely. The mix of final diagnoses in the control group gives reasonable confidence that other intracellular infections, cancers, and noninfectious causes of fever and lymphadenopathy did not substantially contribute to false-positive early presumptive tularemia diagnoses.

We used the data of tularemia patients treated during 2003–2015 and control patients treated during 2012–2015. The use of patients from different periods might have introduced selection bias, but this bias should have been mitigated by the large number of control patients included with complete data available and by the variety of control patient illnesses. That this bias was minimal is supported by the reproducibility of our findings when we performed a comparative analysis restricted to just the tularemia patients and controls treated during 2012–2015.

Serology has been and remains the standard test for tularemia diagnosis for many disease presentations. Other diagnostic tests have drawbacks. The organism is difficult to culture, as demonstrated by only 1 case in this series having a positive blood culture result. Although PCR with an ulcer swab sample

resulted in DNA amplification in 1 case, PCR amplification failed in other cases. Also, only 45.4% of our patient cohort had an easily accessible lesion to swab. We believe that flow cytometry can contribute to tularemia diagnosis better than these other available tests with minimal invasiveness and cost, even when PCR methods become more widely available. In addition, the expansion in the use of PCR will not result in faster tularemia diagnosis because the clinician still needs to suspect tularemia before requesting this test be performed. However, PCR could be used as a confirmatory test for cases with elevated percentages of CD3+/CD4-/CD8- T cells.

The retrospective nature of this study limited our investigations regarding the timing of CD3+/CD4-/CD8- T-cell elevations and *F. tularensis* antibody titer increases in relation to the onset of patient symptoms. In all cases, the flow cytometry test result recorded was that from the first flow cytometry test performed. In contrast, for tularemia serology, the first positive serologic test result was recorded. Most tests were requested when the differential diagnosis first included tularemia. In a small proportion of patients, flow cytometry was performed after a positive serologic test result for tularemia was communicated to the physician; thus, for these patients, flow cytometry results were delayed. The time from symptom onset to elevation of CD3+/CD4-/CD8- T cells that we report does not reflect the timing this cell population increases and how soon this flow cytometry-based diagnostic test can be performed. In addition, in some cases, the diagnostic work-up for tularemia was delayed because of delayed referral of patients to the infectious diseases unit of the hospital. Therefore, we cannot comment on the reliability of the flow cytometry-based method during the first week after symptom onset.

In our study, the rise in the percentage of CD3+/CD4-/CD8- T cells preceded seroconversion even in patients with late referrals. Seroconversion was documented in 53.1% (34/64) of patients with tularemia, many of whom had been treated for tularemia on the basis of raised CD3+/CD4-/CD8- T-cell percentages and were monitored until seroconversion or an alternative diagnosis was obtained.

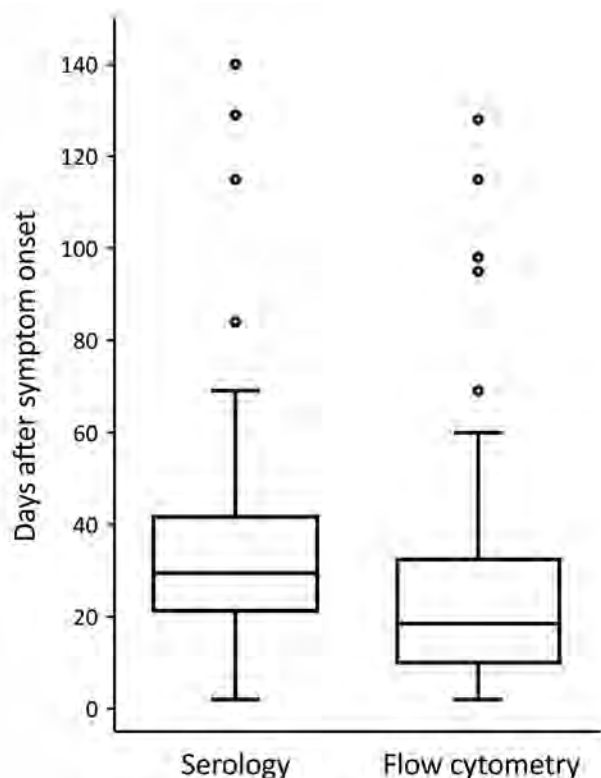


Figure 7. Comparison of time to first positive serologic test result for tularemia and time to raised CD3+/CD4-/CD8- T-cell percentage determined by flow cytometry relative to the time of symptom onset of 58 patients with probable or confirmed tularemia, Czech Republic, 2003–2015. Percentages of CD3+/CD4-/CD8- T cells $\geq 8\%$ were considered raised. A positive serologic test result for tularemia was defined for probable cases as an antibody titer of $\geq 1:20$ in any acute phase blood sample and for confirmed cases as a single antibody titer of $\geq 1:160$ in any blood sample or a seroconversion from negative to positive (any titer) or a 4-fold increase in titer between acute and convalescent patient samples (agglutination test; Tularemia Diagnostic Set, Bioveta a.s., <https://www.bioveta.eu>). Boxes indicate interquartile ranges (IQRs), horizontal lines within boxes indicate medians, whiskers indicate range values $\leq 1.5 \times$ the IQR limits, and circles indicate outliers (i.e., values $> 1.5 \times$ the IQR limits). The CD3+/CD4-/CD8- T cells increased before *Francisella tularensis*-specific antibody titers increased (Wilcoxon signed rank test, $p < 0.0001$).

Including flow cytometry in the tularemia work-up for our cohort contributed to the high percentage of diagnoses confirmed by seroconversion (53.1%), which was much higher than those of other cohorts: 0% in Missouri, USA (7), and Turkey (30); 5% (5/101) in France (8); 35% (9/26) in Sweden (39); and 13.4% (19/142) in Spain (40).

In 25% of the tularemia cases (Table 3), the time from symptom onset to first positive serologic test result was ≥ 22 days, occurring ≥ 14 days after the detection of an elevated CD3+/CD4-/CD8- T-cell percentage, which lends strong support to the use of flow cytometry to identify suspected cases for empirical treatment. Because tularemia might not

have pathognomonic manifestations, adding an extra tube for flow cytometry as part of the diagnostic work-up can help physicians make decisions regarding whether to treat a given health condition as tularemia in cases where serologic results are still negative and the team is waiting for PCR or blood culture results.

In conclusion, in the Czech Republic, flow cytometry analyses of peripheral blood samples showing a percentage of CD3+/CD4-/CD8- T cells $\geq 8\%$ supports a presumptive clinical diagnosis of tularemia and initiation of specific antimicrobial therapy days to weeks before the diagnosis can be confirmed serologically. This more rapid test is a useful addition to the diagnostic work-up for tularemia that can help public health teams managing waterborne outbreaks and inhalation infection clusters speed up diagnosis and treatment and thus contain pathogen spread. In hospital settings, the rapid diagnosis of tularemia afforded with this test might indicate the need for Biosafety Level 3 facilities, required for *F. tularensis* propagation, thereby reducing occupational health risk.

Acknowledgments

The authors are pleased to acknowledge Věra Bártová and Zdeňka Vrajová, who pioneered the use of flow cytometry as a tool to assist in diagnosis of tularemia (28), despite initial skeptical voices of some co-authors of this study.

About the Author

Dr. Chrdle is an infectious disease specialist at the České Budějovice Hospital, České Budějovice, Czech Republic, and the Royal Liverpool University Hospital, Liverpool, UK. His clinical and research interests include *Staphylococcus aureus* bacteremia and zoonotic infections, especially tick-borne encephalitis, Lyme disease, and tularemia.

References

- McCoy GW, Chapin CW. Further observations on a plague-like disease of rodents with a preliminary note on the causative agent, *Bacterium tularensis*. *J Infect Dis*. 1912;10:61–72. <https://doi.org/10.1093/infdis/10.1.61>
- European Centre for Disease Prevention and Control. Tularamia-annual epidemiological report 2016. 2019 Jan 22 [cited 2018 Dec 7]. https://ecdc.europa.eu/sites/portal/files/documents/AER_for_2016-tularamia.pdf
- Sjöstedt A. Tularemia: history, epidemiology, pathogen physiology, and clinical manifestations. *Ann N Y Acad Sci*. 2007;1105:1–29. <https://doi.org/10.1196/annals.1409.009>
- Maurin M, Gyuranez M. Tularamia: clinical aspects in Europe. *Lancet Infect Dis*. 2016;16:113–24. [https://doi.org/10.1016/S1473-3099\(15\)00355-2](https://doi.org/10.1016/S1473-3099(15)00355-2)
- Yapar D, Erenler AK, Terzi Ö, Akdoğan Ö, Ece Y, Baykam N. Predicting tularamia with clinical, laboratory and demographical findings in the ED. *Am J Emerg Med*. 2016;34:218–21. <https://doi.org/10.1016/j.ajem.2015.10.034>
- Tuncer E, Onal B, Simsek G, Elagoz S, Sahpaz A, Kilic S, et al. Tularamia: potential role of cytopathology in differential diagnosis of cervical lymphadenitis: multicenter experience in 53 cases and literature review. *APMIS*. 2014;122:236–42. <https://doi.org/10.1111/apm.12132>

7. Weber IB, Turabelidze G, Patrick S, Griffith KS, Kugeler KJ, Mead PS. Clinical recognition and management of tularemia in Missouri: a retrospective records review of 121 cases. *Clin Infect Dis*. 2012;55:1283–90. <https://doi.org/10.1093/cid/cis706>
8. Maurin M, Pelloux I, Brion JP, Del Banõ JN, Picard A. Human tularemia in France, 2006–2010. *Clin Infect Dis*. 2011;53:e133–41. <https://doi.org/10.1093/cid/cir612>
9. Chu M, Elkins K, Nano F, Titball R. Considerations for handling *F. tularensis*. In: Tärnvik A, editor. WHO guidelines on tularaemia. Geneva: World Health Organization; 2007 [cited 2018 Dec 7]. https://www.who.int/csr/resources/publications/WHO_CDS_EPR_2007_7.pdf?ua=1
10. Esin S, Shigematsu M, Nagai S, Eklund A, Wigzell H, Grunewald J. Different percentages of peripheral blood $\gamma\delta^+$ T cells in healthy individuals from different areas of the world. *Scand J Immunol*. 1996;43:593–6. <https://doi.org/10.1046/j.1365-3083.1996.d01-79.x>
11. Cairo C, Armstrong CL, Cummings JS, Deetz CO, Tan M, Lu C, et al. Impact of age, gender, and race on circulating $\gamma\delta$ T cells. *Hum Immunol*. 2010;71:968–75. <https://doi.org/10.1016/j.humimm.2010.06.014>
12. Bank I, Marcu-Malina V. Quantitative peripheral blood perturbations of $\gamma\delta$ T cells in human disease and their clinical implications. *Clin Rev Allergy Immunol*. 2014;47:311–33. <https://doi.org/10.1007/s12016-013-8391-x>
13. Cibulka M, Selingerová I, Fědorová L, Zdražilová Dubská L. Immunological aspects in oncology—circulating $\gamma\delta$ T-cells [in Czech]. *Klin Onkol*. 2015;28:2S60–8. <http://dx.doi.org/10.14735/amko20152S60>
14. Sumida T, Maeda T, Takahashi H, Yoshida S, Yonaha F, Sakamoto A, et al. Predominant expansion of V γ 9/V δ 2 T cells in a tularemia patient. *Infect Immun*. 1992;60:2554–8.
15. Kroca M, Tärnvik A, Sjöstedt A. The proportion of circulating $\gamma\delta$ T cells increases after the first week of onset of tularaemia and remains elevated for more than a year. *Clin Exp Immunol*. 2000;120:280–4. <https://doi.org/10.1046/j.1365-2249.2000.01215.x>
16. Chen ZW, Letvin NL. V γ 2V δ 2⁺ T cells and anti-microbial immune responses. *Microbes Infect*. 2003;5:491–8. [https://doi.org/10.1016/S1286-4579\(03\)00074-1](https://doi.org/10.1016/S1286-4579(03)00074-1)
17. Tsukaguchi K, Balaji KN, Boom WH. CD4⁺ alpha beta T cell and gamma delta T cell responses to *Mycobacterium tuberculosis*. Similarities and differences in Ag recognition, cytotoxic effector function, and cytokine production. *J Immunol*. 1995;154:1786–96.
18. Kroca M, Johansson A, Sjöstedt A, Tärnvik A. V γ 9V δ 2 T cells in human legionellosis. *Clin Diagn Lab Immunol*. 2001;8:949–54.
19. Hara T, Mizuno Y, Takaki K, Takada H, Akeda H, Aoki T, et al. Predominant activation and expansion of V gamma 9-bearing gamma delta T cells in vivo as well as in vitro in *Salmonella* infection. *J Clin Invest*. 1992;90:204–10. <https://doi.org/10.1172/JCI115837>
20. Bertotto A, Gerli R, Spinozzi F, Muscat C, Scalise F, Castellucci G, et al. Lymphocytes bearing the $\gamma\delta$ T cell receptor in acute *Brucella melitensis* infection. *Eur J Immunol*. 1993;23:1177–80. <https://doi.org/10.1002/eji.1830230531>
21. Kilic SS, Akbulut HH, Ozden M, Bulut V. Gamma/delta T cells in patients with acute brucellosis. *Clin Exp Med*. 2009;9:101–4. <https://doi.org/10.1007/s10238-008-0021-1>
22. Caldwell CW, Everett ED, McDonald G, Jesus YW, Roland WE. Lymphocytosis of $\gamma\delta$ T cells in human ehrlichiosis. *Am J Clin Pathol*. 1995;103:761–6. <https://doi.org/10.1093/ajcp/103.6.761>
23. Schneider T, Jahn HU, Liesenfeld O, Steinhoff D, Riecken EO, Zeitz M, et al. The number and proportion of V γ 9V δ 2 T cells rise significantly in the peripheral blood of patients after the onset of acute *Coxiella burnetii* infection. *Clin Infect Dis*. 1997;24:261–4. <https://doi.org/10.1093/climids/24.2.261>
24. Scalise F, Gerli R, Castellucci G, Spinozzi F, Fabietti GM, Crupi S, et al. Lymphocytes bearing the gamma delta T-cell receptor in acute toxoplasmosis. *Immunology*. 1992;76:668–70.
25. Russo DM, Armitage RJ, Barral-Netto M, Barral A, Grabstein KH, Reed SG. Antigen-reactive gamma delta T cells in human leishmaniasis. *J Immunol*. 1993;151:3712–8.
26. Perera MK, Carter R, Goonewardene R, Mendis KN. Transient increase in circulating gamma/delta T cells during *Plasmodium vivax* malarial paroxysms. *J Exp Med*. 1994;179:311–5. <https://doi.org/10.1084/jem.179.1.311>
27. Schwartz E, Rosenthal E, Bank I. Gamma delta T cells in non-immune patients during primary schistosomal infection. *Immun Inflamm Dis*. 2014;2:56–61. <https://doi.org/10.1002/iid3.18>
28. Bártová V, Žampach P. Certain immune parameters in tularemia [in Czech]. *Klin Mikrobiol Infekc Lek*. 2000;6: 77–8.
29. Mailles A, Vaillant V. 10 years of surveillance of human tularaemia in France. *Euro Surveill*. 2014;19:20956. <https://doi.org/10.2807/1560-7917.ES2014.19.45.20956>
30. Erdem H, Ozturk-Engin D, Yesilyurt M, Karabay O, Elaldi N, Celebi G, et al. Evaluation of tularaemia courses: a multicentre study from Turkey. *Clin Microbiol Infect*. 2014;20:O1042–51. <https://doi.org/10.1111/1469-0691.12741>
31. Centers for Disease Control and Prevention. Tularemia (*Francisella tularensis*). 1999 case definition. [cited 2018 Aug 29]. <https://wwwn.cdc.gov/nndss/conditions/tularemia/case-definition/1999>
32. Centers for Disease Control and Prevention. Tularemia (*Francisella tularensis*). 2017 case definition. [cited 2018 Aug 29]. <https://wwwn.cdc.gov/nndss/conditions/tularemia/case-definition/2017>
33. Rådström P, Bäckman A, Qian N, Kraggsbjerg P, Pålsson C, Olcén P. Detection of bacterial DNA in cerebrospinal fluid by an assay for simultaneous detection of *Neisseria meningitidis*, *Haemophilus influenzae*, and streptococci using a seminested PCR strategy. *J Clin Microbiol*. 1994;32:2738–44.
34. Youden WJ. Index for rating diagnostic tests. *Cancer*. 1950;3:32–5. [http://dx.doi.org/10.1002/1097-0142\(1950\)3:1<32::AID-CNCR2820030106>3.0.CO;2-3](http://dx.doi.org/10.1002/1097-0142(1950)3:1<32::AID-CNCR2820030106>3.0.CO;2-3)
35. Poquet Y, Kroca M, Halary F, Stenmark S, Peyrat MA, Bonnetville M, et al. Expansion of V γ 9V δ 2 T cells is triggered by *Francisella tularensis*-derived phosphoantigens in tularemia but not after tularemia vaccination. *Infect Immun*. 1998;66:2107–14.
36. Bulut OC, Dyckhoff G, Spletstoesser W, Nemeth J, Klauschen F, Penzel R, et al. Unmasked: when a clinically malignant disease turns out infectious. A rare case of tularemia. *Int J Surg Pathol*. 2013;21:76–81. <https://doi.org/10.1177/1066896912448424>
37. Hviid L, Akanmori BD, Loizon S, Kurtzhals JA, Ricke CH, Lim A, et al. High frequency of circulating $\gamma\delta$ T cells with dominance of the V δ 1 subset in a healthy population. *Int Immunol*. 2000;12:797–805. <https://doi.org/10.1093/intimm/12.6.797>
38. Černý Z. Changes of the epidemiology and the clinical picture of tularemia in Southern Moravia (the Czech Republic) during the period 1936–1999. *Eur J Epidemiol*. 2001;17:637–42. <https://doi.org/10.1023/A:1015551213151>
39. Strålin K, Eliasson H, Bäck E. An outbreak of primary pneumonic tularemia. *N Engl J Med*. 2002;346:1027–9. <https://doi.org/10.1056/NEJM200203283461316>
40. Pérez-Castrillón JL, Bachiller-Luque P, Martín-Luquero M, Mena-Martín FJ, Herreros V. Tularemia epidemic in northwestern Spain: clinical description and therapeutic response. *Clin Infect Dis*. 2001;33:573–6. <https://doi.org/10.1086/322601>

Address for correspondence: Aleš Chrdle, České Budějovice Hospital, a.s., Department of Infectious Diseases, B Němcově 54, 37001 České Budějovice, Czech Republic; email: chrdle@email.cz

Control and Elimination of Extensively Drug-Resistant *Acinetobacter baumannii* in an Intensive Care Unit

Amanda Chamieh,¹ Tania Dagher Nawfal,¹
Tala Ballouz,¹ Claude Afif, George Juvelekian,
Sani Hlais, Jean-Marc Rolain, Eid Azar

We decreased antimicrobial drug consumption in an intensive care unit in Lebanon by changing to colistin monotherapy for extensively drug-resistant *Acinetobacter baumannii* infections. We saw a 78% decrease of *A. baumannii* in sputum and near-elimination of *bla*_{oxa-23}-carrying sequence type 2 clone over the 1-year study. Non-*A. baumannii* multidrug-resistant infections remained stable.

The antimicrobial stewardship program (ASP) at Saint Georges Hospital University Medical Center (SGHUMC), a 400-bed tertiary-care center in Beirut, Lebanon, requires an infectious disease (ID) specialist to preauthorize use of restricted broad-spectrum antimicrobial drugs. The ASP regularly monitors the rate of nosocomial infections and the total hospital antimicrobial drug consumption. In the first quarter of 2015, the incidence of extensively drug-resistant (XDR) *Acinetobacter baumannii* bloodstream infections reached its highest level, 0.47/1,000 patient-days (1). Since 2012, the monthly carbapenem consumption increased steadily, reaching 130 defined daily doses (DDD)/1,000 patient-days in 2015, an absolute increase of 30 DDD/1,000 patient-days during that time. Severely ill patients with predisposing conditions are more likely to develop difficult-to-treat *A. baumannii* infections. Despite the existing controversy, this patient population routinely is treated with a carbapenem/colistin combination (2–8).

We evaluated 100 nonduplicate XDR *A. baumannii* isolates at SGHUMC and found no synergy between colistin and carbapenem by the checkerboard technique (9). Consequently, SGHUMC withdrew combination therapy for XDR *A. baumannii* infections. Our aim was to evaluate

the effect of a carbapenem-sparing regimen on ICU antimicrobial consumption, clinical outcome, and microbiological flora.

The Study

The ASP, ID team, and intensive care unit (ICU) physicians approved a plan to reduce use of empiric carbapenems in the ICU and use colistin, tigecycline, or both for patients confirmed with or at high risk for *A. baumannii* infections. ID physicians evaluated the clinical severity and hemodynamic stability of each patient and had final discretion to prescribe either colistin or tigecycline.

We included all ICU admissions in the study, even recurrent admissions. This ICU has a multidrug-resistant organism surveillance program that collects a sputum sample for culture every third day for intubated patients with abundant secretions. We used these cultures for our evaluation. We considered any culture sample outside this practice a duplicate and excluded it from our analysis. During the study period, we did not modify infection control practices. The study was approved by the institutional review board of SGHUMC.

We retrieved data from the hospital's computerized ordering system and examined medical records of all ICU admissions during February 1, 2016–January 31, 2017. Clinical data included patient demographics, admission diagnosis, and presence of mechanical ventilation. During February 1–June 30, 2016 (period 1), patients received colistin/carbapenem combination therapy for *A. baumannii* infections. During July 1, 2016–January 31, 2017 (period 2), we applied our intervention. We recorded the total number of bacterial cultures collected from the ICU and noted the site and date of sampling.

We considered the isolation density the number of clinical isolates/1,000 patient-days and the rate of ventilator-associated pneumonia (VAP) the number of VAP events/1,000 patient-days. We defined variables according to guidelines for XDR *A. baumannii* from the US Centers for Disease Control and Prevention and World Health Organization (10). We calculated case-fatality and VAP rates following guidelines from the American Thoracic Society and Infectious Diseases Society of America (11).

Author affiliations: University of Balamand, Beirut, Lebanon (A. Chamieh, T. Ballouz, C. Afif, G. Juvelekian, E. Azar); Aix-Marseille University, Marseille, France (T.D. Nawfal, J.-M. Rolain); Saint Joseph University and American University of Beirut, Beirut (S. Hlais)

DOI: <https://doi.org/10.3201/eid2509.181626>

¹These authors contributed equally to this article.

We grouped antimicrobial drugs into 5 categories: group 1, antimicrobial drugs that do not require ID preapproval, such as third-generation cephalosporins, amoxicillin/clavulanic acid, and quinolones; group 2, oral vancomycin and metronidazole used for *Clostridioides difficile* therapy; group 3, imipenem and meropenem; group 4, broad-spectrum carbapenem-sparing regimens, including piperacillin/tazobactam, cefepime, ceftazidime, amikacin; and group 5, the XDR *A. baumannii*-active antimicrobial drugs colistin and tigecycline. We measured antimicrobial drug consumption by DDD per 1,000 patient-days (Table 1).

We sent 48 laboratory-confirmed *A. baumannii* isolates, 31 collected during period 1 and 17 during period 2, to IHU-Méditerranée Infection, Aix-Marseille, France, for testing. Samples underwent 4 types of testing: matrix-assisted laser desorption/ionization time-of-flight mass spectrometry (Microflex; Bruker Daltonics, <https://www.bruker.com>); antimicrobial susceptibility testing by disk diffusion method and interpreted according to the European Committee of Antimicrobial Susceptibility Testing 2017; real-time PCR to screen for carbapenemase-encoding genes; and multi-locus sequence typing to determine genetic relationships among the isolates.

The ICU admitted 536 patients during the study period; 3 were readmissions. Patient characteristics between the 2 periods were statistically similar (Table 1). Throughout the study, the incidence of *A. baumannii* VAP decreased from 154.9 to 38/1,000 patient-days ($p = 0.007$) and the *A. baumannii* VAP case-fatality ratio dropped from 79 to 12/1,000 patient-days. Non-*A. baumannii* VAP incidence decreased from 62 to 51/1,000 patient-days. ICU mortality rates from all causes remained unchanged between period 1 and period 2 (Table 1).

Consumption of group 1 and group 4 antimicrobial drugs was statistically similar during the 2 periods (Table 1). Carbapenem consumption decreased by 59%, a total of 318 DDD/1,000 patient-days, and overall restricted antimicrobial drug consumption dropped 637 DDD/1,000 patient-days ($p < 0.005$). Because isolation of *A. baumannii* decreased substantially, colistin consumption also decreased by 55%, from 20 DDD/1,000 patient-days in period 1 to 9 DDD/1,000 patient-days in period 2 ($p = 0.019$) (Figure 2). Tigecycline consumption remained statistically unchanged (84 DDD/1,000 patient-days in period 1, 62 DDD/1,000 patient-days in period 2). Of note, group 2 *C. difficile* therapy consumption dropped by 231 DDD/1,000 patient-days ($p = 0.042$), a 51% decrease that likely mirrors reduction in *C. difficile* infections.

The *A. baumannii* isolate density in sputum cultures decreased by 70.7%, from 82 to 24/1,000 patient-days, positively correlating with the fall in carbapenem consumption

($p = 0.004$) (Figure 1). The number of non-*A. baumannii* multidrug-resistant (MDR) isolates did not increase (Figure 2).

All 48 *A. baumannii* isolates carried extended-spectrum β -lactamase bla_{TEM-1} genes. The 31 isolates from period 1 were XDR; 30 carried the class D carbapenemase bla_{oxa-23}

Table 1. Patient demographics, VAP incidence, treatment courses, and antimicrobial drug consumption in study of carbapenem-sparing regimen for XDR *Acinetobacter baumannii* in an ICU, Beirut, Lebanon*

Characteristics	Period 1†	Period 2‡	p value
Patient data			
No. patients	213	324	NA
Sex			
F	79	144	
M	134	180	
Mean age	69	68	
Mean length of hospital stay, d	6.8	6	
Days in ICU	1,128	1,804	
Type of admission			
Medical	163	253	NA
Surgical	50	71	
Admitted from home or ED	73	114	
Transferred from ward	79	141	
Transferred from other hospital	10	16	
Postoperative	51	57	
Intubation			
At admission	64	85	
After admission	14	16	
Outcome			
<i>A. baumannii</i> VAP incidence, %	15	3.7	0.007
Discharged	170	259	
Deceased	43	64	
Total AB VAP events	32	12	
Deceased during VAP	17	4	
ICU mean mortality rate/month, %	20.4	19.3	0.168
AB VAP case fatality ratio, %	7.9	1.2	0.006
No. XDR <i>A. baumannii</i> VAP courses received			
Colistin and carbapenem	17	2	
Colistin and tigecycline	6	2	
Colistin monotherapy	6	6	
Tigecycline	3	2	
Carbapenem consumption, DDD§			
Group 1	333	320	0.465
Group 2	455	224	0.042
Group 3	541	223	<0.005
Group 4	165	145	0.808
Group 5			
Colistin	20	9	<0.019
Tigecycline	84	62	0.570
Total restricted antimicrobial drugs, DDD	1,265	663	<0.005

*Bold indicates statistical significance. DDD, defined daily doses; ED, emergency department; ESBL, extended-spectrum β -lactamase; ICU, intensive care unit; NA, not applicable; VAP, ventilator-associated pneumonia; XDR, extensively drug-resistant.

†During February 1, 2016–June 30, 2016, ICU patients received colistin/carbapenem therapy for *A. baumannii* infections.

‡During July 1, 2016–January 31, 2017, ICU implemented carbapenem-sparing regimen for *A. baumannii* infections.

§Group 1, antimicrobial drugs that do not require infectious disease specialist preapproval, such as third-generation cephalosporins, amoxicillin/clavulanic acid, and quinolones; group 2, oral vancomycin and metronidazole used for *Clostridioides difficile* therapy; group 3, imipenem and meropenem; group 4, broad-spectrum carbapenem-sparing regimens, including piperacillin/tazobactam, cefepime, ceftazidime, amikacin; and group 5, the XDR *A. baumannii*-active antimicrobial drugs colistin and tigecycline.

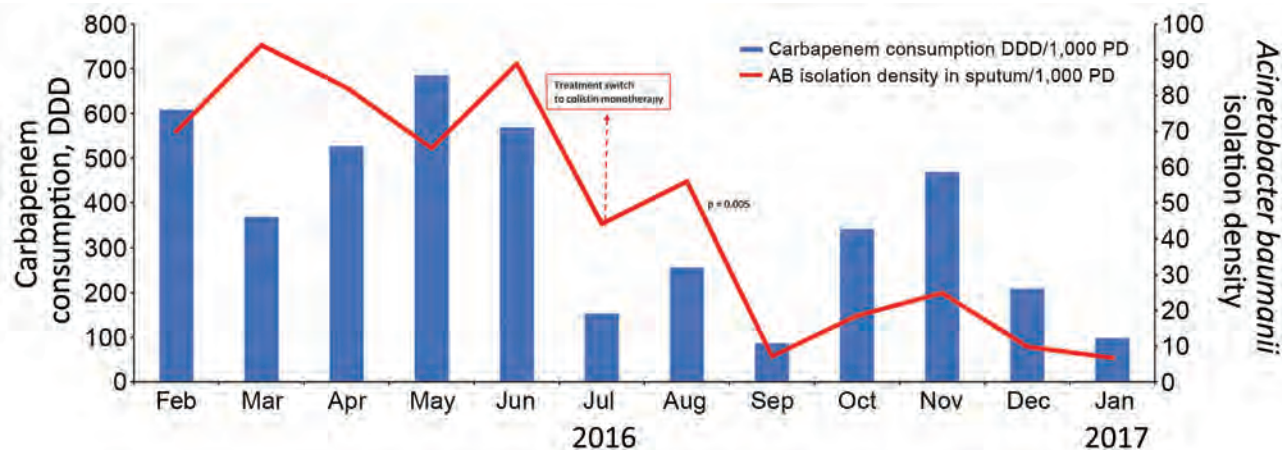


Figure 1. Isolation density of *Acinetobacter baumannii* in sputum cultures versus carbapenem consumption in the intensive care unit (ICU) of Saint Georges Hospital University Medical Center, Beirut, Lebanon, during February 1, 2016–January 31, 2017. Rates are measured per 1,000 patient-days. Dashed arrow represents the beginning of period 2 in which we implemented a carbapenem-sparing regimen. DDD, defined daily dose; PD, patient days.

gene, and 1 carried the *bla*_{oxa-24} gene. Multilocus sequence typing revealed 3 sequence types (STs) in period 1: ST2, 29/31 (93.5%); ST699, 1/31 (3%); and ST627, 1/31 (3%) (Table 2). In period 2, *A. baumannii* ST2 disappeared; 58.8% (10/17) of isolates belonged to ST25 and 5.9% (1/17) belonged to ST99. The remainder belonged to 6 new STs, assigned ST1200, 1201, 1202, 1203, 1204, and 1205 (35.2%). Of the 17 isolates from period 2, 6 carried the *bla*_{oxa-23} gene, 5 the *bla*_{oxa-24} gene, and 3 both genes.

Overall, XDR *A. baumannii* isolation decreased by 64.7% from period 1 to period 2. In addition, isolates from period 2 were more antimicrobial-susceptible than in period 1: 64.8% (11/17) sensitive to ceftazidime and cefepime, 17.6% (3/17) to piperacillin/tazobactam, and 17.6% (3/17) to carbapenems (Table 2).

Conclusions

Our prudent use of antimicrobial drugs did not increase mortality rates and had a dramatic effect on antimicrobial

consumption and MDR *A. baumannii* isolate density. A longer study period and larger sample likely would reveal additional effects on XDR infections and outcomes. Many factors could have affected the study results, including patient referrals and seasonality. However, the microbiological findings strongly point to high rates of carbapenem consumption as a sustaining factor in survival of XDR *A. baumannii* ST2 in our facility. By reducing carbapenem consumption, we broke a vicious cycle.

In the era where clinicians must manage severely ill, MDR-colonized patients, relying on existing guidelines is not enough. A creative, multidisciplinary approach with knowledge of local epidemiology is key to controlling MDR and XDR infections. Investing time in accurate diagnosis and implementing targeted carbapenem-sparing strategies for initial treatment is only possible through trusted collaboration between ID and ICU physicians. The dedication of the ASP and microbiology

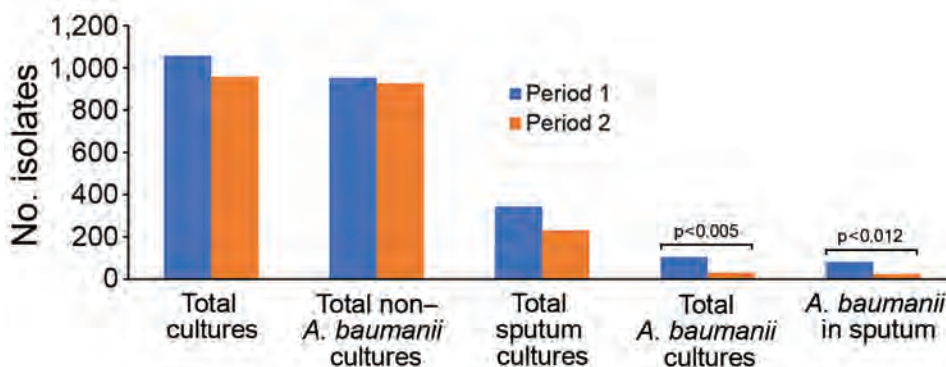


Figure 2. Isolation density of *Acinetobacter baumannii* and non-*A. baumannii* in the intensive care unit (ICU) of Saint Georges Hospital University Medical Center, Beirut, Lebanon, during February 1, 2016–January 31, 2017. Rates are measured in 1,000 patient-days. During period 1, February 1–June 31, 2016, ICU patients received colistin/carbapenem combination therapy for *A. baumannii*. During period 2, July 1, 2016–January 31, 2017, we implemented a carbapenem-sparing regimen in the ICU.

Table 2. Specimen type, site of collection, and microbiologic characteristics in study of carbapenem-sparing regimen for extensively drug-resistant *Acinetobacter baumannii* in an ICU, Beirut, Lebanon*

Specimens and testing	Period 1†	Period 2‡
Specimen type, no.		
Sputum	31	11
Blood	0	3
Wound site or catheter tip	0	3
Site of collection, no.		
Intensive care unit	21	12
Regular floor	10	5
Total no.	31	17
Antimicrobial drug susceptibility testing by disc diffusion, %		
Cefepime/ceftazidime	0	64.7
Piperacillin/tazobactam	0	17.65
Imipenem	0	17.65
Colistin	100	100
Total extensively drug-resistant	100	35.3
Carbapenemase genes, no. (%)§		
ESBL <i>bla</i> _{TEM-1}	31 (100)	17 (100)
<i>bla</i> _{OXA-23}	30 (96.8)	6 (35.3)
<i>bla</i> _{OXA-24}	1 (3.2)	5 (29.4)
<i>bla</i> _{OXA-23} and <i>bla</i> _{OXA-24}	0	3 (17.6)
Sequence type, no. (%)¶		
ST2	29 (93.5)	0
ST699	1 (3.25)	0
ST627	1 (3.25)	0
ST25	0	10 (58.9)
ST99	0	1 (5.8)
New STs, 1200–1206	0	6 (35.3)

*Bold indicates statistical significance. ESBL, extended-spectrum beta-lactamase; ICU, intensive care unit; MLST, multilocus sequence typing; PCR, polymerase chain reaction; ST, sequence type.
†During February 1, 2016–June 30, 2016, ICU patients received colistin/carbapenem therapy for *A. baumannii* infections.
‡During July 1, 2016–January 31, 2017, ICU implemented carbapenem-sparing regimen for *A. baumannii* infections.
§Determined by PCR.
¶Determined by multilocus sequence typing.

departments at this facility is an example of a successful active surveillance program for antimicrobial drug consumption and resistance profiles, especially when developing standards of care tailored to meet an institution's needs.

Acknowledgments

We thank our partners and microbiologists at Méditerranée Infection in Aix-Marseille, France, for conducting antimicrobial susceptibility testing and molecular methods.

About the Author

Dr. Chamieh is an infectious disease specialist and graduate of Saint George Hospital University Medical Center, Beirut, Lebanon, where she is an active member of the Antimicrobial Stewardship and the Infection Control Departments. She is currently pursuing a PhD at Aix-Marseille University, Méditerranée Infection, Marseille, France, in microbiology, with a research focus on antimicrobial resistance mechanisms and surveillance of multidrug resistance.

References

- Ballouz T, Aridi J, Afif C, Irani J, Lakis C, Nasreddine R, et al. Risk factors, clinical presentation, and outcome of *Acinetobacter baumannii* bacteremia. *Front Cell Infect Microbiol*. 2017;7:1–8. <https://doi.org/10.3389/fcimb.2017.00156>
- Falagas ME, Rafailidis PI, Ioannidou E, Alexiou VG, Matthaiou DK, Karageorgopoulos DE, et al. Colistin therapy for microbiologically documented multidrug-resistant Gram-negative bacterial infections: a retrospective cohort study of 258 patients. *Int J Antimicrob Agents*. 2010;35:194–9. <https://doi.org/10.1016/j.ijantimicag.2009.10.005>
- Batirel A, Balkan II, Karabay O, Agalar C, Akalin S, Alici O, et al. Comparison of colistin-carbapenem, colistin-sulbactam, and colistin plus other antibacterial agents for the treatment of extremely drug-resistant *Acinetobacter baumannii* bloodstream infections. *Eur J Clin Microbiol Infect Dis*. 2014;33:1311–22. <https://doi.org/10.1007/s10096-014-2070-6>
- Cai Y, Chai D, Wang R, Liang B, Bai N. Colistin resistance of *Acinetobacter baumannii*: clinical reports, mechanisms and antimicrobial strategies. *J Antimicrob Chemother*. 2012;67:1607–15. <https://doi.org/10.1093/jac/dks084>
- Haddad FA, Van Horn K, Carbonaro C, Agüero-Rosenfeld M, Wormser GP. Evaluation of antibiotic combinations against multidrug-resistant *Acinetobacter baumannii* using the E-test. *Eur J Clin Microbiol Infect Dis*. 2005;24:577–9. <https://doi.org/10.1007/s10096-005-1366-y>
- Rigatto MH, Vieira FJ, Antchevich LC, Behle TF, Lopes NT, Zavascki AP. Polymyxin B in combination with antimicrobials lacking in vitro activity versus polymyxin B in monotherapy in critically ill patients with *Acinetobacter baumannii* or *Pseudomonas aeruginosa* infections. *Antimicrob Agents Chemother*. 2015;59:6575–80. <https://doi.org/10.1128/AAC.00494-15>
- Tripodi MF, Durante-Mangoni E, Fortunato R, Utili R, Zarrilli R. Comparative activities of colistin, rifampicin, imipenem and sulbactam/ampicillin alone or in combination against epidemic multidrug-resistant *Acinetobacter baumannii* isolates producing OXA-58 carbapenemases. *Int J Antimicrob Agents*. 2007;30:537–40. <https://doi.org/10.1016/j.ijantimicag.2007.07.007>
- Liu X, Zhao M, Chen Y, Bian X, Li Y, Shi J, et al. Synergistic killing by meropenem and colistin combination of carbapenem-resistant *Acinetobacter baumannii* isolates from Chinese patients in an in vitro pharmacokinetic/pharmacodynamic model. *Int J Antimicrob Agents*. 2016;48:559–63. <https://doi.org/10.1016/j.ijantimicag.2016.07.018>
- Hajjar Soudeih M, Dahdouh E, Daoud Z, Sarkis DK. Phenotypic and genotypic detection of β -lactamases in *Acinetobacter* spp. isolates recovered from Lebanese patients over a 1-year period. *J Glob Antimicrob Resist*. 2018;12:107–12. <https://doi.org/10.1016/j.jgar.2017.09.016>
- Magiorakos AP, Srinivasan A, Carey RB, Carmeli Y, Falagas ME, Giske CG, et al. Multidrug-resistant, extensively drug-resistant and pandrug-resistant bacteria: an international expert proposal for interim standard definitions for acquired resistance. *Clin Microbiol Infect*. 2012;18:268–81. <https://doi.org/10.1111/j.1469-0691.2011.03570.x>
- Kalil AC, Metersky ML, Klompas M, Muscedere J, Sweeney DA, Palmer LB, et al. Management of adults with hospital-acquired and ventilator-associated pneumonia: 2016 clinical practice guidelines by the Infectious Diseases Society of America and the American Thoracic Society. *Clin Infect Dis*. 2016;63:e61–111. <https://doi.org/10.1093/cid/ciw353>

Address for correspondence: Eid Azar, University of Balamand and Saint George Hospital University Medical Center, PO Box 166378, Achrafieh, Beirut 1100 2807, Lebanon; email: eazar@stgeorgehospital.org

Antigenic Variation of Avian Influenza A(H5N6) Viruses, Guangdong Province, China, 2014–2018

Ru Bai,¹ Reina S. Sikkema,¹ Cong rong Li, Bas B. Oude Munnink, Jie Wu, Lirong Zou, Yi Jing, Jing Lu, Runyu Yuan, Ming Liao, Marion P.G. Koopmans,¹ Chang-wen Ke¹

Market surveillance showed continuing circulation of avian influenza A(H5N6) virus in live poultry markets in Guangdong Province in 2017, despite compulsory vaccination for avian influenza A(H5Nx) and A(H7N9). We analyzed H5N6 viruses from 2014–2018 from Guangdong Province, revealing antigenic drift and decreased antibody response against the vaccine strain in vaccinated chickens.

Human disease from low-pathogenic influenza A(H7N9) infection was first reported in 2013, and a total of 1,567 human cases have been reported (1). During the fifth wave, which started in October 2016, the number of human cases increased steeply, the virus spread into western provinces of China, and a highly pathogenic avian influenza (HPAI) A(H7N9) variant emerged (2). In parallel, HPAI H5 subtype viruses (clade 2.3.4.4 H5Nx) were causing international outbreaks in poultry (3,4) and infecting humans in China (5,6). In July 2017, Guangdong Province implemented a compulsory vaccination strategy for poultry (chickens, ducks, geese, quail, pigeons, and rare birds in captivity) using the combined inactivated influenza vaccine (H5 A/chicken/Guizhou/4/2013 [Re-8] + H7 A/pigeon/Shanghai/S1069/2013 [Re-1]) to prevent the dissemination of HPAI A(H7N9) and A(H5Nx) viruses (7).

Our market surveillance showed that H7N9 viruses almost disappeared from live poultry markets (LPMs), although low-level circulation in poultry and the environment, as well as sporadic human cases, are still reported throughout China (8,9). However, during the same period, H5N6 subtype viruses continued to circulate in LPMs. We report our investigation of the prevalence, evolution, and antigenic variation of H5N6 viruses during 2014–2018 in Guangdong Province.

Author affiliations: Guangdong Provincial Center for Disease Control and Prevention, Guangzhou, China (R. Bai, C. Li, J. Wu, L. Zou, Y. Jing, J. Lu, R. Yuan, C. Ke); Erasmus Medical Centre, Rotterdam, the Netherlands (R.S. Sikkema, B.B. Oude Munnink, M.P.G. Koopmans); Southern Medical University Guangzhou (C. Li, Y. Jing, C. Ke); South China Agricultural University, Guangzhou (M. Liao)

The Study

To investigate the emergence and spread of HPAI H7N9 and H5Nx viruses in LPMs, we collected environmental and poultry samples and a throat swab from an H5N6-infected person in September 2018. We tested samples using reverse transcription PCR (RT-PCR) and real-time RT-PCR (rRT-PCR) to distinguish between subtypes H5 and H7. During January 2016–October 2018, a total of 52,387 environmental samples were collected, of which 1,627 (3.1%) were positive for H5 and 1,303 (2.5%) for H7. All H7-positive samples were of the H7N9 subtype, and 99% of H5-positive samples were of the H5N6 subtype (Figure 1; Appendix 1 Table 1, <https://wwwnc.cdc.gov/EID/article/25/10/19-0274-App1.pdf>). After implementation of poultry vaccination the rate of H7N9 virus-positive samples decreased from 12.8% to 0%, and the average positivity rate for H5-subtype viruses remained ≈20% (Figure 1; Appendix 1 Table 1).

We cultured 883 H5 subtype-positive samples, including the human H5N6 sample. Virus cultivation was successful for 147 environmental samples, 21 poultry samples, and the human sample. We selected 73 H5N6 isolates that were amplified successfully for whole-genome sequencing using the Ion PGM system and the PathAmp FluA reagents (Life Technologies, <https://www.thermofisher.com>). We analyzed data using CLC Genomics Workbench 7.5.1 software (QIAGEN, <https://www.qiagenbioinformatics.com>).

We combined genome sequences from this study with all sequences of H5N6 viruses from China, as well as H3 and H6 subtype viruses available in GenBank and the GISAID database (<https://www.gisaid.org>) for 1996–2018 (Appendix 2 Tables 1, 2, <https://wwwnc.cdc.gov/EID/article/25/10/19-0274-App2.xlsx>). For sequencing, we used MUSCLE version 3.5 (10) and phylogenetic analysis under the general time reversible plus invariant sites plus Γ 4 model (hemagglutinin [HA], neuraminidase [NA], polymerase basic [PB] 1, PB2, polymerase acidic [PA], nucleoprotein [NP]) and the transversion model plus F plus invariant sites plus Γ 4 model (matrix [M], nonstructural [NS]), performed using IQ-TREE (11). Phylogenetic analysis showed that all H5N6 viruses isolated in Guangdong Province descended from the H5N6 viruses that circulated in the province during 2015–2016. However, the currently circulating H5N6

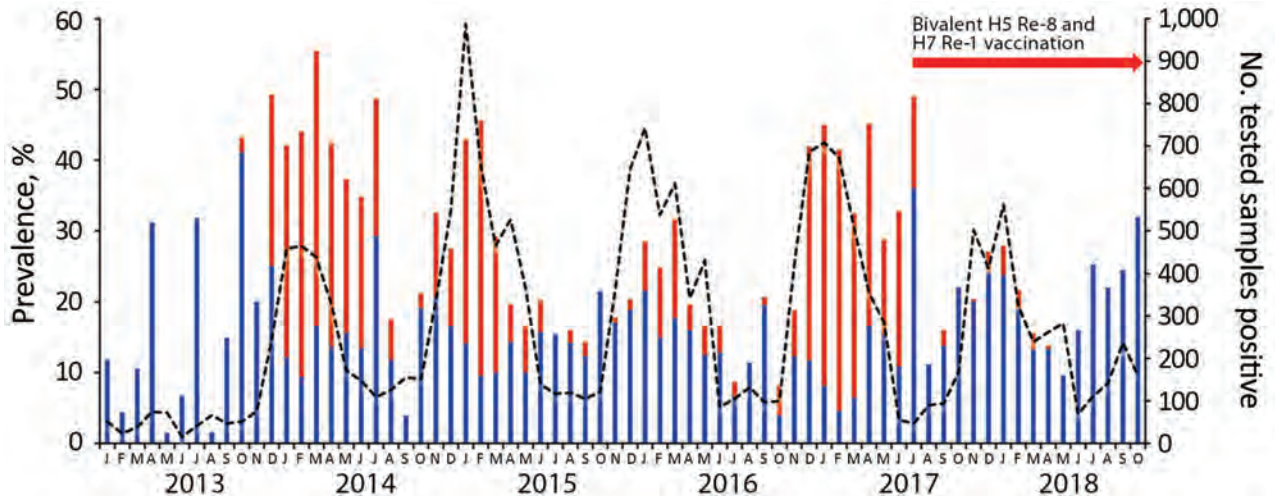


Figure 1. Proportion of H5 (blue bars) and H7 (red bars) subtypes in avian influenza A virus–positive samples (dashed line) from live poultry markets, Guangdong Province, China, January 2013–October 2018. Re-8, A/chicken/Guizhou/4/2013 (Re-8); Re-1, H7 A/pigeon/Shanghai/S1069/2013 (Re-1).

viruses in Guangdong Province cluster separately from the A/chicken/Guizhou/4/2013 (Re-8) vaccine strain, based on HA sequences (Figure 2). All N6 genes belong to the Eurasian lineage. Both HA and NA genes of the human H5N6 virus clustered with the H5N6 viruses found in the environment and poultry in our study (Appendix 1 Figure).

We classified both surface and internal genes of HPAI H5N6 viruses from Guangdong Province into different sublineages according to tree topology and bootstrap values of >85% and further classified the HA and NA genes into 4 subgroups (Figure 2). Phylogeny of the internal genes of the recent clade 2.3.4.4 H5N6 viruses showed they evolved from H5N1 viruses from 2013–2014, in which, from 2015 onward, almost all PB2 genes were replaced by H6 subtype–origin PB2 genes. Substitution of the PB2 gene can change the virulence and pathogenicity in mammals and in different bird species (12). Moreover, from 2016 onward, H5N6 acquired PB1 and PA genes from (avian) H3-like or LPAI gene pools. In 2017, NP, M, and NS genes from H3-like viruses and local LPAI gene pools were first detected in circulating H5N6 viruses (Figure 2). Closely related H5N6 viruses from China with similar internal gene composition did not show any intravenous pathogenicity in ducks and lower intravenous pathogenicity in chickens (13), which could explain the widespread circulation of H5N6 viruses in Guangdong Province.

When we compared the HA gene predicted receptor binding sites and other regions of the H5N6 isolates from Guangdong Province with A/chicken/Guizhou/4/2013 (Re-8), we found 35 positions where >50% of viruses in our study had amino acid substitutions (4). Those mutations (H3 numbering) occurred in sites R50K, D63N, R81S, S94A/T, L122Q, S125R/K, P128S, D129N/S, D130 deletion/E/T, T131S, L133 deletion/S, A137T, A138S, Q142K, M144V, P145A, I155T, N158S, T160A, R173G/K, S185P, N187S, A188V, A189E,

T192A, N193D/K/T/N, T199A/I, R227S/C/Q/G, K238R, V260I, K262T, M272I, H276K/N/Q/S, N278S, and N323S (Appendix 1 Table 2). In addition, we detected several mutations that were exclusively found in >90% of the most recent H5N6 isolates from Guangdong Province (2017–2018), including L122Q, S125R/K, P128S, P145A, K262T, M272I, H276K/N/Q/S, and N401I/S/N. We identified 3 new amino acid substitutions in the NA and PB2 genes of human H5N6 isolate: the Q136H on the NA gene, which might affect its susceptibility to antiviral neuraminidase inhibitors (4), and mutation E627V and A588V in the PB2 gene, of which the influence on its virulence in mammals needs further investigation (4). Furthermore, we found A588V mutations in 64 of 68 PB2 genes of H5N6 viruses from the environment.

We determined HI titers in serum of H5 A/chicken/Guizhou/4/2013 (Re-8)–vaccinated chickens ($n = 5$) and serum from the H5N6 virus–infected human patient to human and environmental H5N6 viral isolates from different time points using a standard protocol (14). Serum from chickens vaccinated with H5 A/chicken/Guizhou/4/2013 (Re-8) showed high titers ($8–10 \log_2$) to the human H5N6 isolates from 2014–2017 and lower titers ($4–6 \log_2$) to the human H5N6 isolate from 2018. We observed a similar trend when using environmental isolates for the HI assays. Conversely, serum from the H5N6-infected human in 2018 showed higher titers to human H5N6 isolates in 2017 and 2018 ($6 \log_2$) than to those from 2014 and 2015 ($4 \log_2$) (Table).

Conclusions

Compulsory vaccination of the combined inactivated influenza vaccine was implemented in Guangdong Province in July 2017. Although the prevalence of H7N9 in LPMs decreased abruptly, we revealed uninterrupted circulation of H5N6 viruses in LPMs after implementation of the

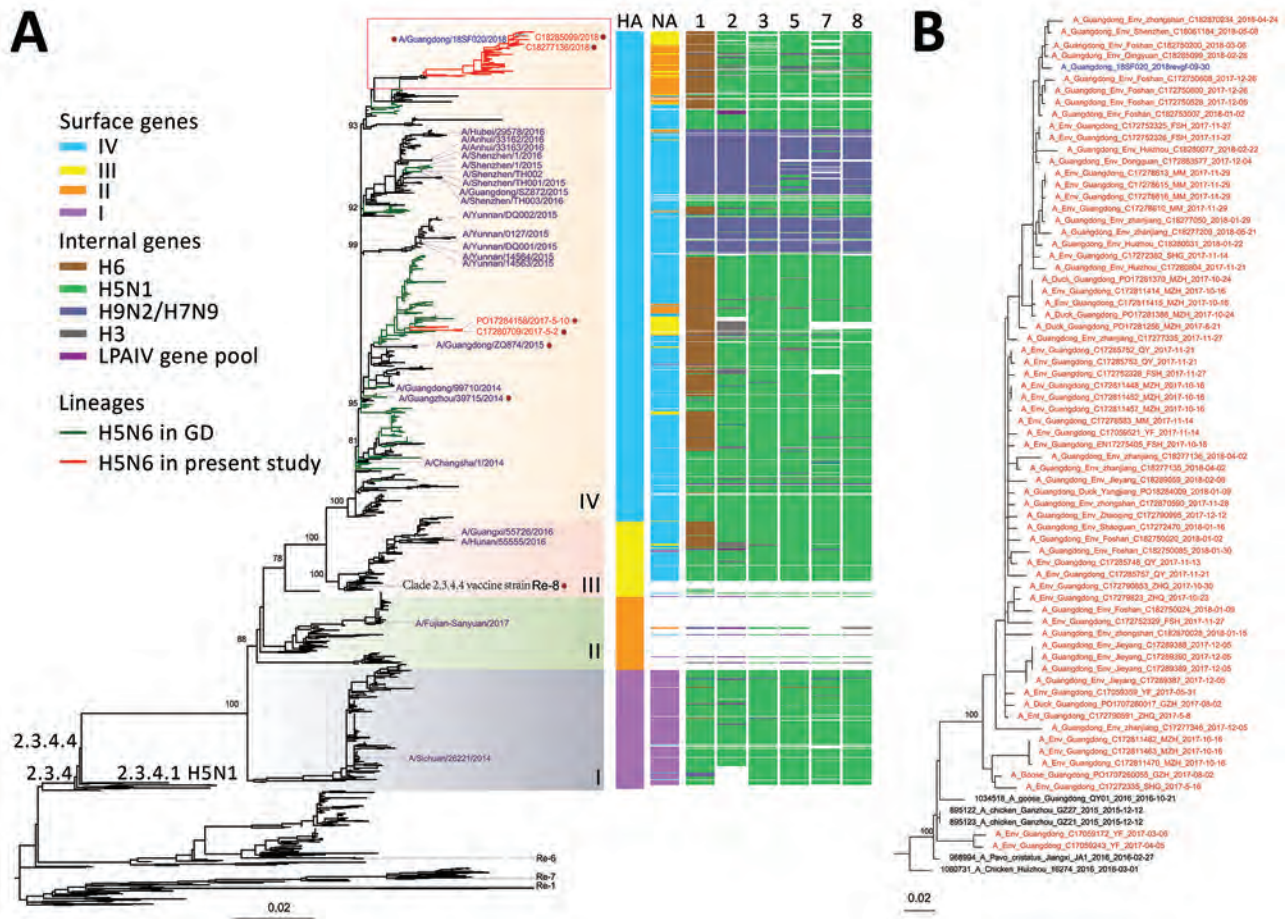


Figure 2. Phylogeny of influenza A(H5N6) viruses collected in Guangdong Province, China, January 2013–October 2018, compared with reference isolates. A) Viruses of clade 2.3.4.4 H5N6 viruses are divided into 4 subgroups (I–IV) on the basis of the surface genes (HA and NA). Colors in key distinguish surface and internal genes. The A/chicken/Guizhou/4/2013 (Re-8) vaccine strain and viral strains used for HI testing are labeled. The 2018 human H5N6 isolate from Guangdong Province is blue, human H5N6 virus sequences since 2013 are purple, human and environmental H5N6 isolates used for the HI test are labeled with a purple dot (except for HA256 human strain, for which no sequence was available). The top part of the tree containing the bulk of the Guangdong Province recent H5N6 viruses and the human case is highlighted with a red box. All branch lengths are scaled according to the number of substitutions per site. Scale bars indicate nucleotide substitutions per site. GD, Guangdong; HA, hemagglutinin gene; LPAIV, low pathogenicity avian influenza virus; NA, neuraminidase gene; 1, polymerase basic 2 gene; 2, polymerase basic 1 gene; 3, polymerase acidic gene; 5, nucleoprotein gene; 7, matrix gene; 8, nonstructural gene. B) An expansion of the phylogenetic tree in the red outlined box of panel A. The sequence in blue is the newly approved vaccine strain 18SF020.

vaccination strategy. Our study shows that H5N6 viruses in Guangdong Province show antigenic drift when compared with the A/chicken/Guizhou/4/2013 (Re-8) vaccine strain, resulting in lower protection of vaccinated chickens against circulating clade 2.3.4.4 H5 viruses. In December 2018, the China government approved a new poultry vaccine (H5 A/duck/Guizhou/S4184/2017 [Re-11], H5 A/chicken/Liaoning/SD007/2017 [Re-12] + H7 A/chicken/Guangxi/SD098/2017 [Re-2]). Moreover, the World Health Organization proposed a new A/Guangdong/18SF020/2018-like H5N6 candidate vaccine virus, which was partly based on strain A/Guangdong/18SF020/2018 reported in this study (15).

Vaccine escape variants remain a risk for human and animal health. Therefore, future policy should focus on preventing the spread of avian influenza viruses along the market chain by strengthening farm-level surveillance and biosecurity, as well as implementing measures to monitor and prevent the spread of avian influenza viruses that have zoonotic potential in the market chain.

Acknowledgments

We thank the 21 collaborating laboratories in Guangdong Province that participated in the longitudinal surveillance.

This work was supported by grants from the National Key Research and Development Program of China (grant

Table. HI titers of influenza A(H5N6) virus strains collected during 2014–2018 in Guangdong Province, China, compared with vaccine strains*

Virus strain†	Sample type	Collection date	HI titers					H5N6-infected human serum
			Postvaccination chicken serum					S6
			S1	S2	S3	S4	S5	
39715	Human	2014 Dec 11	512	512	1024	512	256	16
ZQ874	Human	2015 Dec 31	512	512	512	512	256	16
HA256	Human	2017 Jun 30‡	256	256	512	256	256	64
18SF020-1	Human	2018 Sep 30	32	16	64	32	16	64
C17280709	Environment	2017 May 2	64	64	128	128	64	16
C18277136	Environment	2018 Apr 2	64	32	32	64	16	16
C18285099	Environment	2018 Feb 28	32	32	NT	NT	32	8
PO17284158	Waterfowl	2018 May 10	128	64	NT	NT	NT	NT
A§	Chicken	2018 Nov 19¶	2,048	1,024	4,096	1,024	1,024	NT
B#	Chicken	2018 Sep 20**	32	32	NT	NT	NT	NT

*NT, not tested; S, sample no.

†The name of virus strain is the abbreviation of the original name for each viral isolate.

‡Date isolate received.

§Vaccine strain A/chicken/Guizhou/4/2013 (Re-8) + H7 A/pigeon/Shanghai/S1069/2013 (Re-1).

¶Date vaccine strain tested.

#Vaccine strain H5 A/duck/Guangdong/S1322/2010 (Re-6).

**Date vaccine strain received.

2016YFC1200201), the European Commission's H2020 program under contract number 643476 (<http://www.compare-europe.eu>), and the Royal Netherlands Academy of Arts and Sciences (project number 530-6CDP23).

About the Author

Dr. Bai is a postdoctoral researcher at the Guangdong Provincial Center for Disease Control and Prevention, Guangzhou, China, whose research focuses on the epidemiology, evolution, and transmission of avian influenza viruses in Guangdong Province. Ms. Sikkema is a PhD candidate at the Erasmus Medical Centre, Rotterdam, the Netherlands, whose research focuses on the risk-based surveillance of influenza viruses in the market chain.

References

- World Health Organization. Influenza at the human-animal interface Summary and assessment, 26 January to 2 March 2018. 2018 Mar 2 [cited 2019 May 7], https://www.who.int/influenza/human_animal_interface/Influenza_Summary_IRA_HA_interface_02_03_2018.pdf?ua=1
- Su S, Gu M, Liu D, Cui J, Gao GF, Zhou J, et al. Epidemiology, evolution, and pathogenesis of H7N9 influenza viruses in five epidemic waves since 2013 in China. *Trends Microbiol*. 2017;25:713–28. <https://doi.org/10.1016/j.tim.2017.06.008>
- Poen MJ, Venkatesh D, Bestebroer TM, Vuong O, Scheuer RD, et al. Co-circulation of genetically distinct highly pathogenic avian influenza A clade 2.3.4.4 (H5N6) viruses in wild waterfowl and poultry in Europe and East Asia, 2017–18. *Virus Evol*. 2019; 22:5(1).
- Bi Y, Chen Q, Wang Q, Chen J, Jin T, et al. Genesis, Evolution and Prevalence of H5N6 Avian Influenza Viruses in China. *Cell Host Microbe*. 2016;20:810–21. <https://doi.org/10.1016/j.chom.2016.10.022>
- Yang ZF, Mok CK, Peiris JS, Zhong NS. Human infection with a novel avian influenza A(H5N6) virus. *N Engl J Med*. 2015;373:487–9. <https://doi.org/10.1056/NEJMc1502983>
- Bi Y, Tan S, Yang Y, Wong G, Zhao M, Zhang Q, et al. Clinical and immunological characteristics of human infections with H5N6 avian influenza virus. *Clin Infect Dis*. 2019;68:1100–9. <https://doi.org/10.1093/cid/ciy681>
- Food and Agriculture Organization of the United Nations (FAO). Chinese-origin H7N9 avian influenza spread in poultry and human exposure. 2018 Feb 18 [cited 2019 May 7]. <http://www.fao.org/3/i8705en/i8705EN.PDF>
- Wu J, Ke C, Lau EHY, Song Y, Cheng KL, Zou L, et al. Influenza H5/H7 virus vaccination in poultry and reduction of zoonotic infections, Guangdong province, China, 2017–18. *Emerg Infect Dis*. 2019;25:116–8. <https://doi.org/10.3201/eid2501.181259>
- Food and Agriculture of Organization of the United Nations. FAO H7N9 situation update, 2019 May 8 [cited 2019 Jun 13]. http://www.fao.org/ag/againfo/programmes/en/empres/H7N9/wave_7/Situation_update_2019_05_08.html
- Edgar RC. MUSCLE: multiple sequence alignment with high accuracy and high throughput. *Nucleic Acids Res*. 2004;32:1792–7. <https://doi.org/10.1093/nar/gkh340>
- Nguyen LT, Schmidt HA, von Haeseler A, Minh BQ. IQ-TREE: a fast and effective stochastic algorithm for estimating maximum-likelihood phylogenies. *Mol Biol Evol*. 2015;32:268–74. <https://doi.org/10.1093/molbev/msu300>
- Tada T, Suzuki K, Sakurai Y, Kubo M, Okada H et al. NP Body Domain and PB2 Contribute to Increased Virulence of H5N1 Highly Pathogenic Avian Influenza Viruses in Chickens. *J Virol*. 2011; 85(4):1834–46.14.
- Sun W, Li J, Hu J, Jiang D, Xing C, Zhan T, et al. Genetic analysis and biological characteristics of different internal gene origin H5N6 reassortment avian influenza virus in China in 2016. *Vet Microbiol*. 2018;219:200–11. <https://doi.org/10.1016/j.vetmic.2018.04.023>
- Killian ML. Hemagglutination assay for the avian influenza virus. In: Spackman E, editor. *Avian influenza virus*. New York: Springer; 2008. p. 47–52.
- World Health Organization, Antigenic and genetic characteristics of zoonotic influenza viruses and development of candidate vaccine viruses for pandemic preparedness, 2019 February 21 [cited 2019 August 20] https://www.who.int/influenza/vaccines/virus/201902_zoonotic_vaccinevirusupdate.pdf?ua=1

Address for correspondence: Chang-wen Ke, Guangdong Provincial Center for Disease Control and Prevention, Guangzhou, China; email: kecw1965@aliyun.com; Marion P.G. Koopmans, Erasmus Medical Centre, Viroscience Department, Rotterdam, the Netherlands; email: m.koopmans@erasmusmc.nl

Plasmodium cynomolgi as Cause of Malaria in Tourist to Southeast Asia, 2018

**Gitte N. Hartmeyer, Christen R. Stensvold,
Thilde Fabricius, Ea S. Marmolin,
Silje V. Hoegh, Henrik V. Nielsen,
Michael Kemp, Lasse S. Vestergaard**

We report human infection with simian *Plasmodium cynomolgi* in a tourist from Denmark who had visited forested areas in peninsular Malaysia and Thailand in August and September 2018. Because *P. cynomolgi* may go unnoticed by standard malaria diagnostics, this malaria species may be more common in humans than was previously thought.

Despite marked reductions in the global disease burden, malaria remains a serious threat to persons living in or visiting areas to which it is endemic (1). Traditionally, 4 species of *Plasmodium* parasites (*P. falciparum*, *P. vivax*, *P. ovale*, and *P. malariae*) have been considered to cause natural human malaria; however, several simian *Plasmodium* species have also been found to infect humans (2). *P. knowlesi*, a parasite of forest macaques in Southeast Asia, is regularly detected in human malaria cases, including cases involving tourists (3). Because of morphological similarity, *P. knowlesi* has been widely misdiagnosed as *P. malariae* or *P. falciparum* by microscopy. In Brazil, *P. simium* was initially identified as *P. vivax* during outbreaks in 2015 and 2016 (4), highlighting the need for better methods for accurate identification.

In 2014, another simian *Plasmodium* species, *P. cynomolgi*, was reported to have naturally infected an adult patient (5). Until then, *P. cynomolgi* was known as a human parasite only from experimental studies. In addition to fever, clinical symptoms in humans comprise cephalgia, anorexia, myalgia, and nausea; the prepatent period is 7–16 days and the incubation period is ≈15–20 days, with some variation between different strains of *P. cynomolgi* (2,6).

P. cynomolgi is found in long-tailed macaques across Southeast Asia, often concomitant with other simian malaria parasites such as *P. inui*, *P. coatneyi*, or *P. fieldi* (7).

Author affiliations: Odense University Hospital, Odense, Denmark (G.N. Hartmeyer, T. Fabricius, S.V. Hoegh, M. Kemp); Statens Serum Institut, Copenhagen, Denmark (C.R. Stensvold, H.V. Nielsen, L.S. Vestergaard); Sygehus Lillebælt, Vejle, Denmark (E.S. Marmolin)

DOI: <https://doi.org/10.3201/eid2510.190448>

A recent vector survey in Vietnam demonstrated the presence of *P. cynomolgi* among other human and nonhuman primate *Plasmodium* spp. parasites in *Anopheles dirus*, an important local malaria vector (8). Asymptomatic carriage of *P. cynomolgi* was recently reported in village residents in Cambodia (9). We report a travel-related case of malaria caused by *P. cynomolgi* in a tourist from Denmark who had traveled to forested areas in peninsular Malaysia and Thailand.

The Study

A 37-year-old woman from Denmark with no underlying conditions and no previous history of malaria traveled with her husband and children for 6 weeks in various parts of peninsular Malaysia and Thailand in 2018. None of them took malaria chemoprophylaxis; however, they used mosquito repellents and mosquito nets.

The family traveled by air to Singapore in mid-August 2018 and traveled by bus to Kuala Lumpur, Malaysia. From there, they traveled by air to Kota Bharu on the east coast of peninsular Malaysia and sailed to Perhentian Island, staying for 4 days in a beach cottage, with day trips into the nearby forest. In late August, they returned to Kuala Lumpur and traveled by air to Chiang Mai, Thailand, from which they visited remote mountain villages, hiked through the forest, and stayed overnight in local villages. In early September they traveled by air to Bangkok and traveled onward by train to Khao Sok National Park, Surat Thani Province, where they stayed in treehouses in the jungle for 4 nights. In mid-September they traveled by car and ferry to the island Koh Phangan, where they stayed in beach houses for a week. They then sailed to the island Koh Samui for another week of beach holiday before returning to Denmark.

The patient noted numerous macaque monkeys during the jungle visit in Khao Sok, but not in the other areas. She also reported receiving several mosquito bites while in Khao Sok, despite the use of preventive measures.

We referred the patient to a tertiary hospital for treatment and follow-up. Repeated LAMP was positive for *Plasmodium* DNA, whereas the rapid test was again negative. In-house real-time PCRs were positive for *Plasmodium* (10) but negative for *P. falciparum* (11), *P. vivax* (11,12), *P. ovale* (13), *P. malariae* (13), and *P. knowlesi* (14). A blood sample was analyzed at the National Reference Parasitology Laboratory by PCR

using genus-specific primers (Plasmo F 5'-TTGYCTA-AAATACTTCCATTAATCAAGAACG-3' and Plasmo R 5'-TTTGATTTCTCATAAGGYACTGAAGG-3') and a next-generation sequencing-based (NGS) microbiota assay, described previously (15). Sanger sequencing of the genus-specific PCR product revealed *P. cynomolgi*. The assay identified 2 stage-specific types of nuclear small subunit (SSU) rRNA genes (16), both belonging to *P. cynomolgi*. Clone 1 exhibited 99.51% similarity to GenBank accession no. AB287289 (asexual [A]-type SSU rDNA), and clone 2 had 100% similarity to GenBank accession no. AB287288 (sporozoite [S]-type SSU rDNA), both of which were isolates identified in a long-tailed macaque in Southeast Asia (Figure 2).

The patient received atovaquone/proguanil (1,000/400 mg/d for 4 d), followed by primaquine (26.4 mg/d for 14 d). Symptoms resolved on the second day of treatment, and the patient was discharged for outpatient follow-up. Within a week, platelet count normalized, and S-ALAT further increased to 135 U/L. Results of malaria microscopies

repeated on days 9 and 37 of treatment were negative. The patient fully recovered.

Conclusions

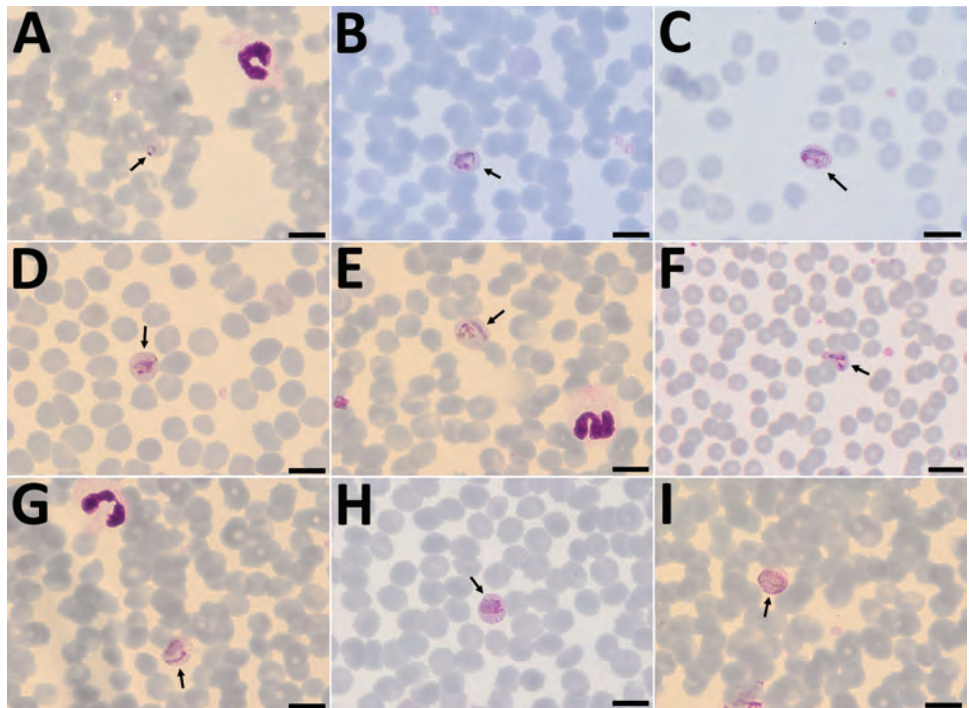
A short-term traveler contracted *P. cynomolgi* malaria during a trip to Southeast Asia. Exactly where the patient became infected is not known. The presence of nocturnal mosquitoes and macaques makes Khao Sok National Park in Thailand a likely site of infection. The time interval of 17 days between her arrival in Khao Sok and the onset of symptoms matches reported incubation periods for human *P. cynomolgi* infections (6).

Surat Thani Province in Thailand is located ≈800 km north of Hulu Terengganu in peninsular Malaysia, where a natural human *P. cynomolgi* infection was only recently reported in a local resident (5). Long-tailed macaques are present in both of these areas, but not around Chiang Mai (3).

We obtained species identification by DNA sequencing only after negative species-specific real-time PCR. Given the challenge of diagnosing *P. cynomolgi* and the

Figure 1. *Plasmodium cynomolgi* parasites (arrows) in Giemsa-stained thin smears of blood from a traveler returning from Southeast Asia to Denmark.

Overall, few parasites were visible in the thin film, and no schizonts were visible at all. A) Young trophozoite. The cytoplasm is ring shaped, and the nucleus is spherical. The erythrocyte is not enlarged, and neither Schüffner's dots nor pigment are visible. B) Growing trophozoite. The young parasite is ring shaped and takes up more than half of the diameter of the host erythrocyte. The cytoplasm has become slightly amoeboid. Schüffner's dots are more prominent than in *P. vivax* at this stage. Pigment is visible as small yellowish granules in the cytoplasm. Erythrocyte enlargement is not evident. C) Growing trophozoite. The cytoplasm appears amoeboid but relatively compact. Schüffner's dots are prominent, but no pigment is seen in the cytoplasm. The erythrocyte is slightly enlarged. D) Growing trophozoite. The cytoplasm appears amoeboid, and the nucleus has increased in size. Schüffner's dots and yellowish pigment are prominent. Enlargement of the erythrocyte is evident. E) Growing trophozoite. The host cell is further enlarged. The cytoplasm is amoeboid as in *P. vivax* at this stage. Schüffner's dots are clearly visible, and yellowish pigment is dispersed within the cytoplasm. F) Growing trophozoite. An infected erythrocyte with major alteration in the shape, similar to that sometimes seen in *P. vivax*-infected erythrocytes. The cytoplasm is amoeboid, with hardly any pigment. Schüffner's dots are prominent, and the host erythrocyte is enlarged. G) Growing trophozoite. The cytoplasm is amoeboid and appears relatively compact. Schüffner's dots are dominant. Pigment is visible in small granules but appears more yellowish-brown and is scattered around in the cytoplasm. H) Near-mature trophozoite. The parasite is becoming more compact with an enlarged nucleus. No ring or amoeboid form is visible. Schüffner's dots are very dense, and abundant yellowish-brown pigment is clearly visible in the cytoplasm. I) Mature microgametocyte. It is round and resembles that of *P. vivax* at the same stage. The nucleus is diffuse and takes up most of the parasite. The stippling of the host cell is forced toward the periphery, as seen for *P. vivax*. Microgametocytes stain reddish-purple (pink hue) in contrast to macrogametocytes, which stain light blue. The yellowish-brown pigment is scattered around in the parasite. Scale bars indicate 100 μm.



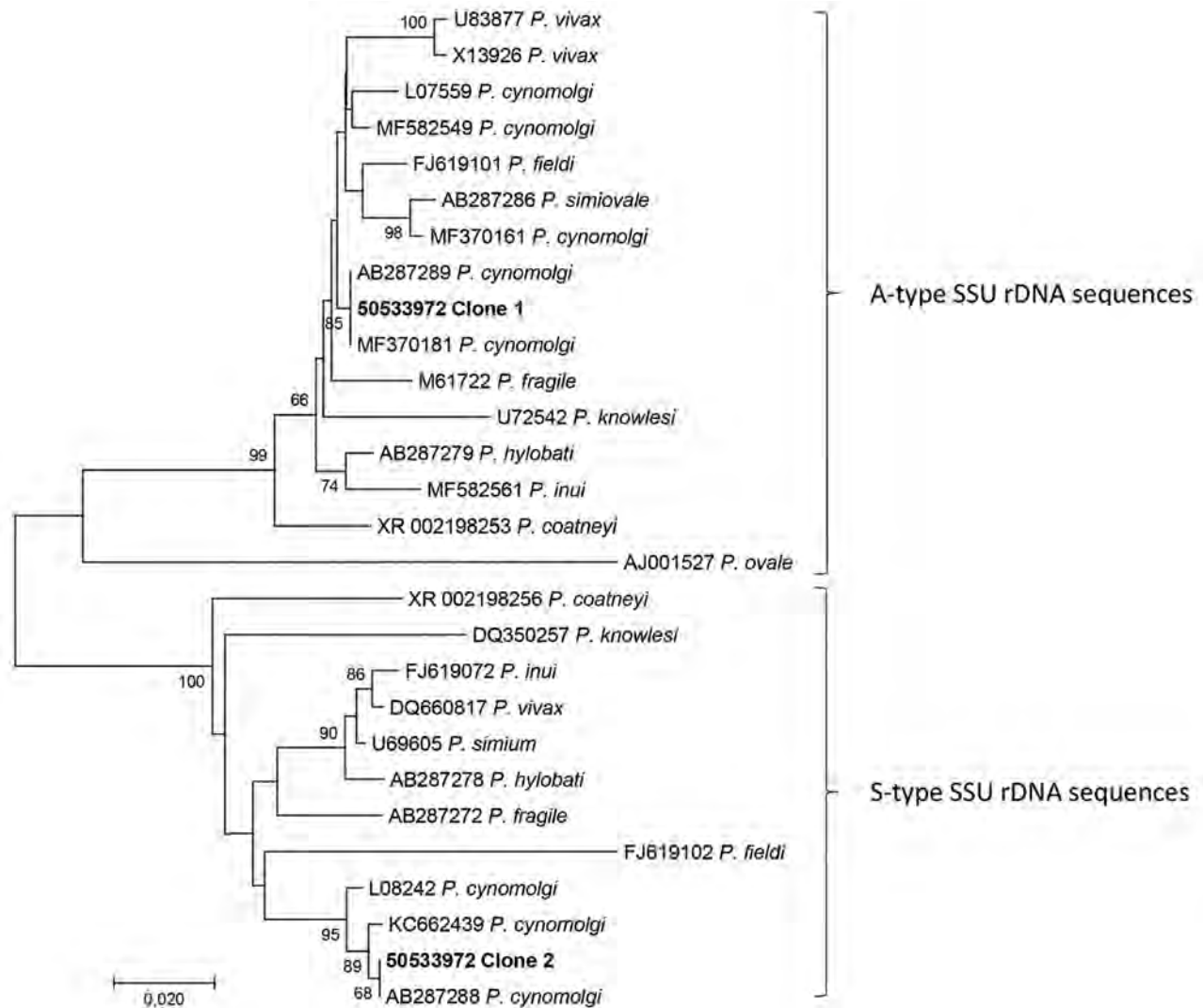


Figure 2. Phylogenetic analysis of the 2 consensus sequences (50533972 clone 1 and 50533972 clone 2) generated by the microbiome assay of blood from a traveler returning from Southeast Asia to Denmark. We used CD-HIT Suite (http://weizhong-lab.ucsd.edu/cdhit_suite/cgi-bin/index.cgi?cmd=cd-hit-est) to cluster sequences reflecting *Plasmodium*-specific DNA amplified and sequenced by our microbiome assay; we generated consensus sequences using an in-house sequence clustering software. We queried the 2 resulting consensus sequences in GenBank, then downloaded examples of DNA sequences with varying genetic similarity and included them in a multiple sequence alignment with the 2 consensus sequences. Phylogenetic analysis revealed that the microbiome assay had amplified asexual stage-specific (A-type) SSU rRNA genes of *Plasmodium cynomolgi*, with 50533972 clone 1 reflecting them, and sporozoite stage-specific (S-type), with 50533972 clone 2 reflecting them. We conducted phylogenetic analysis involving 28 DNA sequences in MEGA7 (<http://www.megasoftware.net>) and included a total of 464 positions in the final dataset. We inferred evolutionary history using the neighbor-joining method. Numbers at the branches show the percentage of replicate trees in which the associated taxa clustered together in the bootstrap test (1,000 replicates). The tree is drawn to scale, with branch lengths in the same units as those of the evolutionary distances used to infer the phylogenetic tree. We computed evolutionary distances using the Kimura 2-parameter method. Scale bar indicates nucleotide substitutions per site.

widespread occurrence of its natural host across Southeast Asia, it is likely that this simian *Plasmodium* sp. is underdiagnosed in both residents and visiting travelers.

Urban development into forested areas leads to closer coexistence of human and monkey. The number of cases in which malaria is transmitted from monkeys to humans may therefore increase. Advanced detection and identification

techniques may improve knowledge of the epidemiology of simian malaria in humans.

About the Author

Dr. Hartmeyer is a consultant in clinical microbiology at Odense University Hospital, Denmark. Her research interests focus on clinical parasitology and epidemiology.

References

1. World Health Organization. World malaria report. 2018 [cited 2019 Jan 16]. <http://www.who.int/malaria/publications/world-malaria-report-2018/report>
2. Coatney GR, Collins WE, Warren M, Contacos PG. The primate malarias. Atlanta: Centers for Disease Control and Prevention; 2003 [cited 2019 Aug 6]. http://www.mcdinternational.org/trainings/malaria/english/DPDx5/HTML/PDF_Files/PrimateMalariasChapters/primate_24.pdf
3. Singh B, Daneshvar C. Human infections and detection of *Plasmodium knowlesi*. *Clin Microbiol Rev*. 2013;26:165–84. <https://doi.org/10.1128/CMR.00079-12>
4. Brasil P, Zalis MG, de Pina-Costa A, Siqueira AM, Júnior CB, Silva S, et al. Outbreak of human malaria caused by *Plasmodium simium* in the Atlantic Forest in Rio de Janeiro: a molecular epidemiological investigation. *Lancet Glob Health*. 2017;10:1038–46. [https://doi.org/10.1016/S2214-109X\(17\)30333-9](https://doi.org/10.1016/S2214-109X(17)30333-9)
5. Ta TH, Hisam S, Lanza M, Jiram AI, Ismail N, Rubio JM. First case of a naturally acquired human infection with *Plasmodium cynomolgi*. *Malar J*. 2014;13:68. <https://doi.org/10.1186/1475-2875-13-68>
6. Contacos PG, Elder HA, Coatney GR, Genter C. Man to man transfer of two strains of *Plasmodium cynomolgi* by mosquito bite. *Am J Trop Med Hyg*. 1962;11:186–93. <https://doi.org/10.4269/ajtmh.1962.11.186>
7. Zhang X, Kadir KA, Quintanilla-Zariñán LF, Villano J, Houghton P, Du H, et al. Distribution and prevalence of malaria parasites among long-tailed macaques (*Macaca fascicularis*) in regional populations across Southeast Asia. *Malar J*. 2016 Sep 2;15(1) [cited 2019 Feb 20]. <https://www.ncbi.nlm.nih.gov/pmc/articles/PMC5010671>
8. Chinh VD, Masuda G, Hung VV, Takagi H, Kawai S, Annoura T, et al. Prevalence of human and non-human primate *Plasmodium* parasites in anopheline mosquitoes: a cross-sectional epidemiological study in southern Vietnam. *Trop Med Health*. 2019;47:9.
9. Imwong M, Madmanee W, Suwannasin K, Kunasol C, Peto TJ, Tripura R, et al. Asymptomatic natural human infections with the simian malaria parasites *Plasmodium cynomolgi* and *Plasmodium knowlesi*. *J Infect Dis*. 2019;219:695–702. <https://doi.org/10.1093/infdis/jiy519>
10. Kamau E, Alemayehu S, Feghali KC, Saunders D, Ockenhouse CF. Multiplex qPCR for detection and absolute quantification of malaria. *PLoS ONE*. 2013;8:e71539.
11. Perandin F, Manca N, Piccolo G, Calderaro A, Galati L, Ricci L, et al. Identification of *Plasmodium falciparum*, *P. vivax*, *P. ovale* and *P. malariae* and detection of mixed infection in patients with imported malaria in Italy. *New Microbiol*. 2003;26:91–100.
12. Rougemont M, Van Saanen M, Sahli R, Hinrikson HP, Bille J, Jaton K. Detection of four *Plasmodium* species in blood from humans by 18S rRNA gene subunit-based and species-specific real-time PCR assays. *J Clin Microbiol*. 2004;42:5636–43. <https://doi.org/10.1128/JCM.42.12.5636-5643.2004>
13. Veron V, Simon S, Carne B. Multiplex real-time PCR detection of *P. falciparum*, *P. vivax* and *P. malariae* in human blood samples. *Exp Parasitol*. 2009;121:346–51. <https://doi.org/10.1016/j.exppara.2008.12.012>
14. Divis PC, Shokoples SE, Singh B, Yanow SK. A TaqMan real-time PCR assay for the detection and quantitation of *Plasmodium knowlesi*. *Malar J*. 2010;9:344. <https://doi.org/10.1186/1475-2875-9-344>
15. Krogsgaard LR, Andersen LO, Johannesen TB, Engsbro AL, Stensvold CR, Nielsen HV, et al. Characteristics of the bacterial microbiome in association with common intestinal parasites in irritable bowel syndrome. *Clin Transl Gastroenterol*. 2018;9:161.
16. Gunderson JH, Sogin ML, Wollett G, Hollingdale M, de la Cruz VF, Waters AP, et al. Structurally distinct, stage-specific ribosomes occur in *Plasmodium*. *Science*. 1987;238:933–7. <https://doi.org/10.1126/science.3672135>

Address for correspondence: Gitte N. Hartmeyer, Odense University Hospital, Department of Clinical Microbiology, Odense, Denmark; email: gitte.hartmeyer@rsyd.dk

EID Podcast Plague in a Dog

Some might think the plague is a relic of the Middle Ages. But *Yersinia pestis* still lingers and has even infected man's best friend.

In this EID podcast, Dr. Joshua Daniels, a bacteriologist at Colorado State University's Veterinary Diagnostic Laboratory, explains how doctors diagnosed this unusual infection.

Visit our website to listen: <https://go.usa.gov/xysvG> **EMERGING
INFECTIOUS DISEASES™**

Bidirectional Human–Swine Transmission of Seasonal Influenza A(H1N1)pdm09 Virus in Pig Herd, France, 2018

Amélie Chastagner,¹ Vincent Enouf,¹
David Peroz, Séverine Hervé, Pierrick Lucas,
Stéphane Quéguiner, Stéphane Gorin,
Véronique Beven, Sylvie Behillil,
Philippe Leneveu, Emmanuel Garin,
Yannick Blanchard, Sylvie van der Werf,
Gaëlle Simon

In 2018, a veterinarian became sick shortly after swabbing sows exhibiting respiratory syndrome on a farm in France. Epidemiologic data and genetic analyses revealed consecutive human-to-swine and swine-to-human influenza A(H1N1)pdm09 virus transmission, which occurred despite some biosecurity measures. Providing pig industry workers the annual influenza vaccine might reduce transmission risk.

In April 2009, a novel influenza A virus (IAV) emerged in humans in North America and spread in the human population worldwide, leading to the first pandemic of the 21st century (1). This virus, influenza A(H1N1)pdm09 (pH1N1), suspected to have resulted from reassortment among IAVs of swine origin, was rapidly transmitted to pig populations. This virus became seasonal in humans (2) and enzootic in several pig populations, including those in Europe (3). Moreover, phylogenetic analyses suggest *de novo* human-to-swine pH1N1 transmission occurs during seasonal epidemics (4–6). In this study, we provide evidence of bidirectional transmission of pH1N1 between humans and pigs in a herd located in France.

The Study

In January of the 2017–18 seasonal influenza epidemic in humans, a farmer reported to a veterinarian an acute

Author affiliations: French Agency for Food, Environmental and Occupational Health, and Safety, Ploufragan, France (A. Chastagner, S. Hervé, P. Lucas, S. Quéguiner, S. Gorin, V. Beven, Y. Blanchard, G. Simon); Institut Pasteur, Paris, France (V. Enouf, S. Behillil, S. van der Werf); Atlantic Vétérinaires, Ancenis, France (D. Peroz); CEVA Santé Animale SA, Libourne, France (P. Leneveu); Coop de France, Paris (E. Garin); Plateforme Epidémiosurveillance Santé Animale, Lyon, France (E. Garin)

respiratory outbreak in the pregnant sows of his farrow-to-wean herd. The animals of this herd (≈1,000 sows) were not vaccinated against swine IAVs. The sows exhibited an influenza-like illness (ILI) of usual intensity (i.e., hyperthermia, apathy, dyspnea, sneezing, and coughing that did not last for >2–3 days for individual animals). On January 17, the veterinarian and a technician handled the animals and, using nasal swabs (MW950Sent2mL Virocult; Kitvia, <https://www.kitvia.com>), collected samples from 3 sows (sample nos. 180028-1, 180028-2, 180028-3), as specified by the National Network for Surveillance of Type A Influenza Virus in Swine (7). The veterinarian (72 hours later) and technician (48 hours later), both not vaccinated against seasonal influenza, had ILI symptoms (i.e., tiredness, runny nose, chills). Neither reported close contact with humans with ILI before their symptom onset. On days 5 and 6 after handling the pigs, the veterinarian self-collected nasal swab samples (sample nos. 180130-1 and 180130-2).

The veterinarian submitted the nasal swab samples from sows to a local veterinary laboratory to determine the diagnosis. This laboratory used quantitative reverse transcription PCR of the influenza matrix gene for IAV detection (8). All 3 samples were positive for IAV and were sent to the National Reference Laboratory (Ploufragan, France) for subtyping. Here, we typed the isolates' hemagglutinin (HA) and neuraminidase genes by using quantitative reverse transcription PCRs specific to swine IAV lineages known to circulate in the pig populations in France (8). The HA and neuraminidase genes we identified were exclusively those of pH1N1. We propagated sample no. 180028-2 through Madin-Darby canine kidney cells (1 passage) to obtain isolate A/sw/France/53-180028/2018. We sequenced the whole genome of this virus using an Ion Proton Sequencer (Thermo Fisher Scientific, <https://www.thermofisher.com>) at the Next-Generation Sequencing Platform of the French Agency for Food, Environmental and Occupational Health, and Safety (Ploufragan, France) (Appendix, <https://wwwnc.cdc.gov/EID/article/25/10/19-0068-App1.pdf>).

In parallel, we amplified the 8 virus genome segments from the 2 veterinarian self-collected nasal swabs and the 3 sow samples using universal primers (9) at the National

Reference Center for Respiratory Viruses (Paris, France). Then, we sequenced them on a NextSeq 500 System (Illumina Inc., <https://www.illumina.com>) at the Mutualized Platform for Microbiology (Paris, France) (Appendix). After cleaning reads, we excluded from analysis data from sample no. 180028-1 because of its low number of residual reads.

In all, we obtained 5 sets of 8 genomic segment sequences (BioProject no. PRJNA507096): 1 from A/sw/France/53-180028/2018, 2 from pigs (sample nos. 180028-2 and 180028-3), and 2 from a human (sample nos. 180130-1 and 180130-2). We found only 3 nucleotide ambiguities supported by >30% of reads: an A-G (45.3%) mixture at position 1,667 in the polymerase basic 2 gene of sample no. 180028-2 and a T-C (49.3%) mixture at position 862 and C-A (34.9%) mixture at position 867 in the HA gene of sample no. 180130-1 (nucleotide numbering starting from first position of coding sequence for all). Excluding these ambiguities, the 5 virus genomes were 100% identical, regardless of source or sequencing pipeline. We compared these virus sequences with those of other pH1N1 strains available in the GISAID database (<https://www.gisaid.org>) using the integrated BLAST program; the highest similarities (up to 99.94% identity) were found with a pH1N1 isolate identified in a population in France during the 2017–18 winter influenza season (Table). We performed maximum-likelihood phylogenetic analyses that included pH1N1 viruses isolated from pigs and humans in France during 2009–2018. Whatever the genomic segment used, be that encoding HA (Figure) or others (data not shown), the isolates from our case study were more closely related to seasonal influenza isolates than isolates from the swine-specific lineage identified in France during 2015–2016 (6), confirming our BLAST results.

The timing of events and results of analyses led to multiple hypotheses: that de novo human-to-swine pH1N1 virus transmission would have been responsible for the first infection in this herd, that swine-to-swine transmission within the herd would have then been responsible for additional animal infections, and that subsequent swine-to-human transmission would have been responsible for the infection in the veterinarian and probably also the one in the technician. Because gilts (i.e., <1-year-old female pigs) were not introduced into the herd during the weeks before

the acute respiratory outbreak, the virus was most probably transmitted to sows by an infected person who entered the farm, probably an employee who, according to the farmer, displayed an ILI a few days before he spotted the first clinical signs in sows. This employee took a shower before entering the breeding area and put on dedicated clothes but did not wear a protective mask or gloves. Likewise, swine-to-human transmission was probably facilitated by the veterinarian and technician not wearing personal protective equipment when handling the sick sows. In either of these situations, transmission probably resulted from contact with respiratory secretions or inhalation of aerosols generated by shedding humans or animals or by contact with contaminated fomites (10).

Serologic investigations have previously suggested that occupational exposure to pigs is a risk factor for human infections (11), but events of bidirectional pH1N1 interspecies transmission have been rarely demonstrated. This report confirms pH1N1 virus can easily be transmitted between pigs and humans. Other swine IAVs were inherited completely or partially from human IAVs, but pH1N1 virus was suspected to be introduced to swine more frequently than other strains, potentially because the virus's origin was probably swine (5). After such reverse zoonotic events, the strain might undergo evolutionary adaptation, as revealed by the previously identified swine-specific genogroup (6); in cases of further antigenic divergence, these strains could constitute novel threats for humans lacking cross-immunity. Moreover, because of co-infections with other swine IAVs, numerous reassortants bearing ≥ 1 pH1N1 genomic segment have been described worldwide, and some of these strains have become enzootic in pig populations (3,5). Such reassortants could also be an increased risk to the public health, as illustrated by many swine-to-human transmission events of swine IAVs containing the pH1N1 matrix gene during exhibition fairs in the United States (12). These transmissions have strongly increased the number of zoonotic infections reported since the last pandemic; only a few cases were reported before 2009 (13,14).

Conclusions

The emergence of novel IAVs that threaten both human and swine health can be facilitated by the virus crossing species

Table. Influenza A(H1N1)pdm09 strains closest related to A/sw/France/53-180028/2018 isolated from a sow in France, 2018*

Influenza A(H1N1)pdm09 strain†	Collection date	Percentage identity								Whole genome
		Segment no. (gene)								
		1 (PB2)	2 (PB1)	3 (PA)	4 (HA)	5 (NP)	6 (NA)	7 (M)	8 (NS)	
A/Haute Normandie/1985/2017	2017 Dec 28	99.96	99.91	100.00	99.88	100.00	99.93	100.00	99.77	99.94
A/Dijon/181/2018	2017 Dec 31	99.96	99.91	99.95	99.82	100.00	99.86	100.00	99.88	99.94
A/Alsace/560/2018	2018 Jan 22	99.91	99.96	100.00	99.82	100.00	99.93	100.00	99.77	99.93
A/Paris/1767/2017	2017 Dec 15	99.96	99.96	99.95	99.76	100.00	100.00	99.90	99.77	99.92

*HA, hemagglutinin; M, matrix; NA, neuraminidase; NP, nucleoprotein; NS, nonstructural protein; PA, polymerase acidic; PB1, polymerase basic 1; PB2, polymerase basic 2.

†Sequences available in GISAID database (<https://www.gisaid.org>) and selected using integrated BLAST program.

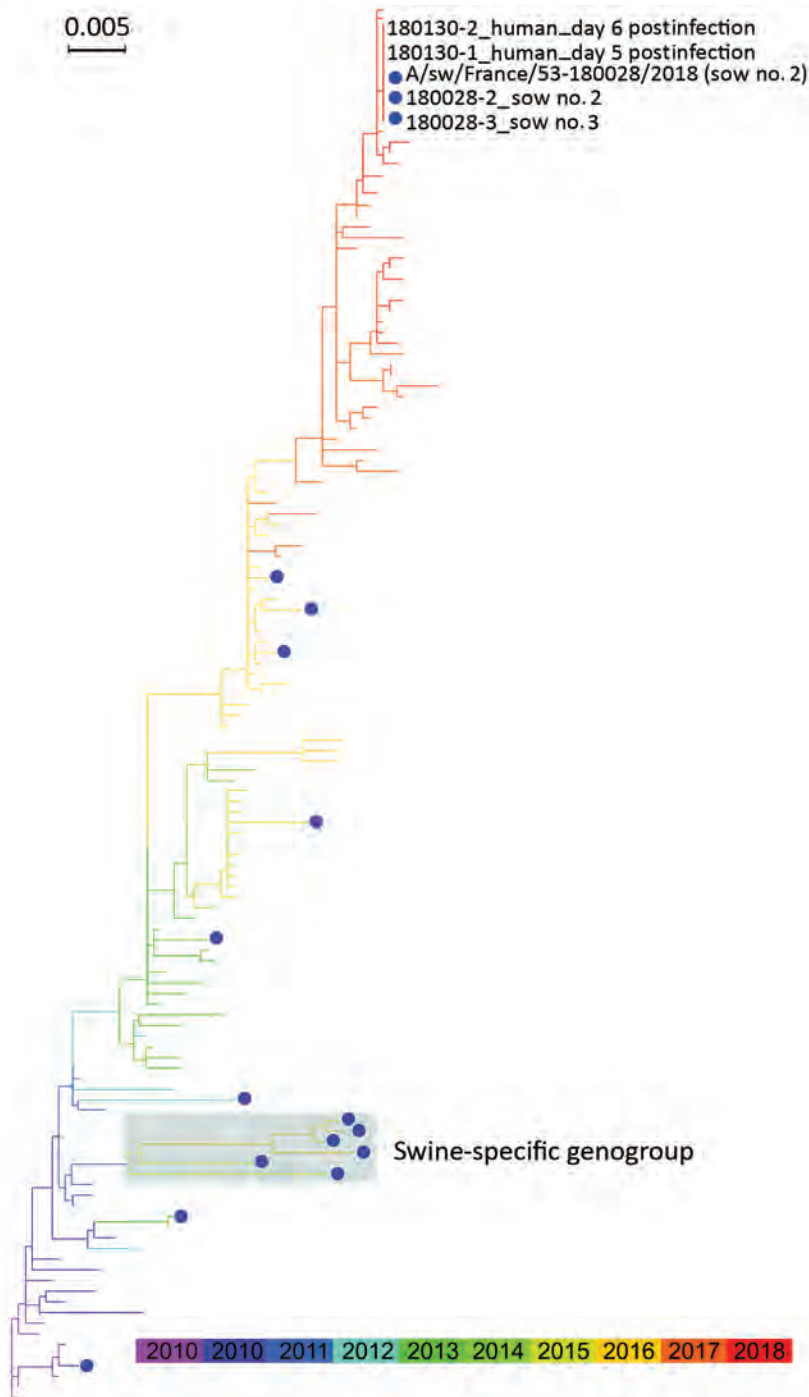


Figure. Maximum-likelihood phylogenetic tree of hemagglutinin segments from influenza A(H1N1) pdm09 isolates from swine (blue dots) and humans, France, 2009–2018. Shaded box indicates swine-specific genogroup previously described by Chastagner et al. (6).

barriers (4,15). The concomitant pH1N1 virus infections we report emphasize the importance of implementing ad hoc biosecurity measures in pig farms to prevent interspecies virus transmission (10). Our evidence supports the One Health perspective of providing pig industry workers the annual seasonal influenza vaccination. This practice can minimize the risk for workers acquiring pH1N1 virus infections from pigs and for workers transmitting human IAVs to pigs.

Acknowledgments

The authors are indebted to all members from RÉSAVIP (Réseau National de Surveillance des Virus Influenza Chez le Porc), also known as the National Network for Surveillance of Type A Influenza Virus in Swine.

This work was partially funded by the European Union Horizon 2020 program 503 COMPARE (Collaborative Management Platform for detection and Analyses of [Re-]emerging and foodborne

outbreaks in Europe; no. 643476) and by Santé Publique France for the coordinating center of the National Reference Center for Respiratory Viruses (including influenza) at Institut Pasteur.

About the Author

Dr. Chastagner is a molecular epidemiologist working in the Swine Virology Immunology Unit and National Reference Laboratory for Swine Influenza at Agence Nationale de Sécurité Sanitaire de l'Alimentation, de l'Environnement et du Travail, Ploufragan, France. Her main research interests are genetic and antigenic evolution of swine influenza viruses.

References

- Smith GJ, Vijaykrishna D, Bahl J, Lycett SJ, Worobey M, Pybus OG, et al. Origins and evolutionary genomics of the 2009 swine-origin H1N1 influenza A epidemic. *Nature*. 2009;459:1122–5. <https://doi.org/10.1038/nature08182>
- Adlhoch C, Broberg E, Beauté J, Snacken R, Bancroft E, Zucs P, et al.; European Influenza Surveillance Network. Influenza season 2013/14 has started in Europe with influenza A(H1)pdm09 virus being the most prevalent subtype. *Euro Surveill*. 2014;19:20686. <https://doi.org/10.2807/1560-7917.ES2014.19.4.20686>
- Simon G, Larsen LE, Dürrwald R, Foni E, Harder T, Van Reeth K, et al.; European Surveillance Network for Influenza in Pigs 3 Consortium. European Surveillance Network for Influenza in Pigs: surveillance programs, diagnostic tools and swine influenza virus subtypes identified in 14 European countries from 2010 to 2013. *PLoS One*. 2014;9:e115815. <https://doi.org/10.1371/journal.pone.0115815>
- Nelson MI, Vincent AL. Reverse zoonosis of influenza to swine: new perspectives on the human-animal interface. *Trends Microbiol*. 2015;23:142–53. <https://doi.org/10.1016/j.tim.2014.12.002>
- Watson SJ, Langat P, Reid SM, Lam TT, Cotten M, Kelly M, et al.; European Surveillance Network for Influenza in Pigs 3 Consortium. Molecular epidemiology and evolution of influenza viruses circulating within European swine between 2009 and 2013. *J Virol*. 2015;89:9920–31. <https://doi.org/10.1128/JVI.00840-15>
- Chastagner A, Hervé S, Bonin E, Quéguiner S, Hirchaud E, Henritzi D, et al. Spatiotemporal distribution and evolution of the A/H1N1 2009 pandemic influenza virus in pigs in France from 2009 to 2017: identification of a potential swine-specific lineage. *J Virol*. 2018;92:e00988–18. <https://doi.org/10.1128/JVI.00988-18>
- Garin E, Hervé S, Rose N, Locatelli C, Lecarpentier L, Ngwa-Mbot D, et al. National Network for Surveillance of Type A Influenza Virus in Swine (RÉSAVIP). Review of operations and surveillance results for 2016 [in French]. *Bull Epidemiol Sante Anim Aliment*. 2017;80:1–5.
- Bonin E, Quéguiner S, Woudstra C, Gorin S, Barbier N, Harder TC, et al. Molecular subtyping of European swine influenza viruses and scaling to high-throughput analysis. *Virol J*. 2018;15:7. <https://doi.org/10.1186/s12985-018-0920-z>
- Watson SJ, Welkers MR, Depledge DP, Coulter E, Breuer JM, de Jong MD, et al. Viral population analysis and minority-variant detection using short read next-generation sequencing. *Philos Trans R Soc Lond B Biol Sci*. 2013;368:20120205. <https://doi.org/10.1098/rstb.2012.0205>
- Centers for Disease Control and Prevention. Flu can spread between pigs and people. 2018 Jul 5 [cited 2019 Jan 14]. <https://www.cdc.gov/flu/pdf/swineflu/transmission-between-pigs-people.pdf>
- Fragaszy E, Ishola DA, Brown IH, Enstone J, Nguyen-Van-Tam JS, Simons R, et al.; Flu Watch Group; Combating Swine Influenza Consortium. Increased risk of A(H1N1)pdm09 influenza infection in UK pig industry workers compared to a general population cohort. *Influenza Other Respir Viruses*. 2016;10:291–300. <https://doi.org/10.1111/irv.12364>
- Bowman AS, Workman JD, Nolting JM, Nelson SW, Slemmons RD. Exploration of risk factors contributing to the presence of influenza A virus in swine at agricultural fairs. *Emerg Microbes Infect*. 2014;3:1–5. <https://doi.org/10.1038/emi.2014.5>
- Myers KP, Olsen CW, Gray GC. Cases of swine influenza in humans: a review of the literature. *Clin Infect Dis*. 2007;44:1084–8. <https://doi.org/10.1086/512813>
- Kuntz-Simon G, Madec F. Genetic and antigenic evolution of swine influenza viruses in Europe and evaluation of their zoonotic potential. *Zoonoses Public Health*. 2009;56:310–25. <https://doi.org/10.1111/j.1863-2378.2009.01236.x>
- Short KR, Richard M, Verhagen JH, van Riel D, Schrauwen EJA, van den Brand JMA, et al. One Health, multiple challenges: the inter-species transmission of influenza A virus. *One Health*. 2015;1:1–13. <https://doi.org/10.1016/j.onehlt.2015.03.001>

Address for correspondence: Gaëlle Simon, ANSES, Laboratoire de Ploufragan-Plouzané-Niort, Rue des Fusillés, Zoopôle Les Croix, BP 53, 22440 Ploufragan, France; email: gaelle.simon@anses.fr

Tick-Borne Encephalitis in Auvergne-Rhône-Alpes Region, France, 2017–2018

Elisabeth Botelho-Nevers,
Amandine Gagneux-Brunon, Aurelie Velay,
Mathilde Guerbois-Galla, Gilda Grard,
Claire Bretagne, Alexandra Mailles,
Paul O. Verhoeven, Bruno Pozzetto,
Sylvie Gonzalo, Samira Fafi-Kremer,
Isabelle Leparc-Goffart, Sylvie Pillet

Three autochthonous cases of tick-borne encephalitis (TBE) acquired in rural areas of France where Lyme borreliosis, but not TBE, is endemic highlight the emergence of TBE in new areas. For patients with neurologic involvement who have been in regions where *Ixodes* ticks circulate, clinicians should test for TBE virus and other tickborne viruses.

Tick-borne encephalitis (TBE) is a zoonotic disease caused by tick-borne encephalitis virus (TBEV), a flavivirus transmitted to humans by the bite of an infected tick (*I*) and usually acquired during outdoor activities in forest regions. Among the different TBEV subtypes (*2*), the European subtype is transmitted by *Ixodes ricinus* ticks (*1*). In France, TBEV infection is predominant in the northeastern part of the country, notably in the Alsace-Lorraine region, where the number of reported cases recently increased (*3–5*). We report 3 autochthonous cases of TBE acquired during the 2017 and 2018 summer seasons in 2 central rural areas of France not previously known to be places of TBEV circulation: Loire (2 cases) and Haute Loire (1 case), located in the Auvergne-Rhône-Alpes region (Tables 1, 2; Figure). The 3 patients provided informed consent to participate in the study.

The Cases

In June 2017, a 76-year-old immunosuppressed man (case-patient 1) was admitted to the emergency department of a

Author affiliations: University Hospital of Saint-Etienne, Saint-Etienne, France (E. Botelho-Nevers, A. Gagneux-Brunon, P.O. Verhoeven, B. Pozzetto, S. Gonzalo, S. Pillet); Strasbourg University, Strasbourg, France (A. Velay, S. Fafi-Kremer); Aix-Marseille University, Marseille, France (M. Guerbois-Galla, G. Grard, I. Leparc-Goffart); Antoine Béclère Hospital, Clamart, France (C. Bretagne); French National Public Health Agency, Saint-Maurice, France (A. Mailles)

DOI: <https://doi.org/10.3201/eid2510.181923>

local hospital for headache and cervicobrachial neuralgia. He reported having been hiking in Haute Loire. After symptom persistence and onset of fever over the next 48 hours, he was transferred to the University Hospital of Saint-Etienne (Saint-Etienne, France). Because clinical presentation was unusual and no etiology was determined, serum and cerebrospinal fluid (CSF) samples were sent to the National Reference Centre for Arboviruses (Marseille, France). ELISA detected IgM against TBEV in both fluids. During follow-up testing, serum TBEV IgM and IgG titers increased. The patient's outcome was favorable, without sequelae.

In September 2017, an 8-year-old boy (case-patient 2) was admitted to the emergency department of the University Hospital of Clamart, near Paris, France, for meningeal syndrome. Two weeks earlier, he had stayed for vacation in the Loire countryside, where he experienced a tick bite. Lumbar puncture results revealed meningitis. A CSF sample was sent to the Borrelia National Reference Centre at the University Hospital of Strasbourg (Strasbourg, France) to rule out Lyme disease; the CSF sample was then transferred to the virology laboratory of the same hospital, where it was positive for TBEV IgM and IgG. The patient recovered without sequelae.

In July 2018, a 66-year-old female farmer (case-patient 3) in Loire, who had been bitten by ticks while working, was first admitted to the emergency department of a local hospital for meningoencephalitis. She was then transferred to the University Hospital of Saint-Etienne. Serologic testing for Lyme disease was positive by ELISA and Western blot for IgG, with no IgM in serum and CSF specimens; Reiber index was <2. Because no alternative etiology was initially found, the patient received treatment for neuroborreliosis. A second lumbar puncture performed 1 week after admission revealed elevated leukocytes (29 cells/mm³; 97% lymphocytes), elevated erythrocytes (136 cells/mm³), elevated protein level (0.72 g/L), and glucose level within reference range (3.02 mmol/L). Serum and CSF specimens were positive for TBEV IgM and IgG, which ruled out neuroborreliosis and led to discontinuation of antimicrobial therapy. Three months after the acute episode, the patient still experienced dizziness and slight motor deficits in her right arm and leg.

Conclusions

These 3 cases of TBE occurred in 2 close areas of the Auvergne-Rhône-Alpes region, France, not previ-

Table 1. Characteristics of 3 case-patients with tick-borne encephalitis acquired in the Auvergne-Rhône-Alpes region of France, 2017–2018*

Characteristic	Case-patient 1	Case-patient 2	Case-patient 3
Medical history	Myelofibrosis associated with a JAK 2 mutation, treated with hydroxycarbamide	None	Zoster Bell palsy in 1990, arterial hypertension, obesity (BMI 34 kg/m ²)
Outdoor activity			
Date/duration	2017 Jun 2/2 d	2017 Aug 13–19	All year
Location	Allègre region (43270, Haute Loire)	Montarcher forest (42380, Loire)	Saint-Bonnet-le-Courreau (42940, Loire)
Type	Hiking for 10 km	Hiking, camping	Farming
Tick exposure	3 nonidentified insect bites on legs and left arm (no eschar, slight erythema at localizations of bites) while hiking	1 tick bite; tick removed 48 h later	Yes, frequent
Clinical manifestations			
Date of symptom onset	2017 Jun 17	2017 Aug 30	2018 Jul 21
Main clinical signs	Headache, left cervicobrachial neuralgia, asthenia, delayed persistent fever (>38.5°C)	Low-grade fever (38.5°C), headache, cervical pain, nausea, vomiting	Dizziness, headache, fever (38.4°C), unable to lift right shoulder
Physical findings	No abnormality	Neck stiffness	Proximal deficit in right arm; 3 days later, light deficit in right leg, inability to walk because of motor deficit and dizziness
Encephalitis	No	No	Yes
Radiologic findings	Unremarkable cerebral CT scan	None	Unremarkable cerebral CT scan and cerebral MRI
Biological parameters			
CSF analysis	2017 Jun 23	2017 Sep 2	2018 Jul 21 (first one)
Leukocytes, cells/mm ³	5	62 (50% PMNs)	195 (88% lymphocytes)
Erythrocytes, cells/mm ³	2	1	51
Proteinorachia, g/L	0.67	0.48	0.77
Glycorachia/glycemia, mmol/L	2.98/5.8	3.4/5.6	3.18/5.68
Etiologic investigations	Absence of HSV, VZV, or enterovirus by PCR or RT-PCR; presence of TBEV IgM	Absence of enterovirus by RT-PCR; presence of TBEV IgM	Absence of HSV, VZV, or enterovirus by PCR or RT-PCR; presence of <i>Borrelia burgdorferi</i> IgG in CSF; Reiber index <2; presence of TBEV IgM
Blood analyses	Blood serology negative for <i>Mycoplasma pneumoniae</i> , <i>Bartonella henselae</i> , <i>Coxiella burnetii</i> , <i>Legionella pneumophila</i> , HIV, hepatitis B and C viruses, <i>B. burgdorferi</i> (both in serum and CSF); positive for cytomegalovirus, Epstein-Barr virus, <i>Toxoplasma gondii</i> , and <i>Chlamydia pneumophila</i> , revealed past immunization	None	Blood serology for <i>B. burgdorferi</i> IgG >0; blood serology negative for <i>M. pneumoniae</i> , <i>B. henselae</i> , <i>C. burnetii</i> , <i>L. pneumophila</i> , HIV, hepatitis B and C viruses
Treatment	2017 Jun 17: paracetamol; 2017 Jun 19: ceftriaxone 1 g/d + levofloxacin 1 g/d; 2017 Jun 23: treatment stopped	2017 Feb 17: ceftriaxone 100 mg/kg/d; 2017 Sep 4: ceftriaxone stopped, switched to doxycycline 200 mg/d	2018 Jul 21: acyclovir 3,000 mg/d amoxicillin 12 g/d; 2018 Jul 27: acyclovir stopped, amoxicillin switched to ceftriaxone 2 g/d for 14 d
Outcome	Headache and asthenia waned progressively, fever disappeared; discharged 2017 Jun 29	Discharge 2017 Sep 4	Discharged 2018 Aug 17 to rehabilitation center because of persistent dizziness and motor deficit in right arm and leg
Follow-up	Consultation 2017 Jul 27; patient felt good, no headache or fever	Consultation 2017 Sep 18: complete recovery	Consultation 2018 Sep 19; patient able to walk alone but always with a slight motor deficit of right arm and leg and dizziness
Sequelae	No	No	Yes

*Case-patient 1, 76-year-old man; case-patient 2, 8-year-old boy; case-patient 3, 66-year-old woman. No patients had been vaccinated against arboviruses. BMI, body mass index; CSF, cerebrospinal fluid; CT, computed tomography; HSV, herpes simplex virus; MRI, magnetic resonance imaging; PMN, polymorphonuclear cell; RT-PCR, reverse transcription PCR; TBEV, tick-borne encephalitis virus; VZV, varicella zoster virus.

Table 2. Results of serologic testing for arboviruses and Lyme disease for 3 patients with tick-borne encephalitis, Loire and Haute Loire, Auvergne-Rhône-Alpes Region, France, 2017–2018*

Case no., sample	Days after clinical onset	TBEV		DENV		CHIKV		ZIKV		WNV		TOSV		<i>Borrelia burgdorferi</i>	
		IgM	IgG	IgM	IgG	IgM	IgG	IgM	IgG	IgM	IgG	IgM	IgG	IgM	IgG
1															
CSF	16	4.3	3.22	1	1.12	<1	<1	<1	1	1	1.14	ND	ND		
Serum	19	6.6	2.94	1.16	1.24	<1	1.1	ND	ND	<1	1.24	<1	1	Neg	Neg
Serum	48	7.1	10.6	1.11	1.10	1	1	ND	ND	ND	ND	ND	ND		
2†															
CSF	15	53.4	748.62	ND	ND	ND	ND	ND	ND	ND	ND	ND	ND	Neg	Neg
3															
CSF	2	2.84	1.74	1.09	<1	<1	<1	<1	<1	<1	1	ND	ND		Pos‡
Serum	ND	ND	ND	ND	ND	ND	ND	ND	ND	ND	ND	ND	ND	Neg	Pos
CSF	10	7.26	6.41	1.05	1.41	<1	1.02	<1	<1	<1	1.39	<1	<1		Pos
Serum‡	10	2.34	3.02	<1	<1	<1	<1	<1	<1	<1	<1	<1	<1	Neg	Pos
Serum	61	4.02	5.19	1.02	2.10	1.02	<1	<1	1	1.06	3.70	ND	ND	ND	ND

*For cases 1 and 3, the results of ELISA serologic testing performed at the National Reference Centre for Arboviruses (Marseille, France) are expressed as the ratio between the optical density obtained with each viral antigen and the optical density with the control antigen. A ratio of <2.5 is considered a negative result; a ratio of 2.5–3.0 is considered an undetermined result; a ratio of >3 is considered a positive result. Lyme borreliosis serology was performed with Vidas immunoassays (bioMérieux, <https://www.biomerieux.com>). Serum specimens reacting for *Borrelia burgdorferi* IgG were also tested with Western blot; reactivity was observed for all cases with the lipoprotein Vlse (a variable surface antigen of *B. burgdorferi*), and 17-, 39-, and 83-KDa proteins. Serologic testing for case-patient 2 was performed at the Laboratory of Virology at Strasbourg (Strasbourg, France) by using commercial assays (SERION ELISA classic TBE Virus IgG/IgM; <https://www.virion-serion.de/en>) and were interpreted according to the manufacturer's instructions; results are expressed as U/mL, and positive cutoff values were 15 U/mL for TBEV IgM and 150 U/mL for TBEV IgG. Lyme borreliosis serology was performed with Enzygnost immunoassays (Siemens, <https://www.siemens-healthineers.com>). Boldface indicates positive results. CHIKV, chikungunya virus; CSF, cerebrospinal fluid; DENV, dengue virus; ND, not done; TBEV, tick-borne encephalitis virus; TOSV, Toscana virus; WNV, West Nile virus; ZIKV, Zika virus.

†Serologic testing could not be performed on serum sample.

‡The Reiber index showed a CSF/serum IgG ratio of 1.03 (i.e., an equivocal result of <2).

ously identified as places of TBEV circulation. TBEV emergence in new regions of Europe has recently been described (5–7). In France, in addition to the Alsace-Lorraine region (3), sporadic cases were reported in other rural and forested regions, such as the Alpine region (2) (Figure), suggesting that circulation of TBEV in France is wider than previously thought. The increasing number and geographic extension of cases can be related to climate changes, importation of infected ticks by animal migration/transportation, modification of lifestyle with travel and exposure to infected ticks by outdoor activities, and more systematic serologic testing for this agent (3,6).

Of note, *I. ricinus* ticks, the vectors of TBEV in western Europe, are also the vectors of *Borrelia burgdorferi*. Co-circulation of both pathogens could then occur in the same area as reported in Alsace, as suggested by the cases reported here and elsewhere (8); Haute Loire and Loire are places with high incidence of Lyme borreliosis (9). The prevalence of TBEV infection in ticks has been reported to be low in Europe, notably in France (10,11). Performance of diagnostic tools for detecting TBEV infection in sentinel animals seems to be better than testing ticks to estimate TBEV circulation in regions where *I. ricinus* ticks are present (10).

In Europe, transmission of TBEV occurs mainly from spring through early autumn (1,4), as found for the 3 cases reported here; this seasonality corresponds to suitable temperatures and humidity required for tick activity (1). The viral cycle involves animal reservoirs, mainly rodents and

deer; humans are incidental hosts. The most common mode of TBEV transmission is the bite of an infected tick; however, transmission by consumption of unpasteurized milk from infected mammals (goats, sheep, cows) is also suspected (6,12,13). For case-patient 1, transmission probably occurred through a tick bite, even if no tick was seen by the patient; the patient denied consumption of at-risk food. For case-patient 2, a tick was attached to the patient some days before symptom onset. For case-patient 3, transmission by a tick bite is also likely because the patient reported having frequently been bitten by ticks during her professional activity.

In TBE-endemic areas of Europe, TBEV infection is a public health concern; in several countries, vaccination is recommended. Indeed, even if most of the infections caused by the TBEV European subtype are clinically inapparent or only mildly symptomatic, the mortality rate is estimated to be ≈1%, and incomplete recovery with long-term neurologic sequelae is reported for 26%–46% of cases (6). Case-patient 1 exhibited atypical and mild symptoms, consisting of headache and fever without neurologic sequelae. Case-patient 2 exhibited the classical biphasic form of the disease with meningitis that evolved favorably. Case-patient 3 had more severe meningoencephalitis with sequelae.

For case-patients 1 and 3, the profile of acute infection suggested by ELISA was confirmed by plaque-reduction neutralization testing (Table 2). This testing could not be done for case-patient 2 (the young boy) because of insufficient CSF volume. For most cases, even if TBEV can be detected by culture or reverse transcription PCR of serum during early infection when the symptoms are not evocative

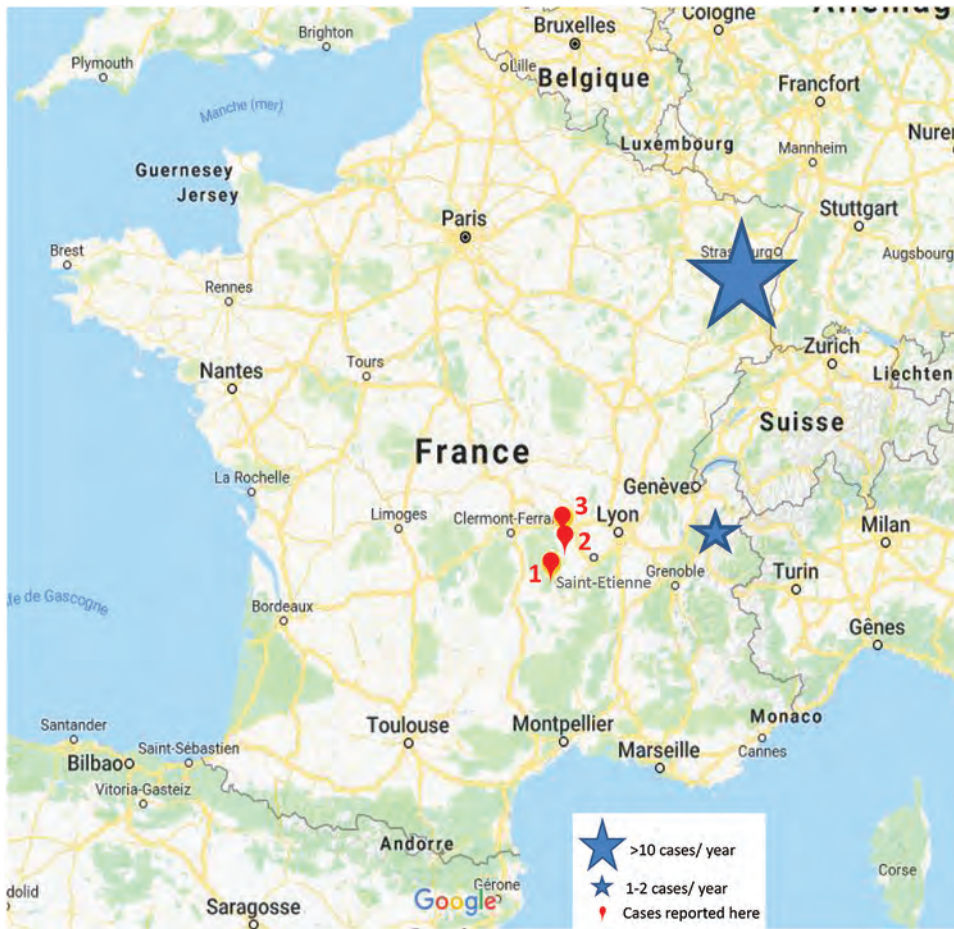


Figure. Areas of the Auvergne-Rhône-Alpes region of France visited by 2 patients and inhabited by 1 patient who acquired tick-borne encephalitis during 2017–2018. Red flags and text indicate locations and case-patient numbers.

of TBE (6,14), a TBE diagnosis is made by serologic testing only. Considering the clinical manifestations, the exposure to tick bites, and serologic results according to the guidelines of the European Academy of Neurology (<https://www.ean.org>), the 3 cases that we report can be classified as confirmed TBEV infection (4).

These cases of TBEV infection highlight the emergence of TBEV in rural and forested areas of France and underline that TBEV infection is probably underdiagnosed in France. Because TBEV and *B. burgdorferi* are carried by the same vector, clinicians with patients who have been bitten by ticks should consider and investigate infection with both pathogens, as well as other tickborne viruses, such as Powassan virus in North America (15). To better document the circulation of these viruses, epidemiologic studies are needed. When diagnosing acute neurologic involvement in patients who stayed in regions where *Ixodes* ticks circulate, serologic testing for TBEV and other tickborne viruses should be performed, according to geographic regions. This testing could improve diagnosis of these infections and, according to the evolution of the epidemiology, might be used to modify the TBEV vaccination policy in areas with high TBE incidence.

About the Author

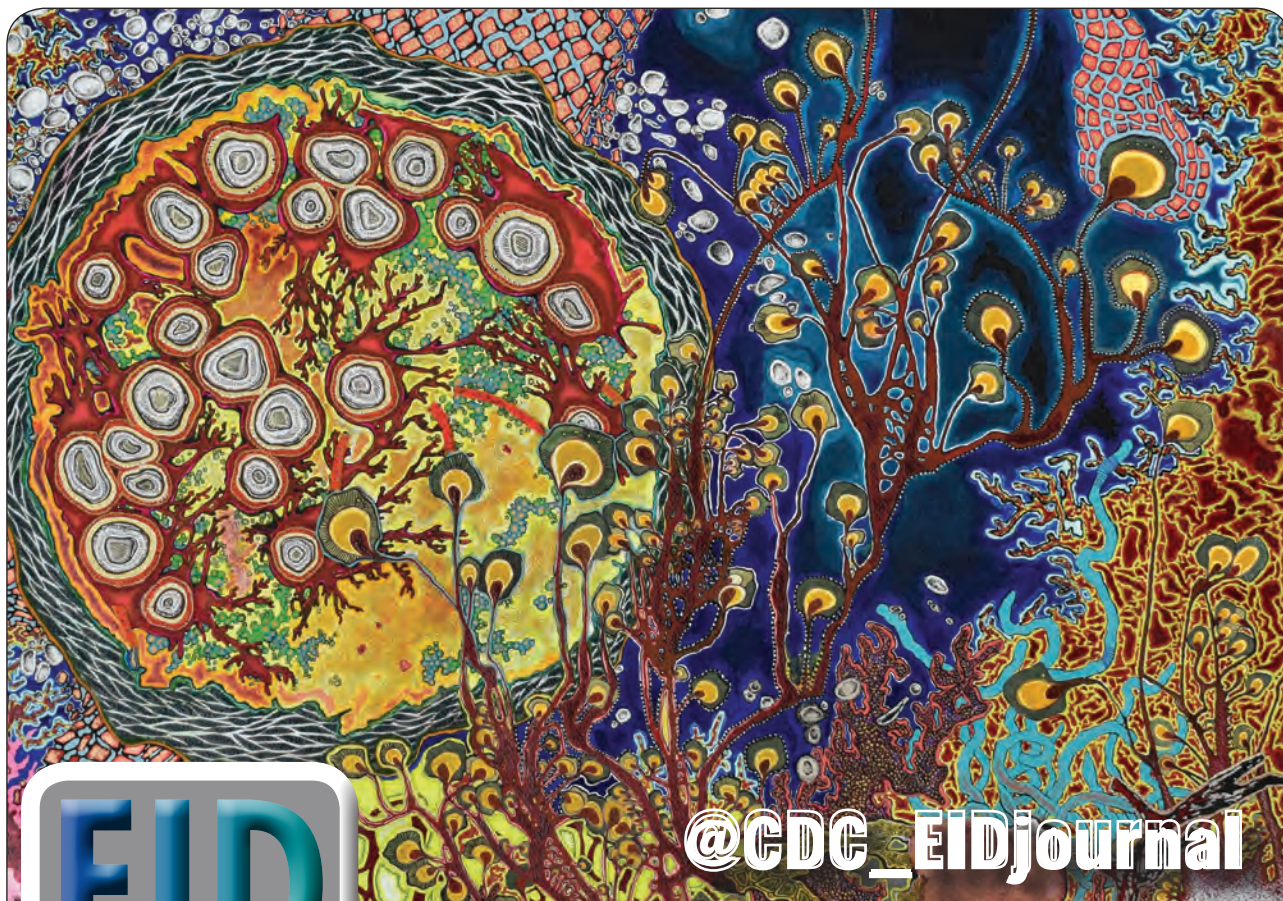
Dr. Botelho-Nevers is a full professor in infectious diseases in Saint-Etienne, France. Her research interest is prevention of healthcare-associated infections.

References

1. Lindquist L, Vapalahti O. Tick-borne encephalitis. *Lancet*. 2008;371:1861–71. [https://doi.org/10.1016/S0140-6736\(08\)60800-4](https://doi.org/10.1016/S0140-6736(08)60800-4)
2. Ruzek D, Avšič Županc T, Borde J, Chrdle A, Eyer L, Karganova G, et al. Tick-borne encephalitis in Europe and Russia: review of pathogenesis, clinical features, therapy, and vaccines. *Antiviral Res*. 2019;164:23–51. <https://doi.org/10.1016/j.antiviral.2019.01.014>
3. Velay A, Solis M, Kack-Kack W, Gantner P, Maquart M, Martinot M, et al. A new hot spot for tick-borne encephalitis (TBE): a marked increase of TBE cases in France in 2016. *Ticks Tick Borne Dis*. 2018;9:120–5. <https://doi.org/10.1016/j.ttbdis.2017.09.015>
4. Beauté J, Spiteri G, Warns-Petit E, Zeller H. Tick-borne encephalitis in Europe, 2012 to 2016. *Euro Surveill*. 2018;23:1800201. <https://doi.org/10.2807/1560-7917.ES.2018.23.45.1800201>
5. Kunze U; the ISW-TBE. Report of the 20th annual meeting of the International Scientific Working Group on Tick-Borne Encephalitis (ISW-TBE): ISW-TBE: 20 years of commitment and still challenges ahead. *Ticks Tick Borne Dis*. 2019;10:13–7. <https://doi.org/10.1016/j.ttbdis.2018.08.004>

6. Taba P, Schmutzhard E, Forsberg P, Lutsar I, Ljøstad U, Mygland Å, et al. EAN consensus review on prevention, diagnosis and management of tick-borne encephalitis. *Eur J Neurol*. 2017;24:1214–e61. <https://doi.org/10.1111/ene.13356>
7. Barzon L. Ongoing and emerging arbovirus threats in Europe. *J Clin Virol*. 2018;107:38–47. <https://doi.org/10.1016/j.jcv.2018.08.007>
8. Thorin C, Rigaud E, Capek I, André-Fontaine G, Oster B, Gastinger G, et al. Séroprévalence de la borréliose de Lyme et de l'encéphalite à tiques chez des professionnels exposés dans le Grand Est de la France. *Med Mal Infect*. 2008;38:533–42. <https://doi.org/10.1016/j.medmal.2008.06.008>
9. Vandenesch A, Turbelin C, Couturier E, Arena C, Jaulhac B, Ferquel E, et al. Incidence and hospitalisation rates of Lyme borreliosis, France, 2004 to 2012. *Euro Surveill*. 2014;19:pii:20883. <https://doi.org/10.2807/1560-7917.ES2014.19.34.20883>
10. Imhoff M, Hagedorn P, Schulze Y, Hellenbrand W, Pfeffer M, Niedrig M. Review: sentinels of tick-borne encephalitis risk. *Ticks Tick Borne Dis*. 2015;6:592–600. <https://doi.org/10.1016/j.ttbdis.2015.05.001>
11. Gondard M, Michelet L, Nisavanh A, Devillers E, Delannoy S, Fach P, et al. Prevalence of tick-borne viruses in *Ixodes ricinus* assessed by high-throughput real-time PCR. *Pathog Dis*. 2018; 76:fty083. <https://doi.org/10.1093/femspd/fty083>
12. Süss J. Tick-borne encephalitis 2010: epidemiology, risk areas, and virus strains in Europe and Asia—an overview. *Ticks Tick Borne Dis*. 2011;2:2–15. <https://doi.org/10.1016/j.ttbdis.2010.10.007>
13. Caini S, Szomor K, Ferenczi E, Szekelyne Gaspar A, Csohan A, Krisztalovics K, et al. Tick-borne encephalitis transmitted by unpasteurised cow milk in western Hungary, September to October 2011. *Euro Surveill*. 2012;17:pii:20128.
14. Veje M, Studahl M, Johansson M, Johansson P, Nolskog P, Bergström T. Diagnosing tick-borne encephalitis: a re-evaluation of notified cases. *Eur J Clin Microbiol Infect Dis*. 2018;37:339–44. <https://doi.org/10.1007/s10096-017-3139-9>
15. Hermance ME, Thangamani S. Powassan virus: an emerging arbovirus of public health concern in North America. *Vector Borne Zoonotic Dis*. 2017;17:453–62. <https://doi.org/10.1089/vbz.2017.2110>

Address for correspondence: Elisabeth Botelho-Nevers, University Hospital, Infectious Diseases Department, Ave Albert Raimond, Saint-Etienne 42055, France; email: elisabeth.botelho-nevers@chu-st-etienne.fr



Want to stay updated on the latest news in Emerging Infectious Diseases? Let us connect you to the world of global health. Discover groundbreaking research studies, pictures, podcasts, and more by following us on Twitter at @CDC_EIDjournal.

Factoring Prior Treatment into Tuberculosis Infection Prevalence Estimates, United States, 2011–2012

Laura A. Vonnahme, Maryam B. Haddad,
Thomas R. Navin

To refine estimates of how many persons in the United States are candidates for treatment of latent tuberculosis, we removed from analysis persons who self-reported prior treatment on the National Health and Nutrition Examination Survey 2011–2012. We estimate that 12.6 million persons could benefit from treatment to prevent active tuberculosis.

In the United States, although tuberculosis (TB) incidence is at historic lows, the average annual rate of decline has slowed to 2% (1). To achieve TB elimination by 2100, sustained annual declines of twice that magnitude are needed (2). Most new cases of TB in the United States result from progression of *Mycobacterium tuberculosis* infections acquired years earlier (3). TB elimination requires scaling up treatment of latent TB infection (LTBI) to prevent progression to active TB. The National Health and Nutrition Examination Survey (NHANES) 2011–2012 determined that ≈5% of the US population had LTBI on the basis of positivity of a tuberculin skin test (TST) or an interferon- γ release assay (IGRA) (4). However, these TB test results may remain positive even after a patient has received effective treatment for active TB or LTBI. Specifically, the TST is widely believed to remain positive for life; whether the IGRA blood test remains positive is still undetermined (5–7). To better estimate the number of persons in the United States who are candidates for LTBI treatment (8), we refined the NHANES-based estimate of the national LTBI prevalence by excluding from analysis persons who reported having received prior treatment for active TB or LTBI.

The Study

The only nationally representative survey that reflects both TST and IGRA results is the NHANES 2011–2012. NHANES cross-sectional surveys are implemented in consecutive 2-year cycles and are designed to assess the health

and nutritional status of the civilian, noninstitutionalized US population (9). To obtain this nationally representative sample, NHANES uses complex, stratified, multistage probability cluster sampling (10). The survey consists of questionnaires administered in the home, followed by a medical examination conducted in a mobile examination center. The NHANES 2011–2012 questionnaire included questions about participants' history of TB testing and diagnosis and any prior treatment for active TB or LTBI (9). The medical examinations included a TST and an IGRA for TB infection for participants ≥ 6 years of age (4).

We defined a positive test result for TB infection as a positive result for an IGRA administered by NHANES according to manufacturer's standards (11) or a TST reaction of ≥ 10 mm. Self-reported prior treatment was defined as a participant's answer of yes to NHANES questions about having ever been prescribed medicine for TB disease or to keep from getting sick with TB (i.e., LTBI treatment). We ascertained prevalence estimates of self-reported prior treatment among persons ≥ 6 years of age who had a positive result for TB infection for a test conducted by NHANES. We assessed treatment history among subgroups with IGRA positivity, TST positivity, TST or IGRA positivity, or dual TST and IGRA positivity. For comparison, we also assessed treatment history among persons with dual TST and IGRA negativity. We stratified subgroups by birthplace. We calculated population prevalence estimates and corresponding 95% CIs by using SAS software (<https://www.sas.com>), which accounted for the complex survey design, the 2-year examination weights, and population denominators from the 2011 American Community Survey data.

All NHANES participants or their proxies provided informed consent, and the Research Ethics Review Board of the National Center for Health Statistics reviewed all procedures and protocols. All data used for this analysis are publicly available (<https://www.cdc.gov/nchs/nhanes>).

Having already been treated for active TB or for LTBI was self-reported by 12.2% (95% CI 8.5%–15.8%) participants, or 1.8 (95% CI 1.1–2.3) million of the 14.1 (95% CI 11.9–16.4) million persons in the civilian, noninstitutionalized US population with a positive IGRA blood test result for TB infection. This finding suggests that as

Author affiliation: Centers for Disease Control and Prevention, Atlanta, Georgia, USA

DOI: <https://doi.org/10.3201/eid2510.190439>

of 2011–2012, 12.6 (95% CI 10.5–14.7) million persons could still benefit from LTBI treatment after further evaluation (i.e., after obtaining radiologic evidence to help exclude a diagnosis of active TB disease).

Stratification by birthplace did not reveal substantial differences for prevalence of prior treatment for TB disease or LTBI; 11.3% (95% CI 5.5%–17.1%) of persons born in the 50 US states or the District of Columbia (US-born) and 13.0% (95% CI 9.5%–16.5%) of non-US-born persons with a positive IGRA result reported having received prior treatment (Figure). Excluding those persons, an estimated 6.5 (95% CI 4.4–8.5) million US-born persons and 5.5 (95% CI 4.6–6.3) million non-US-born persons with a positive IGRA result reported no prior treatment.

When also considering TST results in the definition of a positive test result for TB infection, the prevalence of self-reported prior TB treatment among persons with TB infection ranged from 11.9% to 16.4%, with overlapping CIs (Figure). Among subgroups, the prevalence range for prior treatment was wider overall among US-born persons (11.3%–22.5%) than among non-US-born persons (10.9%–14.1%); the highest rate of self-reported prior TB treatment was among US-born persons with dual-positive results for the TST and the IGRA: 22.5% (95% CI 10.9%–34.0%).

Among persons with dual-negative results for the TST and IGRA, the prevalence of prior TB treatment was 0.6% (95% CI 0.3%–0.9%). Prevalence was higher among non-US-born (2.5% [95% CI 1.2%–3.7%]) than among US-born (0.3% [95% CI 0.1%–0.6%]) persons.

Conclusions

An estimated 12.6 (95% CI 10.5–14.7) million persons living in the United States with evidence of TB infection by IGRA result reported no prior TB treatment. This number excludes \approx 12% of persons in previously reported estimates of the number of persons with LTBI in the United States (4). In estimating the potential effect of interventions to expand screening and treatment for LTBI, our estimate of 12.6 million untreated TB-infected persons is a more meaningful measure for determining potential individual and societal benefits of LTBI treatment.

A limitation of this analysis is that previous medication history was self-reported only. Recall bias might have resulted in the misreporting of prior treatment. In addition, we cannot assume that all persons who reported prior treatment completed the regimen, although partial treatment of TB has been shown to be effective (12). However, because the questionnaire was administered several days before the medical examination, knowledge of the outcome of the NHANES test for *M. tuberculosis* infection would not have influenced this response. A treatment adherence question was included in the survey; however, a positive response to the question was not used to define prior treatment because it pertained only to completing treatment for LTBI, and $>$ 90% reported treatment completion. In addition, a single 2-year NHANES cycle is not designed to provide stable prevalence estimates for detailed subpopulations (e.g., non-US-born persons with a certain test result); consecutive NHANES cycles of at least 4 or 6 years would provide more precise estimates (8,9).

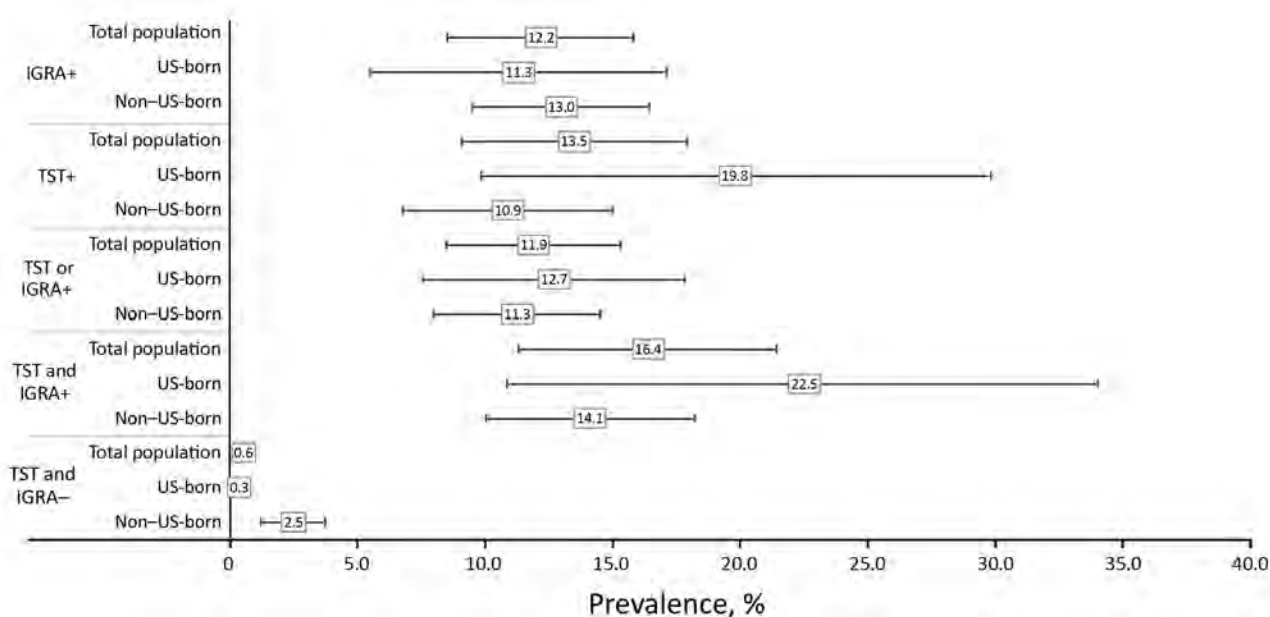


Figure. Estimated prevalence of prior treatment among persons tested for tuberculosis infection, United States, 2011–2012. Boxes represent prevalence estimates and corresponding horizontal lines represent 95% CIs. IGRA, interferon- γ release assay; TST, tuberculin skin test; +, positive; –, negative.

The higher prevalence of self-reported prior treatment among persons with a positive test result for *M. tuberculosis* infection helps validate the 2 implicit assumptions that anyone who had received prior treatment would have had at that time a positive test result (or a diagnosis of active TB disease) and that the result would have remained positive at the time of the NHANES examination. Conversely, the <1% prevalence of prior treatment history among those with negative TST and IGRA results suggests that some test results became negative after treatment or that some uninfected participants inaccurately recalled having taken medication for active TB disease or LTBI.

Regardless of which diagnostic test for TB infection was considered, consistently ≈12% of those with positive results during the NHANES 2011–2012 self-reported prior TB treatment. In conclusion, we estimate that the other 88% (i.e., ≈6.5 million US-born persons and ≈5.5 million non-US-born persons living in the United States) could benefit from interventions to expand screening and treatment for LTBI.

Acknowledgments

We acknowledge Andrew Hill and Rachel Yelk-Woodruff for their contributions to the successful completion of this analysis.

About the Author

Ms. Vonnahme is an epidemiologist with the Division of Tuberculosis Elimination, National Center for HIV/AIDS, Viral Hepatitis, STD, and TB Prevention, Centers for Disease Control and Prevention, Atlanta, GA. Her primary research interests are LTBI and health disparities among migrant populations.

References

- Centers for Disease Control and Prevention. Reported tuberculosis in the United States, 2011 [cited 2019 Jul 29]. <https://www.cdc.gov/mmwr/preview/mmwrhtml/mm6111a2.htm>
- Hill AN, Becerra JE, Castro KG. Modelling tuberculosis trends in the USA. *Epidemiol Infect.* 2012;140:1862–72.
- Yuen CM, Kammerer JS, Marks K, Navin TR, France AM. Recent transmission of tuberculosis—United States, 2011–2014. *PLoS One.* 2016;11:e0153728.
- Miramontes R, Hill AN, Yelk Woodruff RS, Lambert LA, Navin R, Castro KG, et al. Tuberculosis infection in the United States: prevalence estimates from the National Health and Nutrition Examination Survey, 2011–2012. *PLoS One.* 2015;10:e0140881. <https://doi.org/10.1371/journal.pone.0140881>
- Menzies D. Interpretation of repeated tuberculin tests: boosting, conversion, and reversion. *Am J Respir Crit Care Med.* 1999;159:15–21.
- Chee CBE, Khinmar KW, Gan SH, Barkham TM, Koh CK, Shen L, et al. Tuberculosis treatment effect on T-cell interferon- γ responses to *Mycobacterium tuberculosis* specific antigens. *Eur Respir J.* 2010;36:355–61.
- Pollock NR, Kashino SS, Napolitano DR, Sloutsky A, Joshi S, Guillet J, et al. Evaluation of the effect of treatment of latent tuberculosis infection on QuantiFERON-TB gold assay results. *Infect Control Hosp Epidemiol.* 2009;30:392–5. <https://doi.org/10.1086/596606>
- National Tuberculosis Controllers Association; Centers for Disease Control and Prevention. Guidelines for the investigation of contacts of persons with infectious tuberculosis. *MMWR Recomm Rep.* 2005;16:1–47.
- Centers for Disease Control and Prevention (CDC). NHANES 2011–2012 overview [cited 2019 July 6]. <https://wwwn.cdc.gov/nchs/nhanes/ContinuousNhanes/Overview.aspx?BeginYear=2011>
- Johnson C, Dohrmann S, Burt V, Mohadjer L. National Health and Nutrition Examination Survey: sample design, 2011–2014. *Vital Health Stat.* 2014;162:1–33.
- Centers for Disease Control and Prevention. National Health and Nutrition Examination Survey (NHANES) Laboratory Procedures Manual. Atlanta: The Centers; 2014.
- Reichler MR, Khan A, Sterling TR, Zhao H, Moran J, McAuley J, et al. Risk and timing of tuberculosis among close contacts of persons with infectious tuberculosis. *J Infect Dis.* 2018;218:1000–8. <https://doi.org/10.1093/infdis/jiy265>

Address for correspondence: Laura A. Vonnahme, Centers for Disease Control and Prevention, 1600 Clifton Rd NE, Mailstop US12-4, Atlanta, GA 30329-4027, USA; email: kdy1@cdc.gov

Melioidosis after Hurricanes Irma and Maria, St. Thomas/St. John District, US Virgin Islands, October 2017

Irene Guendel,¹ Lisa LaPlace Ekpo,¹
Mary K. Hinkle, Cosme J. Harrison,
David D. Blaney, Jay E. Gee, Mindy G. Elrod,
Sandra Boyd, Christopher A. Gulvik, Lindy Liu,
Alex R. Hoffmaster, Brett R. Ellis,
Tai Hunte-Cesar, Esther M. Ellis

We report 2 cases of melioidosis in women with diabetes admitted to an emergency department in the US Virgin Islands during October 2017. These cases emerged after Hurricanes Irma and Maria and did not have a definitively identified source. Poor outcomes were observed when septicemia and pulmonary involvement were present.

Melioidosis is caused by *Burkholderia pseudomallei*, a saprophytic, gram-negative bacillus endemic to tropical regions worldwide (1). Diagnosis is difficult because of wide-ranging clinical manifestations (2), and this bacterium is innately resistant to many antimicrobial drugs, making treatment options limited, complex, and lengthy (3). Infection occurs by percutaneous exposure, inhalation, or ingestion.

Melioidosis is rare in the United States, and cases are usually travel related (4,5). However, regional endemicity has been documented in Puerto Rico (6), and sporadic human cases have been reported in the Caribbean (5,7). In September 2017, the US Virgin Islands were affected by 2 category 5 hurricanes, Irma and Maria; widespread flooding continued for weeks. We describe the clinical manifestations, management, and outcome of posthurricane melioidosis cases in 2 women in St. Thomas and St. John, US Virgin Islands.

The Study

Despite major damage to the 2 hospitals in the territory during the 2 hurricanes, the Virgin Islands Department of Health (VIDOH) maintained surveillance at both emergency

departments. Two isolates were recovered from each patient. Local specimen analysis for organism identification was performed by using the MicroScan WalkAway System (Siemens Healthcare Diagnostics, <https://www.siemens-healthineers.com>). All isolates were confirmed as *B. pseudomallei* at the Centers for Disease Control and Prevention (CDC; Atlanta, GA, USA). Whole-genome sequencing and single-nucleotide polymorphism analysis were performed (National Center for Biotechnology Information, <https://www.ncbi.nlm.nih.gov>, Project PRJNA488733). Genomes from a given patient were clonal to each other. However, representative genomes from both patients had differences (>5,600 single-nucleotide polymorphisms), indicating the presence of different strains in these infections. Genomic comparison with a reference panel indicated that the isolates were within the previously described Western Hemisphere clade and subclade associated with the Caribbean (8).

Patient 1 was an 80-year-old female resident of St. Thomas who had a history of cardiomyopathy and type II diabetes mellitus. She came to the emergency department (ED) at Schneider Regional Medical Center (St. Thomas, US Virgin Islands) because of shortness of breath (symptom onset 28 days after Hurricane Irma and 9 days after Hurricane Maria). Her symptoms were worsened orthopnea, increased abdominal girth, and edema, consistent with her symptoms at previous admissions. The patient was admitted for management of acute decompensated heart failure.

The patient had a temperature of 98.5°F; diffuse pulmonary crackles; jugular venous distension; normal heart sounds; and bilateral, lower extremity pitting edema. Examination showed a focal area on the anterior left thigh that had a central, firm, warm, erythematous, tender, subcutaneous nodule ≈2 cm in diameter with a central fluctuant area and a small pinhole. Incision and drainage was performed, and a swab specimen of purulent drainage was sent for culture.

The patient was given intravenous clindamycin (600 mg every 8 h for 5 d) and was discharged while receiving oral clindamycin, but the treatment course was not completed. Cultured wound showed growth of *B. pseudomallei* at ≈5 days. However, culture growth was not yet positive before patient discharge. The isolate was susceptible to trimethoprim/sulfamethoxazole (Table 1).

Author affiliations: Virgin Islands Department of Health, St. Thomas, Virgin Islands, USA (I. Guendel, L. LaPlace Ekpo, C.J. Harrison, B.R. Ellis, T. Hunte-Cesar, E.M. Ellis); Walter Reed Army Institute of Research, Silver Spring, Maryland, USA (M.K. Hinkle); Centers for Disease Control and Prevention, Atlanta, Georgia, USA (D.D. Blaney, J.E. Gee, M.G. Elrod, S. Boyd, C.A. Gulvik, L. Liu, A.R. Hoffmaster)

DOI: <https://doi.org/10.3201/eid2510.180959>

¹These authors contributed equally to this article.

Table 1. Culture results and antimicrobial drug susceptibility for *Burkholderia pseudomallei* isolated from 2 case-patients with melioidosis after Hurricanes Irma and Maria, St. Thomas/St. John District, US Virgin Islands, October 2017*

Patient, culture	Drug	MicroScan Walk Away		CDC MIC, $\mu\text{g/mL}$	Result
		System MIC, $\mu\text{g/mL}$ †	Result		
1, first wound culture	Amoxicillin/clavulanate	NT	NA	4/2	S
	Ceftazidime	>16	R	4	S
	Doxycycline	NT	NA	1	S
	Imipenem	NT	NA	0.5	S
	Tetracycline	NT	NA	4	S
	Trimethoprim/sulfamethoxazole	$\leq 2/38$	S	$\leq 0.5/9.5$	S
	Meropenem	NT	NA	1	‡
1, second wound culture	Amoxicillin/clavulanate	NT	NA	4/2	S
	Ceftazidime	>16	R	2	S
	Doxycycline	NT	NA	1	S
	Imipenem	NT	NA	0.5	S
	Tetracycline	NT	NA	4	S
	Trimethoprim/sulfamethoxazole	$\leq 2/38$	S	$\leq 0.5/9.5$	S
	Meropenem	NT	NA	1	‡
2, sputum culture	Amoxicillin/clavulanate	NT	NA	4/2	S
	Ceftazidime	4	S	4	S
	Doxycycline	NT	NA	1	S
	Imipenem	NT	NA	0.5	S
	Tetracycline	NT	NA	4	S
	Trimethoprim/sulfamethoxazole	$\leq 2/38$	S	$\leq 0.5/9.5$	S
	Meropenem	NT	NA	1	‡

*CDC, Centers for Disease Control and Prevention; NA, not applicable; NT, not tested; R, resistant; S, susceptible.

†Siemens Healthcare Diagnostics, <https://www.siemens-healthineers.com>.

‡There are no published breakpoints in the Clinical and Laboratory Standards Institute M45 (9).

Patient 1 returned to the ED 2 weeks later because of manifestations similar to those at the first visit. She was afebrile and admitted for diuresis. The left thigh lesion had progressed into a 2-cm, tender, shallow ulcer productive of purulent material surrounded by erythema and a focal area of induration (Figure). Laboratory data reflected a leukocyte count within reference ranges and mild renal insufficiency with estimated glomerular filtration rate of 40.47 mL/min (Table 2).

A second wound culture was collected, and the patient was given intravenous meropenem (1 g every 8 h). Culture was presumptively positive for *B. pseudomallei* and *Serratia marcescens* after ≈ 48 hours, confirmed after 8 days. Both isolates showed the same resistance pattern and were susceptible to meropenem and trimethoprim/sulfamethoxazole: the MIC for meropenem was $<1 \mu\text{g/mL}$ (Table 2). Meropenem was continued for 8 days, and ulcer improvement was observed. The patient was discharged while receiving oral trimethoprim/sulfamethoxazole (800 mg/160 mg 2 \times /d) to complete maintenance therapy. The patient completed a 3-month course of trimethoprim/sulfamethoxazole and achieved resolution.

Patient 2 was a 60-year-old female who was a resident of St. John who had diabetes. She was referred to the ED at Schneider Regional Medical Center by her primary care physician because of hyperglycemia, productive cough, and malaise for 1 week (symptom onset 46 days after Hurricane Irma and 33 days after Hurricane Maria). The patient was admitted to the intensive care unit because of community-acquired pneumonia.

The patient was lethargic and had a temperature of 101°F; heart rate was 99 beats/min, respiratory rate 22 breaths/min, and blood pressure 142/81 mm Hg. Blood gas



Figure. Cutaneous melioidosis lesion in case-patient 1 after Hurricanes Irma and Maria, St. Thomas/St. John District, US Virgin Islands, October 2017. This lesion was on the left anterior thigh and had a diameter of 2 cm. Shown is a tender, shallow, ulcer productive of purulent material surrounded by erythema and a focal area of induration. Scale bar indicates 1 cm.

Table 2. Laboratory values for 2 case-patients with melioidosis after Hurricanes Irma and Maria, St. Thomas/St. John District, US Virgin Islands, October, 2017*

Parameter	Patient 1			Patient 2			Reference range
	Oct 18	Oct 21	Oct 24	Oct 26	Oct 27	Oct 30	
Leukocytes	4.2	NT	4.1	28.3	18.1	12.6	4.8–10.8 × 10 ³ /mm ³
Hemoglobin B	11.9	NT	15.5	11.3	10.4	8.1	12.0–14.0 g/L
Hematocrit	38.1	NT	48.9	34.6	31.5	24.0	36.0–42.0%
Platelets	185	NT	174	441	345	201	140–440 × 10 ³ /mm ³
Neutrophils	67.0	NT	46.2	92.5	89.5	92.6	40.0%–75.0%
Lymphocytes	20.8	NT	38.2	1.8	2.4	5.1	15.0%–45.5%
Monocytes	9.6	NT	10.8	4.9	5.3	2.2	0.0%–10.0%
Eosinophils	0.6	NT	3.7	0.7	2.7	0.0	0.0%–6.0%
Basophils	2.0	NT	1.1	0.1	0.1	0.1	0.0%–2.0%
Sodium	134	127	NT	125	130	137	136–145 mmol/L
Potassium	4.8	3.6	NT	3.5	2.9	3.2	3.6–5.2 mmol/L
Chloride	100	91	NT	87	95	104	98–107 mmol/L
Bicarbonate	28.0	31.3	NT	17.5	21.5	16.5	21–32 mmol/L
Blood urea nitrogen	23	18	NT	17	17	63	7–18 mg/dL
Creatinine	1.58	1.26	NT	1.19	1.07	3.92	0.6–1.3 mg/dL
Glucose	169	213	NT	367	235	404	70–110 mg/dL
Hemoglobin A1C	NT	NT	NT	NT	NT	11	4.5%–6.2%
Calcium	8.2	9.1	NT	10.2	9.0	8.3	8.5–10.5 mg/dL
Phosphorus	NT	3.3	NT	NT	NT	1.9	2.4–4.9 mg/dL
Magnesium	NT	NT	NT	NT	NT	1.9	1.8–2.4 mg/dL
Total bilirubin	0.6	NT	NT	1.5	1.5	2.3	0.0–1.0 mg/dL
Direct bilirubin	NT	NT	NT	NT	NT	2.0	0.0–0.3 mg/dL
AST	32	NT	NT	34	52	49	15–37 U/L
ALT	27	NT	NT	25	25	34	12–78 U/L
Alkaline phosphatase	94	NT	NT	155	138	142	50–136 U/L
Total protein	7.2	NT	NT	8.0	6.4	5.1	6.4–8.2 g/dL
Albumin	3.10	2.70	NT	2.10	1.6	0.8	3.4–5.0 g/dL

*Units for laboratory values are shown in the reference range column. ALT, alanine aminotransferase; AST, aspartate aminotransferase; hemoglobin A1C, glycated hemoglobin; NT, not tested.

testing showed pO₂ of 47.6 mm Hg with an oxygen saturation of 87.2% on 2-liter nasal cannula. A chest radiograph showed a left-sided mild infiltrate, and her leukocyte count was markedly increased (28.3 × 10³ cells/mm³) (Table 2).

The patient was given intravenous ceftriaxone (1 g/d) and azithromycin (500 mg/d) after blood and sputum cultures were prepared. She required bilevel positive airway pressure but eventually required mechanical ventilation. The patient then became hypotensive and required norepinephrine to maintain a mean arterial pressure ≥65 mm Hg. Ceftriaxone was discontinued, and she was given intravenous piperacillin/tazobactam (3.375 g every 6 h). Trimethoprim/sulfamethoxazole- and ceftazidime-sensitive *B. pseudomallei* were identified from sputum culture after 72 hours (Table 1). Methicillin-sensitive *Staphylococcus aureus* and *Candida glabrata* were also identified. One of 2 blood cultures was positive for gram-negative rods. Piperacillin/tazobactam was discontinued, and the patient was given meropenem (1 g every 8 h).

The patient remained critically ill and was transferred to a tertiary care hospital in the continental United States. She died in a long-term care facility during October 2018 without showing signs of neurologic improvement.

Isolates from both patients showed susceptibility to routinely tested antimicrobial drugs (10,11). Isolates from patient 1 showed resistance to ceftazidime during preliminary analysis (Table 1). However, broth microdilution

confirmatory testing performed at CDC indicated ceftazidime susceptibility, highlighting the need for additional antimicrobial resistance confirmation.

Both patients were interviewed to determine travel history and possible exposure sources. Patient 1 traveled occasionally to the southeastern United States; her last travel date was 3 months before her illness. This patient reported flooding and water damage to her home from the hurricanes, but did not report contact with flood waters. Patient 2 reported no travel history before the hurricanes.

VIDOH has investigated and confirmed a subsequent case-patient with pulmonary melioidosis in St. Thomas during December 2018 (I. Guendel et al., unpub. data). This case-patient reported no recent travel and might have had occupational exposure as a professional gardener. This person had 2 risk factors (type II diabetes mellitus and heavy use of alcohol).

Conclusions

Given regional occurrence, detection of melioidosis in the US Virgin Islands is not surprising. Furthermore, emergence of melioidosis after extreme weather events has been well documented, and cases were likely acquired locally from storm-related exposure to flooded soil, surface water runoff, or generation of coarse aerosols (12,13). Although detection of *B. pseudomallei* has yet to be confirmed in the environment, it might be endemic to the US Virgin Islands, as in Puerto Rico.

In January 2018, melioidosis was listed as a reportable disease in the US Virgin Islands. Future actions include disease education efforts for physicians and laboratory staff because misdiagnosis is common (14). Awareness campaigns highlighting preventive measures for the public are necessary because risk factors are prevalent in the local population (e.g., diabetes and other chronic disease) and might be exacerbated under disaster settings (e.g., respiratory effects and open wounds). VIDOH has implemented rapid diagnostic testing by using Active Melioidosis Detect (InBios International, <https://inbios.com>) on suspected specimens for prompt on-island case identification while routine ED diagnostic cultures are performed (5). All confirmatory testing is conducted at CDC.

Acknowledgments

We thank Beulah Pinney, LaToya Harrigan, Maritza Phillip, and infection control staff from Schneider Regional Medical Center for providing assistance.

This study was supported by the Epidemiology and Laboratory Capacity for Infectious Diseases Cooperative Agreement from the Centers for Disease Control and Prevention.

About the Author

Dr. Guendel is an epidemiologist at the US Virgin Islands Department of Health. Her research interests are emerging and reemerging infectious diseases.

References

1. Wiersinga WJ, Currie BJ, Peacock SJ. Melioidosis. *N Engl J Med*. 2012;367:1035–44. <https://doi.org/10.1056/NEJMra1204699>
2. Cheng AC, Currie BJ. Melioidosis: epidemiology, pathophysiology, and management. *Clin Microbiol Rev*. 2005;18:383–416. <https://doi.org/10.1128/CMR.18.2.383-416.2005>
3. Wuthiekanun V, Amornchai P, Saiprom N, Chantratita N, Chierakul W, Koh GC, et al. Survey of antimicrobial resistance in clinical *Burkholderia pseudomallei* isolates over two decades in northeast Thailand. *Antimicrob Agents Chemother*. 2011;55:5388–91. <https://doi.org/10.1128/AAC.05517-11>
4. Stewart T, Engelthaler DM, Blaney DD, Tuanyok A, Wangsness E, Smith TL, et al. Epidemiology and investigation of melioidosis, southern Arizona. *Emerg Infect Dis*. 2011;17:1286–8. <https://doi.org/10.3201/eid1707.100661>
5. Benoit TJ, Blaney DD, Doker TJ, Gee JE, Elrod MG, Rolim DB, et al. A review of melioidosis cases in the Americas. *Am J Trop Med Hyg*. 2015;93:1134–9. <https://doi.org/10.4269/ajtmh.15-0405>
6. Doker TJ, Sharp TM, Rivera-Garcia B, Perez-Padilla J, Benoit TJ, Ellis EM, et al. Contact investigation of melioidosis cases reveals regional endemicity in Puerto Rico. *Clin Infect Dis*. 2015;60:243–50. <https://doi.org/10.1093/cid/ciu764>
7. Sanchez-Villamil JI, Torres AG. Melioidosis in Mexico, Central America, and the Caribbean. *Trop Med Infect Dis*. 2018;3:pil:24.
8. Gee JE, Gulvik CA, Elrod MG, Batra D, Rowe LA, Sheth M, et al. Phylogeography of *Burkholderia pseudomallei* isolates, Western Hemisphere. *Emerg Infect Dis*. 2017;23:1133–8. <https://doi.org/10.3201/eid2307.161978>
9. Clinical and Laboratory Standards Institute. Methods for antimicrobial dilution and disk susceptibility testing of infrequently isolated or fastidious bacteria. 3rd ed (M45). Wayne (PA): The Institute; 2016.
10. Limmathurotsakul D, Peacock SJ. Melioidosis: a clinical overview. *Br Med Bull*. 2011;99:125–39. <https://doi.org/10.1093/bmb/ldr007>
11. Wuthiekanun V, Peacock SJ. Management of melioidosis. *Expert Rev Anti Infect Ther*. 2006;4:445–55. <https://doi.org/10.1586/14787210.4.3.445>
12. Cheng AC, Jacups SP, Gal D, Mayo M, Currie BJ. Extreme weather events and environmental contamination are associated with case-clusters of melioidosis in the Northern Territory of Australia. *Int J Epidemiol*. 2006;35:323–9. <https://doi.org/10.1093/ije/dyi271>
13. Merritt AJ, Inglis TJ. The role of climate in the epidemiology of melioidosis. *Curr Trop Med Rep*. 2017;4:185–91. <https://doi.org/10.1007/s40475-017-0124-4>
14. Hemarajata P, Baghdadi JD, Hoffman R, Humphries RM. *Burkholderia pseudomallei*: challenges for the clinical microbiology laboratory. *J Clin Microbiol*. 2016;54:2866–73. <https://doi.org/10.1128/JCM.01636-16>

Address for correspondence: Esther M. Ellis, Virgin Islands Department of Health, 1303 Hospital Ground Rd, Ste 10, VI 00802, USA; email: esther.ellis@doh.vi.gov

Possible Prognostic Value of Serial Brain Magnetic Resonance Imaging for Powassan Virus Encephalitis

Joshua Allgaier, Ryan Quarles, Daniel Skiest

Powassan virus (POWV) encephalitis is a rare tickborne illness. We describe the clinical course, laboratory findings, and imaging for a patient with POWV in Massachusetts, USA. Clinical presentation and laboratory findings were nonspecific. Improvement on brain magnetic resonance imaging after 2 weeks preceded clinical improvement by months, suggesting possible prognostic value.

Powassan virus (POWV) is a tickborne virus that can cause disease in humans, sometimes in the form of encephalitis. Although rare, encephalitis caused by this virus has been increasingly recognized, especially in the New England and northern Midwest regions of the United States. Clinical course, laboratory findings, and imaging findings are variable, with a few commonly seen trends. Antibody testing diagnoses POWV, but this test is currently done only by the US Centers for Disease Control and Prevention. Treatment options are primarily supportive; no prognostic indicators have been described. We describe the clinical course of POWV encephalitis in a man living in Massachusetts.

The Case

A 55-year-old male truck driver with no major medical history developed acute onset of confusion preceded by 2 days of nausea, vomiting, and headache in November 2017. He was found by his co-workers driving his truck in circles and was brought to the hospital by his family, whom he reportedly did not recognize. The patient denied substance abuse or recent travel but was an avid hunter with multiple recent tick bites. Initial vital signs were temperature 101.7°F, blood pressure 124/73 mm Hg, and heart rate 80 bpm. His neck was supple, and he had no rash or focal neurologic deficits.

Hematologic laboratory values were leukocytes 12.5×10^9 cells/mL (reference range $4\text{--}11 \times 10^9$ cells/mL) with 9.1×10^9 cells/mL neutrophils (reference range $1.3\text{--}7.0 \times 10^9$ cells/mL); notable metabolic laboratory values were blood urea nitrogen 27 mg/dL (reference range 6–20 mg/dL) and creatinine 1.3 mg/dL (reference

range 0.7–1.2 mg/dL). Levels of ammonia, copper, B_{12} , and carbon monoxide, as well as liver and thyroid function, were normal. Serologic results were negative for Lyme disease, tularemia, West Nile virus (WNV), HIV, and eastern equine encephalitis virus. Serum PCR results were negative for ehrlichiosis and anaplasmosis. Cerebrospinal fluid (CSF) showed elevated protein (64 mg/dL) and 88 leukocytes/mm³ (4% neutrophils, 84% lymphocytes, and 12% monocytes). CSF testing with the FilmArray meningitis/encephalitis panel (BioFire Diagnostics, <https://www.biofire.com>) was negative for DNA of *Escherichia coli* K1, *Haemophilus influenzae*, *Listeria monocytogenes*, *Neisseria meningitidis*, *Streptococcus agalactiae*, *Streptococcus pneumoniae*, cytomegalovirus, enterovirus, herpes simplex virus-1 and -2, human herpesvirus-6, human parechovirus, varicella zoster virus, and *Cryptococcus neoformans/gattii*. CSF cytology revealed no abnormalities.

After a largely negative workup for the patient's unusual memory deficit, we performed brain magnetic resonance imaging (MRI) with and without contrast; results showed symmetric T2 hyperintensities in the bilateral caudate, putamen, and hippocampus, nonspecific findings suggestive of inflammatory encephalitis (Figure). Diffusion-weighted imaging also showed enhancement of the hippocampus (data not shown). These studies were completed during the patient's ongoing memory deficit and fever with persistent lack of other neurologic findings on examination. A video electroencephalogram identified temporal lobe seizures with mild to moderate generalized background slowing.

We treated the patient empirically for bacterial meningitis with ceftriaxone (2 g every 12 h) and for tickborne illness with doxycycline (100 mg every 12 h). When cultures of blood and CSF remained sterile for 48 hours, we stopped all antimicrobial drugs. Over the next 2 weeks, the patient's memory improved, including better recognition of staff and family. A repeat MRI showed improvement of the previously seen T2 hyperintensities (Figure) and resolution of the hippocampal enhancement on diffusion-weighted imaging (data not shown). The patient was discharged to home the next week with a persistent short-term memory deficit, requiring 24-hour supervision.

Author affiliation: Baystate Medical Center, Springfield, Massachusetts, USA

DOI: <https://doi.org/10.3201/eid2510.181262>

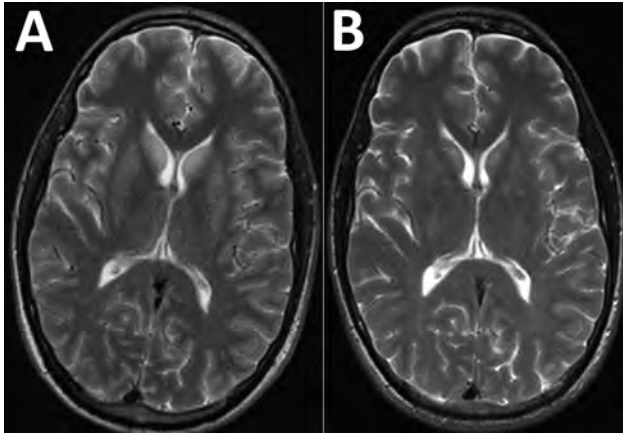


Figure. Magnetic resonance imaging (MRI) of the brain of a patient with encephalitis caused by Powassan virus, Massachusetts, USA, 2017. A) Initial brain MRI showing high T2 signal abnormality in the bilateral caudate and putamen. B) Noticeable improvement on repeat brain MRI 2 weeks later.

One month after discharge, POWV-specific IgM and plaque reduction neutralization tests of the CSF and serum (performed at CDC) confirmed infection. Five months after initial hospitalization, the patient returned to the neurologist, who reported that the patient's mental status had returned to baseline.

Conclusions

Since POWV was isolated in Powassan, Ontario, in 1958, just over 100 cases have been described (1–4). POWV is a flavivirus with 2 serologically indistinguishable lineages (1,2). Lineage 1 is isolated predominantly from *Ixodes cookei* ticks and lineage 2 (deer tick virus) is isolated predominantly from *I. scapularis* ticks (2,5). Rarely, POWV has been isolated from other tick species, such as *I. marxi*, *I. spinipalpus*, and *Dermacentor andersoni* (3). Other than in humans, evidence of infection has been documented in woodchucks and 37 other mammal species, including red squirrels, chipmunks, and skunks (2,4). The virus has been detected from Virginia to Nova Scotia, Canada, and in Michigan, Wisconsin, and Minnesota (lineage 1) (2). More recently, human cases have been increasingly reported in New England (lineage 2) (4).

The clinical course and outcomes of POWV infection are variable and nonspecific. After an incubation period of 1–5 weeks, the most common clinical manifestation is a febrile illness with sore throat, drowsiness, headache, and disorientation (2). Other manifestations include rash; gastrointestinal symptoms (4); or encephalitis manifesting as vomiting, prolonged fever, respiratory distress, discoordination, difficulty speaking, and seizures (2). CSF findings are generally nonspecific and often include elevated protein and lymphocytic pleocytosis (4). MRI findings often show T2/FLAIR abnormalities commonly

affecting the basal ganglia and thalamus, with noncontiguous lesions in the brainstem, cortex, and periventricular white matter (2,4). In some cases, brain MRI has been normal, whereas others have reported atypical findings such as microhemorrhages (4). Initial MRI findings are sometimes consistent with eventual clinical outcomes, but no definitive correlation has been demonstrated (4). Follow-up brain MRI has not been studied previously, and no case reports include mention of evolution of lesions seen on MRI.

Detection of virus-specific IgM- and IgG-neutralizing antibodies of serum or CSF diagnoses POWV infection (6). Viremia usually resolves before encephalitis symptoms, possibly implicating the immune response as a likely cause of clinical manifestations. Approximately 10%–15% of cases with POWV-associated encephalitis are fatal (1). Long-term neurologic deficits persist in about half of survivors (4). There are isolated case reports of lower mortality with high-dose corticosteroids; however, the number of reported cases is low, and thus no correlation with outcomes has been determined (2,4). Similarly, the use of intravenous immunoglobulin has been reported, but with minimal apparent impact on outcomes (2,4).

WNV is a better-understood flavivirus that shares similarities with POWV. Both can manifest as nonspecific encephalitis that can be clinically indistinguishable from each other and with nonspecific CSF findings, usually lymphocytic pleocytosis (7). Both WNV and POWV patients show MRI abnormalities predominantly in the thalamus, basal ganglia, and brainstem. Outcomes are similar regarding potential for long-term neurologic deficits and death. Among reported WNV patients, <1% develop meningoencephalitis, but 10% of those develop flaccid paralysis, with a 10% death rate (7–9). In the few previous case reports of WNV meningoencephalitis that report serial brain MRIs, persistent MRI abnormalities in the posterior fossa were associated with poor outcomes; 1 patient with bilateral edema and hyperintensity of the basal ganglia and thalamus on initial MRI later improved both on MRI and clinically (9,10). Although a correlation of serial MRI findings with clinical outcomes cannot be concluded from these few previous case reports and our report, they suggest the possibility of prognostic value of serial MRI.

The case we describe is typical of reported cases of POWV encephalitis: nonspecific cognitive impairment, elevated CSF protein and lymphocytic pleocytosis, and T2 hyperintense lesions on brain MRI. The improvement in MRI at 2 weeks preceded our patient's clinical improvement, suggesting that repeat MRI might have prognostic value. Clinicians in New England and North Central states should consider POWV as a possible etiology in patients with encephalitis in late spring through the fall, during seasonal tick activity.

Acknowledgment

The authors thank Eugene Kang for review of the MRI findings.

About the Author

Dr. Allgaier is a hospitalist at Baystate Medical Center in Springfield, Massachusetts, USA. His primary interest is in patient care, including novel approaches to diagnostics and treatment.

References

1. Pastula DM, Smith DE, Beckham JD, Tyler KL. Four emerging arboviral diseases in North America: Jamestown Canyon, Powassan, chikungunya, and Zika virus diseases. *J Neurovirol*. 2016;22:257–60. <https://doi.org/10.1007/s13365-016-0428-5>
2. Hermance ME, Thangamani S. Powassan virus: an emerging arbovirus of public health concern in North America. *Vector Borne Zoonotic Dis*. 2017;17:453–62. <https://doi.org/10.1089/vbz.2017.2110>
3. Centers for Disease Control and Prevention. Outbreak of Powassan encephalitis—Maine and Vermont, 1999–2001. *MMWR Morb Mortal Wkly Rep*. 2001;50:761–4.
4. Piantadosi A, Rubin DB, McQuillen DP, Hsu L, Lederer PA, Ashbaugh CD, et al. Emerging cases of Powassan virus encephalitis in New England: clinical presentation, imaging, and review of the literature. *Clin Infect Dis*. 2016;62:707–13. <https://doi.org/10.1093/cid/civ1005>
5. Ebel GD, Spielman A, Telford SR III. Phylogeny of North American Powassan virus. *J Gen Virol*. 2001;82:1657–65. <https://doi.org/10.1099/0022-1317-82-7-1657>
6. Thomm AM, Schotthoefer AM, Dupuis AP II, Kramer LD, Frost HM, Fritsche TR, et al. Development and validation of a serologic test panel for detection of Powassan virus infection in U.S. patients residing in regions where Lyme disease is endemic. *mSphere*. 2018;3:e00467-17. <https://doi.org/10.1128/mSphere.00467-17>
7. Thomas SJ, Endy TP, Rothman AL, Barrett AD. Flaviviruses (dengue, yellow fever, Japanese encephalitis, West Nile encephalitis, St. Louis encephalitis, tick-borne encephalitis, Kyasanur forest disease, Alkhurma hemorrhagic fever, Zika). In: Bennett JE, Dolin R, Blaser MJ, editors. *Mandell, Douglas, and Bennett's principles and practice of infectious diseases*, 8th ed. Philadelphia: Elsevier/Saunders; 2015. p. 1881–903.
8. Ali M, Safriel Y, Sohi J, Llave A, Weathers S. West Nile virus infection: MR imaging findings in the nervous system. *AJNR Am J Neuroradiol*. 2005;26:289–97.
9. Petropoulou KA, Gordon SM, Prayson RA, Ruggieri PM. West Nile virus meningoencephalitis: MR imaging findings. *AJNR Am J Neuroradiol*. 2005;26:1986–95.
10. Mainali S, Afshani M, Wood JB, Levin MC. The natural history of West Nile virus infection presenting with West Nile virus meningoencephalitis in a man with a prolonged illness: a case report. *J Med Case Rep*. 2011;5:204. PubMed <https://doi.org/10.1186/1752-1947-5-204>

Address for correspondence: Joshua Allgaier, Baystate Medical Center Internal Medicine, 759 Chestnut St, Springfield, MA, 01199, USA; email: Joshua.AllgaierDO@bhs.org

EID Podcast

Candida auris in New York Healthcare Facilities

When patients at various New York City healthcare centers began showing symptoms of fungal infection, labs struggled to identify the source: *Candida auris*, a yeast that is often resistant to antimicrobial medications.

In this EID podcast, Dr. Eleanor Adams, a public health physician with the New York Metropolitan Region Healthcare Epidemiology & Infection Control Program, discusses a fungal outbreak in New York City healthcare facilities.

Visit our website to listen: <https://go.usa.gov/xy6Uz> **EMERGING INFECTIOUS DISEASES**

Rapid Screening of *Aedes aegypti* Mosquitoes for Susceptibility to Insecticides as Part of Zika Emergency Response, Puerto Rico

Ryan R. Hemme, Lucrecia Vizcaino,
Angela F. Harris, Gilberto Felix,
Michael Kavanaugh, Joan L. Kenney,
Nicole M. Nazario, Marvin S. Godsey,
Roberto Barrera, Julieanne Miranda,
Audrey Lenhart

In response to the 2016 Zika outbreak, *Aedes aegypti* mosquitoes from 38 locations across Puerto Rico were screened using Centers for Disease Control and Prevention bottle bioassays for sensitivity to insecticides used for mosquito control. All populations were resistant to pyrethroids. Naled, an organophosphate, was the most effective insecticide, killing all mosquitoes tested.

The first case of autochthonous Zika virus infection in the Western Hemisphere was reported in Brazil in 2015, followed by reports from 26 countries and territories in the Caribbean and Central and South America (1,2). On December 31, 2015, the Puerto Rico Department of Health reported the first autochthonous case of Zika virus infection, and by the end of 2016, ≈35,000 cases had been reported (1,3).

During 1945–1955, as part of a broader campaign to eliminate *Aedes aegypti* mosquitoes from the Western Hemisphere, vector-control efforts used DDT to control these mosquitoes in Puerto Rico, primarily through residual treatments in houses; resistance in *Ae. aegypti* mosquitoes to organochlorine insecticides (DDT and dieldrin) was reported as early as 1961 (4,5). The first reports of resistance to organophosphate insecticides were published in the 1970s, and by the 1980s, *Ae. aegypti* mosquitoes in Puerto Rico had developed resistance to synthetic pyrethroids (5,6). At the

time of the Zika virus outbreak, vector-control authorities in Puerto Rico used cleanup campaigns, community education, and adulticiding with ultralow-volume (ULV) truck-mounted sprayers to control *Ae. aegypti* mosquitoes. Commercial products containing the pyrethroid insecticide permethrin were most commonly used in ULV applications, and a few municipalities used a formulation that contained a proprietary mixture of botanical compounds. The heavy reliance on permethrin-based products raised concerns, given recent reports that *Ae. aegypti* populations in 8 municipalities were already highly resistant to it (7).

During outbreaks, vector-control strategies must rapidly suppress adult mosquito populations to interrupt disease transmission (8,9). In March 2016, in response to the Zika virus outbreak, the World Health Organization released special guidance on reducing human–vector contact, recommending the use of targeted residual spraying and ULV spraying against adult mosquitoes; larval control, including source reduction; and personal protective measures, including the use of topical repellents (8,9). To learn which adult mosquito-control products would have the greatest likelihood of rapidly suppressing *Ae. aegypti* mosquito populations, during early 2016 we conducted an emergency islandwide screening in Puerto Rico for susceptibility to insecticides in products available for public health use in areas of active or at high risk for Zika virus transmission.

The Study

Sampling sites for this investigation comprised municipalities with large urban populations and other potential areas at high risk for Zika virus transmission islandwide. We collected *Ae. aegypti* eggs from 38 neighborhoods (clusters of ≈200 houses) within 23 municipalities in Puerto Rico (Figure) using standard black ovitraps containing 10% hay infusion and seed germination paper as the oviposition substrate (10). We placed 2–4 ovitraps at homes within sampling neighborhoods (120 ovitraps per neighborhood) after acquiring verbal consent from the homeowners. Ovitrap remained in the field for 4 days, after which they were retrieved and the germination papers containing eggs were dried until hatching.

We hatched eggs and reared mosquitoes under insectary conditions using standardized protocols (11). When the

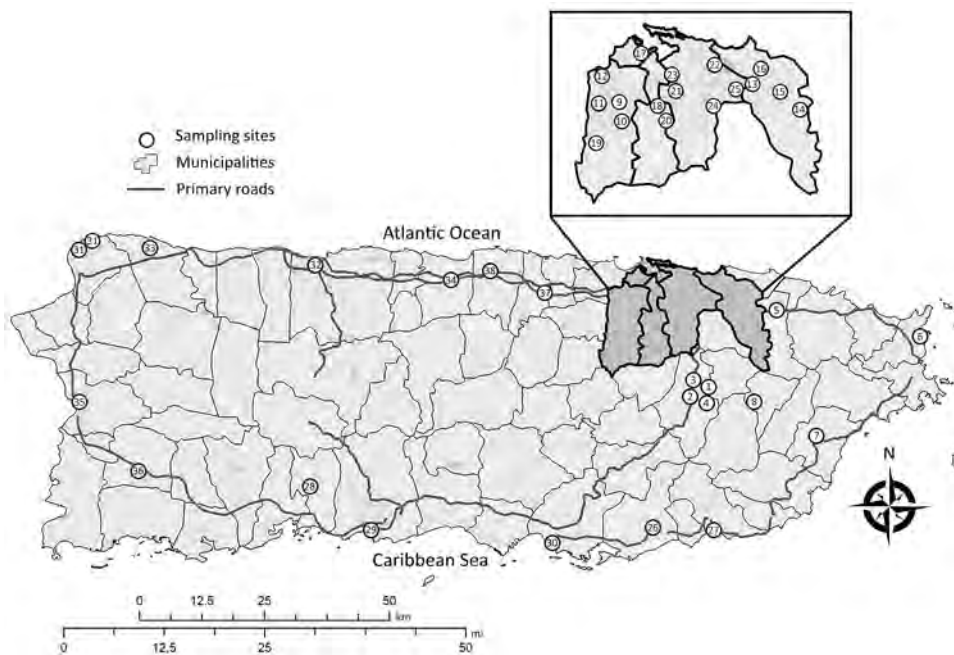
Author affiliations: Centers for Disease Control and Prevention, San Juan, Puerto Rico, USA (R.R. Hemme, A.F. Harris, G. Felix, R. Barrera); Centers for Disease Control and Prevention, Atlanta, Georgia, USA (L. Vizcaino, A. Lenhart); United States Navy, Jacksonville, Florida, USA (M. Kavanaugh); Centers for Disease Control and Prevention, Fort Collins, Colorado, USA (J.L. Kenney, M.S. Godsey); Puerto Rico Vector Control Unit, San Juan (N.M. Nazario, J. Miranda)

DOI: <https://doi.org/10.3201/eid2510.181847>

Figure. Locations of *Aedes aegypti* egg collections

for insecticide resistance testing, Puerto Rico, 2016.

Municipalities or barrios: 1, Caguas, Condado Moderno; 2, Caguas, Urb Idamaris Garden; 3, Caguas, Villa Blanca; 4, Caguas, Villa de Castro; 5, Canóvanas; 6, Fajardo; 7, Humacao; 8, Juncos; 9, Bayamón; 10, Bayamón, Irlanda; 11, Bayamón, Pájaros; 12, Bayamón, Teresita; 13, Carolina, El Comandante; 14, Carolina, Los Colobos; 15, Carolina, Villa Carolina; 16, Carolina, Vistamar; 17, Cataño; 18, Guaynabo, Ponce de León; 19, Guaynabo, Sabana; 20, Guaynabo, Villa Clementina; 21, San Juan, Caparra Terrace; 22, San Juan, Israel; 23, San Juan, Puerto Nuevo; 24, San Juan, Venus Garden; 25, San Juan, El Comandante; 26, Guayama; 27, Patillas; 28, Peñuelas; 29, Ponce; 30, Salinas; 31, Aquadilla; 32, Arecibo; 33, Isabela; 34, Manati; 35, Mayagüez; 36, San German; 37, Vega Alta; 38, Vega Baja. Inset shows closer view of dark gray shaded area.



mosquitoes were 2–5 days old, we evaluated non-blood-fed females for resistance to insecticides using the standard Centers for Disease Control and Prevention bottle bioassay protocol (12). We screened populations for susceptibility to 11 insecticides and scored mortality at a 30-minute diagnostic time for all insecticides (Table, <https://wwwnc.cdc.gov/EID/article/25/10/18-1847-T1.htm>). We used the insecticide-susceptible Rockefeller strain of *Ae. aegypti* mosquitoes as a control. We conducted bioassays during March–June 2016; partial findings were initially published on the Centers for Disease Control and Prevention website in April 2016 (<https://www.cdc.gov/zika/vector/testing-puertorico.html>).

The World Health Organization recommends that insecticide resistance, partial resistance, and susceptibility for mosquito populations are interpreted from bioassay data at <90%, 91%–98%, and >98% mortality, respectively. All populations we tested were resistant to permethrin, and results of initial testing with phenothrin, etofenprox, and tetramethrin suggested that populations were highly resistant across the simple pyrethroids (Table). Because these preliminary findings suggested that simple pyrethroids would not be effective against *Ae. aegypti* mosquitoes in Puerto Rico, we did not test all populations against this class of insecticide, opting instead to focus on screening alternatives. Of the 3 cyano-pyrethroids tested, deltamethrin was effective in more populations; we found fully susceptible *Ae. aegypti* populations in 5 municipalities,

and results from 4 additional municipalities showed partial resistance (Table). Overall, the organophosphate naled was the most promising insecticide tested; all *Ae. aegypti* populations showed 100% susceptibility (Table). However, efforts to launch a naled-based response to the Zika epidemic led to strong public opposition and were ultimately canceled. Although currently no product containing bendiocarb is registered for public health use by the US Environmental Protection Agency, we screened its effectiveness against *Ae. aegypti* mosquitoes as an alternative insecticide in 6 populations, and all were susceptible (Table).

Conclusions

The primary objective of our survey was to rapidly screen key *Ae. aegypti* mosquito populations in Puerto Rico for susceptibility to insecticides that could be quickly deployed to address the Zika outbreak. Our results strongly suggested that the use of simple pyrethroids should be avoided because of widespread insecticide resistance. Results from the cyano-pyrethroid and malathion assays were less straightforward because resistance was geographically heterogeneous. This survey did not include mosquito populations from all municipalities; therefore, the resistance profiles of *Ae. aegypti* mosquitoes from large portions of Puerto Rico remain unknown, making islandwide policy recommendations difficult. Furthermore, the high degree

of fine-scale spatial heterogeneity in the resistance profiles indicated that a mosaic insecticide treatment strategy that applied different products in different locations based on their resistance profile would be logistically challenging.

This study illustrates the challenges in translating laboratory findings into actionable vector-control strategies in the field, especially during an arbovirus outbreak. We did not find, as hoped, 1 insecticide effective at killing *Ae. aegypti* adults islandwide in Puerto Rico and available to municipalities for ground-based ULV spraying. The most effective insecticide, naled, can be applied only from the air, according to its Environmental Protection Agency label. In addition to concerns about insecticide efficacy and acceptability, products can vary greatly in their cost. For example, switching from a permethrin-based product to a deltamethrin-based product for use in truck-mounted ULV spraying would substantially increase program costs. The most commonly used permethrin product that is commercially available in Puerto Rico carries a local cost of \$0.55 per acre, whereas a commercial product containing deltamethrin costs \$1.99 per acre to apply, a cost increase of 260%.

Our results provide a rapid snapshot of resistance to key insecticides across Puerto Rico during the Zika emergency response. The findings highlight the importance of collecting routine data on insecticide resistance to develop vector-control strategies based on evidence from long-term trends. Routine and systematic surveillance of insecticide resistance should be used to guide vector-control policies for outbreak response and routine vector control. These results also underscore the importance of vector-control approaches that do not rely on insecticides as part of an integrated vector management strategy for Puerto Rico.

Acknowledgments

We thank Manuel Amador and Veronica Acevedo for their help in collecting the eggs from southern and western Puerto Rico. We also thank Stephanie Martinez-Conde for producing the map of sampling locations and her assistance with geographic information systems.

The Centers for Disease Control and Prevention provided funding for this study.

About the Author

Dr. Hemme is a research biologist in the Dengue Branch, Division of Vector-Borne Diseases, National Center for

Emerging and Zoonotic Infectious Diseases, Centers for Disease Control and Prevention, in San Juan, Puerto Rico. His primary research interests include mosquito ecology and behavior, and vector–pathogen interactions.

References

1. Thomas DL, Sharp TM, Torres J, Armstrong PA, Munoz-Jordan J, Ryff KR, et al. Local transmission of Zika virus—Puerto Rico, November 23, 2015–January 28, 2016. *MMWR Morb Mortal Wkly Rep*. 2016;65:154–8. <https://doi.org/10.15585/mmwr.mm6506e2>
2. Zanluca C, Melo VC, Mosimann AL, Santos GI, Santos CN, Luz K. First report of autochthonous transmission of Zika virus in Brazil. *Mem Inst Oswaldo Cruz*. 2015;110:569–72. <https://doi.org/10.1590/0074-02760150192>
3. Centers for Disease Control and Prevention. Zika virus: case counts in the US 2016 [cited 2018 Oct 10]. <https://www.cdc.gov/zika/reporting/2016-case-counts.html>
4. Flynn AD, Schoof HF, Morlan HB, Porter JE. Susceptibility of seventeen strains of *Aedes aegypti* (L.) from Puerto Rico and the Virgin Islands to DDT, dieldrin, and malathion. *Mosq News*. 1964;24:118–23.
5. Fox I. Malathion resistance in *Aedes aegypti* of Puerto Rico induced by selection pressure on larvae. *Am J Trop Med Hyg*. 1980;29:1456–9. <https://doi.org/10.4269/ajtmh.1980.29.1456>
6. Hemingway J, Boddington RG, Harrisa J, Sumbar SJ. Mechanisms of insecticide resistance in *Aedes aegypti* (L.) (Diptera: Culicidae) from Puerto Rico. *Bull Entomol Res*. 1989;79:79. <https://doi.org/10.1017/S0007485300018630>
7. Ponce-García G, Del Río-Galvan S, Barrera R, Saavedra-Rodriguez K, Villanueva-Segura K, Felix G, et al. Knockdown resistance mutations in *Aedes aegypti* (Diptera: Culicidae) from Puerto Rico. *J Med Entomol*. 2016;53:1410–4. <https://doi.org/10.1093/jme/tjw115>
8. World Health Organization. Vector control operations framework for Zika virus. Geneva: The Organization; 2016.
9. World Health Organization. Mosquito (vector) control emergency response and preparedness for Zika virus. Geneva: The Organization; 2016.
10. Reiter P, Amador MA, Colon N. Enhancement of the CDC ovitrap with hay infusions for daily monitoring of *Aedes aegypti* populations. *J Am Mosq Control Assoc*. 1991;7:52–5.
11. Hemme RR, Poole-Smith BK, Hunsperger EA, Felix GE, Horiuchi K, Biggerstaff BJ, et al. Non-human primate antibody response to mosquito salivary proteins: implications for dengue virus transmission in Puerto Rico. *Acta Trop*. 2016;164:369–74. <https://doi.org/10.1016/j.actatropica.2016.08.027>
12. Centers for Disease Control and Prevention. Guideline for evaluating insecticide resistance in vectors using the CDC bottle bioassay [cited 2017 Apr 12]. https://www.cdc.gov/malaria/resources/pdf/fsp/ir_manual/ir_cdc_bioassay_en.pdf

Address for correspondence: Ryan R. Hemme, Centers for Disease Control and Prevention, 1324 Calle Cañada, San Juan, PR 00920, USA; email: rhemme@cdc.gov

New Exposure Location for Hantavirus Pulmonary Syndrome Case, California, USA, 2018

Anne M. Kjemtrup, Sharon Messenger,
Amy M. Meza, Tina Feiszli,
Melissa Hardstone Yoshimizu,
Kerry Padgett, Sunita Singh

We describe a case of hantavirus pulmonary syndrome in a patient exposed to Sin Nombre virus in a coastal county in California, USA, that had no previous record of human cases. Environmental evaluation coupled with genotypic analysis of virus isolates from the case-patient and locally trapped rodents identified the likely exposure location.

Hantavirus pulmonary syndrome (HPS), which is caused by infection with Sin Nombre virus (SNV), was made nationally notifiable in the United States in 1995. Since then, 71 cases in California residents have been reported (range 0–8 cases/y) (1). Persons are usually exposed to SNV through inhalation of aerosolized excreta (e.g., saliva, urine, and feces) from infected rodents, typically deer mice (*Peromyscus maniculatus*) (2), although other wild mice, such as the cactus mouse (*P. eremicus*), have been implicated as reservoirs in California (3). SNV has been documented in deer mice throughout California (4), but exposure for most human cases has been in noncoastal, mountainous (>900 m elevation), rural areas of the state.

Disease onset occurs after a 2–8-week incubation (5); onset for 70% of California cases has occurred during May–September. Laboratory confirmation includes serologic testing (e.g., ELISA, IgM, and IgG), reverse transcription PCR (RT-PCR) testing of serum or respiratory samples, or immunohistochemistry to identify virus antigen in tissue (5). Sequencing of viral RNA (most commonly glycoprotein or nucleoprotein open reading frames) is used to infer relationships of hantavirus strains from humans and rodents (3,6). We report a case of HPS in a patient exposed to SNV in a coastal county in California, USA, that had no previous record of human cases.

Author affiliations: California Department of Public Health, Sacramento, California, USA (A.M. Kjemtrup); California Department of Public Health, Richmond, California, USA (S. Messenger, T. Feiszli, M. Hardstone Yoshimizu, K. Padgett); County of Santa Cruz Public Health Department, Santa Cruz, California, USA (A.M. Meza); Sutter Health Santa Cruz Center, Santa Cruz (S. Singh)

DOI: <https://doi.org/10.3201/eid2510.190058>

The Study

The adult patient (age 35–40 years) sought care at a local urgent-care facility in April 2018 for a 2-day history of fever (38.8°C), chills, muscle aches, nausea, dizziness, shortness of breath, and cough. Initially diagnosed with a viral illness, the patient returned 2 days later with worsening symptoms, including nuchal rigidity and photophobia. The patient was referred to a local emergency department because of concerns about meningitis.

At hospital admission, a computed tomography scan of the lungs showed bilateral perihilar air space consolidation, increased lung density (ground glass), and moderate bilateral pleural effusion. Clinical laboratory values demonstrated thrombocytopenia ($\approx 46,000$ cells/mL [reference 150,000–400,000 cells/mL]), elevated creatinine (1.5 mg/dL [reference 0.6–1.3 mg/dL]), elevated leukocytes (12,400 cells/mL [reference 3,900–11,700 cells/mL]), neutropenia (8.9% [reference 45%–70%]), and lymphopenia (17.3% [reference 18%–48%]). One day later, the patient was transferred to a hospital with a higher acute care level, intubated, and placed on extracorporeal membrane oxygenation.

Serum collected 4 days after illness onset tested negative at the local public health laboratory for influenza A and B. At a commercial laboratory, serum test results were urine antigen–negative for leptospirosis and legionella, antibody–negative for coccidioidomycosis, and PCR–negative for *Yersinia enterocolitica* but were IgM- and IgG-positive for hantavirus. The California Department of Public Health Viral and Rickettsial Disease Laboratory tested an additional serum sample collected 7 days after illness onset, confirmed the positive serologic results, and detected SNV RNA by using a previously described RT-PCR (7). The patient remained on extracorporeal membrane oxygenation for 10 days, was extubated on day 18, and was released 20 days after illness onset.

The case-patient lives and works on a farm at ≈ 20 m elevation in Santa Cruz County, along the north coast of California. An interview with the family initially suggested a rural work exposure in San Mateo County, north of the farm residence, at ≈ 400 m elevation, where both the case-patient and a family member worked outdoors in a dusty, rodent-infested environment 18 days before illness onset. The family did not recall a substantial rodent exposure on the farm except for the case-patient cleaning a shed ≥ 1 week before illness onset.

The California Department of Public Health Vector-Borne Disease Section collaborated with county vector-

control agencies to evaluate the case-patient's place of residence, farm, and rural workplace for potential exposure to SNV. At the farm, rodent access, feces, and nesting material were present in multiple outbuildings and structures in and around the home. Of 105 Sherman traps set, 19 rodents were captured (18% trap success) from the farm, including 18 deer mice and 1 Western harvest mouse (*Reithrodontomys megalotis*). Rodents were anesthetized, bled through a retro-orbital blood collection technique, and humanely euthanized. Five (28%) of the deer mice and the harvest mouse were serologically positive for SNV, including 1 deer mouse from inside the shed that the case-patient cleaned and 1 from the basement of the house. Blood from 4 of the 5 deer mice and the harvest mouse were positive for SNV by RT-PCR.

The rural San Mateo County workplace location could not be investigated directly; however, trapping and habitat evaluation were conducted at public areas near the

worksite. Rodents captured in 35 of 100 traps (35% trap success) included 15 parasitic mice (*P. californicus*) and 20 piñon mice (*P. truei*) but no deer mice. One piñon mouse tested serologically positive for SNV, but no viral RNA was detected by RT-PCR.

We conducted phylogenetic analysis to compare the case-patient's isolate to other California hantavirus sequences, including those from the farm where the case-patient lived and worked. Because no PCR-positive rodents were collected near the rural worksite, archived sequences from SNV-positive deer mice collected in previous years (2014, 2016, and 2018) from 2 different sites in the same county as the rural worksite (San Mateo County) were included in our analysis. We found that the SNV glycoprotein sequence from the case-patient was genetically related most closely to the hantavirus sequences recovered from the case-patient's farm (Figure). The sequences from the 2 sites in San Mateo County each form separate monophyletic

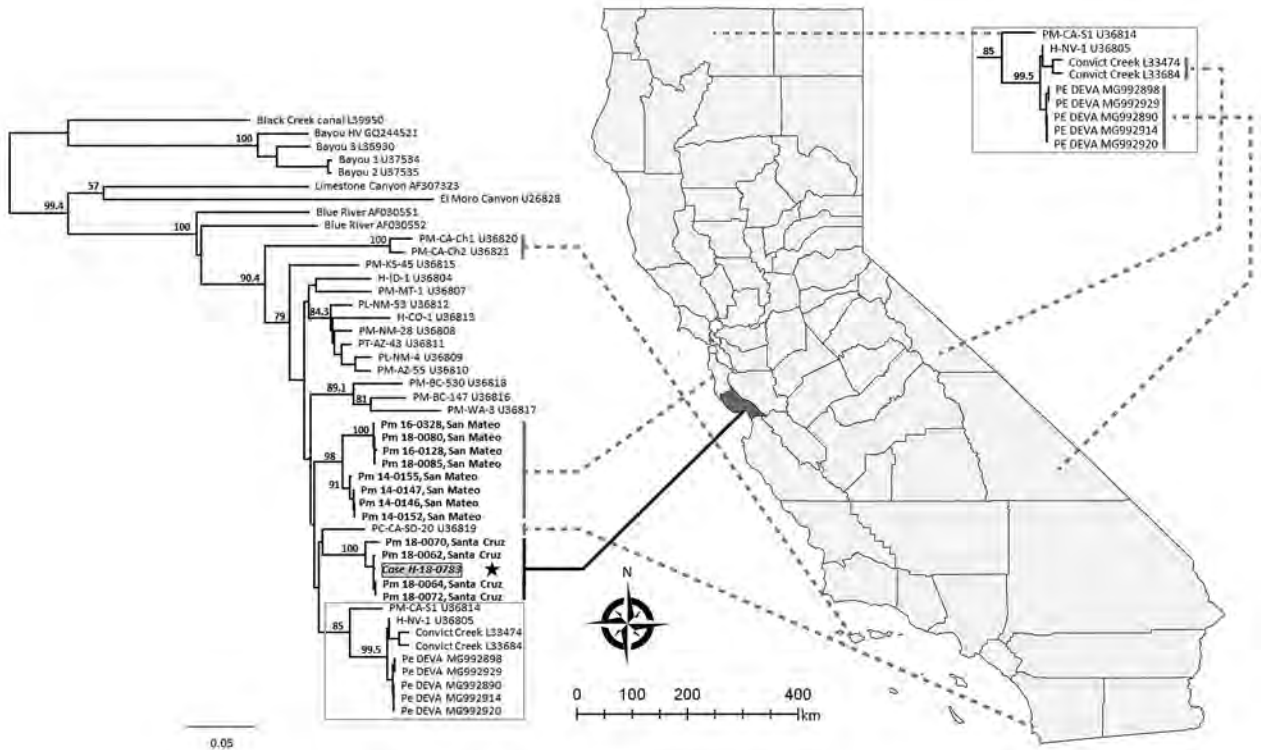


Figure. Phylogenetic tree of hantavirus Gn glycoprotein sequences from isolates collected in California, USA, and reference sequences. The hantavirus sequence from the case-patient described in this study (gray box) is shown in comparison to sequences from the case-patient farm in Santa Cruz County and archived samples from neighboring San Mateo County (bold). Dotted lines indicate general geographic origins of California sequences. Representative reference sequences of hantaviruses were downloaded from Genbank (accession numbers included in taxon labels). H indicates sequences from human cases; all other sequences are from small rodents. The tree was reconstructed by analysis of 848 bases of the glycoprotein precursor gene by using the neighbor-joining method and employing the Hasegawa-Kishino-Yano model to estimate genetic distances with Geneious 10.0 (<https://www.geneious.com>). We estimated support for relationships by using a nonparametric bootstrap analysis (1,000 replicates). Nodes with bootstrap percentages >50% are indicated. Similar tree topologies were generated from maximum-likelihood (RAXML) and Bayesian (Mr. Bayes) phylogenetic analyses (data not shown). Genbank accession numbers: Case H-18-0783, MK386451; Pm-18-0062, Santa Cruz, MK386452; Pm-18-0064, Santa Cruz, MK386453; Pm-18-0070, Santa Cruz, MK386454; Pm-18-0072, Santa Cruz, MK386455; Pm-14-0146, San Mateo, MK386456; Pm-14-0147, San Mateo, MK386457; Pm-14-0152, San Mateo, MK386458; Pm-14-0155, San Mateo, MK386459; Pm-16-0128, San Mateo, MK386460; Pm-16-0328, San Mateo, MK386461; Pm-18-0080, San Mateo, MK386462; and Pm-18-0085, San Mateo, MK386463. Scale bars represent the genetic distance (nucleotide substitutions per site).

clades that cluster together, despite collections over several years, and are distinct from all samples from Santa Cruz County. Thus, exposure most likely occurred at the farm where the case-patient lived and worked. Although the type of exposure of opening poorly ventilated outbuildings and performing activities that raise dust is typical for hantavirus exposure, the geographic location in this coastal California county has not been previously implicated in SNV exposure leading to HPS. Follow-up visits by county vectorborne disease officials provided information to the family on rodent exclusion and other prevention measures to reduce the risk for subsequent exposure to SNV.

Conclusions

The prevalence of hantavirus in deer mice in the counties surrounding Santa Cruz ranged from 0% to 12% during 1975–2017 (4); however, human HPS cases have not been documented previously from this area. Typically, HPS cases are associated with higher elevations (8,9). The rural workplace was the first focus of this exposure investigation because it was at a higher elevation and the initial interview with the family suggested rodent exposure. Ultimately, however, the environmental investigation identified the most likely exposure location was the case-patient's farm in Santa Cruz County. The high abundance of deer mice reported by the family, coupled with the presence of SNV in the mice found near the case-patient's farm, likely contributed to elevated exposure risk. The environmental investigation of this case highlights the importance of evaluating all possible places of exposure to minimize future risk for illness and death from HPS. Molecular analysis of case-patient and rodent sequences was a valuable tool to identify the likely exposure locale.

The comprehensive epidemiologic investigation, including molecular sequencing, prompted public health messaging on hantavirus prevention to the public and medical community in a region where a hantavirus case had not previously been identified. Evaluation of the case-patient's residence provided an opportunity for recommendations to decrease risk for ongoing exposure to the case-patient's family. Findings from this environmental investigation might guide future public health interventions in California, including surveillance and public health messaging.

Acknowledgments

We thank Chris Conroy for mammal species confirmation, Santa Cruz County Mosquito Abatement/Vector Control and San Mateo County Mosquito Vector Control District for environmental support, Greg Hacker for the map, Bryan Jackson for rodent necropsy, and Vicki Kramer for manuscript review.

This work was determined exempt for a human subject protocol by the California Office of State Health and Planning. Animal handling protocol #2014-18, approved by the California Department of Public Health, was followed. Wildlife sampling permits are not required for animals taken by state public health officials, pursuant to California Fish and Game Code 4011 (6)(b).

About the Author

Dr. Kjemtrup is a research scientist and epidemiologist with the California Department of Public Health Vector-Borne Disease Section. She focuses on the surveillance and prevention of rodentborne and tickborne diseases.

References

1. California Department of Public Health. Vector-Borne Disease Section Annual Report, 2017. Sacramento: California Department of Public Health; 2018.
2. Childs JE, Ksiazek TG, Spiropoulou CF, Krebs JW, Morzunov S, Maupin GO, et al. Serologic and genetic identification of *Peromyscus maniculatus* as the primary rodent reservoir for a new hantavirus in the southwestern United States. *J Infect Dis.* 1994;169:1271–80. <https://doi.org/10.1093/infdis/169.6.1271>
3. Burns JE, Metzger ME, Messenger S, Fritz CL, Vilcins IE, Enge B, et al. Novel focus of Sin Nombre virus in *Peromyscus eremicus* mice, Death Valley National Park, California, USA. *Emerg Infect Dis.* 2018;24:1112–5. <https://doi.org/10.3201/eid2406.180089>
4. California Department of Public Health. Hantavirus in California—an interactive story map [cited 2018 Jul 26]. <https://cdphdata.maps.arcgis.com/apps/MapSeries/index.html?appid=31fd0ca80e264cbd9bba7d54952194de>
5. Núñez JJ, Fritz CL, Knust B, Buttke D, Enge B, Novak MG, et al.; Yosemite Hantavirus Outbreak Investigation Team. Hantavirus infections among overnight visitors to Yosemite National Park, California, USA, 2012. *Emerg Infect Dis.* 2014;20:386–93. <https://doi.org/10.3201/eid2003.131581>
6. Hjelle B, Lee SW, Song W, Torrez-Martinez N, Song JW, Yanagihara R, et al. Molecular linkage of hantavirus pulmonary syndrome to the white-footed mouse, *Peromyscus leucopus*: genetic characterization of the M genome of New York virus. *J Virol.* 1995;69:8137–41.
7. Bagamian KH, Towner JS, Kuenzi AJ, Douglass RJ, Rollin PE, Waller LA, et al. Transmission ecology of Sin Nombre hantavirus in naturally infected North American deer mouse populations in outdoor enclosures. *PLoS One.* 2012;7:e47731. <https://doi.org/10.1371/journal.pone.0047731>
8. Glass GE, Shields T, Cai B, Yates TL, Parmenter R. Persistently highest risk areas for hantavirus pulmonary syndrome: potential sites for refugia. *Ecol Appl.* 2007;17:129–39. [https://doi.org/10.1890/1051-0761\(2007\)017\[0129:PHRAFH\]2.0.CO;2](https://doi.org/10.1890/1051-0761(2007)017[0129:PHRAFH]2.0.CO;2)
9. Jay M, Ascher MS, Chomel BB, Madon M, Sesline D, Enge BA, et al. Seroepidemiologic studies of hantavirus infection among wild rodents in California. *Emerg Infect Dis.* 1997;3:183–90. <https://doi.org/10.3201/eid0302.970213>

Address for correspondence: Anne M. Kjemtrup, California Department of Public Health, Vector-Borne Disease Section, 1616 Capitol Ave, Mailstop 7307, PO Box 997377, Sacramento, CA 95899-7377, USA; email: anne.kjemtrup@cdph.ca.gov

Two Cases of *Borrelia miyamotoi* Meningitis, Sweden, 2018

Anna J. Henningsson, Hilmir Asgeirsson,
Berit Hammas, Elias Karlsson,
Åsa Parke, Dieuwertje Hoornstra,
Peter Wilhelmsson, Joppe W. Hovius

We report 2 human cases of *Borrelia miyamotoi* disease diagnosed in Sweden, including 1 case of meningitis in an apparently immunocompetent patient. The diagnoses were confirmed by 3 different independent PCR assays and DNA sequencing from cerebrospinal fluid, supplemented by serologic analyses.

Borrelia miyamotoi is the cause of an emerging disease in the Northern Hemisphere, transmitted by hard (*Ixodes*) ticks. The bacterial species, described in Japan in 1995 (1), is genetically related to the relapsing fever borreliae and may be divided into Siberian, European, and American genotypes (2). *B. miyamotoi* disease (BMD), described in case series from Russia (3) and the United States (4,5), is a systemic illness causing relapsing fever, headache, myalgia, arthralgia, elevated liver enzymes, neutropenia, and thrombocytopenia. In addition, 3 cases of meningoencephalitis caused by *B. miyamotoi* have been reported worldwide, 2 from Europe and 1 from the United States, all in highly immunocompromised patients (6–8). We report 2 human cases of BMD diagnosed in Sweden, including 1 case of meningitis in an apparently immunocompetent patient.

The Patients

On July 29, 2018, a 53-year-old woman (patient A) sought care at a hospital for headache, neck stiffness, and high-grade fever that had progressively worsened during the preceding week (Figure 1, panel A). Her medical history included previous cholecystectomy and gastric bypass surgery. Her sole medication was oxycodone (an opioid drug used to manage

pain), which she was taking because of a recent elbow fracture. She had not been abroad during the preceding months but she had removed an attached tick while staying in Stockholm County 6 weeks earlier. No subsequent erythema appeared around the bite site. At admission, we found no neurologic deficits or signs of impaired consciousness. Cerebrospinal fluid (CSF) analysis showed total leukocyte count 321 cells/ μ L (reference ≤ 5 cells/ μ L), mononuclear cells 276 cells/ μ L (reference ≤ 5 cells/ μ L), and albumin 1,270 mg/L (reference < 420 mg/L). Bacterial culture; anti-*Borrelia* antibody testing; and PCR for herpes simplex virus, varicella zoster virus, and enterovirus were negative in CSF. Serologic test results for tickborne encephalitis were negative. Viral meningitis was suspected.

The next day, clinical improvement occurred, and the patient was discharged. However, the patient's condition then worsened, with more pronounced headache and neck pain, and she was readmitted on August 6. Blood cell and platelet counts and C-reactive protein levels were normal. CSF analysis showed total leukocyte count 517 cells/ μ L (reference ≤ 5 cells/ μ L), mononuclear cells 354 cells/ μ L (reference ≤ 5 cells/ μ L), and CXCL13 327 pg/mL (reference < 190 pg/mL). We initiated intravenous treatment with ampicillin to cover *Listeria* meningitis; the fever resolved within 1 day. The CSF *Borrelia* antibody index came back weakly positive for IgM (Table) and, under the diagnosis of (atypical) Lyme neuroborreliosis (LNB), oral doxycycline was initiated (200 mg 2 \times /d for 14 d). Panbacterial *16S* rRNA gene sequencing (9) of the CSF sample suggested *B. miyamotoi*, a finding that later was confirmed by specific PCR, sequencing, and serologic testing (Table).

At follow-up on August 24, the patient showed continued improvement without any fever relapses. Complementary tests for immunodeficiency showed normal serum levels of immunoglobulins. We analyzed convalescent serum using several commercially available tests for laboratory diagnosis of Lyme borreliosis (Table); all results were negative.

A 66-year-old woman (patient B) living in Stockholm County was referred in August 2018 for 6 weeks of intermittent high-grade fever and 9 months of various other symptoms (Figure 1, panel B). She had rheumatoid arthritis, treated with methotrexate together with rituximab twice a year since 2011, but had been physically very active. Her symptoms began with headache and increasing fatigue in November 2017, a few days after returning from a 2-week

Author affiliations: Linköping University, Linköping, Sweden (A.J. Henningsson, P. Wilhelmsson); County Hospital Ryhov, Jönköping, Sweden (A.J. Henningsson, P. Wilhelmsson); Karolinska Institutet, Stockholm, Sweden (H. Asgeirsson); Karolinska University Hospital, Stockholm (H. Asgeirsson, B. Hammas, Å. Parke); Danderyd University Hospital, Stockholm (E. Karlsson); Academic Medical Center, Amsterdam, the Netherlands (D. Hoornstra, J.W. Hovius)

DOI: <https://doi.org/10.3201/eid2510.190416>

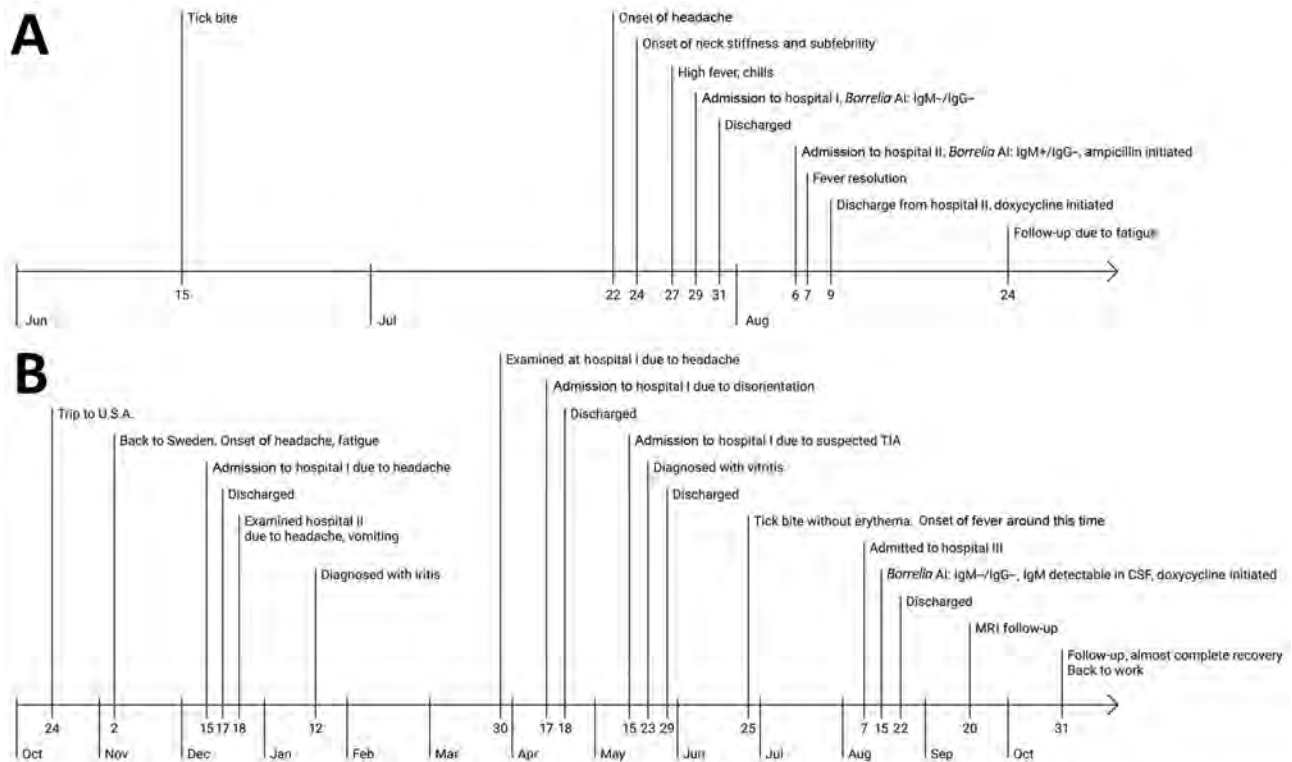


Figure 1. Time course of *Borrelia miyamotoi* meningitis in 2 patients, Sweden, 2018. A) Patient A, a 53-year-old immunocompetent woman; B) patient B, a 66-year-old immunocompromised woman. AI, antibody index; CSF, cerebrospinal fluid; MRI, magnetic resonance imaging; TIA, transient ischemic attack.

trip to California and Nevada, USA. She had not noticed any tick bites during the trip but had had several tick bites in Sweden during the summer of 2017. She subsequently started experiencing progressing difficulties with concentration and memory and had relapsing febrile episodes. In January 2018, she received diagnoses of uveitis and iritis; vitritis of unknown cause was later diagnosed. She also had progressive hearing loss, and hearing aids were prescribed.

In addition, she had loss of appetite and weight (15 kg within 6 months). In May she had a short episode of left-sided weakness, and transient ischemic attack was suspected. All this resulted in her quitting her work as an accountant and hardly being able to leave her house.

Upon referral, we performed a lumbar puncture, which showed total CSF leukocytes of 331 cells/ μ L (reference \leq 5 cells/ μ L), 273 cells/ μ L mononuclear (reference \leq 5 cells/

Table. Confirmatory analyses performed on cerebrospinal fluid and serum/plasma samples from 2 patients with diagnoses of meningitis caused by *Borrelia miyamotoi*, Sweden, 2018*

Analysis	Patient A, dates samples collected					Patient B, dates samples collected			
	Jul 30		Aug 6		Aug 24	Aug 9		Oct 31	
Sample	Serum	CSF	Serum	CSF	Serum	Serum	Plasma	CSF	Serum
BM-specific PCR	-	+	+	+	NA	NA	+	+	NA
BM-specific serologic testing	IgM+, (GlpQ, Vlp5), IgG-	NA	IgM+ (GlpQ, Vlp5), IgG+ (GlpQ)	NA	IgM+ (GlpQ, Vsp1), IgG+ (GlpQ, Vlp15/16)	IgM+ (GlpQ), IgG-	NA	NA	IgM+ (GlpQ), IgG-
LB serology†	-	-	-	IgM AI+	-‡	-	NA	IgM detectable, but AI-	-‡
Culture attempts	-	-	-	-	NA	NA	-	NA	NA

*Patient A: a 53-year-old immunocompetent woman; patient B: a 66-year-old immunocompromised woman. AI, antibody index; BM, *Borrelia miyamotoi*; CSF, cerebrospinal fluid; GlpQ, glycerophosphodiester-phosphodiesterase; LB, Lyme borreliosis; NA, not analyzed; Vlp, variable large protein; Vsp, variable small protein; +, positive; -, negative.

†LIAISON *Borrelia burgdorferi* (DiaSorin, <https://www.diasorin.com>).

‡In addition to LIAISON, the sample was analyzed by Enzygnost Lyme link VlsE IgG and Enzygnost Borreliosis IgM (DADE Behring, <https://www.siemens.com>), recomBead *Borrelia* IgM and IgG (Mikrogen GmbH, <https://www.mikrogen.de>), C6 Lyme ELISA Kit (Immunetics, <https://immunetics.com>), and Anti-*Borrelia* EUROLINE-RN-AT IgG and IgM (EUROIMMUN, <http://www.euroimmun.com>). All test results were negative.

μL), albumin 1,550 mg/L (reference <420 mg/L), lactate 4.2 mmol/L (reference 1.2–2.1 mmol/L), and CXCL13 >500 pg/mL (reference <250 pg/mL). Magnetic resonance imaging showed contrast enhancement in both oculomotor nerves and the left trigeminal nerve, as well as thickening of the pituitary stalk. CSF was PCR negative for herpes simplex virus, varicella zoster virus, enterovirus, *Mycoplasma*, and *Toxoplasma*. Bacterial, mycobacterial, and fungal CSF cultures were negative. Serologic results for tickborne encephalitis and Lyme borreliosis were negative, with the exception of detectable *B. burgdorferi* IgM in CSF (Table). The 16S rRNA gene sequencing (9) was positive for *B. miyamotoi*.

We treated the patient with doxycycline (200 mg 2×/d for 14 d); within 5 days, the patient regained her hearing, and the fever and headache disappeared. MRI 1 month later showed an almost complete regression of the contrast enhancement of the cranial nerves. By follow-up 2 months after finishing the treatment, the patient had resumed employment and felt almost completely recovered.

We performed *B. miyamotoi* quantitative PCR (qPCR) targeting the flagellin gene, slightly modified from Hovius et al. (6) (Appendix, <http://wwwnc.cdc.gov/EID/article/25/10/19-0416-App1.pdf>). The 2 successive CSF samples and 1 serum

sample from patient A were positive by qPCR, as were the CSF and plasma samples from patient B (Table).

From 1 of the CSF samples from patient A and the CSF sample from patient B, we confirmed the presence of *B. miyamotoi* by nested PCR amplification and sequencing of the glycerophosphodiester-phosphodiesterase (*glpQ*) and *p66* genes (6), as well as a fragment of the intergenic spacer (IGS) between the 16S rRNA and 23S rRNA genes (10) (Appendix). The DNA sequences of the 16S-23S IGS (Figure 2), *glpQ*, and *p66* from patients A and B were identical to *B. miyamotoi* sequences derived from Europe but different from sequences derived from Asia and North America, indicating BMD contracted in Europe.

We tested for GlpQ and variable major proteins (Vmps) IgM and IgG by ELISA, as described previously (11,12) (Table). A clear seroconversion from IgM to IgG against GlpQ was demonstrated in patient A, whereas patient B merely demonstrated IgM reactivity against GlpQ. However, in patient A, but not in patient B (the immunosuppressed patient), we could demonstrate IgM and IgG against different Vmps over time.

Finally, we pursued culture attempts in MKP-F media on CSF and serum samples drawn before initiation of

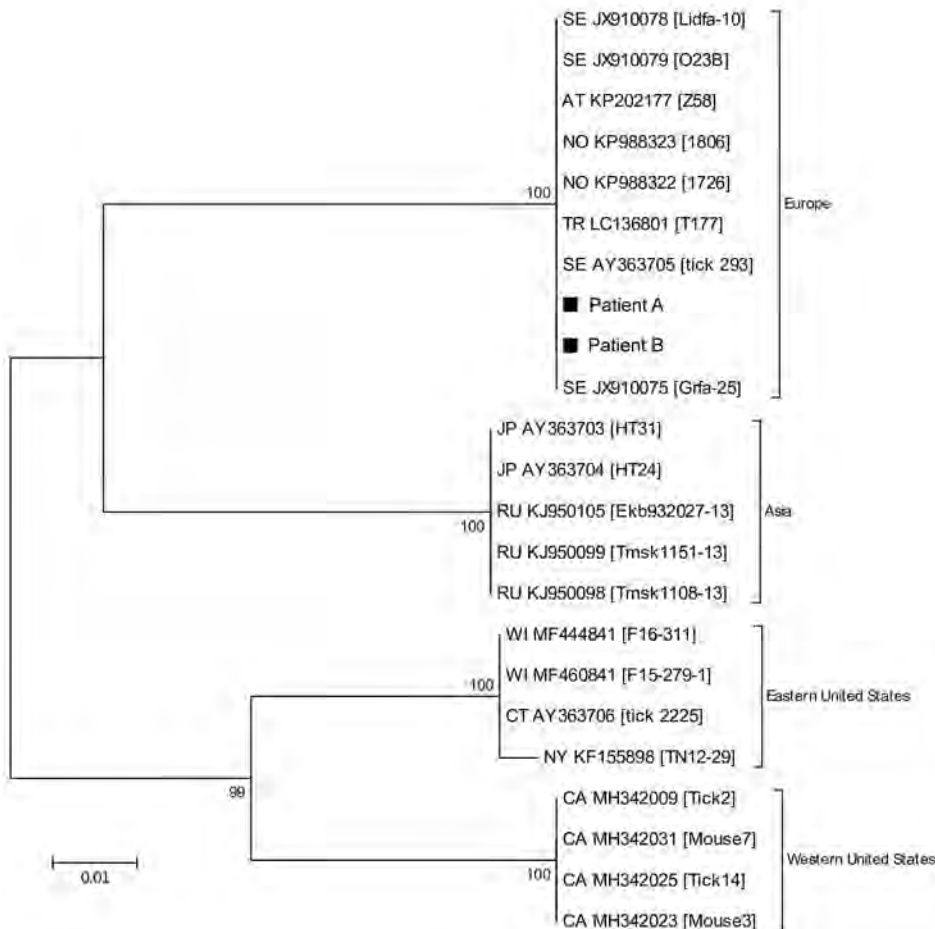


Figure 2. Phylogenetic tree based on 16S-23S intergenic spacer region sequences of *Borrelia miyamotoi* from 2 patients in Sweden, 2018 (patients A and B, black squares), and reference sequences. Tree constructed using the maximum-likelihood method based on the Tamura-Nei model and complete deletion. Sequences detected from patients in this study were deposited into GenBank under accession nos. MK458687 (patient A) and MK458688 (patient B). The source of each reference sequence is indicated by an accession number preceded by a state or country code: AT, Austria; CA, California; CT, Connecticut; JP, Japan; NO, Norway; NY, New York; RU, Russian Federation; SE, Sweden; TR, Turkey; WI, Wisconsin. The accession number is followed by the isolate name in brackets. The reliability of the tree was tested by 500 bootstrap replicate analyses; only values >50% are shown. The phylogenetic relationship between the *B. miyamotoi* strains detected in our patients was corroborated by the DNA sequences obtained from the *glpQ* and *p66* genes (data not shown). Scale bar indicates nucleotide substitutions per site.

antimicrobial drug treatment, retrieved from -80°C (Table), as described by Koetsveld et al. (13). After 2 months of culture, all samples remained negative.

Conclusions

Epidemiologic surveillance of emerging tickborne pathogens is crucial to increase awareness of the diseases that can be contracted after tick bites. Previous studies have shown that *B. miyamotoi* is present in *Ixodes ricinus* ticks in Scandinavia (14,15), but no human cases of BMD have been reported, and public health importance has been uncertain. Until now, severe disease, including slowly progressive CNS symptoms (6,7), has been reported in immunocompromised patients, but our findings indicate that *B. miyamotoi* may also cause CNS infection in immunocompetent persons (patient A). The clinical presentation differs from that of LNB, and results of serologic tests that are routinely used for LNB diagnosis can be negative. Therefore, we need to raise awareness of BMD among healthcare providers and ensure that adequate diagnostic methods are available. BMD should be a differential diagnosis in cases of fever and CNS symptoms after a tick bite in both immunosuppressed and immunocompetent persons.

Acknowledgments

We thank the patients for giving us their permission to report about their clinical symptoms and disease course. We also thank Gärda Andersson for laboratory support.

Confirmatory tests were performed at the laboratory for Clinical Microbiology, Division of Laboratory Medicine, Region Jönköping County, Sweden (molecular analyses), and Center for Experimental and Molecular Medicine, Academic Medical Center, University of Amsterdam, the Netherlands (serological analyses and propagation attempts).

A.J.H. and P.W. were supported by the EU Interreg V program as part of the project ScandTick Innovation (project ID 20200422, reference no. 2015-000167), and D.H. and J.W.H. were supported by ZonMW as part of the project “Ticking on Pandora’s Box, a study into tick-borne pathogens in Europe” (project no. 50-52200-98-313).

About the Author

Dr. Henningsson is a specialist in infectious diseases and clinical microbiology with a position as senior consultant in Region Jönköping County and as associate professor at Linköping University. Her primary research interest is tickborne diseases.

References

1. Fukunaga M, Takahashi Y, Tsuruta Y, Matsushita O, Ralph D, McClelland M, et al. Genetic and phenotypic analysis of *Borrelia miyamotoi* sp. nov., isolated from the ixodid tick *Ixodes*

2. persulcatus, the vector for Lyme disease in Japan. Int J Syst Bacteriol. 1995;45:804–10. <https://doi.org/10.1099/00207713-45-4-804>
2. Talagrand-Reboul E, Boyer PH, Bergström S, Vial L, Boulanger N. Relapsing fevers: neglected tick-borne diseases. Front Cell Infect Microbiol. 2018;8:98. <https://doi.org/10.3389/fcimb.2018.00098>
3. Platonov A, Karan LS, Kolyasnikova NM, Makhneva NA, Toporkova MG, Maleev VV, et al. Humans infected with relapsing fever spirochete *Borrelia miyamotoi*, Russia. Emerg Infect Dis. 2011;17:1816–23. <https://doi.org/10.3201/eid1710.101474>
4. Krause PJ, Narasimhan S, Wormser GP, Rollend L, Fikrig E, Lepore T, et al. Human *Borrelia miyamotoi* infection in the United States. N Engl J Med. 2013;368:291–3. <https://doi.org/10.1056/NEJMc1215469>
5. Molloy PJ, Telford SR III, Chowdri HR, Lepore TJ, Gugliotta JL, Weeks KE, et al. *Borrelia miyamotoi* disease in the northeastern United States: a case series. Ann Intern Med. 2015;163:91–8. <https://doi.org/10.7326/M15-0333>
6. Hovius JW, de Wever B, Sohne M, Brouwer MC, Coumou J, Wagemakers A, et al. A case of meningoencephalitis by the relapsing fever spirochaete *Borrelia miyamotoi* in Europe. Lancet. 2013;382:658. [https://doi.org/10.1016/S0140-6736\(13\)61644-X](https://doi.org/10.1016/S0140-6736(13)61644-X)
7. Gugliotta JL, Goethert HK, Berardi VP, Telford SR III. Meningoencephalitis from *Borrelia miyamotoi* in an immunocompromised patient. N Engl J Med. 2013;368:240–5. <https://doi.org/10.1056/NEJMoa1209039>
8. Boden K, Lobenstein S, Hermann B, Margos G, Fingerle V. *Borrelia miyamotoi*-associated neuroborreliosis in immunocompromised person. Emerg Infect Dis. 2016;22:1617–20. <https://doi.org/10.3201/eid2209.152034>
9. Beser J, Hallström BM, Advani A, Andersson S, Östlund G, Winięcka-Krusnell J, et al. Improving the genotyping resolution of *Cryptosporidium hominis* subtype IbA10G2 using one step PCR-based amplicon sequencing. Infect Genet Evol. 2017;55:297–304. <https://doi.org/10.1016/j.meegid.2017.08.035>
10. Bunikis J, Garpmo U, Tsao J, Berglund J, Fish D, Barbour AG. Sequence typing reveals extensive strain diversity of the Lyme borreliosis agents *Borrelia burgdorferi* in North America and *Borrelia afzelii* in Europe. Microbiology. 2004;150:1741–55. <https://doi.org/10.1099/mic.0.26944-0>
11. Wagemakers A, Koetsveld J, Narasimhan S, Wickel M, Deponte K, Bleijlevens B, et al. Variable major proteins as targets for specific antibodies against *Borrelia miyamotoi*. J Immunol. 2016;196:4185–95. <https://doi.org/10.4049/jimmunol.1600014>
12. Koetsveld J, Kolyasnikova NM, Wagemakers A, Stukolova OA, Hoorstra D, Sarkisyan DS, et al. Serodiagnosis of *Borrelia miyamotoi* disease by measuring antibodies against GlpQ and variable major proteins. Clin Microbiol Infect. 2018;24:1338.e1–7. <https://doi.org/10.1016/j.cmi.2018.03.009>
13. Koetsveld J, Kolyasnikova NM, Wagemakers A, Toporkova MG, Sarkisyan DS, Oei A, et al. Development and optimization of an in vitro cultivation protocol allows for isolation of *Borrelia miyamotoi* from patients with hard tick-borne relapsing fever. Clin Microbiol Infect. 2017;23:480–4. <https://doi.org/10.1016/j.cmi.2017.01.009>
14. Wilhelmsson P, Fryland L, Börjesson S, Nordgren J, Bergström S, Ernerudh J, et al. Prevalence and diversity of *Borrelia* species in ticks that have bitten humans in Sweden. J Clin Microbiol. 2010;48:4169–76. <https://doi.org/10.1128/JCM.01061-10>
15. Kjelland V, Rollum R, Korslund L, Slettan A, Tveitnes D. *Borrelia miyamotoi* is widespread in *Ixodes ricinus* ticks in southern Norway. Ticks Tick Borne Dis. 2015;6:516–21. <https://doi.org/10.1016/j.ttbdis.2015.04.004>

Address for correspondence: Anna J. Henningsson, Region Jönköping County Clinical Microbiology, Sjukhusgatan 1 County Hospital Ryhov, Jönköping 55466, Sweden; email: anna.jonsson.henningsson@rjl.se

Susceptibility of Influenza A, B, C, and D Viruses to Baloxavir¹

Vasilii P. Mishin, Mira C. Patel, Anton Chesnokov, Juan De La Cruz, Ha T. Nguyen, Lori Lollis, Erin Hodges, Yunho Jang, John Barnes, Timothy Uyeki, Charles T. Davis, David E. Wentworth, Larisa V. Gubareva

Baloxavir showed broad-spectrum in vitro replication inhibition of 4 types of influenza viruses (90% effective concentration range 1.2–98.3 nmol/L); susceptibility pattern was influenza A > B > C > D. This drug also inhibited influenza A viruses of avian and swine origin, including viruses that have pandemic potential and those resistant to neuraminidase inhibitors.

Influenza viruses are classified into 4 types: A, B, C, and D (1). Influenza A viruses infect a wide range of species and pose threats to human and animal health. Influenza A viruses belonging to 16 hemagglutinin and 9 neuraminidase subtypes have been identified in the natural reservoir (wild birds). Zoonotic infections with avian H5N1, H5N6, and H7N9 viruses are concerning because of their high fatality rates in humans and pandemic risk (2).

Swine are recognized as mixing vessels because influenza A viruses from multiple hosts can infect pigs and produce novel reassortants. Numerous subtypes of reassortant swine influenza A viruses are enzootic throughout North America and pose a threat to human health. For instance, H3N2 triple reassortant viruses caused a multi-state outbreak affecting hundreds of persons in the United States during 2012, and a quadruple reassortant H1N1 virus caused the 2009 pandemic and now circulates as a seasonal virus (2,3).

Influenza B viruses are considered strictly human pathogens, although occasional outbreaks in aquatic mammals have been reported (1). Influenza C viruses are known to infect humans, pigs, camels, and dogs (1). Unlike influenza A and B viruses, influenza C viruses typically cause

mild illness. However, in recent years, severe illness in children infected by influenza C virus has raised concerns over the lack of virus-specific therapeutics and vaccines (4). Recently discovered influenza D viruses were isolated from swine and bovines. No virologically confirmed human infections have been reported, but influenza D virus antibodies have been found in persons exposed to cattle (1). Evolutionarily, influenza C and D viruses are more closely related to each other than to influenza A or B viruses (1).

Antiviral drugs have been used to mitigate zoonotic virus outbreaks and are central to pandemic preparedness. However, therapeutic options remain limited and drug-resistant viruses can emerge after treatment, spontaneous mutation, or reassortment. Until recently, only matrix (M) 2 blockers and neuraminidase inhibitors (NAIs) were approved to control influenza. M2 blockers are effective only against influenza A viruses and are not recommended because of widespread resistance. NAIs are used for treatment of influenza A and B virus infections, but NAI-resistant viruses have emerged (5). NAI-resistant seasonal influenza H1N1 viruses circulated worldwide during late 2007 through early 2009 (6) and raised concerns over limited therapeutic options.

In 2014, favipiravir was licensed in Japan for restricted use in the event of a drug-resistant influenza pandemic (7). Favipiravir is a broad-spectrum antiviral drug that inhibits viral RNA polymerase, an enzyme recognized as an attractive target because of its critical role in virus replication and high degree of conservation (8). In 2018, another inhibitor of the viral RNA polymerase, baloxavir marboxil, was approved in Japan and the United States for treatment of influenza A and B virus infections (9). Its active metabolite, baloxavir acid, inhibits cap-dependent endonuclease activity of polymerase acidic (PA) protein (10). Amino acid substitutions at position 38 in the PA active site were recognized as the primary pathway to baloxavir resistance (11). PA substitutions at this and other positions have variable impact on resistance and are rarely found in nature (11,12). The purpose of this study was to determine the effectiveness of baloxavir against the 4 types of influenza viruses.

Author affiliations: Centers for Disease Control and Prevention, Atlanta, Georgia, USA (V.P. Mishin, M.C. Patel, A. Chesnokov, J. De La Cruz, H.T. Nguyen, L. Lollis, E. Hodges, Y. Jang, J. Barnes, T. Uyeki, C.T. Davis, D.E. Wentworth, L.V. Gubareva); Battelle Memorial Institute, Atlanta (M.C. Patel, J. De La Cruz, H.T. Nguyen, L. Lollis)

DOI: <https://doi.org/10.3201/eid2510.190607>

¹Preliminary results from this study were presented at the 6th International Society for Influenza and Other Respiratory Virus Diseases Antiviral Group Conference; November 13–15, 2018; Rockville, Maryland, USA.

The Study

The active site of the PA protein (P3 in C and D viruses) is nearly identical in all 4 influenza virus types (1,8). Therefore, we hypothesized that baloxavir would inhibit replication of not only influenza A and B viruses but also influenza C and D viruses. First, we tested 2 viruses of each type by using a virus yield reduction assay. We used baloxavir acid (baloxavir) in experiments and included favipiravir as a control.

Baloxavir broadly inhibited virus replication of all 4 types (Table 1). On the basis of 90% effective concentration values determined at 48 hours postinfection, influenza A viruses were most susceptible to baloxavir and influenza D viruses least susceptible. Baloxavir susceptibility for influenza B viruses was \approx 3-fold lower and that for influenza C viruses was \approx 6-fold lower than that for influenza A viruses. Analysis of 34 P3 sequences of influenza D virus and 221 of influenza C virus (retrieved from GISAID, <https://www.gisaid.org>, and GenBank) showed that all influenza D viruses have valine at position 38, whereas influenza C viruses have isoleucine, similar to most influenza A and B viruses. Nevertheless, valine at 38 in influenza A and B viruses had little or no effect (\leq 3-fold) on baloxavir susceptibility (10–12). Favipiravir also showed inhibitory effects against all virus types, although much higher concentrations were required to achieve similar levels of reduction (Table 1).

Although the virus yield reduction assay has been used to assess baloxavir susceptibility of seasonal and avian viruses (10,13), other phenotypic assays, such as the focus-reduction assay (FRA) and the high-content imaging neutralization test (HINT), offer an improved throughput (12,14,15). Regardless of the assay used, baloxavir effective concentrations for influenza A viruses were similar (\approx 0.1–3 nmol/L) (10,12–15). Unlike the FRA, HINT

relies on single-cycle virus replication, which is achieved by withdrawing trypsin needed to activate infectivity of progeny virus. HINT eliminates variance caused by different replication kinetics. However, the FRA is optimal for testing highly pathogenic avian viruses because multicycle replication of these viruses is trypsin independent. We used 2 seasonal A(H1N1)pdm09 viruses, one of which contains the naturally occurring substitution PA-I38L, for reference purposes (12) (Table 2).

First, we tested 25 influenza viruses of avian origin, representing H5, H6, H7, H9, and H10 subtypes, by using FRA or HINT as described (12) (Table 2; Appendix Table 1, <https://wwwnc.cdc.gov/EID/article/25/10/19-0607-App1.pdf>). Most viruses were isolated from infected humans. Most viruses had markers of M2 resistance and some had NAI-resistance markers. Data showed that these diverse viruses were susceptible to baloxavir and had 50% effective concentration (EC_{50}) values in a low nanomolar range (Table 2; Appendix Table 1). In the FRA, favipiravir EC_{50} values were much higher than those for baloxavir (Appendix Table 1). However, favipiravir did not produce a measurable antiviral effect by HINT because this drug requires several hours for activation in cells. Baloxavir susceptibility of 30 swine-origin viruses, representing different lineages and subtypes and collected over many years, demonstrated HINT EC_{50} values comparable to avian and seasonal influenza A viruses (Table 2; Appendix Table 2) (10,12,13).

It is prudent to analyze PA sequences of emerging influenza A viruses for markers previously associated with reduced baloxavir susceptibility (11,12). Among swine-origin viruses available for testing in this study, polymorphism PA-38I/M was detected in A/Iowa/33/2017 (H1N1) v. Virus populations with either PA-I38 or PA-I38M were recovered by biologic cloning and tested by using HINT.

Table 1. Drug susceptibility of influenza A, B, C, and D viruses by viral yield reduction assay in MDCK cells*

Type	Virus	Virus titer, log ₁₀ TCID ₅₀ /mL†		EC ₉₀ , nmol/L		
				Baloxavir, mean \pm SD		Favipiravir
		24 hpi	48 hpi	24 hpi	48 hpi	48 hpi
A	A/Texas/138/2018 (H1N1)pdm09	6.4 \pm 0.5	9.1 \pm 0.1	0.8 \pm 0.2	1.2 \pm 0.1	NT
	A/Illinois/08/2018 (H1N1)pdm09	5.8 \pm 0.5	8.9 \pm 0.3	2.7 \pm 0.5	3.3 \pm 0.2	3,005
B	B/Maryland/29/2018	3.5 \pm 0.5	7.1 \pm 0.6	8.9 \pm 1.6	5.8 \pm 1.1	1,789
	B/Iowa/18/2018	3.5 \pm 0.5	7.6 \pm 0.4	13.8 \pm 2.0	7.8 \pm 1.7	1,635
C	C/Taylor/1233/47	<1.5	5.9 \pm 0.5	NA	13.0 \pm 3.3	27,476
	C/Aomori/74	<1.5	4.9 \pm 0.4	NA	18.4 \pm 6.5	31,603
D	D/swine/Oklahoma/13334/2011	4.4 \pm 0.3	7.7 \pm 0.1	110.2 \pm 27.6	98.3 \pm 23.9	2,764
	D/bovine/Oklahoma/660/2013	4.8 \pm 0.0	8.0 \pm 0.5	105.6 \pm 37.0	64.3 \pm 16.2	3,106

*Cell monolayers were inoculated at a multiplicity of infection of 0.0005 and virus was allowed to adsorb for 1 h. Virus inoculum was removed, serially diluted drug (baloxavir: 0.5–500 nmol/L; favipiravir: 310–318,000 nmol/L) was added, and cells were incubated at 33°C in a 5% CO₂ incubator. At 24 and 48 hpi, cell culture supernatants were harvested to determine infectious virus titers. Replication of influenza A and B viruses was detected by neuraminidase activity (Fluor-NA Kit; Applied Biosystems, <https://www.thermofisher.com>), and replication of influenza C and D viruses by esterase activity (3-acetyl-umbelliferone in 20 mmol/L Tris-HCl, pH 8.0, reaction buffer (Sigma-Aldrich, <https://www.sigmaaldrich.com>)). The EC₉₀ corresponds to a drug concentration causing a 90% reduction in virus titer compared with control wells without drug. The EC₉₀ for each virus and drug were determined by using nonlinear regression analysis (GraphPad, <https://www.graphpad.com>). For baloxavir, results are shown as mean \pm SD of 3 independent experiments; favipiravir results are shown as single or average of 2 independent experiments. EC₉₀, 90% effective concentration; hpi, hours postinfection; NA, not applicable; NT, not tested; TCID₅₀, 50% tissue culture infectious dose.

†Virus titers were determined in control wells without drug.

Table 2. Baloxavir susceptibility of zoonotic and animal influenza A viruses in MDCK-SIAT1 cells*

Virus subtype	FRA		HINT	
	No. viruses tested	EC ₅₀ , nmol/L, mean ± SD†	No. viruses tested	EC ₅₀ , nmol/L, mean ± SD†
Avian origin				
H5N6‡	3	0.31 ± 0.19	–	–
H6N1	1	0.12	1	0.48
H7N9	19	0.48 ± 0.32	9	1.44 ± 1.08
H9N2§	1	0.18	1	0.53
H10N8	1	0.30	1	0.63
Swine origin				
H1N1¶	–	–	3	0.72 ± 0.27
H1N1v	–	–	3	0.51 ± 0.12
H1N2v	–	–	9	1.19 ± 0.36
H3N2v	–	–	15	0.86 ± 0.50
Reference viruses#				
A/Illinois/08/2018 (H1N1)pdm09 PA-I38		2.12	–	1.75 ± 0.59
A/Illinois/37/2018 (H1N1)pdm09 PA-I38L		14.96 (7-fold)**	–	13.09 ± 3.56 (8-fold)**

*Both assays were conducted by using MDCK-SIAT1 cells. Details on viruses tested are in the Appendix (<https://wwwnc.cdc.gov/EID/article/25/10/19-0607-App1.pdf>). According to World Health Organization nomenclature, the swine-origin influenza viruses isolated from humans are named variant viruses (e.g., A[H1N1]v). EC₅₀, 50% effective concentration; FRA, focus reduction assay; HINT, high-content imaging neutralization test; –, not tested.

†Mean ± SD or average of 2 test results.

‡One of 3 viruses was isolated from chicken (Appendix Table 1).

§Virus was isolated from chicken (Appendix Table 1).

¶All 3 viruses were isolated from swine (Appendix Table 2).

#A pair of seasonal influenza A(H1N1)pdm09 viruses were included in each test as reference viruses (12).

**Fold change to EC₅₀ of virus carrying PA-I38L compared with sequence-matched control virus carrying PA-I38.

Substitution PA-I38M conferred 12-fold reduced baloxavir susceptibility, consistent with previous reports for PA-I38M-containing H3N2 viruses (11,12). Analysis of PA sequences from 2,485 H7N9 viruses (from GISAID and GenBank) showed 1 virus with PA-I38M, 2 with PA-E199G, and 1 with PA-A36V (11,12). The effect of these substitutions on baloxavir susceptibility for H7N9 viruses is currently unknown. Moreover, PA sequence of 1 swine influenza A virus showed PA-I38T, a marker associated with clinically relevant baloxavir resistance (11). None of these viruses were available for phenotypic testing.

Conclusions

Baloxavir displayed broad antiviral activity against diverse influenza viruses, including all 4 types and animal-origin influenza A viruses with pandemic potential. Our findings suggest that baloxavir might offer the first therapeutic option against influenza C virus infections. Further studies are needed to provide comprehensive assessment of baloxavir susceptibility by using a large panel of representative influenza C viruses. Ongoing monitoring of baloxavir susceptibility of emerging avian and swine influenza A viruses with pandemic potential is needed to inform clinical management and public health preparedness efforts.

Acknowledgments

We thank Shionogi and Co., Ltd. (Osaka, Japan), for kindly providing baloxavir acid; the China Centers for Disease Control and Prevention and other partners from the World Health Organization Global Influenza Surveillance and Response System for providing influenza A viruses; Christine Warnes for providing influenza C virus isolates; Richard J. Webby for providing influenza D virus

isolates; and the US Department of Agriculture, Agricultural Research Service and National Veterinary Services Laboratories, for providing viruses collected from birds and animals.

This study was supported by the Influenza Division, National Center for Immunization and Respiratory Diseases, CDC.

About the Author

Dr. Mishin is a biologist in the Influenza Division, National Center for Immunization and Respiratory Diseases, Centers for Disease Control and Prevention, Atlanta, GA. His primary research interests are influenza viruses, antiviral drugs, development and optimization of in vitro assays for monitoring drug susceptibility, and influenza antigenic characterization.

References

1. Asha K, Kumar B. Emerging influenza D virus threat: what we know so far! *J Clin Med*. 2019;8:E192. <https://doi.org/10.3390/jcm8020192>
2. Uyeki TM, Katz JM, Jernigan DB. Novel influenza A viruses and pandemic threats. *Lancet*. 2017;389:2172–4. [https://doi.org/10.1016/S0140-6736\(17\)31274-6](https://doi.org/10.1016/S0140-6736(17)31274-6)
3. Garten RJ, Davis CT, Russell CA, Shu B, Lindstrom S, Balish A, et al. Antigenic and genetic characteristics of swine-origin 2009 A(H1N1) influenza viruses circulating in humans. *Science*. 2009;325:197–201. <https://doi.org/10.1126/science.1176225>
4. Njouom R, Monamele GC, Ermetal B, Tchatchouang S, Moyo-Tetang S, McCauley JW, et al. Detection of influenza C virus infection among hospitalized patients, Cameroon. *Emerg Infect Dis*. 2019;25:607–9. <https://doi.org/10.3201/eid2503.181213>
5. Hu Y, Lu S, Song Z, Wang W, Hao P, Li J, et al. Association between adverse clinical outcome in human disease caused by novel influenza A H7N9 virus and sustained viral shedding and emergence of antiviral resistance. *Lancet*. 2013;381:2273–9. [https://doi.org/10.1016/S0140-6736\(13\)61125-3](https://doi.org/10.1016/S0140-6736(13)61125-3)

6. Hurt AC. The epidemiology and spread of drug resistant human influenza viruses. *Curr Opin Virol*. 2014;8:22–9. <https://doi.org/10.1016/j.coviro.2014.04.009>
7. Furuta Y, Komeno T, Nakamura T. Favipiravir (T-705), a broad spectrum inhibitor of viral RNA polymerase. *Proc Jpn Acad, Ser B, Phys Biol Sci*. 2017;93:449–63. <https://doi.org/10.2183/pjab.93.027>
8. DuBois RM, Slavish PJ, Baughman BM, Yun MK, Bao J, Webby RJ, et al. Structural and biochemical basis for development of influenza virus inhibitors targeting the PA endonuclease. *PLoS Pathog*. 2012;8:e1002830. <https://doi.org/10.1371/journal.ppat.1002830>
9. Hayden FG, Sugaya N, Hirotsu N, Lee N, de Jong MD, Hurt AC, et al.; Baloxavir Marboxil Investigators Group. Baloxavir marboxil for uncomplicated influenza in adults and adolescents. *N Engl J Med*. 2018;379:913–23. <https://doi.org/10.1056/NEJMoa1716197>
10. Noshi T, Kitano M, Taniguchi K, Yamamoto A, Omoto S, Baba K, et al. In vitro characterization of baloxavir acid, a first-in-class cap-dependent endonuclease inhibitor of the influenza virus polymerase PA subunit. *Antiviral Res*. 2018;160:109–17. <https://doi.org/10.1016/j.antiviral.2018.10.008>
11. Omoto S, Speranzini V, Hashimoto T, Noshi T, Yamaguchi H, Kawai M, et al. Characterization of influenza virus variants induced by treatment with the endonuclease inhibitor baloxavir marboxil. *Sci Rep*. 2018;8:9633. <https://doi.org/10.1038/s41598-018-27890-4>
12. Gubareva LV, Mishin VP, Patel MC, Chesnokov A, Nguyen HT, De La Cruz J, et al. Assessing baloxavir susceptibility of influenza viruses circulating in the United States during the 2016/17 and 2017/18 seasons. *Euro Surveill*. 2019;24. <https://doi.org/10.2807/1560-7917.ES.2019.24.3.1800666>
13. Taniguchi K, Ando Y, Nobori H, Toba S, Noshi T, Kobayashi M, et al. Inhibition of avian-origin influenza A(H7N9) virus by the novel cap-dependent endonuclease inhibitor baloxavir marboxil. *Sci Rep*. 2019;9:3466. <https://doi.org/10.1038/s41598-019-39683-4>
14. Kozalka P, Tilmanis D, Roe M, Vijaykrishna D, Hurt AC. Baloxavir marboxil susceptibility of influenza viruses from the Asia–Pacific, 2012–2018. *Antiviral Res*. 2019;164:91–6. <https://doi.org/10.1016/j.antiviral.2019.02.007>
15. Takashita E, Morita H, Ogawa R, Nakamura K, Fujisaki S, Shirakura M, et al. Susceptibility of influenza viruses to the novel cap-dependent endonuclease inhibitor baloxavir marboxil. *Front Microbiol*. 2018;9:3026. <https://doi.org/10.3389/fmicb.2018.03026>

Address for correspondence: Larisa V. Gubareva, Centers for Disease Control and Prevention, 1600 Clifton Rd NE, Mailstop H17-5, Atlanta, GA 30329-4027, USA; email: lgubareva@cdc.gov

Emerging Infectious Diseases Spotlight Topics



etymologia

Antimicrobial resistance • Ebola • Etymologia
Food safety • HIV-AIDS • Influenza
Lyme disease • Malaria • MERS • Pneumonia
Rabies • Tuberculosis • Ticks • Zika
<https://wwwnc.cdc.gov/eid/page/spotlight-topics>

EID's spotlight topics highlight the latest articles and information on emerging infectious disease topics in our global community.

Genetic Characterization and Zoonotic Potential of Highly Pathogenic Avian Influenza Virus A(H5N6/H5N5), Germany, 2017–2018

Anne Pohlmann,¹ Donata Hoffmann,¹
Christian Grund, Susanne Koethe,
Daniela Hüsey, Simone M. Meier,
Jacqueline King, Jan Schinköthe,
Reiner Ulrich, Timm Harder, Martin Beer

We genetically characterized highly pathogenic avian influenza virus A(H5N6) clade 2.3.4.4b isolates found in Germany in 2017–2018 and assessed pathogenicity of representative H5N5 and H5N6 viruses in ferrets. These viruses had low pathogenicity; however, continued characterization of related isolates is warranted because of their high potential for reassortment.

During winter 2016–17, outbreaks of highly pathogenic avian influenza (HPAI) virus A(H5N8) clade 2.3.4.4b caused substantial losses in wild water birds and domestic poultry across Europe (1–4). This virus is related to strains from China and Mongolia and has a high potential for reassortment (4–6). Genetic and temporal analysis of these isolates revealed multiple reassortant events, indicating multiple independent entries into Europe; the outbreaks in Germany were dominated by 5 independent reassortant groups of HPAI virus H5N8 (5). Several outbreaks of HPAI virus H5Nx strains in wild birds confirmed the continued presence of H5 clade 2.3.4.4b in Europe well into the summer of 2017. This virus's high tendency to reassort raised concerns that further reassorted strains could dominate in HPAI outbreaks in Europe or become enzootic in wild bird populations in the future. In this study, we set out to characterize related reassortant viruses of subtype H5N6 or H5N5 isolated in Germany during 2017–2018 and delineate their zoonotic potential in ferrets.

Author affiliations: Friedrich-Loeffler-Institut, Greifswald-Insel Riems, Germany (A. Pohlmann, D. Hoffmann, C. Grund, S. Koethe, J. King, J. Schinköthe, R. Ulrich, T. Harder, M. Beer); Institute of Virology and Immunology, Mittelhäusern, Switzerland (D. Hüsey); Vetsuisse Faculty Zurich, Zurich, Switzerland (S.M. Meier)

DOI: <https://doi.org/10.3201/eid2510.181931>

The Study

Starting in November 2017, H5 HPAI viruses, classified as clade 2.3.4.4b according to their hemagglutinin (HA) segments, carrying N6 segments were detected in the Netherlands (7), United Kingdom, Switzerland, and Germany (8). We used samples mostly from the outbreaks in Germany collected during December 2017–August 2018 (Appendix Table 1, <https://wwwnc.cdc.gov/EID/article/25/10/18-1931-App1.pdf>). We sequenced (Appendix) and analyzed these viruses and found they carried a neuraminidase (NA) segment of subtype N6 with a high similarity to low pathogenicity avian influenza (LPAI) viruses identified in Asia during 2015–2017 (Appendix Table 2).

According to a full-genome analysis, these H5N6 viruses represent 2 mosaic reassortants of HPAI virus H5N8 found in Europe during the epizootic of 2016–17 (Figure, panel A). Reassortant group I shares all but the NA segment with viruses from the epizootic of 2016–17 (Appendix Figure 1), and because of distinct homologies in the HA, matrix, and nonstructural protein gene segments (Appendix Figure 1), these viruses were further divisible into 3 subgroups, which we designated Gre-02-17-N6, Tai-12-17-N6, and Kor-12-17-N6 (Figure, panel A). The divergence within this reassortant group might have been caused by genetic drift and would be in line with their temporal and geographic patterns of occurrence (Figure, panel B). In contrast, reassortant group II (designated Ger-12-17-N6; Figure) comprises a more homogeneous group of H5N6 viruses from Western and Central Europe. Reassortant group II is genetically distinguishable from reassortant group I by separate clustering of the polymerase acidic (PA) and polymerase basic 2 (PB2) genes (Appendix Figure 1). Group II viruses were detected in Germany during December 2017–August 2018. Their PA segment is similar to that of the HPAI virus A(H5N8) found in the Netherlands in November and December 2016, and their PB2 segment is similar to that of LPAI viruses in Europe and, to a lesser extent, HPAI H5N5 and H5N8 2.3.4.4b isolates from the epizootic of 2016–17 (Appendix Figure 1). This find-

¹These authors contributed equally to this article.

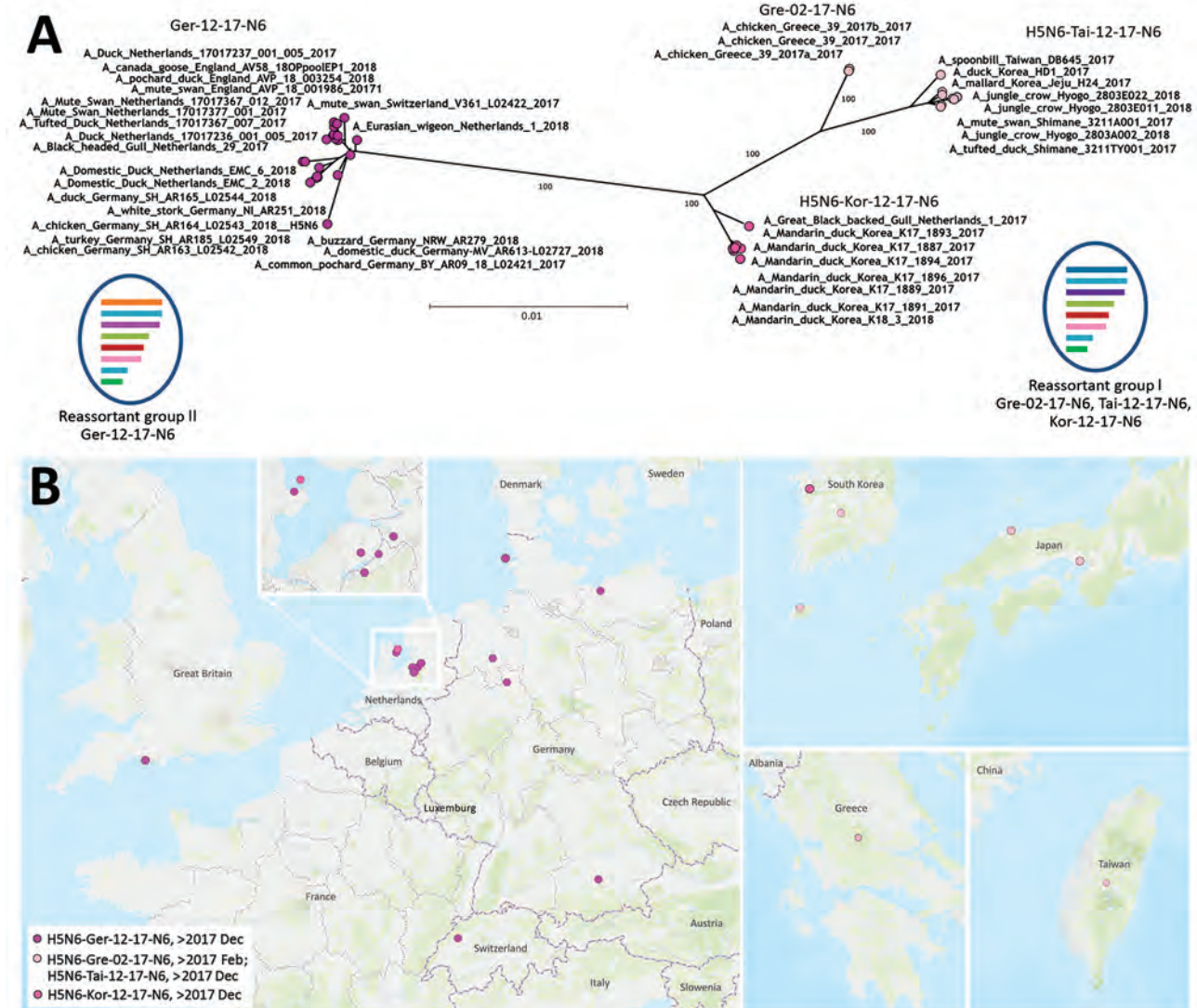


Figure. Phylogenetic clustering and geographic distribution of highly pathogenic avian influenza A(H5N6) viruses, Europe, 2017–2018. A) Supernetwork generated by using maximum-likelihood trees of influenza virus full genomes with RAxML (<https://cme.h-its.org/exelixis/web/software/raxml/index.html>) and 1,000 bootstrap iterations followed by network analysis with SplitsTree4 (<http://ab.inf.uni-tuebingen.de/software/splitstree4>). Reassortant viruses are grouped according to their phylogenetic results. Scale bar indicates nucleotide substitutions per site. The mosaic genome structure of reassortant groups I and II is also provided. Gene segment descriptions are given in Appendix Figure 1 (<https://wwwnc.cdc.gov/EID/article/25/10/18-1931-App1.pdf>). B) Geographic locations of cluster isolates. Inset of cluster in the Netherlands is provided for easier visualization.

ing underscores the ability of HPAI virus clade 2.3.4.4b from the epizootic of 2016–17 to frequently reassort, probably empowered by its genome constellation, especially its HA segment.

H5N6 viruses of clades 2.3.4.4c and 2.3.4.4d and an H5 virus of clade 2.3.4.4b (A/Fujian-Sanyuan/21099/2017) have been reported in cases of human influenza; thus, concerns have been raised about these viruses' zoonotic potential (9). Several clade 2.3.4.4b H5 HPAI viruses isolated in South Korea (Appendix Table 3) have already been evaluated in multiple animal models and showed no zoonotic propensity in ferrets (10,11). These results concur with

our previous analysis of cluster 2.3.4.4b HPAI virus H5N8 from Germany (A/tufted_duck_Germany/AR8444/2016) in human lung explants and in ferrets (12).

We extended the zoonotic risk assessment of these viruses by using a reassortant group II HPAI H5N6 virus (AR09/18, A/common_pochard/Germany-BY/AR09-18-L02421/2017). For comparison, we included a related reassortant HPAI H5N5 clade 2.3.4.4b virus (AR425/17, A/turkey/Germany-SH/R425/2017) with 3 genes, NA (Appendix Table 2), polymerase basic 1, and nucleoprotein, related to LPAI viruses from different countries and 4 genes, PB2, PA, matrix, and nonstructural protein,

related to HPAI viruses isolated during the epizootic of 2016–17 (5).

We inoculated 10 ferrets intranasally with either the H5N6 or H5N5 virus (Appendix). None of the animals displayed any respiratory signs; the only change observed was a minor, short-lived increase in body temperature. Only 1 of the 5 ferrets inoculated with H5N5 exhibited body temperatures >40°C for 3 consecutive days (5–7 days postinfection [dpi]). This particular animal also exhibited a mild gait disorder at 5 dpi, and because these atactic movements persisted (a sign qualifying for termination), the ferret was euthanized at 7 dpi. The viral RNA loads in the nasal washings of animals inoculated with H5N5 and H5N6 were low up through 7 dpi (Table), and RNA excretion ceased thereafter. However, at 7 dpi, the H5N5-inoculated ferret showing mild ataxia displayed a peak of 100 copies/μL of extracted RNA (input volume 100 μL) in the nasal washing fluid (Table).

Nucleoprotein antibody-specific seroconversion (Table) was detected in all inoculated ferrets surviving until euthanasia at 14 dpi. The serum sample of the atactic animal euthanized at 7 dpi scored reactive but not positive.

We dissected all euthanized animals and analyzed spleens, tracheas, lungs, conchae, cerebellum, and cerebrum for viral genome loads, as described previously (12). All organ samples taken at 14 dpi were negative; however, the cerebrum, trachea, and nasal concha of the single animal exhibiting disease euthanized at 7 dpi had a low viral load of 7–25 copies/μL of extracted RNA from ≈2 mm³ tissue material homogenized in 1 mL of medium (input volume 100 μL).

Histopathologic workup of the sick ferret revealed mild, subacute necrotizing rhinitis; moderate, oligofocal,

subacute necrotizing bronchointerstitial pneumonia; moderate, multifocal necrotizing hepatitis; severe necrotizing salpingitis; and the focal-to-multifocal intralesional presence of influenza virus matrix protein (Appendix Figure 2) consistent with systemic virus spread. Only 1 of 4 of the H5N5-infected ferrets and 2 of 5 of the H5N6-infected ferrets necropsied at 14 dpi revealed inflammatory lung lesions, yet all were negative for matrix protein by immunohistochemical staining (Appendix Table 4). Considering the low morbidity rate (10%), these H5 viruses have a mild pathogenic potential in the ferret model compared with other HPAI viruses (13).

Conclusions

The genetic makeup of HPAI H5 clade 2.3.4.4b viruses fosters reassortment, which can expand their evolutionary capacity. Segment reassortment bears a concomitant danger of the emergence of strains that are more pathogenic or zoonotic or that have a higher potential to evolve to propagate in avian hosts with different migratory behaviors. H5N6 and H5N5 viruses of this clade have been continuously present in Europe since 2017, necessitating continuous surveillance and virus characterization. Our study excludes the possibility of enhanced zoonotic potential for the analyzed H5N5 and H5N6 2.3.4.4b clade viruses. Nonetheless, existing reports of clade 2.3.4.4c HPAI H5N6 virus infections in mammals and clade 2.3.4.4b-2.3.4.4d virus co-infections in humans indicate a continued risk for zoonotic events with H5Nx reassortants (9). Continued surveillance and characterization of these viruses is crucial to reduce the risk for outbreaks with burgeoning HPAI isolates of the goose/Guangdong lineage.

Acknowledgments

We thank Kathrin Steffen and Patrick Zitzow for excellent technical assistance and Andrea Vöglin for providing material.

This work was in part financed by the European Union Horizon 2020 program grant agreement COMPARE (COLlaborative Management Platform for detection and Analyses of [Re-]emerging and foodborne outbreaks in Europe; no. 643476) and DELTA-FLU (no. 727922).

About the Author

Dr. Pohlmann is a senior scientist and expert for influenza virus sequence analysis within the Institute of Diagnostic Virology of the Friedrich-Loeffler-Institut, Greifswald-Insel Riems, Germany. Her research interests are focused on the sequencing, genetic characterization, and classification of influenza viruses and their molecular epidemiology.

Table. Viral RNA loads in nasal washing samples from ferrets infected with highly pathogenic avian influenza A(H5N6/H5N5) clade 2.3.4.4b virus isolates from Germany, 2017–2018, and seroconversion in study assessing virus zoonotic risk*

Group	Day postinfection, viral RNA load, genome copies/μL						Seroconversion†
	0	1	3	5	7	9	
Controls	–	–	–	–	–	–	–
H5N5	–	0.2	0.2	0.1	100.6	ND‡	+/-§
	–	1.2	2.8	0.1	–	–	+
	–	1.9	0.9	2.9	–	–	+
	–	1.2	–	0.1	–	–	+
	–	0.1	–	8.2	0.9	–	+
H5N6	–	–	0.8	1.3	1.3	–	+
	–	0.2	1.9	13.8	3.2	–	+
	–	0.2	–	0.2	0.2	–	+
	–	–	–	–	–	–	+
	–	0	1.3	0.2	4.2	–	+

*ND, not done; –, negative.

†Seroconversion measured with sensitive nucleoprotein ELISA (ID Screen Influenza A Antibody Competition ELISA Kit; ID.Vet, https://www.idvet.com) with day 14 or 7 serum sample, depending on day of animal sacrifice, and compared with preinoculation serum sample.

‡Sacrificed day 7 because animal displayed neurologic symptoms.

§Reaction interpreted as reactive but not positive.

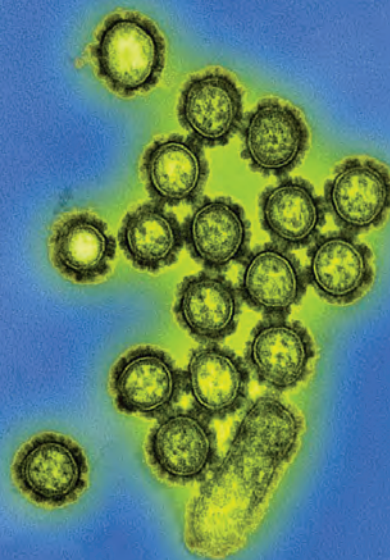
References

1. Pohlmann A, Starick E, Harder T, Grund C, Höper D, Globig A, et al. Outbreaks among wild birds and domestic poultry caused by reassorted influenza A(H5N8) clade 2.3.4.4 viruses, Germany, 2016. *Emerg Infect Dis.* 2017;23:633–6. <https://doi.org/10.3201/eid2304.161949>
2. Kleyheeg E, Slaterus R, Bodewes R, Rijks JM, Spiereburg MAH, Beerens N, et al. Deaths among wild birds during highly pathogenic avian influenza A(H5N8) virus outbreak, the Netherlands. *Emerg Infect Dis.* 2017;23:2050–4. <https://doi.org/10.3201/eid2312.171086>
3. Globig A, Staubach C, Sauter-Louis C, Dietze K, Homeier-Bachmann T, Probst C, et al. Highly pathogenic avian influenza H5N8 clade 2.3.4.4b in Germany in 2016/2017. *Front Vet Sci.* 2017;23:1543–7. <https://doi.org/10.3201/eid2309.170539>
4. Fusaro A, Monne I, Mulatti P, Zecchin B, Bonfanti L, Ormelli S, et al. Genetic diversity of highly pathogenic avian influenza A(H5N8/H5N5) viruses in Italy, 2016–17. *Emerg Infect Dis.* 2017;23:1543–7. <https://doi.org/10.3201/eid2309.170539>
5. Pohlmann A, Starick E, Grund C, Höper D, Strebelow G, Globig A, et al. Swarm incursions of reassortants of highly pathogenic avian influenza virus strains H5N8 and H5N5, clade 2.3.4.4b, Germany, winter 2016/17. *Sci Rep.* 2018;8:15. <https://doi.org/10.1038/s41598-017-16936-8>
6. Beerens N, Heutink R, Bergervoet SA, Harders F, Bossers A, Koch G. Multiple reassorted viruses as cause of highly pathogenic avian influenza A(H5N8) virus epidemic, the Netherlands, 2016. *Emerg Infect Dis.* 2017;23:1974–81. <https://doi.org/10.3201/eid2312.171062>
7. Beerens N, Koch G, Heutink R, Harders F, Vries DPE, Ho C, et al. Novel highly pathogenic avian influenza A(H5N6) virus in the Netherlands, December 2017. *Emerg Infect Dis.* 2018;24:770–3. <https://doi.org/10.3201/eid2404.172124>
8. Poen MJ, Venkatesh D, Bestebroer TM, Vuong O, Scheuer RD, Oude Munnink BB, et al. Co-circulation of genetically distinct highly pathogenic avian influenza A clade 2.3.4.4 (H5N6) viruses in wild waterfowl and poultry in Europe and East Asia, 2017–18. *Virus Evol.* 2019;5:vez004. <http://dx.doi.org/10.1093/ve/vez004>
9. World Health Organization. Antigenic and genetic characteristics of zoonotic influenza viruses and development of candidate vaccine viruses developed for pandemic preparedness. 2018 Feb [cited 2018 Feb 22]. http://www.who.int/entity/influenza/vaccines/virus/201802_zoonotic_vaccinevirusupdate.pdf?ua=1
10. Noh JY, Lee DH, Yuk SS, Kwon JH, Tseren-Ochir EO, Hong WT, et al. Limited pathogenicity and transmissibility of Korean highly pathogenic avian influenza H5N6 clade 2.3.4.4 in ferrets. *Transbound Emerg Dis.* 2018;65:923–6. <https://doi.org/10.1111/tbed.12869>
11. Kwon HI, Kim EH, Kim YI, Park SJ, Si YJ, Lee IW, et al. Comparison of the pathogenic potential of highly pathogenic avian influenza (HPAI) H5N6, and H5N8 viruses isolated in South Korea during the 2016–2017 winter season. *Emerg Microbes Infect.* 2018;7:29. <https://doi.org/10.1038/s41426-018-0029-x>
12. Grund C, Hoffmann D, Ulrich R, Naguib M, Schinköthe J, Hoffmann B, et al. A novel European H5N8 influenza A virus has increased virulence in ducks but low zoonotic potential. *Emerg Microbes Infect.* 2018;7:132. <https://doi.org/10.1038/s41426-018-0130-1>
13. Belsler JA, Johnson A, Pulit-Penalosa JA, Pappas C, Pearce MB, Tzeng WP, et al. Pathogenicity testing of influenza candidate vaccine viruses in the ferret model. *Virology.* 2017;511:135–41. <https://doi.org/10.1016/j.virol.2017.08.024>

Address for correspondence: Martin Beer, Friedrich-Loeffler-Institut, Institute of Diagnostic Virology, Suedufer 10, Greifswald-Insel Riems 17493, Germany; email: martin.beer@fli.de

EID SPOTLIGHT TOPIC

Influenza



Influenza is a contagious respiratory illness caused by influenza viruses. It can cause mild to severe illness. Serious outcomes of influenza infection can result in hospitalization or death. Some people, such as older people, young children, and people with certain health conditions, are at high risk for serious influenza complications. The best way to prevent the flu is by getting vaccinated each year.

<http://wwwnc.cdc.gov/eid/page/influenza-spotlight>

**EMERGING
INFECTIOUS DISEASES®**

Lassa Virus in Pygmy Mice, Benin, 2016–2017

Anges Yadouleton, Achaz Agolinou, Fodé Kourouma, Raoul Saizonou, Meike Pahlmann, Sonia Kossou Bedié, Honoré Bankolé, Beate Becker-Ziaja, Fernand Gbaguidi, Anke Thielebein, N’Faly Magassouba, Sophie Duraffour, Jean-Pierre Baptiste, Stephan Günther, Elisabeth Fichet-Calvet

Author affiliations: Laboratoire des Fièvres Hémorragiques Virales, Cotonou, Benin (A. Yadouleton, A. Agolinou); Ministry of Health, Cotonou (A. Yadouleton, H. Bankolé, F. Gbaguidi); Laboratoire des Fièvres Hémorragiques Virales, Conakry, Guinea (F. Kourouma, N. Magassouba); World Health Organization, Cotonou (R. Saizonou, S.K. Bedié, J.-P. Baptiste); Bernhard-Nocht Institute for Tropical Medicine, Hamburg, Germany (M. Pahlmann, B. Becker-Ziaja, A. Thielebein, S. Duraffour, S. Günther, E. Fichet-Calvet)

DOI: <https://doi.org/10.3201/eid2510.180523>

Lassa virus has been identified in 3 pygmy mice, *Mus baoulei*, in central Benin. The glycoprotein and nucleoprotein sequences cluster with the Togo strain. These mice may be a new reservoir for Lassa virus in Ghana, Togo, and Benin.

Lassa fever has recently emerged in Benin and Togo, where it had been unknown until 2014. In November 2014, two persons died of confirmed Lassa virus (LASV) infection at Saint Jean de Dieu Hospital, in Tanguieta, northern Benin. During January–February 2016, a second outbreak with 11 confirmed cases of Lassa fever occurred in the communes of Tchaourou and Parakou, department of Borgou, central Benin. These 11 cases were diagnosed at the Irrua Specialist Teaching Hospital (Irrua, Nigeria) and the Bernhard-Nocht Institute for Tropical Medicine (Hamburg, Germany). During the same period, 2 cases from neighboring Togo were also confirmed as Lassa fever (1,2).

In July 2016, to enable the affected countries to quickly detect new cases of Lassa fever, the Bernhard-Nocht Institute for Tropical Medicine and the German Ministry of Cooperation established LASV diagnostic capacity in Cotonou (Benin) and Lomé (Togo). In 2017, another 2 cases occurred in central Benin.

The need to understand the epidemiology of Lassa fever in Benin and the involvement of rodents in the transmission of the disease led us to investigate the small mammal community living in and around the dwellings in

villages where the index case-patients lived. To identify these villages, a first expedition in October 2016 traced back confirmed and probable cases according to the health registers of the local hospital in Tchaourou and the teaching hospital in Parakou. An investigation of several villages enabled us to record some evidence from the nurses in the health centers.

On the basis of these findings, a second expedition in September 2017 used Sherman traps (<https://www.shermantraps.com>) to capture small mammals in 6 villages in Tchaourou. The animals were sampled in several habitats: houses (inside, 80 traps) and fields and savannah (outside, 120 traps). The animals were then killed with an overdose of halothane, and necropsies were performed in situ according to Biosafety Level 3 security procedures (3).

We collected blood and organs (including spleen and liver) and identified the animals morphologically, according to standard measurements: body weight; body, tail, hindfoot, and ear lengths. Because of possible sibling species among *Mastomys* spp. and *Mus* spp. rodents, we performed molecular identification through a PCR targeting cytochrome b. Distribution of the small mammals was 210 *Praomys daltoni* mice, 14 *Mus baoulei* mice, 12 *Rattus rattus* rats, 10 *Lemniscomys striatus* mice, 7 *Mus mattheyi* mice, 6 *Mastomys natalensis* mice, and 26 *Crocidura* spp. shrews (Appendix Table 1, <https://wwwnc.cdc.gov/EID/article/25/10/18-0523-App1.pdf>). The surprising finding was the scarcity of *M. natalensis* mice, the most probable reservoir of LASV; we trapped only 3 of these mice inside and 3 outside. In that area, the commensal rodent was *P. daltoni*, as is often found in Ghana and Nigeria (4,5).

We screened all samples for LASV by using 2 reverse transcription PCRs: 1 specific for LASV and 1 for panarenaviruses (6,7). The 2 tests enabled us to detect 3 LASV-positive animals, all pygmy mice (*M. baoulei*). To determine phylogeny more reliably than we could by using short fragments issued from the diagnostic tests, we performed additional PCRs on glycoprotein (GP) and nucleoprotein (NP) genes located on the small RNA segment (primers in Appendix Table 2). GP sequence of 1,408 nt and NP sequences of 1,654 nt were aligned with 31 LASV sequences belonging to all lineages.

The phylogenetic analyses performed with a Bayesian approach on GP and NP alignments shows that the 3 new sequences (Worogui50, Worogui51, and Odo-Akaba13) clustered with Jirandogo76, from the same species (*M. baoulie*) collected in Ghana in 2011 (Figure). Furthermore, the analysis showed strong support with the strains from humans in Togo, which clustered with the sequences from humans in Benin (S. Günther, E. Fichet-Calvet, unpub. data). The differences between the 3 GP sequences in mice from Benin and the strain from humans in Togo ranged from 20.8% to 21.7% (8.5% to 10.3% at the amino

reservoirs could still be implicated in the recent events of LASV transmission to humans.

Our findings strongly point toward *M. baoulei* mice as a potential candidate for LASV spreading in Benin, Togo, and Ghana. Together with the multimammate mice *M. natalensis* and *Mastomys erythroleucus* and the soft-furred mouse *Hylomyscus pamfi* (10), the fourth rodent species reservoir of LASV is *M. baoulei* pygmy mice.

Acknowledgments

We express our gratitude to Eléonore Gandjeto and Lucien Toko, who facilitated our research in Benin. We are particularly grateful to the field assistants who participated in the rodent sampling: Moussa Fofana, Edwige Kpodo, Zita Sagbohan, and Morlaye Sylla.

Authorization for rodent trapping was granted by the Ministry of Agriculture (014/MAEP/SGM/DE/SSA/SE). This research was funded by the German Research Foundation (DFG FI 1781/2-1 and GU 883/4-1) and the Global Health Protection program, supported by the Federal Ministry of Health (ZMV11-2516-GHP-704).

About the Author

Dr. Yadouleton is a medical entomologist in the Centre de Recherche Entomologique de Cotonou, Benin, head of the Laboratoire des Fièvres Hémorragiques in Cotonou, and a teacher at the University of Natitingou, Benin. His research interests include mosquito control and the diagnosis of viral hemorrhagic fevers.

References

- Whitmer SLM, Strecker T, Cadar D, Dienes HP, Faber K, Patel K, et al. New lineage of Lassa virus, Togo, 2016. *Emerg Infect Dis*. 2018;24:599–602. <https://doi.org/10.3201/eid2403.171905>
- World Health Organization. Lassa fever—Benin [cited 2016 July 1]. <http://www.who.int/csr/don/13-june-2016-lassa-fever-benin>
- Fichet-Calvet E. Lassa fever: a rodent-human interaction. In: Johnson N, editor. *The role of animals in emerging viral diseases*. London: Elsevier; 2014. p. 89–123.
- Kronmann KC, Nimo-Printsil S, Guirguis F, Kronmann LC, Bonney K, Obiri-Danso K, et al. Two novel arenaviruses detected in pygmy mice, Ghana. *Emerg Infect Dis*. 2013;19:1832–5. <https://doi.org/10.3201/eid1911.121491>
- Olayemi A, Obadare A, Oyeyiola A, Fasogbon A, Igbokwe J, Igbahenah F, et al. Small mammal diversity and dynamics within Nigeria, with emphasis on reservoirs of the Lassa virus. *Syst Biodivers*. 2017;15:1–10.
- Olschläger S, Lelke M, Emmerich P, Panning M, Drosten C, Hass M, et al. Improved detection of Lassa virus by reverse transcription-PCR targeting the 5' region of S RNA. *J Clin Microbiol*. 2010;48:2009–13. <https://doi.org/10.1128/JCM.02351-09>
- Vieth S, Drosten C, Lenz O, Vincent M, Omilabu S, Hass M, et al. RT-PCR assay for detection of Lassa virus and related Old World arenaviruses targeting the L gene. *Trans R Soc Trop Med Hyg*. 2007;101:1253–64. <https://doi.org/10.1016/j.trstmh.2005.03.018>
- Drummond AJ, Suchard MA, Xie D, Rambaut A. Bayesian phylogenetics with BEAUti and the BEAST 1.7. *Mol Biol Evol*. 2012;29:1969–73. <https://doi.org/10.1093/molbev/mss075>
- Bowen MD, Rollin PE, Ksiazek TG, Hustad HL, Bausch DG, Demby AH, et al. Genetic diversity among Lassa virus strains. *J Virol*. 2000;74:6992–7004. <https://doi.org/10.1128/JVI.74.15.6992-7004.2000>
- Olayemi A, Cadar D, Magassouba N, Obadare A, Kourouma F, Oyeyiola A, et al. New hosts of the Lassa virus. *Sci Rep*. 2016;6:25280. <https://doi.org/10.1038/srep25280>

Address for correspondence: Elisabeth Fichet-Calvet, Bernhard-Nocht Institute for Tropical Medicine, Virology, Bernhard-Nocht Str. 74, Hamburg 20359, Germany; email: fichet-calvet@bnitm.de

Genomic Characterization of Rift Valley Fever Virus, South Africa, 2018

Antoinette van Schalkwyk, Marco Romito

Author affiliation: Onderstepoort Veterinary Institute, Onderstepoort, South Africa

DOI: <https://doi.org/10.3201/eid2510.181748>

An isolated Rift Valley fever (RVF) outbreak was reported in 2018 in Free State Province, South Africa. Phylogenetic analyses based on complete genome sequences of 3 RVF viruses from blood and tissue samples indicated that they were related to a virus isolated in 2016 from a man returning to China from Angola.

Rift Valley fever (RVF) is endemic to sub-Saharan Africa; major outbreaks were reported in South Africa during the 1950s, the 1970s, and 2008–2011 (1). Molecular classification of RVF viruses (RVFVs) isolated from 16 countries showed that these viruses cluster into 15 lineages (A–O) (2). Viral sequences from the previous outbreaks in South Africa clustered in lineage C (2008–2009), lineage H (2009–2010), lineage I (1951), and lineage L (1974–1975); 1 isolate in 2009 from Kakamas in the Northern Cape Province was in lineage K (Figure) (2). Lineage K contains the hepatotropic Entebbe-44 virus isolated from mosquitoes in Uganda in 1944 and its derivative, the Smithburn neurotropic vaccine strain (SNS) commercially available in South Africa (2). RVFV was identified by unbiased deep

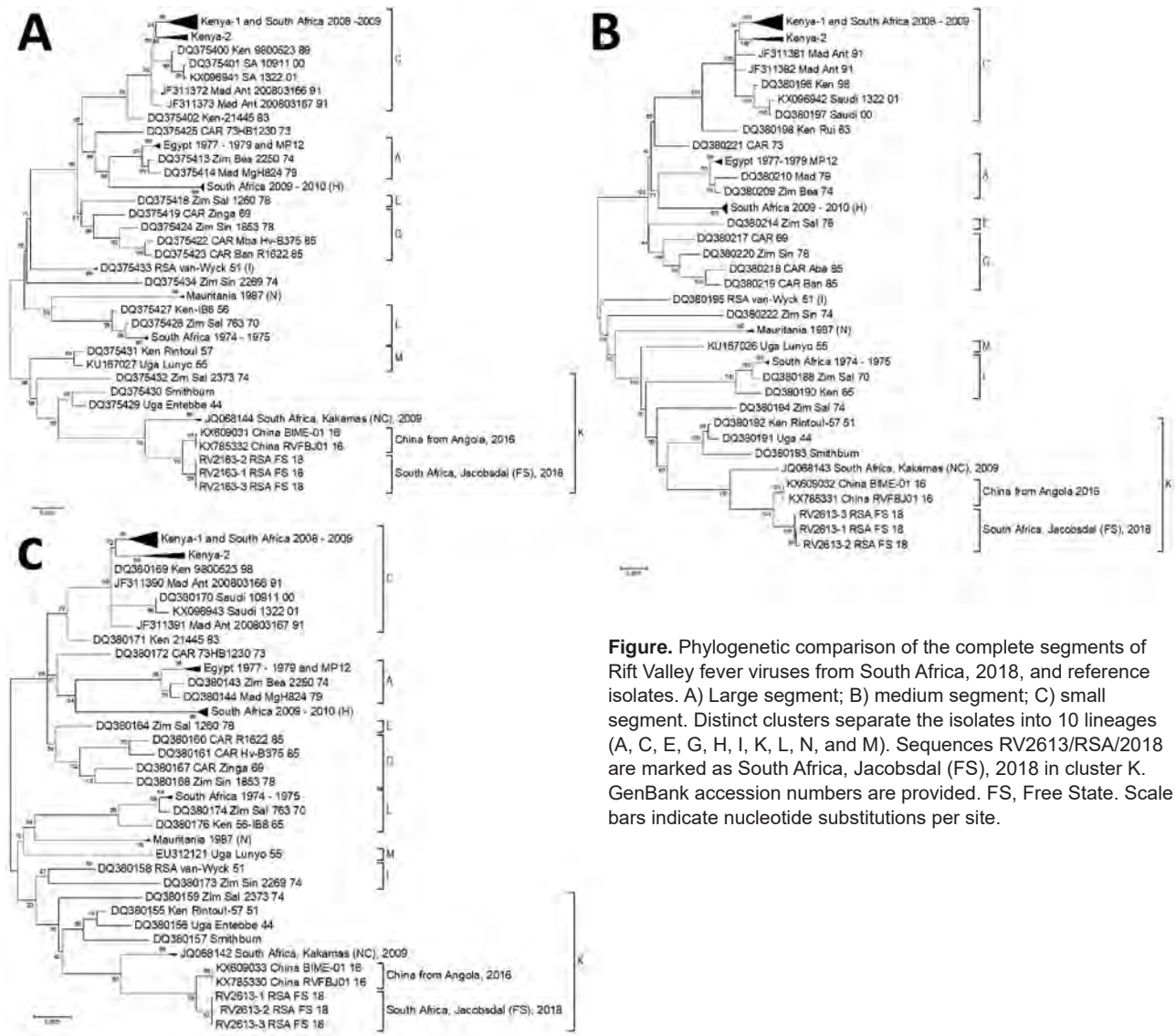


Figure. Phylogenetic comparison of the complete segments of Rift Valley fever viruses from South Africa, 2018, and reference isolates. A) Large segment; B) medium segment; C) small segment. Distinct clusters separate the isolates into 10 lineages (A, C, E, G, H, I, K, L, N, and M). Sequences RV2613/RSA/2018 are marked as South Africa, Jacobsdal (FS), 2018 in cluster K. GenBank accession numbers are provided. FS, Free State. Scale bars indicate nucleotide substitutions per site.

sequencing of the virus genome (isolate BIME-01) from a man returning to China in 2016 with fever and jaundice after a 22-month stay in Angola (3). Phylogenetic analysis of the complete RVFV genome of sample BIME-01 and the Vero cell culture isolate of the virus (RVFBJ01) showed that it clustered together with the Kakamas/2009 virus in lineage K (3).

On April 28, 2018, an outbreak of suspected RVF was reported on a sheep farm in the Jacobsdal area of the Free State Province of South Africa. The illness rate was ≈55.8% and the case-fatality-rate 100% (335 sheep died) (4). Six persons either working or residing on the farm reported symptoms compatible with RVFV infection, but no human fatalities occurred (5). Clinical specimens from affected sheep were submitted to the Onderstepoort Veterinary Institute Agricultural Research Council

(Onderstepoort, South Africa) for laboratory confirmation of the outbreak.

We used flocculated nylon swabs (FLOQswabs, COPAN, <http://www.copanusa.com>) to pierce and swab the tissue pools and then placed the swabs into Eppendorf tubes containing 700 μL phosphate-buffered saline (pH 7.0). After agitation, we removed 200 μL buffer for total nucleic acid extraction. We used either whole blood in EDTA (RV2613-1/RSA/2018) or a combination of tissue swab specimens from liver, spleen, and kidney for extractions (RV2613-2/RSA/2018 and RV2613-3/RSA/2018) using the MagNA Pure 96 (Roche Molecular Systems, <https://www.roche.com>). We detected the presence of RVFV RNA using real-time reverse transcription PCR (RT-PCR) (6). We used the same 3 nucleic acid extracts as templates in 8 individual RT-PCRs (A–H), designed to

overlap the entire genome (Appendix Table 1, <http://www.wnc.cdc.gov/EID/article/25/10/18-1748-App1.pdf>). We used the SuperScript III One-Step RT-PCR System with Platinum Taq DNA polymerase (Invitrogen, <https://www.thermofisher.com>) in a 20- μ L reaction with 0.25 μ mol/L of each primer (Appendix Table 1) at an annealing temperature of 53°C for 45 cycles. The resulting amplicons overlapped regions of all 3 genome segments: large (A, B, C, and H), medium (D, E, and F), and small (H). We submitted the 8 amplicons to Inqaba Biotechnical Industries, Pretoria, South Africa (<https://www.inqababiotec.co.za>), for Sanger sequencing, using the primers incorporated during the generation of the amplicons and 9 additional primers (Appendix Table 1). We constructed the complete viral genome sequences from the 3 field specimens and submitted them to GenBank (accession nos. MK134834–42).

The 3 sequences (RV2613-1/RSA/2018, RV2613-2/RSA/2018, and RV2613-3/RSA/2018) were similar to one another: no nucleotide differences in the large segment, 2 in the medium segment, and 1 in the small segment. The high sequence identity among these 3 viruses and the lack of segment reassortment, together with the isolated geographic distribution of the outbreak, indicate a single introduction. After phylogenetic analysis, we clustered the 3 viruses into lineage K, with their closest known relatives BIM-01/2016, isolated from a worker from China in Angola, and the virus RVFBJ01/2016 derived from cell culture (Figure). We assessed each genome segment and found <1% sequence difference between any of the 3 South Africa viruses and the virus from Angola and <2.11% sequence difference for Kakamas/2009 (Appendix Table 2). Evolutionary analysis of segment M using Bayesian inference with BEAST version 1.8.1 (<https://beast.community>) under the Hasegawa-Kishino-Yano substitution model, a strict molecular clock, and a constant population size estimated that RV2613/RSA/2018 and BIM-01/2016 had a common ancestor \approx 7 years ago that shared a common ancestor with Kakamas/2009 \approx 28 years ago. Virus RV2613/RSA/2018 had a higher sequence identity with the original Entebbe-44 isolate than the SNS vaccine or vaccine-derived Ken Rintoul-57 (Appendix Table 2). This result indicates that Kakamas/2009, BIM-01/2016, and RV2613/RSA/2018 probably evolved from a common ancestor of Entebbe-44 and not from its derivative SNS vaccine.

The sequence data imply that this outbreak was likely the result of a single introduction of virus that probably remained localized to 1 farm because of the onset of colder winter temperatures and a decline in rainfall. The phylogenetic relationship of this virus to known others suggests a persistent, yet largely unnoticed, low-level spread of RVFVs in southern Africa. This finding reemphasizes the importance of active disease surveillance programs with diligent reporting of suspected cases, as well as suitable vaccination regimens.

Funding for this project was obtained from the National Research Foundation of South Africa, under Competitive Support for Unrated Researchers Grant CSUR160418162303.

About the Author

Dr. van Schalkwyk is a researcher at the Agricultural Research Council, Onderstepoort Veterinary Institute, in South Africa. Her primary research interest is molecular epidemiology and virus evolution.

References

- Pienaar NJ, Thompson PN. Temporal and spatial history of Rift Valley fever in South Africa: 1950 to 2011. *Onderstepoort J Vet Res.* 2013;80:384. <http://doi.org/10.4102/ojvr.v80i1.384>
- Grobbelaar AA, Weyer J, Leman PA, Kemp A, Paweska JT, Swanepoel R. Molecular epidemiology of Rift Valley fever virus. *Emerg Infect Dis.* 2011;17:2270–6. <https://doi.org/10.3201/eid1712.111035>
- Liu W, Sun F-J, Tong Y-G, Zhang S-Q, Cao W-C. Rift Valley fever virus imported into China from Angola. *Lancet Infect Dis.* 2016;16:1226. [https://doi.org/10.1016/S1473-3099\(16\)30401-7](https://doi.org/10.1016/S1473-3099(16)30401-7)
- World Organization for Animal Health (OIE). Rift Valley fever South Africa. 2018 [cited 2018 May 31]. http://www.oie.int/wahis_2/public/wahid.php/Reviewreport/Review?page_refer=MapFullEventReport&reportid=26639
- Jansen van Vuren P, Kgaladi J, Patharoo V, Ohaebosim P, Msimang V, Nyokong B, et al. Human cases of Rift Valley fever in South Africa, 2018. *Vector Borne Zoonotic Dis.* 2018;18:713–5. <https://doi.org/10.1089/vbz.2018.2357>
- Drosten C, Götting S, Schilling S, Asper M, Panning M, Schmitz H, et al. Rapid detection and quantification of RNA of Ebola and Marburg viruses, Lassa virus, Crimean-Congo hemorrhagic fever virus, dengue virus, and yellow fever virus by real-time reverse transcription-PCR. *J Clin Microbiol.* 2002;40:2323–30. <https://doi.org/10.1128/JCM.40.7.2323-2330.2002>

Address for correspondence: Antoinette van Schalkwyk, ARC Onderstepoort Veterinary Institute, MED, Old Soutpan Road, Onderstepoort, Pretoria, Gauteng 0110, South Africa; email: VanSchalkwykA1@arc.agric.za

Estimated Incubation Period and Serial Interval for Human-to-Human Influenza A(H7N9) Virus Transmission

Lei Zhou, Qun Li, Timothy M. Uyeki

Author affiliations: Peking University Health Science Center, Beijing, China (L. Zhou); Chinese Center for Disease Control and Prevention, Beijing (L. Zhou, Q. Li); Centers for Disease Control and Prevention, Atlanta, Georgia, USA (T.M. Uyeki)

DOI: <https://doi.org/10.3201/eid2510.190117>

We estimated the incubation period and serial interval for human-to-human-transmitted avian influenza A(H7N9) virus infection using case-patient clusters from epidemics in China during 2013–2017. The median incubation period was 4 days and serial interval 9 days. China's 10-day monitoring period for close contacts of case-patients should detect most secondary infections.

As of April 2019, a total of 1,568 confirmed cases of avian influenza A(H7N9) virus infection acquired in China have been reported in humans since the virus emerged in spring 2013 (1,2). A large increase in infections occurred in China during the fifth H7N9 virus epidemic (2016–17), prompting concerns of increased H7N9 virus transmissibility in humans (3). However, as of June 2019, only evidence of limited, nonsustained human-to-human transmission has been reported (3).

Field investigations of case-patients with confirmed H7N9 virus infections are critical to assessing possible human-to-human transmission. The incubation period for H7N9 virus infection has been estimated to be 3–7 days (4–6). However, the incubation period estimated in these studies primarily reflects sporadic poultry-to-human transmission; no study has specifically focused on the incubation period for human-to-human H7N9 virus transmission. Although the kinds of exposures, amount of virus per exposure, and routes of exposure might differ between poultry-to-human and limited human-to-human H7N9 virus transmission, whether the incubation periods differ is unknown. Data on the incubation period for H7N9 virus in the setting of human-to-human transmission can help determine the appropriate duration for monitoring exposed close contacts, including healthcare personnel, of confirmed H7N9 case-patients.

We analyzed the data on all clusters of epidemiologically linked H7N9 case-patients collected during field investigations of 5 epidemics that occurred in mainland China during 2013–2017 and that were reported to the Chinese Center for Disease Control and Prevention (China CDC).

We focused on clusters involving probable human-to-human transmission in which no poultry exposure, including visits to live poultry markets, was reported for epidemiologically linked secondary case-patients exposed to a symptomatic index case-patient, as previously described (3). We defined the incubation period for a secondary case-patient as days from the date of an unprotected exposure within 1 meter to an index case-patient for any duration beginning, at the earliest, the day before illness onset of the index case-patient to the date of illness onset of the secondary case-patient. The exposures and dates of illness onset were determined through field investigations of each H7N9 case-patient. For a secondary case-patient with multiple days of exposure to an ill index case-patient, we used the earliest exposure date to define the maximum incubation period and the last exposure date (such as the index case-patient's date of hospital isolation) to define the minimum incubation period. We estimated incubation periods using median values, as done previously (1,7), and compared them by epidemic. We calculated serial intervals using the reported illness onset dates of index and secondary case-patients. We classified secondary case-patients as blood related or unrelated and compared median serial intervals by subgroup and epidemic.

Among 14 secondary H7N9 case-patients in 14 clusters of probable human-to-human transmission, the overall median estimated incubation period was 4 (range 1–12) days (Table). The median overall and medians of the minimum and maximum incubation periods estimated for secondary case-patients in the fifth epidemic were not significantly different than those estimated for case-patients in previous epidemics (Table). The estimated median serial interval among secondary case-patients who were blood related to an index case-patient ($n = 6$; 9.5 [range 5–12] days) and unrelated to an index case-patient ($n = 8$; 8 [range 6–15] days) were not significantly different (Appendix Table, <https://wwwnc.cdc.gov/EID/article/25/10/19-0117-App1.pdf>). The median serial interval for H7N9 virus infection among all clusters from the 5 epidemics was 9 (range 6–11) days and was not significantly different between epidemics (data not shown).

Overall, the incubation period and serial interval for limited human-to-human H7N9 virus transmission (including blood-related and unrelated persons) were unchanged during 2013–2017. Limitations to this study that could have affected our estimates include a small sample size of 14 secondary case-patients and the potential to misclassify secondary case-patients as a result of unrecognized or unreported poultry exposure. However, data on human, poultry, and environmental exposures and dates of illness onset included in our analyses were collected during detailed field investigations that were initiated promptly among close contacts of index case-patients after laboratory confirmation of H7N9 virus infection and reported to the China CDC.

Table. Estimated incubation periods for avian influenza A(H7N9) virus infection in the setting of probable human-to-human transmission among 14 epidemiologically linked clusters of case-patients from 5 epidemic waves in mainland China, 2013–2017*

Incubation period, d, median (range); p value	Epidemic wave, no. secondary case-patients					
	All, n = 14	First, n = 2	Second, n = 3	Third, n = 2	Fourth, n = 3	Fifth, n = 4
Overall	4 (1–12)	6.5 (1–12); 0.297	3.5 (1–7); 0.295	4.5 (1–7); 0.857	6 (1–11); 0.517	3.5 (1–8); 0.735
Minimum	1 (1–7)	3 (1–5); 0.830	1 (1–3); 0.519	2 (1–3); 0.914	1 (1–7); 1.000	2 (1–6); 0.581
Maximum	6.5 (3–12)	10 (8–12); 0.072	4 (4–7); 0.199	6.5 (6–7); 0.920	8 (5–11); 0.304	4 (3–8); 0.231

*After the first epidemic wave of infections, defined as March–August 2013, an epidemic wave was defined as September 1–August 31 of the following year. Thirteen secondary case-patients had multiple exposure dates and 1 secondary case-patient had 1 exposure date to an index case-patient. The incubation period for secondary case-patients was defined as the time in days from the date of an unprotected exposure within 1 meter to an index case-patient for any duration beginning at the earliest date before illness onset of the index case-patient to the date of illness onset of the secondary case-patient. For secondary case-patients with multiple days of exposure to an ill index case-patient, we used the earliest exposure date to define the maximum incubation period and last exposure date (such as the date of hospital isolation of the index case-patient) to define the minimum incubation period. We compared the median incubation period for each epidemic wave with the 4 other epidemic waves. We used Wilcoxon rank-sum test to compare the distribution of median incubation periods; a p value <0.05 was considered statistically significant.

Our use of median values to describe the epidemiologic parameters for H7N9 case-patients in the 14 clusters might have led to an overestimation of the incubation period and serial interval for human-to-human H7N9 virus transmission. For example, parametric analyses performed with data from much larger datasets (mostly H7N9 cases resulting from poultry exposures), in which data with right-skewed distributions were censored, were reported to provide shorter estimated incubation periods (4–6,8). The incubation period could also have been overestimated among case-patients with multiple exposure days to an index case-patient, if infection did not occur on the first day of exposure. Therefore, further comprehensive epidemiologic investigations to better define the transmission dynamics of human-to-human H7N9 virus transmission are critical. Nevertheless, our findings suggest that China's policy since 2013 for a 10-day monitoring period for close contacts of H7N9 case-patients should detect most symptomatic secondary infections.

Acknowledgments

We thank the local and provincial Chinese CDC staff for providing assistance with data collection, Yuelong Shu and colleagues for their contributions to laboratory testing, Ruiqi Ren for help with data collection and analyses, and Carolyn M. Greene for assistance with interpretation of study results.

About the Author

Dr. Zhou is chief of the Branch for Emerging Infectious Diseases, Public Health Emergency Center, China CDC, Beijing, China. Her research interests are prevention and control of emerging infectious diseases and pandemic influenza preparedness and response.

References

- Li Q, Zhou L, Zhou M, Chen Z, Li F, Wu H, et al. Epidemiology of human infections with avian influenza A(H7N9) virus in China. *N Engl J Med*. 2014;370:520–32. <https://doi.org/10.1056/NEJMoa1304617>
- World Health Organization. Influenza at the human-animal interface. Summary and assessment, 13 February to 9 April 2019. 2019 [cited 2019 Jun 5]. https://www.who.int/influenza/human_animal_interface/Influenza_Summary_IRA_HA_interface_09_04_2019.pdf?ua=1
- Zhou L, Chen E, Bao C, Xiang N, Wu J, Wu S, et al. Clusters of human infection and human-to-human transmission of avian influenza A(H7N9) virus, 2013–2017. *Emerg Infect Dis*. 2018;24:397–400. <https://doi.org/10.3201/eid2402.171565>
- Cowling BJ, Jin L, Lau EH, Liao Q, Wu P, Jiang H, et al. Comparative epidemiology of human infections with avian influenza A H7N9 and H5N1 viruses in China: a population-based study of laboratory-confirmed cases. *Lancet*. 2013;382:129–37. [https://doi.org/10.1016/S0140-6736\(13\)61171-X](https://doi.org/10.1016/S0140-6736(13)61171-X)
- Virlogeux V, Li M, Tsang TK, Feng L, Fang VJ, Jiang H, et al. Estimating the distribution of the incubation periods of human avian influenza A(H7N9) virus infections. *Am J Epidemiol*. 2015;182:723–9. <https://doi.org/10.1093/aje/kwv115>
- Virlogeux V, Yang J, Fang VJ, Feng L, Tsang TK, Jiang H, et al. Association between the severity of influenza A(H7N9) virus infections and length of the incubation period. *PLoS One*. 2016;11:e0148506. <https://doi.org/10.1371/journal.pone.0148506>
- Huai Y, Xiang N, Zhou L, Feng L, Peng Z, Chapman RS, et al. Incubation period for human cases of avian influenza A (H5N1) infection, China. *Emerg Infect Dis*. 2008;14:1819–21. <http://dx.doi.org/10.3201/eid1411.080509>
- Lessler J, Reich NG, Brookmeyer R, Perl TM, Nelson KE, Cummings DA. Incubation periods of acute respiratory viral infections: a systematic review. *Lancet Infect Dis*. 2009;9:291–300. [https://doi.org/10.1016/S1473-3099\(09\)70069-6](https://doi.org/10.1016/S1473-3099(09)70069-6)

Address for correspondence: Qun Li, Chinese Center for Disease Control and Prevention, Public Health Emergency Center, No. 155 Changbai Rd, Changping District, Beijing, 102206, China; email: liqun@chinacdc.cn

Pulmonary Infection Associated with *Mycobacterium canariasense* in Suspected Tuberculosis Patient, Iran

Fatemeh Sakhaee, Farzam Vaziri, Golnaz Bahramali, Kambiz Taremiyan, Seyed Davar Siadat, Abolfazl Fateh

Author affiliations: Pasteur Institute of Iran, Tehran, Iran (F. Sakhaee, F. Vaziri, G. Bahramali, S.D. Siadat, A. Fateh); Mohammad Medical Imaging Center, Varamin, Iran (K. Taremiyan)

DOI: <https://doi.org/10.3201/eid2510.190156>

Mycobacterium canariasense had only been isolated in humans from blood and contaminated catheters. We report a case of pulmonary disease associated with *M. canariasense* infection that was identified by multilocus sequence analysis; the illness was initially ascribed to *M. tuberculosis*. *M. canariasense* should be considered a cause of respiratory infection.

Mycobacterium tuberculosis is a widely known cause of pulmonary disease, specifically tuberculosis (TB). However, its symptoms may be similar to those of pulmonary infections caused by other pathogens. We document a case in which disease initially ascribed to *M. tuberculosis* was ruled out through testing and a different mycobacterium, *M. canariasense*, was identified as the likely cause.

The patient was a 67-year-old woman with pulmonary infection living in a village in Afghanistan who traveled to Iran for treatment. Her signs and symptoms included fever, cough, sputum, weight loss, chest pain, and night sweats; the fever and cough had persisted for 6 months. Forty-six years earlier, at 21 years of age, she had experienced a pulmonary TB episode, which was treated with anti-TB drugs. She had no history of smoking or taking immunosuppressive drugs. No other pulmonary diseases were reported.

Results of clinical parameters were normal, apart from an elevated C-reactive protein (CRP) rate (72.4 mg/L) and erythrocyte sedimentation (ESR) rate (85 mm/h). The induration from a tuberculin skin test was 21 mm. A computed tomography scan indicated calcified mediastinal lymph nodes, nodular opacities, and fibrotic changes in the left lower lobe (Appendix Figure, <https://wwwnc.cdc.gov/EID/article/25/10/19-0156-App1.pdf>). The physician assumed a TB reactivation, and chemotherapy was initiated with isoniazid, rifampin, ethambutol, and pyrazinamide. However, the pulmonary symptoms did not disappear after 4 months.

Five sputum samples from the patient were sent to the Pasteur Institute of Iran (Tehran, Iran) in August 2017 for *M. tuberculosis* testing. Results of smear tests indicated partially acid-fast bacilli, whereas all of the samples showed negative results when evaluated by insertion sequence 6110 PCR assay for *M. tuberculosis*. A culture of sputum samples on Lowenstein-Jensen medium after 3 days showed rapidly growing mycobacteria with smooth, small, shiny, and nonpigmented colonies, which turned pale yellow and shinier after 4 days. Phenotypic tests of the isolate were positive on MacConkey agar without crystal violet, urease, Tween 80 hydrolysis, heat-resistant catalase, and arylsulfatase tests. On the other hand, nitrate reductase, growth in 5% NaCl, tellurite, and niacin accumulation tests were negative.

Multilocus sequence analysis was performed for partial *hsp65* and *rpoB* genes and full *16S rRNA* gene, as described in the literature (1–3), and results indicated 100% homology to *M. canariasense* (Figure). This organism was described by Jiménez et al. in a suspected nosocomial outbreak infecting 17 patients during January 2000–September 2002 at a tertiary care hospital in the Canary Islands in Spain (4,5). The phenotypic and genotypic characteristics of the isolate agreed with those for *M. canariasense*, on the basis of guidelines of the American Thoracic Society and the Infectious Disease Society of America (6).

The results of susceptibility testing, performed according to Clinical and Laboratory Standards Institute guidelines (7), indicated that the *M. canariasense* isolate was highly resistant to isoniazid, rifampin, ethambutol, and streptomycin; extremely susceptible to amikacin, levofloxacin, clarithromycin, ceftiofloxacin, ciprofloxacin, imipenem, doxycycline, minocycline, and trimethoprim/sulfamethoxazole; and intermediately susceptible to vancomycin. On the basis of these results, the patient was treated with levofloxacin and amikacin for 17 days. After treatment, sputum samples were collected from the patient over 5 days. The results of smear and culture tests were negative for partially acid-fast bacilli, and the results of a computed tomography scan and CRP and ESR measurements were normal.

Previously, *M. canariasense* had only been detected in the blood of patients and in contaminated catheters (8,9); no study had reported pulmonary infections associated with this isolate. Our results reveal that clinical and radiographic findings of *M. canariasense* pulmonary infection are similar in appearance to those of TB and other nontuberculous mycobacteria infections. However, these findings and improved radiological findings and ESR and CRP levels due to chemotherapy, indicating that *M. canariasense* had been eliminated, strongly suggest that the bacterium could have been the cause of pulmonary disease in this patient.

Although no specific treatment has been recommended for *M. canariasense* infection, combination therapy with

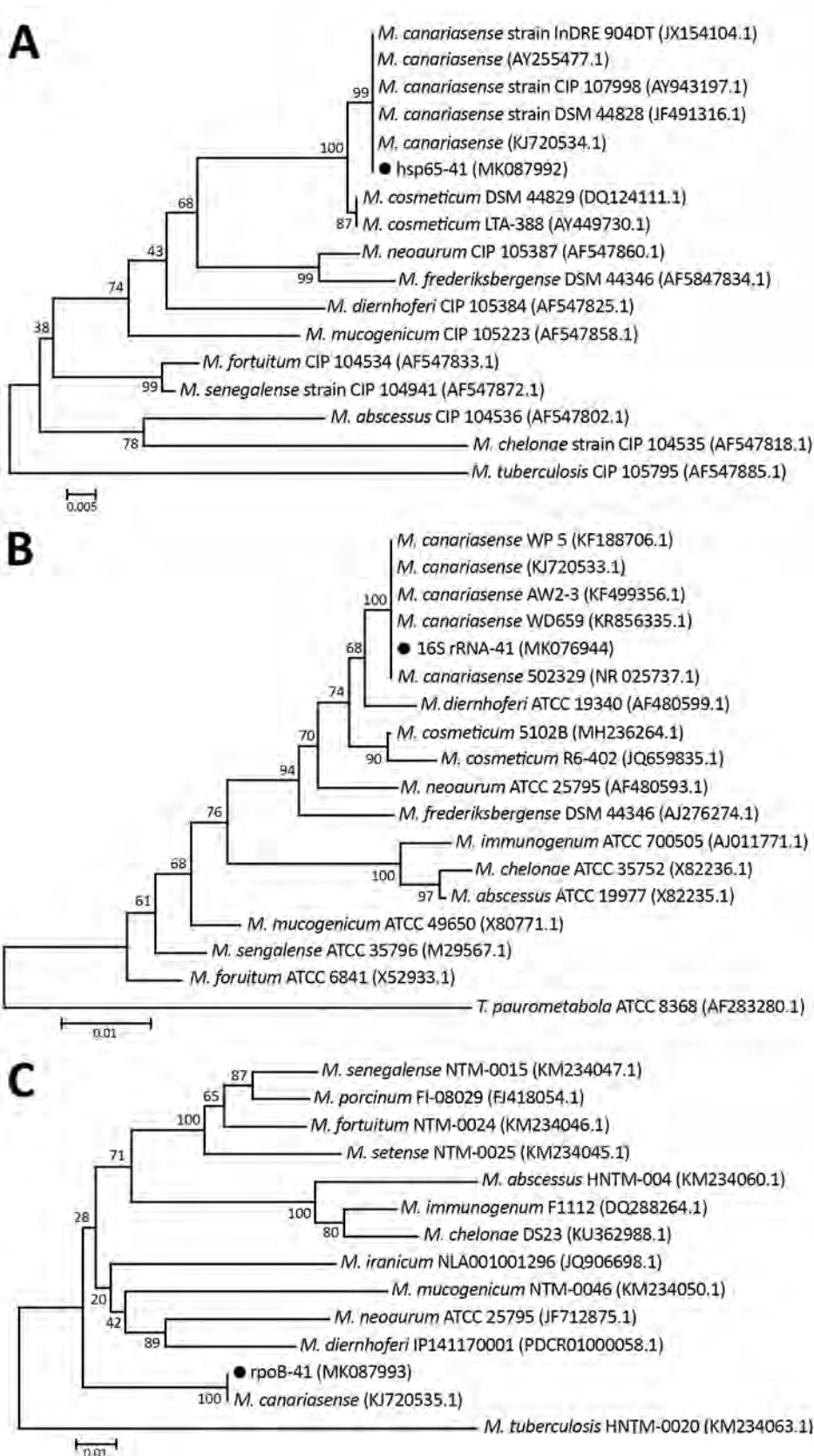


Figure. Neighbor-joining tree of the *hsp65* (A), 16S *rRNA* (B), and *rpoB* (C) genes of an isolate from a patient infected with *Mycobacterium canariasisense*, Tehran, Iran (black dots), and other rapidly growing mycobacteria. Outgroup for *hsp65/rpoB* genes was *Mycobacterium tuberculosis* and for the 16S *rRNA* gene was *Tsukamurella paurometabola*. Bootstrap values are represented on branch nodes. GenBank accession numbers are given in parentheses for reference sequences. The nucleotide sequences identified in this study were submitted to GenBank under the following accession numbers: *hsp65*, MK087992; *rpoB*, MK087993; and 16S *rRNA*, MK076944. Scale bars indicate nucleotide substitutions per site.

levofloxacin and amikacin produced a successful outcome in this case; no recurrent pulmonary disease was reported in the patient. However, treatment with other drugs to which *M. canariensis* is susceptible might also succeed. In a 2006 report, Campos-Herrero et al. noted the favorable outcomes produced by fluoroquinolones and amikacin (8). However, the optimal antimycobacterial regimen for *M. canariensis* infection needs to be clearly established in more cases.

Acknowledgments

We thank all the personnel of the Department of Mycobacteriology and Pulmonary Research, Pasteur Institute of Iran, for their assistance in this project. Funding: This study was funded by a grant from the Pasteur Institute of Iran (no. 866).

About the Author

Miss Sakhaee is an expert clinical microbiologist at the Pasteur Institute of Iran. Her primary research interests focus on epidemiologic and clinical aspects of mycobacterial infections.

References

1. Telenti A, Marchesi F, Balz M, Bally F, Böttger EC, Bodmer T. Rapid identification of mycobacteria to the species level by polymerase chain reaction and restriction enzyme analysis. *J Clin Microbiol.* 1993;31:175–8.
2. Turenne CY, Tschetter L, Wolfe J, Kabani A. Necessity of quality-controlled 16S rRNA gene sequence databases: identifying nontuberculous *Mycobacterium* species. *J Clin Microbiol.* 2001;39:3637–48. <https://doi.org/10.1128/JCM.39.10.3638-3648.2001>
3. Adékambi T, Colson P, Drancourt M. rpoB-based identification of nonpigmented and late-pigmenting rapidly growing mycobacteria. *J Clin Microbiol.* 2003;41:5699–708. <https://doi.org/10.1128/JCM.41.12.5699-5708.2003>
4. Jiménez MS, Campos-Herrero MI, García D, Luquin M, Herrera L, García MJ. *Mycobacterium canariensis* sp. nov. *Int J Syst Evol Microbiol.* 2004;54:1729–34. <https://doi.org/10.1099/ijs.0.02999-0>
5. Tortoli E. The new mycobacteria: an update. *FEMS Immunol Med Microbiol.* 2006;48:159–78. <https://doi.org/10.1111/j.1574-695X.2006.00123.x>
6. Griffith DE, Aksamit T, Brown-Elliott BA, Catanzaro A, Daley C, Gordin F, et al.; ATS Mycobacterial Diseases Subcommittee; American Thoracic Society; Infectious Disease Society of America. An official ATS/IDSA statement: diagnosis, treatment, and prevention of nontuberculous mycobacterial diseases. *Am J Respir Crit Care Med.* 2007;175:367–416. <https://doi.org/10.1164/rccm.200604-571ST>
7. Clinical and Laboratory Standards Institute. Susceptibility testing of mycobacteria, nocardiae, and other aerobic actinomycetes—second edition: approved standard (M24-A2). Wayne (PA): The Institute; 2011.
8. Campos-Herrero MI, García D, Figuerola A, Suárez P, Campo C, García MJ. Bacteremia caused by the novel species *Mycobacterium canariensis*. *Eur J Clin Microbiol Infect Dis.* 2006;25:58–60. <https://doi.org/10.1007/s10096-005-0079-6>
9. Paniz-Mondolfi A, Ladutko L, Brown-Elliott BA, Vasireddy R, Vasireddy S, Wallace RJ, Jr, et al. First report of *Mycobacterium canariensis* catheter-related bacteremia in the Americas. *J Clin Microbiol.* 2014;52:2265–9. <https://doi.org/10.1128/JCM.03103-13>

Address for correspondence: Abolfazl Fateh, Pasteur Institute of Iran, Department of Mycobacteriology and Pulmonary Research, No. 69, 12th Farwardin Ave, Tehran, Iran; email: afateh2@gmail.com

Mycobacterium conceptionense Pneumonitis in Patient with HIV/AIDS¹

Sarah M. Michienzi, Rodrigo M. Burgos, Richard M. Novak

Author affiliations: University of Illinois at Chicago College of Pharmacy, Chicago, Illinois, USA (S.M. Michienzi, R.M. Burgos); University of Illinois at Chicago College of Medicine, Chicago (R.M. Novak)

DOI: <https://doi.org/10.3201/eid2510.190444>

Approximately 21 human cases of infection with *Mycobacterium conceptionense* have been reported. However, most cases were outside the United States, and optimal treatment remains uncertain. We report a case of *M. conceptionense* pneumonitis in a patient with HIV/AIDS in the United States. The patient was cured with azithromycin and doxycycline.

Mycobacterium conceptionense is a nonpigmented, rapidly growing, nontuberculous mycobacterium, first isolated in France in 2006 (1). Approximately 21 cases of human infection have been reported (1–10). However, excluding the case we report here, only 2 cases have been reported in the United States (2). Optimal treatment for *M. conceptionense* infection remains uncertain. We report the clinical course and management of *M. conceptionense* pneumonitis in a patient with HIV/AIDS in the United States.

A 47-year-old black cisgender man sought care at an emergency department during 2015 for cough, shortness of

¹Results from this study were presented at the American College of Clinical Pharmacy 2018 Global Conference, October 20–23, 2018, Seattle, Washington, USA.

breath, and diarrhea. He denied travel outside of the United States. The patient had HIV/AIDS, which was diagnosed during the 1980s but was untreated until this admission. He also had chronic hepatitis C, which was diagnosed during this admission. He was positive for HLA-B*5701, indicating hypersensitivity to the antiretroviral drug abacavir, but had no other known allergies to medications.

At admission, the patient was febrile (temperature 38.9°C) and had tachycardia (heart rate 112 beats/min) with low oxygen saturation (92% on room air), bibasilar rales, and poor inspiratory effort. Baseline laboratory test values were compiled (Table). A baseline chest radiograph showed increased interstitial marking and bibasilar patchy opacities. A baseline chest computed tomography scan showed bilateral interstitial and ground-glass opacities and a 6-mm nodule in the right middle lobe.

The patient was given empiric antimicrobial drugs (azithromycin 250 mg/d and ceftriaxone 1 g/d, both intravenously [IV]) for presumptive community-acquired pneumonia and trimethoprim/sulfamethoxazole (TMP/SMX; 800/160 mg every 6 h IV) for presumptive *Pneumocystis jirovecii* pneumonia (PJP). On day 4, ceftriaxone and azithromycin were discontinued. Induced sputum culture obtained on day 2 showed acid-fast bacilli (AFB) on day 8.

Infection with *M. tuberculosis* was not suspected because of the patient's clinical manifestations and fast growth of the organism. The symptoms improved after admission. On day 11, he was discharged from the hospital and received oral TMP/SMX equivalent to that for intravenous dosing for PJP treatment. In addition, he erroneously received oral azithromycin (1,250 mg/wk) for *M. avium* complex prophylaxis.

On day 22, the patient returned to the ambulatory care clinic at the same institution. At this time, additional induced sputum cultures from days 3 and 4 were positive for AFB. His TMP/SMX treatment course was completed and decreased to 800/160 mg/day orally for secondary PJP prophylaxis. Azithromycin was corrected to treatment doses and increased to 250 mg/d orally. Baseline HIV genotyping showed wild-type virus, and antiretroviral therapy (ART) was initiated with elvitegravir/cobicistat/emtricitabine/tenofovir alafenamide (E/c/F/TAF) in a fixed-dose combination.

At day 43, the pneumonitis had clinically resolved, and repeat computed tomography and AFB culture showed negative results. A diagnosis of infection with *M. conceptionense* was confirmed from 3 induced sputum cultures obtained during days 2–4. Growth of *M. conceptionense* was identified by *rpoB* gene sequencing. Testing was performed at National Jewish Mycobacteriology Reference Laboratory (Denver, CO, USA). Drug susceptibility testing was not performed. An environmental source of the infection was not sought. Doxycycline (100 mg 2×/day orally)

Table. Pertinent baseline laboratory test results for a 47-year-old man with *Mycobacterium conceptionense* pneumonitis and HIV/AIDS, United States*

Laboratory test	Value or result
Serum creatinine	0.89 mg/dL
Aspartate aminotransferase	25 U/L
Alanine aminotransferase	23 U/L
HIV RNA	25,611 copies/mL
CD4 cells	19 cells/μL (5%)
Hepatitis C virus antibody	Positive
Leukocytes	$2.3 \times 10^3/\mu$L
Neutrophils	$1.9 \times 10^3/\mu$ L
Lymphocytes	$0.2 \times 10^3/\mu$L
Lactate dehydrogenase	546 U/L
<i>Histoplasma</i> antigen	Negative
Rapid plasma reagin	1:0
<i>Clostridioides difficile</i>	Negative
Stool culture	Negative

*Abnormal values are indicated in bold.

was given in addition to azithromycin because of lack of susceptibility information and previous case reports using dual therapy, although there is no clear guidance for management. ART with E/c/F/TAF was continued.

The patient is still profoundly immunosuppressed (CD4 cell count 60 cells/ μ L [6%]) because of nonadherence to ART. Darunavir (800 mg/day orally) was added to E/c/F/TAF because of development of resistance to ART, most notably the M184V pathway. We plan to continue oral azithromycin and doxycycline at current doses until immune reconstitution is achieved.

Cases of infection with *M. conceptionense* have been reported in immunocompetent and immunocompromised patients and in traumatic (e.g., after surgery or injury) and nontraumatic situations (1–10). The lungs are the most common site for *M. conceptionense* infection, comprising 7 of the ≈ 21 cases reported (1–4). Our patient was immunocompromised because of infection with HIV. Pathogen entry occurred by inhalation in a nontraumatic fashion and led to pneumonitis.

Outside the United States, *M. conceptionense* infection has been reported in France, Iran, Taiwan, South Korea, China, and Japan (1,3–10). The only 2 previously reported case-patients with *M. conceptionense* infection in the United States were also in Chicago but were epidemiologically unrelated to the patient we describe (2).

Similar to other reported case-patients, this patient was given broad-spectrum antimicrobial drugs, which were tailored once diagnosis of nontuberculous mycobacterium was confirmed. In vitro drug susceptibility data from rapidly growing mycobacteria indicate that *M. conceptionense* is susceptible to clarithromycin, doxycycline, and fluoroquinolones but resistant to sulfamethoxazole (3). In addition, macrolides, fluoroquinolones, or doxycycline have been used for treatment of *M. conceptionense* infections in case reports. (1–10) These cases have assisted our choice of treatment for this case. In summary, our case report shows

clinical and microbiological cure of *M. conceptionense* pneumonitis by using azithromycin and doxycycline in a patient with HIV/AIDS in the United States.

About the Author

Dr. Michienzi is a clinical assistant professor and pharmacist at the University of Illinois at Chicago College of Pharmacy, Chicago, IL. Her research interests are HIV–hepatitis C virus co-infection, HIV in incarcerated and underserved populations, and pharmacist roles in care.

References

- Adékambi T, Stein A, Carvajal J, Raoult D, Drancourt M. Description of *Mycobacterium conceptionense* sp. nov., a *Mycobacterium fortuitum* group organism isolated from a posttraumatic osteitis inflammation. *J Clin Microbiol*. 2006; 44:1268–73. <https://doi.org/10.1128/JCM.44.4.1268-1273.2006>
- Oda G, Winters M, Pacheco SM, Sikka M, Bleasdale S, Dunn B, et al. Identical strain of *Mycobacterium conceptionense* isolated from patients at 2 veterans affairs medical centers within the same metropolitan area over a 4-year period. Abstract no. 648. In: Abstracts of ID Week 2017, San Diego, October 4–8, 2017. Arlington (VA): Infectious Diseases Society of America; 2017.
- Kim SY, Kim MS, Chang HE, Yim JJ, Lee JH, Song SH, et al. Pulmonary infection caused by *Mycobacterium conceptionense*. *Emerg Infect Dis*. 2012;18:174–6. <https://doi.org/10.3201/eid1801.110251>
- Shojaei H, Hashemi A, Heidarieh P, Ataei B, Naser AD. Pulmonary and extrapulmonary infection caused by *Mycobacterium conceptionense*: the first report from Iran. *JRSM Short Rep*. 2011;2:31. <https://doi.org/10.1258/shorts.2010.010103>
- Liao CH, Lai CC, Huang YT, Chou CH, Hsu HL, Hsueh PR. Subcutaneous abscess caused by *Mycobacterium conceptionense* in an immunocompetent patient. *J Infect*. 2009;58:308–9. <https://doi.org/10.1016/j.jinf.2009.02.012>
- Lee KH, Heo ST, Choi SW, Park DH, Kim YR, Yoo SJ. Three cases of postoperative septic arthritis caused by *Mycobacterium conceptionense* in the shoulder joints of immunocompetent patients. *J Clin Microbiol*. 2014;52:1013–5. <https://doi.org/10.1128/JCM.02652-13>
- Yang HJ, Yim HW, Lee MY, Ko KS, Yoon HJ. *Mycobacterium conceptionense* infection complicating face rejuvenation with fat grafting. *J Med Microbiol*. 2011;60:371–4. <https://doi.org/10.1099/jmm.0.024554-0>
- Zhang X, Liu W, Liu W, Jiang H, Zong W, Zhang G, et al. Cutaneous infections caused by rapidly growing mycobacteria: case reports and review of clinical and laboratory aspects. *Acta Derm Venereol*. 2015;95:985–9. <https://doi.org/10.2340/00015555-2105>
- Yaita K, Matsunaga M, Tashiro N, Sakai Y, Masunaga K, Miyoshi H, et al. *Mycobacterium conceptionense* bloodstream infection in a patient with advanced gastric carcinoma. *Jpn J Infect Dis*. 2017;70:92–5. <https://doi.org/10.7883/yoken.JJID.2015.626>
- Thibeaut S, Levy PY, Pelletier ML, Drancourt M. *Mycobacterium conceptionense* infection after breast implant surgery, France. *Emerg Infect Dis*. 2010;16:1180–1. <https://doi.org/10.3201/eid1607.090771>

Address for correspondence: Sarah M. Michienzi, University of Illinois at Chicago, College of Pharmacy, Pharmacy Practice (MC 886), 833 S Wood St, Ste 164, Chicago, IL 60612, USA; email: msarah@uic.edu

Emergence of Influenza A(H7N4) Virus, Cambodia

Dhanasekaran Vijaykrishna, Yi-Mo Deng, Miguel L. Grau, Matthew Kay, Annika Suttie, Paul F. Horwood, Wantanee Kalpravidh, Filip Claes, Kristina Osbjør, Phillipe Dussart, Ian G. Barr, Erik A. Karlsson

Author affiliations: Peter Doherty Institute for Infection and Immunity, Melbourne, Victoria, Australia (D. Vijaykrishna, Y.-M. Deng, M. Kay, I.G. Barr); Monash University, Melbourne (D. Vijaykrishna, M.L. Grau); Institut Pasteur du Cambodge, Phnom Penh, Cambodia (A. Suttie, P.F. Horwood, P. Dussart, E.A. Karlsson); James Cook University, Townsville, Queensland, Australia (P.F. Horwood); Food and Agriculture Organization of the United Nations, Bangkok, Thailand (W. Kalpravidh, F. Claes); Food and Agriculture Organization of the United Nations, Phnom Penh, Cambodia (K. Osbjør)

DOI: <https://doi.org/10.3201/eid2510.190506>

Active surveillance in high-risk sites in Cambodia has identified multiple low-pathogenicity influenza A(H7) viruses, mainly in ducks. None fall within the A/Anhui/1/2013(H7N9) lineage; however, some A(H7) viruses from 2018 show temporal and phylogenetic similarity to the H7N4 virus that caused a nonfatal infection in Jiangsu Province, China, in December 2017.

Avian influenza virus (AIV) subtype A(H7) is of concern because it has been a leading cause of zoonotic infections over the past 2 decades (1). The A/Anhui/1/2013-lineage A(H7N9) viruses, a leading cause of zoonotic infections in Asia since 2013, have not been detected in the Greater Mekong Subregion, but independent H7 lineages, including H7N3, H7N7, and H7Nx, have been detected occasionally in Cambodia since 2009 (2–4). H7N3 virus was detected from a duck mortality event in Kampong Thom during January 2017 (2), and H7N7 virus was detected in a live-bird market (LBM) in Takeo in September 2017 (4). Furthermore, highly pathogenic avian influenza (HPAI) A(H5N1) and low-pathogenicity avian influenza (LPAI) A(H9N2) are endemic in Cambodia (5); 59 poultry outbreaks of AIV and 56 human HPAI A(H5N1) cases have occurred since 2006. Although the exact ecologic links are unknown, serologic studies suggest that AIVs of multiple subtypes are frequently introduced into poultry in Cambodia, possibly through cross-border trade or through wild birds (2,6,7).

In December 2017, a 68-year-old woman in Jiangsu, China, who had underlying medical conditions was infected by an LPAI influenza A(H7N4) virus, which led to severe pneumonia and intensive care unit admission, but

she recovered and left the hospital after 21 days (8,9). Genetically similar H7N4 viruses were subsequently detected in contact chickens (9,10) and aquatic poultry in Jiangsu (GISAID, <https://www.gisaid.org>), substantiating that the infection was zoonotic and raising concerns of endemicity of H7N4 in the region. Because of the antigenic differences between the A/Jiangsu/1/2018-like A(H7N4) virus and other H7 lineages (10), including A/Anhui/1/2013(H7N9) lineage, this newly detected H7N4 virus has been proposed as a vaccine candidate for pandemic preparedness (10).

Beginning in February 2018, 2 months after the H7N4 case in China, this virus was detected in ducks in Cambodia; the frequency of detection increased in March and April (4). Therefore, because of the novelty of the strain and the association with human infection, we sought to understand the genomic diversity of H7 viruses in Cambodia.

We characterized the whole genomes (for sequencing methods, see Appendix, <http://wwwnc.cdc.gov/EID/article/25/10/19-0506-App1.pdf>) of 16 viruses collected during

2015–2018 subtyped by reverse transcription PCR (RT-PCR) as having an H7 hemagglutinin (HA) gene or an N4 neuraminidase (NA) gene; we also included viruses for which the HA or NA could not be typed but that were epidemiologically associated with A(H7) viruses (Appendix Table). We obtained samples from poultry swabs collected across multiple LBMs, slaughterhouses, and poultry collection centers in Cambodia; most H7 viruses originated from domestic ducks (4).

All AIV samples collected during February–April 2018 in Cambodia ($n = 9$) (Appendix Table 1, Figure 1) contained ≥ 1 segment with high similarity and common evolutionary origins to the Jiangsu H7N4 samples, whereas AIV collected before this period formed other independent lineages derived from wild birds. Seven H7-HA from viruses collected in 2018 in Cambodia (4 H7N4, 1 H7N5, 1 H7Nx, and 1 H7 with mixed N4 and N7 segments) were most closely related to the HA and NA genes of Jiangsu H7N4 isolates; all 6 N4 NA were most closely related to the NA genes of Jiangsu H7N4 isolates (Figure). We also

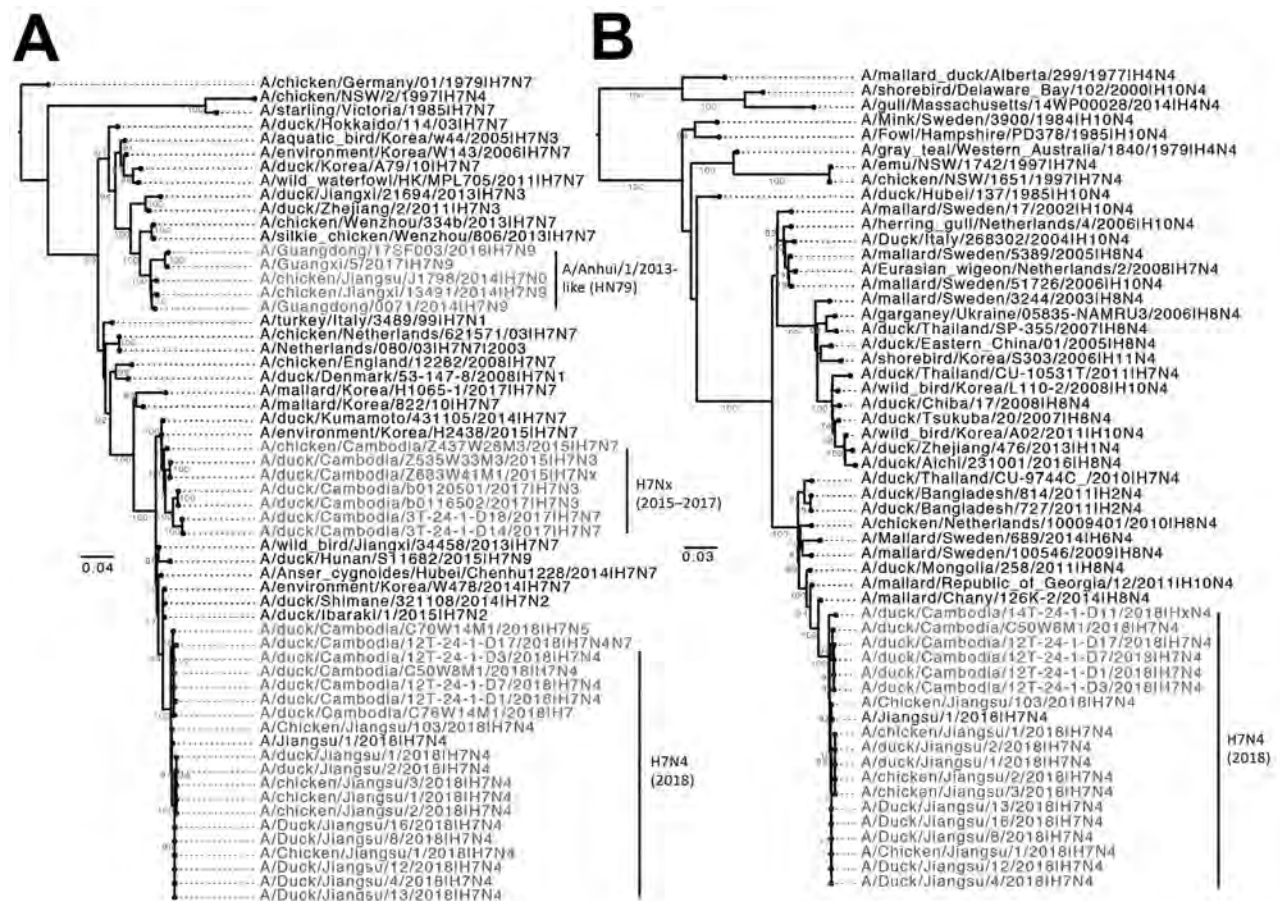


Figure. Maximum-likelihood phylogeny of the evolutionary origins of influenza A(H7N4) virus in Cambodia and comparison with reference isolates. H7 hemagglutinin (A) and N4 neuraminidase (B) genes were inferred using a general time-reversible nucleotide substitution model with a gamma distribution of among-site rate variation in RAXML version 8 (<https://cme.h-its.org/exelixis/web/software/raxml/>) and visualized using Figtree version 1.4 (<http://tree.bio.ed.ac.uk/software/figtree/>). Branch support values were generated using 1,000 bootstrap replicates. Scale bars represent nucleotide substitutions per site. A color version of this figure is available online (<https://wwwnc.cdc.gov/EID/article/25/10/19-0506-F1.htm>).

observed close relationships between the Jiangsu and Cambodia isolates in the internal segments polymerase basic protein 2 (PB2), polymerase acidic protein (PA), and nucleoprotein (NP); most viruses carried a common PA gene (Appendix Figure 1). However, none of the H7N4 viruses from Cambodia shared all segments with Jiangsu isolates, indicating continual reassortment with AIV co-circulating in the region.

Phylogenetic analysis showed that the Cambodia–Jiangsu H7-HA genes emerged during late 2017 (mean time to most recent common ancestor November 2017; 95% CI August 2016–July 2017) and were derived from H7N7 and H7N2 viruses previously detected in aquatic birds in east Asia (Appendix Figure 2). In contrast, the N4-NA exhibited a greater diversity in Cambodia (mean time to most recent common ancestor January 2016; 95% CI January 2015–November 2016) and were derived from H10N4 and H8N4 viruses previously detected in Georgia, Russia, and Mongolia.

Our results show that H7N4 is a newly developing virus lineage that originated from divergent avian lineages within the Eurasian AIV gene pool. The dispersed genetic origins from locations in Europe and central Asia and the similarity of the Cambodia and Jiangsu H7N4 samples indicates that the H7N4 virus was generated in aquatic birds, likely just before their first detection. Detection of H7N4 in LBMs in Cambodia in such a short span of time at such a large spatial distance highlights the risk and potential for rapid spread of AIV lineages throughout the region. The ability to infect a human subject, the continual reassortment and antigenic evolution of this lineage, and the endemicity of numerous LPAI and HPAI viruses may further increase the risk for zoonotic infections and warrants vigilant, active surveillance in wild birds and poultry in the region.

Acknowledgments

The investigators thank everyone on the Influenza Team in the Virology Unit at Institut Pasteur du Cambodge (IPC) who contributed to this study, including Viseth Srey Horm, Songha Tok, Phalla Y, Ponnarath Keo, Sereyath Sun, Sonita Kol, Chiva Sum, Sarath Sin, Kim Lay Chea, and Sokhoun Yann. In addition, we thank Veasna Duong. We also thank all of the support teams at IPC, including the drivers and facilities personnel who make these studies possible, as well as all the local teams, epidemiologists, veterinary officers, and other staff from the National Health and Production Research Institute. We also thank everyone from the regional and country Food and Agriculture Organization of the United Nations (FAO) offices, especially Makara Hak and Aurelie Brioudes.

Work at Institut Pasteur in Cambodia was supported by the Office of the Assistant Secretary for Preparedness and Response,

US Department of Health and Human Services (grant no. IDSEP 140020-01-00; <http://www.asideproject.org>), and by the FAO, with funding from the United States Agency for International Development (USAID) under the Emerging Pandemics Threats 2 (EPT-2) project. The Melbourne WHO Collaborating Centre for Reference and Research on Influenza is supported by the Australian Government Department of Health. D.V. and M.L.G. are supported by contract no. HHSN27220140006C from the National Institute of Allergy and Infectious Diseases, National Institutes of Health, US Department of Health and Human Services.

About the Author

Dr. Vijaykrishna is an evolutionary biologist based at the Biomedicine Discovery Institute in Melbourne, working closely with staff and students at IPC and World Health Organization Collaborating Centre, Melbourne. His primary research interests are in using disease surveillance and comparative genomics to track and solve problems in clinical and veterinary virology.

References

1. Abdelwhab EM, Veits J, Mettenleiter TC. Prevalence and control of H7 avian influenza viruses in birds and humans. *Epidemiol Infect.* 2014;142:896–920. <https://doi.org/10.1017/S0950268813003324>
2. Suttie A, Yann S, Y P, Tum S, Deng YM, Hul V, et al. Detection of low pathogenicity influenza A(H7N3) virus during duck mortality event, Cambodia, 2017. *Emerg Infect Dis.* 2018;24:1103–7. <https://doi.org/10.3201/eid2406.172099>
3. World Health Organization. Cumulative number of confirmed human cases for avian influenza A(H5N1) reported to WHO, 2003–2018. 2018 [cited 2018 Dec 13]. https://www.who.int/influenza/human_animal_interface/H5N1_cumulative_table_archives
4. Karlsson EA, Horm SV, Tok S, Tum S, Kalpravidh W, Claes F, et al. Avian influenza virus detection, temporality and co-infection in poultry in Cambodian border provinces, 2017–2018. *Emerg Microbes Infect.* 2019;8:637–9. <https://doi.org/10.1080/22221751.2019.1604085>
5. Suttie A, Karlsson EA, Deng YM, Horm SV, Yann S, Tok S, et al. Influenza A(H5N1) viruses with A(H9N2) single gene (matrix or PB1) reassortment isolated from Cambodian live bird markets. *Virology.* 2018;523:22–6. <https://doi.org/10.1016/j.virol.2018.07.028>
6. Horm SV, Tarantola A, Rith S, Ly S, Gambaretti J, Duong V, et al. Intense circulation of A/H5N1 and other avian influenza viruses in Cambodian live-bird markets with serological evidence of sub-clinical human infections. *Emerg Microbes Infect.* 2016;5:e70. <https://doi.org/10.1038/emi.2016.69>
7. Van Kerkhove MD, Vong S, Guitian J, Holl D, Mangtani P, San S, et al. Poultry movement networks in Cambodia: implications for surveillance and control of highly pathogenic avian influenza (HPAI/H5N1). *Vaccine.* 2009;27:6345–52. <https://doi.org/10.1016/j.vaccine.2009.05.004>
8. Gao P, Du H, Fan L, Chen L, Liao M, Xu C, et al. Human infection with an avian-origin influenza A (H7N4) virus in Jiangsu: a potential threat to China. *J Infect.* 2018;77:249–57. <https://doi.org/10.1016/j.jinf.2018.07.005>

9. Tong XC, Weng SS, Xue F, Wu X, Xu TM, Zhang WH. First human infection by a novel avian influenza A(H7N4) virus. *J Infect*. 2018;77:249–57. <https://doi.org/10.1016/j.jinf.2018.06.002>
10. World Health Organization. Human infection with avian influenza A(H7N4) virus—China. *Disease Outbreak News (DON)* 2018 [cited 2018 Dec 17]. <https://www.who.int/csr/don/22-february-2018-ah7n4-china>

Address for Correspondence: Erik A. Karlsson, Institut Pasteur du Cambodge Virology Unit, 5 Monivong Blvd, PO Box 983, Phnom Penh, Cambodia; email: ekarlsson@pasteur-kh.org

***Mycobacterium marseillense* Infection in Human Skin, China, 2018**

Bibo Xie,¹ Yanqing Chen,¹ Jian Wang, Wei Gao, Haiqing Jiang, Jiya Sun, Xindong Jin, Xudong Sang, Xiaobing Yu, Hongsheng Wang

Author affiliations: Institute of Dermatology, Chinese Academy of Medical Sciences and Peking Union Medical College, Nanjing, China (B. Xie, Y. Chen, W. Gao, H. Jiang, H. Wang); Zhejiang Institute of Dermatology, Deqing, China (B. Xie, J. Wang, X. Jin, X. Sang, X. Yu); Jiangsu Key Laboratory of Molecular Biology for Skin Diseases and STIs, Nanjing (Y. Chen, W. Gao, H. Jiang, H. Wang); Suzhou Institute of Systems Medicine, Chinese Academy of Medical Sciences, Suzhou, China (J. Sun); Centre for Global Health, Nanjing Medical University, Nanjing (H. Wang)

DOI: <https://doi.org/10.3201/eid2510.190695>

We describe a case of facial skin infection and sinusitis caused by *Mycobacterium marseillense* in an immunocompetent woman in China in 2018. The infection was cleared with clarithromycin, moxifloxacin, and amikacin. Antimicrobial drug treatments could not be predicted by genetic analyses; further genetic characterization would be required to do so.

Mycobacterium marseillense is a member of the *M. avium* complex (1) that has caused infections with lymphatic or pulmonary involvement sporadically in humans (2–4). We report *M. marseillense* infection involving facial skin in an immunocompetent woman in eastern China.

¹These authors contributed equally to this article.

In April 2018, a 59-year-old woman was referred to our institute (Institute of Dermatology, Chinese Academy of Medical Sciences and Peking Union Medical College, Nanjing, China) for a 4-year history of an erythematous plaque with ulceration located on the right cheek. The primary lesion was a small erythematous patch that gradually developed into an asymptomatic ulcerative plaque (i.e., the plaque had no heat, swelling, pain, or pruritus). She also reported occasional bloody, purulent nasal discharge over the course of 2 years. Two years before visiting our hospital, cutaneous tuberculosis was suspected, so she received treatment for tuberculosis (rifampin, isoniazid, ethambutol, pyrazinamide) for 10 months. No obvious improvement was observed with this treatment. Her medical history was otherwise unremarkable.

On physical examination, an infiltrated erythematous plaque with yellow scales and crusts on the right cheek was visible (Figure, panel A). Routine laboratory tests showed no remarkable findings. The results of autoantibody and HIV tests were negative, and immune subset cell counts were unremarkable. Histologic examination showed infiltration of a large number of lymphocytes, plasma cells, and neutrophils and some tissue cells in the dermis (Appendix Figure 1, <https://wwwnc.cdc.gov/EID/article/25/10/19-0695-Appl.pdf>). Computed tomography scan of the paranasal sinuses showed bilateral maxillary, right ethmoid, and frontal sinusitis (Figure, panel C). Culture and PCR for mycobacteria in nasal discharge yielded negative findings.

After 3 weeks of skin tissue culture at 32°C in Löwenstein–Jensen medium, we observed smooth, yolk-yellow bacterial colonies (Appendix Figure 2). Ziehl–Neelsen staining confirmed the cultured organism was acid-fast bacilli. Sequence analysis indicated that the complete genetic sequence of 16S rRNA was 99.0%, *hsp65* 100%, and *rpoB* 99.8% homologous with *M. marseillense* strain FLAC0026. Phylogenetic analysis of the 16S rRNA sequence showed the isolate clustered with *M. chimaera* and *M. intracellulare* (Figure, panel D). Although the 16S rRNA gene sequence of the isolate was 100% similar to *M. intracellulare* subsp. *yongonense* 05-1390, the sequence similarities to *hsp65* and *rpoB* were relatively low. Sequence analyses suggested *M. marseillense* infection.

Referring to the guidelines for pulmonary *M. avium* complex disease, we treated the patient with the antimicrobial drugs clarithromycin, rifampin, and ethambutol (5). Afterward, in vitro drug susceptibility testing showed the isolate was sensitive to clarithromycin, azithromycin, and amikacin; moderately sensitive to moxifloxacin; and resistant to ethambutol and rifampin. Therefore, 3 months after initiating treatment, we changed the regimen to clarithromycin, moxifloxacin, and amikacin, which she received for 2 months. The patient's skin lesions healed gradually, and nasal symptoms disappeared, but a scar and erythema

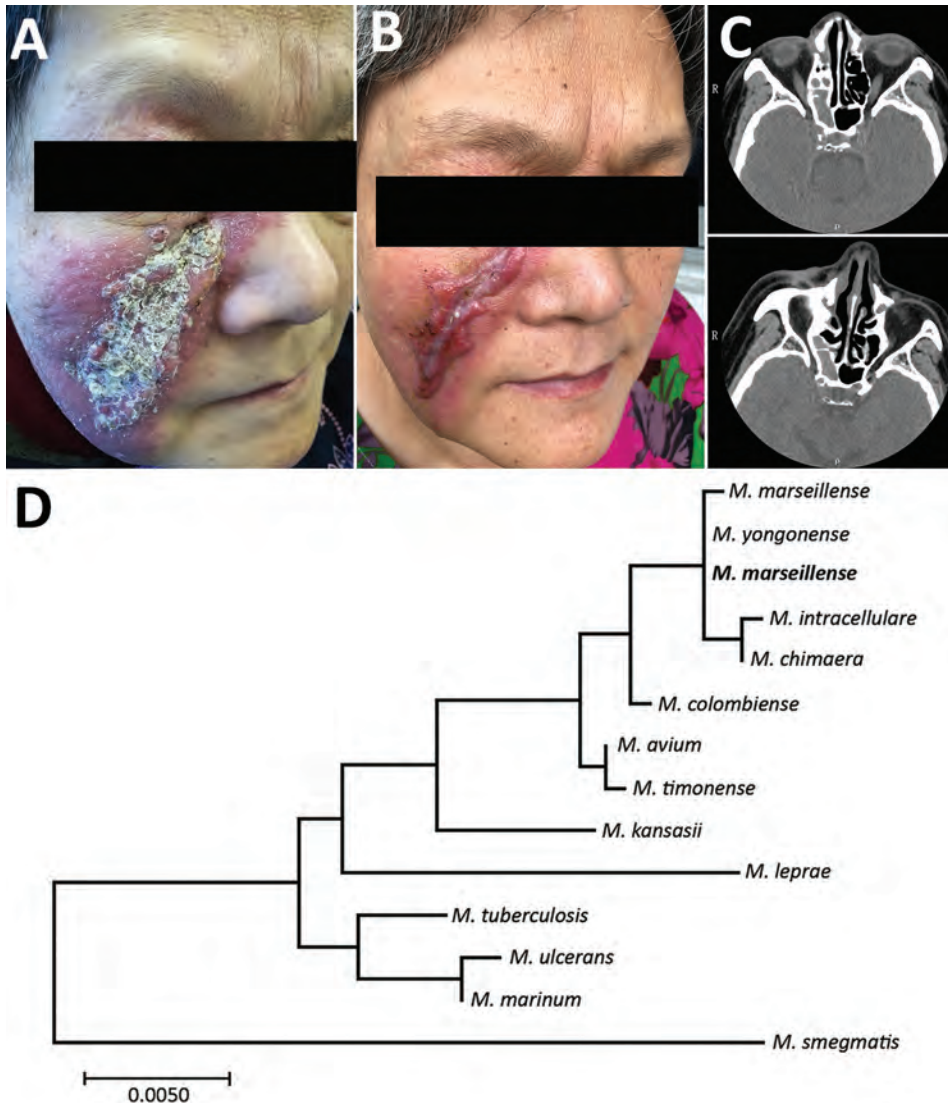


Figure. Skin lesions and computer tomography scans of woman with *Mycobacterium marseillense* skin infection, China, 2018, and genomic analysis of isolate. A, B) Facial skin lesion of woman with *M. marseillense* infection before and after treatment. Infiltrated erythematous plaque with yellowish scales and crusts (A) resolved to a scar after clearance of infection (B). C) Computed tomography imaging before treatment (top) shows heterogeneous hypersignal in right ethmoid sinus and after treatment (bottom) shows recovery of right ethmoid sinus. P, posterior; R, right. D) Phylogenetic tree constructed with 16S rRNA gene sequence of isolate from patient (bold) and other species. Scale bar indicates nucleotide substitutions per site.

remained (Figure, panel B). Computed tomography scans of the paranasal sinuses showed the reduction of sinusitis (Figure, panel C). No recurrence was observed during 4 months of monitoring.

We characterized this isolate's genome (GenBank accession no. VASI0000000) further to help determine the cause of its virulence and resistance (Appendix Figure 3). Genetic analyses indicated the genome ($\approx 5,706,022$ bp) contained 5,343 predicted genes, 3 rRNAs, and 48 tRNAs and had a GC content of 67.73%. We annotated the genes functionally through multiple databases (Appendix Table 1, Figure 4). Using the Virulence Factors of Pathogenic Bacteria database, we identified 137 potential virulence genes (identity $>95.0\%$, E value $<1 \times 10^{-5}$), such as type VII secretion system genes (e.g., *esxH*, *esxC*, *esxH*, and *esxC*) (6), in the isolate's genome (Appendix 2, <https://wwwnc.cdc.gov/EID/article/25/10/19-0695-App2.xlsx>). In Comprehensive Antibiotic Resistance Database searches,

we detected the antimicrobial drug resistance genes *mtrA*, *murA*, and *gyrA* (identity $>90.0\%$, E value $<1 \times 10^{-5}$; Appendix Table 2); *mtrA* modulates antimicrobial drug efflux, *murA* encodes the fosfomycin resistance protein, and *gyrA* encodes the fluoroquinolone resistance protein.

M. marseillense infections are rare in humans. Our case demonstrates that *M. marseillense* can cause infections in immunocompetent persons. For facial skin infection with *M. marseillense*, this and similar (7) reports indicate the need for vigilance of paranasal sinus infection. Although many potential virulence factors could be detected by genomic analysis, cases of infection and transmission with this bacterium are rarely reported, suggesting the presence of other influencing factors.

The drug resistance mechanisms of *M. marseillense* have not been completely elucidated. The drug susceptibility test results and treatment response we observed were generally consistent with those previously reported for

cases of pulmonary infection, although sensitivity to rifampin and quinolones yielded various results (2–4). Drug susceptibility testing indicated that the isolate we obtained was resistant to ethambutol and rifampin. However, in genetic analyses, mutations associated with ethambutol and rifampin resistance were not detected. According to the Comprehensive Antibiotic Resistance Database, our isolate was resistant to fluoroquinolone, but drug susceptibility test results were inconsistent. Our results indicate that drug susceptibility testing should be performed for *M. marseillense* to guide antimicrobial drug treatment. If drug susceptibility results are absent, treatments including macrolides and amikacin appear to be reasonable.

Acknowledgments

We thank Jun Chen and Ying Shi for data analysis.

This manuscript was supported by grants from the Chinese Academy of Medical Science Innovation Fund for Medical Science (2017-I2M-B&R-14, 2016-I2M-1-005), Jiangsu Provincial Science and Technology Project (BE2018619), National Science and Technology Major Project (2018ZX10101-001), Graduate Innovation Foundation of Peking Union Medical College (2018-1002-02-13), and Jiangsu Natural Science Foundation (BK20160377).

About the Author

Dr. Xie is a physician in the Department of Dermatology, Zhejiang Institute of Dermatology, Deqing, China, and formerly studied at the Institute of Dermatology, Chinese Academy of Medical Sciences and Peking Union Medical College, Nanjing, China. His major research interest is infectious diseases of the skin.

References

1. Ben Salah I, Cayrou C, Raoult D, Drancourt M. *Mycobacterium marseillense* sp. nov., *Mycobacterium timonense* sp. nov. and *Mycobacterium bouchedurhonense* sp. nov., members of the *Mycobacterium avium* complex. *Int J Syst Evol Microbiol*. 2009;59:2803–8. <https://doi.org/10.1099/ijs.0.010637-0>
2. Grottola A, Roversi P, Fabio A, Antenora F, Apice M, Tagliazucchi S, et al. Pulmonary disease caused by *Mycobacterium marseillense*, Italy. *Emerg Infect Dis*. 2014;20:1769–70. <https://doi.org/10.3201/eid2010.140309>
3. Kim SY, Yoo H, Jeong BH, Jeon K, Ha YE, Huh HJ, et al. First case of nontuberculous mycobacterial lung disease caused by *Mycobacterium marseillense* in a patient with systemic lupus erythematosus. *Diagn Microbiol Infect Dis*. 2014;79:355–7. <https://doi.org/10.1016/j.diagmicrobio.2014.03.019>
4. Azzali A, Montagnani C, Simonetti MT, Spinelli G, de Martino M, Galli L. First case of *Mycobacterium marseillense* lymphadenitis in a child. *Ital J Pediatr*. 2017;43:92. <https://doi.org/10.1186/s13052-017-0413-5>
5. Griffith DE, Aksamit T, Brown-Elliott BA, Catanzaro A, Daley C, Gordin F, et al.; American Thoracic Society Mycobacterial Diseases Subcommittee; American Thoracic Society; Infectious Disease Society of America. An official ATS/IDSA statement: diagnosis, treatment, and prevention of nontuberculous mycobacterial diseases. (Erratum in: *Am J Respir Crit Care Med* 2007;175:744–5.) *Am J Respir Crit Care Med*. 2007;175:367–416. <https://doi.org/10.1164/rccm.200604-571ST>
6. Abdallah AM, Gey van Pittius NC, DiGiuseppe Champion PA, Cox J, Luirink J, Vandenbroucke-Grauls CMJE, et al. Type VII secretion—mycobacteria show the way. *Nat Rev Microbiol*. 2007;5:883–91. <https://doi.org/10.1038/nrmicro1773>
7. Chen Y, Jiang J, Jiang H, Chen J, Wang X, Liu W, et al. *Mycobacterium gordonae* in patient with facial ulcers, nosebleeds, and positive T-SPOT.TB test, China. *Emerg Infect Dis*. 2017;23:1204–6. <https://doi.org/10.3201/eid2307.162033>

Address for correspondence: Hongsheng Wang, Chinese Academy of Medical Sciences and Peking Union Medical College, Institute of Dermatology, St 12 Jiangwangmiao, Nanjing, Jiangsu, 210042, China; email: whs33@vip.sina.com

Geospatial Variation in Rotavirus Vaccination in Infants, United States, 2010–2017

Mary A.M. Rogers, Catherine Kim, Annika M. Hofstetter

Author affiliations: University of Michigan, Ann Arbor, Michigan, USA (M.A.M. Rogers, C. Kim); University of Washington and Seattle Children's Research Institute, Seattle, Washington, USA (A.M. Hofstetter)

DOI: <https://doi.org/10.3201/eid2510.190874>

We evaluated rotavirus vaccination rates in the United States by using records from a nationwide health database. From data on 519,697 infants, we found 68.6% received the entire rotavirus vaccine series. We noted pockets of under-vaccination in many states, particularly in the Northeast and in some western states.

Vaccination coverage in the United States frequently is evaluated with telephone and mailed surveys (1). However, telephone response rates have declined over the past 2 decades (2) and parents who choose not to vaccinate their children might be less likely to participate in surveys (3).

The Advisory Committee on Immunization Practices (ACIP) recommends routine vaccination among US infants to prevent rotavirus infection, the most common cause of gastroenteritis in children worldwide (4). We designed a study to evaluate rotavirus vaccination rates using nationwide health insurance records.

We conducted a longitudinal study of rotavirus vaccination rates during January 1, 2010–June 30, 2017. We obtained deidentified data from Clinformatics Data Mart (Optum, <https://www.optum.com>), an integrated database containing demographic, service type (inpatient and outpatient), medication, and laboratory data for ≈ 77.8 million privately insured persons of all ages across 50 states. We included data on infants (≤ 1 year of age) with continuous health insurance enrollment from birth to 1 year of age and an available residential ZIP code. We determined completion of the rotavirus vaccine series by using Current Procedural Terminology (CPT) codes and data on vaccine administration, including vaccine type, date, and location. Vaccine completion requires 2 doses of monovalent Rotarix (Glaxo-SmithKline, <https://www.gsk.com>; CPT 90681) or 3 doses of pentavalent RotaTeq (Merck and Company, <https://www.merck.com>; CPT 90680). To evaluate geographic variation,

we used the first 3 digits of residential ZIP codes and excluded areas with <20 infants to provide stability of the estimates. The study was reviewed and deemed exempt by the institutional review board of the University of Michigan.

We identified 526,376 infants with continuous health insurance for ≥ 1 year during 2010–2017. We excluded 5,708 (1.1%) with no known residential ZIP code and 971 (0.2%) from areas with <20 infants. Our final cohort contained 519,697 eligible infants; 99.8% had no copayment for vaccine administrations. The number of infants in each 3-digit ZIP code area was 20–9,426 (median 223; interquartile range 85–682).

In our cohort, 68.6% (95% CI 68.5%–68.8%) of infants completed the rotavirus vaccine series; 15.9% completed only part of the series, and 15.5% received no rotavirus vaccine. Of infants completing the vaccine series, 79% received RotaTeq, 19% received Rotarix, and 2% received both. The mean interval between vaccine doses was 64.9 days.

Rotavirus vaccination rates were higher in eastern states, although some states in the Northeast had low proportions of vaccination (Figure). Alaska had considerably lower vaccination rates, ranging from 17% to 28%. Series completion was lowest in northeastern Wyoming at 9%

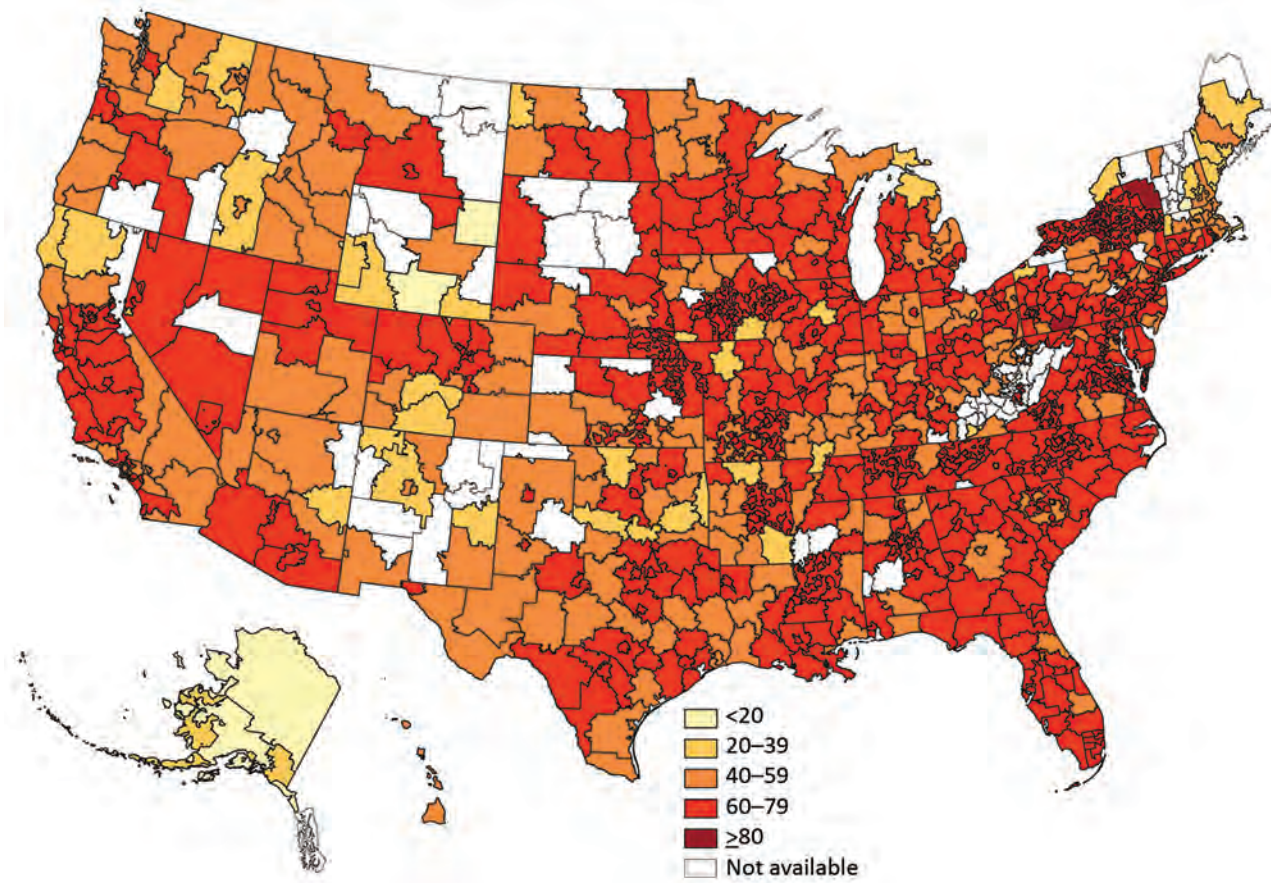


Figure. Percentage of infants (≤ 1 year of age) covered by private health insurance who completed the rotavirus vaccination series in the United States, 2010–2017.

(95% CI 4%–17%) and highest (>80%) in upstate New York, several areas of Pennsylvania, and 1 suburb of San Francisco, California.

Rotavirus vaccination coverage varied considerably across the United States, with pockets of undervaccination in many states. National Immunization Survey (NIS) data show \approx 59.2% of infants completed the rotavirus vaccine series in 2010 and \approx 73.2% completed the series in 2017 (1,5). Our overall estimate was 68.6% during 2010–2017 among privately insured infants. However, we note several differences in these samples. NIS used a nationwide sample of 15,333 children in 2017, whereas our study used 34 \times that number (519,697), giving us an opportunity to assess vaccination rates in local areas. NIS weights for nonparticipation but could underestimate coverage rates in less densely populated areas (6). Our use of deidentified data rather than telephone surveys might provide an opportunity to include vaccine-hesitant populations (3). However, our sample does not shed light on vaccination rates in children covered under Medicaid or the Children’s Health Insurance Program or those with no insurance coverage.

Parents’ decision to vaccinate their children involves a complex interplay between advice from family and friends; school and institutional mandates; experience with health-care professionals; personal beliefs; and social impacts, including media coverage, access, and transportation issues (7). The geographic variation in vaccination rates we found might reflect some of these determinants. For instance, low coverage in remote areas may reflect an inability to travel to providers; lower overall vaccination rates have been found in children living in rural areas (1,8). Because 99.8% of our cohort did not have a copayment, we do not believe there was financial disincentive, but other financial obstacles could exist. Previous studies suggest rotavirus vaccination is lower among persons with public or no insurance (9). Therefore, vaccination rates might be <68% in geographic regions with a high number of uninsured or underinsured children.

The 15.9% of infants in our cohort who did not complete the vaccination series could reflect an inability to meet the start- and end-date requirements. Rotavirus vaccination has an exceptionally narrow window of administration; ACIP recommends the first dose at <15 weeks of age and conclusion of all doses before 8 months of age.

In summary, we found considerable geographic variation in rotavirus vaccination rates in the United States. We recommend additional efforts at the local and county levels to address pockets of rotavirus undervaccination.

Acknowledgments

This study was funded by the National Institutes of Health (grant no. UL1TR000433) and was carried out in accordance with National Institutes of Health guidelines for studies that utilize deidentified data from humans.

About the Author

Dr. Rogers is an epidemiologist and research associate professor at the University of Michigan, Ann Arbor, Michigan, USA. Her research interests include preventive medicine and translational research.

References

- Hill HA, Elam-Evans LD, Yankey D, Singleton JA, Kang Y. Vaccination coverage among children aged 19–35 months—United States, 2017. *MMWR Morb Mortal Wkly Rep.* 2018; 67:1123–8. <https://doi.org/10.15585/mmwr.mm6740a4>
- Nishimura R, Wagner J, Elliott MR. Alternative indicators for the risk of non-response bias: a simulation study. *Int Stat Rev.* 2016;84:43–62. <https://doi.org/10.1111/instr.12100>
- Salmon DA, Moulton LH, Omer SB, DeHart MP, Stokley S, Halsey NA. Factors associated with refusal of childhood vaccines among parents of school-aged children: a case-control study. *Arch Pediatr Adolesc Med.* 2005;159:470–6. <https://doi.org/10.1001/archpedi.159.5.470>
- Centers for Disease Control and Prevention. Prevention of rotavirus gastroenteritis among infants and children: recommendations of the Advisory Committee on Immunization Practices (ACIP). *MMWR Morb Mortal Wkly Rep.* 2009;58(RR02):1–25.
- Centers for Disease Control and Prevention. National and state vaccination coverage among children aged 19–35 months—United States, 2010. *MMWR Morb Mortal Wkly Rep.* 2011; 60:1157–63.
- Groves RM, Peytcheva E. The impact of nonresponse rates on nonresponse bias: a meta-analysis. *Public Opin Q.* 2008; 72:167–89. <https://doi.org/10.1093/poq/nfn011>
- Sturm LA, Mays RM, Zimet GD. Parental beliefs and decision making about child and adolescent immunization: from polio to sexually transmitted infections. *J Dev Behav Pediatr.* 2005; 26:441–52. <https://doi.org/10.1097/00004703-200512000-00009>
- O’Leary ST, Barnard J, Lockhart S, Kolasa M, Shmueli D, Dickinson LM, et al. Urban and rural differences in parental attitudes about influenza vaccination and vaccine delivery models. *J Rural Health.* 2015;31:421–30. <https://doi.org/10.1111/jrh.12119>
- Aliabadi N, Wikswo ME, Tate JE, Cortese MM, Szilagyi PG, Staat MA, et al. Factors associated with rotavirus vaccine coverage. *Pediatrics.* 2019;143:e20181824. <https://doi.org/10.1542/peds.2018-1824>

Address for correspondence: Mary A.M. Rogers, University of Michigan, Bldg 16, Rm 422W, North Campus Research Complex, 2800 Plymouth Rd, Ann Arbor, MI 48109–2800, USA; email: maryroge@umich.edu

Databases for Research and Development

Michael G. Head

Author affiliation: University of Southampton, Hampshire, UK

DOI: <https://doi.org/10.3201/eid2510.181411>

To the Editor: I welcome the findings of Mehand et al. in putting together a methodology that can prioritize emerging infectious diseases in need of research and development (1). These approaches are vital in establishing how global research funders and research institutions can best contribute to establishing a knowledge base around what diseases to address and how.

There is also a distinct need to understand ongoing research portfolios at international and national levels. The data emerging from these projects can provide further knowledge and impact in health policy and inform further research priorities.

Our ongoing project involves the Research Investments in Global Health (ResIn) study. ResIn has described research portfolios for cancer and infectious disease research in the United Kingdom (2,3). Internationally, the study has covered investments into global pneumonia research (4) and malaria research across Africa (5). Findings have examined, for example, the burden of disease alongside levels of investment, as well as providing informed comment on research gaps. ResIn also considers how best to implement findings from a research database into health policy and practice, and has presented results and sought opinion from meetings with key stakeholders, including the World Health Organization (WHO), European Commission, and Wellcome Trust.

I encourage WHO and other stakeholders to consider an open-access global research investments portfolio for all areas of health, using open datasets to describe spending on research alongside other areas, such as burden of disease. Alongside the WHO R&D Blueprint (<https://www.who.int/blueprint>), this resource can support decision-making around research knowledge and innovation.

References

1. Mehand MS, Millett P, Al-Shorbaji F, Roth C, Kienny MP, Murgue B. World Health Organization methodology to prioritize emerging infectious diseases in need of research and development. *Emerg Infect Dis*. 2018;24. <http://dx.doi.org/10.3201/eid2409.171427>
2. Maruthappu M, Head MG, Zhou CD, Gilbert BJ, El-Harasis MA, Raine R, et al. Investments in cancer research awarded to UK institutions and the global burden of cancer 2000–2013: a systematic analysis. *BMJ Open*. 2017;7:e013936. <http://dx.doi.org/10.1136/bmjopen-2016-013936>
3. Head MG, Fitchett JR, Nageshwaran V, Kumari N, Hayward A, Atun R. Research investments in global health: a systematic analysis of UK infectious disease research funding and global

health metrics, 1997–2013. *EBioMedicine*. 2015;3:180–90. <http://dx.doi.org/10.1016/j.ebiom.2015.12.016>

4. Brown RJ, Head MG. Sizing up pneumonia research. Southampton (United Kingdom): University of Southampton; 2018 [cited 2019 Aug 3]. https://figshare.com/articles/Sizing_Up_Pneumonia_Investment/6143060
5. Head MG, Goss S, Gelister Y, Alegana V, Brown RJ, Clarke SC, et al. Global funding trends for malaria research in sub-Saharan Africa: a systematic analysis. *Lancet Glob Health*. 2017;5:e772–81. [http://dx.doi.org/10.1016/S2214-109X\(17\)30245-0](http://dx.doi.org/10.1016/S2214-109X(17)30245-0)

Address for correspondence: Michael G. Head, University of Southampton, Clinical Informatics Research Unit, Faculty of Medicine, Coxford Road, University Hospital, Southampton, Southampton SO16 6YD, UK; email: m.head@soton.ac.uk

Self-Flagellation as Possible Route of Human T-Cell Lymphotropic Virus Type 1 Transmission

Claire E. Styles, Veronica C. Hoad, Paula Denham-Ricks, Dianne Brown, Clive R. Seed

Author affiliations: Australian Red Cross Blood Service, Perth, Western Australia, Australia (C.E. Styles, V.C. Hoad, C.R. Seed); Australian Red Cross Blood Service, Melbourne, Victoria, Australia (P. Denham-Ricks, D. Brown)

DOI: <https://doi.org/10.3201/eid2510.190484>

To the Editor: Blood donors in Australia who test positive for transfusion-transmissible infections, including human T-lymphotropic virus (HTLV), hepatitis B virus (HBV), hepatitis C virus, and HIV, undergo posttest counseling, as previously described (1). Similar to Tang et al. (2), we identified self-flagellation as a possible unique risk factor for HTLV-1 infection. History of self-flagellation was elicited in 7 (28%) of 25 HTLV-1–positive donors identified during January 2012–December 2018. All 7 donors were men 20–37 years of age, of whom 5 were born in Pakistan and 2 in India; 6 had given blood in Victoria, Australia. The 18 remaining HTLV-1–positive donors were 29–68 years of age; 10 (56%) were men; 1 was born in India and none in Pakistan; and 7 (39%) gave blood in Victoria.

HBV shares transmission routes with HTLV-1 and is highly infectious, including through minor blood exposures

(3). After discussion of recognized infective risk factors, the 610 HBV-positive donors from the same period, of whom 83 were born in India or Pakistan, were asked about any other potential blood exposures. None reported self-flagellation.

At the time of posttest counseling, no previous HTLV results were available for donors reporting self-flagellation or for their family members. Until the known modes of vertical and sexual transmission have been excluded by such results, the likelihood of self-flagellation as an infective risk factor remains unclear. Although India and Pakistan are not known to be geographic risk areas for HTLV-1, few prevalence studies are available (4), and HTLV-1 is commonly present in small geographic foci (5). In addition, a noticeable degree of transmission through communal self-flagellation would first require a raised prevalence of infection among the practicing group. We look forward to further research that may clarify the apparent link between self-flagellation and HTLV-1 infection.

Australian governments fund the Australian Red Cross Blood Service for the provision of blood, blood products, and services to the Australian community.

References

1. Polizzotto MN, Wood EM, Ingham H, Keller AJ; Australian Red Cross Blood Service Donor and Product Safety Team. Reducing the risk of transfusion-transmissible viral infection through blood donor selection: the Australian experience 2000 through 2006. *Transfusion*. 2008;48:55–63.
2. Tang AR, Taylor GP, Dhasmana D. Self-flagellation as possible route of human T-cell lymphotropic virus type-1 transmission. *Emerg Infect Dis*. 2019;25:811–3. <https://doi.org/10.3201/eid2504.180984>
3. Trépo C, Chan HL, Lok A. Hepatitis B virus infection. *Lancet*. 2014; 384:2053–63. [https://doi.org/10.1016/S0140-6736\(14\)60220-8](https://doi.org/10.1016/S0140-6736(14)60220-8)
4. Niazi SK, Bhatti FA, Salamat N. Seroprevalence of human T-cell lymphotropic virus-1/2 in blood donors in northern Pakistan: implications for blood donor screening. *J Coll Physicians Surg Pak*. 2015;25:874–7.
5. Gessain A, Cassar O. Epidemiological aspects and world distribution of HTLV-1 infection. *Front Microbiol*. 2012;3:388. <https://doi.org/10.3389/fmicb.2012.00388>

Address for correspondence: Claire E. Styles, Australian Red Cross Blood Service, GPO Box B80, Perth, Western Australia 6838, Australia; email: cstyles@redcrossblood.org.au

Corrections

Vol. 25, No. 3

Figure 2 contained incorrect values in Cross-Border Movement of Highly Drug-Resistant *Mycobacterium tuberculosis* from Papua New Guinea to Australia through Torres Strait Protected Zone, 2010–2015 (A. Bainomugisa et al.). The corrected figure is provided, and the article has been corrected online (https://wwwnc.cdc.gov/eid/article/25/3/18-1003_article).

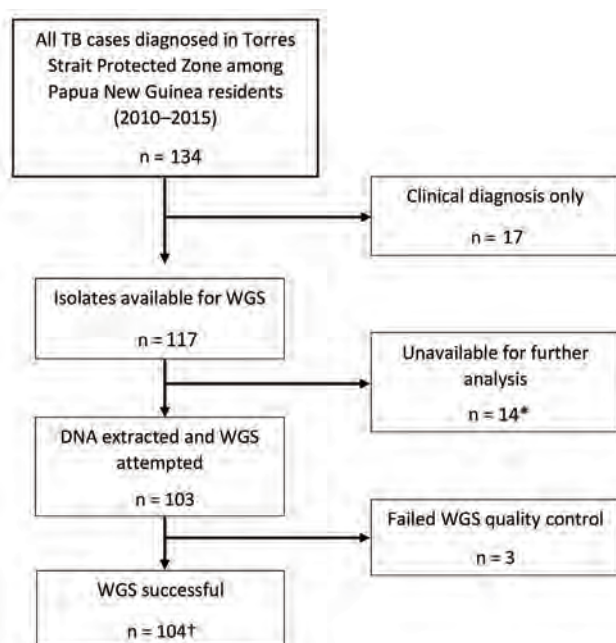


Figure 2. Flow diagram of included *Mycobacterium tuberculosis* isolates from Papua New Guinea citizens residing in Torres Strait Protected Zone, 2010–2015. *Isolates unable to grow or were contaminated. †Included were 4 additional isolates among Queensland residents that were a part of an epidemiologic cluster linked to the Torres Strait Protected Zone. TB, tuberculosis; WGS, whole-genome sequencing.

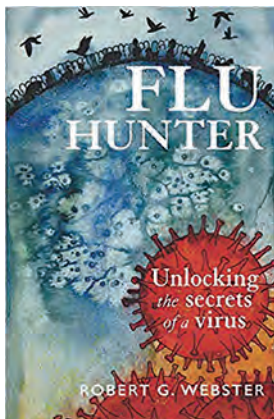
Vol. 25, No. 9

Clostridioides was misspelled in Risk for *Clostridioides difficile* Infection among Older Adults with Cancer (M. Kamboj et al.). The article has been corrected online (https://wwwnc.cdc.gov/eid/article/25/9/18-1142_article).

Flu Hunter: Unlocking the Secrets of a Virus

Robert G. Webster, Otago University Press, Dunedin, New Zealand, 2018; ISBN-10: 1988531314; ISBN-13: 978-1988531311; Pages: 220; Price: \$24.99 (Paperback)

Flu Hunter: Unlocking the Secrets of a Virus offers an engaging and highly readable homage to the influenza virus by one of the world's preeminent influenza virologists, Dr. Robert Webster. Although the book is nominally an autobiographical account of Webster's career, the central figure is often the influenza virus itself, with each of the 17 chapters focusing on an influenza-related event from the past century. Drawing on experience from 50 years as a virologist, Webster provides a first-person account of what happened in each event, and why and how it happened.



Webster points out that it was the heavy toll in human suffering caused by the devastating 1918 Spanish flu pandemic that jump-started influenza research and ultimately led the international scientific community to implement many clinical and public health improvements. Research from this and subsequent influenza events, including the 2009 H1N1 “swine flu” pandemic, has shaped our current understanding of influenza as a continuously mutating pathogen that demands constant global attention.

Two themes appear throughout the book. The first is that influenza is a quintessential One Health pathogen that can only be understood when studied in humans and other animals but especially in both its wild and domestic bird reservoirs. Throughout his career, Webster has championed this approach, which has led to many of the breakthroughs in how we approach influenza prevention and control today. The second theme is the need for

collaboration and cooperation to successfully address the challenges posed by influenza, an idea Webster has lived out by mentoring and working with influenza scientists throughout the world.

Webster weaves anecdotes throughout the book about himself, his family, and his colleagues, among these a walk on an Australian beach littered with dead birds that led to his lifelong interest in influenza. There are wonderful descriptions of his involvement in field expeditions to the Great Barrier Reef, horseshoe crab nesting sites on Delaware Bay, and Spitsbergen, Norway. However, some sections of the book focus so intently on describing influenza viruses or the work of other investigators that readers may be left wanting to hear more of the remarkable personal stories he has to tell.

The book does not entirely shy away from controversial topics. In the latter sections of the book, Webster addresses the pros and cons, from scientific and societal perspectives, of reconstituting the 1918 influenza virus. This section includes a discussion of gain of function research into the potential transmissibility of novel influenza viruses—research that might be used for the benefit or to the detriment of humankind. Webster concludes the book with a discussion of as-yet unanswered questions about the virus and how prepared the world is for an inevitable future pandemic.

Flu Hunter: Unlocking the Secrets of a Virus offers a welcome addition to the bookshelf of anyone wanting to know more about the science of influenza, whether as an interested observer or a seasoned virologist. Indeed, science aside, this story of a remarkable, rewarding, and impactful career and life makes for compelling reading on its own.

Sameh W. Boktor, Stephen Ostroff

Author affiliation: Pennsylvania Department of Health, Harrisburg, Pennsylvania, USA (S.W. Boktor); S Ostroff Consulting, Harrisburg (S. Ostroff)

DOI: <https://doi.org/10.3201/eid2510.190880>

Address for correspondence: Sameh W. Boktor, Pennsylvania Department of Health, 625 Forster St, Rm 933, Harrisburg, PA 17120, USA; email: sboktor@pa.gov



Robert Lee Kocher (1929–), *Two Birds* (1959). Oil on wood, 12 in × 7.75 in/30.5 cm × 19.7 cm. Image used by permission of the artist. Private collection, Fayetteville, Georgia, USA. Photography by James Gathany.

A Study in Stillness and Symmetry

Byron Breedlove

With an MA degree in art from the University of Missouri, Robert Lee Kocher pondered a career illustrating medical textbooks. Instead, his passion for painting led him to pursue a course that allowed him full immersion in art as both an academic and an artist. Kocher served as chair of the art department at Coe College in Cedar Rapids, Iowa USA, where he is the Marvin D. Cone Professor of Art, Emeritus. Cone, who preceded Kocher at Coe College, was a close friend of a famous painter associated with Cedar Rapids, Grant Wood (P. Kocher, pers. comm., email, 2019 Aug 4).

Author affiliation: Centers for Disease Control and Prevention, Atlanta, Georgia, USA

DOI: <https://doi.org/10.3201/eid2510.AC2510>

Throughout his career, Kocher found opportunities to explore myriad styles and formats. Many of his works are drenched in color, whereas others feature deliberately limited palettes. His versatility is underscored by the contrast between his vivid abstract works overlaid with petroglyphs that he created in New Mexico and his more subdued rendering of a row house near the South Carolina coast. Kocher sometimes painted directly on wood instead of traditional surfaces, using the textures from the wood as another distinctive element.

Two Birds, appearing on this month's cover, is one of Kocher's more somber paintings. The artist depicts a pair of common grackles (*Quiscalus quiscula*) perched on a tree branch, visible from a window in his late mother's home. The distinct symmetry of dark and light tones instills a

palpable sense of stillness and quiet. He matches the dark colors of the birds and the tree but varies their textures. Kocher's grackles are nearly all black: purple, green, and blue iridescence is muted in the filtered sunlight of an overcast winter's afternoon.

Native to North America, grackles forage in farm fields, rural pastures, suburban lawns, cattle feedlots, and marshes. Their song is a cacophonous crackling and high-pitched screech that the National Audubon Society guide likens to the sound made by a rusty hinge. In his poem "The Grackle," Ogden Nash does not flatter the species, writing, "I cannot help but deem the grackle / an ornithological debacle."

Kocher's painting, however, offers a different perspective on this common bird. Kocher probably looked out that window many times before he noticed the symmetry and contrast that prompted him to paint *Two Birds*. His grackles are subdued, claws tightly clenched as they huddle, their curved silhouettes edged by the cold Iowa winter. The bare tree branches that bisect the lower part of the painting extend beyond the edges of the painting, like unclenched claws grasping for warmth in cold sunlight. Kocher focuses on a pair of grackles, but his painting serves as a quiet reminder that birds are our ubiquitous neighbors.

Indeed, tallying the number of individual birds on Earth is a challenging endeavor. Some bird experts suggest an upper range of 200 to 400 billion, or 40 to 60 birds for every human. Birds are incredibly diverse—a recent study suggests there are more than 18,000 species—and very mobile. The interconnections among birds, humans, domestic animals, and wildlife are intricate and of concern to public health.

Wild and domestic birds carry various emerging and reemerging pathogens, including some that can be transmitted to humans. For example, soils with large accumulations of bird droppings may expose humans to potentially infectious fungal pathogens such as *Cryptococcus neoformans* or *Histoplasma capsulatum*, although the human respiratory infections caused by those pathogens—cryptococcosis or histoplasmosis—are rare. Avian influenza A

viruses have sporadically caused severe, sometimes fatal, infections in humans. *Chlamydia psittaci* has caused rare zoonotic respiratory infections.

A safe and healthy world depends on animal, environmental, and human health. Birds are found in virtually every ecosystem, so studying their worldwide population numbers provides compelling evidence for gauging the overall health of our environments. Because pathogens can mutate and gain the ability to spread among people, scientists must vigilantly monitor avian populations for telltale signs that could signal a spillover event. Not to do those things would be, to revisit Nash's poem, a very serious ornithological debacle.

Bibliography

1. Audubon Guide to North American Birds. Common grackle [cited 2019 Aug 13]. <https://www.audubon.org/field-guide/bird/common-grackle>
2. Audubon. New study doubles the world's number of bird species by redefining 'species' [cited 2019 Aug 13]. <https://www.audubon.org/news/new-study-doubles-worlds-number-bird-species-redefining-species>
3. Barrowclough GF, Cracraft J, Klicka J, Zink RM. How many kinds of birds are there and why does it matter? PLoS One. 2016;11:e0166307. <https://doi.org/10.1371/journal.pone.0166307>
4. Centers for Disease Control and Prevention. Avian influenza A virus infections in humans [cited 2019 Aug 11]. <https://www.cdc.gov/flu/avianflu/avian-in-humans.htm>
5. Centers for Disease Control and Prevention. Birds kept as pets [cited 2019 Aug 11]. <https://www.cdc.gov/healthypets/pets/birds.html>
6. European Centre for Disease Prevention and Control. Facts about avian influenza in humans [cited 2019 Aug 11]. <https://ecdc.europa.eu/en/avian-influenza-humans/facts>
7. Reed KD, Meece JK, Henkel JS, Shukla SK. Birds, migration and emerging zoonoses: West Nile virus, Lyme disease, influenza A and enteropathogens. Clin Med Res. 2003;1:5–12. <https://doi.org/10.3121/cmr.1.1.5>
8. World Health Organization. Influenza (avian and other zoonotic). Key facts [cited 2019 Aug 11]. [https://www.who.int/news-room/fact-sheets/detail/influenza-\(avian-and-other-zoonotic\)](https://www.who.int/news-room/fact-sheets/detail/influenza-(avian-and-other-zoonotic))

Address for correspondence: Byron Breedlove, EID Journal, Centers for Disease Control and Prevention, 1600 Clifton Rd NE, Mailstop H16-2, Atlanta, GA 30329-4027, USA; email: wbb1@cdc.gov

EMERGING INFECTIOUS DISEASES®

Upcoming Issue

- Vaccine-Derived Poliovirus Infection among Patients with Primary Immunodeficiency and Impact of Patient Screening on Disease Outcomes, Iran
- Rare Detection of *Bordetella pertussis* Pertactin-Deficient Strains in Argentina
- Clinical and Molecular Epidemiology of Invasive Group B Streptococcus Disease among Infants, China
- Lack of Efficacy of High-Titered Immunoglobulin in Patients with West Nile Virus Central Nervous System Disease
- Molecular and Clinical Comparison of Enterovirus D68 Outbreaks among Hospitalized Children, Ohio, USA, 2014 and 2018
- *Mansonella ozzardi* Infection in the Amazon Region, Ecuador
- Human-to-Human Transmission of Influenza A(H3N2) Virus with Reduced Susceptibility to Baloxavir, Japan, February 2019
- Preventing Sexual Transmission of Zika Virus Infection During Pregnancy, Puerto Rico, USA, 2016
- Endemicity of Yaws Shown by *Treponema pallidum* Antibodies in Nonhuman Primates, Kenya
- Middle East Respiratory Syndrome Coronavirus, Saudi Arabia, 2017–2018
- Unavailability of Injectable Antimicrobial Drugs to Treat Gonorrhea and Syphilis, United States, 2016
- Mutation and Diversity of Diphtheria Toxin in *Corynebacterium ulcerans*
- Molecular Epidemiology of Hantaviruses in the Czech Republic
- Psittacosis Outbreak at Chicken Slaughter Plants, Virginia and Georgia, USA, 2018
- *Mycobacterium microti* Infection in Free-ranging Wild Boar, Spain, 2017–2019
- Drug-Susceptible and Multidrug-Resistant *Mycobacterium tuberculosis* in a Single Patient
- Outbreak of *Achromobacter xylosoxidans* and *Ochrobactrum anthropi* Infections after Prostate Biopsies, France, 2014
- Macrolide-Resistant *Mycoplasma genitalium* in Southeastern Region of the Netherlands, 2014–2017

Complete list of articles in the November issue at
<http://www.cdc.gov/eid/upcoming.htm>

Upcoming Infectious Disease Activities

November 20–24, 2019

ASTMH

American Society of Tropical Medicine and Hygiene

68th Annual Meeting

National Harbor, MD, USA

<https://www.astmh.org/>

January 28–30, 2020

American Society for Microbiology

2020 ASM Biothreats

Arlington, VA, USA

<https://www.asm.org/Events/ASM-Biothreats/Home>

February 20–23, 2020

International Society for Infectious Diseases

Kuala Lumpur, Malaysia

<https://www.isid.org/>

March 8–11, 2020

CROI

Conference on Retroviruses and Opportunistic Infections

Boston, MA, USA

<https://www.croiconference.org/>

March 26–30, 2020

SHEA

Conference on Retroviruses and Opportunistic Infections

Boston, MA, USA

<https://www.croiconference.org/>

March 26–30, 2020

SHEA

Conference on Retroviruses and Opportunistic Infections

Boston, MA, USA

<https://www.croiconference.org/>

6th International Conference on Healthcare Associated Infections

Atlanta, GA, USA

<https://decennial2020.org>

April 18–21, 2020

ECCMID 2020

European Congress of Clinical Microbiology and Infectious Diseases

Paris, France

https://www.eccmid.org/eccmid_2020/

June 18–22, 2020

American Society for Microbiology

ASM Microbe

Chicago, IL, USA

<https://www.asm.org/Events/ASM-Microbe/Home>

Announcements

Email announcements to EIDEditor

(eideditor@cdc.gov). Include the event's

date, location, sponsoring organization, and

a website. Some events may appear only on

EID's website, depending on their dates.

Earning CME Credit

To obtain credit, you should first read the journal article. After reading the article, you should be able to answer the following, related, multiple-choice questions. To complete the questions (with a minimum 75% passing score) and earn continuing medical education (CME) credit, please go to <http://www.medscape.org/journal/eid>. Credit cannot be obtained for tests completed on paper, although you may use the worksheet below to keep a record of your answers.

You must be a registered user on <http://www.medscape.org>. If you are not registered on <http://www.medscape.org>, please click on the “Register” link on the right hand side of the website.

Only one answer is correct for each question. Once you successfully answer all post-test questions, you will be able to view and/or print your certificate. For questions regarding this activity, contact the accredited provider, CME@medscape.net. For technical assistance, contact CME@medscape.net. American Medical Association’s Physician’s Recognition Award (AMA PRA) credits are accepted in the US as evidence of participation in CME activities. For further information on this award, please go to <https://www.ama-assn.org>. The AMA has determined that physicians not licensed in the US who participate in this CME activity are eligible for AMA PRA Category 1 Credits™. Through agreements that the AMA has made with agencies in some countries, AMA PRA credit may be acceptable as evidence of participation in CME activities. If you are not licensed in the US, please complete the questions online, print the AMA PRA CME credit certificate, and present it to your national medical association for review.

Article Title

***Edwardsiella tarda* Bacteremia, Okayama, Japan, 2005–2016**

CME Questions

1. Your patient is a 75-year-old man with a liver tumor who is suspected of having *Edwardsiella tarda* bacteremia (ETB). According to the clinical series of 26 patients with ETB by Kamiyama and colleagues, which of the following statements about the clinical epidemiology and characteristics of ETB is correct?

- A. The most common clinical manifestation was urinary tract infection
- B. Patients with ETB were older than patients with nonbacteremic *E. tarda* infection and had higher rates of hepatobiliary infections and solid tumors
- C. The most common underlying disease was hematologic malignancy
- D. More than half of the patients had hospital-acquired bloodstream infections

2. According to the clinical series of patients with ETB by Kamiyama and colleagues, which of the following statements about treatment and outcomes of ETB is correct?

- A. *E. tarda* strains isolated from blood cultures were resistant to most tested antibiotics
- B. More than half of patients in this cohort died within 90 days of developing ETB
- C. *E. tarda* is naturally resistant to benzylpenicillin, colistin, and polymyxin B
- D. ETB could not be successfully treated with ampicillin

3. According to the clinical series of patients with ETB by Kamiyama and colleagues, which of the following statements about seasonal distribution and other clinical implications is correct?

- A. In this series, *E. tarda* infection more likely occurred during summer and autumn
- B. This series showed that ETB is relatively common
- C. Mortality of ETB in this series was higher than previously reported
- D. *E. tarda* is a rare human pathogen causing salmonella-like gastrointestinal disease, usually self-limited enteritis, in ≈80% of infections

Earning CME Credit

To obtain credit, you should first read the journal article. After reading the article, you should be able to answer the following, related, multiple-choice questions. To complete the questions (with a minimum 75% passing score) and earn continuing medical education (CME) credit, please go to <http://www.medscape.org/journal/eid>. Credit cannot be obtained for tests completed on paper, although you may use the worksheet below to keep a record of your answers.

You must be a registered user on <http://www.medscape.org>. If you are not registered on <http://www.medscape.org>, please click on the “Register” link on the right hand side of the website.

Only one answer is correct for each question. Once you successfully answer all post-test questions, you will be able to view and/or print your certificate. For questions regarding this activity, contact the accredited provider, CME@medscape.net. For technical assistance, contact CME@medscape.net. American Medical Association’s Physician’s Recognition Award (AMA PRA) credits are accepted in the US as evidence of participation in CME activities. For further information on this award, please go to <https://www.ama-assn.org>. The AMA has determined that physicians not licensed in the US who participate in this CME activity are eligible for AMA PRA Category 1 Credits™. Through agreements that the AMA has made with agencies in some countries, AMA PRA credit may be acceptable as evidence of participation in CME activities. If you are not licensed in the US, please complete the questions online, print the AMA PRA CME credit certificate, and present it to your national medical association for review.

Article Title

Case Studies and Literature Review of Pneumococcal Septic Arthritis in Adults

CME Questions

1. Your patient is a 62-year-old woman with severe bronchitis and presumed pneumococcal septic arthritis (SA). According to results from the retrospective case series and literature review by Dernoncourt and colleagues, which of the following statements about clinical and epidemiological features of pneumococcal SA in adults >18 years old reported to the “Picardie Regional Pneumococcal Network” from January 2005 to December 2016 is correct?

- A. SA accounted for 0.5% of cases of invasive pneumococcal disease
- B. SA prevalence increased significantly from 0.69% in 2005–2010 to 2.47% in 2011–2016 ($p = 0.02$) after introduction of pneumococcal 13-valent conjugate vaccine
- C. Most patients had no predisposing comorbid condition
- D. Most patients had polyarticular infection of the knee and shoulders

2. According to results from the retrospective case series and literature review by Dernoncourt and colleagues, which of the following statements about diagnosis and treatment of pneumococcal SA in adults >18 years old reported to the “Picardie Regional Pneumococcal Network” from January 2005 to December 2016 is correct?

- A. Median interval between admission and diagnosis was 15 days
- B. Leukocyte scintigraphy and positron emission tomography scan did not contribute to diagnosis in any patient
- C. All patients received 2 intravenous antibiotics followed by oral antibiotics for >42 days alone or in combination
- D. Joint fluid and blood cultures were both *Streptococcus pneumoniae*-positive for one-quarter of recovered strains

3. According to the retrospective case series and literature review by Dernoncourt and colleagues, which of the following statements about outcomes and implications of pneumococcal SA in adults >18 years old reported to the “Picardie Regional Pneumococcal Network” from January 2005 to December 2016 is correct?

- A. 57% of cases completely recovered, 36% had moderately reduced range of motion of the affected joint, and 1 died from colchicine-related multiple organ failure 2 days after admission
- B. Vaccination would have been unlikely to prevent any of the SA cases
- C. The rate of concomitant extra-articular infection in this study was higher than that of previous studies
- D. Treatment of choice for SA is antibiotic therapy alone

Earning CME Credit

To obtain credit, you should first read the journal article. After reading the article, you should be able to answer the following, related, multiple-choice questions. To complete the questions (with a minimum 75% passing score) and earn continuing medical education (CME) credit, please go to <http://www.medscape.org/journal/eid>. Credit cannot be obtained for tests completed on paper, although you may use the worksheet below to keep a record of your answers.

You must be a registered user on <http://www.medscape.org>. If you are not registered on <http://www.medscape.org>, please click on the “Register” link on the right hand side of the website.

Only one answer is correct for each question. Once you successfully answer all post-test questions, you will be able to view and/or print your certificate. For questions regarding this activity, contact the accredited provider, CME@medscape.net. For technical assistance, contact CME@medscape.net. American Medical Association’s Physician’s Recognition Award (AMA PRA) credits are accepted in the US as evidence of participation in CME activities. For further information on this award, please go to <https://www.ama-assn.org>. The AMA has determined that physicians not licensed in the US who participate in this CME activity are eligible for AMA PRA Category 1 Credits™. Through agreements that the AMA has made with agencies in some countries, AMA PRA credit may be acceptable as evidence of participation in CME activities. If you are not licensed in the US, please complete the questions online, print the AMA PRA CME credit certificate, and present it to your national medical association for review.

Article Title

Risk for Invasive Streptococcal Infections among Adults Experiencing Homelessness, Anchorage, Alaska, USA, 2002–2015

CME Questions

1. You are in the clinic preparing to see a 40-year-old gentleman with a past history of experiencing homelessness and a chief complaint of rash. What should you consider regarding the epidemiology and health risks for homelessness before you enter the room?

- A. The total population of persons experiencing homelessness (PEH) in the United States has increased steadily for decades
- B. The population of PEH in the United States was >550,000 in 2017
- C. PEH have higher risks for tuberculosis but not hepatitis C virus infection
- D. PEH have higher risks for HIV infection but not tuberculosis

2. The patient appears to have cellulitis of the left leg. You inquire about his health history. Which of the following characteristics was less common among PEH vs. the general population with infection in the current study?

- A. Diabetes
- B. Alcohol abuse
- C. Diagnosis of pneumonia
- D. Younger age

3. You suspect this patient has infection with a gram-positive bacteria. People experiencing homelessness had higher rates of which of the following types of infection vs. the general population in the current study?

- A. Group A Streptococcus (GAS) only
- B. GAS and Group B Streptococcus (GBS) only
- C. Invasive pneumococcal only
- D. GAS, GBS, and invasive pneumococcal

4. What should you consider regarding the types of bacteria identified among PEH in the current study?

- A. There was no correlation between bacterial types in the PEH and general populations
- B. The most common type of GAS identified in the PEH and general populations was emm1
- C. Only isolates of invasive pneumococcal infection were the same in the PEH and general populations
- D. The GAS strains more common in PEH are associated with skin infections

Emerging Infectious Diseases is a peer-reviewed journal established expressly to promote the recognition of new and reemerging infectious diseases around the world and improve the understanding of factors involved in disease emergence, prevention, and elimination.

The journal is intended for professionals in infectious diseases and related sciences. We welcome contributions from infectious disease specialists in academia, industry, clinical practice, and public health, as well as from specialists in economics, social sciences, and other disciplines. Manuscripts in all categories should explain the contents in public health terms. For information on manuscript categories and suitability of proposed articles, see below and visit <http://wwwnc.cdc.gov/eid/pages/author-resource-center.htm>.

Summary of Authors' Instructions

Authors' Instructions. For a complete list of EID's manuscript guidelines, see the author resource page: <http://wwwnc.cdc.gov/eid/page/author-resource-center>.

Manuscript Submission. To submit a manuscript, access Manuscript Central from the Emerging Infectious Diseases web page (www.cdc.gov/eid). Include a cover letter indicating the proposed category of the article (e.g., Research, Dispatch), verifying the word and reference counts, and confirming that the final manuscript has been seen and approved by all authors. Complete provided Authors Checklist.

Manuscript Preparation. For word processing, use MS Word. Set the document to show continuous line numbers. List the following information in this order: title page, article summary line, keywords, abstract, text, acknowledgments, biographical sketch, references, tables, and figure legends. Appendix materials and figures should be in separate files.

Title Page. Give complete information about each author (i.e., full name, graduate degree(s), affiliation, and the name of the institution in which the work was done). Clearly identify the corresponding author and provide that author's mailing address (include phone number, fax number, and email address). Include separate word counts for abstract and text.

Keywords. Use terms as listed in the National Library of Medicine Medical Subject Headings index (www.ncbi.nlm.nih.gov/mesh).

Text. Double-space everything, including the title page, abstract, references, tables, and figure legends. Indent paragraphs; leave no extra space between paragraphs. After a period, leave only one space before beginning the next sentence. Use 12-point Times New Roman font and format with ragged right margins (left align). Italicize (rather than underline) scientific names when needed.

Biographical Sketch. Include a short biographical sketch of the first author—both authors if only two. Include affiliations and the author's primary research interests.

References. Follow Uniform Requirements (www.icmje.org/index.html). Do not use endnotes for references. Place reference numbers in parentheses, not superscripts. Number citations in order of appearance (including in text, figures, and tables). Cite personal communications, unpublished data, and manuscripts in preparation or submitted for publication in parentheses in text. Consult List of Journals Indexed in Index Medicus for accepted journal abbreviations; if a journal is not listed, spell out the journal title. List the first six authors followed by "et al." Do not cite references in the abstract.

Tables. Provide tables within the manuscript file, not as separate files. Use the MS Word table tool, no columns, tabs, spaces, or other programs. Footnote any use of bold-face. Tables should be no wider than 17 cm. Condense or divide larger tables. Extensive tables may be made available online only.

Figures. Submit editable figures as separate files (e.g., Microsoft Excel, PowerPoint). Photographs should be submitted as high-resolution (600 dpi) .tif or .jpg files. Do not embed figures in the manuscript file. Use Arial 10 pt. or 12 pt. font for lettering so that figures, symbols, lettering, and numbering can remain legible when reduced to print size. Place figure keys within the figure. Figure legends should be placed at the end of the manuscript file.

Videos. Submit as AVI, MOV, MPG, MPEG, or WMV. Videos should not exceed 5 minutes and should include an audio description and complete captioning. If audio is not available, provide a description of the action in the video as a separate Word file. Published or copyrighted material (e.g., music) is discouraged and must be accompanied by written release. If video is part of a manuscript, files must be uploaded with manuscript submission. When uploading, choose "Video" file. Include a brief video legend in the manuscript file.

Types of Articles

Perspectives. Articles should not exceed 3,500 words and 50 references. Use of subheadings in the main body of the text is recommended. Photographs and illustrations are encouraged. Provide a short abstract (150 words), 1-sentence summary, and biographical sketch. Articles should provide insightful analysis and commentary about new and reemerging infectious diseases and related issues. Perspectives may address factors known to influence the emergence of diseases, including microbial adaptation and change, human demographics and behavior, technology and industry, economic development and land use, international travel and commerce, and the breakdown of public health measures.

Synopses. Articles should not exceed 3,500 words in the main body of the text or include more than 50 references. Use of subheadings in the main body of the text is recommended. Photographs and illustrations are encouraged. Provide a short abstract (not to exceed 150 words), a 1-line summary of the conclusions, and a brief

biographical sketch of first author or of both authors if only 2 authors. This section comprises case series papers and concise reviews of infectious diseases or closely related topics. Preference is given to reviews of new and emerging diseases; however, timely updates of other diseases or topics are also welcome. If detailed methods are included, a separate section on experimental procedures should immediately follow the body of the text.

Research. Articles should not exceed 3,500 words and 50 references. Use of subheadings in the main body of the text is recommended. Photographs and illustrations are encouraged. Provide a short abstract (150 words), 1-sentence summary, and biographical sketch. Report laboratory and epidemiologic results within a public health perspective. Explain the value of the research in public health terms and place the findings in a larger perspective (i.e., "Here is what we found, and here is what the findings mean").

Policy and Historical Reviews. Articles should not exceed 3,500 words and 50 references. Use of subheadings in the main body of the text is recommended. Photographs and illustrations are encouraged. Provide a short abstract (150 words), 1-sentence summary, and biographical sketch. Articles in this section include public health policy or historical reports that are based on research and analysis of emerging disease issues.

Dispatches. Articles should be no more than 1,200 words and need not be divided into sections. If subheadings are used, they should be general, e.g., "The Study" and "Conclusions." Provide a brief abstract (50 words); references (not to exceed 15); figures or illustrations (not to exceed 2); tables (not to exceed 2); and biographical sketch. Dispatches are updates on infectious disease trends and research that include descriptions of new methods for detecting, characterizing, or subtyping new or reemerging pathogens. Developments in antimicrobial drugs, vaccines, or infectious disease prevention or elimination programs are appropriate. Case reports are also welcome.

Research Letters Reporting Cases, Outbreaks, or Original Research. EID publishes letters that report cases, outbreaks, or original research as Research Letters. Authors should provide a short abstract (50-word maximum), references (not to exceed 10), and a short biographical sketch. These letters should not exceed 800 words in the main body of the text and may include either 1 figure or 1 table. Do not divide Research Letters into sections.

Letters Commenting on Articles. Letters commenting on articles should contain a maximum of 300 words and 5 references; they are more likely to be published if submitted within 4 weeks of the original article's publication.

Commentaries. Thoughtful discussions (500–1,000 words) of current topics. Commentaries may contain references (not to exceed 15) but no abstract, figures, or tables. Include biographical sketch.

Another Dimension. Thoughtful essays, short stories, or poems on philosophical issues related to science, medical practice, and human health. Topics may include science and the human condition, the unanticipated side of epidemic investigations, or how people perceive and cope with infection and illness. This section is intended to evoke compassion for human suffering and to expand the science reader's literary scope. Manuscripts are selected for publication as much for their content (the experiences they describe) as for their literary merit. Include biographical sketch.

Books, Other Media. Reviews (250–500 words) of new books or other media on emerging disease issues are welcome. Title, author(s), publisher, number of pages, and other pertinent details should be included.

Conference Summaries. Summaries of emerging infectious disease conference activities (500–1,000 words) are published online only. They should be submitted no later than 6 months after the conference and focus on content rather than process. Provide illustrations, references, and links to full reports of conference activities.

Online Reports. Reports on consensus group meetings, workshops, and other activities in which suggestions for diagnostic, treatment, or reporting methods related to infectious disease topics are formulated may be published online only. These should not exceed 3,500 words and should be authored by the group. We do not publish official guidelines or policy recommendations.

Photo Quiz. The photo quiz (1,200 words) highlights a person who made notable contributions to public health and medicine. Provide a photo of the subject, a brief clue to the person's identity, and five possible answers, followed by an essay describing the person's life and his or her significance to public health, science, and infectious disease.

Etymologia. Etymologia (100 words, 5 references). We welcome thoroughly researched derivations of emerging disease terms. Historical and other context could be included.

Announcements. We welcome brief announcements of timely events of interest to our readers. Announcements may be posted online only, depending on the event date. Email to eideditor@cdc.gov.

December, 2019 *Emerging Infectious Diseases* marks the final issue that will be published in print. We encourage you to make the transition with us. Read the journal and sign up for table of contents alerts: <https://wwwnc.cdc.gov/eid>

Official Business
Penalty for Private Use \$300
Return Service Requested



DEPARTMENT OF
HEALTH & HUMAN SERVICES
Public Health Service
Centers for Disease Control and Prevention (CDC)
Molokop H16-2, Atlanta, GA 30329-4027

Robert Lee Kocher (1929–), *Two Birds* (1959). Oil on wood, 12 in x 7.75 in/30.5 cm x 19.7 cm. Image used by permission of the artist. Private collection, Fayetteville, Georgia, USA. Photography by James Galthany



MEDIA MAIL
POSTAGE & FEES PAID
PHS/CDC
Permit No. G 284

ISSN 1080-6040